NASA/TM—2017–219094

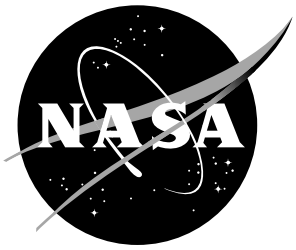

Blade Displacement Measurements During the NFAC UH-60A Airloads Test

Volume I—Methodology, System Development, and Data Analysis Techniques

Larry A. Meyn and Anita I. Abrego
Ames Research Center, Moffett Field, California

Danny A. Barrows
Langley Research Center, Hampton, Virginia

Alpheus W. Burner
Jacobs Technology, Hampton, Virginia

August 2017

NASA STI Program. . . in Profile

Since its founding, NASA has been dedicated to the advancement of aeronautics and space science. The NASA scientific and technical information (STI) program plays a key part in helping NASA maintain this important role.

The NASA STI Program operates under the auspices of the Agency Chief Information Officer. It collects, organizes, provides for archiving, and disseminates NASA's STI. The NASA STI Program provides access to the NASA Aeronautics and Space Database and its public interface, the NASA Technical Report Server, thus providing one of the largest collection of aeronautical and space science STI in the world. Results are published in both non-NASA channels and by NASA in the NASA STI Report Series, which includes the following report types:

- TECHNICAL PUBLICATION. Reports of completed research or a major significant phase of research that present the results of NASA programs and include extensive data or theoretical analysis. Includes compilations of significant scientific and technical data and information deemed to be of continuing reference value. NASA counterpart of peer-reviewed formal professional papers, but having less stringent limitations on manuscript length and extent of graphic presentations.
- TECHNICAL MEMORANDUM. Scientific and technical findings that are preliminary or of specialized interest, e.g., quick release reports, working papers, and bibliographies that contain minimal annotation. Does not contain extensive analysis.
- CONTRACTOR REPORT. Scientific and technical findings by NASA-sponsored contractors and grantees.
- CONFERENCE PUBLICATION. Collected papers from scientific and technical conferences, symposia, seminars, or other meetings sponsored or co-sponsored by NASA.
- SPECIAL PUBLICATION. Scientific, technical, or historical information from NASA programs, projects, and missions, often concerned with subjects having substantial public interest.
- TECHNICAL TRANSLATION. English-language translations of foreign scientific and technical material pertinent to NASA's mission.

Specialized services also include organizing and publishing research results, distributing specialized research announcements and feeds, providing information desk and personal search support, and enabling data exchange services.

For more information about the NASA STI Program, see the following:

- Access the NASA STI program home page at http://www.sti.nasa.gov
- E-mail your question to help@sti.nasa.gov
- Phone the NASA STI Information Desk at 757-864-9658
- Write to:
  NASA STI Information Desk
  Mail Stop 148
  NASA Langley Research Center
  Hampton, VA 23681-2199

NASA/TM—2017–219094

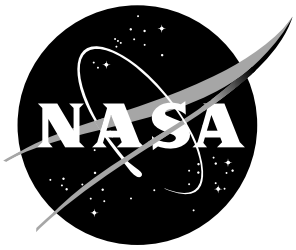

Blade Displacement Measurements During the NFAC UH-60A Airloads Test

Volume I—Methodology, System Development, and Data Analysis Techniques

Larry A. Meyn and Anita I. Abrego
Ames Research Center, Moffett Field, California

Danny A. Barrows
Langley Research Center, Hampton, Virginia

Alpheus W. Burner
Jacobs Technology, Hampton, Virginia

National Aeronautics and
Space Administration

Ames Research Center
Moffett Field, CA 94035-1000

August 2017

Available from:

NASA STI Support Services
Mail Stop 148
NASA Langley Research Center
Hampton, VA 23681-2199
757-864-9658

National Technical Information Service
5301 Shawnee Road
Alexandria, VA 22312
webmail@ntis.gov
703-605-6000

This report is also available in electronic form at:

http://ntrs.nasa.gov

Table of Contents

Table of Contents (cont.)

Nomenclature

α	shaft angle of attack, deg
α_c	corrected shaft angle, positive aft, deg
α_s	geometric shaft angle, positive aft, deg
β	blade flapping angle, positive up, deg
$\Delta twist$	elastic deformation of the blade about the 1/4-chord axis, positive nose up, deg
Δx	elastic deformation of the blade along the x-axis, in.
Δy	elastic deformation of the blade along the y-axis, in.
Δz	elastic deformation of the blade along the z-axis, in.
κ	rotation angle about the z-axis, positive counterclockwise
κ_{dynt}	angle offset, in rotation about the z-axis, for the hub under dynamic loading with respect to the hub under static loading
κ_{hat}	angle offset of the instrumentation hat with respect to the hub in rotation about the z-axis
μ	advance ratio
ω	rotation angle about the x-axis, positive counterclockwise
ω_{dyn}	angle offset, in rotation about the x-axis, for the hub under dynamic loading with respect to the hub under static loading
ω_{hat}	angle offset of the instrumentation hat with respect to the hub in rotation about the x-axis
ψ	azimuth, deg (0° is in the aft direction)
ψ_{shaft}	azimuth angle of the rotor shaft, equal to zero when Blade 1 is downstream of the hub and aligned with the longitudnal, x, axis of the body coordinate system, deg
ψ_N	azimuth offset angle from shaft azimuth for blade, N, deg
ψ_{offset}	angular offset of the longitudnal axis of the Large Rotor Test Apparatus from the test section centerline, deg
σ	rotor solidity, 0.0826
φ	rotation angle about the y-axis, positive counterclockwise
φ_{dyn}	angle offset, in rotation about the y-axis, for the hub under dynamic loading with respect to the hub under static loading
φ_{hat}	angle offset of the instrumentation hat with respect to the hub in rotation about the y-axis
ϑ	transverse location of rotor hub center in the test section coordinate system
ζ	blade lag angle, positive aft, deg

Nomenclature (cont.)

c	blade chord, in.
C_Q	rotor torque coefficient
C_T	rotor thrust coefficient
M_{tip}	hover tip Mach number
R	rotor radius, 322 in.
r	rotor radial coordinate, in.
x	streamwise or chordwise coordinate, in.
x_{dyn}	streamwise deflection of rotor hub center due to dynamic loads
x_{hat}	streamwise offset of the instrumentation hat axes origin from the hub axes origin
x_{hub}	streamwise location of rotor hub center in the test section coordinate system
x_{pivotH}	streamwise location of the angle-of-attack pivot point in the rotor hub coordinate system
x_{pivot}	streamwise location of the angle-of-attack pivot point in the wind tunnel coordinate system
y	lateral or spanwise coordinate, in.
y_{dyn}	lateral deflection of rotor hub center due to dynamic loads
y_{hat}	lateral offset of the instrumentation hat axes origin from the hub axes origin
y_{hub}	lateral location of rotor hub center in the test section coordinate system
y_{pivotH}	lateral location of the angle-of-attack pivot point in the rotor hub coordinate system
y_{pivot}	lateral location of the angle-of-attack pivot point in the wind tunnel coordinate system
z	vertical coordinate, in.
z_{dyn}	vertical deflection of rotor hub center due to dynamic loads
z_{hat}	vertical offset of the instrumentation hat axes origin from the hub axes origin
z_{hub}	vertical location of rotor hub center in the test section coordinate system
z_{pivotH}	vertical location of the angle-of-attack pivot point in the rotor hub coordinate system
z_{pivot}	vertical location of the angle-of-attack pivot point in the wind tunnel coordinate system
θ	blade pitch angle, deg
θ_0	collective pitch angle, deg
CCD	charge-coupled device, a type of digital camera sensor
PC	personal computer

Summary

Blade displacement measurements using multi-camera photogrammetry techniques were acquired for a full-scale UH-60A rotor, tested in the National Full-Scale Aerodynamics Complex (NFAC) 40- by 80-Foot Wind Tunnel. The measurements, acquired over the full rotor azimuth, encompassed a range of test conditions that included advance ratios from 0.15 to 1.0, thrust coefficient to rotor solidity ratios from 0.01 to 0.13, and rotor shaft angles from -10.0 to 8.0 degrees. The objective was to measure the blade displacements and deformations of the four rotor blades and provide a benchmark blade displacement database to be used in the development and validation of rotorcraft prediction techniques. The blade displacement measurement methodology, system development, and data analysis techniques are presented. Sample results are shown based on the final set of camera calibrations, data reduction procedures, and estimated corrections that account for registration errors due to blade elasticity.

1 Introduction

In May 2010, a full-scale wind tunnel test of the UH-60A Airloads rotor was completed in the USAF National Full-Scale Aerodynamics Complex (NFAC) 40- by 80-Foot Wind Tunnel at NASA Ames Research Center.[1] The test was a joint venture between NASA and the U.S. Army to acquire an expanded database, supplementing the widely used and extensive 1993 UH-60A airloads flight test data.[2] Unique measurement techniques, such as blade displacement multi-camera photogrammetry, were implemented to expand the airloads database and assist with the validation of rotorcraft predictive tools.

Blade displacement measurements are used to resolve rotor blade shape and position, including blade pitch, flap, lag, and elastic deformations. When combined with blade airloads and wake measurements, a comprehensive dataset is formed that directly relates rotor performance to the physical properties of the flow. The accurate prediction of rotor blade rigid body motion and elastic displacements is a key goal in the development of improved rotorcraft design and analysis techniques. Furthermore, the availability of detailed experimental measurements obtained under conditions representative of the actual flight environment may lead to more tightly coupled multi-disciplinary, higher fidelity rotorcraft aeromechanics analysis techniques.

Traditionally, blade displacements have been derived from strain gauges imbedded in the rotor blades. Due to blade size limitations and the limited availability of rotating instrumentation channels, the number of possible sensors is usually insufficient to fully resolve the blade motion. As an alternative, optical methods can be used to provide a description of the blade geometry over much of its length with the added benefit of reduced fabrication costs and sensor count.[3]

High-quality and comprehensive rotor blade displacement data sets are relatively rare. A Blade Deformation Measurement System using CCD cameras imbedded in the hub to measure blade movement and deformation of a Ka-25 helicopter blade was reported in 1997.[4] In 2001 stereo pattern recognition was used for the Higher Harmonic Control Aeroacoustic Rotor Test (HART II) to measure blade position and displacement of a 40-percent Mach scaled, 2-meter-radius BO-105 model rotor.[5] The technique used was based on a 3-dimensional (3D) reconstruction of visible marker locations using stereo photogrammetry, which provided the blade motion parameters in flap, lag, and torsion.

More recently, in preparation for the UH-60A Airloads wind tunnel test, rotor blade displacement measurements were acquired during two earlier wind tunnel tests in the NFAC 40- by 80-Foot Wind Tunnel. Blade displacement measurements were briefly used in 2008 during the Smart Material Actuated Rotor Technology (SMART) test and then again in 2009 during the

Individual Blade Control (IBC) test.[6,7] For these two wind tunnel tests and then for the Airloads test discussed here, the photogrammetry system progressively doubled in size and complexity for each test. A single PC assembly with two cameras was used for the SMART test, two PCs with four cameras were used for the IBC test, and four PCs with eight cameras were used for the final and much more extensive Airloads test. The final test included 27 sets of data for all four blades over the full rotor azimuth and many additional limited sets tracking all four blades, but only over a single quadrant. The measurement efforts during the first two test entries, while brief, significantly influenced and improved the final system design for the detailed blade displacement measurements during the more comprehensive Airloads test.

An overview of the blade displacement measurements for the NFAC Airloads Test and initial results were first presented by Abrego et al.[8] The objective of that report was to provide an overview and update of the blade displacement measurement methodology and system development used for the NFAC Airloads Test. Also presented were descriptions of image processing, uncertainty considerations, preliminary results covering static and moderate advance ratio test conditions, and initial comparisons with computational results.

2 Test Description

The 2010 Airloads test conducted in the NFAC 40- by 80-Foot Wind Tunnel used a Sikorsky Aircraft UH-60A rotor system mounted on the NASA Large Rotor Test Apparatus (LRTA) as shown in Fig. 1. The test section of the 40- by 80-Foot Wind Tunnel has semicircular sides, a flat ceiling, and a flat floor. The test section is lined with sound-absorbing material to reduce acoustic reflections, which reduces its cross section to 39 feet high by 79 feet wide. The test section is 80 feet long between the upstream contraction and downstream diffuser. The maximum test section velocity of the facility is approximately 300 knots. The LRTA, a special-purpose drive and support system designed to test helicopters and tilt rotors in the NFAC,[9] was mounted on three struts, allowing for an angle of attack range of +15° to -15°.

The UH-60A has a four-bladed articulated rotor system consisting of a hub, blade pitch controls, bifilar vibration absorbers, and main rotor blades. The blades used in this wind tunnel test were the same four rotor blades flown during the UH-60A Airloads Program.[2] Two blades were heavily instrumented, one with 242 dynamic pressure transducers (Blade 1) and the other with a mix of strain gauges and accelerometers (Blade 3). A summary of the rotor system parameters is provided in Table 1.

Table 1. UH-60A rotor parameters.

Parameter	**Value**
Number of blades	4
Radius, in.	322
Nominal chord, in.	20.76
Blade tip sweep, deg aft	20
Geometric solidity ratio	0.0826
Airfoil section designation	SC1095/SC1094R8
Thickness, % chord	9.5
100% RPM	258

Figure 1. UH-60A Airloads rotor installed on the Large Rotor Test Apparatus (LRTA) in the NFAC 40- by 80-Foot Wind Tunnel.

Although the UH-60A is classified as an articulated or hinged helicopter, there are no actual hinges at the blade root. Rather, the blade motions occur through elastomeric bearings and the "hinges" are the focal points of the bearings. During both the flight and wind tunnel tests, measurements of the blade motions about these focal points were accomplished through a combination of Rotary Variable Differential Transformer (RVDT) sensors and links, referred to as the Blade Motion Hardware (BMH) or "crab arm." A crab arm is installed on each blade and provides measurements of the blade flap, lead-lag, and pitch angles.

A second blade motion measurement system, composed of four sets of three laser distance transducers (one set mounted to each hub arm), was also used.[1] The calibration of both systems was performed simultaneously in the wind tunnel. Both of these measurement systems have troublesome interactions between the measured parameters that were largely corrected for during calibration. These interactions, if not properly accounted for, may lessen the confidence in the measured parameters from these systems.

2.1 Test Conditions

The primary wind tunnel test data were acquired during speed sweeps at 1-g simulated flight conditions up to an advance ratio of $\mu = 0.4$, and during parametric thrust sweeps (up to and including stall) at various combinations of shaft angles and forward speeds. Data were also acquired at conditions matching previous full-scale flight tests, small-scale wind tunnel tests, and while

performing unique slowed-rotor simulations at reduced RPM (40 and 65 percent), up to an advance ratio of μ =1.0. Detailed descriptions of these test conditions are presented by Norman et al.[1] A summary of the wind tunnel test conditions for the Airloads test is provided in Appendix A. The subset of test conditions chosen for detailed blade displacement measurements are listed in Appendix B.

3 Geometry

Three coordinate systems were used in the analysis of the photogrammetry data in the UH-60A Airloads Test: the wind tunnel coordinate system, the rotor hub coordinate system, and the rotor blade coordinate system. The photogrammetry system measured all target locations in the wind tunnel coordinate system. Targets located on the test section ceiling were used in the wind tunnel coordinate system for calibration of camera locations, pointing angles, and distortion coefficients. However, targets on the rotor hub and blades need to be transformed to the rotor hub and rotor blade coordinate systems, respectively.

3.1 Wind Tunnel Coordinate System

The UH-60A Rotor was mounted on the Large Rotor Test Apparatus (LRTA) for testing in the 40- by 80-Foot Wind Tunnel. Photogrammetric measurements were made in the wind tunnel coordinate system, which is depicted schematically in Fig. 2. (See Fig. 1 for an image.) The origin of the wind tunnel coordinate system is directly above the turntable center at the streamwise test section centerline. The x-axis is positive downstream, the z-axis is positive in the vertical direction, and the y-axis, defined by the right-hand rule, is positive in the starboard direction. The center of the UH-60A rotor hub at 0° angle of attack is located directly over the main support struts of the wind tunnel, approximately 85.9 inches upstream of the turntable center.

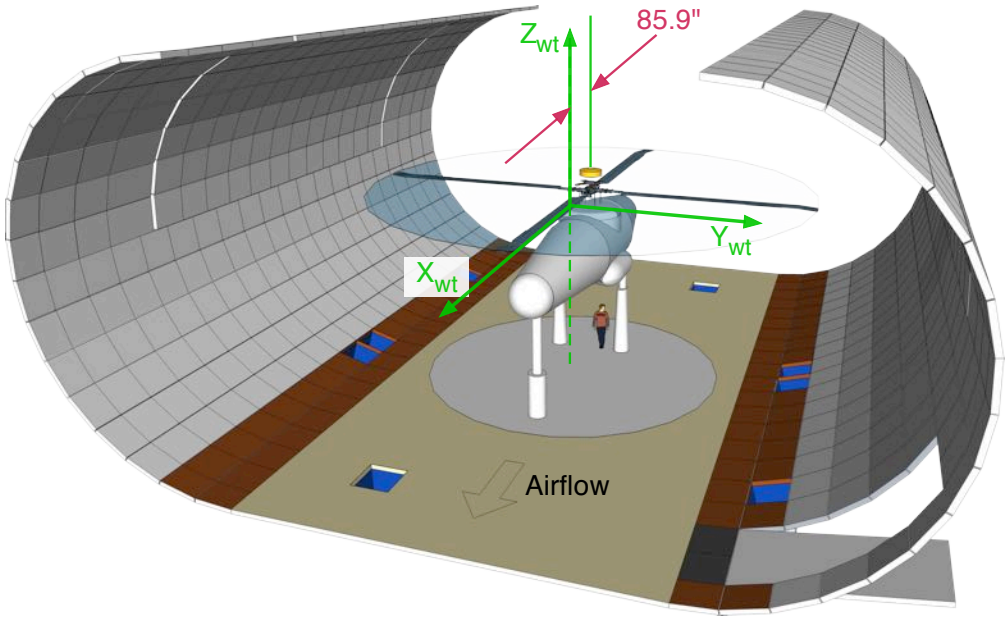

Figure 2. Orientation of the UH-60A/LRTA in the 40- by 80-Foot Wind Tunnel test section coordinate system.

The hub coordinate system is aligned with the LRTA body axis. The LRTA is not perfectly aligned with the test section centerline, but has a slight angular offset of 0.23° toward the starboard as shown in Fig. 3.* The locations of important hub and LRTA reference points in the vertical dimension are depicted in Fig. 4, and are referenced with respect to the hub moment center. The ball socket centerline is the location about which the model is rotated to set angle of attack, α. As shown, the hub moment center is 243.48 inches above the surface of the acoustic floor. The surface of the acoustic floor is 234 inches below the test section centerline (20 feet minus the 6-inch depth of the acoustic floor.) This dimension was used to determine the Z-axis locations of the UH-60A/LRTA reference locations presented in Table 2.

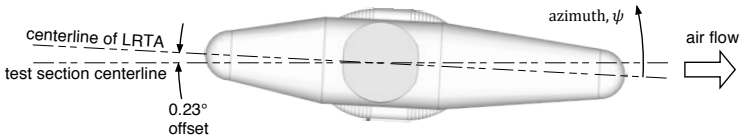

Figure 3. Overhead view of the alignment of the LRTA with the 40- by 80-Foot Wind Tunnel test section centerline.

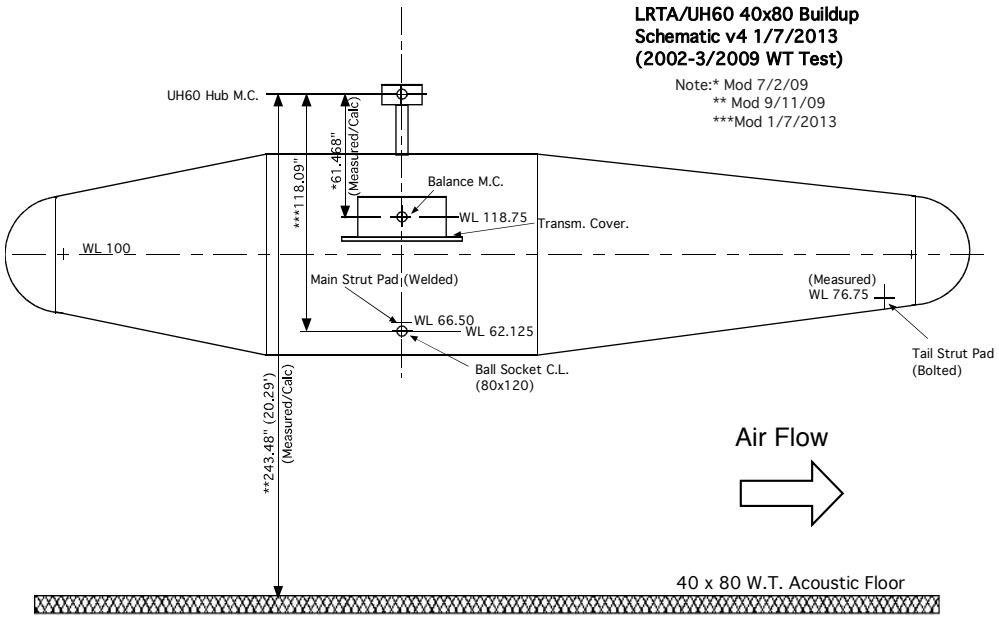

Figure 4. Profile view of the UH-60A rotor and the LRTA in the wind tunnel.

Table 2. UH-60A/LRTA reference locations in the wind tunnel coordinate system.

	X (in.)	**Y (in.)**	**Z (in.)**
Rotor Hub Center	-85.9	0	9.48
Angle of Attack Pivot Point	-85.9	0	-108.61
Balance Moment Center	-85.9	0	-51.988

*Per email from Justin McLellan on July 30, 2008: "Correction: The model was yawed slightly so that the nose is pointed to the starboard _not_ port side. Again the model is off by .23 degrees."

3.2 Hub and Rotor Blade Coordinate Systems

Rotor blade positions and orientations are referenced to the center and plane of rotation of the hub. When the LRTA is at a nonzero angle of attack, the hub center and its plane of rotation are rotated about the ball socket depicted in Fig. 4, which results in a rotation and translation of the hub coordinate system that is used for rotor blade positions and orientations. The UH-60A has four rotor blades numbered 1 through 4 as shown in Fig. 5. The rotor hub/shaft rotation angle about the shaft, or shaft azimuth, ψ_{shaft}, is defined as zero when the principal quarter-chord line of Blade 1, at zero lag angle, is aligned with the aft centerline of the LRTA. Blade position and orientation is defined by four rigid body rotation angles applied with respect to the reference orientation of each blade at 0° azimuth. These four angles, in the order of application, are pitch, θ, flap, β, lag, ζ, and azimuth, ψ.

The following simplified representations of the rotor blade show how these four angles are defined. The UH-60A rotor blade has a complex shape. The airfoil profile, twist, and sweep all vary along the span, as described in Appendix F. However, pitch, flap, lag, and elastic deformations can be thought of as being applied to a rectangular cylinder or bounding box that encompasses the blade in 3D space. Figure 6 shows an end view of this bounding box with a selection of the UH-60A airfoil profiles from different radial stations. Pitch, θ, is the first rotation angle applied to the reference geometry of the blade. As shown in Fig. 7, for pitch the blade is rotated in the vertical yz plane about its quarter-chord line, which is coincident with the x-axis of

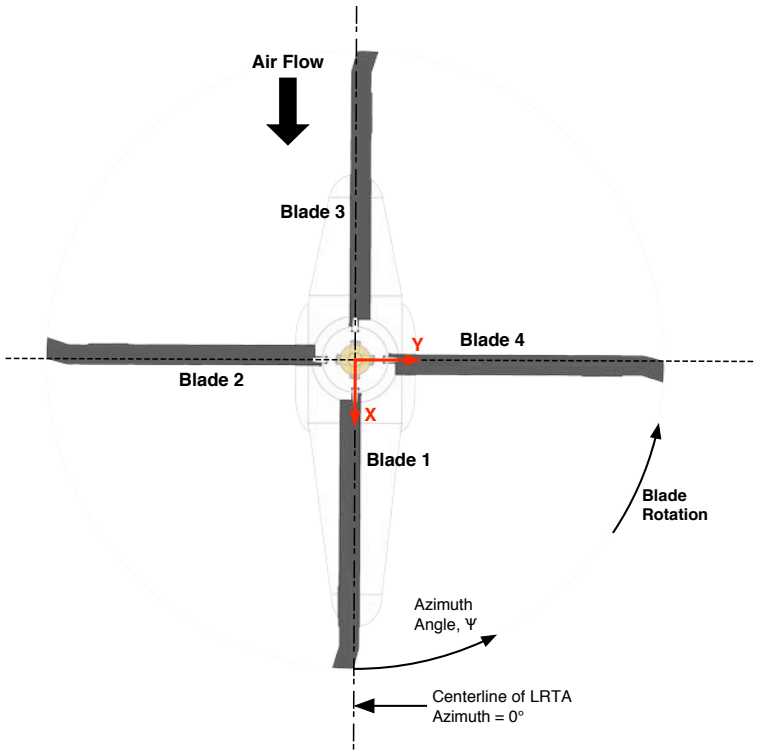

Figure 5. Top-view schematic of the test installation. All blades are shown with zero lag. The quarter-chord line of Blade 1 is aligned with the downstream LRTA centerline, which defines the zero azimuth position for the rotor hub and shaft.

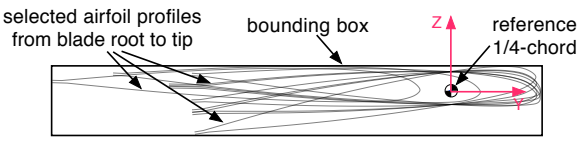

Figure 6. End view of the bounding box encompassing the UH-60A rotor blade.

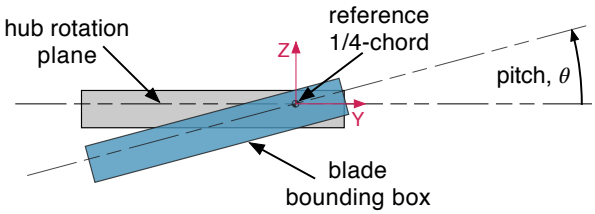

Figure 7. Pitch angle definition.

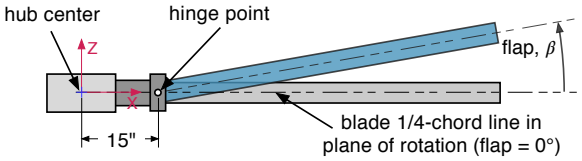

Figure 8. Flap angle definition.

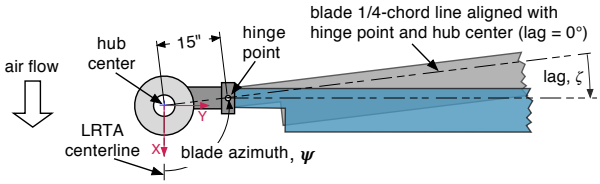

Figure 9. Blade azimuth and lag angle definitions.

the hub coordinate system. Second, the blade is rotated in the vertical xz plane about its hinge point by the flap angle, β, as shown in Fig. 8. Third, as shown in Fig. 9, a horizontal rotation about the hinge point by the lag angle, ζ, is applied to the blade. Finally, the blade and hub are rotated together in the hub rotation plane about the hub center by the blade azimuth angle, ψ, as shown in Fig. 9.

3.2.1 Elastic Blade Deformations

Elastic blade deformation variables represent the subtraction, in the blade reference coordinate system, of rigid blade geometry from the measured, elastically deformed blade geometry. These variables, Δx, Δy, Δz, and Δtwist, are defined for the locations along the quarter chord as shown in Fig. 10. It is assumed that the rigid blade and the elastically deformed blade have the same pitch, flap, lag, and azimuth orientation at the blade root. Errors in the estimated blade root orientation propagate into errors in the elastic deformation variables.

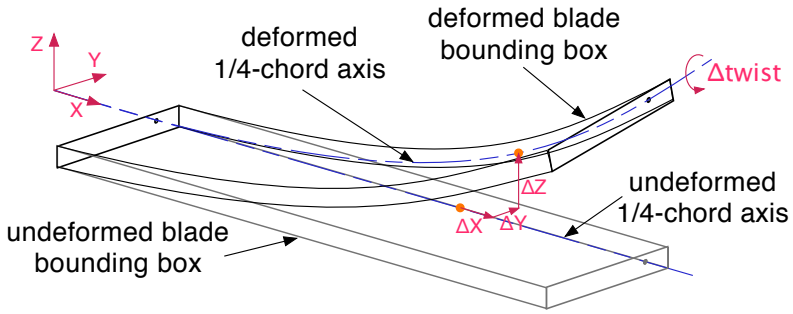

Figure 10. Rotor blade deformation variable definitions.

4 Blade Displacement System

The blade displacement experimental technique is based on the principles of digital close-range photogrammetry.[10] The optical method of photogrammetry has been used in a number of wind tunnels to measure aeroelastic deformations.[11,12] In this application for the Airloads test, multiple cameras were used to determine the spatial coordinates of retro-reflective targets attached to the lower surface of the blade. These coordinates were then used to extract pitch, flap, and lag angles, along with elastic bending and twist for each blade of the rotor system. An overview of the test hardware preparation, camera selection, hardware installation, and image processing are presented below. This system has also been documented in prior publications.[6,8]

4.1 Hardware Preparation

Retro-reflective targets were cut from 4-mil-thick, 3M Scotchlite 7610, high-reflectance adhesive tape and applied to both the lower surface of the blades and the test section ceiling (Fig. 11). Forty-eight 2-inch-diameter retro-reflective targets, three per radial station, uniformly spaced at approximately 0.05R intervals between the blade cuff and blade tip, were applied to each blade, covering the blade span from approximately r/R = 0.20 to 0.97 (Fig. 12). Figure 12(a) shows the targets on the lower surface of Blade 4. The additional targets shown in this image were applied to aid in the target location measurement process as described in Appendix I. Figure 12(b) is a schematic showing the location of the target centroids in the blade coordinate system. Small blade-to-blade variations in target locations were needed to avoid other surface-mounted blade instrumentation. Eighty-four, six-inch-diameter targets were also installed on the test section ceiling. Next to each ceiling target was a small cluster of 0.5-inch-diameter coded targets to assist with automated target recognition, in addition to a single 0.5-inch-diameter control target. Blade and ceiling target spatial locations were measured using the V-STARS commercial photogrammetry system, developed by Geodetic Systems Inc.[13] The standard deviations of the mappings for the ceiling and the blade target measurements were typically less than 0.04 inch and 0.001 inch, respectfully. Further details of the V-STARS measurements are described by Barrows et al.[7] Table 3 gives the ceiling target locations. Additional details on blade target measurements are presented in Appendix H.

The mappings of each blade in an un-deformed state, as measured in a laboratory setting, serve as reference geometries. The measured spatial data for the blades at any azimuth are then transformed to align with the reference geometries aligned at 0° azimuth to determine pitch, flap, lag, elastic twist, elastic flap bending, elastic lag bending, and radial deformations. For each blade the rigid body motion estimates, as determined from the 12 targets at the 4 inboard radial stations, r/R = 0.20 to 0.35, are used to transform all targets. All available blade targets are then used in the computation of elastic deformations. More detail about the calculation of blade orientation and deformations is presented in Section 4.5.

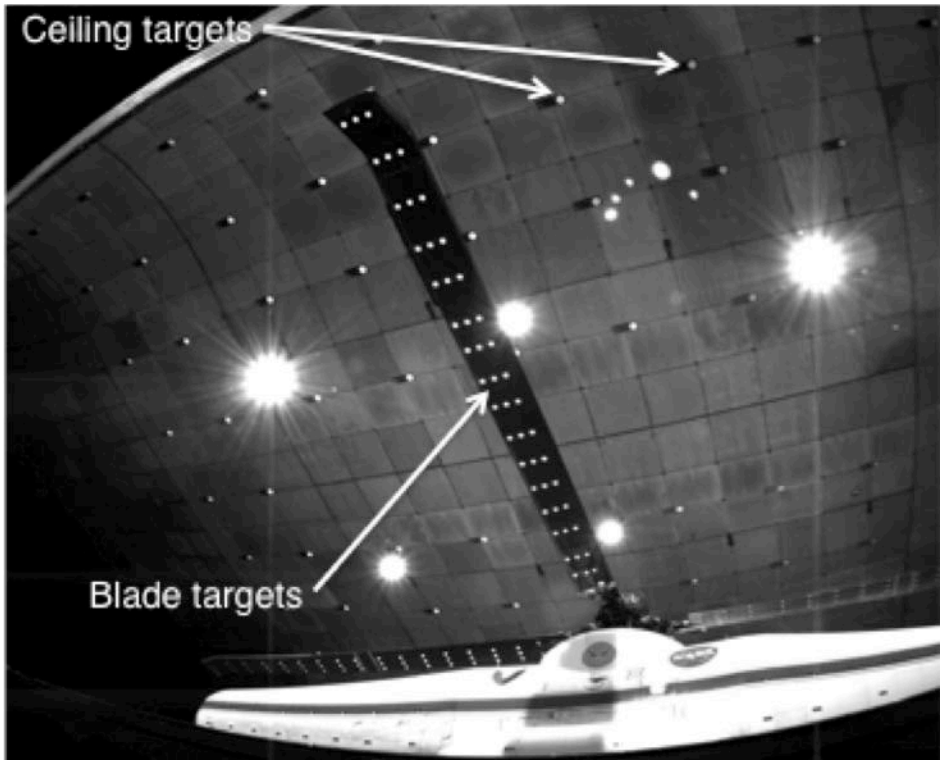

Figure 11. Rotor blade and test section ceiling retro-reflective targets.

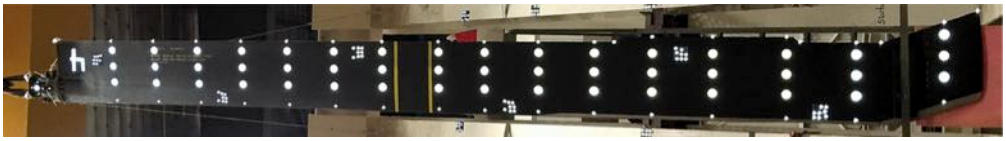

(a)

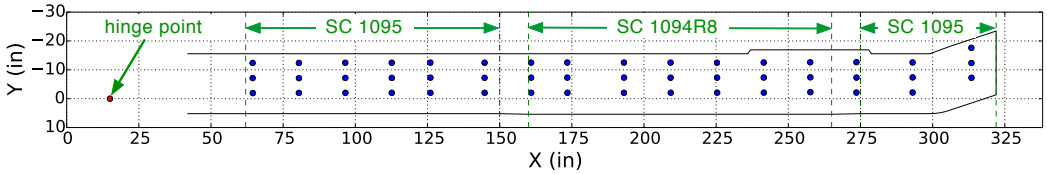

(b)

Figure 12. Target locations on the lower surface of the rotor blades: (a) photograph of targets on Blade 4, (b) schematic showing the blade lower surface planform with the target locations and the extent of airfoil profile sections.

Table 3. 40- by 80- Foot Wind Tunnel test section ceiling registration target locations.

Target Number	X(in.)	Y(in.)	Z(in.)	Target Number	X(in.)	Y(in.)	Z(in.)
1	-514.8296	370.0277	193.7674	**49**	300.9476	0.2063	234.5381
2	-418.8300	370.0428	193.9490	**50**	397.0012	-0.0051	234.6746
3	-310.1473	370.2541	194.2991	**51**	-514.8605	-96.1164	232.9658
4	-211.7249	370.5374	194.2451	**52**	-418.6617	-95.6765	233.0417
5	-113.2534	370.7880	194.3015	**53**	-310.1861	-98.1224	233.4856
6	-15.1983	370.6130	194.4887	**54**	-211.7024	-98.3226	233.6068
7	83.5031	370.9901	194.5390	**55**	-113.2205	-98.1700	233.8217
8	181.8699	371.0486	194.5439	**56**	-14.7615	-97.9884	233.9959
9	300.8676	371.0865	194.8728	**57**	83.7641	-97.9025	234.0715
10	396.9173	371.1691	194.9859	**58**	182.2275	-97.8864	234.2845
11	-514.9937	285.9451	228.6496	**59**	301.1806	-95.6231	234.5431
12	-419.0126	285.9025	228.7873	**60**	397.1488	-95.6337	234.7159
13	-310.3037	285.6269	229.1434	**61**	-514.9183	-192.1084	233.0860
14	-211.8955	286.0277	229.1559	**62**	-419.0298	-191.7238	233.1699
15	-113.5574	285.9565	229.2302	**63**	-310.5000	-204.0356	233.4892
16	-14.9306	286.1022	229.3912	**64**	-211.8311	-203.7290	233.6264
17	83.2740	286.1577	229.5351	**65**	-113.3429	-203.9685	233.8340
18	181.8315	286.1911	229.7300	**66**	-14.8127	-203.8228	233.9310
19	300.9482	285.9109	230.0822	**67**	83.6703	-204.0642	234.1183
20	397.1399	286.1695	230.2383	**68**	181.8035	-203.7213	234.2574
21	-514.7547	192.0638	233.1380	**69**	300.9483	-191.6311	234.5315
22	-418.7933	192.0475	233.2683	**70**	396.9169	-191.6036	234.6978
23	-310.5521	204.7111	233.6154	**71**	-514.5749	-285.4166	228.6704
24	-212.0481	204.1346	233.6076	**72**	-418.6132	-285.3816	228.6312
25	-113.6932	204.2821	233.6347	**73**	-310.4228	-285.7264	228.7940
26	-15.2085	204.2763	233.9089	**74**	-212.0374	-285.6640	229.1155
27	83.1926	204.1543	234.0591	**75**	-113.3260	-285.7392	229.3258
28	181.8539	204.3638	234.3156	**76**	-14.8999	-285.8102	229.4668
29	300.8318	192.1105	234.3779	**77**	83.5367	-285.8432	229.6192
30	396.8665	192.1427	234.6470	**78**	181.9964	-285.5708	229.8344
31	-515.0281	96.2116	233.1606	**79**	301.2281	-285.7920	230.0140
32	-418.7238	96.2496	233.3295	**80**	397.2115	-285.4644	230.2434
33	-310.3325	98.3783	233.4967	**81**	-514.5851	-369.8649	193.6221
34	-211.9004	98.7286	233.5668	**82**	-418.6759	-370.0070	193.6175
35	-113.4123	98.3396	233.9010	**83**	-310.4386	-370.2129	193.8719
36	-15.0089	98.6414	233.9736	**84**	-211.9506	-370.2896	194.0154
37	83.4239	98.5032	234.0117	**85**	-113.2431	-370.3734	194.2639
38	181.8694	98.6585	234.2860	**86**	-14.8870	-370.2674	194.4810
39	301.1896	96.4362	234.4942	**87**	83.5439	-370.3855	194.5796
40	396.8961	96.0973	234.7073	**88**	181.8167	-370.6249	194.4764
41	-514.9676	0.0004	233.1288	**89**	301.2128	-370.7809	194.7187
42	-419.0426	0.2222	233.1871	**90**	397.2873	-370.4284	195.0357

4.2 Cameras

The blade displacement system used eight 4-megapixel, 12-bit CCD progressive scan Imperx IPX-4M15-L digital cameras, with a resolution of 2048 × 2048 pixels. To capture the full motion of each rotor blade with at least two cameras, each camera's image field-of-view included a blade azimuth range of at least 90°. The overall translational movement experienced by the rotor blades due to angle of attack changes, blade flapping, and elastic blade deformations further expanded the lens field-of-view requirements. As a result, to encompass the full range of of blade motion and camera installation constraints of the test section, Nikon 10.5 mm f/2.8 DX (fish-eye) lenses were selected as a compromise. Such short focal length "fish-eye" lenses are not typically used in photogrammetry applications because of the difficulty in obtaining sufficiently accurate distortion corrections. Lens calibrations, mentioned in Barrows et al.,[7] can partially correct the troubling lens distortions that otherwise reduce the accuracy of the measurements.

4.3 Installation

Prior to the start of the UH-60A full-scale wind tunnel test, the blade displacement system setup concentrated on ensuring high image quality (particularly lighting), optimal orientation angles of the cameras, and adequate coverage on the camera image planes across the complete rotor disk for the anticipated test conditions. A top-view schematic of the LRTA, rotor blades, camera locations, and quadrant identifications is illustrated in Fig. 13.

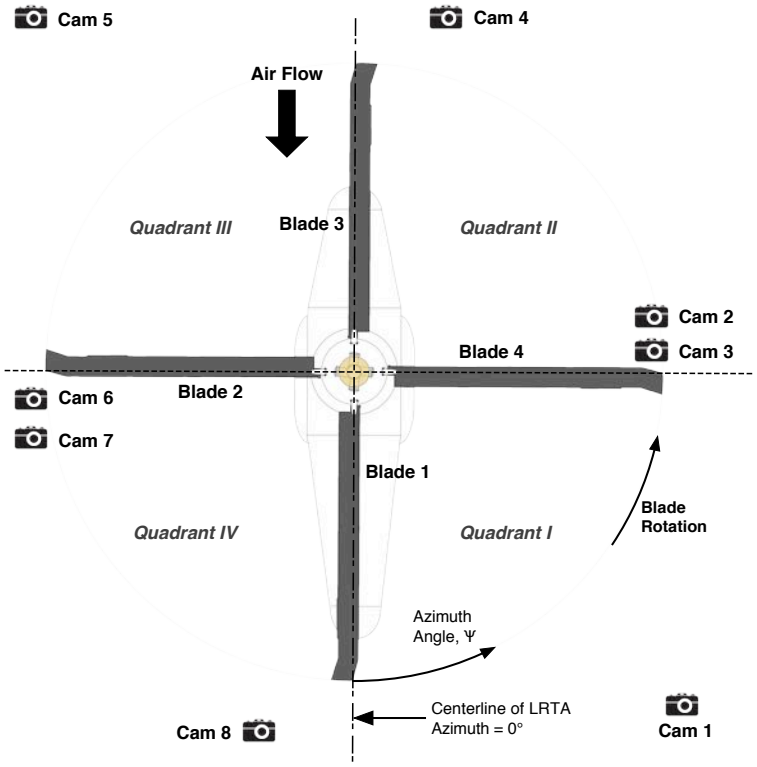

Figure 13. Top-view schematic of the test installation with blade numbers, cameras, and rotor quadrants identified. All blades are shown with zero lag. The quarter-chord line of Blade 1 is aligned with the downstream LRTA centerline, which defines the zero azimuth position for the rotor hub and shaft.

The blades, numbered 1 to 4, rotate counterclockwise when viewed from above. The 0° azimuth location of each blade is defined as aft, over the tail of the LRTA. The four quadrants that make up the rotor disk are designated as Q-I thru Q-IV. Since the rotary shaft encoder 1/rev signal is referenced to Blade 1, the azimuth angles of the other three blades must be calculated from the azimuth position of Blade 1. The eight blade displacement cameras were positioned such that two cameras predominantly viewed each rotor quadrant. Cameras 1 and 2 viewed Q-I, cameras 3 and 4 viewed Q-II, etc. The camera locations were not symmetrical about the rotor shaft due to differences in blade motion on the advancing and retreating side of the rotor, based on experience from the SMART and IBC tests. Fig. 14 illustrates the camera viewport locations in the test section. Although each camera pair was arranged to view a single rotor quadrant, the view from a given camera was not necessarily limited to that specified quadrant. In particular, a blade could often be viewed by more than two cameras, resulting in potential multi-camera photogrammetric intersections of the blade targets at many azimuths.

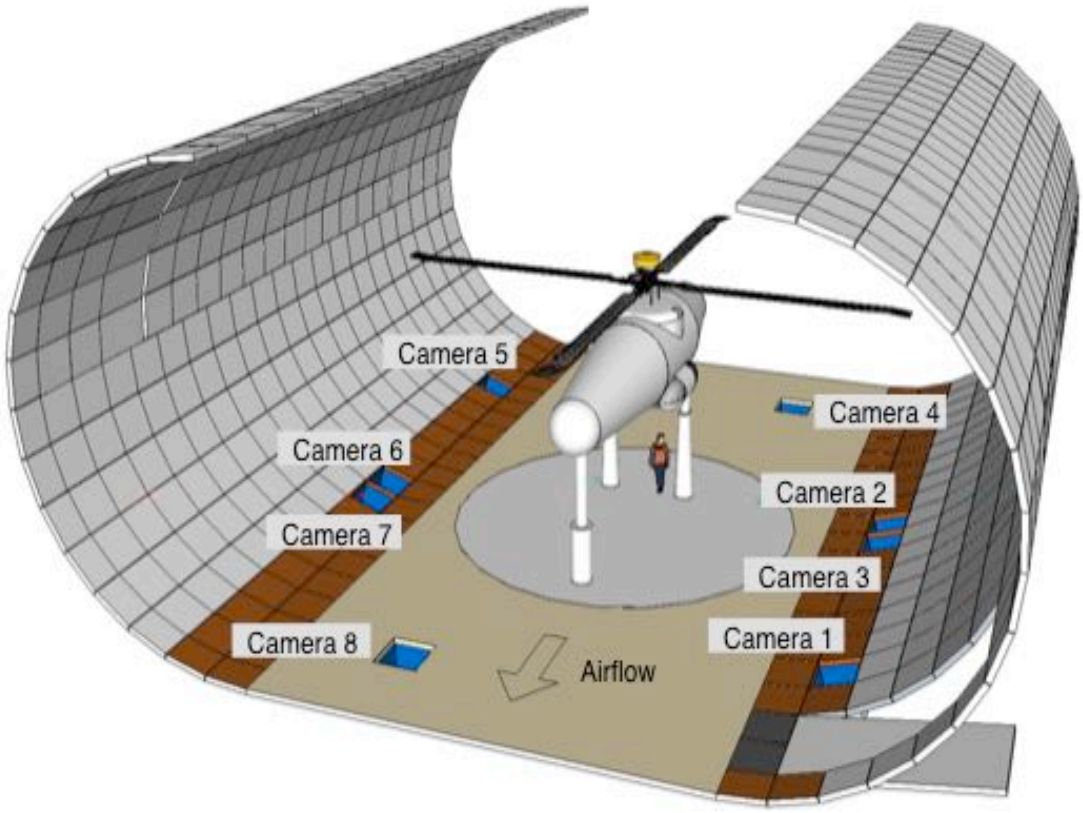

Figure 14. Test section schematic illustrating camera viewport locations.

The cameras were securely anchored inside the test section floor camera viewports, facing upward to view the lower surfaces of the blades through protective, low-reflectance glass windows (Fig. 15). The low-reflectance windows were procured especially for the UH-60A test to reduce troublesome reflections from the fiber-optic bundle illuminators that interfere with target centroiding. Target illumination was provided by Perkin-Elmer Machine Vision 7060-10 xenon flash-lamp 50-mJ strobes with a pulse duration of 10 microseconds (full width at 1/3 maximum). Fiber-optic bundles positioned as near as possible to the optical axis of each camera lens routed the light from each strobe to illuminate the targets. This near on-axis lighting maximized the signal return from the blade and ceiling retro-reflective targets. On average, there were eight 0.25-inch-diameter fiber-optic bundles encompassing each camera lens to help distribute the emitted strobe light equally across the blades. Roughly 50 percent of the fiber bundles were capped with focusing lenses to further increase strobe illumination in areas of the rotor disk where the light return from the retro-reflective targets was lower because of the highly oblique viewing angle.

Figure 15. Camera installation inside test section floor cavity.

4.4 Data Acquisition

The blade displacement image acquisition hardware consisted of components in both the wind tunnel computer room and in the test section viewports. The data acquisition system consisted of four PC's running Windows XP Professional®, each with a Matrox Helios PCIX® frame grabber board that was interfaced via Camera Link® through fiber-optic cables. Due to the extreme distances (> 250 ft) between the cameras and the blade displacement data acquisition system, Camera Link fiber-optic (FO) extender units were required to connect data via fiber from the cameras to the PC frame grabber boards. Software included NASA-developed Rotor Azimuth Synchronization Program (RASP) rotor encoder[14] and WingViewer image acquisition software.[15] A digital/delay pulse generator provided the synchronized trigger to all strobes and cameras based on the image acquisition software and RASP selection of azimuth. The master blade displacement data acquisition system configuration, which enabled RASP to control the synchronized strobe, camera, and acquisition triggers to the other three systems, is illustrated in Fig. 16.

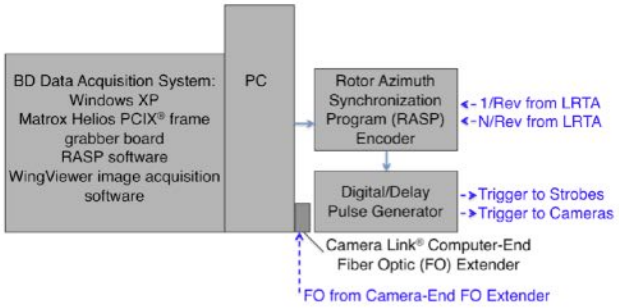

Figure 16. Master blade displacement data acquisition system computer room components.

The strobes and cameras were triggered such that the strobe light pulses occurred within the integration time of the CCD video cameras and with respect to the desired blade azimuth location in increments of 0.35° (degree/effective shaft encoder count). All cameras and strobes

were synchronized with the rotor shaft encoder to simultaneously capture the retro-reflective targets on the lower surface of each blade at an image-set acquisition rate of once per rotor revolution. Fig. 17 illustrates a typical test section camera viewport installation and LRTA encoder channels.

Image data were taken for up to 60 consecutive revolutions to document the instantaneous and mean (via sample average) deformation of each blade at a specified rotor azimuth. This process was repeated for up to 40 rotor azimuth locations to document the deformation of each blade throughout the entire rotor disk. For the nominal rotor rotation rate of 258 RPM, one image per each of the eight cameras was captured every 0.23 seconds.

Blade displacement image data sets were categorized as either primary or secondary. For 28 of the 29 Airloads primary blade displacement test conditions, images were acquired for 60 revolutions of data per azimuth, with 8 cameras and 40 rotor azimuths, producing 19,200 individual images. (At one primary test condition, only 15 images were acquired at each azimuth for each camera.) The time required to acquire 60 images at each of the 40 rotor azimuths was approximately 14 seconds, leading to a total data acquisition time approaching 10 minutes. The data acquisition time proportionally increased during slowed rotor testing performed at 167 and 105 RPM. Secondary data sets consisted of 12 images per rotor azimuth that recorded a single blade per rotor quadrant for a data set of 11 azimuth positions over a range of 95°. Acquisition time for secondary data sets was approximately 1 minute. These secondary data sets were acquired during the majority of the Airloads wind tunnel test, during test conditions not identified as blade displacement primary data sets. Appendix B lists the blade displacement data sets that were analyzed for this report.

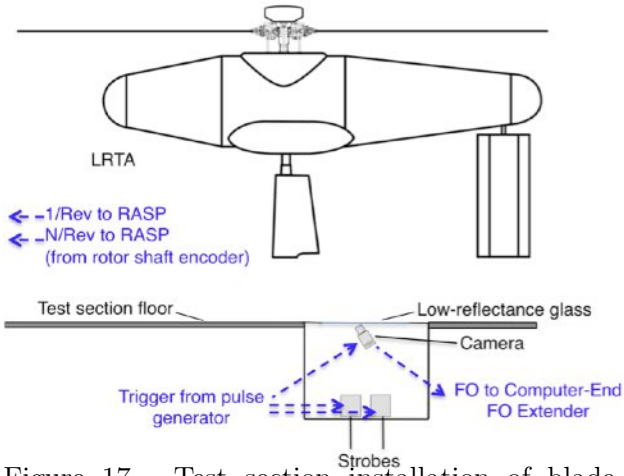

Figure 17. Test section installation of blade displacement data acquisition components in camera viewport and LRTA encoder signals.

4.5 Data Analysis

4.5.1 Camera Calibration

Photogrammetry requires a set of equations for each camera that maps coordinates in three-dimensional space to coordinates in a two-dimensional camera image. These are referred to as collinearity equations, and the specific set of coefficients used for each camera is referred to as the camera's calibration. The form of the collinearity equations used for data analysis in this report is described in References 11 and 12. However, an additional coefficient, for a third radial distortion parameter, was added as described in Reference 16.

Typically cameras are calibrated in a lab environment and then the calibrations are adjusted in the field to account for changes in the camera's "exterior" coefficients due to camera position and orientation. This procedure did not work well for this test, as mean calibration errors of a pixel or more were evident when comparing the calculated location of the ceiling targets in a camera image with the centroids of visible ceiling targets in the image. The source of this error was not determined, but it was quite possibly due to the cameras being installed behind windows that caused

image distortion. Instead, each camera was calibrated in situ using the ceiling targets. The cameras were recalibrated following any activity that could possibly alter camera alignment. For these in situ calibrations, the mean calibration errors for each camera were 0.16 pixels or less.

4.5.2 Image Processing

Each set of images was digitally processed to calculate centroid locations of discrete targets on the rotor blades and test section ceiling. For image processing and data reduction, a suite of custom designed image processing and data reduction functions was developed using the Mathworks® Matlab software environment. Supporting functions for image processing, photogrammetry, and coordinate transformations were provided via a custom Matlab Photogrammetry Toolbox developed for NASA by Western Michigan University.[16] This toolbox, in conjunction with the Matlab Image Processing and Statistics Toolboxes, was integrated into a NASA rotor-specific toolbox suite of functions. The NASA Rotor Toolbox makes use of moderately automated post-test image processing procedures that identify and calculate the image plane centroid spatial coordinates for each target. The Rotor Toolbox also contains a number of specialty scripts and functions for camera calibration, determining camera location and pointing angles, and performing multi-camera intersections to determine 3D spatial coordinates for computing pitch, flap, and lag angles, as well as elastic deformations.

An interactive graphical user interface (GUI) is used for image processing of targets and target centroid inspections. The GUI provides some automation of the centroiding process, but manual inputs and visual inspection of image are required to detect and avoid some issues. A detailed description of the GUI and its use is provided in Appendix D. Figure 18 shows a sample of the blade centroids being identified by this initial processing step. After target numbering is properly identified using the first image, the computation of target centroids for the second image through the end of the image sequence is fully automated. Targets on the LRTA fuselage, test section ceiling, and instrumentation hat are useful visual guides during this processing step.

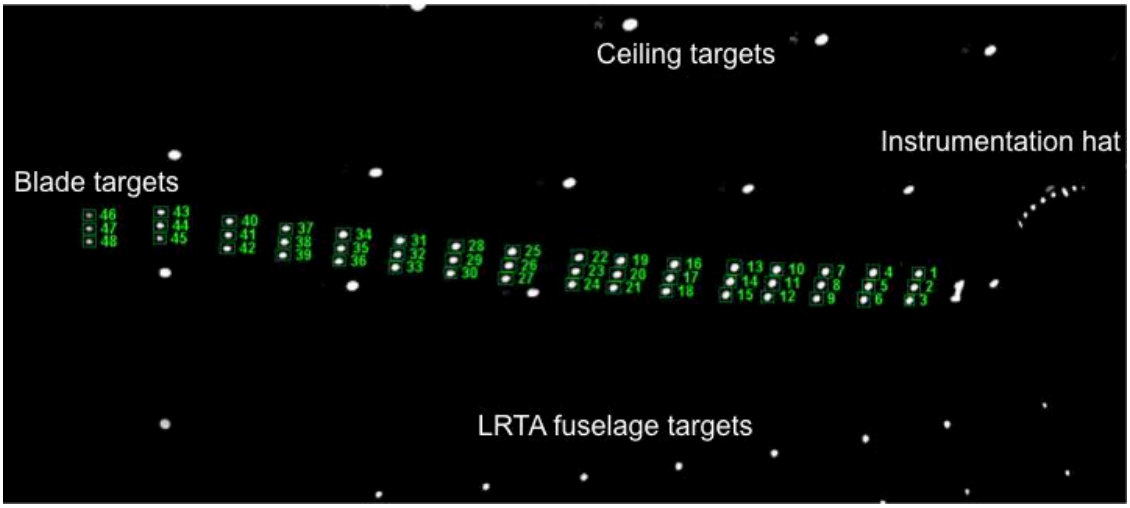

Figure 18. Example data image with the various types of targets identified. Blade targets are identified by target number and outlined by green rectangles.

4.5.3 Centroid Validation

Centroid validation is necessary because partially blocked targets are sometimes identified as full-size targets and they can be difficult to detect. These occurrences are problematic because the partially blocked targets are not properly defined and their identified centroid locations are offset. Due to the movement of the rotor blades about the image plane and target numbering complications caused by blocked targets, a user interface is necessary for the first image of each data sequence. To avoid or correct partially blocked targets, centroid data for all images in a set must be inspected and validated. A separate centroid validation Matlab function was developed to locate mislabeled or suspect centroid data that may require manual correction. For example, slowed-rotor, high-advance-ratio test conditions proved to be particularly challenging due to the extreme image-to-image blade motion (compared to lower advance ratios). This holds true even near the inboard portion of the rotor blades. Also, ceiling targets and strobe window reflections have the potential to interfere with the accurate identification of blade target centroid locations.

It is important to review all images in a set because targets may appear in several images but then disappear (either fully or partially) in later images of the same sequence (Fig. 19). Figure 19(a) is a long-exposure close-up of the LRTA and inboard portion of the rotor blades with the blade area of interest indicated within the red box. Figures 19(b) and 19(c) are two data images from the same image sequence where the trailing-edge targets of Blade 1 can be seen in Fig. 19(b), but are no longer visible in the next image, Fig. 19(c). As the blade flaps, the trailing-edge targets are intermittently blocked by the LRTA fuselage. This is common for the inboard targets and caused difficulty in automating the image processing.

Another example of a centroid validation challenge are the strobe reflections off the camera viewport windows. Light from a xenon strobe, reflecting off the camera viewport window, can be seen in each image (Fig. 20). Although the reflection intensity was reduced by a factor of approximately four by replacing the standard glass camera viewport windows with low-reflectance coated windows,[8] it continued to pose potential complications with image processing automation. The reflections generally affect only a few targets on each blade at a single blade azimuth position per camera (Fig. 20(a)). Consequently, rev-to-rev variations in blade position can cause the strobe reflections to intermittently merge with blade targets. Figure 20(b) illustrates two blade targets near the vicinity of a strobe reflection where the blade target is properly discriminated. However, in the same image sequence, the strobe reflection can merge with an adjacent target as indicated by the shaded red area of Fig. 20(c), causing an error in the centroid location. More effective means for dealing with these occurrences would greatly improve the level of automation.

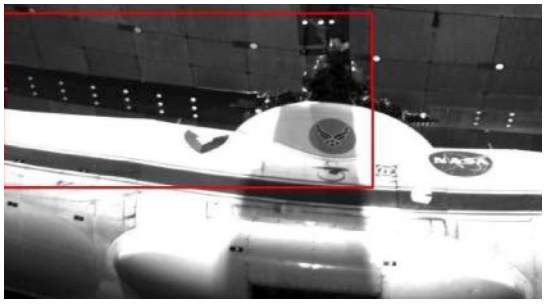

(a) Close-up of LRTA in region of interest.

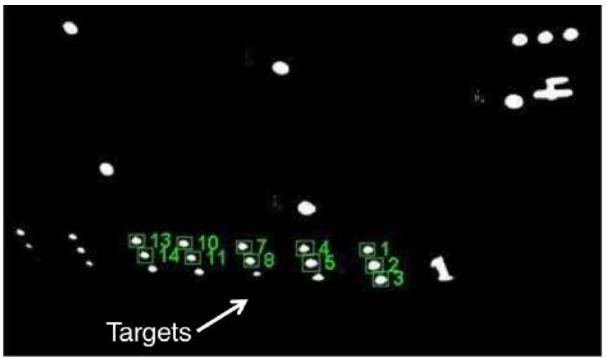

(b) Trailing-edge targets of Blade 1 are visible.

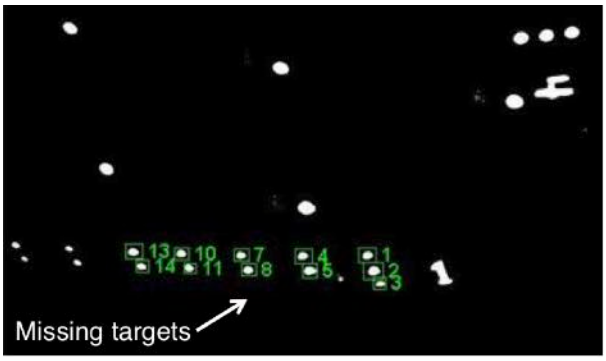

(c) Trailing-edge targets of Blade 1 are blocked by the LRTA fuselage.

Figure 19. Image processing example with the identification of rotor blade targets.

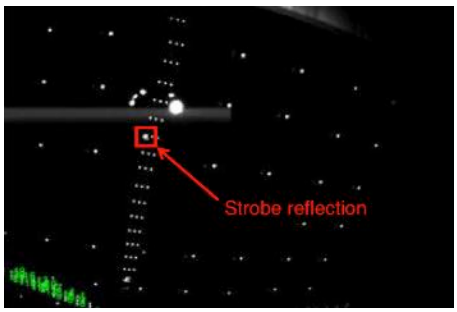

(a) Typical image with strobe reflection near the vicinity of blade targets; red box indicates area of interest for (b) and (c).

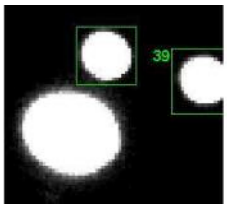

(b) Image showing strobe reflection distinct from targets.

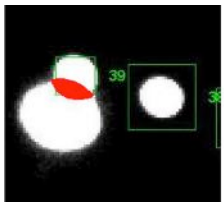

(c) Image showing strobe reflection overlapping blade target; red region indicates combined grayscale.

Figure 20. Effect of strobe light reflection on target centroiding.

4.5.4 Target Locations

To determine the location of the targets in the wind tunnel coordinate system, the target centroids need to be available for two or more cameras. Photogrammetry provides a relationship, known as collinearity, between the three-dimensional locations of the targets and the corresponding, two-dimensional centroid locations in simultaneous camera images.[11,12] The collinearity equations relating the target location (X, Y, Z) in object space to the corresponding point (x, y) in the image plane for two or more cameras, were used to estimate the (X, Y, Z) locations that yield the minimum least-squares error. Each combination of cameras used to determine the (X, Y, Z) target locations is referred to as an "intersection." The (X, Y, Z) target locations for all possible intersections were determined for each blade, for each image set, and for each data record point.[†] Ideally, the data for all of the intersections could be combined to yield a robust set of target location for all targets visible to two or more cameras. A weighted average of all intersections with the target locations weighted inversely by the square of the standard deviation (or variance) of their least-squares estimates is one way to accomplish this. Unfortunately, the current camera calibrations each have regional variations in their errors, which results in inconsistent location estimates when all of the weighted intersections do not contain the identical sets of targets. This can result in large, false discontinuities in the spanwise variation of blade deformations.

To avoid these inconsistencies and discontinuities, the (X, Y, Z) target locations from only one of the available intersections is used to subsequently estimate blade orientation and deformation. The algorithm used to select the "best" intersection uses three metrics—the number of targets available, the mean total standard deviation for target locations, and the maximum intra-target distance error. The total standard deviation for target locations is based on the least-squares error statistics for each target in the intersection. The total standard deviation for a target is the root-mean-square of the x, y, and z error standard deviations for the target.

Intra-target distance is calculated as follows. First, the distance between all adjacent targets is calculated for an intersection's target locations. From these values, the corresponding distance determined from the reference target locations is subtracted. The absolute value of these distance differences is the intra-target distance "error." Because the blades deform, zero intra-target distance error is not expected. However, errors due to deformation alone should be relatively small. Large errors are then likely due to misidentified targets, centroiding errors, or large local inconsistencies between camera calibrations.

The "best" intersection selection algorithm uses the following selection steps.

1. The maximum target count, $MaxTargs$, of all the available intersections is determined.
2. Candidate intersections are limited to intersection target counts greater than $MaxTargs - 7$.
3. The candidate intersections are then restricted to those with a maximum intra-target distance error of 0.25 inches. If none of the intersection meet this criteria, then this restriction is skipped.
4. Of the remaining candidates, the one with the lowest mean total standard deviation is chosen as the "best" intersection.

The "best" intersection determined via this algorithm is then used to estimate blade orientation and deformation.

[†]Intersections for cameras 2 and 3 and for cameras 6 and 7 are ignored due to the small angular separation of the camera views.

4.5.5 Blade Position, Orientation, and Deformation

The blade position and orientation variables are pitch, θ, flap, β, lag, ζ, and azimuth, ψ. The blade deformation variables are Δx, Δy, Δz, and Δtwist. The definitions for these variables are presented in Section 3.2. The blade target locations are measured in the wind tunnel coordinate system. The initial estimate of blade position and orientation is based on a specific series of geometric rotations and translations needed to closely map reference blade target locations to measured blade target locations. The translations in the x, y, and z directions are t_x, t_y, and t_z, respectively. The rotations about the x, y, and z axes are ω, ϕ, and κ, respectively, as shown in Fig. 21. Details on these geometric transformations are provided in Appendix C.

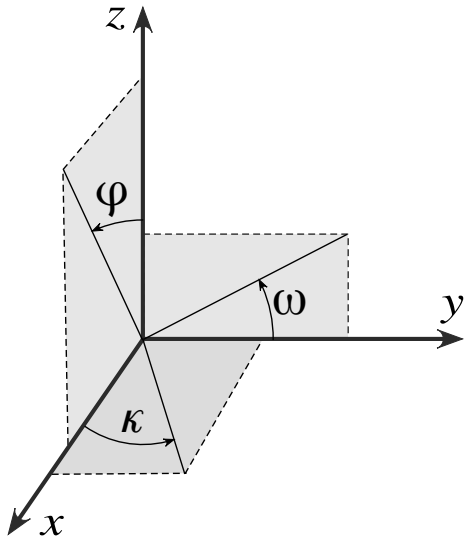

Figure 21. Coordinate system for 3D rotations.

The first step in the process is the adjustment of the measured target coordinates for angle of attack, α, by rotating them about the y-axis by $-\alpha$. Then the `conformal3DNLLS` routine, from the Photogrammetry Toolbox, is used to determine the rotation and translation values that best map the reference blade target locations to the measured blade target locations, for the 12 most inboard targets, using a nonlinear least-squares algorithm. The rotation angles are then used to determine pitch, flap, and lag. The translation values are currently unused. Equations 1, 2, and 3 are used to calculate the pitch, flap, and lag angles, respectively. The lag angle equation requires the blade's azimuth angle, ψ, and the LRTA alignment offset, ψ_{offset}. The azimuth angle of the blade is determined using Eqn. 4. This equation requires the azimuth angle of the rotor shaft, ψ_{shaft}, which is provided by the rotor data system and ψ_N, the azimuth offset angle from the shaft azimuth for blade N. ψ_N is 0°, 270°, 180°, and 90°, respectively, for blades 1 through 4.

$$\theta = -\omega \tag{1}$$

$$\beta = \phi \tag{2}$$

$$\zeta = mod(\kappa + \psi + \psi_{offset}, 360) \tag{3}$$

$$\psi = \psi_{shaft} + \psi_N \tag{4}$$

The deformation values, Δx, Δy, Δz, and Δtwist, are determined by applying the inverse of the calculated transformation to all the measured target location values using the `conformal3Dinv` routine, from the Photogrammetry Toolbox,[16] which applies a rigid-body transformation of the measured target locations to the blade coordinate system. Deviations of

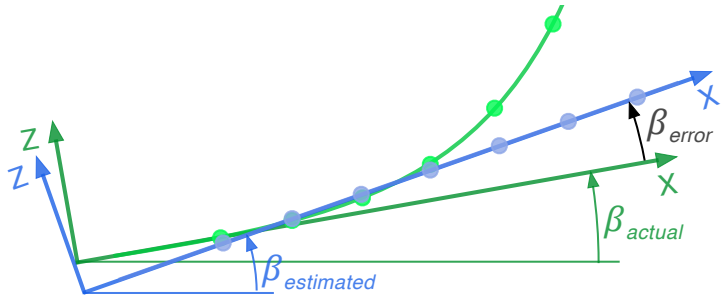

Figure 22. Illustration of flap angle estimate error due to blade elasticity.

these transformed target locations are due to blade deformations and measurement error. The deformation values are determined for each spanwise station that has a full row with three targets.[‡] Values of t_x, t_y, and t_z, and ω are calculated with the `conformal3DNLLS` function to provide the best rigid-body transformation of the three reference target locations at each station to the measured target locations. The transformation coefficients t_x, t_y, and t_z, and ω are direct equivalents of the deformation values Δx, Δy, Δz, and Δtwist.

4.5.6 Position and Orientation Errors Due to Blade Elasticity

As previously mentioned, the first four inboard rows of targets are used to estimate the pitch, flap, and lag of a blade from the measured target locations. This provides the initial, uncorrected pitch, flap, lag, and deformation values.

Due to elastic deformation of the measured blade at these inboard locations, this registration process can lead to errors in the estimated blade position and orientation with corresponding errors in the deformation values. This is illustrated in Fig. 22, which shows a hypothetical registration to estimate the flap angle. The green xz axes show the actual flap angle, β_{actual}, with the green line representing the deformed quarter-chord line of the measured blade. The dots along the line represent registration target rows. The blue xz axes show the estimated flap angle, $\beta_{estimated}$, that is found when fitting the reference target locations for the first four rows to the corresponding measured target locations. The difference in these two angles is the flap angle error due to blade elasticity. Similar errors occur for pitch and lag.

The following assumptions and procedures are used to correct pitch, flap, and lag for these elasticity errors.

1. For the pitch angle correction, it is assumed that Δtwist is zero at the hinge point and that the first derivative of Δtwist with respect to x is also zero at the hinge point. The pitch angle correction is based on a cubic fit of the inital Δtwist estimates for the first three inboard rows. (Use of less than three rows often produced spurious results due to the scatter Δtwist estimates.) Application of the pitch angle correction results in a zero value for Δtwist at the hinge point.

2. For the flap angle correction, it is assumed that Δz is zero at the hinge point and that the first and second derivatives of Δz with respect to x are also zero at the hinge point. The flap angle correction is based on a cubic fit of the Δz estimates for the first five inboard rows after the

[‡]For the pitch angle correction, it is assumed that Δtwist is zero at the hinge point and that the first derivative of Δtwist with respect to x is also zero at the hinge point.

pitch angle correction has been applied. (Cubic fits often did not fit the data well when using more than five rows due to higher order deformation behavior.) The Δz correction enforces a zero value for Δz at the hinge point. The flap angle and Δz corrections are applied, and the deformation values are recalculated for the next step.

3. For the lag angle correction, it is assumed that Δy is zero at the hinge point and that the first and second derivatives of Δy with respect to x are also zero at the hinge point. The lag angle correction is based on a cubic fit of the Δy estimates for the first five inboard rows after the pitch, flap, and Δz corrections have been applied. Both a lag angle correction and a Δy correction are determined. The Δy correction is determined and applied to enforce a zero value for Δy at the hinge point. The lag angle and Δy corrections are applied and the deformation values are recalculated. This step completes the correction procedure.

5 Measurement Process Uncertainty Considerations

5.1 Estimates of Static Precision and Limited Bias

The uncertainty of blade displacement measurements consists of both precision and bias errors. Precision errors of the measurement process define the variation (or scatter) in repeat measurements due to random processes. It is a measure of the capability of the experimental technique to discriminate between two measurements. The precision error of the measurement process can be estimated from the standard deviation of repeat measurements when everything is held constant. It is important to separate the precision of the blade displacement measurement technique from the experimental variations that occur when the blade oscillates (especially evident when the blade is rotating and under flow conditions). For instance, large values of the standard deviation noted during blade rotation and with flow are mostly due to blade motion. For repeat images of a given blade at fixed azimuth the scatter of the various parameters due to the measurement technique is typically a much smaller component of the total standard deviation derived from that image set. The other component of the uncertainty, bias (or systematic) error, are those errors that do not contribute to the scatter. The bias error can be thought of as a mean offset from the true value with a scatter about that mean given by the precision. Bias errors for optical measurement techniques applied to wind tunnels are particularly difficult to accurately quantify. However, a limited first estimate of the precision and bias errors for the blade displacement measurements in a static measurement situation can be very useful to identify and possibly improve the uncertainty of the measurements without the complications of rotating blades and airflow. The limited and incomplete results presented here, while not a formal uncertainty analysis, can help explain the strengths and weaknesses of the blade displacement measurement system. A more extensive uncertainty analysis should include the effects of a rotor operating in forward flight.

In order to provide an estimate of the static precision and bias of the measurement technique without the complications of rotating blades and airflow, a static wind-off azimuth sweep over 360° was taken. Forty blade azimuth angles were set by manually positioning Blade 4 over a range of 360°. The LRTA shaft encoder determined the azimuth for Blade 1 at each azimuth position. The azimuths of the other three blades were then calculated based on the azimuth of Blade 1. The initial estimate of static precision is taken to be the standard deviation of repeat measurements at a single azimuth. A total of 160 data points (40 for each blade) at three images per data point were taken. The mean of the standard deviations of the 160 points for each parameter is used to approximate the standard deviation of repeat measurements at a single azimuth to yield a rough estimate of static precision.

Table 4. Estimates of static precision and bias based on static, wind-off measurements over 360°.

	Precision	Bias
Pitch	0.007°	0.267°
Flap	0.007°	0.372°
Lag	0.002°	0.366°

Table 5. Estimates of static precision and bias based on static, wind-off measurements over 360° at inboard (r/R = 0.20) and outboard (r/R = 0.97) stations on the blades.

	r/R	Precision	Bias
Elastic ΔZ	0.20	0.002 in.	0.098 in.
Elastic ΔTwist	0.20	0.012°	0.200°
Z	0.20	0.002 in.	0.432 in.
Elastic ΔZ	0.97	0.038 in.	1.122 in.
Elastic ΔTwist	0.97	0.025°	0.229°
Z	0.97	0.066 in.	1.429 in.

During the static azimuthal sweep, each blade should have nearly identical values of pitch, flap, lag, elastic bending, and twist independent of azimuth. Thus deviations from the mean value over 360° azimuth indicate error in the blade displacement measurement, which contributes to the total bias error. This component of the bias error is a function of azimuth and, if found to be repeatable, could be removed from subsequent measurements. The limited bias errors representing variations with azimuth were computed as the standard deviation of the 160 sample means over 360°. The results for initial estimates of precision and the azimuthal component of bias error from a static sweep for pitch, flap, and lag in terms of one standard deviation are presented in Table 4. Other important factors leading to additional error in the measurement process not reflected in the following two tables are discussed later in this section.

Similarly computed results for elastic bending in Z and elastic twist, along with the inboard and outboard Z-coordinate of a single target, are presented in Table 5. Note the good precision at a single azimuth for Table 4 and for the inboard data of Table 5. This data emphasizes the ability to discriminate rev-to-rev differences over time for a blade at a given azimuth and condition, even in the presence of significant bias error. In addition, blade-to-blade differences at a given azimuth can be effectively discriminated.

It is important here to separate the precision of the measurement technique from the experimental variations that occur when the blade oscillates in the vertical direction. This is especially evident when the blade is rotating and under flow conditions. An example of blade motion can be seen even in the static data of Table 5 by comparing the precision at the inboard and outboard radial blade positions, r/R = 0.20 and 0.97, respectively. For the inboard radial position, r/R = 0.20, the movement of the blade during image acquisition is nearly negligible and more indicative of the precision of the measurement technique. However, at the outboard radial position, r/R = 0.97, significant and measurable vertical blade motions occur as the blade is moved to a new azimuth, mainly due to the sizable length (322 inches) of the rather narrow blades (≈21-inch chord). For the static sweep, Blade 4 was manually positioned to the desired azimuth at a rate of about one-point-per-minute. The manual pushing of Blade 4 to each new azimuth caused a 2× change in lag variation compared to the other three blades. The one-point-per-minute manual positioning of the blades did not allow enough time for the induced blade motion to settle

Table 6. Mean bias offset error based on static, wind-off measurements over 360° for r/R = 0.97.

	Bias
Pitch	0.102°
Elastic ΔTwist	-0.023°

before taking image data and moving on to the next azimuth position. Thus the data at r/R = 0.97 includes both experimental technique precision (of the order shown by the inboard data at r/R = 0.20) as well as the variation in the blade motion. For example, the Z-coordinate near the tip, on average, has a value 33 times greater than the inboard portion of the blade in Table 5. Therefore the inboard data is a better indicator of the experimental technique static precision for elastic ΔZ and elastic Δtwist. Note that generally pitch, flap, and lag are determined from the inboard portion of the blade from r/R = 0.20 to 0.35, so that their values of precision presented in Table 4 are impacted much less by blade motion during the static experiment.

As is often the case for optical techniques applied to wind tunnel measurements, the bias errors are larger (and generally more difficult to quantify) than the precision. Over a range of 360°, the static bias errors for the parameters pitch, flap, lag, elastic ΔZ, and elastic twist can be significant. Part of the bias error is caused by the use of a different set of cameras to measure a given blade as it rotates about the shaft. Enhancements to the data reduction procedures that have been investigated include optimization of camera calibration coefficients, alternate fish-eye corrections based on equisolid angle projection, and weighting of multiple intersection XYZ results by the variance. None of these investigations have significantly reduced the bias error.

5.2 Mean Bias Offset for Pitch, Lag, and Elastic Twist

The values of flap angle, lag angle, and elastic ΔZ are not necessarily known for the static sweep, thus their mean values over 360° cannot be easily compared to known reference values to determine a measure of bias offset error. However, the root collective pitch angle was set to 0° and the elastic twist is expected to be near zero throughout the static azimuthal sweep. Thus for these two parameters the mean difference from zero over the 360° azimuthal sweep can be viewed as a bias offset error. The mean bias offset error over 360° for pitch and elastic Δtwist are presented in Table 6 at the radial station r/R = 0.97. For comparison, note that the error in the root collective is thought to be around 0.2°.

5.3 Error Due to Rigid Body Transformation

A source of bias error not reflected in the tables and previous discussion is the use of inboard targets from r/R = 0.20 to 0.35 for the 3D nonlinear least-squares coordinate transformation of the blades to each of the four blade reference geometries at 0° azimuth. This transformation is necessary in order to separate and resolve the much smaller elastic deformations from the rigid body motion that occurs as the blade rotates about the shaft, coupled with additional changes in pitch, flap, and lag angles that are azimuth dependent. It is important to emphasize that the blade displacement values of pitch, flap, and lag, while useful for comparisons and validation with crab-arm and laser measurements, are primarily used to remove rigid body motion in order to compute the elastic deformations. It is the elastic deformations that are the most important product (and the most difficult to accurately obtain) of the blade displacement measurements.

The determination of the rigid body motion of the blade targets begins with a 3D conformal transformation about the cross-flow coordinate of the wind tunnel based on the facility value of the shaft geometrical angle of attack, α_s. This is a forward transformation and no additional parameters are determined from this operation. The α_s transformation is used to align the z-axis of the blade target data parallel with the rotor shaft. Any error in the facility value of α_s causes error in pitch, which varies as the sine of azimuth and error in flap angle, which varies as the cosine of azimuth. There should be little error in lag due to error in α_s. A jitter test with $\pm 1^\circ$ error in α_s for a $\mu = 0.30$ flow case confirms the sine and cosine dependences for pitch and lag to within 0.04° worst case. This same jitter test produces a worst-case error for lag of 0.08°. The error is less than 0.01 inch and 0.01° for elastic ΔZ and Δtwist for a $\pm 1^\circ$ error in α_s. The reason negligible error is noted for elastic ΔZ and Δtwist is that the computed transformation coefficients completely compensate for any error in α_s.

The bias errors for pitch and lag, while not negligible, do not indicate a major concern for the computation of elastic deformation at this time. However, that is not the case for flap, which has a much larger potential bias error. While little flap angle bias error is noted for near-zero bending, significant bias error in flap is noted for non-zero elastic bending. The error in flap is a direct consequence of the slope in the Z-coordinates as a function of r/R due to residual elastic bending from r/R = 0.20 to 0.35. The bias error in flap leads to slope error in the 3D coordinate transformation to the reference geometry. The slope error in the 3D coordinate transformation causes a slope error in elastic bending and twist that causes those results to be underestimated if not corrected as described previously in the Section 4.5.6, "Position and Orientation Errors Due to Blade Elasticity."

5.4 Bias Error Correlation for Elastic Deformation

The bias error for the elastic deformations is lessened significantly for closely spaced targets since their bias error in Z is correlated. For example, the bias error for elastic twist has extreme sensitivity to errors in the Z-coordinate of a single leading- or trailing-edge target at a given normalized radial position, r/R. The limited separation of leading- and trailing-edge targets, L, places a lower limit on the error in the determination of elastic twist. As a simple limited example, if the total error in Z between the leading- and trailing-edge targets, δZ, is 0.01 inch, the error in elastic twist angle, δtwist, (neglecting any error in the separation of the targets) is 0.05° based on a simplified error expression using the arcsin of the ratio of δZ to L with L $\approx$10.5 inches. Note however, the more important error in the difference between leading- and trailing-edge targets can actually be much smaller than the absolute error in the Z-coordinate of either target due to correlation in the error. Thus elastic twist and out-of-plane bending (Z) can be determined to an uncertainty significantly less than that indicated by considering the bias errors in Z separately (and uncorrelated). In fact, the uncertainty can even approach the much smaller values of precision for very closely spaced targets. The degree of error correlation depends primarily on the separation of the targets on the image plane. Closely spaced targets on the image plane will have similar correlated errors, even when the following error sources are present: (1) incomplete distortion correction, (2) fundamental limitations due to camera view geometry, (3) errors in camera parameters such as camera constant, photogrammetric principal point, horizontal and vertical pixel spacing, (4) image sensor non-uniformities, (5) error in camera location and pointing angles, and (6) errors in the mathematical model used for distortion correction. As the separation between targets increases, such as from near the tip to inboard, the correlation decreases markedly. Little error correlation occurs for large changes in azimuth. This discussion should not be interpreted to mean that closely spaced targets are desirable for angle measurements since generally a larger spacing would yield less error in angle. This discussion simply states that

when forced to place targets relatively close together (for instance because of limitations of chord length), bias errors, which vary across the image plane, will be similar for closely spaced targets and, due to correlation, tend to partially cancel out.

6 Results and Discussion

An extensive compilation of blade displacement measurement results is provided in the second volume of this report, "Volume II—Selected Data and Plots." This volume contains plots and tables for all of the primary blade displacement data sets, for selected secondary data sets, and for several reference data sets where the rotor was set to a common reference condition. Volume II presents plots and lists blade orientation and elastic blade deformation averages derived from the multiple image sets obtained for each of the selected data sets listed in Table B1. The data and plots presented are derived from the latest camera calibrations and data reduction procedures. These include estimated corrections that account for registration errors due to blade elasticity as presented in Section 4.5.6, "Position and Orientation Errors Due to Blade Elasticity." A text-file database is also provided, with the same averaged data presented in Volume II, and in addition it includes data for individual image sets as well as the values of the estimated pitch, flap, and lag angle corrections used to account for registration errors due to blade bending.

Preliminary blade displacement measurement results have been previously presented in several papers,[6,7,8,17,18] Those results are now superseded by the results presented in Volume II. In general, the changes in blade pitch, flap, and lag between the prior, preliminary presentations and the current results are not very significant. However, even small changes in estimated flap and pitch can lead to significant differences in the blade elasticity values ΔZ and Δtwist. (Values for elastic ΔX and ΔY were not included in any of the prior presentations.) Examples of these changes are presented in Figs. 23 and 24, which depict the uncorrected and corrected values for elastic ΔZ and Δtwist as a function of rotor radius for the test conditions originally included in the paper by Abrego, et al.[8] These figures include the CFD/CSD predictions of elastic ΔZ and Δtwist presented in that paper. The "uncorrected" values for elastic ΔZ and Δtwist are very nearly the same as those presented in that paper, but are instead based on the most recent camera calibrations and data reduction procedures, excluding the registration error corrections. The "corrected" values include the registration error corrections.

Figure 23 shows estimated elastic ΔZ deformations from CFD/CSD predictions and from photogrammetry measurements at 0°, 150°, and 255° blade-azimuth (ψ) locations for $\mu = 0.30$ and $CT/\sigma = 0.10$. The "Uncorrected Measurement" values represented by green circles do not incorporate corrections to flap angle due to registration errors, which are included in the corrected values shown by the blue squares. The flap angle correction rotates the blade reference position, resulting in larger ΔZ corrections as the radial station increases, which is why the curve representing the corrected values looks somewhat like a rotation of the uncorrected curve. To give an idea of how different flap angle corrections would affect the ΔZ values, curves representing the ΔZ values for $\pm$20 and $\pm$50 percent deviations in the estimated flap angle correction are provided. For all three figures, the flap angle correction looks more realistic in that elastic ΔZ values asymptotically approach zero as r/R approaches zero. Figures 23 (a) and (c) show much better agreement between the CFD/CSD predictions and the corrected measurement values out to an r/R of about 0.6. While the agreement did not improve for Fig. 23 (b), it is clear that in adjusting the flap angle correction by -50 percent, it very nearly matches the CFD/CSD prediction. However, no adjustment of the flap angle correction would make the CFD/CSD predictions match

the measured data for Figs. 23 (a) and (c) over the entire span of the rotor. This would indicate that these CFD/CSD predictions are not fully capturing the spanwise elastic behavior at these azimuths.

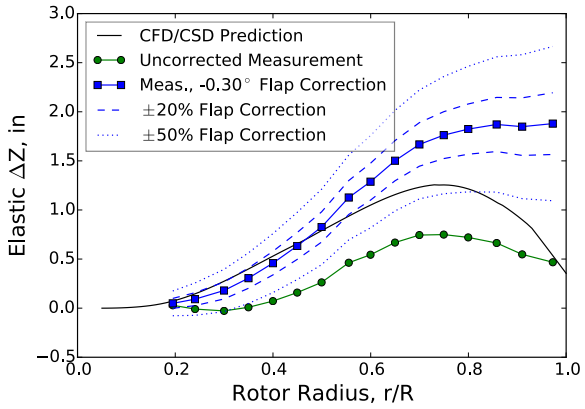

(a) $\psi = 0°$

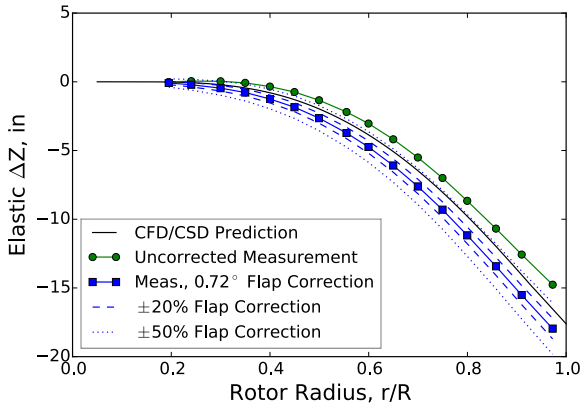

(b) $\psi = 150°$

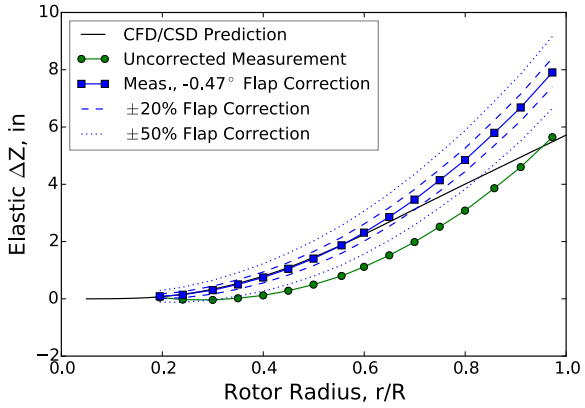

(c) $\psi = 255°$

Figure 23. Estimated elastic ΔZ deformations from CFD/CSD, and from corrected and uncorrected photogrammetry measurements at three blade-azimuth, ψ, locations for $\mu = 0.30$ and $CT/\sigma = 0.10$.

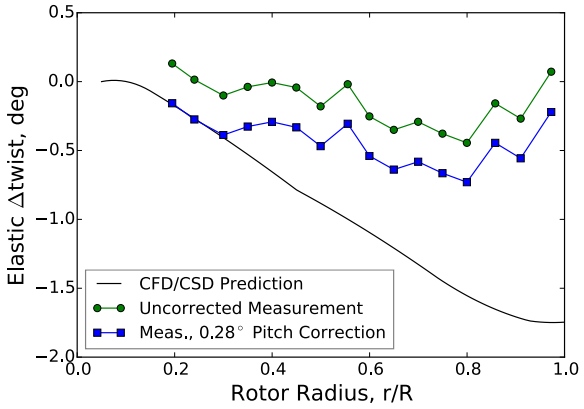

(a) $\psi = 0°$

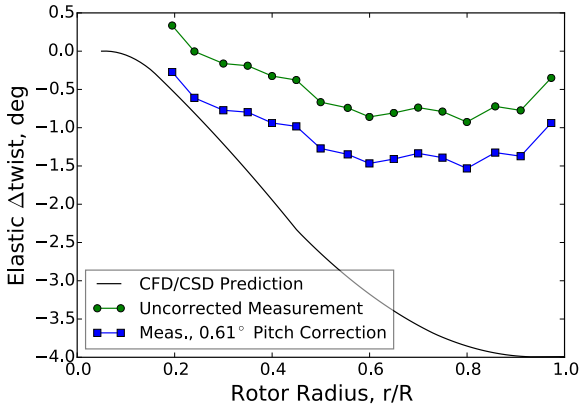

(b) $\psi = 150°$

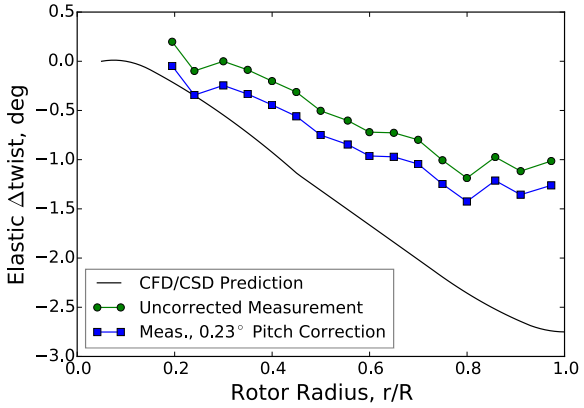

(c) $\psi = 255°$

Figure 24. Estimated elastic Δtwist deformations from CFD/CSD, and from corrected and uncorrected photogrammetry measurements at three blade-azimuth, ψ, locations for $\mu = 0.30$ and $CT/\sigma = 0.10$.

Figure 24 shows estimated elastic Δtwist deformations from CFD/CSD predictions and from photogrammetry measurements for the same test conditions and blade azimuths as provided in Fig. 23. For elastic Δtwist deformations, the correction for the registration error due to blade deformation is a correction in the blade pitch angle, which simply shifts the elastic Δtwist values by an offset that is constant over the span of the rotor. Since it is easy to visualize how such offsets would affect the data, percentage variations in the value of the correction, as provided for Fig. 23, are not provided in Fig. 24. Elastic Δtwist estimates from the photogrammetric measurements have more uncertainty and show more scatter. This is primarily due to the angle measurements being essentially the derivative of measured target positions, whereas the ΔZ values are determined directly from measured target positions after blade orientation transformations are made.

In Fig. 24 (a) the corrected Δtwist measurements for the first three radial stations fall right on top of the CFD/CSD prediction. However, the CFD/CSD prediction shows the Δtwist values becoming increasingly more negative as the radius increases, whereas the measured Δtwist values tend to level out. Changing the value of the correction used would not improve the comparison of the measured values to the CFD/CSD prediction. In Figs. 24 (b) and (c), a small change in the value of the pitch correction would make the measured Δtwist values more closely match the CFD/CSD predictions at the inboard stations. However, the CFD/CSD predictions still show a strong trend of increasingly negative Δtwist values with radial station that is not shown by the measured values.

6.1 Data Issues

While the blade displacement team has high confidence in most of the data presented here, there are a couple of caveats. First, the estimate lag angle values may have significant offset errors due to the potential that the rotor azimuth values used in data reduction may have had errors of 1 to 2 degrees. This was initially suspected because the estimated lag values differed by 1 to 2 degrees from the lag measured using hub mounted instrumentation. Examination of targets on the instrumentation hat, as presented in Appendix E.3, show run-to-run discrepancies of hat target locations for identical rotor azimuth values. This would indicate that there may be an issue with the value of the rotor azimuth used in reducing the data. The source of this discrepancy is not known, but it may be due to a time lag in either receiving the azimuth value from the wind tunnel data system or in triggering the photogrammetry data acquisitions. This may correctable by using the hat targets to determine azimuth, but this process was not developed due to time and resource constraints.

The second caveat is that there are occasional data outliers. Some of these may be due to centroiding errors, but an effort was made to find and correct most of these. A second source of outliers in spanwise deformation data is when the data is determined from more than one set of camera combinations. Each camera calibration has bias errors, which leads to bias errors in target positions determined for each set of camera combinations. When the same set of cameras is used for all targets on a blade, they have a common bias error. This common bias error will affect pitch, flap, and lag angle estimates, but should not affect the spanwise variation of elastic deformation estimates. However, if the inboard targets use one set of cameras and the outboard targets use a different set of cameras, the different bias errors for the two sets may cause a discontinuity in the spanwise distribution of estimated target positions, which results in a discontinuity in the spanwise variation of elastic deformation estimates. For most of the data presented, only one set of cameras was used for all targets on a blade for a specific azimuth and test condition. However, there are some cases where all the targets were not visible to each camera used, so more than one camera combination was used to get data for all of the visible targets. In these cases the differing bias errors can result in discontinuities in the spanwise variation of elastic deformation estimates.

Be aware that if outliers are present in the first few spanwise radial stations of the elastic deformation data for a blade, their presence may lead to errors in the corresponding estimates of the pitch, flap, and lag angles.

References

1. Norman, T. R., Shinoda, P., Peterson, R. L., and Datta, A., "Full-Scale Wind Tunnel Test of the UH-60A Airloads Rotor," *American Helicopter Society 67th Annual Forum, Virginia Beach, VA*, May 2011.

2. Kufeld, R. M., Balough, D. L., Cross, J. L., Studebaker, K. F., Jennison, C. D., and Bousman, W. G., "Flight Testing of the UH-60A Airloads Aircraft," *American Helicopter Society 50th Annual Forum, Washington D.C.*, May 1994.

3. Jenkins, L. N., Barrows, D. A., Cheung, B. K., Lau, B. H., Okojie, R. S., Wadcock, A. J., Watkins, A. N., and Yao, C. S., *A Status of NASA Rotorcraft Research*, NASA TP-2009-215369 Chapter 5 – Experimental Capabilities, National Aeronautics and Space Administration, Sept. 2009.

4. Bosnyakov, S., Bykov, A., Coulech, V., Fonov, S., Morozov, A., and Moskalik, V., "Blade Deformation and PSP Measurements on the Large Scale Rotor by Videometric System," *Instrumentation in Aerospace Simulation Facilities, 1997. ICIASF '97 Record., International Congress on*, Sept. 1997, pp. 95–104.

5. Schneider, O. and Van der Wall, B. G., "Final Analysis of HART II Blade Deflection Measurement," *29th European Rotorcraft Forum, Friedrichshafen, Germany*, Sept. 16–18 2003.

6. Olson, L. E., Abrego, A., Barrows, D., and Burner, A. W., "Blade Deflection Measurements of a Full-Scale UH-60A Rotor System," *American Helicopter Socieity Aeromechanics Specialist Conference, San Francisco, CA*, American Helicopter Socieity, Jan. 20 2010.

7. Barrows, D. A., Olson, L. E., Abrego, A. I., and Burner, A. W., "Blade Displacement Measurements of the Full-Scale UH-60A Airloads Rotor," *29th AIAA Applied Aerodynamics Conference*, American Institute of Aeronautics and Astronautics, Nov. 2011.

8. Abrego, A. I., Olson, L. E., Romander, E. A., Barrows, D. A., and Burner, A. W., "Blade Displacement Measurement Technique Applied to a Full-Scale Rotor Test," *American Helicopter Society 68th Annual Forum*, Fort Worth, Texas, May 1–3, 2012.

9. Norman, T. R., Shinoda, P. M., Kitaplioglu, S. A., Jacklin, S. A., and Sheikman, A., "Low-Speed Wind Tunnel Investigation of a Full-Scale UH-60 Rotor System," *American Helicopter Society 58th Annual Forum, Montreal, Canada*, June 2002.

10. Luhmann, T., Robson, S., Kyle, S., and Harley, I., *Close Range Photogrammetry: Principles, Techniques and Applications*, John Wiley and Sons, 2006.

11. Burner, A. W. and Liu, T., "Videogrammetric Model Deformation Measurement Technique," *Journal of Aircraft*, Vol. 38, No. 4, Nov. 2001, pp. 745–754.

12. Barrows, D. A., "Videogrammetric Model Deformation Measurement Technique for Wind Tunnel Applications," *45th AIAA Aerospace Sciences Meeting and Exhibit*, American Institute of Aeronautics and Astronautics, Jan. 8–11, 2007.

13. Geodetic Systems, Inc., *V-STARS*, http://www.geodetic.com/.

14. Fleming, G. A., "RASP: Rotor Azimuth Synchronization Program (RASP) User's Guide, Version 1.3," Tech. Rep., NASA Langley Research Center, Feb. 6, 2008.

15. Amer, T. R. and Goad, W. K., "WingViewer: Data Acquisition Software for PSP/TSP Wind Tunnel Cameras," Tech. Rep. LAR-16474-1, NASA Langley Research Center, Oct. 2005.

16. Liu, T. and Burner, A. W., "Photogrammetry Toolbox Reference Manual," NASA/CR 2014-218518, NASA Langley Research Center, Hampton, VA, Sept. 2014.

17. Romander, E. A., Meyn, L. A., Barrows, D., and Burner, A., "Blade Motion Correlation for the Full-Scale UH-60A Airloads Rotor," *Fifth Decennial AHS Aeromechanics Specialists' Conference*, San Francisco, California, Jan. 22–24 2014.

18. Biedron, R. T. and Lee-Rausch, E. M., "Blade Displacement Predictions for the Full-Scale UH-60A Airloads Rotor," *American Helicopter Society 70th Annual Forum*, Montreal, Quebec, May 20, 2014.

Appendix A

UH-60A Airloads Wind Tunnel Test Conditions

The following tables, from Norman et al.,[A1] summarize the UH-60A Airloads wind tunnel test conditions with blade displacement primary conditions highlighted in bold.

Table A1. Parametric sweep test conditions.

M_{tip}	α_s	μ	C_T/σ
0.650	-8	0.30	.02 to .12
		0.35	.02 to .11
		0.37	.02 to .11
	-4	**0.15**	**0.08**
		0.24	.02 to .126
		0.30	.02 to .118
		0.35	.02 to .11
	0	**0.15**	.04 to .13 (**.08**)
		0.20	.04 to .13
		0.24	.02 to .127 (**0.13**)
		0.30	.02 to .124 (**0.10**)
		0.35	.02 to .11
	4	**0.15**	.06 to .13 (**0.08**)
		0.20	.02 to .12
		0.24	.02 to .12
		0.30	.06 to .08 (**0.08**)
	8	**0.15**	.06 to .12 (**0.08**)
		0.20	.06 to .12
		0.24	.06 to .12
		0.30	0.08
0.625	0	0.24	.02 to .131
		0.30	.02 to .125
0.675	-8	0.35	.02 to .10
		0.37	.02 to .10
		0.385	.02 to .09

[A1] T. R. Norman, P. Shinoda, R. L. Peterson, and A. Datta, "Full-Scale Wind Tunnel Test of the UH-60A Airloads Rotor," in American Helicopter Society 67th Annual Forum, Virginia Beach, VA, May 2011. Available: http://rotorcraft.arc.nasa.gov/Publications/files/AHS11_TestSummary_Norman.pdf

Table A2. Slowed rotor test conditions.

M_{tip}	α_s	μ	Collective Pitch Angles, θ_0
0.650	0	0.30	0, 2, 3, 4, 6, 8, 10
		0.40	0.5, 2, 3, 4, 6, 8
	2	0.30	0, 2, 3, 4, 6, 8, 10
		0.40	0, 2, 3, 4, 6, 8
	4	0.30	0, 2, 3, 4, 6
		0.40	0, 2, 3, 4, 6
0.420	**0**	0.30	0, 2, 3, 4, 6, 8
		0.40	0, 2, 3, 4, 6, 8
		0.50	0, 2, 3, 4, 6, 8
		0.60	**0**, 2, 3, 4, 6, 8
0.260	**0**	0.30	0, 2, 3, 4, 6, 8
		0.40	0, 2, 3, 4, 6, 8
		0.50	0, 2, 3, 4, 6, 8
		0.60	**0**, 2, 3, 4, 6, 8
		0.70	0, 2, 3, 4, 6, 8
		0.80	0, 2, 3, 4, 6, 8
		0.90	0, 2, 3, 4
		1.00	**0**, 1, 2
	2	0.30	2
		0.40	2
		0.50	2
		0.60	**2**
		0.70	2
		0.80	2
		0.90	2
		1.00	**1**
	4	0.30	0, 2, 3, 4, 6, 8
		0.40	0, 2, 3, 4, 6, 8
		0.50	0, 2, 3, 4, 6, 8
		0.60	**0**, 2, 3, 4, 6, 8
		0.70	0, 2, 3, 4, 6, 8
		0.80	0, 2, 3, 4, 6, 8
		0.90	0, 2, 3, 6
		1.00	**0,** 2

Table A3. 1-g level flight test conditions.

C_L/σ	M_{tip}	Advance Ratios, μ
0.08	**0.650**	**0.15,** 0.20, 0.24, 0.30, **0.35**, **0.37,** 0.385, **0.40**
0.09	0.650	0.15, 0.20, 0.24, 0.30, 0.35, 0.37, 0.385, 0.40
0.10	0.650	0.15, 0.20, 0.24, 0.30, 0.35, 0.37, 0.385

Table A4. Flight/DNW test simulation conditions.

Test	Test Pt #	M_{tip}	μ	C_T/σ
Flight	**C8424**	**0.638**	**0.30**	**0.087**
	C8525	0.643	0.23	0.077
	C9020	**0.669**	**0.245**	**0.118**
DNW	**11.24**	**0.629**	**0.30**	**0.10**
	13.12	**0.638**	**0.30**	**0.07**
	13.2	**0.637**	**0.15**	**0.07**

Table A5. PIV test conditions.

M_{tip}	α_s	μ	C_T/σ	Azimuth Delays (deg)
0.650	0	0.15	0.08	5, 15, 30, 45, 60, 75, 95, 135, 185, 225, 275, 315
0.650	4	0.15	0.08	5, 15, 30, 45, 60, 75, 95, 135, 185, 225, 275, 315
0.638	4.82	0.30	0.087	5, 15, 30, 45, 60, 75, 95
0.650	0	0.24	0.07, 0.09	5
0.650	**0**	**0.24**	**0.11**	**5, 15, 30, 45, 60, 75, 95, 185, 275**
0.650	0	0.15	0.07, 0.09, 0.11, 0.12	15
0.650	**-6.9**	**0.35**	**0.08**	**5, 10, 15, 20, 30, 45, 60, 75, 95, 185, 275**

Appendix B

Blade Displacement Measurement Sets

The Blade Displacement Airloads data sets processed to date, including Primary, Secondary, and Reference sets, are listed in Table B1. Hover and Static data, the first two runs in the list, were taken very early in the test, before serious testing began. The static data, collected during wind-off conditions, recorded only three images per point, as described in Section E.2. The remaining sets of data include 12 to 15 images per point for Secondary and Reference sets, and 60 images per point for Primary sets. Since the run and point numberings for the Blade Displacement (BD) system were different from the run and point numberings used by the National Full-Scale Aerodynamics Complex (NFAC), both numbering sets are included in the table. Table B2 lists just the Primary data sets along with information about test conditions during each set.

Table B1. Full range of available BD measurement sets.

No.	NFAC Run	NFAC Point(s)	Data Set	BD Run	BD Points
1.	15	20	Hover	10	229-268
2.	N/A	N/A	Static	12	277-317
3.	38	19-23	Primary	17	562-601
4.	38	27-27	Primary	17	602-641
5.	40	29-34	Primary	18	650-689
6.	42	7	Reference	19	690-700
7.	42	11-14	Primary	19	722-761
8.	42	21	Reference	19	826-836
9.	42	43	Secondary	19	1079-1089
10.	42	44	Secondary	19	1090-1100
11.	42	46-49	Primary	19	1112-1152
12.	42	60-63	Primary	19	1263-1302
13.	43	7	Reference	20	1367-1377
14.	43	8-11	Primary	20	1378-1417
15.	43	28-31	Primary	20	1587-1626
16.	45	7	Reference	21	1627-1637
17.	45	34	Secondary	21	1917-1927
18.	45	51	Secondary	21	2106-2116
19.	45	52	Secondary	21	2117-2127
20.	47	8	Reference	22	2208-2218
21.	47	9	Secondary	22	2219-2229
22.	47	10-15	Primary	22	2233-2272
23.	47	30	Secondary	22	2282-2292
24.	47	33-37	Primary	22	2304-2343
25.	47	52-58	Primary	22	2355-2394
26.	50	12-15	Primary	24	2495-2534
27.	50	23	Reference	24	2612-2622
28.	52	11	Reference	25	2623-2633
29.	52	20	Secondary	25	2722-2732
30.	52	28	Secondary	25	2815-2825

Table B1. Full range of available BD measurement sets.

No.	NFAC Run	NFAC Point(s)	Data Set	BD Run	BD Points
31.	52	29	Secondary	25	2826-2836
32.	52	49	Secondary	25	3046-3056
33.	52	50	Secondary	25	3057-3067
34.	52	55	Reference	25	3112-3122
35.	53	11	Reference	26	3123-3133
36.	53	13	Secondary	26	3145-3155
37.	53	14	Secondary	26	3156-3166
38.	53	20	Primary	26	3222-3261
39.	53	26	Secondary	26	3262-3272
40.	53	32	Secondary	26	3328-3338
41.	53	33	Secondary	26	3339-3349
42.	53	34-39	Primary	26	3350-3389
43.	53	40	Secondary	26	3390-3400
44.	57	7	Reference	27	3412-3422
45.	60	28-29	Primary	28	4024-4063
46.	61	9	Reference	29	4064-4074
47.	63	8	Reference	30	4328-4338
48.	63	10	Secondary	30	4350-4360
49.	63	11	Secondary	30	4361-4371
50.	63	12	Secondary	30	4372-4382
51.	63	13	Secondary	30	4383-4393
52.	63	22	Secondary	30	4482-4492
53.	63	23	Secondary	30	4493-4503
54.	63	24	Secondary	30	4504-4514
55.	66	20	Secondary	31	4784-4794
56.	66	36	Secondary	31	4960-4970
57.	66	38	Reference	31	4982-4992
58.	67	9	Reference	32	4993-5003
59.	67	11	Secondary	32	5004-5014
60.	67	13	Secondary	32	5021-5031
61.	67	14-18	Primary	32	5032-5071
62.	67	33	Secondary	32	5072-5082
63.	67	34-39	Primary	32	5083-5122
64.	67	47	Reference	32	5123-5133
65.	69	7	Reference	33	5134-5144
66.	69	56	Reference	33	5667-5677
67.	73	59	Reference	34	5722-5732
68.	75	7	Reference	35	5733-5743
69.	75	53	Reference	35	5777-5787
70.	77	8	Reference	36	5788-5798
71.	77	11	Secondary	36	5799-5809
72.	77	14	Secondary	36	5810-5820
73.	77	16	Reference	36	5821-5831
74.	78	7	Reference	37	5832-5842

Table B1. Full range of available BD measurement sets.

No.	NFAC Run	NFAC Point(s)	Data Set	BD Run	BD Points
75.	78	10	Secondary	37	5844-5854
76.	78	32	Secondary	37	5855-5865
77.	78	34	Reference	37	5866-5876
78.	81	7	Reference	38	5878-5888
79.	81	12-16	Primary	38	5889-5928
80.	81	50	Secondary	38	5929-5939
81.	81	53	Reference	38	5940-5950
82.	83	7	Reference	39	5951-5961
83.	83	33	Secondary	39	6006-6016
84.	83	70-74	Primary	39	6017-6056
85.	83	77	Reference	39	6057-6067
86.	85	15	Reference	40	6068-6078
87.	85	47	Reference	40	6421-6431
88.	87	17	Secondary	41	6498-6508
89.	87	37-41	Primary	41	6723-6762
90.	87	42	Secondary	41	6763-6773
91.	87	46	Secondary	41	6807-6817
92.	91	18	Secondary	42	6906-6916
93.	91	37-40	Primary	42	7123-7162
94.	91	66	Secondary	42	7433-7443
95.	91	67	Secondary	42	7444-7454
96.	91	68-73	Primary	42	7455-7494
97.	91	74	Secondary	42	7495-7505
98.	93	8	Secondary	43	7550-7560
99.	93	11	Secondary	43	7583-7593
100.	93	14	Secondary	43	7616-7626
101.	93	32-36	Primary	43	7792-7831
102.	95	30	Secondary	44	8164-8174
103.	95	31-36	Primary	44	8177-8216
104.	95	37	Secondary	44	8217-8227
105.	96	9-13	Primary	45	8283-8322
106.	96	14	Secondary	45	8323-8333
107.	96	17-21	Primary	45	8356-8395
108.	98	13	Reference	46	8407-8417
109.	98	16-19	Primary	46	8440-8479
110.	98	39	Secondary	46	8690-8700
111.	98	40	Secondary	46	8701-8711
112.	98	41-44	Primary	46	8712-8751
113.	98	45	Secondary	46	8752-8762
114.	98	48-51	Primary	46	8785-8824
115.	98	52	Reference	46	8825-8835

Table B2. Primary data sets for blade displacement measurements.

NFAC Run	NFAC Point Start	NFAC Point End	BD Run	BD Point Start	BD Point End	Number of Images	Advance Ratio	C_T/σ	Angle of Attack	Tip Mach	Notes
38	19	23	17	562	601	60	0.15	0.08	-1.7	0.65	1-G Level Flight 1
38	27	27	17	602	641	15	0.24	0.08	-3.0	0.65	1-G Level Flight 1, only 15 images per BD data point.
40	29	34	18	650	689	60	0.35	0.08	-6.9	0.65	1-G Level Flight 1
42	11	14	19	722	761	60	0.15	0.08	0.0	0.65	Parametric Sweep 1
42	46	49	19	1112	1152	60	0.24	0.13	0.0	0.65	Parametric Sweep 1
42	60	63	19	1263	1302	60	0.3	0.10	0.0	0.65	Parametric Sweep 1
43	8	11	20	1378	1417	60	0.15	0.08	-4.0	0.65	Parametric Sweep 2
43	28	31	20	1587	1626	60	0.15	0.08	-4.0	0.65	Parametric Sweep 2
47	10	15	22	2233	2272	60	0.30	0.087	-4.82	0.64	Airloads Match 1 (Airloads C8424)
47	33	37	22	2304	2343	60	0.30	0.10	-4.5	0.63	DNW Data Point 13.20
47	52	58	22	2355	2394	60	0.24	0.12	-1.37	0.67	Airloads Data Point C9017.But did not match 9017.
50	12	15	24	2495	2534	60	0.15	0.08	4.0	0.65	Parametric Sweep 4
53	20	25	26	3222	3261	60	0.37	0.08	-8.4	0.65	1-G Level Flight
53	34	39	26	3350	3389	60	0.40	0.08	-10.0	0.65	1-G Level Flight
60	28	29	28	4024	4063	60	0.25	0.12	-1.9	0.67	Airloads Data Point C9020
67	14	18	32	5032	5071	60	0.30	0.07	-0.6	0.64	DNW Data Point 13.12
67	34	39	32	5083	5122	60	0.15	0.07	4.76	0.64	DNW Data Point 11.24
81	12	16	38	5889	5928	60	0.24	0.11	0.0	0.65	Parametric Sweep 1 (PIV4a)
83	70	74	39	6017	6056	60	0.35	0.08	-6.9	0.65	1-G Level Flight (PIV5a)
87	37	41	41	6723	6762	60	0.60	0.01	0.0	0.42	Tip=0.421 (65% Nom Tip)
91	37	40	42	7123	7162	60	0.60	0.02	0.0	0.26	Tip=0.260 (40% Nom Tip)
91	68	73	42	7455	7494	60	1.00	0.02	0.0	0.26	Tip=0.260 (40% Nom Tip)
93	32	36	43	7792	7831	60	0.60	0.05	4.0	0.26	Tip=0.260 (40% Nom Tip)
95	31	36	44	8177	8216	60	1.00	0.06	4.0	0.26	Tip=0.260 (40% Nom Tip)
96	9	13	45	8283	8322	60	0.60	0.05	2.0	0.26	Tip=0.260 (40% Nom Tip)
96	17	21	45	8356	8395	60	1.00	0.04	2.0	0.26	Tip=0.260 (40% Nom Tip)
98	16	19	46	8440	8479	60	0.15	0.08	8.0	0.65	Parametric Sweep 4 (Alternate)
98	41	44	46	8712	8751	60	0.30	0.08	8.0	0.65	Parametric Sweep 4 (Alternate)
98	48	51	46	8785	8824	60	0.30	0.08	4.0	0.65	Parametric Sweep 4 (Alternate)

Appendix C

Coordinate Transformations

For this test, several different coordinate systems were used. These included the test section coordinate system, the hub/body coordinate system, and the blade coordinate system. Each of these is a right-handed coordinate system having x, y, and z axes. The angles ω, φ, and κ are rotations about the x, y, and z axes, respectively, defined as positive in the counterclockwise direction when viewing down the axis toward the origin, as shown in Fig. C1. For various analyses it is necessary to transform the coordinates for one system into coordinates for another system. The conventions and equations used for these transformations are presented in this appendix.

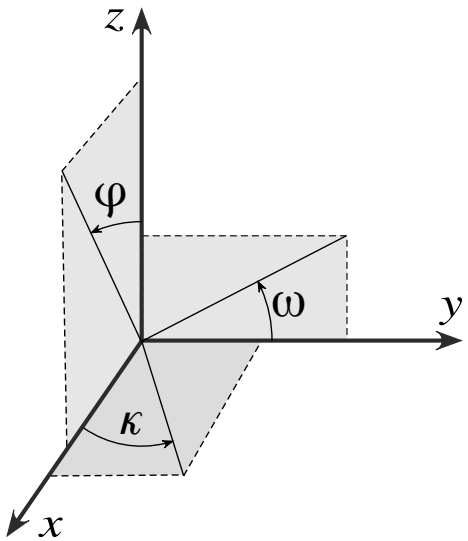

Figure C1. Coordinate system for 3D rotations, where rotations about axes are positive in the counterclockwise direction.

C.1 Basic Transformation Equations

A point is defined as a set of x, y, and z values that gives the location of the point in a coordinate system. Transforming a point's location from one coordinate system to another is accomplished through a sequence of translations and rotations. There are two possible conventions for transforming the coordinates of a point from one coordinate system to another. The axes could be considered as fixed and the transformations applied to the point, or alternatively, the point could be considered as fixed and the transformations applied to the axes. The first is sometimes referred to as active transformation and the second as passive transformation. The transformation equations presented here are for passive transformation in which the rotations and translations are applied to the axes.

C.1.1 Translation and Rotation

Translations are defined by Equation C1.

$$\begin{aligned} x' &= x - t_x \\ y' &= y - t_y \\ z' &= z - t_z \end{aligned} \tag{C1}$$

Rotations are defined as rotations of the axes about the origin. For rotations about the x-axis:

$$\begin{aligned} x' &= x \\ y' &= y\cos(\omega) + z\sin(\omega) \\ z' &= -y\sin(\omega) + z\cos(\omega) \end{aligned} \tag{C2}$$

For rotations about the y-axis:

$$\begin{aligned} x' &= x\cos(\varphi) - z\sin(\varphi)) \\ y' &= y \\ z' &= x\sin(\varphi) + z\cos(\varphi) \end{aligned} \tag{C3}$$

For rotations about the z-axis:

$$\begin{aligned} x' &= x\cos(\kappa) + y\sin(\kappa) \\ y' &= -x\sin(\kappa) + y\cos(\kappa) \\ z' &= z \end{aligned} \tag{C4}$$

C.1.2 Elementary Rotation Matrices

These rotation equations can be expressed by the following matrix equation, where $\mathbf{p}$ is the vector representing the coordinates x, y, and z, and $\mathbf{p}'$ is the vector representing the transformed coordinates, while i denotes the rotation axis and θ denotes the rotation angle.

$$\mathbf{p}' = \mathbf{R}_i(\theta)\mathbf{p} \tag{C5}$$

The three rotation matrices would then be defined by the following three equations,
Eqn. C6, for rotations about the x-axis:

$$\mathbf{R}_x(\omega) = \begin{bmatrix} 1 & 0 & 0 \\ 0 & \cos(\omega) & \sin(\omega) \\ 0 & -\sin(\omega) & \cos(\omega) \end{bmatrix} \tag{C6}$$

Eqn. C7, for rotations about the y-axis:

$$\mathbf{R}_y(\varphi) = \begin{bmatrix} \cos(\varphi) & 0 & -\sin(\varphi) \\ 0 & 0 & 0 \\ \sin(\varphi) & 0 & \cos(\varphi) \end{bmatrix} \tag{C7}$$

And Eqn. C8, for rotations about the z-axis:

$$\mathbf{R}_z(\kappa) = \begin{bmatrix} \cos(\kappa) & \sin(\kappa) & 0 \\ -\sin(\kappa) & \cos(\kappa) & 0 \\ 0 & 0 & 1 \end{bmatrix} \tag{C8}$$

C.1.3 Concatenated Elementary Rotations

Rotation matrices can be concatenated to represent a sequence of rotations. However, since matrix multiplication in general is not commutative, the order of the matrices is important. For example, the transformation matrix that represents a rotation in ω, followed by a rotation in φ and then in κ, would be the product of the three rotation matrices, $\mathbf{R}_z(\kappa)\mathbf{R}_y(\varphi)\mathbf{R}_x(\omega)$, which are ordered right to left. The resultant matrix, after the three rotations, is shown in Eqn. C9 as $\boldsymbol{R}(\omega, \varphi, \kappa)$:

$$\boldsymbol{R}(\omega, \varphi, \kappa) = \begin{bmatrix} c_\kappa c_\varphi & c_\kappa s_\varphi s_\omega + s_\kappa c_\omega & -c_\kappa s_\varphi c_\omega + s_\kappa s_\omega \\ -s_\kappa c_\varphi & -s_\kappa s_\varphi s_\omega + c_\kappa c_\omega & s_\kappa s_\varphi c_\omega + c_\kappa s_\omega \\ s_\varphi & -c_\varphi s_\omega & c_\varphi c_\omega \end{bmatrix} \tag{C9}$$

$$c_\omega \triangleq \cos(\omega),\ s_\omega \triangleq \sin(\omega),\ \ldots$$

C.2 Homogeneous Transformation Equations

It is useful to include translations along with rotations when concatenating a sequence of transformations. Homogeneous coordinates are one method to accomplish this, by representing the three-vector (x, y, z) as a four-vector $(x, y, z, 1)$. When using this system, translation can be expressed as the matrix multiplication shown in Eqn. C10. The homogeneous matrices for rotation are presented in Eqns. C11, C12, and C13.

$$\boldsymbol{T}(\boldsymbol{t}) = \begin{bmatrix} 1 & 0 & 0 & -t_x \\ 0 & 1 & 0 & -t_y \\ 0 & 0 & 1 & -t_z \\ 0 & 0 & 0 & 1 \end{bmatrix} \tag{C10}$$

$$\boldsymbol{R}_x(\omega) = \begin{bmatrix} 1 & 0 & 0 & 0 \\ 0 & \cos(\omega) & \sin(\omega) & 0 \\ 0 & -\sin(\omega) & \cos(\omega) & 0 \\ 0 & 0 & 0 & 1 \end{bmatrix} \tag{C11}$$

$$\boldsymbol{R}_y(\varphi) = \begin{bmatrix} \cos(\varphi) & 0 & -\sin(\varphi) & 0 \\ 0 & 1 & 0 & 0 \\ \sin(\varphi) & 0 & \cos(\varphi) & 0 \\ 0 & 0 & 0 & 1 \end{bmatrix} \tag{C12}$$

$$\boldsymbol{R}_z(\kappa) = \begin{bmatrix} \cos(\kappa) & \sin(\kappa) & 0 & 0 \\ -\sin(\kappa) & \cos(\kappa) & 0 & 0 \\ 0 & 0 & 1 & 0 \\ 0 & 0 & 0 & 1 \end{bmatrix} \tag{C13}$$

Concatenating a series of transformations will yield a matrix $\mathbf{M}$, which can be used to transform coordinate $\mathbf{p}$ to $\mathbf{p}'$ according to Eqn. C14.

$$\mathbf{p}' = \mathbf{M}\mathbf{p} \tag{C14}$$

The vector and matrix components of this equation for homogeneous transformations are shown in Eqn. C15. The last row of M will always be $(0, 0, 0, 1)$, the terms m_{14}, m_{24}, and m_{34} represent translation, and the remaining m_{ij} term represents rotation.

$$\begin{bmatrix} x' \\ y' \\ z' \\ 1 \end{bmatrix} = \begin{bmatrix} m_{11} & m_{12} & m_{13} & m_{14} \\ m_{21} & m_{22} & m_{23} & m_{24} \\ m_{31} & m_{32} & m_{33} & m_{34} \\ 0 & 0 & 0 & 1 \end{bmatrix} \begin{bmatrix} x \\ y \\ z \\ 1 \end{bmatrix} \tag{C15}$$

C.3 Transformation Equations for the UH-60A Airloads Test

Three coordinate systems were used in the analysis of the photogrammetry data in the UH-60A Airloads Test. These were the wind tunnel coordinate system, the rotor hub coordinate system, and the rotor blade coordinate system. The photogrammetry system measures all target locations in the wind tunnel coordinate system. Target locations on the test section ceiling were used in the wind tunnel coordinate system for calibration of camera locations, pointing angles, and distortion coefficients. However, targets on the rotor hub and blades needed to be transformed to the rotor hub and rotor blade coordinate systems, respectively.

C.3.1 Wind Tunnel to Hub Transformations

With zero angle of attack, the origin of the hub coordinate system is designated as $\mathbf{p}_{hub}$. The transformation matrix for this translation is $\mathbf{T}(\mathbf{p}_{hub})$, where $\mathbf{p}_{hub}$ is $(x_{hub}, y_{hub}, z_{hub}, 1)$. From Table 2, $\mathbf{p}_{hub}$ is (-85.9, 0, 9.48, 1). If the LRTA is set to a nonzero angle of attack, then a rotation of the coordinate system about the angle-of-attack pivot point is required. This rotation is accomplished by translating the axes origin to the pivot point, rotating the axes about the y-axis by the angle of attack, α, and then reversing the translation to the pivot point. The location of the angle-of-attack pivot point in the wind tunnel coordinate system is designated as $\mathbf{p}_{pivot}$, which is (-85.9, 0, -108.61, 1), as shown in Table 2.

The rotation about the pivot point takes place after the coordinate axes have been translated to the nominal origin of the hub coordinate system. The pivot point in the hub coordinate system, designated as $\mathbf{p}_{pivotH}$, is calculated using Eqn. C16.

$$\mathbf{p}_{pivotH} = \mathbf{T}(\mathbf{p}_{hub})\mathbf{p}_{pivot} \tag{C16}$$

Rotation of the coordinate system by α about the pivot can be represented by concatenating $\mathbf{T}(-\mathbf{p}_{pivotH})$, $\mathbf{R}_y(\alpha)$, and $\mathbf{T}(\mathbf{p}_{pivotH})$. The next step in transforming from the wind tunnel coordinate system to the hub coordinate system is a rotation about the z-axis, $\mathbf{R}_z(\psi_{offset})$, to correct for the -0.23° misalignment of the longitudinal axis of the LRTA with the wind tunnel centerline as shown in Fig. 3. The final step is to rotate about the z-axis by rotor shaft azimuth, ψ_{shaft}. Concatenating all of the transformations yields the transformation matrix for converting from wind tunnel coordinates to hub coordinates, $\mathbf{M}_{wind2hub}$, which is given by Eqn. C17.

$$\mathbf{M}_{wind2hub} = \mathbf{R}_z(\psi_{shaft})\mathbf{R}_z(\psi_{offset})\mathbf{T}(-\mathbf{p}_{pivotH})\mathbf{R}_y(\alpha)\mathbf{T}(\mathbf{p}_{pivotH})\mathbf{T}(\mathbf{p}_{hub}) \tag{C17}$$

Eqn. C17can be simplified by replacing $\mathbf{R}_z(\psi_{shaft})\mathbf{R}_z(\psi_{offset})$ with $\mathbf{R}_z(\psi_{shaft} + \psi_{offset})$, as shown in Eqn. C18.

$$\mathbf{M}_{wind2hub} = \mathbf{R}_z(\psi_{shaft} + \psi_{offset})\mathbf{T}(-\mathbf{p}_{pivotH})\mathbf{R}_y(\alpha)\mathbf{T}(\mathbf{p}_{pivotH})\mathbf{T}(\mathbf{p}_{hub}) \tag{C18}$$

The inverse of $\mathbf{M}_{wind2hub}$ can be used to transform coordinates in the hub coordinate system to the wind tunnel coordinate system. This matrix, $\mathbf{M}_{hub2wind}$, can also be calculated by reversing the sequence of transformations, as shown in Eqn. C19.

$$\mathbf{M}_{hub2wind} = \mathbf{T}(-\mathbf{p}_{hub})\mathbf{T}(-\mathbf{p}_{pivotH})\mathbf{R}_y(-\alpha)\mathbf{T}(\mathbf{p}_{pivotH})\mathbf{R}_z(-\psi_{shaft} - \psi_{offset}) \tag{C19}$$

The values for the variables in homogeneous form (x, y, z, 1) used in these transformations are given in Table C1.

These equations assume that α and ψ_{shaft} are the only dynamic variables affecting the hub's position and orientation in the wind tunnel. Not only may the values for α and ψ_{shaft} have errors, but aerodynamic loads and rotor forces may cause deflections of the structures supporting the hub. Appendix E provides details on how targets on the instrumentation hat, rigidly mounted on top of the hub, can be used to estimate the hub position and orientation.

Table C1. Values for the variables used to transform wind tunnel coordinates to hub coordinates.

Variable	**Value**
$\mathbf{p}_{hub}$	$(-85.9, 0, 9.48, 1)$
$\mathbf{p}_{pivot}$	$(-85.9, 0, -108.61, 1)$
$\mathbf{p}_{pivotH}$	$(0, 0, -118.09, 1)$
ψ_{offset}	$-0.23°$

Appendix D

Image Processing Software Usage

The image data from the Airloads NFAC Test were digitally processed to calculate centroid locations of discrete targets on the rotor blades and test section ceiling. A suite of custom designed image processing and data reduction functions were developed using the Mathworks® Matlab software environment for this effort. Supporting functions for image processing, photogrammetry, and coordinate transformations were provided via a custom Matlab Photogrammetry Toolbox developed for NASA by Western Michigan University.[D1] The suite of custom designed image processing and data reduction functions, using additional selected functions from the Matlab Image Processing and Statistics Toolboxes, were integrated into a NASA rotor-specific toolbox. The NASA Rotor Toolbox makes use of moderately automated post-test image processing procedures that identify and calculate the image plane centroid spatial coordinates for each target. The Rotor Toolbox also contains a number of specialty scripts and functions for implementing camera calibration, determining camera location and pointing angles, performing multi-camera intersections to determine 3D spatial coordinates, and computing pitch, flap, and lag angles, as well as elastic bending and twist.

The Rotor Toolbox contains an interactive graphical user interface (GUI) to process image targets and enable target centroid inspections (Fig. D1). The GUI panel displays the Project, Centroid, and Image paths (Fig. D1(a)) of the current data point. Options are available for selecting the BD run, point, camera, and blade numbers (Fig. D1(b)). Earlier versions of the GUI had an interactive image grayscale threshold input option, which was replaced with a more robust, automated adaptive thresholding algorithm.

There are several centroid processing and inspection features within the GUI. For example, specified image sets can be processed to compute grayscale centroids by using the "process images" feature (Fig. D1(c)). Once the centroids have been identified, they can be superimposed onto

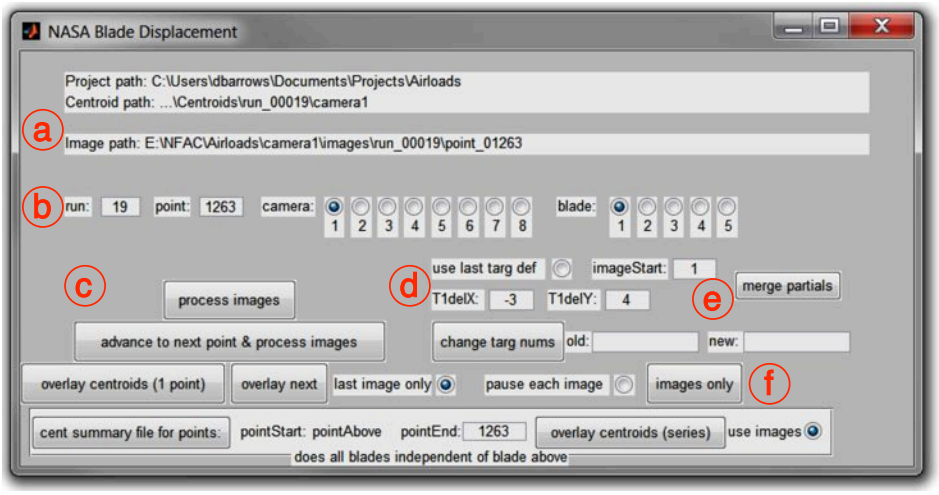

Figure D1. Graphical User Interface (GUI) from the Matlab Rotor Toolbox for image processing and centroid inspections. The red circled numbers are illustrative locations on the GUI.

[D1] Liu, T. and Burner, A. W., "Photogrammetry Toolbox Reference Manual," NASA/CR 2014-218518, NASA Langley Research Center, Hampton, VA, Sept. 2014.

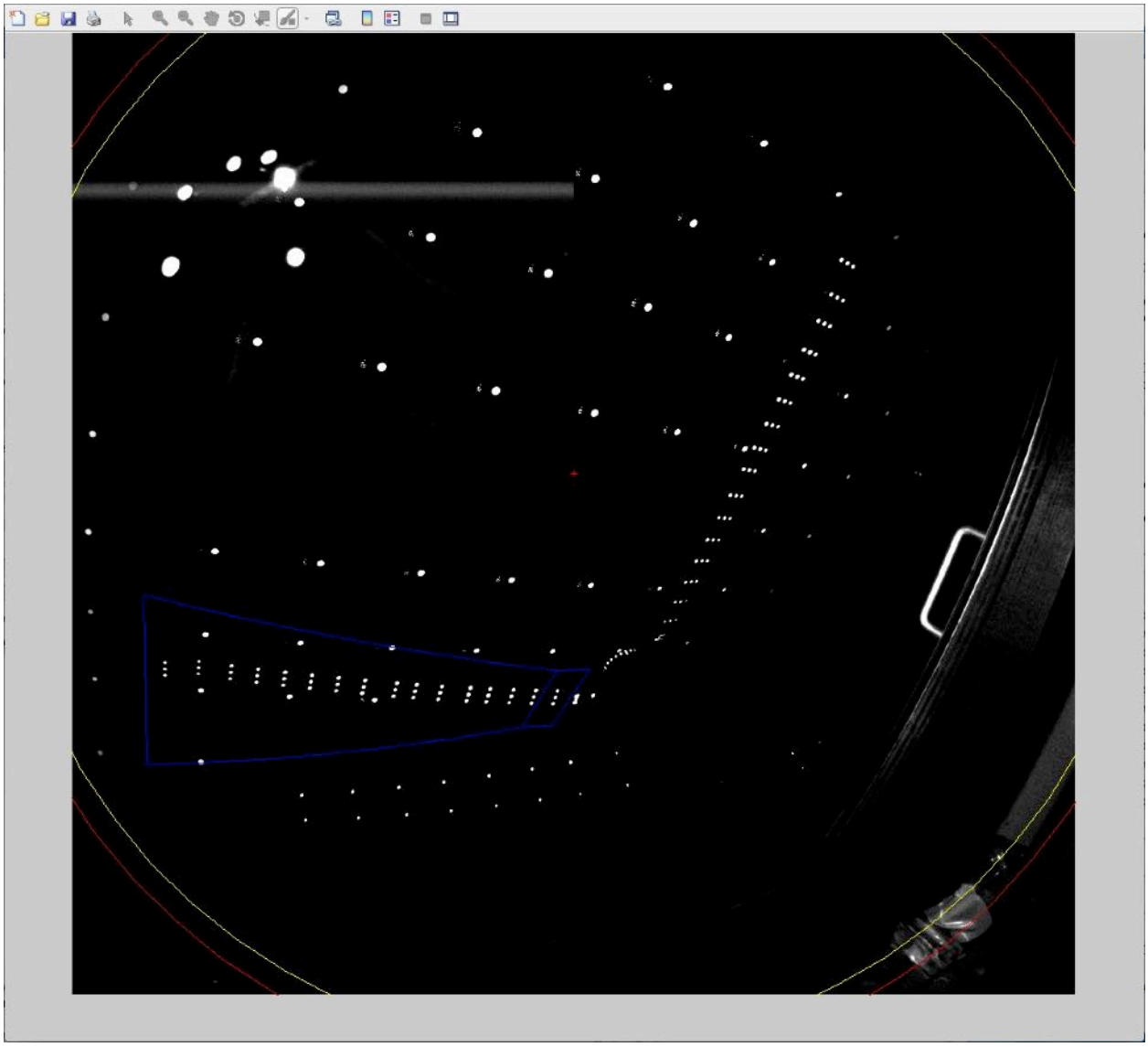

Figure D2. Figure window used for initial selection of blade targets.

the original images for data inspection using "overlay centroids (1 point)," also shown in Fig. D1(c). The Matlab zoom feature in figure mode allows for more detailed interrogation in the areas of interest during an inspection.

The image processing begins with selecting the run, point, camera, and blade number in the GUI. A figure window (Fig. D2) illustrating the first image from the specified data point opens and the blade of interest is indicated by the blue outlined polygon within the figure. For the convenience and ease of processing, the chosen blade selection is transformed to a horizontal axis, as seen in Fig. D3. The root of the blade is positioned to the left in the figure window. Figure D3a shows all visible targets in the specified blade region, including false targets. The blade targets need to be manually confirmed or identified (Fig. D3b) and the false targets need to be deselected. Once all the visible targets are identified, the automated processing for the remaining images will proceed. When all the blade targets are not visible, a target selection GUI window (Fig. D4) is used to select the correct target numbers to those selected in the image.

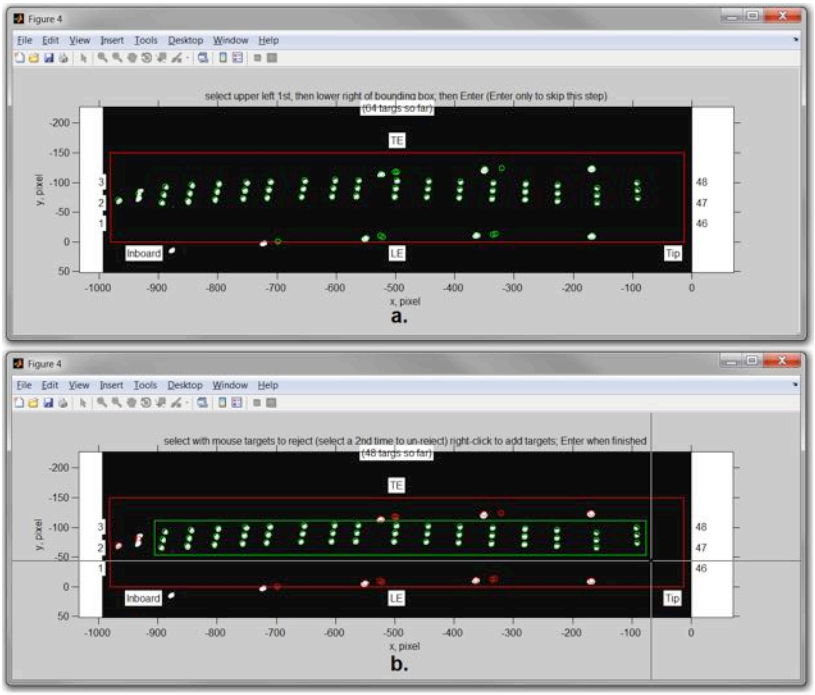

Figure D3. Matlab figure windows, computing grayscale centroids: a) all available targets; b) blade targets only, unwanted others removed.

This initial manual interaction with the first image of a data set is required at the start of the image processing because of discernible complex details within the images. Full automation is difficult to govern due to the blade motion and the variation in visible targets. Targets on the LRTA fuselage, test section ceiling, and instrumentation hat are useful visual guides during this manual processing step. When the image set automated processing step is complete, a new blade image displaying the superimposed centroids opens. This centroid inspection image is important and is highly recommended to ensure the accuracy of the identified centroids. Any discrepancies requiring changes to the data can be easily performed at this time. Options to accomplish this, without having to reprocess from the beginning, are available in the main processing GUI (Fig. D1).

The main processing GUI also contains two "advance to the next point" features to help streamline the data processing and inspection routines. When processing the images in an azimuth sweep, the "advance to next point & process images" feature (Fig. D1(c)) advances to the next grayscale data point to be processed. Similarly, when inspecting a series of centroids of an azimuth sweep, an "overlay next" feature can advance the point number and superimpose the centroids onto the matching images. Additional inspection features provide alternate ways to look at the centroid overlays and images, such as "last image only" and "pause

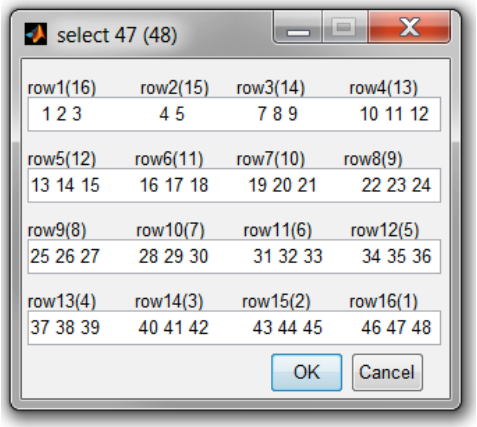

Figure D4. GUI target selection window with target number 6 removed.

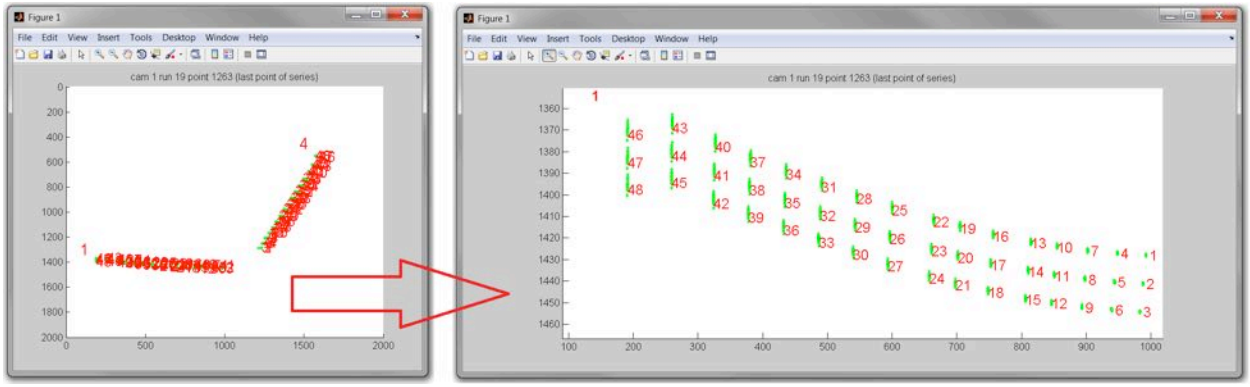

Figure D5. Display of rev-to-rev spread of target centroids on a single plot, minus the image.

each image," shown in figure D1(f). Both of these features are self-explanatory, but when neither "last image only" nor "pause each image" are utilized the program will quickly step through the sequence of images (and overlays) without pausing. These GUI features not only offer useful ways to view and inspect superimposed centroids, but also to view the images only, without centroids, using "overlay centroids (1 point)," "overlay next," "images only," and "overlay centroids (series)." The "last image only" option is the default for these features.

A display of the rev-to-rev spread of all the visible target centroids, for all of the visible blades, can be viewed in a single figure using "overlay centroids (series)" shown in figure D1(f). A starting point number (Fig. D1(b)) and an ending point number (Fig. D1(f)) provide the chosen range of point numbers for the rev-to-rev centroid inspection. Another convenient option of the "overlay centroids (series)" feature, particularly when images are not available, is the "use images" option (Fig. D1(f)). A rev-to-rev spread of target centroid locations in a single figure can be viewed, as shown in figure D5, for every blade revolution without superimposing them onto the images.

When inspecting any superimposed centroids using the overlay features, mislabeled or unwanted targets are sometimes discovered. The "change targ nums" feature (Fig. D1(d)) makes individual target identification corrections to the centroid files without having to reprocess the entire file. For instance, if one or more targets are improperly labeled, "change targ nums," provides a convenient correction to unwanted target values. To rename a mislabeled target, there is an input for the "old" target number (Fig. D1(e)) and an input for the "new" target number. These inputs allow the user to make changes to existing target numbers, including targets that need to be removed from a file. Unwanted target label(s) can be replaced with "nan" to completely disassociate any labels from unwanted targets. However, the "change targ nums" feature does not create new centroids. It only allows existing target labels to be relabeled or removed.

Occasionally, a number of ensuing data points being processed can have an identical pattern of targets, with fewer than the 48 total. These patterns, or sometimes unusually troublesome arrangements of scattered targets on a blade, might require multiple centroiding attempts before being processed correctly. The "use last target def" feature (Fig. D1(d)) bypasses the GUI target selection window (Fig. D4) by retaining the numbering definitions appointed in the prior processing attempt. This handy option is often useful for repeat processing attempts and can help speed things up. Use caution, however, when using this feature because the numbering definitions will remain in place until "use last target def" is turned off.

During some more aggressive tunnel conditions that experience slowed rotor, high advance ratio situations, partially blocked targets become difficult to track because they can have the appearance of being full-size usable targets. These tunnel conditions were particularly challenging because

of extreme image-to-image, or rev-to-rev, blade motion. This, in part, increases the difficulty in automating the image processing. Any and all partially blocked targets are considered unusable and should be omitted because they reduce centroiding accuracy. A "merge partials" feature (Fig. D1(e)) supports troublesome data points that do not fully process. If the processing procedure stops short of finishing the complete data set of images, a partial centroid data file is created. An attempt can be made to create a subsequent partial centroid data file using the "imageStart" feature (Fig. D1(e)) that begins with the last image number used, plus one, from the previous file. When completed, the two partial files can be combined using "merge partials."

Centroid tracking during slowed rotor, high advance ratio tunnel conditions can cause the tracking algorithm to experience difficulty staying locked onto the targets. The "T1delX" and "T1delY" variables (Fig. D1(d)) are used occasionally to fine-tune the search region of interest for the most inboard row of targets when the default settings fail.

A separate centroid validation Matlab function, plotXY_Pixels.m, was developed to locate mislabeled or suspect centroid data that may require manual correction. Slowed-rotor, high advance ratio test conditions proved to be particularly challenging due to the extreme image-to-image blade motion (compared to lower advance ratios). This holds true even near the inboard portion of the rotor blades. Ceiling targets and strobe window reflections have the potential to interfere with the accurate identification of blade target centroid locations. The plotXY_Pixels.m function checks for mistakes in centroiding by looking for a lack of "smoothness" in plots and comparing blade-to-blade plots, and checks for targets whose maxROI/minROI ratio, across all images for that point, exceed some specified value.

Appendix E

Hub Location and Orientation Using Instrumentation Hat Targets

The photogrammetric blade displacement measurements were acquired in the wind tunnel coordinate system. However, the essential blade orientation data consisting of pitch, flap, and lag, are referenced to the hub coordinate system along with the azimuth rotation. This required that the location and orientation of the hub be measured or estimated in order to calculate blade orientation. The position and orientation was dependent on the model angle of attack, α, and the shaft azimuth, ψ_{shaft}. These measurements provided known and expected adjustments to the hub coordinate system.

However, there are several other ways that the hub location and orientation could be altered. First, the hub position and orientation may change due to aerodynamic and mechanical loads deflecting the hub's support structure. Second, it is possible that the signal used to synchronize the photogrammetry images to the rotor azimuth position has a delay, leading to an error in the estimated lag. Both of these factors can be compensated for by measuring the hub location and orientation using the same photogrammetry system used to capture rotor blade data, provided that two or more cameras viewed common targets that rotated with the hub.

Visual access to the main rotor hub was obscured due to interference of the blade assembly at the hub, assorted instrumentation, and other flight hardware, as illustrated in Fig. E1. However, there was a protective instrumentation canister mounted on top of the hub that is relatively unobstructed. This canister, referred to as the Rotating Data Acquisition System (RDAS), or instrumentation hat, provided a locale for instrumentation wiring and the Rotor Mounted Data Acquisition and Transmission System.[E1]Since the instrumentation hat was rigidly mounted to the hub, it consequently rotated and moved with the hub. Thus measurements of the hat location and orientation could be used to provide hub location and orientation.

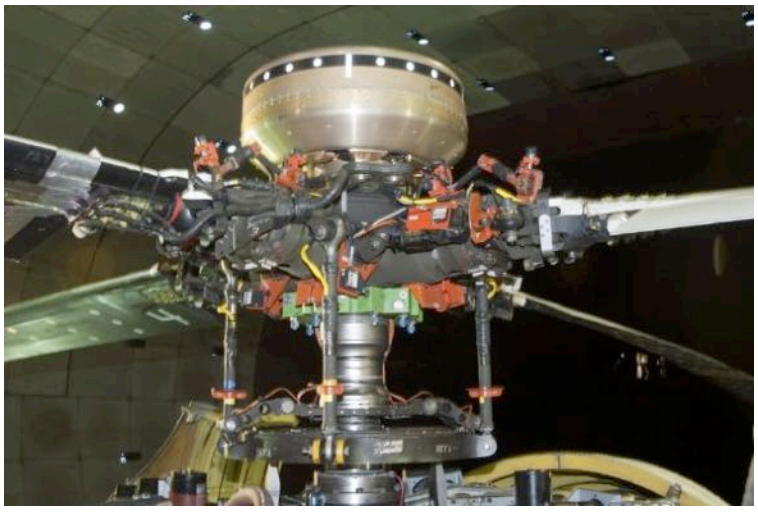

Figure E1. Close-up of UH-60A rotating hardware with the instrumentation hat above the rotor hub.

[E1]Norman, T. R., Shinoda, P., Peterson, R. L., and Datta, A., "Full-Scale Wind Tunnel Test of the UH-60A Airloads Rotor," *American Helicopter Society 67th Annual Forum*, Virginia Beach, VA, May 2011.

The locations of a ring of targets applied to the circumference of the instrumentation hat to assist with determining the hat location and orientation were measured in a laboratory. These target locations were transformed to the wind tunnel coordinate system after the instrumentation hat was installed in the tunnel with the model in a static, unloaded condition. Then, with the model operating under load and the hat targets imaged concurrently with the blade targets, translation and rotation values due to loading and any azimuth signal delay could be determined. These translation and rotation values could then be used to correct the azimuth used for the blade target measurements and hence improve photogrammetrically determined lag measurements.

E.1 Hat Target Location Measurements

Twenty, one-inch-diameter retro-reflective targets were attached to the circumference of the hat in four groups of five targets each. These groups were separated by 1- by 3-inch rectangular, retro-reflective markers designated as M1-M5, in Fig. E2. Each target was separated by approximately 4 inches between centers, when measured along the circumference. The target numbering and positions, with respect to the numbered rotor blades, are shown in Fig. E2. The setup to independently measure the hat target locations, using the V-STARS System, is shown in Fig. E3. The radius of the hat targets 15.903 inches with center at x = -16.172 inches and y = 0.010 inches was calculated from the coordinates in Table E1.

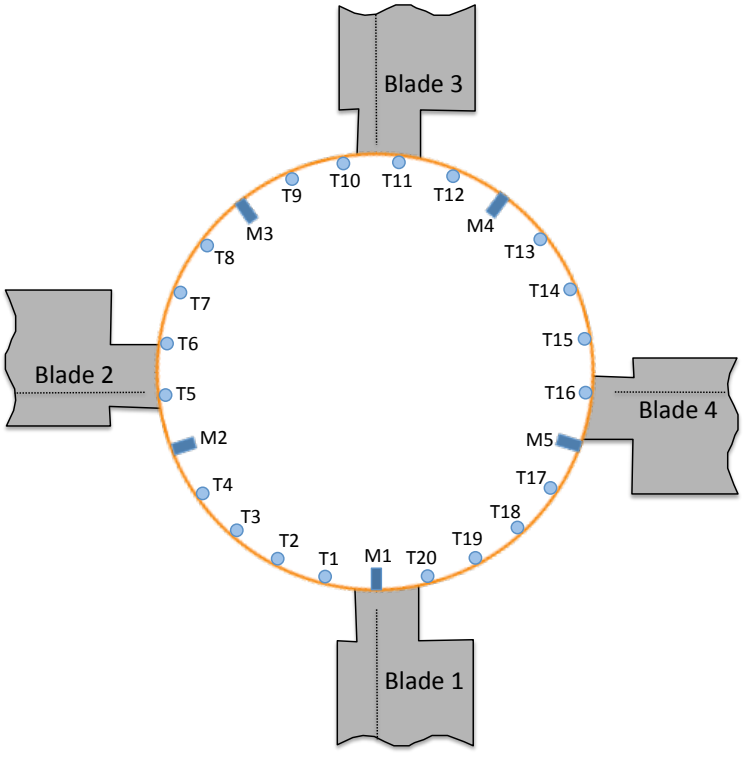

Figure E2. Instrumentation hat target numbering. Tn denotes 20 1-inch-diameter targets and Mn denotes 5 1- by 3-inch rectangular markers.

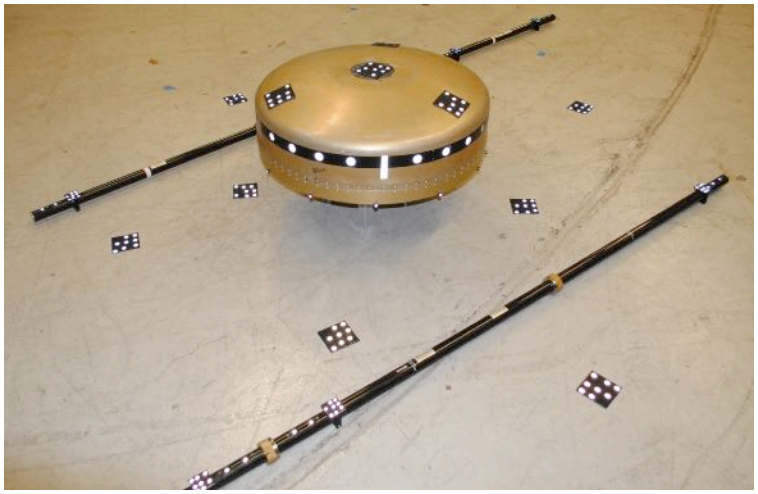

Figure E3. V-STARS setup for instrumentation hat target location measurements.

Table E1. Instrument hat target locations.

Target Number	X(in.)	Y(in.)	Z(in.)
1	-0.8596	-4.1717	5.8885
2	-2.3677	-7.8663	5.8741
3	-4.7496	-11.0579	5.8681
4	-7.8631	-13.5603	5.8789
5	-15.4303	-15.8907	5.9382
6	-19.4118	-15.5686	5.9335
7	-23.1836	-14.2601	5.9117
8	-26.5203	-12.065	5.9019
9	-31.0648	-5.5804	5.9259
10	-31.9879	-1.6989	5.9536
11	-31.9104	2.2913	5.9498
12	-30.8299	6.1299	5.9200
13	-26.0222	12.4770	5.9180
14	-22.6488	14.5288	5.9227
15	-18.8229	15.6887	5.9736
16	-14.8300	15.8661	5.9748
17	-7.3724	13.2887	5.9278
18	-4.3473	10.6687	5.8825
19	-2.0643	7.3703	5.8894
20	-0.7066	3.6224	5.8810

E.2 Static Location of the Hat Targets in Hub and Wind Tunnel Coordinates

Table E1 shows the hat target locations in the instrumentation hat coordinate system established by the V-STARS measurements. To be more useful, the target locations would need to be transformed from these coordinates to the hub and wind tunnel coordinate systems. This could be done by determining the origin of the hat coordinate system as measured in the hub coordinate system,

and designated as $\mathbf{p}_{hat}$, which represents the homogeneous point $(x_{hat}, y_{hat}, z_{hat}, 1)$. There is also a possibility the hat coordinate axes may have some angular offsets from the hub coordinate axes. The offsets, ω_{hat}, φ_{hat}, and κ_{hat}, represent rotations about the x-axis, y-axis, and z-axis, respectively. The transformation matrix, $\mathbf{M}_{hat2hub}$, used to convert locations in the hat coordinate system to the hub coordinate system, is given in Eqn. E1.

$$\mathbf{M}_{hat2hub} = \mathbf{R}_z(-\kappa_{hat})\mathbf{R}_y(-\varphi_{hat})\mathbf{R}_x(-\omega_{hat})\mathbf{T}(-\mathbf{p}_{hat}) \tag{E1}$$

Even though the hat coordinate system origin and orientation values could be estimated using fabrication drawings, the actual values could differ due to variances in fabrication and installation, in addition to positioning of the hat and references during the V-STARS target measurements. A more desirable option would be to measure the installed hat target locations using blade displacement photogrammetry while in the wind tunnel coordinate system, and ultimately transform V-STARS hat target locations to the wind tunnel coordinate system. The transformation matrix, $\mathbf{M}_{hat2wind}$, could be calculated using $\mathbf{M}_{hub2wind}$ (defined in Eqn. C19), as shown in Eqn. E2, which would be valid when the test article is in a static, unloaded condition.

$$\mathbf{M}_{hat2wind} = \mathbf{M}_{hub2wind}\mathbf{M}_{hat2hub} \tag{E2}$$

The equation to convert target locations in the hat coordinate system, $\mathbf{x}_{hat}$, to target locations in the wind tunnel coordinate system, $\mathbf{x}_{wind}$, is given in Eqn. E3.

$$\mathbf{x}_{wind} = \mathbf{M}_{hub2wind}\mathbf{M}_{hat2hub}\mathbf{x}_{hat} \tag{E3}$$

The hat target centroid data from a wind-off tunnel condition was used to determine $\mathbf{M}_{hat2hub}$, where the rotor hub and blades were manually rotated over the full 360° azimuth. A total of 40 different shaft azimuth positions were recorded during this series of three-image-per-point sets, at angles of attack of 0°, 10°, and -10°. The progression of work to follow entailed calculating predicted target centroids for each observed target centroid. The predicted centroids were a result of the observed centroid calculated 3D wind tunnel coordinates from Eqn. E3 and the V-STARS target location values in Table E1. A transformation of these 3D coordinate locations back to 2D centroid locations was accomplished, using each of the camera's calibrated transform function, in order to compare the predicted centroids with the observed centroids. A nonlinear least-squares solver was used to find the hat-to-hub transformation variables, shown in Table E2, which minimized the difference between the observed and predicted centroids. These transformation variables were then used to calculate the hat target locations in the hub coordinate system, which are presented in Table E3.

Table E2. Hat-to-hub transformation variables.

Variable	**Value**	**Standard Deviation**
κ_{hat} (deg)	-0.0367	0.0059
ω_{hat} (deg)	0.0164	0.0111
φ_{hat} (deg)	0.0956	0.0111
x_{hat} (in.)	16.1461	0.0035
y_{hat} (in.)	-0.0113	0.0035
z_{hat} (in.)	14.0909	0.0019

Table E3. Instrument hat target locations in the hub coordinate system.

Target Number	X(in.)	Y(in.)	Z(in.)
1	15.3171	-4.1985	19.9527
2	13.8067	-7.8921	19.9398
3	11.4227	-11.0822	19.9368
4	8.3076	-13.5826	19.9521
5	0.7390	-15.9082	20.0234
6	-3.2423	-15.5835	20.0254
7	-7.0132	-14.2726	20.0103
8	-10.3485	-12.0754	20.0067
9	-14.8888	-5.5879	20.0401
10	-15.8094	-1.7058	20.0705
11	-15.7294	2.2844	20.0677
12	-14.6465	6.1223	20.0372
13	-9.8347	12.4663	20.0289
14	-6.4600	14.5159	20.0286
15	-2.6333	15.6734	20.0734
16	1.3597	15.8482	20.0680
17	8.8156	13.2661	20.0078
18	11.8389	10.6441	19.9567
19	14.1198	7.3443	19.9589
20	15.4751	3.5955	19.9472

E.3 Hat Target Camera Intersections in Quadrant IV

Discrepancies between lag angle measurements from the blade displacement system and hub mounted instrumentation led to concerns about the validity of the blade displacement system lag measurements. An analysis was conducted to see if the hat targets could be used to improve the values of shaft azimuth angle, and hence lag measurements. This analysis focused on selected hat targets from two reference run/points (run 85, points 15 and 47) that were recorded on the same day, separated by about 2 hours, 20 minutes. Both reference runs experienced similar tunnel and rotor conditions, meaning the calculated mean lag results between the two should have been comparable. However, the mean lag values from the two points differed by about 1 degree (see Fig. E4). Analysis of the hat targets also showed about 1 degree difference in location between the two points for the same shaft azimuths. Yet, the measured angle between targets for these two runs, when compared to V-STARS, differed by only a few hundredths of a degree. This indicates the blade displacement system has some unknown error source that impacts the azimuth used in data reduction, which in turn, leads to an error in estimated lag. However, it is believed the estimated pitch and flap values should be unaffected by this error.

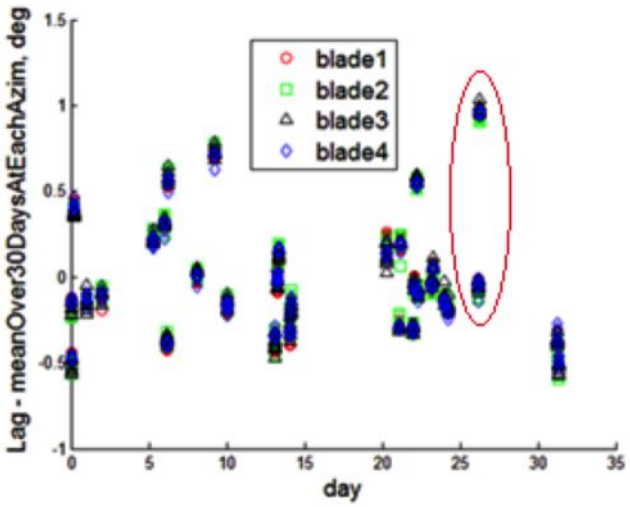

Figure E4. Lag scatter of reference runs over 30 days. Run 85, points 15 and 47 circled in red.

When Blade 1 is at Az = 0°, Blade 2 is at Az = 270°. The best visible hat targets for camera intersection are when targets 2, 3, and 4 (Fig. E2) are in quadrant IV of the rotor disc. These targets remain visible in the camera views as Blade 2 advances from Az = 270°, Az = 275°, to Az = 285° at alpha = 0°. However, the image quality of target 2 begins to weaken as the hub azimuth advances. This possibly explains why the data output for target 2 gradually drifts away from targets 3 and 4 in Fig. E5. The measured angle between targets for run 85, points 15 and 47, minus matching V-STARS measurements, are shown in Fig. E6.

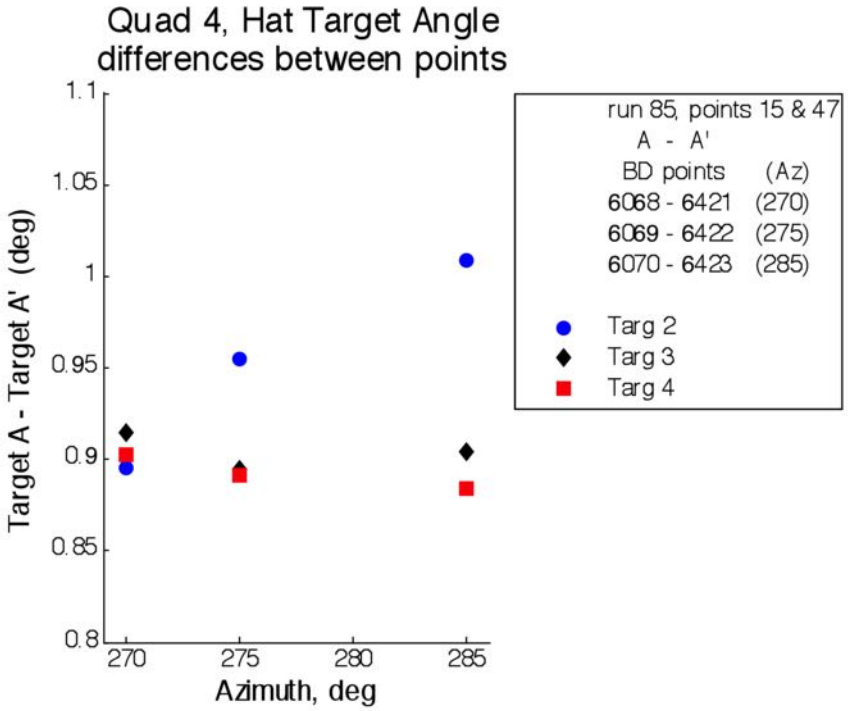

Figure E5. Target angle differences for like reference points (15 and 47) at the same azimuth.

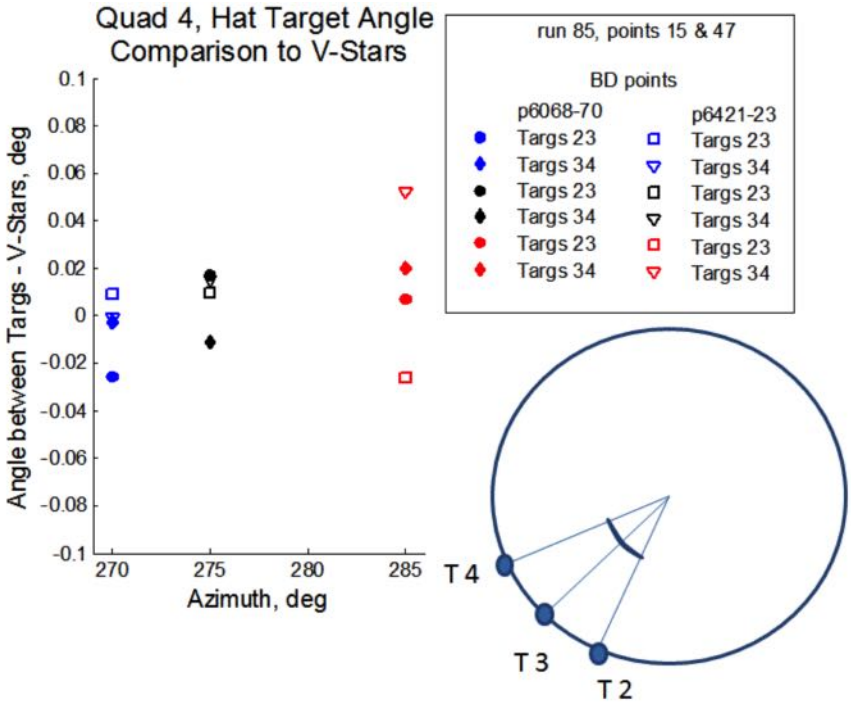

Figure E6. Target angle comparisons to V-STARS for like reference points (15 and 47).

Appendix F

UH-60A Rotor Blade Geometry

The blade displacement data reduction procedures rely on reference measurements of blade targets on the actual blades in a static, undeformed state. Thus detailed geometric design information on the UH-60A rotor blades was not essential to the blade displacement measurements. However, the geometric design information was used to make slight alignment adjustments to the measured target coordinates to reduce possible pitch, flap, and lag errors due to misalignment of the coordinate system used for the reference measurements. A NASA Technical Publication by William Bousman[F1] was the primary source of UH-60A rotor blade geometry information. Additional information on the blade twist distribution was obtained from papers by J. P. Shanley[F2] and Jasim Ahmad.[F3]

The 2D, chordwise airfoil sections of the UH-60A rotor blade are based on SC1095 and SC1094 R8 airfoils, which are described in more detail in Bousman's paper. Figure F1 and Table F1, from Bousman's paper, show how the airfoil section profiles are distributed along the span of the blade. (Note: the quarter-chord location value for the 322-inch radial station in Table F1 has a correction that is consistent with Bousman's description of the blade planform.)

The distribution of blade aerodynamic twist, also from Bousman's paper, is shown in Fig. F2, where the twist angle is defined by the airfoil section mean chord line. As such, there is a –1° shift for the radial stations that use the SC1094 R8 airfoil. It is important to note that there is no equivalent twist offset in the structural spar over the span where the SC1094 R8 airfoil is used. Bousman's paper does not supply tabulated values of the twist distribution, but the data in Fig. F2 is most likely from Shanley's paper, which validated UH-60A input data used in CAMRAD simulations. More recent computational models use a slightly different twist distribution, as is shown in Fig. F3 from Ahmad's paper. Dr. Jasim Ahmad also supplied a listing of the twist distribution that he used in his computational models of the UH-60A rotor blades.[F4]

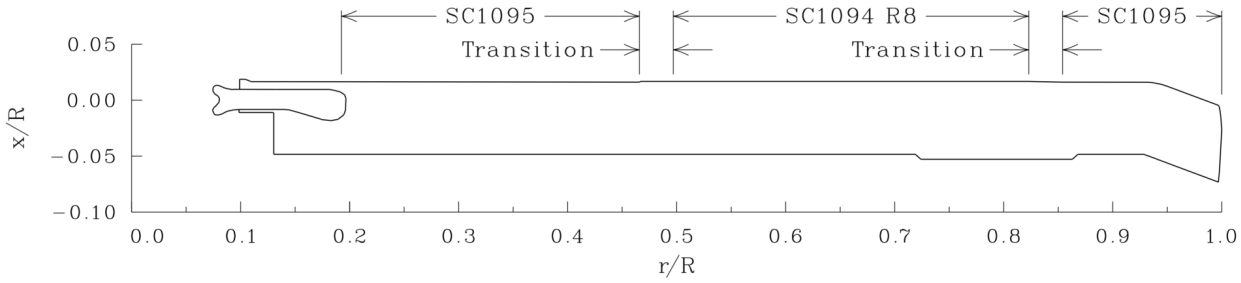

Figure F1. Layout of SC1095 and SC1094 R8 airfoils on a UH-60A planform (Bousman).

[F1] Bousman, W.G., "Aerodynamic Characteristics of SC1095 and SC1094 R8 Airfoils," NASA TP 212265, Sept. 2003. http://www.dtic.mil/get-tr-doc/pdf?AD=ADA480634

[F2] Shanley, W.G. , "Validation of UH-60A CAMRAD/JA Input Model," Sikorsky Aircraft, SER 70279-1, Nov. 1991.

[F3] Ahmad, J. and Biedron, R., "Code-to-Code Comparison of CFD/CSD Simulation for a Helicopter Rotor in Forward Flight," in 29th AIAA Applied Aerodynamics Conference, Sept. 2011. http://dx.doi.org/10.2514/6.2011-3819

[F4] Email correspondence from Dr. Jasim Ahmad on June 13, 2012.

Table F1. UH-60A blade profile distribution (Bousman).

Section characteristic	Radial location, in.	Radial location, r/R	Chord, in (includes trim tab)	Quarter chord, in. (Relative to SC1095 quarter chord, positive forward.)
Root cutout	42.00	0.13	20.76	0.00
SC1095 (inner/inner)	62.00	0.19	20.76	0.00
SC1095 (outer/inner)	150.00	0.47	20.76	0.00
SC1094 R8 (inner)	160.00	0.50	20.97	0.15
SC1094 R8 (tab, inner)	236.91	0.74	22.32	-0.18
SC1094 R8 (outer)	265.00	0.82	22.32	-0.18
SC1095 (inner/outer)	275.00	0.85	22.11	-0.34
SC1095 (tab, outer/outer)	277.86	0.86	22.11	-0.34
SC1095 (sweep, inner)	299.00	0.93	20.76	0.00
SC1095 (sweep, tip)	322.00	1.00	22.09	-7.37

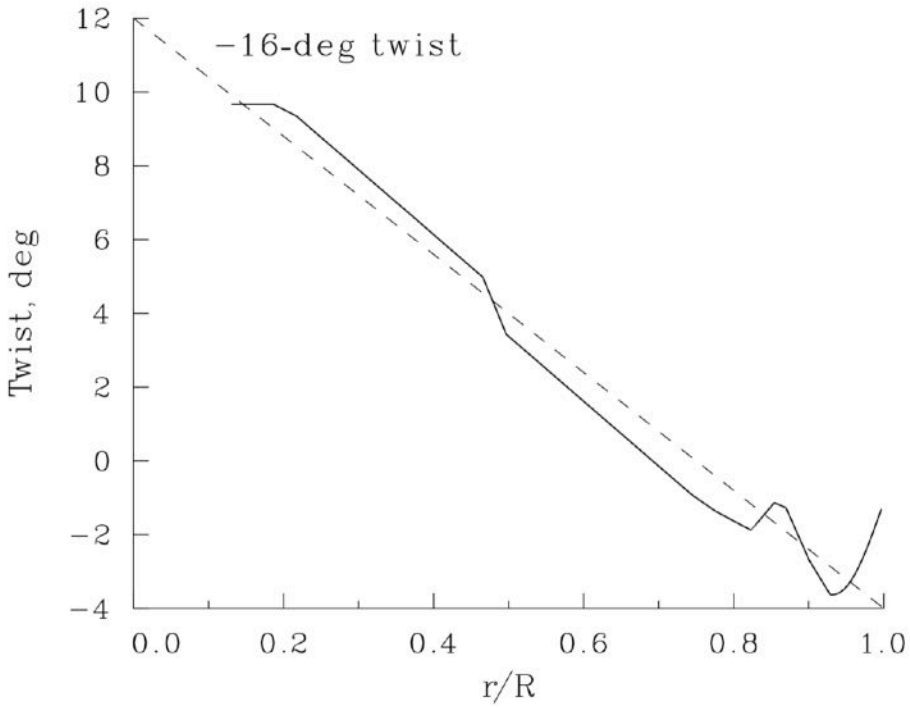

Figure F2. Aerodynamic twist of UH-60A blade based on mean chord line (Bousman).

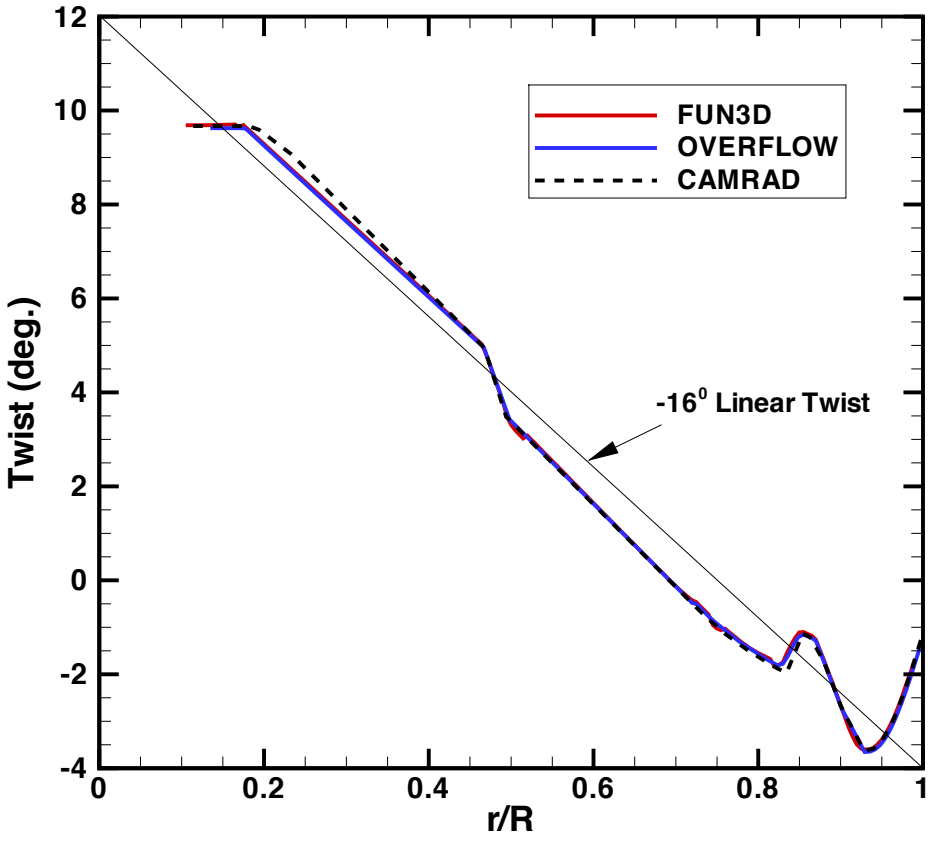

Figure F3. Computed twist distributions for independently generated reference blades, compared with twist distribution used in CAMRAD II (Ahmad).

Appendix G

Blade Identification and Locations for UH-60A Airloads Tests

Table G1 lists the UH-60A rotor blades used in Airloads Wind Tunnel Test, the IBC Wind Tunnel Test, and the Airloads Flight Test. Unknown or uncertain data is denoted by question marks.

Table G1. Blade identification and location for UH-60A tests.

Airloads Wind Tunnel Test

Identification	**Position on Hub**	Blade **Color**	**Tip Accelerometers**
Pressure Blade	1	Red	No
Standard Blade	2	Black	Yes
Strain Gauge Blade	3	White?	No
Standard Blade	4	Blue	Yes
Standard Blade	off	Yellow	?

IBC Wind Tunnel Test

Identification	**Position on Hub**	Blade **Color**	**Tip Accelerometers**
Strain Gauge Blade	1	Red position / White blade	No
Standard Blade	2	Black	Yes
Standard Blade	3	Yellow	?
Standard Blade	4	Black	?
Pressure Blade	off	Blue	No

Airloads Flight Test

Identification	**Position on Hub**	Blade **Color**	**Tip Accelerometers**
Pressure Blade	1	?	?
Standard Blade	2	?	?
Instrumented Blade	3	?	?
Standard Blade	4	?	?

Appendix H

Blade Target Registration

The determination of blade orientation and deformation was based on the comparison of the blade target locations measured during the test to blade target locations measured in the blade reference coordinate system. For each Blade Displacement data point obtained under test conditions, the measured blade target locations were compared to their reference locations in order to estimate pitch, flap, lag, and deformation values. Each blade had rows of 3 targets at 16 spanwise stations, for a total of 48 reference targets. The reference location measurements of these targets were made several times from September 2008 and September 2012 in support of the Individual Blade Control (IBC) and the NFAC UH-60A Airloads Tests in the USAF National Full-Scale Aerodynamics Complex (NFAC) 40- by 80-Foot Wind Tunnel.[H1,H2,H3] Prior to 2012, these measurements were taken with the blades supported in a horizontal orientation as shown in Fig. H1.

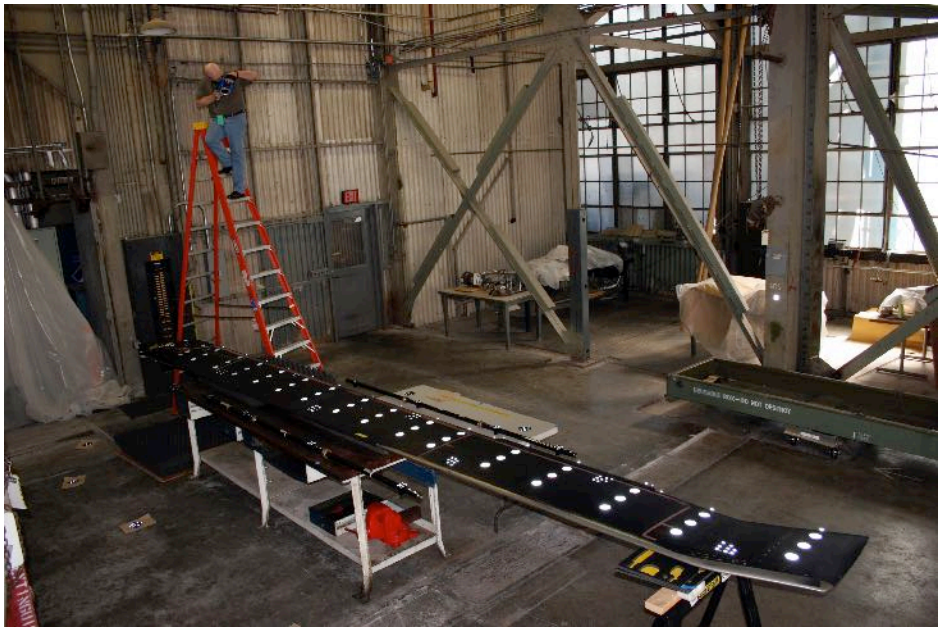

Figure H1. Horizontal UH-60A blade target registration setup.

[H1] Olson, L. E., Abrego, A., Barrows, D., and Burner, A. W., "Blade Deflection Measurements of a Full- Scale UH-60A Rotor System," *American Helicopter Society Aeromechanics Specialist Conference*, San Francisco, CA, American Helicopter Socieity, Jan. 20 2010.

[H2] Barrows, D. A., Olson, L. E., Abrego, A. I., and Burner, A. W., "Blade Displacement Measurements of the Full-Scale UH-60A Airloads Rotor," *29th AIAA Applied Aerodynamics Conference*, American Institute of Aeronautics and Astronautics, Nov. 2011.

[H3] Abrego, A. I., Olson, L. E., Romander, E. A., Barrows, D. A., and Burner, A. W., "Blade Displacement Measurement Technique Applied to a Full-Scale Rotor Test," *American Helicopter Society 68th Annual Forum*, Fort Worth, Texas, May 1–3, 2012.

The reference target location measurements were made using a V-STARS[H4] camera and software. To facilitate the registration measurements, additional, temporary, targets were also applied to the blades.These included small, magnetic button targets that were attached to the trailing edge of the blades and targets in the bolt holes of the tang at the blade root. Small groups of targets, referred to as coded targets, were also applied as part of the measurement procedure. These coded targets were also placed on the surface around the blade and on two "scale bars" that can be seen on either side of the blade in Fig. H1.

Any errors in the reference target locations propagate to subsequent blade orientation and deformation estimates, so great care was taken in aligning and supporting the blades to minimize errors. However the blades have a complex geometry with spanwise variation in the airfoil section, twist about the quarter-chord line, and sweep at the tip, which makes it difficult to visually detect misalignment or bending. In 2012, the existing blade target registration data were compared to an "as-designed" geometric model derived from data and descriptions in Bousman.[H5] It is expected that the "as-built" geometry will deviate from the "as-designed" geometry, but the comparisons indicated that there may have been some gravity-induced bending of the blades due to the horizontal supports that were used. This led to the decision to repeat the reference target measurements with the blades suspended from the ceiling as shown in Fig. H2.

Figure H2. Vertically suspended UH-60A blade target registration setup.

The blades were suspended by an attachment to the tang at the blade root, which was the only support. To keep the blades from moving due to air motion or vibrations, the blades were slightly restrained near the tip by foam attached to wood planks as shown in Fig. H2. Temporary targets were applied as described for the previous registration measurements, with the addition of targets near the leading edge for each row and a target near the trailing-edge tip.

Software was developed to map the V-STARS target locations to the "as-designed" geometry model using a series of rigid-body geometry transformations. First the trailing-edge targets were used to determine adjustments to the lag angle and x coordinate, and then all targets were used to determine the remaining geometric transformation adjustments. Due to measurement error and differences between the "as-built" and "as-designed" geometries, the geometric transformations were

[H4]Geodetic Systems, Inc., V-STARS, http://www.geodetic.com/.

[H5]Bousman, W.G., "Aerodynamic Characteristics of SC1095 and SC1094 R8 Airfoils," NASA TP 212265, Sept. 2003. http://www.dtic.mil/get-tr-doc/pdf?AD=ADA480634

determined so as to minimize the least-square differences between the "as-built" and "as-designed" target locations. The geometric transformations will vary depending on which targets are used to determine them. Calculations using both the first 6 rows and the first 15 rows of targets were made, but only the results based on the first 6 rows were used. Details about the registration data and calculation results for the vertically suspended blade measurements are found in the blade registration reports presented in Appendix I.

Figure H3 is a historical view of the difference between the measured and "as-designed" z coordinate of the quarter-chord line for Blade 2 for several spanwise stations based on all of the V-STARS measurement data. The August and September 2012 data were acquired with the vertically suspended blade, the others were acquired with the blade suspended horizontally. Figures H4 and H5 show a comparison between the measured and "as-designed" z location and twist along the quarter-chord line for each of the four blades based on the most recent V-STARS data for vertically suspended blades.[H6]

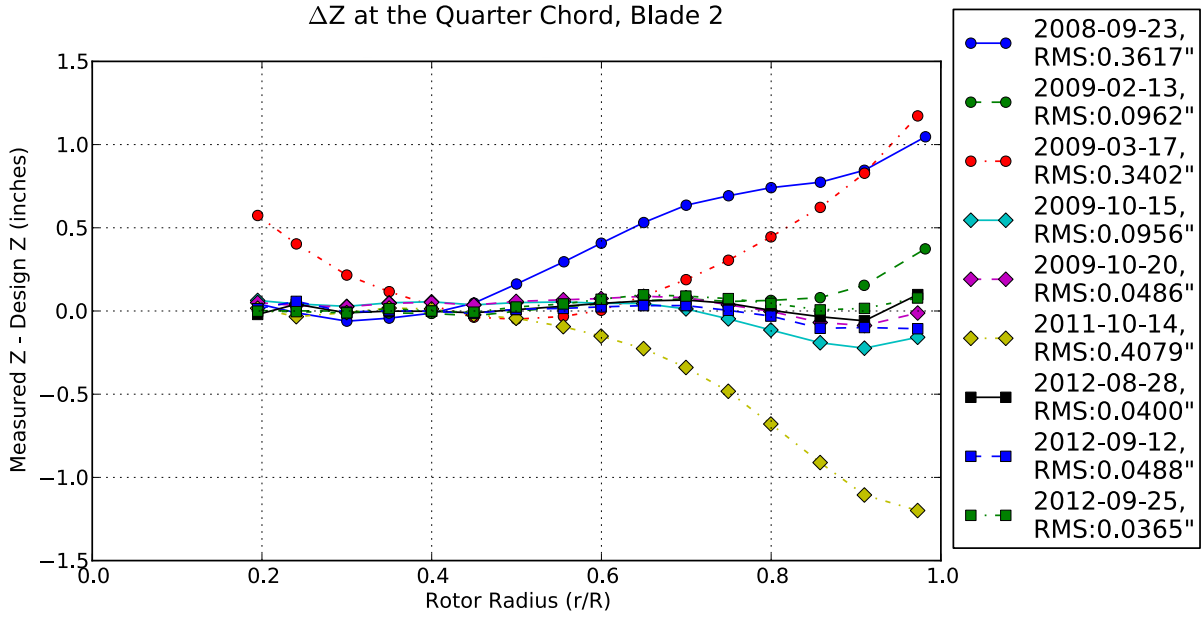

Figure H3. Historical differences between the measured z locations and the "as-designed" z locations along the quarter-chord line.

[H6]Due to exposure to dirt and oil, a few of the targets on some blades could not be measured using the V-STARS system. Their positions were interpolated from previous measurements.

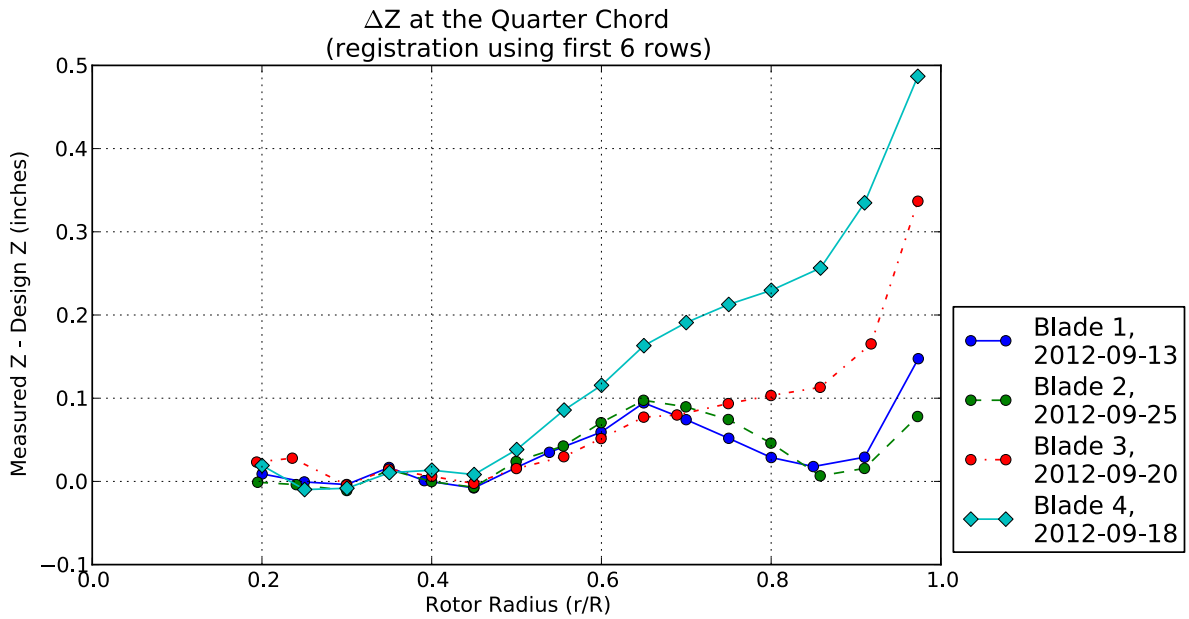

Figure H4. Differences between the measured (2012) z locations and the "as-designed" z locations along the quarter-chord line for each blade.

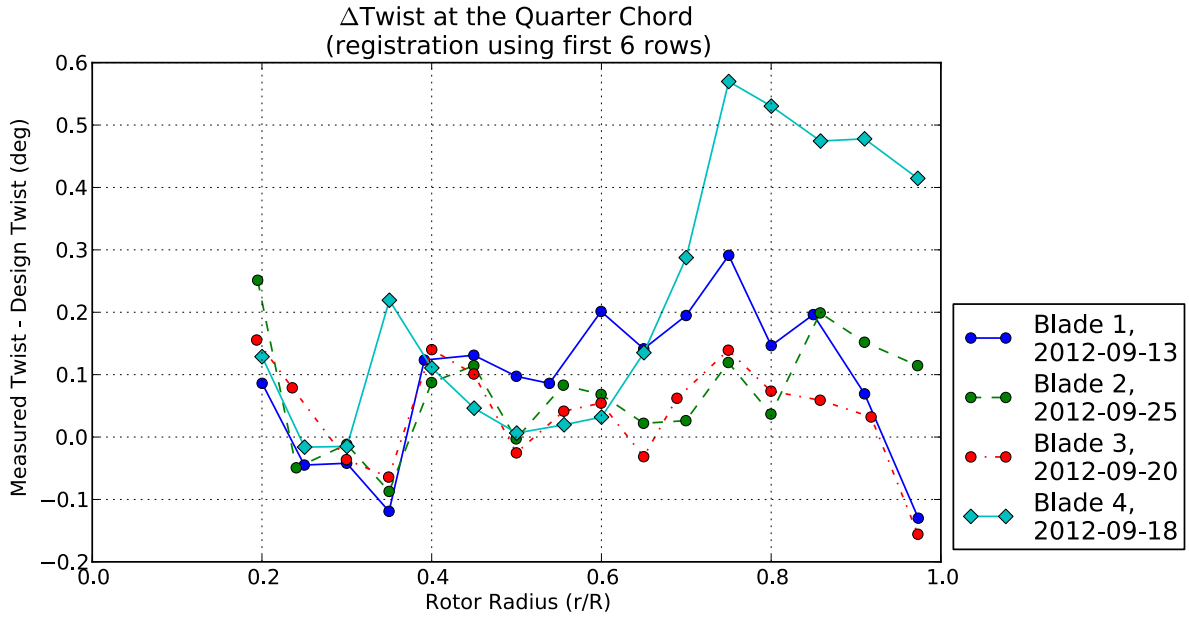

Figure H5. Differences between the measured (2012) twist and the "as-designed" twist along the quarter-chord line for each blade.

Appendix I

Blade Target Registration Reports

The attached blade target registration reports are based on the most recent V-STARS data for vertically suspended blades. The target locations based on registrations using the first six rows of targets, with corrections for lag, flap, and ΔZ, are the locations used in calculating blade orientation and deformations for the NFAC Airloads Test.

I.1 Blade 1

The blade target registration report for Blade 1 is included here. It is based on the most recent V-STARS target location data for the vertically suspended blade. The condition of targets 2 and 47 had degraded too much for the V-STARS system to measure them for this last measurement session, so their locations were estimated based on their relative distance to nearby targets from previous V-STARS measurements.

Blade Target Registration

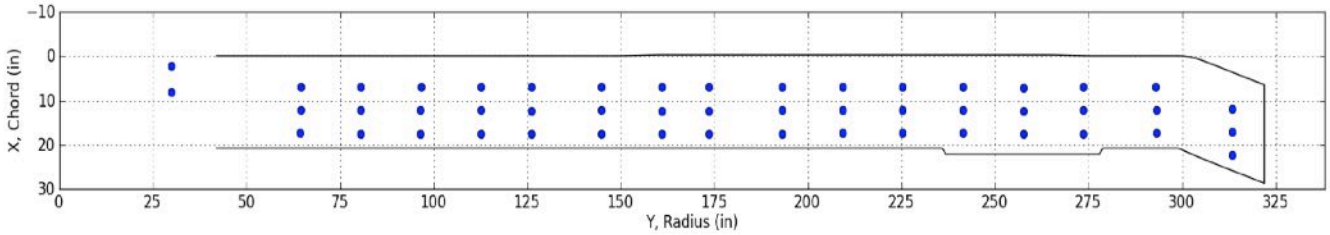

Registration Report for Blade Number 1

File: Blade 1 091312 vertical(1)_2_47.csv

Z reference allowed ±2.00 inches of travel

Aeromechanics Branch
Flight Vehicle Research and Technology Division
NASA Ames Research Center
Moffett Field, CA 94035

Chapter 1: VSTARS Target Location Data

Table 1-1. VSTARS target measurements (inches).

Name	Number	X	Y	Z	sigma X	sigma Y	sigma Z
B1_R20_C05		0.8603	64.48	-0.3321	0.0004	0.0004	0.0007
B1_R20_C36	1	7.0097	64.496	-1.5055	0.0004	0.0005	0.0008
B1_R20_C86	3	17.432	64.437	-2.6037	0.0006	0.0005	0.0008
B1_R20_C99		20.37	64.389	-3.1398	0.0003	0.0004	0.0005
B1_R25_C05		0.9178	80.484	-0.4478	0.0003	0.0004	0.0006
B1_R25_C36	4	7.0324	80.453	-1.5603	0.0004	0.0004	0.0008
B1_R25_C61	5	12.15	80.489	-2.0785	0.0004	0.0004	0.0007
B1_R25_C86	6	17.404	80.476	-2.5076	0.0004	0.0005	0.0007
B1_R25_C99		20.37	80.501	-3.0595	0.0003	0.0003	0.0005
B1_R30_C05		0.8533	96.548	-0.5457	0.0003	0.0004	0.0006
B1_R30_C36	7	7.0394	96.582	-1.5469	0.0005	0.0006	0.001
B1_R30_C61	8	12.194	96.559	-2.0329	0.0005	0.0006	0.0008
B1_R30_C86	9	17.453	96.53	-2.378	0.0006	0.0008	0.001
B1_R30_C99		20.4	96.466	-2.8972	0.0003	0.0003	0.0005
B1_R35_C05		0.8687	112.6	-0.6185	0.0003	0.0004	0.0006
B1_R35_C36	10	7.0118	112.64	-1.5494	0.0005	0.0005	0.0007
B1_R35_C61	11	12.181	112.64	-1.9582	0.0003	0.0004	0.0005
B1_R35_C86	12	17.428	112.64	-2.2297	0.0003	0.0003	0.0005
B1_R35_C99		20.431	112.62	-2.6896	0.0003	0.0003	0.0005
B1_R40_C05		0.8185	126.02	-0.7255	0.0003	0.0004	0.0006
B1_R40_C36	13	6.9988	126.03	-1.5538	0.0005	0.0005	0.0007
B1_R40_C61	14	12.237	126.03	-1.8979	0.0004	0.0005	0.0006
B1_R40_C86	15	17.451	126.01	-2.0792	0.0004	0.0005	0.0006
B1_R40_C99		20.422	126.03	-2.5068	0.0003	0.0004	0.0005
B1_R45_C05		0.7631	144.78	-0.8341	0.0003	0.0004	0.0006
B1_R45_C36	16	6.9697	144.81	-1.5778	0.0003	0.0004	0.0006
B1_R45_C61	17	12.155	144.79	-1.8218	0.0004	0.0004	0.0008
B1_R45_C86	18	17.399	144.8	-1.9259	0.0003	0.0004	0.0005
B1_R45_C99		20.427	144.83	-2.2814	0.0003	0.0004	0.0005
B1_R50_C05		0.7533	160.95	-1.1153	0.0003	0.0004	0.0005
B1_R50_C36	19	6.9516	160.93	-1.5674	0.0004	0.0005	0.0007
B1_R50_C61	20	12.189	160.92	-1.7386	0.0003	0.0004	0.0005
B1_R50_C86	21	17.409	160.9	-1.7639	0.0003	0.0004	0.0005
B1_R50_C99		20.433	160.9	-2.079	0.0003	0.0004	0.0005
B1_R55_C05		0.8113	173.51	-1.1852	0.0003	0.0004	0.0005
B1_R55_C36	22	6.945	173.49	-1.5406	0.0005	0.0005	0.0008
B1_R55_C61	23	12.191	173.45	-1.6796	0.0005	0.0005	0.0009
B1_R55_C86	24	17.415	173.45	-1.6205	0.0003	0.0004	0.0005
B1_R55_C99		20.434	173.47	-1.8927	0.0003	0.0004	0.0005
B1_R60_C05		0.7716	193.03	-1.2723	0.0003	0.0004	0.0005
B1_R60_C36	25	6.8915	193.07	-1.5478	0.0005	0.0005	0.0012
B1_R60_C61	26	12.166	193.1	-1.5392	0.0006	0.0009	0.0008
B1_R60_C86	27	17.376	193.09	-1.3775	0.0003	0.0004	0.0005
B1_R60_C99		20.409	193.07	-1.5985	0.0003	0.0004	0.0005
B1_R65_C05		0.7176	209.29	-1.3396	0.0003	0.0004	0.0005
B1_R65_C36	28	6.8932	209.28	-1.5023	0.0006	0.001	0.0009
B1_R65_C61	29	12.101	209.24	-1.4468	0.0005	0.0006	0.0008
B1_R65_C86	30	17.336	209.24	-1.201	0.0004	0.0006	0.0007
B1_R65_C99		20.376	209.21	-1.3765	0.0003	0.0004	0.0005
B1_R70_C05		0.642	225.38	-1.4632	0.0003	0.0004	0.0005
B1_R70_C36	31	6.8957	225.35	-1.5265	0.0003	0.0004	0.0006

Name	Number	X	Y	Z	sigma X	sigma Y	sigma Z
B1_R70_C61	32	12.098	225.33	-1.3753	0.0006	0.0011	0.0009
B1_R70_C86	33	17.276	225.32	-1.0638	0.0005	0.0008	0.0009
B1_R70_C99		20.367	225.39	-1.1797	0.0003	0.0004	0.0005
B1_R75_C05		0.8455	241.53	-1.592	0.0003	0.0004	0.0006
B1_R75_C36	34	6.8827	241.52	-1.5589	0.0003	0.0004	0.0006
B1_R75_C61	35	12.11	241.52	-1.3155	0.0003	0.0004	0.0006
B1_R75_C86	36	17.321	241.51	-0.924	0.0006	0.001	0.0009
B1_R75_C105		21.87	241.53	-0.8848	0.0003	0.0004	0.0005
B1_R80_C05		0.7776	257.63	-1.6859	0.0004	0.0004	0.0006
B1_R80_C36	37	7.025	257.65	-1.5918	0.0004	0.0004	0.0007
B1_R80_C61	38	12.163	257.65	-1.3126	0.0005	0.0005	0.0015
B1_R80_C86	39	17.372	257.62	-0.8652	0.0005	0.0005	0.0016
B1_R80_C105		21.799	257.74	-0.7535	0.0003	0.0004	0.0006
B1_R86_C05		0.7502	273.59	-1.6216	0.0004	0.0004	0.0007
B1_R86_C36	40	6.8593	273.6	-1.611	0.0005	0.0005	0.0012
B1_R86_C61	41	12.047	273.63	-1.2816	0.0006	0.0006	0.0017
B1_R86_C86	42	17.394	273.62	-0.8007	0.0007	0.0013	0.0012
B1_R86_C105		21.73	273.66	-0.6468	0.0004	0.0004	0.0006
B1_R91_C05		0.6908	292.99	-1.7448	0.0004	0.0005	0.0008
B1_R91_C36	43	6.8462	293.08	-1.5639	0.0011	0.0014	0.0019
B1_R91_C61	44	12.07	293.09	-1.1019	0.0008	0.0009	0.0014
B1_R91_C86	45	17.269	293.08	-0.4273	0.0009	0.0011	0.0016
B1_R91_C99		20.284	293.16	-0.2982	0.0004	0.0005	0.0007
B1_R97_C05		4.4336	313.42	-1.4244	0.0005	0.0006	0.0012
B1_R97_C36	46	11.918	313.47	-1.2468	0.0007	0.0012	0.0012
B1_R97_C86	48	22.286	313.44	-0.2557	0.0007	0.0014	0.0013
B1_R97_C99		25.248	313.36	-0.2063	0.0004	0.0006	0.0008
Blade Tip		27.982	320.95	-0.2752	0.0004	0.0005	0.0007
HUB_LE		2.1917	30	-3.5001	0.0004	0.0005	0.0006
HUB_TE		8.1883	30	-3.4999	0.0004	0.0005	0.0006
B1_R20_C61	2	12.217	64.445	-2.1171	0.0005	0.0006	0.0011
B1_R97_C61	47	17.043	313.47	-0.79895	0.0007	0.0008	0.0011

Chapter 2: Bolt Hole Target Alignment

The measured X, Y, and Z locations of the bolt hole targets are compared to their "as designed" locations. X, Y, and Z translation errors, along with pitch and lag errors, are estimated, and compensating translations and rotations are then applied to all target measurements.

2.1: Bolt Hole Alignment Errors

Table 2-1. Measured(1) vs "as designed"(2) in inches.

Name	X1	Y1	Z1	X2	Y2	Z2	dX	dY	dZ	dR
HUB_LE	2.1917	30	-3.5001	2.19	30	-3.5	0.0017	0	-0.0001	0.0017029
HUB_TE	8.1883	30	-3.4999	8.19	30	-3.5	-0.0017	0	0.0001	0.0017029
RMS Errors:							0.0017	0	0.0001	0.0017029

Table 2-2. Initial alignment errors.

Alignment Error	Value
X Error	-8.8818e-16
Y Error	0
Z Error	0
Pitch Error	-0.0019109
Lag Error	0

2.2: Corrected Bolt Hole Alignment

Table 2-3. Measured(1) with alignment correction vs "as designed"(2) in inches.

Name	X1	Y1	Z1	X2	Y2	Z2	dX	dY	dZ	dR
HUB_LE	2.1917	30	-3.5001	2.19	30	-3.5	0.0017	0	-0.0001	0.0017029
HUB_TE	8.1883	30	-3.4999	8.19	30	-3.5	-0.0017	0	0.0001	0.0017029
RMS Errors:							0.0017	0	0.0001	0.0017029

Table 2-4. Errors after hole alignment correction.

Alignment Error	Value
X Error	-8.8818e-16
Y Error	0
Z Error	0
Pitch Error	-0.0019109
Lag Error	0

Chapter 3: Trailing-Edge Alignment

The measured X locations of the trailing-edge targets, excluding those on the tab and swept tip, are compared to the "as designed" locations. An estimated lag error, for rotation about the centroid of the two bolt hole targets, and an estimated centroid offset in the X direction that minimize the root-mean-square of the ΔX values with respect to the "as designed" trailing-edge X location, are determined and applied to all target measurements.

3.1: Trailing-Edge Alignment Errors

Table 3-1. Measured(1) vs "as designed"(2) in inches.

Name	X1	Y1	Z1	X2	Y2	Z2	dX	dY	dZ	dR
B1_R20_C05	0.8603	64.48	-0.3321	0.8603	64.48	0.14268	0	0	-0.47478	0.47478
B1_R20_C36	7.0097	64.496	-1.5055	7.0097	64.496	-1.1098	0	0	-0.39574	0.39574
B1_R20_C61	12.217	64.445	-2.1171	12.217	64.445	-1.7752	0	0	-0.34188	0.34188
B1_R20_C86	17.432	64.437	-2.6037	17.432	64.437	-2.2608	0	0	-0.34286	0.34286
B1_R20_C99	20.37	64.389	-3.1398	20.506	64.389	-2.8207	-0.13533	0	-0.3191	0.34661
B1_R25_C05	0.9178	80.484	-0.4478	0.9178	80.484	0.057317	0	0	-0.50512	0.50512
B1_R25_C36	7.0324	80.453	-1.5603	7.0324	80.453	-1.0852	0	0	-0.47513	0.47513
B1_R25_C61	12.15	80.489	-2.0785	12.15	80.489	-1.6675	0	0	-0.411	0.411
B1_R25_C86	17.404	80.476	-2.5076	17.404	80.476	-2.0844	0	0	-0.42322	0.42322
B1_R25_C99	20.37	80.501	-3.0595	20.544	80.501	-2.604	-0.17366	0	-0.45551	0.48749
B1_R30_C05	0.8533	96.548	-0.5457	0.8533	96.548	0.023019	0	0	-0.56872	0.56872
B1_R30_C36	7.0394	96.582	-1.5469	7.0394	96.582	-1.0581	0	0	-0.48879	0.48879
B1_R30_C61	12.194	96.559	-2.0329	12.194	96.559	-1.5712	0	0	-0.46169	0.46169
B1_R30_C86	17.453	96.53	-2.378	17.453	96.53	-1.9139	0	0	-0.46412	0.46412
B1_R30_C99	20.4	96.466	-2.8972	20.579	96.466	-2.3894	-0.17911	0	-0.50777	0.53843
B1_R35_C05	0.8687	112.6	-0.6185	0.8687	112.6	-0.043745	0	0	-0.57476	0.57476
B1_R35_C36	7.0118	112.64	-1.5494	7.0118	112.64	-1.0276	0	0	-0.52178	0.52178
B1_R35_C61	12.181	112.64	-1.9582	12.181	112.64	-1.4705	0	0	-0.4877	0.4877
B1_R35_C86	17.428	112.64	-2.2297	17.428	112.64	-1.7393	0	0	-0.49039	0.49039
B1_R35_C99	20.431	112.62	-2.6896	20.611	112.62	-2.1723	-0.18017	0	-0.51735	0.54782
B1_R40_C05	0.8185	126.02	-0.7255	0.8185	126.02	-0.074549	0	0	-0.65095	0.65095
B1_R40_C36	6.9988	126.03	-1.5538	6.9988	126.03	-1.0039	0	0	-0.54985	0.54985
B1_R40_C61	12.237	126.03	-1.8979	12.237	126.03	-1.391	0	0	-0.50693	0.50693
B1_R40_C86	17.451	126.01	-2.0792	17.451	126.01	-1.5966	0	0	-0.48262	0.48262
B1_R40_C99	20.422	126.03	-2.5068	20.635	126.03	-1.9919	-0.2135	0	-0.5149	0.55741
B1_R45_C05	0.7631	144.78	-0.8341	0.7631	144.78	-0.12368	0	0	-0.71042	0.71042
B1_R45_C36	6.9697	144.81	-1.5778	6.9697	144.81	-0.97074	0	0	-0.60706	0.60706
B1_R45_C61	12.155	144.79	-1.8218	12.155	144.79	-1.2716	0	0	-0.55015	0.55015
B1_R45_C86	17.399	144.8	-1.9259	17.399	144.8	-1.395	0	0	-0.53091	0.53091
B1_R45_C99	20.427	144.83	-2.2814	20.666	144.83	-1.7388	-0.23853	0	-0.5426	0.59271
B1_R50_C05	0.7533	160.95	-1.1153	0.7533	160.95	-0.45309	0	0	-0.66221	0.66221
B1_R50_C36	6.9516	160.93	-1.5674	6.9516	160.93	-0.94786	0	0	-0.61954	0.61954
B1_R50_C61	12.189	160.92	-1.7386	12.189	160.92	-1.1736	0	0	-0.56498	0.56498
B1_R50_C86	17.409	160.9	-1.7639	17.409	160.9	-1.2185	0	0	-0.54537	0.54537
B1_R50_C99	20.433	160.9	-2.079	20.695	160.9	-1.5143	-0.26244	0	-0.56472	0.62272
B1_R55_C05	0.8113	173.51	-1.1852	0.8113	173.51	-0.51237	0	0	-0.67283	0.67283
B1_R55_C36	6.945	173.49	-1.5406	6.945	173.49	-0.92572	0	0	-0.61488	0.61488
B1_R55_C61	12.191	173.45	-1.6796	12.191	173.45	-1.0896	0	0	-0.59001	0.59001
B1_R55_C86	17.415	173.45	-1.6205	17.415	173.45	-1.0721	0	0	-0.5484	0.5484
B1_R55_C99	20.434	173.47	-1.8927	20.712	173.47	-1.3279	-0.27832	0	-0.56481	0.62966
B1_R60_C05	0.7716	193.03	-1.2723	0.7716	193.03	-0.58905	0	0	-0.68325	0.68325
B1_R60_C36	6.8915	193.07	-1.5478	6.8915	193.07	-0.89044	0	0	-0.65736	0.65736
B1_R60_C61	12.166	193.1	-1.5392	12.166	193.1	-0.95826	0	0	-0.58094	0.58094
B1_R60_C86	17.376	193.09	-1.3775	17.376	193.09	-0.84449	0	0	-0.53301	0.53301

Name	X1	Y1	Z1	X2	Y2	Z2	dX	dY	dZ	dR
B1_R60_C99	20.409	193.07	-1.5985	20.734	193.07	-1.0371	-0.32556	0	-0.56144	0.649
B1_R65_C05	0.7176	209.29	-1.3396	0.7176	209.29	-0.65206	0	0	-0.68754	0.68754
B1_R65_C36	6.8932	209.28	-1.5023	6.8932	209.28	-0.86379	0	0	-0.63851	0.63851
B1_R65_C61	12.101	209.24	-1.4468	12.101	209.24	-0.85224	0	0	-0.59456	0.59456
B1_R65_C86	17.336	209.24	-1.201	17.336	209.24	-0.65895	0	0	-0.54205	0.54205
B1_R65_C99	20.376	209.21	-1.3765	20.748	209.21	-0.79738	-0.37249	0	-0.57912	0.68857
B1_R70_C05	0.642	225.38	-1.4632	0.642	225.38	-0.71358	0	0	-0.74962	0.74962
B1_R70_C36	6.8957	225.35	-1.5265	6.8957	225.35	-0.83752	0	0	-0.68898	0.68898
B1_R70_C61	12.098	225.33	-1.3753	12.098	225.33	-0.74653	0	0	-0.62877	0.62877
B1_R70_C86	17.276	225.32	-1.0638	17.276	225.32	-0.47676	0	0	-0.58704	0.58704
B1_R70_C99	20.367	225.39	-1.1797	20.759	225.39	-0.55697	-0.39165	0	-0.62273	0.73565
B1_R75_C05	0.8455	241.53	-1.592	0.8455	241.53	-0.78846	0	0	-0.80354	0.80354
B1_R75_C36	6.8827	241.52	-1.5589	6.8827	241.52	-0.81405	0	0	-0.74485	0.74485
B1_R75_C61	12.11	241.52	-1.3155	12.11	241.52	-0.65032	0	0	-0.66518	0.66518
B1_R75_C86	17.321	241.51	-0.924	17.321	241.51	-0.30556	0	0	-0.61844	0.61844
B1_R80_C05	0.7776	257.63	-1.6859	0.7776	257.63	-0.83381	0	0	-0.85209	0.85209
B1_R80_C36	7.025	257.65	-1.5918	7.025	257.65	-0.7919	0	0	-0.7999	0.7999
B1_R80_C61	12.163	257.65	-1.3126	12.163	257.65	-0.56965	0	0	-0.74295	0.74295
B1_R80_C86	17.372	257.62	-0.8652	17.372	257.62	-0.16498	0	0	-0.70022	0.70022
B1_R86_C05	0.7502	273.59	-1.6216	0.7502	273.59	-0.63671	0	0	-0.98489	0.98489
B1_R86_C36	6.8593	273.6	-1.611	6.8593	273.6	-0.77734	0	0	-0.83366	0.83366
B1_R86_C61	12.047	273.63	-1.2816	12.047	273.63	-0.51529	0	0	-0.76631	0.76631
B1_R86_C86	17.394	273.62	-0.8007	17.394	273.62	-0.057232	0	0	-0.74347	0.74347
B1_R91_C05	0.6908	292.99	-1.7448	0.6908	292.99	-0.72165	0	0	-1.0231	1.0231
B1_R91_C36	6.8462	293.08	-1.5639	6.8462	293.08	-0.72156	0	0	-0.84234	0.84234
B1_R91_C61	12.07	293.09	-1.1019	12.07	293.09	-0.27884	0	0	-0.82306	0.82306
B1_R91_C86	17.269	293.08	-0.4273	17.269	293.08	0.34494	0	0	-0.77224	0.77224
B1_R91_C99	20.284	293.16	-0.2982	20.755	293.16	0.50234	-0.471	0	-0.80054	0.92882
B1_R97_C05	4.4336	313.42	-1.4244	4.4336	313.42	-0.44778	0	0	-0.97662	0.97662
B1_R97_C36	11.918	313.47	-1.2468	11.918	313.47	-0.48907	0	0	-0.75773	0.75773
B1_R97_C61	17.043	313.47	-0.79895	17.043	313.47	-0.083438	0	0	-0.71551	0.71551
B1_R97_C86	22.286	313.44	-0.2557	22.286	313.44	0.49439	0	0	-0.75009	0.75009
B1_R97_C99	25.248	313.36	-0.2063	25.98	313.36	0.64097	-0.73246	0	-0.84727	1.12
HUB_LE	2.1917	30	-3.5001	2.19	5.19	-3.5	0.0017	24.81	-0.0001	24.81
HUB_TE	8.1883	30	-3.4999	8.19	5.19	-3.5	-0.0017	24.81	0.0001	24.81
RMS Errors:							0.13863	3.9476	0.62879	3.9997

The estimated lag error is -0.08836°.

The estimated X error is 0.073435 inches.

3.2: Corrected Trailing-Edge Alignment

Table 3-2. Measured(1) with lag correction vs "as designed"(2) in inches.

Name	X1	Y1	Z1	X2	Y2	Z2	dX	dY	dZ	dR
B1_R20_C05	0.98691	64.486	-0.3321	0.98691	64.486	0.089392	0	0	-0.42149	0.42149
B1_R20_C36	7.1363	64.493	-1.5055	7.1363	64.493	-1.1283	0	0	-0.37723	0.37723
B1_R20_C61	12.343	64.434	-2.1171	12.343	64.434	-1.7892	0	0	-0.32789	0.32789
B1_R20_C86	17.559	64.418	-2.6037	17.559	64.418	-2.2715	0	0	-0.33225	0.33225
B1_R20_C99	20.497	64.365	-3.1398	20.506	64.365	-2.821	-0.0088214	0	-0.31878	0.3189
B1_R25_C05	1.0691	80.491	-0.4478	1.0691	80.491	-3.0408e-05	0	0	-0.44777	0.44777
B1_R25_C36	7.1836	80.45	-1.5603	7.1836	80.45	-1.1051	0	0	-0.45522	0.45522
B1_R25_C61	12.302	80.478	-2.0785	12.302	80.478	-1.6821	0	0	-0.39644	0.39644
B1_R25_C86	17.555	80.457	-2.5076	17.555	80.457	-2.0949	0	0	-0.41271	0.41271
B1_R25_C99	20.522	80.478	-3.0595	20.544	80.478	-2.6043	-0.022308	0	-0.45519	0.45574
B1_R30_C05	1.0294	96.555	-0.5457	1.0294	96.555	-0.044096	0	0	-0.5016	0.5016
B1_R30_C36	7.2155	96.579	-1.5469	7.2155	96.579	-1.0788	0	0	-0.46812	0.46812
B1_R30_C61	12.37	96.548	-2.0329	12.37	96.548	-1.5857	0	0	-0.44725	0.44725
B1_R30_C86	17.629	96.511	-2.378	17.629	96.511	-1.9236	0	0	-0.45441	0.45441
B1_R30_C99	20.576	96.442	-2.8972	20.579	96.442	-2.3897	-0.0031427	0	-0.50745	0.50746
B1_R35_C05	1.0695	112.6	-0.6185	1.0695	112.6	-0.11523	0	0	-0.50327	0.50327
B1_R35_C36	7.2127	112.63	-1.5494	7.2127	112.63	-1.0485	0	0	-0.50093	0.50093
B1_R35_C61	12.382	112.63	-1.9582	12.382	112.63	-1.4841	0	0	-0.47407	0.47407
B1_R35_C86	17.629	112.62	-2.2297	17.629	112.62	-1.7475	0	0	-0.48216	0.48216
B1_R35_C99	20.632	112.6	-2.6896	20.611	112.6	-2.1726	0.020709	0	-0.51703	0.51744
B1_R40_C05	1.04	126.02	-0.7255	1.04	126.02	-0.15365	0	0	-0.57185	0.57185
B1_R40_C36	7.2203	126.03	-1.5538	7.2203	126.03	-1.0244	0	0	-0.52941	0.52941
B1_R40_C61	12.458	126.02	-1.8979	12.458	126.02	-1.4033	0	0	-0.49456	0.49456
B1_R40_C86	17.672	125.99	-2.0792	17.672	125.99	-1.603	0	0	-0.47616	0.47616
B1_R40_C99	20.643	126	-2.5068	20.635	126	-1.9922	0.0080494	0	-0.51458	0.51465
B1_R45_C05	1.0135	144.78	-0.8341	1.0135	144.78	-0.21238	0	0	-0.62172	0.62172
B1_R45_C36	7.2202	144.81	-1.5778	7.2202	144.81	-0.98982	0	0	-0.58798	0.58798
B1_R45_C61	12.406	144.78	-1.8218	12.406	144.78	-1.2816	0	0	-0.54021	0.54021
B1_R45_C86	17.65	144.78	-1.9259	17.65	144.78	-1.3982	0	0	-0.52773	0.52773
B1_R45_C99	20.678	144.81	-2.2814	20.666	144.81	-1.7391	0.012009	0	-0.54228	0.54241
B1_R50_C05	1.0287	160.95	-1.1153	1.0287	160.95	-0.48675	0	0	-0.62855	0.62855
B1_R50_C36	7.2269	160.93	-1.5674	7.2269	160.93	-0.96464	0	0	-0.60276	0.60276
B1_R50_C61	12.465	160.9	-1.7386	12.465	160.9	-1.1804	0	0	-0.55819	0.55819
B1_R50_C86	17.684	160.89	-1.7639	17.684	160.89	-1.2179	0	0	-0.54602	0.54602
B1_R50_C99	20.708	160.88	-2.079	20.695	160.88	-1.5146	0.012878	0	-0.56437	0.56451
B1_R55_C05	1.1061	173.51	-1.1852	1.1061	173.51	-0.54412	0	0	-0.64108	0.64108
B1_R55_C36	7.2397	173.49	-1.5406	7.2397	173.49	-0.94018	0	0	-0.60042	0.60042
B1_R55_C61	12.486	173.43	-1.6796	12.486	173.43	-1.0933	0	0	-0.58629	0.58629
B1_R55_C86	17.71	173.43	-1.6205	17.71	173.43	-1.0679	0	0	-0.55264	0.55264
B1_R55_C99	20.729	173.45	-1.8927	20.712	173.45	-1.3282	0.016391	0	-0.56446	0.5647
B1_R60_C05	1.0965	193.03	-1.2723	1.0965	193.03	-0.61841	0	0	-0.65389	0.65389
B1_R60_C36	7.2164	193.07	-1.5478	7.2164	193.07	-0.90049	0	0	-0.64731	0.64731
B1_R60_C61	12.491	193.08	-1.5392	12.491	193.08	-0.95631	0	0	-0.58289	0.58289
B1_R60_C86	17.701	193.07	-1.3775	17.701	193.07	-0.83372	0	0	-0.54378	0.54378
B1_R60_C99	20.734	193.05	-1.5985	20.734	193.05	-1.0374	-0.0006275	0	-0.56108	0.56108
B1_R65_C05	1.0675	209.3	-1.3396	1.0675	209.3	-0.67918	0	0	-0.66042	0.66042
B1_R65_C36	7.2431	209.28	-1.5023	7.2431	209.28	-0.8692	0	0	-0.6331	0.6331
B1_R65_C61	12.451	209.23	-1.4468	12.451	209.23	-0.84489	0	0	-0.60191	0.60191
B1_R65_C86	17.686	209.22	-1.201	17.686	209.22	-0.64197	0	0	-0.55903	0.55903
B1_R65_C99	20.726	209.19	-1.3765	20.748	209.19	-0.79773	-0.022683	0	-0.57877	0.57921
B1_R70_C05	1.0168	225.39	-1.4632	1.0168	225.39	-0.73898	0	0	-0.72422	0.72422

Name	X1	Y1	Z1	X2	Y2	Z2	dX	dY	dZ	dR
B1_R70_C36	7.2704	225.35	-1.5265	7.2704	225.35	-0.83757	0	0	-0.68893	0.68893
B1_R70_C61	12.473	225.32	-1.3753	12.473	225.32	-0.73287	0	0	-0.64243	0.64243
B1_R70_C86	17.651	225.3	-1.0638	17.651	225.3	-0.45284	0	0	-0.61096	0.61096
B1_R70_C99	20.742	225.36	-1.1797	20.759	225.36	-0.55732	-0.016902	0	-0.62238	0.62261
B1_R75_C05	1.2452	241.54	-1.592	1.2452	241.54	-0.80553	0	0	-0.78647	0.78647
B1_R75_C36	7.2823	241.52	-1.5589	7.2823	241.52	-0.80858	0	0	-0.75032	0.75032
B1_R75_C61	12.509	241.51	-1.3155	12.509	241.51	-0.63009	0	0	-0.68541	0.68541
B1_R75_C86	17.72	241.49	-0.924	17.72	241.49	-0.27436	0	0	-0.64964	0.64964
B1_R80_C05	1.2021	257.64	-1.6859	1.2021	257.64	-0.84833	0	0	-0.83757	0.83757
B1_R80_C36	7.4495	257.64	-1.5918	7.4495	257.64	-0.78086	0	0	-0.81094	0.81094
B1_R80_C61	12.588	257.64	-1.3126	12.588	257.64	-0.54318	0	0	-0.76942	0.76942
B1_R80_C86	17.797	257.61	-0.8652	17.797	257.61	-0.12695	0	0	-0.73825	0.73825
B1_R86_C05	1.1993	273.6	-1.6216	1.1993	273.6	-0.7218	0	0	-0.8998	0.8998
B1_R86_C36	7.3084	273.59	-1.611	7.3084	273.59	-0.76248	0	0	-0.84852	0.84852
B1_R86_C61	12.497	273.62	-1.2816	12.497	273.62	-0.48395	0	0	-0.79765	0.79765
B1_R86_C86	17.843	273.6	-0.8007	17.843	273.6	-0.013452	0	0	-0.78725	0.78725
B1_R91_C05	1.1698	293	-1.7448	1.1698	293	-0.82123	0	0	-0.92357	0.92357
B1_R91_C36	7.3253	293.07	-1.5639	7.3253	293.07	-0.68931	0	0	-0.87459	0.87459
B1_R91_C61	12.549	293.08	-1.1019	12.549	293.08	-0.22889	0	0	-0.87301	0.87301
B1_R91_C86	17.748	293.06	-0.4273	17.748	293.06	0.40808	0	0	-0.83538	0.83538
B1_R91_C99	20.763	293.13	-0.2982	20.755	293.13	0.50167	0.0082247	0	-0.79987	0.79991
B1_R97_C05	4.9441	313.42	-1.4244	4.9441	313.42	-0.57924	0	0	-0.84516	0.84516
B1_R97_C36	12.428	313.46	-1.2468	12.428	313.46	-0.456	0	0	-0.7908	0.7908
B1_R97_C61	17.554	313.45	-0.79895	17.554	313.45	-0.033324	0	0	-0.76562	0.76562
B1_R97_C86	22.797	313.42	-0.2557	22.797	313.42	0.55814	0	0	-0.81384	0.81384
B1_R97_C99	25.758	313.33	-0.2063	25.969	313.33	0.64213	-0.21059	0	-0.84843	0.87417
HUB_LE	2.2651	30.005	-3.5001	2.19	5.19	-3.5	0.075139	24.815	-0.0001	24.815
HUB_TE	8.2617	29.995	-3.4999	8.19	5.19	-3.5	0.071732	24.805	0.0001	24.805
RMS Errors:							0.027017	3.9475	0.62143	3.9962

3.3: Trailing-Edge Registration Plots

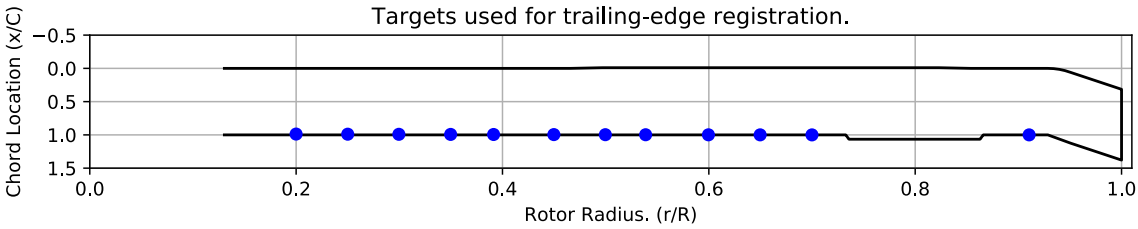

Figure 3-1. Targets used for trailing-edge alignment.

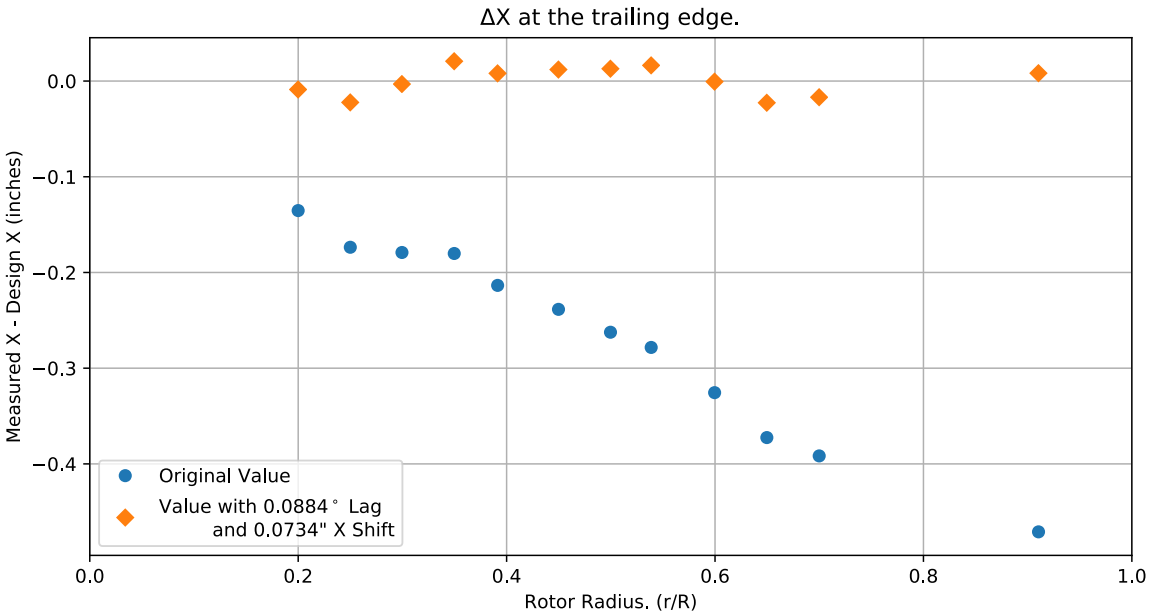

Figure 3-2. Trailing-edge ΔX error vs rotor radius.

Chapter 4: Flap Only Registration (6 rows)

The targets at the 6 spanwise stations nearest the root are used to determing the flap offset.

The estimated flap error is -0.32002°.

4.1: Target Location Errors After Flap Target Registration

Table 4-1. Measured(1) with flap registration vs "as designed"(2) in inches.

Name	X1	Y1	Z1	X2	Y2	Z2	dX	dY	dZ	dR
B1_R20_C05	0.98691	64.468	-0.13953	0.98691	64.468	0.08946	0	0	-0.22899	0.22899
B1_R20_C36	7.1363	64.481	-1.3129	7.1363	64.481	-1.1283	0	0	-0.18459	0.18459
B1_R20_C61	12.343	64.426	-1.9248	12.343	64.426	-1.7893	0	0	-0.13553	0.13553
B1_R20_C86	17.559	64.413	-2.4115	17.559	64.413	-2.2715	0	0	-0.13996	0.13996
B1_R20_C99	20.497	64.362	-2.9479	20.506	64.362	-2.8211	-0.0088151	0	-0.12681	0.12712
B1_R25_C05	1.0691	80.473	-0.16584	1.0691	80.473	3.3949e-05	0	0	-0.16587	0.16587
B1_R25_C36	7.1836	80.438	-1.2785	7.1836	80.438	-1.1051	0	0	-0.17345	0.17345
B1_R25_C61	12.302	80.47	-1.7966	12.302	80.47	-1.6821	0	0	-0.11446	0.11446
B1_R25_C86	17.555	80.451	-2.2258	17.555	80.451	-2.095	0	0	-0.13083	0.13083
B1_R25_C99	20.522	80.474	-2.7776	20.544	80.474	-2.6044	-0.022301	0	-0.17322	0.17465
B1_R30_C05	1.0294	96.537	-0.17401	1.0294	96.537	-0.044033	0	0	-0.12998	0.12998
B1_R30_C36	7.2155	96.567	-1.1751	7.2155	96.567	-1.0788	0	0	-0.09626	0.09626
B1_R30_C61	12.37	96.539	-1.6612	12.37	96.539	-1.5857	0	0	-0.075516	0.075516
B1_R30_C86	17.629	96.504	-2.0065	17.629	96.504	-1.9237	0	0	-0.082853	0.082853
B1_R30_C99	20.576	96.438	-2.5261	20.579	96.438	-2.3898	-0.0031335	0	-0.1363	0.13633
B1_R35_C05	1.0695	112.59	-0.15717	1.0695	112.59	-0.11516	0	0	-0.042002	0.042002
B1_R35_C36	7.2127	112.62	-1.0879	7.2127	112.62	-1.0485	0	0	-0.039397	0.039397
B1_R35_C61	12.382	112.62	-1.4967	12.382	112.62	-1.4842	0	0	-0.012519	0.012519
B1_R35_C86	17.629	112.61	-1.7683	17.629	112.61	-1.7476	0	0	-0.02064	0.02064
B1_R35_C99	20.632	112.59	-2.2283	20.611	112.59	-2.1727	0.02072	0	-0.055634	0.059367
B1_R40_C05	1.04	126.01	-0.18921	1.04	126.01	-0.15359	0	0	-0.035617	0.035617
B1_R40_C36	7.2203	126.01	-1.0175	7.2203	126.01	-1.0244	0	0	0.0069185	0.0069185
B1_R40_C61	12.458	126.01	-1.3616	12.458	126.01	-1.4034	0	0	0.041787	0.041787
B1_R40_C86	17.672	125.99	-1.5431	17.672	125.99	-1.6031	0	0	0.060094	0.060094
B1_R40_C99	20.643	126	-1.9706	20.635	126	-1.9923	0.0080617	0	0.021707	0.023156
B1_R45_C05	1.0135	144.77	-0.19302	1.0135	144.77	-0.21232	0	0	0.019292	0.019292
B1_R45_C36	7.2202	144.79	-0.93659	7.2202	144.79	-0.98985	0	0	0.053252	0.053252
B1_R45_C61	12.406	144.77	-1.1807	12.406	144.77	-1.2817	0	0	0.10093	0.10093
B1_R45_C86	17.65	144.77	-1.2848	17.65	144.77	-1.3983	0	0	0.11345	0.11345
B1_R45_C99	20.678	144.8	-1.6402	20.666	144.8	-1.7392	0.012022	0	0.099067	0.099793
B1_R50_C05	1.0287	160.94	-0.3839	1.0287	160.94	-0.48669	0	0	0.10278	0.10278
B1_R50_C36	7.2269	160.91	-0.83616	7.2269	160.91	-0.96467	0	0	0.12851	0.12851
B1_R50_C61	12.465	160.89	-1.0075	12.465	160.89	-1.1805	0	0	0.17302	0.17302
B1_R50_C86	17.684	160.87	-1.0329	17.684	160.87	-1.218	0	0	0.18514	0.18514
B1_R50_C99	20.708	160.87	-1.348	20.695	160.87	-1.5148	0.012893	0	0.16675	0.16725
B1_R55_C05	1.1061	173.5	-0.38365	1.1061	173.5	-0.54406	0	0	0.16042	0.16042
B1_R55_C36	7.2397	173.48	-0.73919	7.2397	173.48	-0.94021	0	0	0.20102	0.20102
B1_R55_C61	12.486	173.42	-0.87849	12.486	173.42	-1.0934	0	0	0.2149	0.2149
B1_R55_C86	17.71	173.42	-0.81942	17.71	173.42	-1.068	0	0	0.24859	0.24859
B1_R55_C99	20.729	173.44	-1.0915	20.712	173.44	-1.3284	0.016405	0	0.23691	0.23747
B1_R60_C05	1.0965	193.02	-0.36173	1.0965	193.02	-0.61836	0	0	0.25663	0.25663
B1_R60_C36	7.2164	193.05	-0.63703	7.2164	193.05	-0.90052	0	0	0.26349	0.26349

Name	X1	Y1	Z1	X2	Y2	Z2	dX	dY	dZ	dR
B1_R60_C61	12.491	193.07	-0.62834	12.491	193.07	-0.9564	0	0	0.32806	0.32806
B1_R60_C86	17.701	193.05	-0.46673	17.701	193.05	-0.83389	0	0	0.36716	0.36716
B1_R60_C99	20.734	193.04	-0.68783	20.734	193.04	-1.0376	-0.00061445	0	0.34978	0.34978
B1_R65_C05	1.0675	209.28	-0.33817	1.0675	209.28	-0.67912	0	0	0.34095	0.34095
B1_R65_C36	7.2431	209.26	-0.501	7.2431	209.26	-0.86923	0	0	0.36823	0.36823
B1_R65_C61	12.451	209.22	-0.44576	12.451	209.22	-0.84499	0	0	0.39923	0.39923
B1_R65_C86	17.686	209.2	-0.20003	17.686	209.2	-0.64216	0	0	0.44213	0.44213
B1_R65_C99	20.726	209.17	-0.3757	20.748	209.17	-0.79795	-0.022672	0	0.42225	0.42286
B1_R70_C05	1.0168	225.37	-0.37191	1.0168	225.37	-0.73892	0	0	0.36701	0.36701
B1_R70_C36	7.2704	225.34	-0.43542	7.2704	225.34	-0.83759	0	0	0.40218	0.40218
B1_R70_C61	12.473	225.3	-0.28439	12.473	225.3	-0.73297	0	0	0.44858	0.44858
B1_R70_C86	17.651	225.28	0.026991	17.651	225.28	-0.45304	0	0	0.48003	0.48003
B1_R70_C99	20.742	225.35	-0.088551	20.759	225.35	-0.55756	-0.016893	0	0.46901	0.46931
B1_R75_C05	1.2452	241.52	-0.4105	1.2452	241.52	-0.80548	0	0	0.39498	0.39498
B1_R75_C36	7.2823	241.51	-0.37749	7.2823	241.51	-0.80861	0	0	0.43112	0.43112
B1_R75_C61	12.509	241.49	-0.13418	12.509	241.49	-0.63018	0	0	0.496	0.496
B1_R75_C86	17.72	241.47	0.25722	17.72	241.47	-0.27453	0	0	0.53175	0.53175
B1_R80_C05	1.2021	257.63	-0.41447	1.2021	257.63	-0.8483	0	0	0.43383	0.43383
B1_R80_C36	7.4495	257.63	-0.32035	7.4495	257.63	-0.78088	0	0	0.46053	0.46053
B1_R80_C61	12.588	257.62	-0.04119	12.588	257.62	-0.54325	0	0	0.50206	0.50206
B1_R80_C86	17.797	257.59	0.40603	17.797	257.59	-0.1271	0	0	0.53313	0.53313
B1_R86_C05	1.1993	273.58	-0.26103	1.1993	273.58	-0.72202	0	0	0.46099	0.46099
B1_R86_C36	7.3084	273.58	-0.25046	7.3084	273.58	-0.76252	0	0	0.51207	0.51207
B1_R86_C61	12.497	273.61	0.079095	12.497	273.61	-0.48411	0	0	0.56321	0.56321
B1_R86_C86	17.843	273.58	0.55987	17.843	273.58	-0.013767	0	0	0.57363	0.57363
B1_R91_C05	1.1698	292.98	-0.27587	1.1698	292.98	-0.82114	0	0	0.54527	0.54527
B1_R91_C36	7.3253	293.06	-0.094552	7.3253	293.06	-0.68936	0	0	0.59481	0.59481
B1_R91_C61	12.549	293.06	0.36747	12.549	293.06	-0.22912	0	0	0.59658	0.59658
B1_R91_C86	17.748	293.04	1.042	17.748	293.04	0.40759	0	0	0.63437	0.63437
B1_R91_C99	20.763	293.11	1.1715	20.755	293.11	0.50106	0.0082049	0	0.67041	0.67046
B1_R97_C05	4.9441	313.4	0.15858	4.9441	313.4	-0.58057	0	0	0.73915	0.73915
B1_R97_C36	12.428	313.45	0.33643	12.428	313.45	-0.45556	0	0	0.79199	0.79199
B1_R97_C61	17.554	313.43	0.78421	17.554	313.43	-0.032334	0	0	0.81654	0.81654
B1_R97_C86	22.797	313.39	1.3272	22.797	313.39	0.55978	0	0	0.76746	0.76746
B1_R97_C99	25.758	313.31	1.3762	25.96	313.31	0.64297	-0.20226	0	0.7332	0.76059
HUB_LE	2.2651	30.005	-3.5001	2.19	30	-3.5	0.075139	0.0045111	-7.4805e-05	0.075274
HUB_TE	8.2617	29.995	-3.4999	8.19	30	-3.5	0.071732	-0.0047376	7.354e-05	0.071888
RMS Errors:							0.026199	0.00073601	0.36807	0.369

4.2: Flap Registration Plots (6 rows)

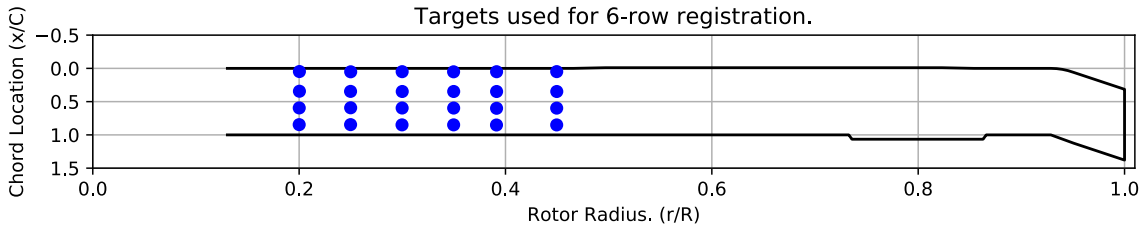

Figure 4-1. Targets used for 6 row root registration.

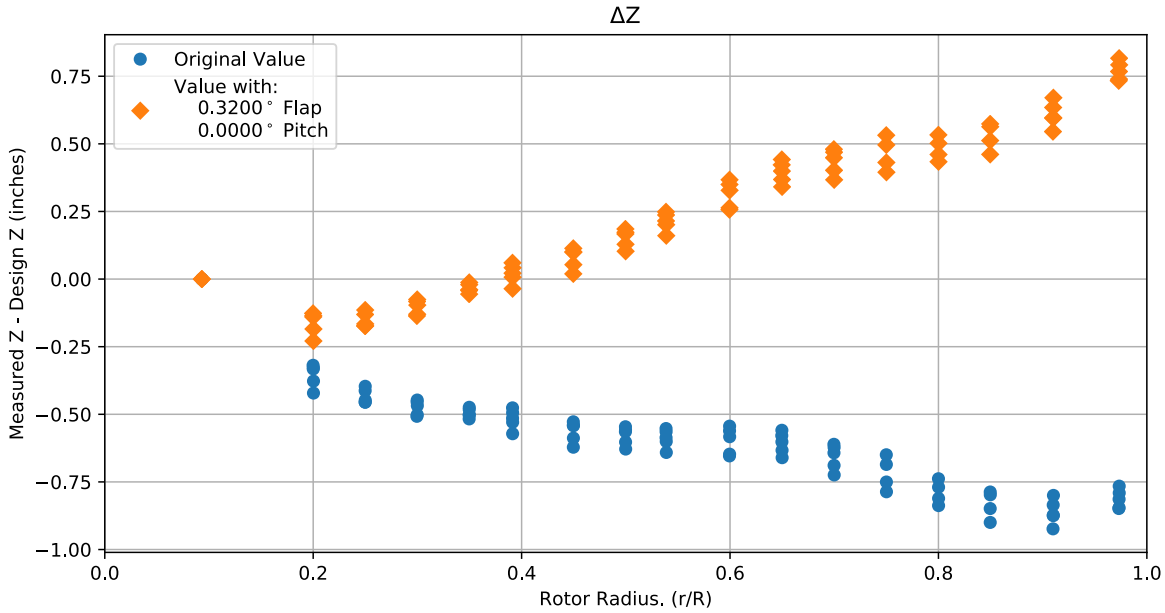

Figure 4-2. Flap target registration, ΔZ error vs rotor radius.

Note: the “as designed” geometry used for the swept tip may have some inaccuracies.

4.3: Estimated Bending and Twist at the Quarter Chord

The error bars shown represent the residual errors for fitting the measure target locations to the "as designed" geometry. These errors are generally much larger than those due to the VSTARS measurement errors. Therefore, the most likely source of these errors is the placement of the trailing-edge targets, differences between the "as designed" and "as built" geometries, and blade deformation during measurement. In the future, iterative adjustment of the "as designed" twist angle may be implemented to see if it reduces the fit error in delta twist. Note: The "as designed" geometry used for the swept tip may have some inaccuracies.

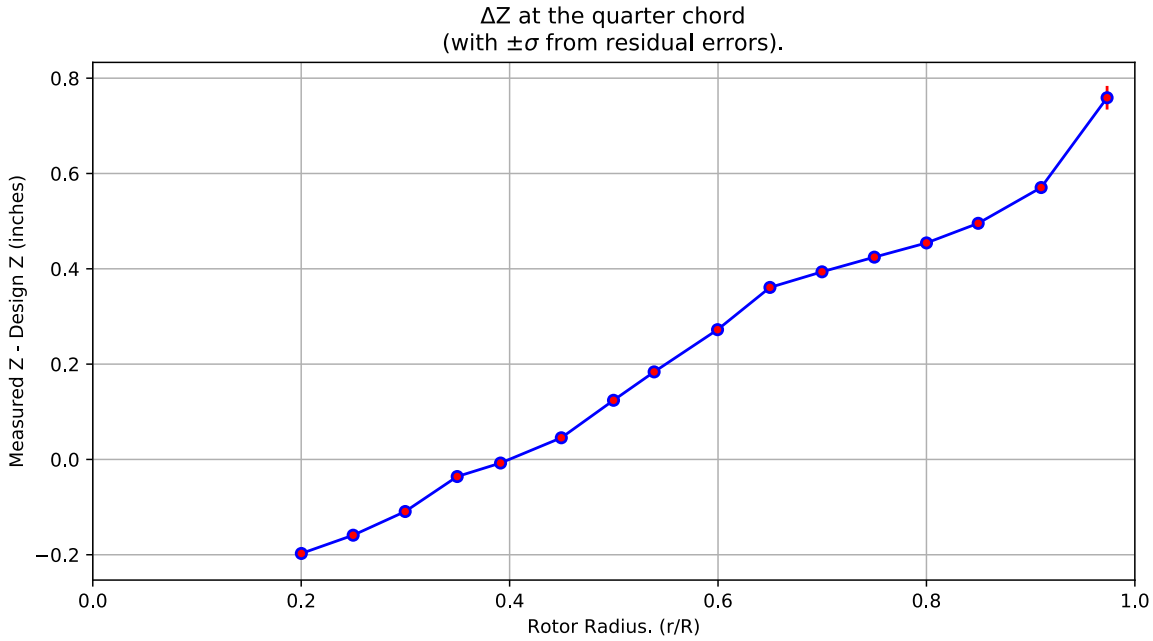

Figure 4-3. ΔZ error at the quarter chord vs rotor radius.

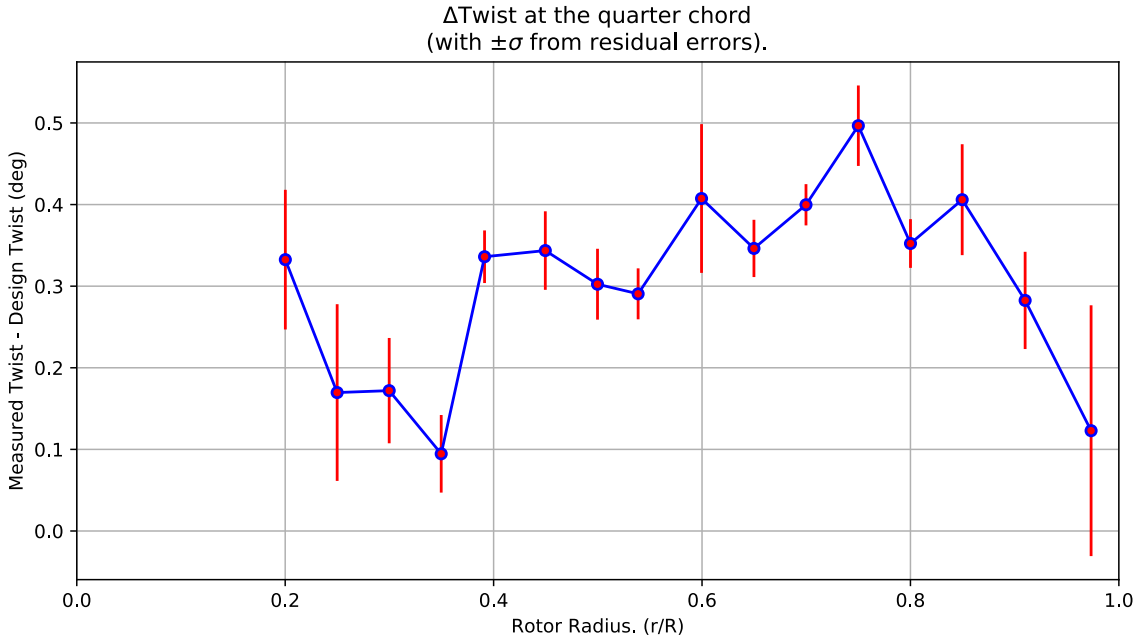

Figure 4-4. ΔTwist error at the quarter chord vs rotor radius.

Table 4-2. Quarter-chord bending and twist statistics.

r	r/R	dZ 1/4-chord	dT	sigma dZ meas	sigma dT meas	sigma dZ res	sigma dT res	n	t_conf
64.447	0.20015	-0.19732	0.3325	6.1099e-10	4.6611e-09	0.0064466	0.085569	4	4.3027
80.458	0.24987	-0.15899	0.16964	6.1328e-10	4.691e-09	0.0081962	0.10827	4	4.3027
96.537	0.2998	-0.10927	0.172	6.1343e-10	4.6585e-09	0.0049227	0.06453	4	4.3027
112.61	0.34972	-0.035876	0.094592	6.1443e-10	4.6677e-09	0.003637	0.04754	4	4.3027
126	0.39131	-0.0075579	0.33607	6.1448e-10	4.6431e-09	0.0024801	0.032237	4	4.3027
144.77	0.44961	0.045446	0.34364	6.1343e-10	4.6463e-09	0.0036795	0.048105	4	4.3027
160.9	0.4997	0.12408	0.3024	6.1438e-10	4.6372e-09	0.0033436	0.043429	4	4.3027
173.45	0.53867	0.18369	0.29061	6.1658e-10	4.6501e-09	0.0024226	0.031224	4	4.3027
193.05	0.59953	0.27229	0.40742	6.1603e-10	4.6475e-09	0.0070572	0.091143	4	4.3027
209.24	0.64982	0.36091	0.34625	6.1543e-10	4.6492e-09	0.002708	0.035087	4	4.3027
225.32	0.69977	0.39366	0.39974	6.1479e-10	4.6446e-09	0.0019467	0.025276	4	4.3027
241.5	0.75	0.42446	0.49663	6.2078e-10	4.6849e-09	0.003871	0.049292	4	4.3027
257.62	0.80005	0.45429	0.35228	6.2298e-10	4.66e-09	0.00238	0.029844	4	4.3027
273.59	0.84965	0.49543	0.40597	6.2002e-10	4.6453e-09	0.0053633	0.067954	4	4.3027
293.04	0.91005	0.57053	0.28254	6.1994e-10	4.6581e-09	0.0046877	0.059578	4	4.3027
313.42	0.97335	0.75896	0.1229	8.6108e-10	4.3467e-09	0.024783	0.15366	4	4.3027

4.4: Section Plots

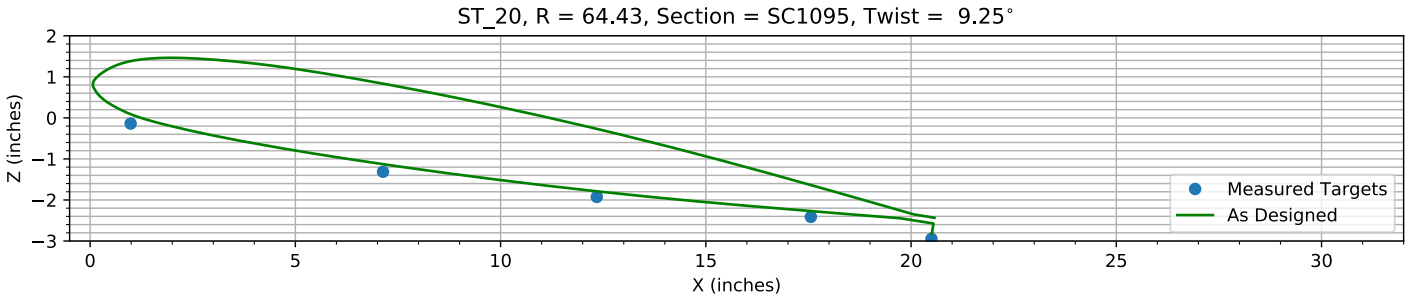

Figure 4-5. Target locations vs section profile at station 20.

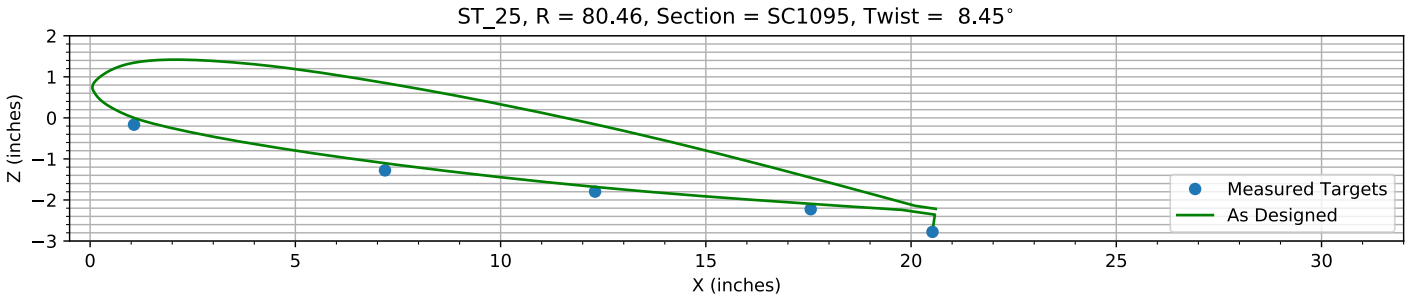

Figure 4-6. Target locations vs section profile at station 25.

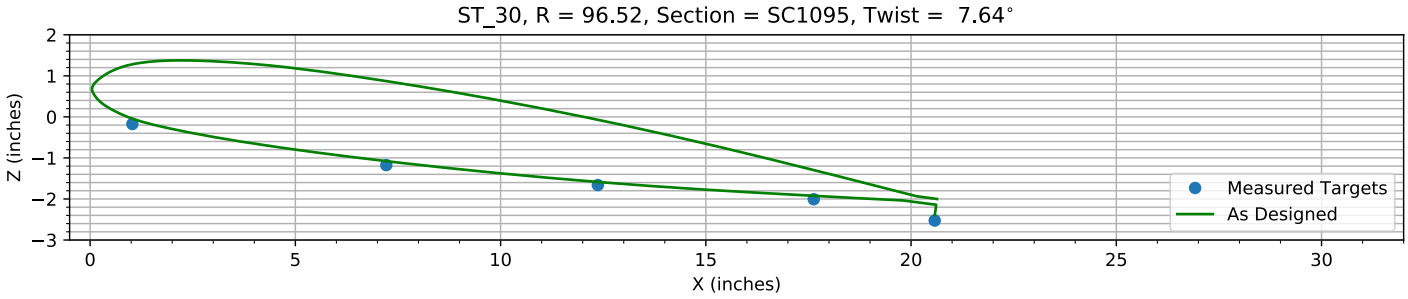

Figure 4-7. Target locations vs section profile at station 30.

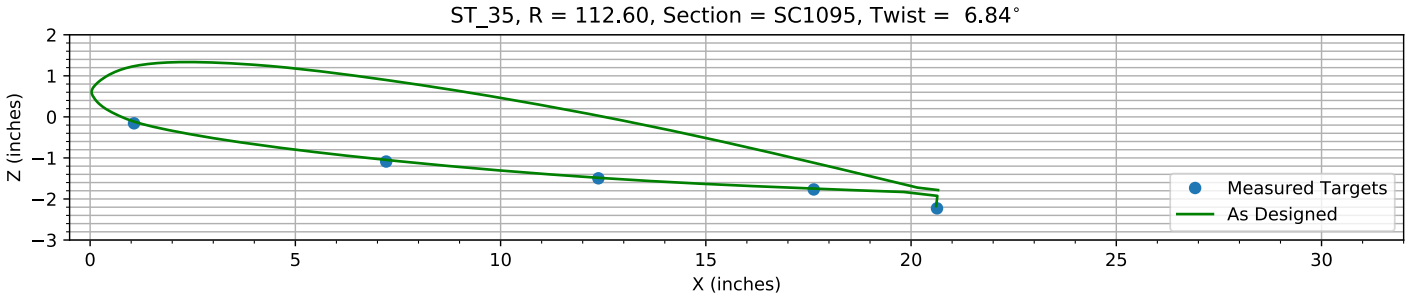

Figure 4-8. Target locations vs section profile at station 35.

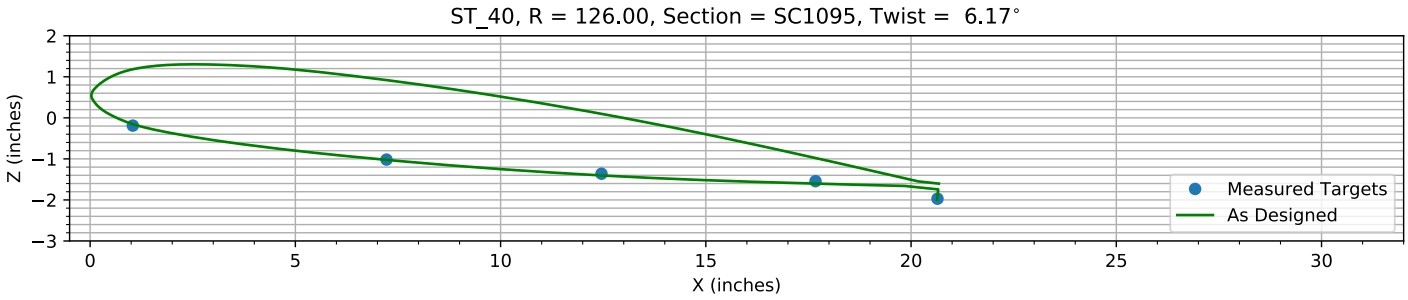

Figure 4-9. Target locations vs section profile at station 40.

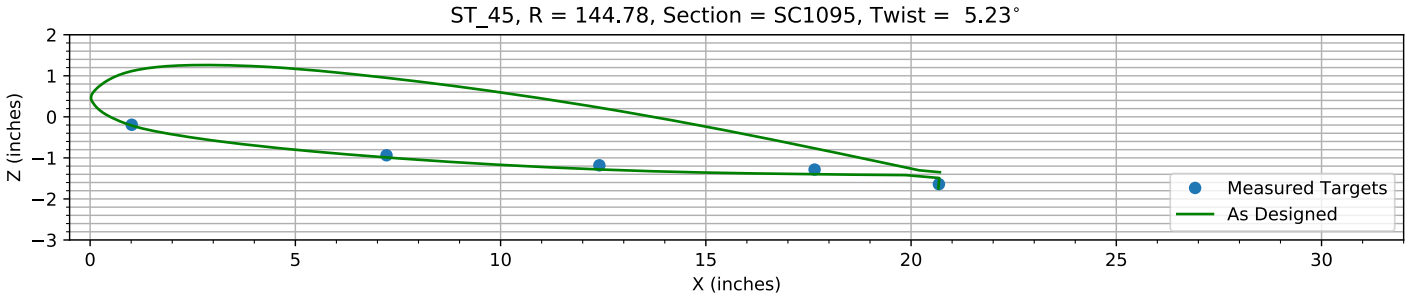

Figure 4-10. Target locations vs section profile at station 45.

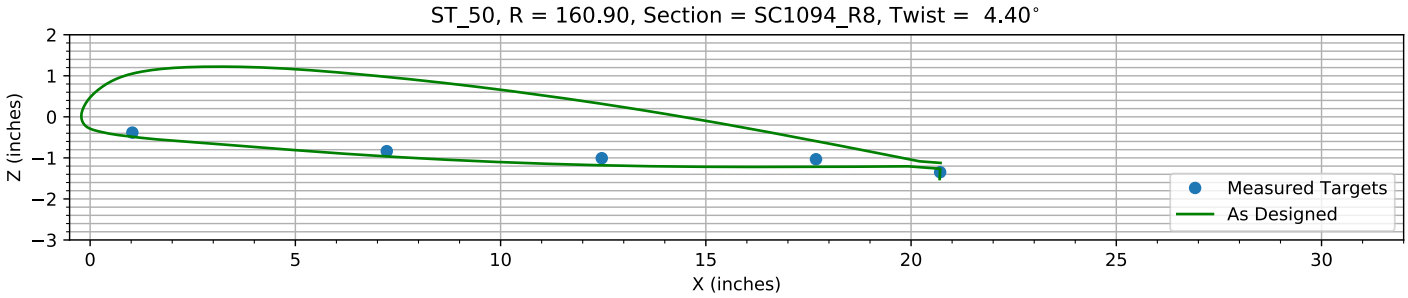

Figure 4-11. Target locations vs section profile at station 50.

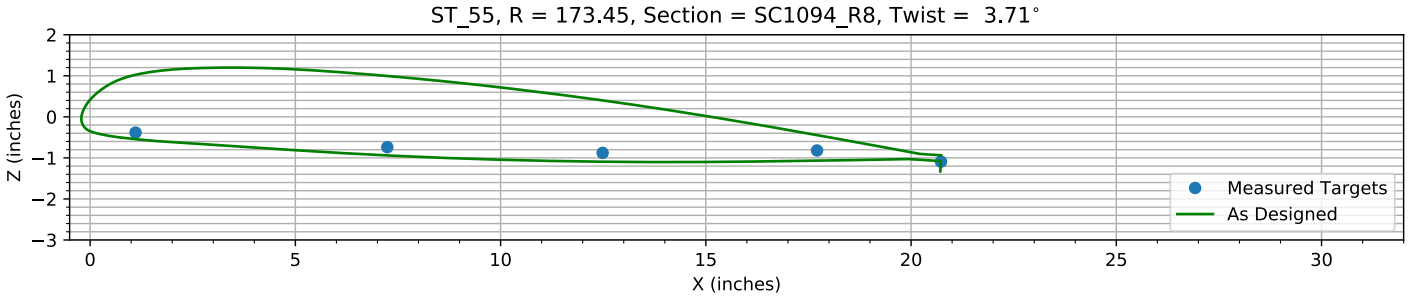

Figure 4-12. Target locations vs section profile at station 55.

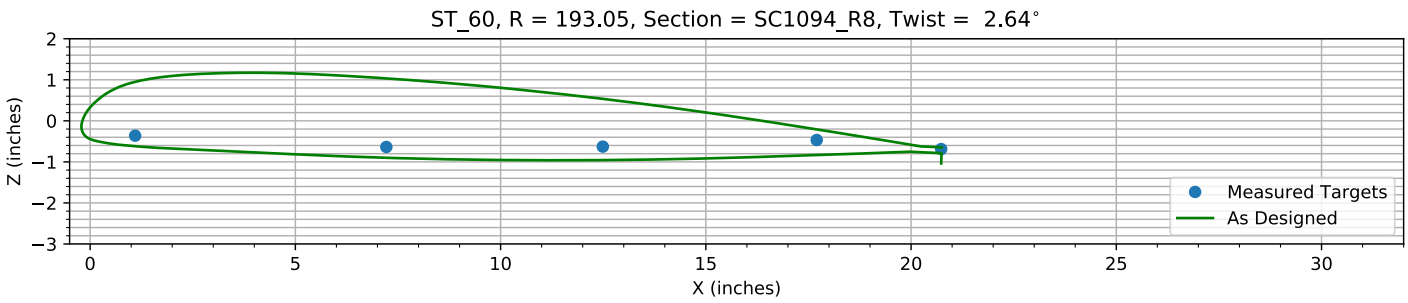

Figure 4-13. Target locations vs section profile at station 60.

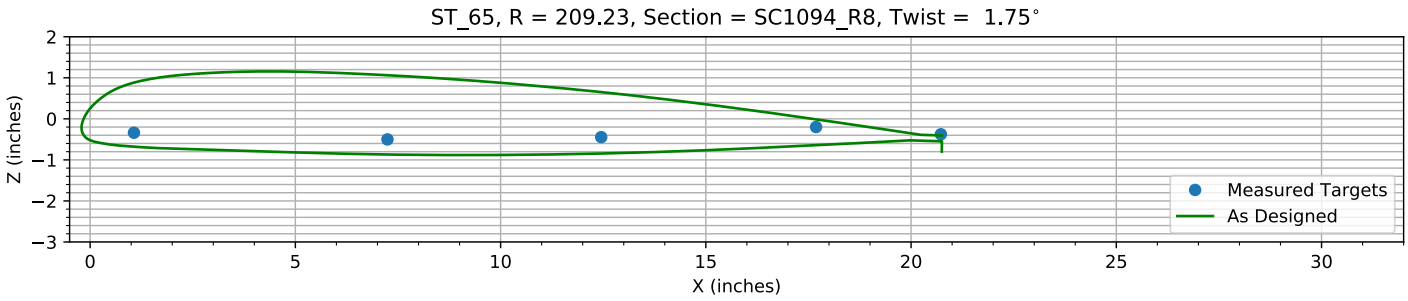

Figure 4-14. Target locations vs section profile at station 65.

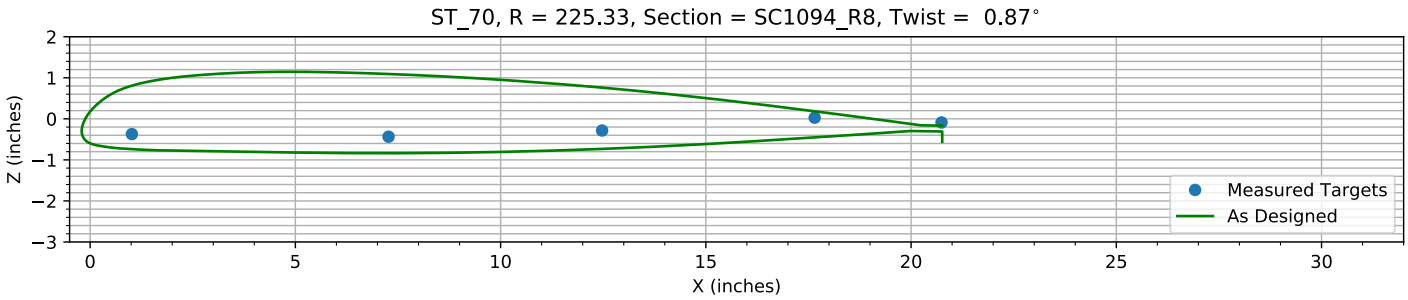

Figure 4-15. Target locations vs section profile at station 70.

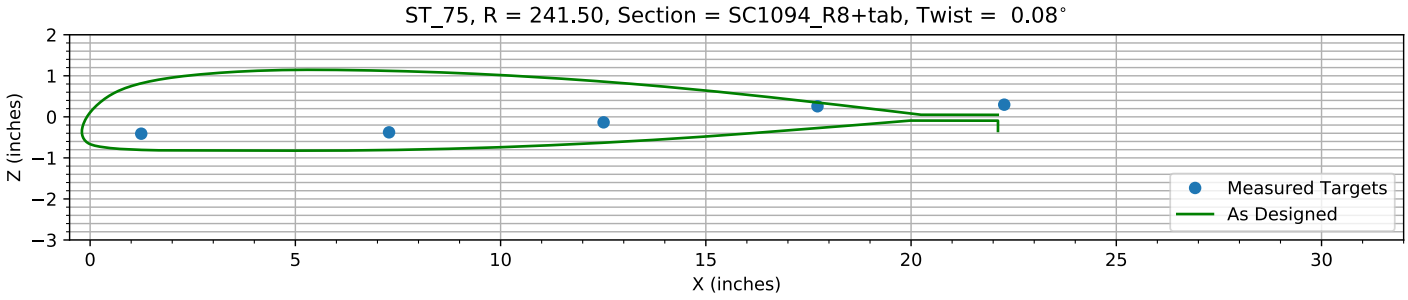

Figure 4-16. Target locations vs section profile at station 75.

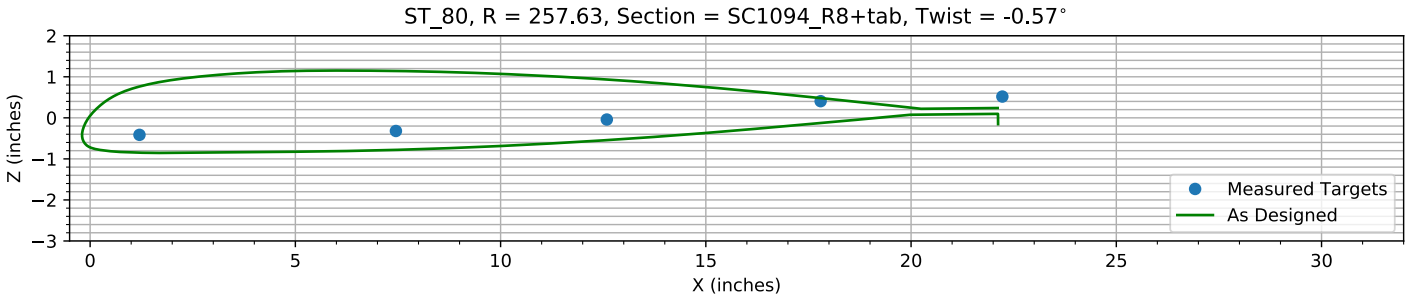

Figure 4-17. Target locations vs section profile at station 80.

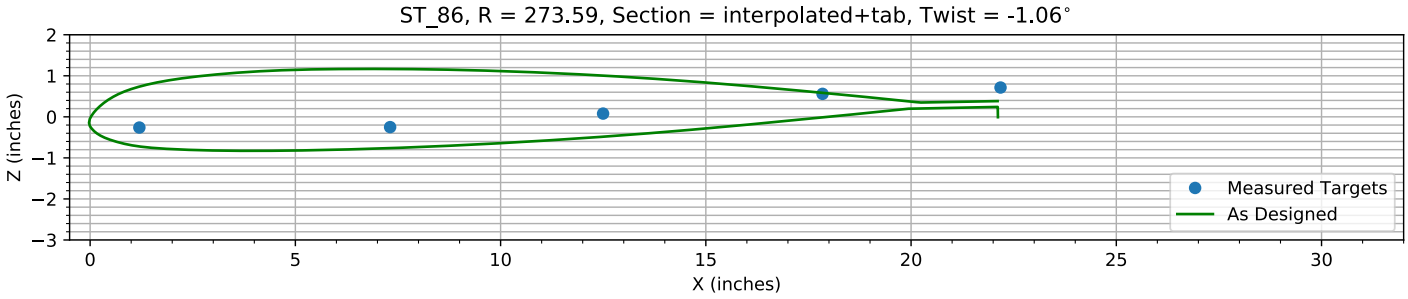

Figure 4-18. Target locations vs section profile at station 86.

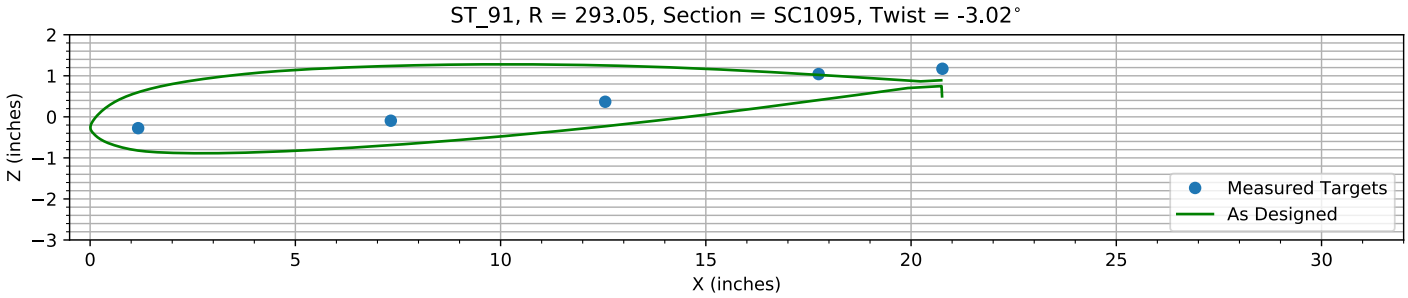

Figure 4-19. Target locations vs section profile at station 91.

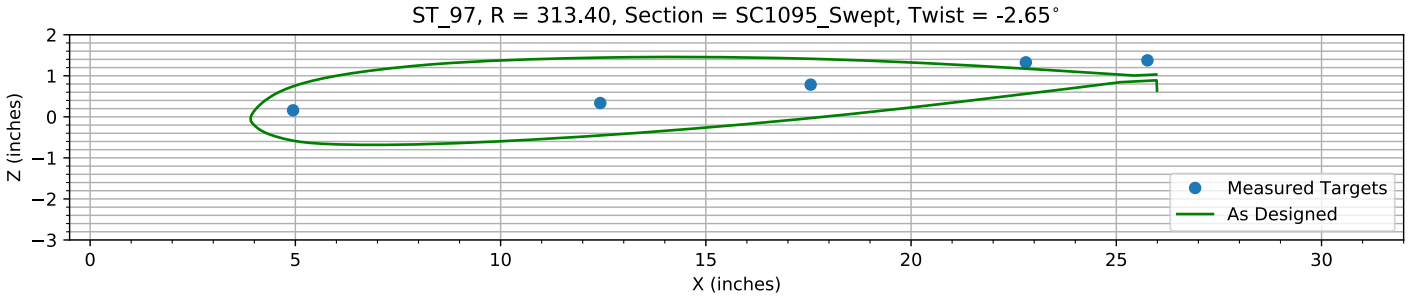

Figure 4-20. Target locations vs section profile at station 97.

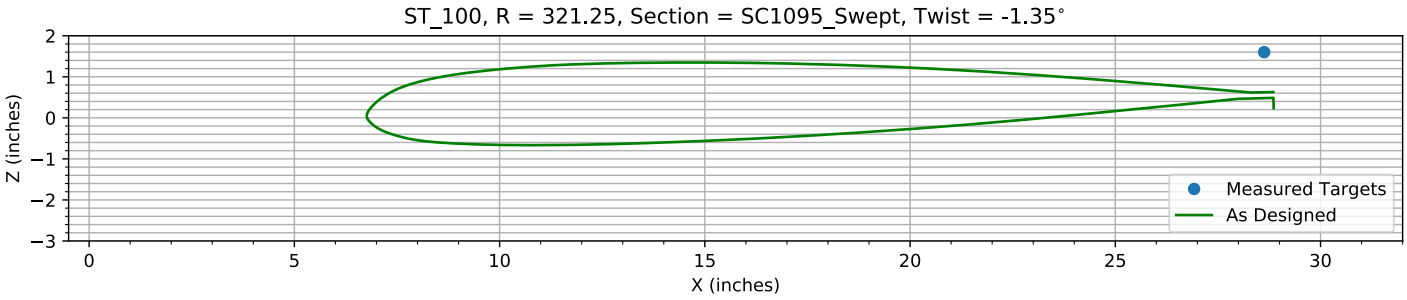

Figure 4-21. Target locations vs section profile at station 100.

Chapter 5: Flap Only Registration (15 rows)

The targets at the 15 spanwise stations nearest the root are used to determing the flap offset.

The estimated flap error is -0.2302°.

5.1: Target Location Errors After Flap Target Registration

Table 5-1. Measured(1) with flap registration vs "as designed"(2) in inches.

Name	X1	Y1	Z1	X2	Y2	Z2	dX	dY	dZ	dR
B1_R20_C05	0.98691	64.473	-0.19357	0.98691	64.473	0.089441	0	0	-0.28301	0.28301
B1_R20_C36	7.1363	64.484	-1.3669	7.1363	64.484	-1.1283	0	0	-0.23865	0.23865
B1_R20_C61	12.343	64.428	-1.9788	12.343	64.428	-1.7893	0	0	-0.18952	0.18952
B1_R20_C86	17.559	64.414	-2.4654	17.559	64.414	-2.2715	0	0	-0.19393	0.19393
B1_R20_C99	20.497	64.363	-3.0017	20.506	64.363	-2.821	-0.0088172	0	-0.18069	0.18091
B1_R25_C05	1.0691	80.478	-0.24497	1.0691	80.478	1.5312e-05	0	0	-0.24498	0.24498
B1_R25_C36	7.1836	80.441	-1.3576	7.1836	80.441	-1.1051	0	0	-0.25253	0.25253
B1_R25_C61	12.302	80.472	-1.8757	12.302	80.472	-1.6821	0	0	-0.1936	0.1936
B1_R25_C86	17.555	80.453	-2.3049	17.555	80.453	-2.0949	0	0	-0.20994	0.20994
B1_R25_C99	20.522	80.476	-2.8567	20.544	80.476	-2.6043	-0.022303	0	-0.25236	0.25335
B1_R30_C05	1.0294	96.542	-0.27833	1.0294	96.542	-0.044051	0	0	-0.23427	0.23427
B1_R30_C36	7.2155	96.57	-1.2794	7.2155	96.57	-1.0788	0	0	-0.20063	0.20063
B1_R30_C61	12.37	96.541	-1.7655	12.37	96.541	-1.5857	0	0	-0.17985	0.17985
B1_R30_C86	17.629	96.506	-2.1108	17.629	96.506	-1.9236	0	0	-0.18714	0.18714
B1_R30_C99	20.576	96.439	-2.6303	20.579	96.439	-2.3898	-0.0031365	0	-0.24047	0.24049
B1_R35_C05	1.0695	112.59	-0.28664	1.0695	112.59	-0.11518	0	0	-0.17146	0.17146
B1_R35_C36	7.2127	112.62	-1.2174	7.2127	112.62	-1.0485	0	0	-0.16893	0.16893
B1_R35_C61	12.382	112.62	-1.6262	12.382	112.62	-1.4842	0	0	-0.14206	0.14206
B1_R35_C86	17.629	112.61	-1.8978	17.629	112.61	-1.7476	0	0	-0.15018	0.15018
B1_R35_C99	20.632	112.59	-2.3578	20.611	112.59	-2.1726	0.020716	0	-0.18514	0.18629
B1_R40_C05	1.04	126.01	-0.33972	1.04	126.01	-0.15361	0	0	-0.18611	0.18611
B1_R40_C36	7.2203	126.02	-1.168	7.2203	126.02	-1.0244	0	0	-0.14361	0.14361
B1_R40_C61	12.458	126.01	-1.5121	12.458	126.01	-1.4034	0	0	-0.10875	0.10875
B1_R40_C86	17.672	125.99	-1.6935	17.672	125.99	-1.6031	0	0	-0.090416	0.090416
B1_R40_C99	20.643	126	-2.1211	20.635	126	-1.9923	0.0080577	0	-0.12882	0.12907
B1_R45_C05	1.0135	144.77	-0.37295	1.0135	144.77	-0.21233	0	0	-0.16062	0.16062
B1_R45_C36	7.2202	144.8	-1.1166	7.2202	144.8	-0.98984	0	0	-0.12672	0.12672
B1_R45_C61	12.406	144.77	-1.3607	12.406	144.77	-1.2816	0	0	-0.079023	0.079023
B1_R45_C86	17.65	144.77	-1.4648	17.65	144.77	-1.3982	0	0	-0.066512	0.066512
B1_R45_C99	20.678	144.8	-1.8201	20.666	144.8	-1.7392	0.012018	0	-0.080944	0.081831
B1_R50_C05	1.0287	160.94	-0.58918	1.0287	160.94	-0.48671	0	0	-0.10248	0.10248
B1_R50_C36	7.2269	160.92	-1.0414	7.2269	160.92	-0.96466	0	0	-0.076734	0.076734
B1_R50_C61	12.465	160.9	-1.2127	12.465	160.9	-1.1805	0	0	-0.032212	0.032212
B1_R50_C86	17.684	160.88	-1.2381	17.684	160.88	-1.218	0	0	-0.020081	0.020081
B1_R50_C99	20.708	160.87	-1.5532	20.695	160.87	-1.5147	0.012888	0	-0.038455	0.040558
B1_R55_C05	1.1061	173.5	-0.60862	1.1061	173.5	-0.54408	0	0	-0.064534	0.064534
B1_R55_C36	7.2397	173.48	-0.96412	7.2397	173.48	-0.9402	0	0	-0.023915	0.023915
B1_R55_C61	12.486	173.43	-1.1033	12.486	173.43	-1.0934	0	0	-0.0099697	0.0099697
B1_R55_C86	17.71	173.42	-1.0443	17.71	173.42	-1.068	0	0	0.023705	0.023705
B1_R55_C99	20.729	173.44	-1.3164	20.712	173.44	-1.3284	0.016401	0	0.011982	0.020311
B1_R60_C05	1.0965	193.02	-0.6173	1.0965	193.02	-0.61837	0	0	0.0010767	0.0010767
B1_R60_C36	7.2164	193.06	-0.89265	7.2164	193.06	-0.90051	0	0	0.0078573	0.0078573

Name	X1	Y1	Z1	X2	Y2	Z2	dX	dY	dZ	dR
B1_R60_C61	12.491	193.07	-0.88399	12.491	193.07	-0.95637	0	0	0.072384	0.072384
B1_R60_C86	17.701	193.06	-0.72236	17.701	193.06	-0.83384	0	0	0.11148	0.11148
B1_R60_C99	20.734	193.04	-0.94343	20.734	193.04	-1.0375	-0.00061862	0	0.094124	0.094126
B1_R65_C05	1.0675	209.29	-0.61924	1.0675	209.29	-0.67914	0	0	0.059902	0.059902
B1_R65_C36	7.2431	209.27	-0.78203	7.2431	209.27	-0.86922	0	0	0.087184	0.087184
B1_R65_C61	12.451	209.22	-0.72672	12.451	209.22	-0.84496	0	0	0.11824	0.11824
B1_R65_C86	17.686	209.21	-0.48097	17.686	209.21	-0.6421	0	0	0.16113	0.16113
B1_R65_C99	20.726	209.18	-0.65659	20.748	209.18	-0.79788	-0.022676	0	0.14129	0.1431
B1_R70_C05	1.0168	225.38	-0.6782	1.0168	225.38	-0.73894	0	0	0.060741	0.060741
B1_R70_C36	7.2704	225.34	-0.74165	7.2704	225.34	-0.83758	0	0	0.095935	0.095935
B1_R70_C61	12.473	225.31	-0.59058	12.473	225.31	-0.73294	0	0	0.14236	0.14236
B1_R70_C86	17.651	225.29	-0.27916	17.651	225.29	-0.45298	0	0	0.17382	0.17382
B1_R70_C99	20.742	225.35	-0.3948	20.759	225.35	-0.55748	-0.016896	0	0.16268	0.16356
B1_R75_C05	1.2452	241.53	-0.74211	1.2452	241.53	-0.8055	0	0	0.063386	0.063386
B1_R75_C36	7.2823	241.51	-0.70908	7.2823	241.51	-0.8086	0	0	0.099522	0.099522
B1_R75_C61	12.509	241.5	-0.46574	12.509	241.5	-0.63015	0	0	0.16441	0.16441
B1_R75_C86	17.72	241.48	-0.074314	17.72	241.48	-0.27448	0	0	0.20017	0.20017
B1_R80_C05	1.2021	257.63	-0.77132	1.2021	257.63	-0.84831	0	0	0.07699	0.07699
B1_R80_C36	7.4495	257.63	-0.67721	7.4495	257.63	-0.78087	0	0	0.10366	0.10366
B1_R80_C61	12.588	257.63	-0.39804	12.588	257.63	-0.54322	0	0	0.14519	0.14519
B1_R80_C86	17.797	257.59	0.049236	17.797	257.59	-0.12705	0	0	0.17629	0.17629
B1_R86_C05	1.1993	273.59	-0.6429	1.1993	273.59	-0.72194	0	0	0.079044	0.079044
B1_R86_C36	7.3084	273.58	-0.63232	7.3084	273.58	-0.76251	0	0	0.13019	0.13019
B1_R86_C61	12.497	273.61	-0.30281	12.497	273.61	-0.48406	0	0	0.18125	0.18125
B1_R86_C86	17.843	273.59	0.178	17.843	273.59	-0.013666	0	0	0.19166	0.19166
B1_R91_C05	1.1698	292.99	-0.68816	1.1698	292.99	-0.82117	0	0	0.13301	0.13301
B1_R91_C36	7.3253	293.06	-0.50696	7.3253	293.06	-0.68935	0	0	0.18239	0.18239
B1_R91_C61	12.549	293.07	-0.04494	12.549	293.07	-0.22904	0	0	0.1841	0.1841
B1_R91_C86	17.748	293.05	0.62959	17.748	293.05	0.40775	0	0	0.22184	0.22184
B1_R91_C99	20.763	293.12	0.75897	20.755	293.12	0.50125	0.0082112	0	0.25772	0.25785
B1_R97_C05	4.9441	313.41	-0.28572	4.9441	313.41	-0.58012	0	0	0.29441	0.29441
B1_R97_C36	12.428	313.45	-0.10794	12.428	313.45	-0.45571	0	0	0.34777	0.34777
B1_R97_C61	17.554	313.44	0.33986	17.554	313.44	-0.032657	0	0	0.37252	0.37252
B1_R97_C86	22.797	313.4	0.88296	22.797	313.4	0.55926	0	0	0.32371	0.32371
B1_R97_C99	25.758	313.32	0.93202	25.963	313.32	0.6427	-0.20492	0	0.28932	0.35454
HUB_LE	2.2651	30.005	-3.5001	2.19	30	-3.5	0.075139	0.004511	-8.1877e-05	0.075274
HUB_TE	8.2617	29.995	-3.4999	8.19	30	-3.5	0.071732	-0.0047375	8.0967e-05	0.071888
RMS Errors:							0.02646	0.00073599	0.16721	0.16929

5.2: Flap Registration Plots (15 rows)

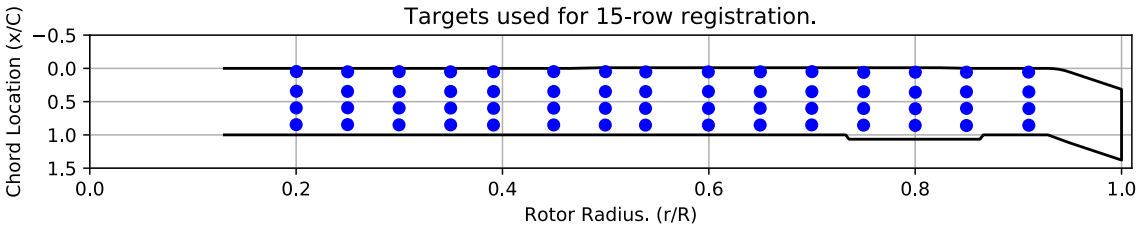

Figure 5-1. Targets used for 15 row root registration.

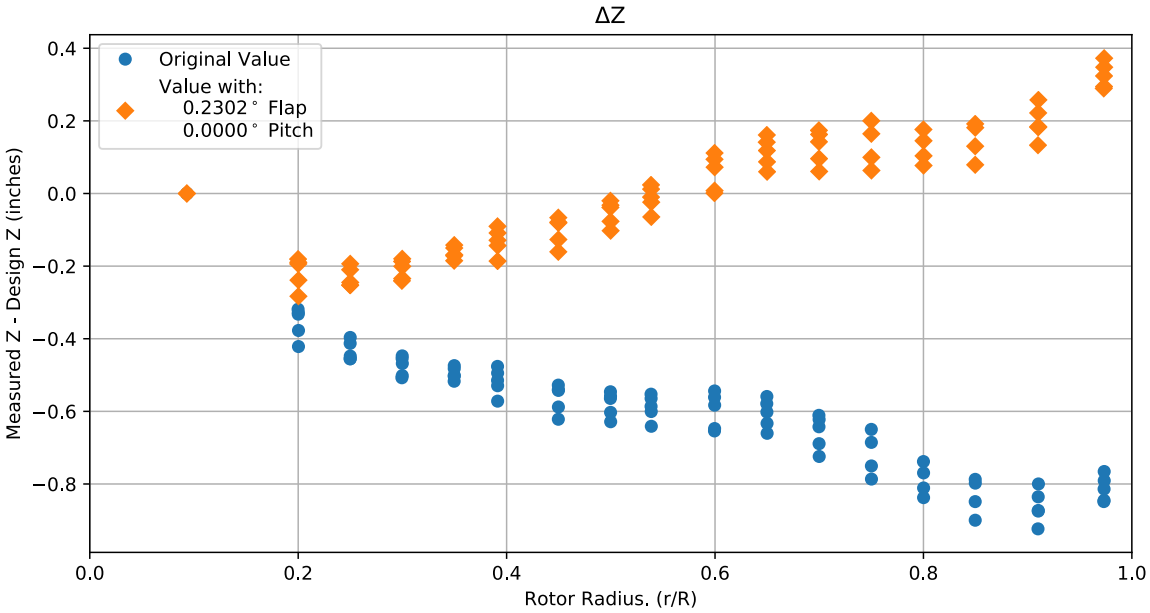

Figure 5-2. Flap target registration, ΔZ error vs rotor radius.

Note: the “as designed” geometry used for the swept tip may have some inaccuracies.

5.3: Estimated Bending and Twist at the Quarter Chord

The error bars shown represent the residual errors for fitting the measure target locations to the "as designed" geometry. These errors are generally much larger than those due to the VSTARS measurement errors. Therefore, the most likely source of these errors is the placement of the trailing-edge targets, differences between the "as designed" and "as built" geometries, and blade deformation during measurement. In the future, iterative adjustment of the "as designed" twist angle may be implemented to see if it reduces the fit error in delta twist. Note: The "as designed" geometry used for the swept tip may have some inaccuracies.

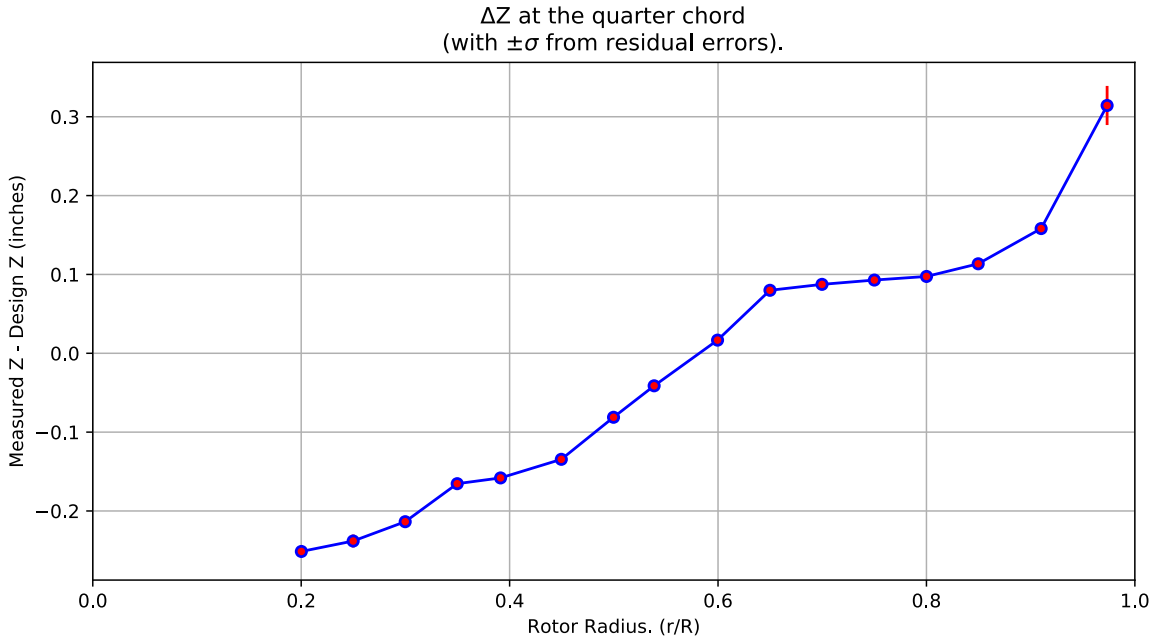

Figure 5-3. ΔZ error at the quarter chord vs rotor radius.

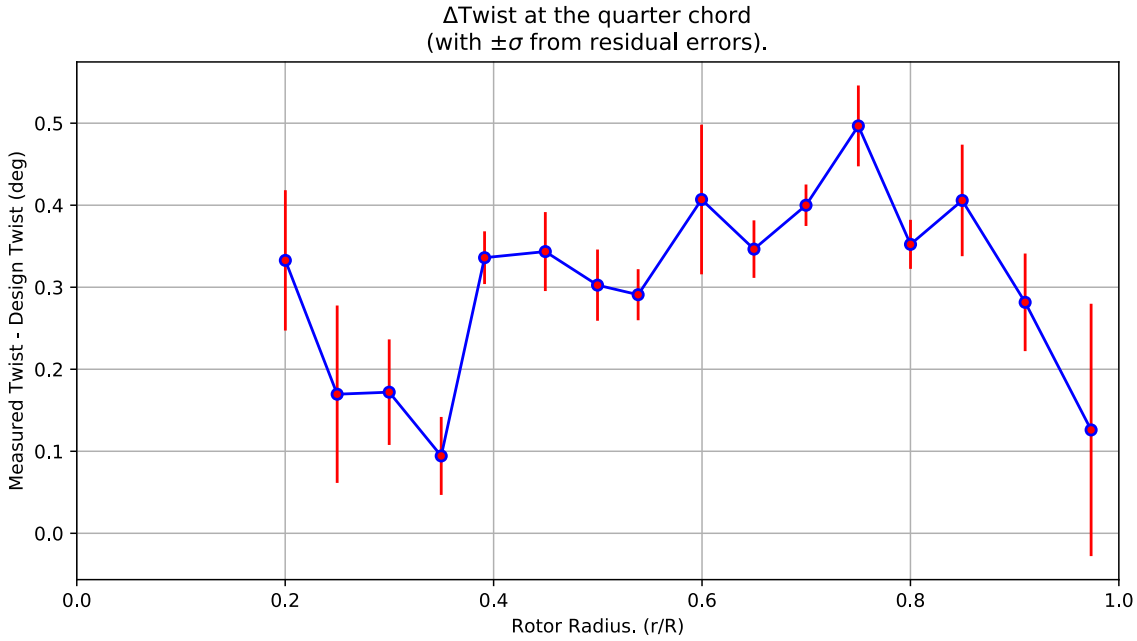

Figure 5-4. ΔTwist error at the quarter chord vs rotor radius.

Table 5-2. Quarter-chord bending and twist statistics.

r	r/R	dZ 1/4-chord	dT	sigma dZ meas	sigma dT meas	sigma dZ res	sigma dT res	n	t_conf
64.45	0.20016	-0.25134	0.33274	6.1099e-10	4.6611e-09	0.0064454	0.085553	4	4.3027
80.461	0.24988	-0.2381	0.16957	6.1328e-10	4.691e-09	0.0081864	0.10814	4	4.3027
96.54	0.29981	-0.2136	0.17205	6.1343e-10	4.6585e-09	0.0049091	0.064351	4	4.3027
112.61	0.34973	-0.16537	0.094326	6.1443e-10	4.6677e-09	0.0036368	0.047537	4	4.3027
126.01	0.39133	-0.15807	0.33601	6.1448e-10	4.6431e-09	0.0024732	0.032148	4	4.3027
144.78	0.44962	-0.13449	0.34348	6.1343e-10	4.6463e-09	0.003682	0.048138	4	4.3027
160.91	0.49972	-0.081168	0.30254	6.1438e-10	4.6372e-09	0.0033437	0.04343	4	4.3027
173.46	0.53869	-0.041246	0.29088	6.1658e-10	4.6501e-09	0.0024152	0.031129	4	4.3027
193.05	0.59954	0.016691	0.40696	6.1603e-10	4.6475e-09	0.0070635	0.091224	4	4.3027
209.25	0.64983	0.079876	0.34646	6.1543e-10	4.6492e-09	0.0027062	0.035064	4	4.3027
225.33	0.69978	0.08741	0.39997	6.1479e-10	4.6446e-09	0.0019472	0.025282	4	4.3027
241.5	0.75001	0.092868	0.49668	6.2078e-10	4.6849e-09	0.0038711	0.049293	4	4.3027
257.62	0.80006	0.097439	0.35228	6.2298e-10	4.66e-09	0.0023835	0.029887	4	4.3027
273.59	0.84967	0.11351	0.40583	6.2002e-10	4.6453e-09	0.0053656	0.067983	4	4.3027
293.04	0.91007	0.15818	0.2816	6.1994e-10	4.6581e-09	0.0046804	0.059486	4	4.3027
313.42	0.97337	0.31427	0.12603	8.6108e-10	4.3467e-09	0.024809	0.15382	4	4.3027

5.4: Section Plots

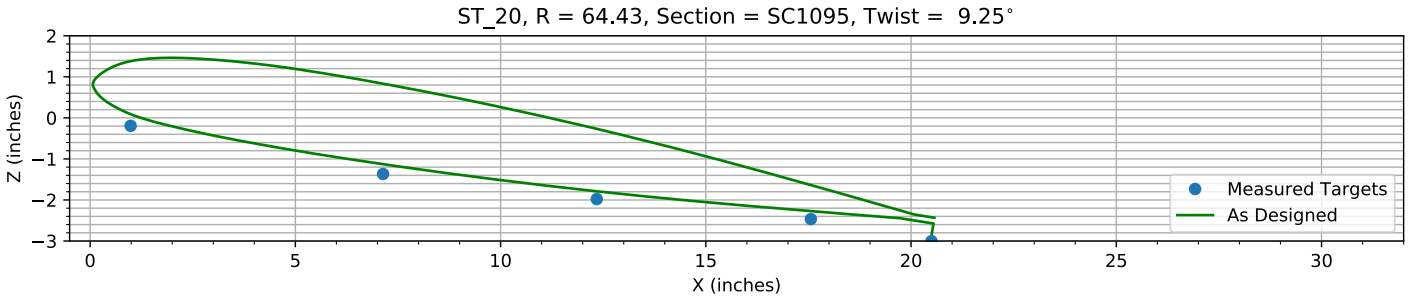

Figure 5-5. Target locations vs section profile at station 20.

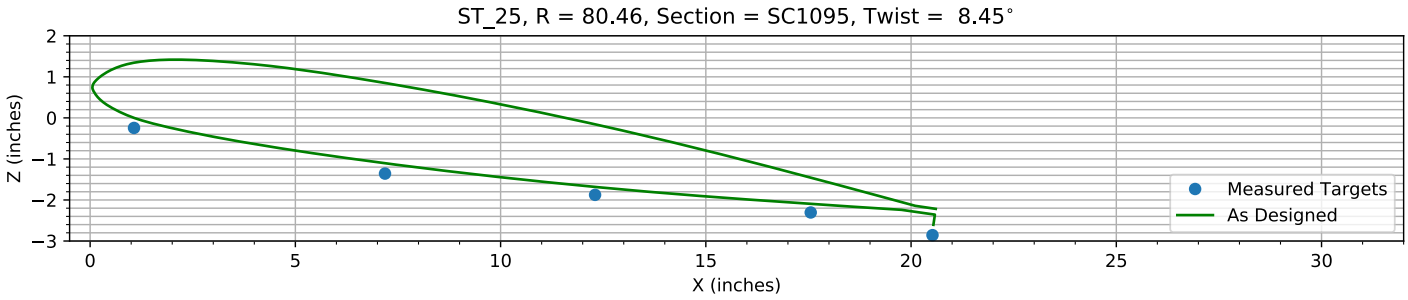

Figure 5-6. Target locations vs section profile at station 25.

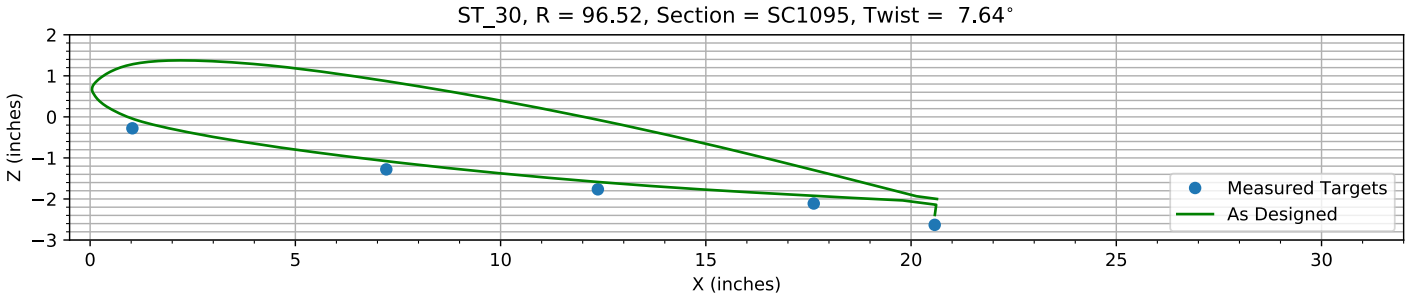

Figure 5-7. Target locations vs section profile at station 30.

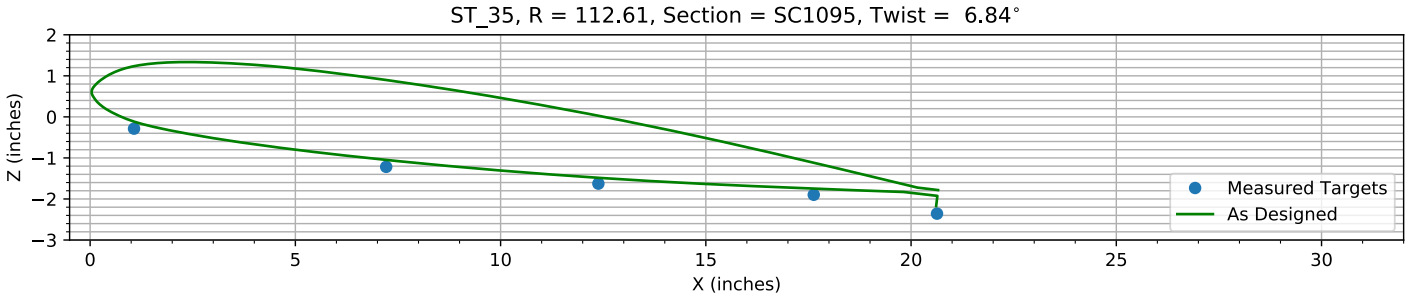

Figure 5-8. Target locations vs section profile at station 35.

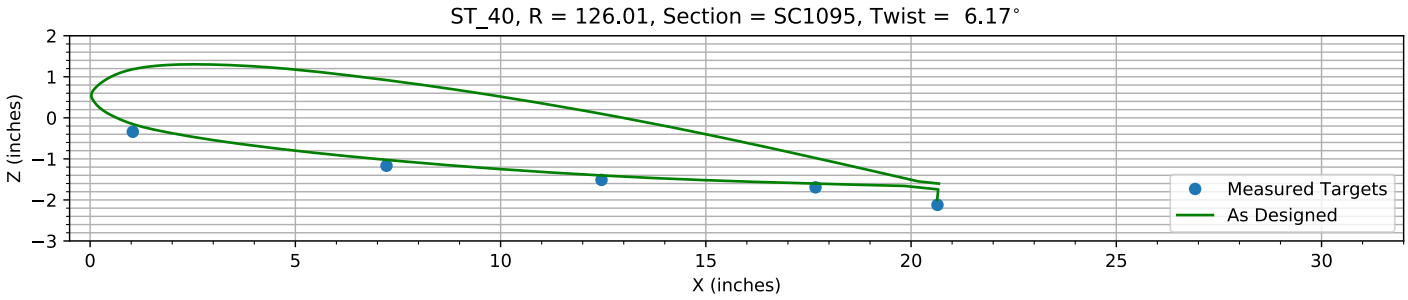

Figure 5-9. Target locations vs section profile at station 40.

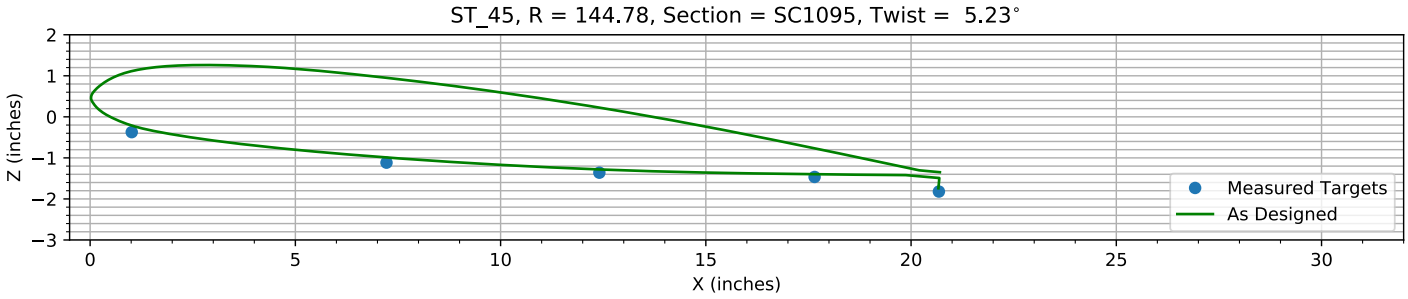

Figure 5-10. Target locations vs section profile at station 45.

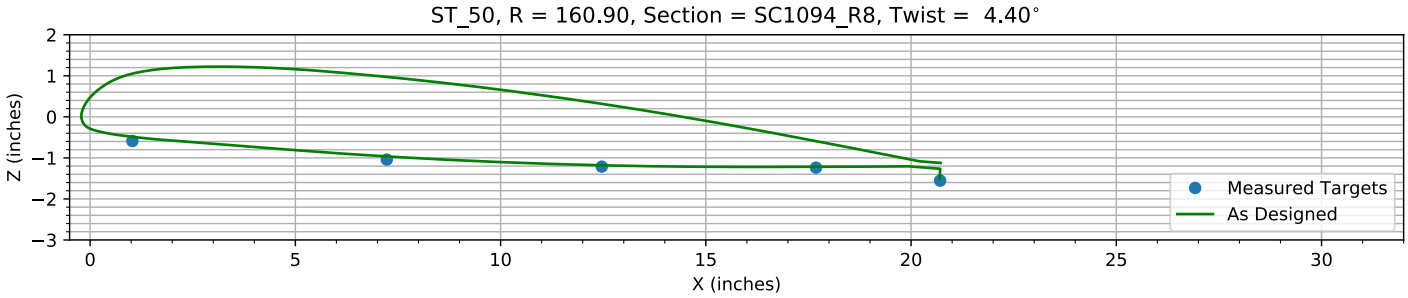

Figure 5-11. Target locations vs section profile at station 50.

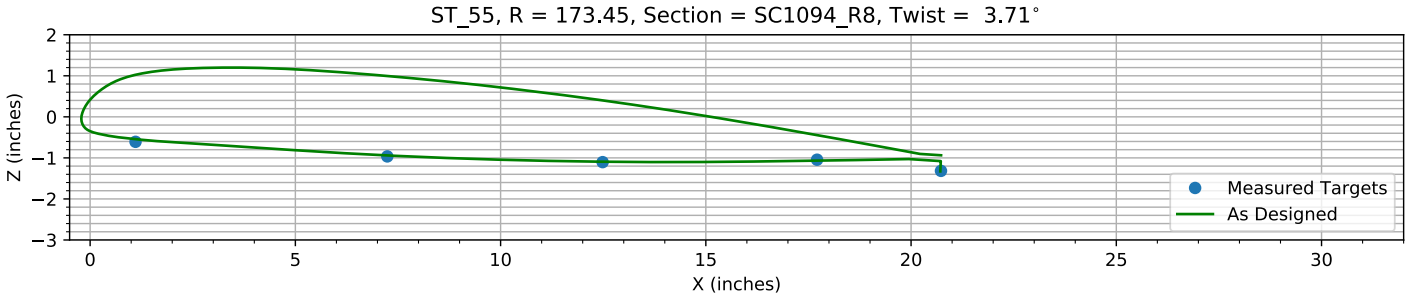

Figure 5-12. Target locations vs section profile at station 55.

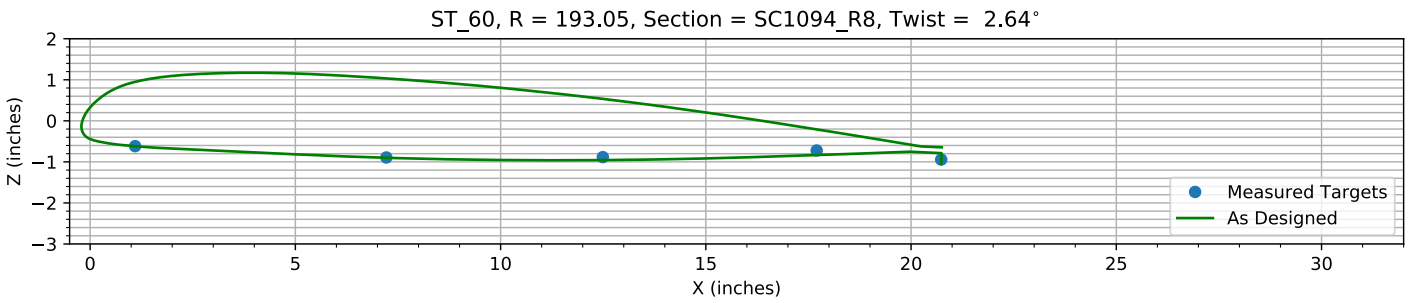

Figure 5-13. Target locations vs section profile at station 60.

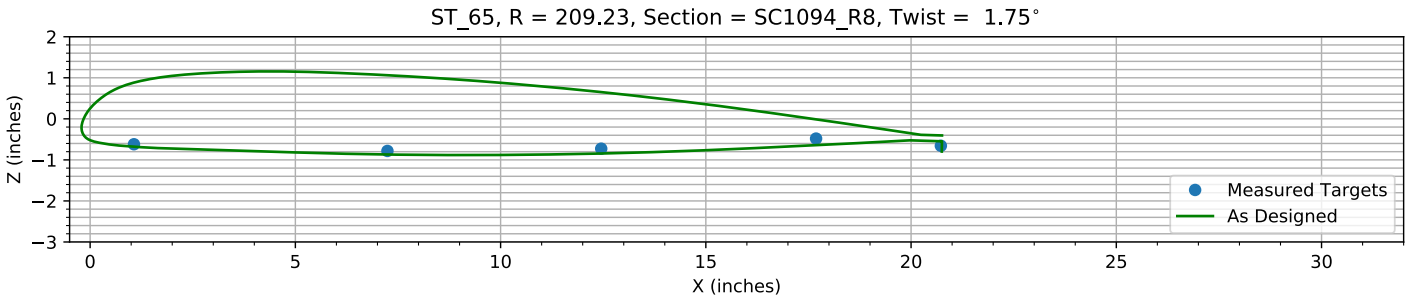

Figure 5-14. Target locations vs section profile at station 65.

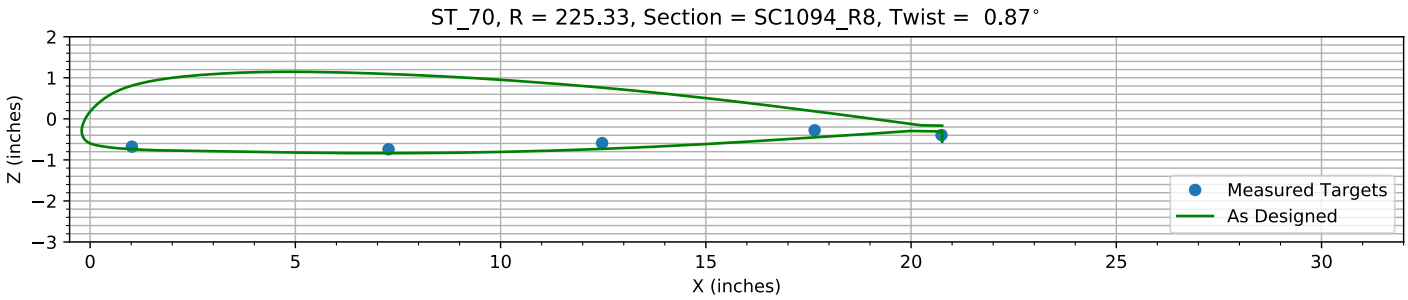

Figure 5-15. Target locations vs section profile at station 70.

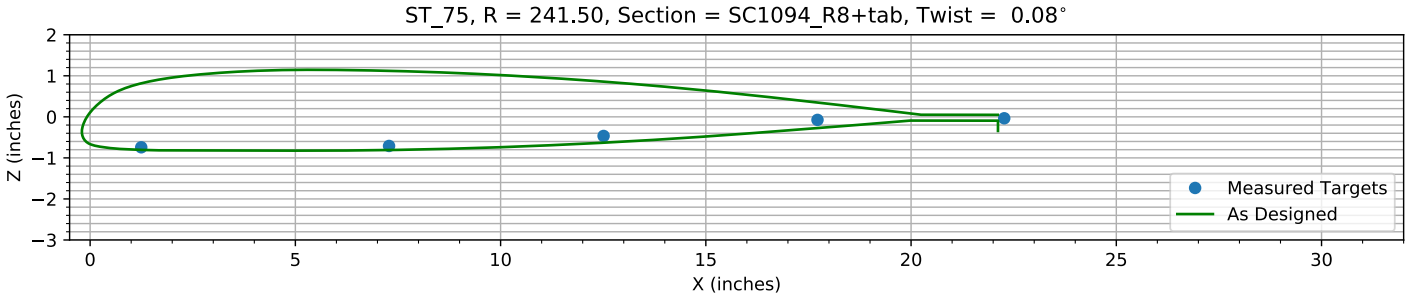

Figure 5-16. Target locations vs section profile at station 75.

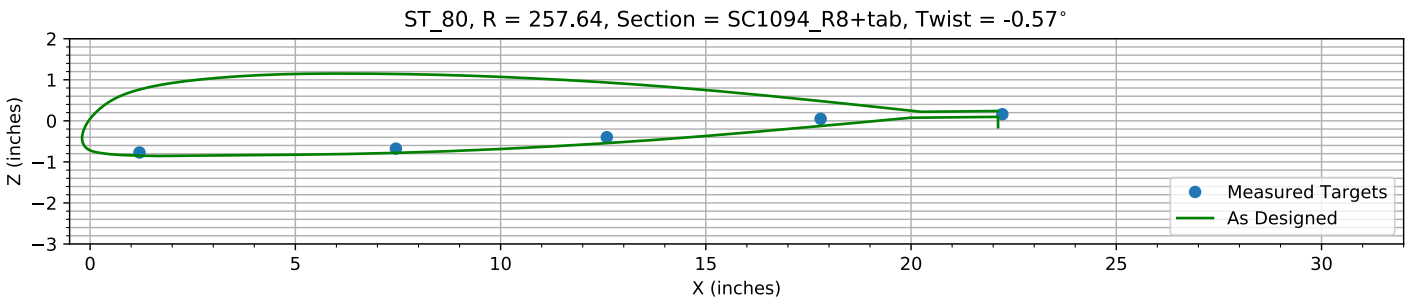

Figure 5-17. Target locations vs section profile at station 80.

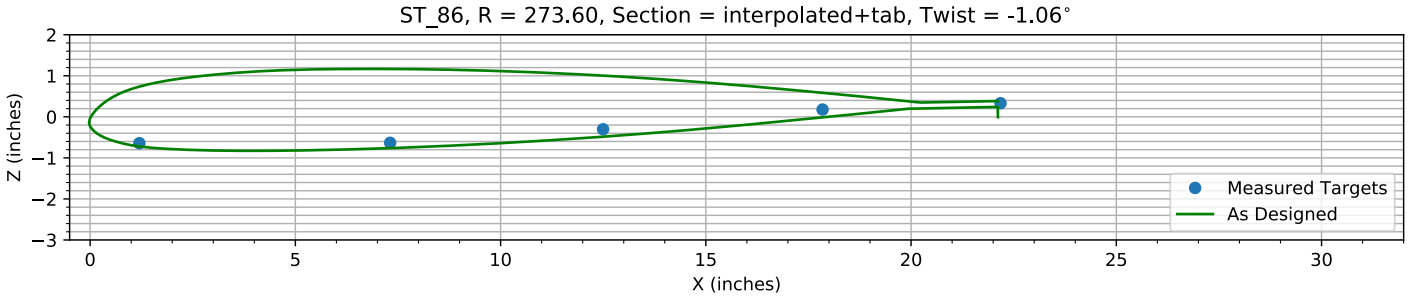

Figure 5-18. Target locations vs section profile at station 86.

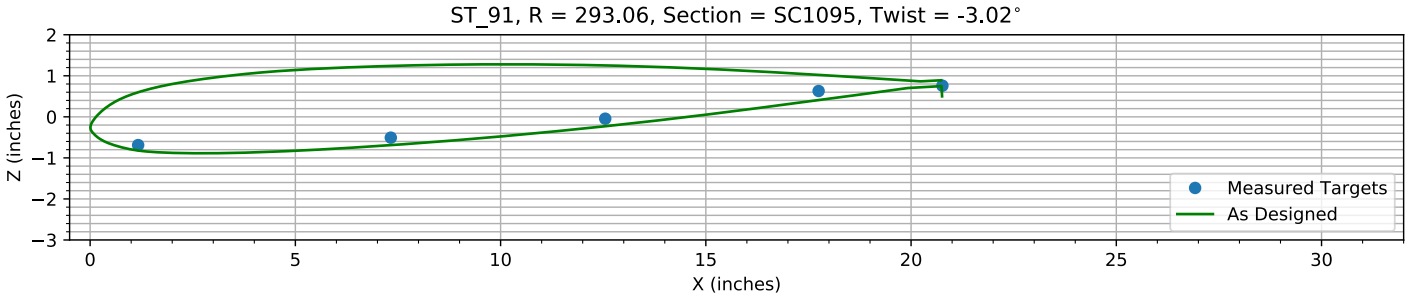

Figure 5-19. Target locations vs section profile at station 91.

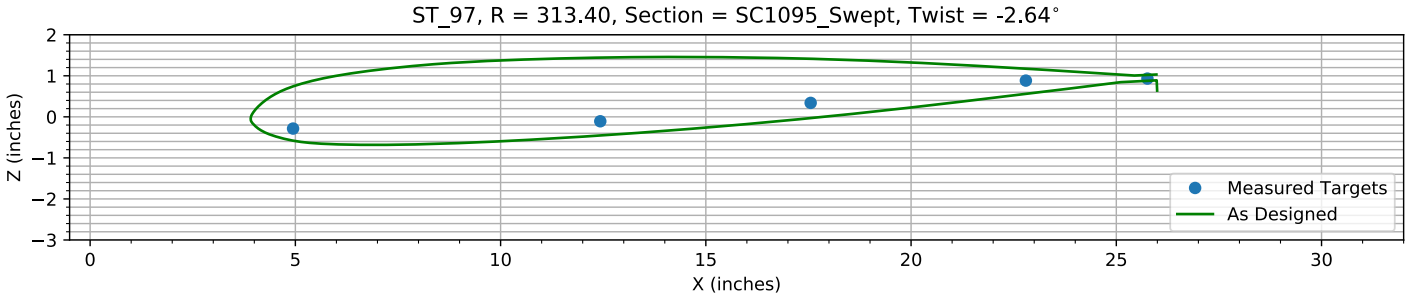

Figure 5-20. Target locations vs section profile at station 97.

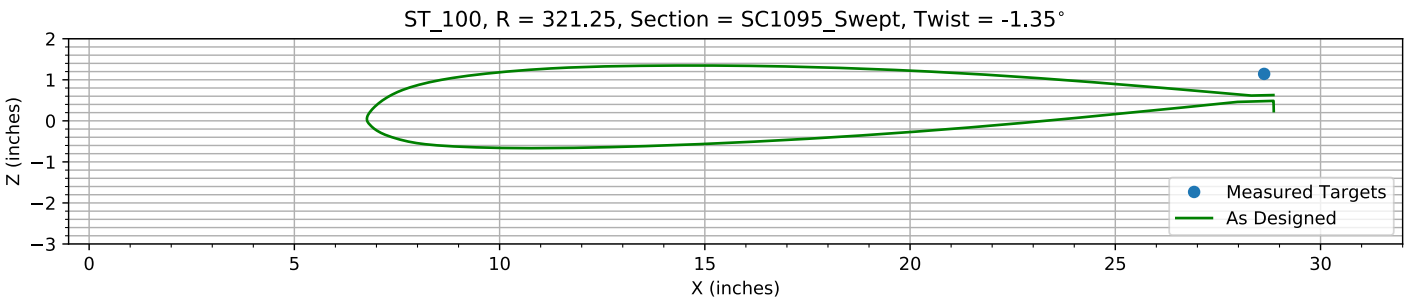

Figure 5-21. Target locations vs section profile at station 100.

Chapter 6: Flap and ΔZ Registration (6 rows)

The targets at the 6 spanwise stations nearest the root are used to determing the Z and flap offset.

The estimated Z error, -0.32754 inches, is within an allowed range of ±2.000 inches.

The estimated flap error is -0.11428°.

6.1: Target Location Errors After Flap Target Registration

Table 6-1. Measured(1) with flap registration vs as designed(2) in inches.

Name	X1	Y1	Z1	X2	Y2	Z2	dX	dY	dZ	dR
B1_R20_C05	0.98691	64.479	0.06422	0.98691	64.479	0.089419	0	0	-0.025199	0.025199
B1_R20_C36	7.1363	64.488	-1.1092	7.1363	64.488	-1.1283	0	0	0.01911	0.01911
B1_R20_C61	12.343	64.43	-1.7209	12.343	64.43	-1.7893	0	0	0.068351	0.068351
B1_R20_C86	17.559	64.416	-2.2075	17.559	64.416	-2.2715	0	0	0.06397	0.06397
B1_R20_C99	20.497	64.364	-2.7437	20.506	64.364	-2.821	-0.0088179	0	0.077321	0.077823
B1_R25_C05	1.0691	80.484	-0.019558	1.0691	80.484	-5.7209e-06	0	0	-0.019552	0.019552
B1_R25_C36	7.1836	80.445	-1.1321	7.1836	80.445	-1.1051	0	0	-0.027053	0.027053
B1_R25_C61	12.302	80.475	-1.6503	12.302	80.475	-1.6821	0	0	0.031806	0.031806
B1_R25_C86	17.555	80.455	-2.0794	17.555	80.455	-2.0949	0	0	0.015501	0.015501
B1_R25_C99	20.522	80.476	-2.6313	20.544	80.476	-2.6043	-0.022304	0	-0.02695	0.034982
B1_R30_C05	1.0294	96.548	-0.085416	1.0294	96.548	-0.044072	0	0	-0.041344	0.041344
B1_R30_C36	7.2155	96.574	-1.0866	7.2155	96.574	-1.0788	0	0	-0.00778	0.00778
B1_R30_C61	12.37	96.544	-1.5726	12.37	96.544	-1.5857	0	0	0.013047	0.013047
B1_R30_C86	17.629	96.508	-1.9178	17.629	96.508	-1.9236	0	0	0.0058257	0.0058257
B1_R30_C99	20.576	96.44	-2.4371	20.579	96.44	-2.3898	-0.0031385	0	-0.047362	0.047466
B1_R35_C05	1.0695	112.6	-0.1262	1.0695	112.6	-0.1152	0	0	-0.011001	0.011001
B1_R35_C36	7.2127	112.63	-1.057	7.2127	112.63	-1.0485	0	0	-0.0085647	0.0085647
B1_R35_C61	12.382	112.62	-1.4659	12.382	112.62	-1.4842	0	0	0.018302	0.018302
B1_R35_C86	17.629	112.61	-1.7374	17.629	112.61	-1.7476	0	0	0.010198	0.010198
B1_R35_C99	20.632	112.59	-2.1973	20.611	112.59	-2.1726	0.020713	0	-0.024713	0.032246
B1_R40_C05	1.04	126.02	-0.20644	1.04	126.02	-0.15363	0	0	-0.052808	0.052808
B1_R40_C36	7.2203	126.02	-1.0347	7.2203	126.02	-1.0244	0	0	-0.010338	0.010338
B1_R40_C61	12.458	126.01	-1.3788	12.458	126.01	-1.4034	0	0	0.024523	0.024523
B1_R40_C86	17.672	125.99	-1.5602	17.672	125.99	-1.6031	0	0	0.042892	0.042892
B1_R40_C99	20.643	126	-1.9878	20.635	126	-1.9923	0.0080543	0	0.0044772	0.0092151
B1_R45_C05	1.0135	144.78	-0.27762	1.0135	144.78	-0.21235	0	0	-0.065264	0.065264
B1_R45_C36	7.2202	144.8	-1.0213	7.2202	144.8	-0.98983	0	0	-0.031441	0.031441
B1_R45_C61	12.406	144.78	-1.2653	12.406	144.78	-1.2816	0	0	0.01629	0.01629
B1_R45_C86	17.65	144.78	-1.3694	17.65	144.78	-1.3982	0	0	0.028789	0.028789
B1_R45_C99	20.678	144.8	-1.7249	20.666	144.8	-1.7392	0.012014	0	0.014299	0.018676
B1_R50_C05	1.0287	160.95	-0.52656	1.0287	160.95	-0.48672	0	0	-0.039839	0.039839
B1_R50_C36	7.2269	160.92	-0.97872	7.2269	160.92	-0.96465	0	0	-0.01407	0.01407
B1_R50_C61	12.465	160.9	-1.15	12.465	160.9	-1.1804	0	0	0.030475	0.030475
B1_R50_C86	17.684	160.88	-1.1753	17.684	160.88	-1.2179	0	0	0.042628	0.042628
B1_R50_C99	20.708	160.87	-1.4904	20.695	160.87	-1.5147	0.012883	0	0.024271	0.027478
B1_R55_C05	1.1061	173.51	-0.57141	1.1061	173.51	-0.5441	0	0	-0.027309	0.027309
B1_R55_C36	7.2397	173.48	-0.92686	7.2397	173.48	-0.94019	0	0	0.013332	0.013332
B1_R55_C61	12.486	173.43	-1.066	12.486	173.43	-1.0933	0	0	0.027368	0.027368

Name	X1	Y1	Z1	X2	Y2	Z2	dX	dY	dZ	dR
B1_R55_C86	17.71	173.42	-1.0069	17.71	173.42	-1.0679	0	0	0.061032	0.061032
B1_R55_C99	20.729	173.44	-1.279	20.712	173.44	-1.3283	0.016396	0	0.049264	0.051921
B1_R60_C05	1.0965	193.03	-0.61958	1.0965	193.03	-0.61839	0	0	-0.001187	0.001187
B1_R60_C36	7.2164	193.06	-0.89501	7.2164	193.06	-0.9005	0	0	0.0054934	0.0054934
B1_R60_C61	12.491	193.08	-0.88638	12.491	193.08	-0.95634	0	0	0.069965	0.069965
B1_R60_C86	17.701	193.06	-0.72471	17.701	193.06	-0.83378	0	0	0.10908	0.10908
B1_R60_C99	20.734	193.04	-0.94574	20.734	193.04	-1.0375	-0.00062277	0	0.091743	0.091745
B1_R65_C05	1.0675	209.29	-0.65443	1.0675	209.29	-0.67916	0	0	0.024727	0.024727
B1_R65_C36	7.2431	209.27	-0.81718	7.2431	209.27	-0.86921	0	0	0.052029	0.052029
B1_R65_C61	12.451	209.23	-0.76177	12.451	209.23	-0.84493	0	0	0.083157	0.083157
B1_R65_C86	17.686	209.21	-0.516	17.686	209.21	-0.64204	0	0	0.12604	0.12604
B1_R65_C99	20.726	209.18	-0.69156	20.748	209.18	-0.79781	-0.022679	0	0.10625	0.10865
B1_R70_C05	1.0168	225.38	-0.74594	1.0168	225.38	-0.73896	0	0	-0.0069844	0.0069844
B1_R70_C36	7.2704	225.35	-0.80932	7.2704	225.35	-0.83758	0	0	0.028258	0.028258
B1_R70_C61	12.473	225.31	-0.65818	12.473	225.31	-0.7329	0	0	0.074723	0.074723
B1_R70_C86	17.651	225.29	-0.34672	17.651	225.29	-0.45291	0	0	0.10619	0.10619
B1_R70_C99	20.742	225.36	-0.46249	20.759	225.36	-0.55741	-0.016899	0	0.094913	0.096405
B1_R75_C05	1.2452	241.53	-0.84253	1.2452	241.53	-0.80551	0	0	-0.037018	0.037018
B1_R75_C36	7.2823	241.52	-0.80946	7.2823	241.52	-0.80859	0	0	-0.00086909	0.00086909
B1_R75_C61	12.509	241.5	-0.56609	12.509	241.5	-0.63012	0	0	0.064031	0.064031
B1_R75_C86	17.72	241.48	-0.17463	17.72	241.48	-0.27442	0	0	0.099796	0.099796
B1_R80_C05	1.2021	257.63	-0.90431	1.2021	257.63	-0.84832	0	0	-0.055992	0.055992
B1_R80_C36	7.4495	257.64	-0.81021	7.4495	257.64	-0.78086	0	0	-0.029343	0.029343
B1_R80_C61	12.588	257.63	-0.53102	12.588	257.63	-0.5432	0	0	0.01218	0.01218
B1_R80_C86	17.797	257.6	-0.083683	17.797	257.6	-0.127	0	0	0.04332	0.04332
B1_R86_C05	1.1993	273.59	-0.80818	1.1993	273.59	-0.72187	0	0	-0.086307	0.086307
B1_R86_C36	7.3084	273.59	-0.79759	7.3084	273.59	-0.76249	0	0	-0.035097	0.035097
B1_R86_C61	12.497	273.62	-0.46814	12.497	273.62	-0.48401	0	0	0.015873	0.015873
B1_R86_C86	17.843	273.59	0.01272	17.843	273.59	-0.013561	0	0	0.026281	0.026281
B1_R91_C05	1.1698	292.99	-0.89269	1.1698	292.99	-0.8212	0	0	-0.071485	0.071485
B1_R91_C36	7.3253	293.07	-0.71164	7.3253	293.07	-0.68933	0	0	-0.022308	0.022308
B1_R91_C61	12.549	293.07	-0.24963	12.549	293.07	-0.22896	0	0	-0.020663	0.020663
B1_R91_C86	17.748	293.05	0.42494	17.748	293.05	0.40791	0	0	0.017029	0.017029
B1_R91_C99	20.763	293.13	0.55418	20.755	293.13	0.50146	0.0082179	0	0.052721	0.053357
B1_R97_C05	4.9441	313.41	-0.53156	4.9441	313.41	-0.57969	0	0	0.048132	0.048132
B1_R97_C36	12.428	313.46	-0.35387	12.428	313.46	-0.45585	0	0	0.10198	0.10198
B1_R97_C61	17.554	313.45	0.093962	17.554	313.45	-0.032989	0	0	0.12695	0.12695
B1_R97_C86	22.797	313.41	0.63714	22.797	313.41	0.5587	0	0	0.078438	0.078438
B1_R97_C99	25.758	313.32	0.68637	25.966	313.32	0.64242	-0.20775	0	0.043951	0.21234
HUB_LE	2.2651	30.004	-3.1726	2.19	30	-3.5	0.075139	0.0038575	0.32745	0.33598
HUB_TE	8.2617	29.995	-3.1724	8.19	30	-3.5	0.071732	-0.0053906	0.32763	0.33543
RMS Errors:							0.026737	0.00074579	0.073792	0.07849

6.2: Flap Registration Plots (6 rows)

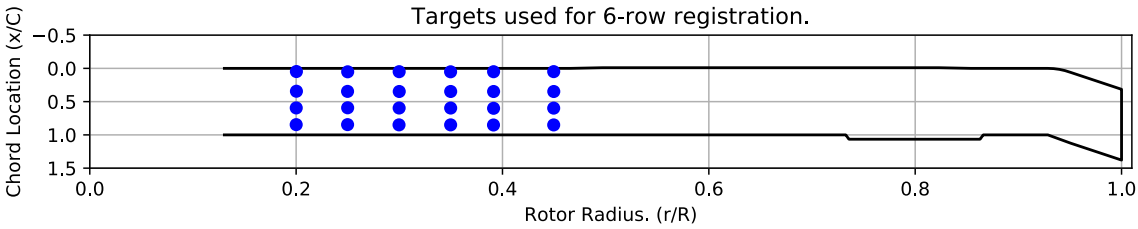

Figure 6-1. Targets used for 6 row root registration.

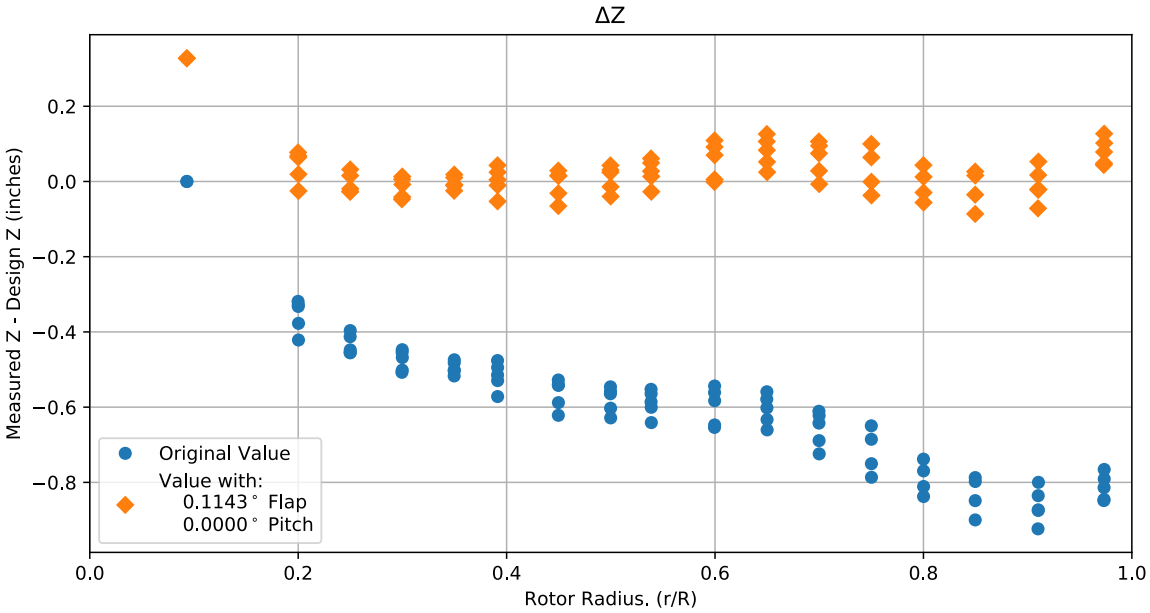

Figure 6-2. Flap target registration, ΔZ error vs rotor radius.

Note: the “as designed” geometry used for the swept tip may have some inaccuracies.

6.3: Estimated Bending and Twist at the Quarter Chord

The error bars shown represent the residual errors for fitting the measure target locations to the "as designed" geometry. These errors are generally much larger than those due to the VSTARS measurement errors. Therefore, the most likely source of these errors is the placement of the trailing-edge targets, differences between the "as designed" and "as built" geometries, and blade deformation during measurement. In the future, iterative adjustment of the "as designed" twist angle may be implemented to see if it reduces the fit error in delta twist. Note: The "as designed" geometry used for the swept tip may have some inaccuracies.

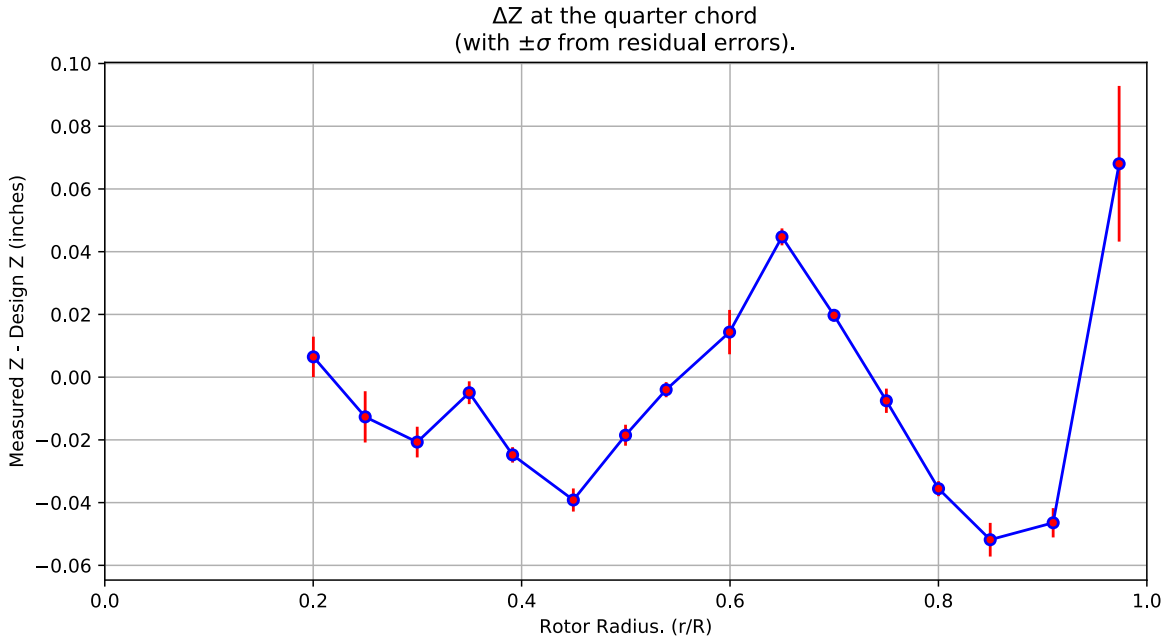

Figure 6-3. ΔZ error at the quarter chord vs rotor radius.

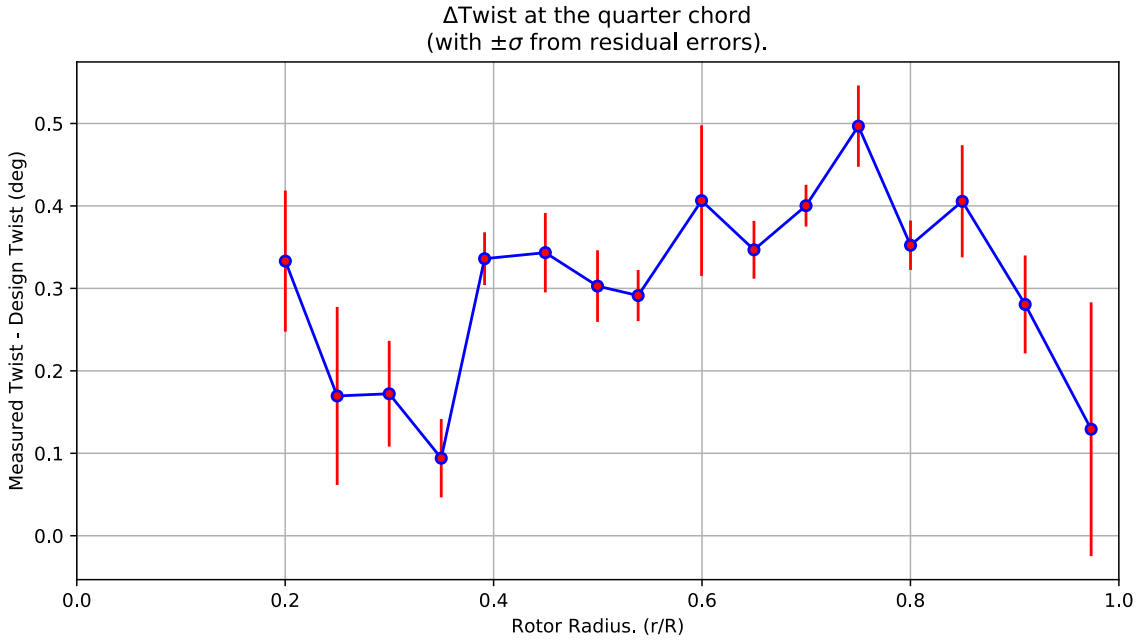

Figure 6-4. ΔTwist error at the quarter chord vs rotor radius.

Table 6-2. Quarter-chord bending and twist statistics.

r	r/R	dZ 1/4-chord	dT	sigma dZ meas	sigma dT meas	sigma dZ res	sigma dT res	n	t_conf
64.453	0.20017	0.0064632	0.33311	6.1099e-10	4.6611e-09	0.006444	0.085535	4	4.3027
80.465	0.24989	-0.01266	0.16956	6.1328e-10	4.691e-09	0.0081737	0.10797	4	4.3027
96.544	0.29982	-0.020699	0.1722	6.1343e-10	4.6585e-09	0.0048918	0.064124	4	4.3027
112.62	0.34974	-0.0049615	0.094051	6.1443e-10	4.6677e-09	0.0036365	0.047533	4	4.3027
126.01	0.39134	-0.024782	0.33601	6.1448e-10	4.6431e-09	0.0024646	0.032036	4	4.3027
144.78	0.44963	-0.039168	0.34335	6.1343e-10	4.6463e-09	0.0036854	0.048183	4	4.3027
160.91	0.49973	-0.018513	0.30279	6.1438e-10	4.6372e-09	0.0033438	0.043433	4	4.3027
173.46	0.5387	-0.0039942	0.29129	6.1658e-10	4.6501e-09	0.0024056	0.031006	4	4.3027
193.06	0.59956	0.014367	0.40644	6.1603e-10	4.6475e-09	0.0070714	0.091327	4	4.3027
209.25	0.64985	0.044724	0.3468	6.1543e-10	4.6492e-09	0.0027036	0.035031	4	4.3027
225.33	0.6998	0.019716	0.40032	6.1479e-10	4.6446e-09	0.0019477	0.025289	4	4.3027
241.51	0.75003	-0.0075277	0.4968	6.2078e-10	4.6849e-09	0.0038711	0.049293	4	4.3027
257.63	0.80008	-0.035555	0.35232	6.2298e-10	4.66e-09	0.0023879	0.029943	4	4.3027
273.6	0.84968	-0.051827	0.40565	6.2002e-10	4.6453e-09	0.0053664	0.067994	4	4.3027
293.05	0.91009	-0.046429	0.28053	6.1994e-10	4.6581e-09	0.0046712	0.059369	4	4.3027
313.43	0.97339	0.068035	0.12922	8.6108e-10	4.3467e-09	0.024819	0.15389	4	4.3027

6.4: Section Plots

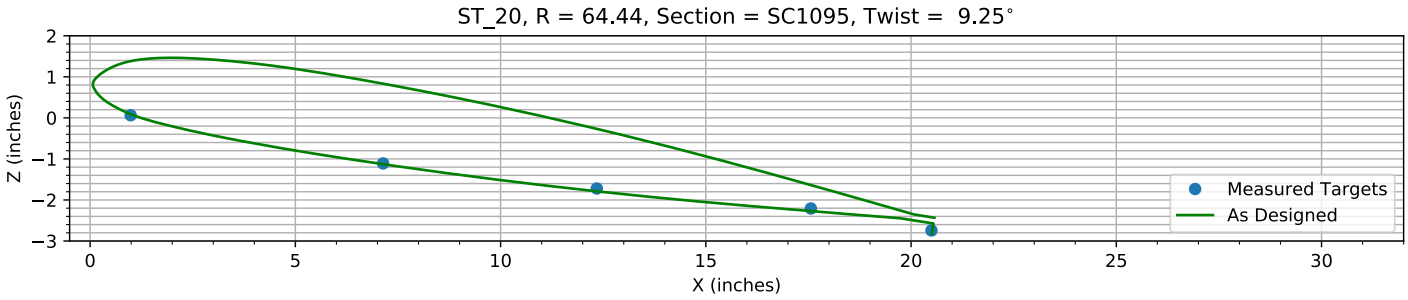

Figure 6-5. Target locations vs section profile at station 20.

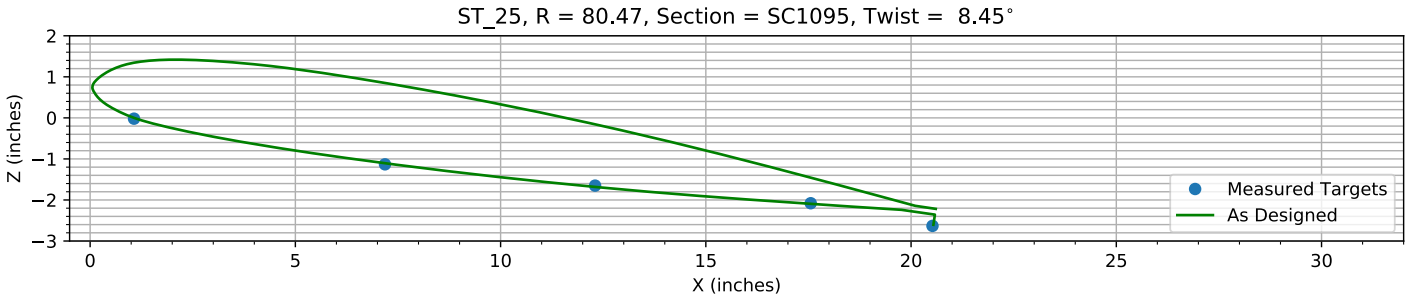

Figure 6-6. Target locations vs section profile at station 25.

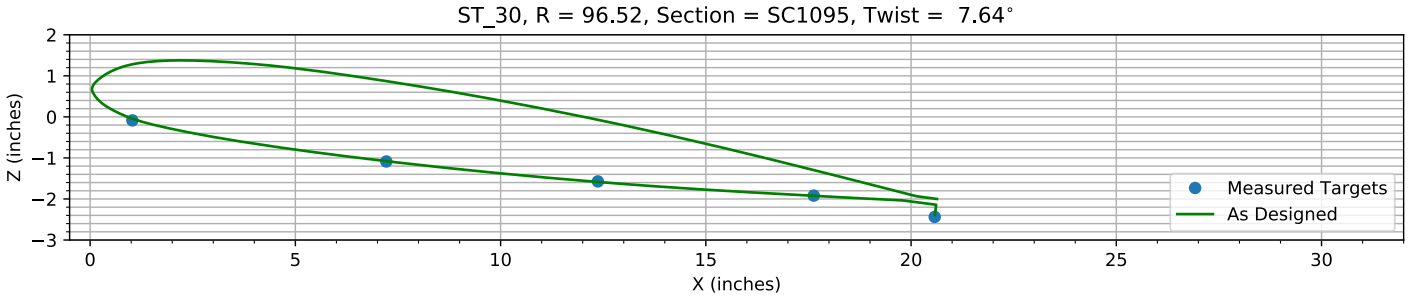

Figure 6-7. Target locations vs section profile at station 30.

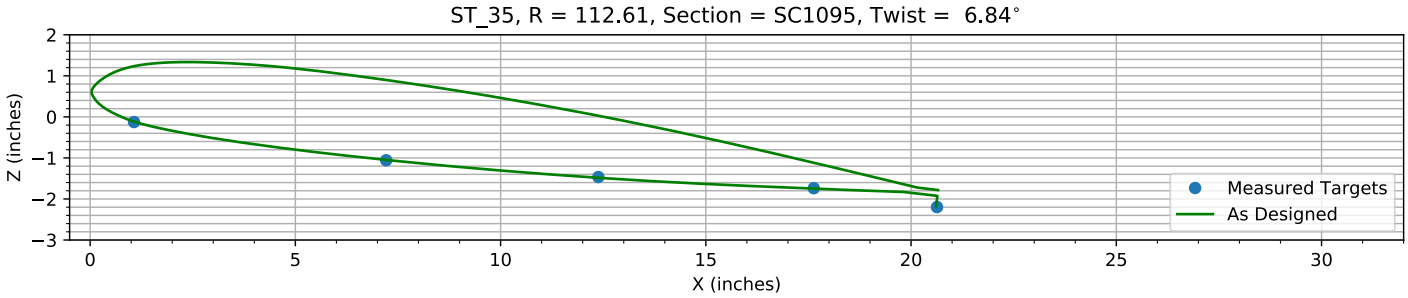

Figure 6-8. Target locations vs section profile at station 35.

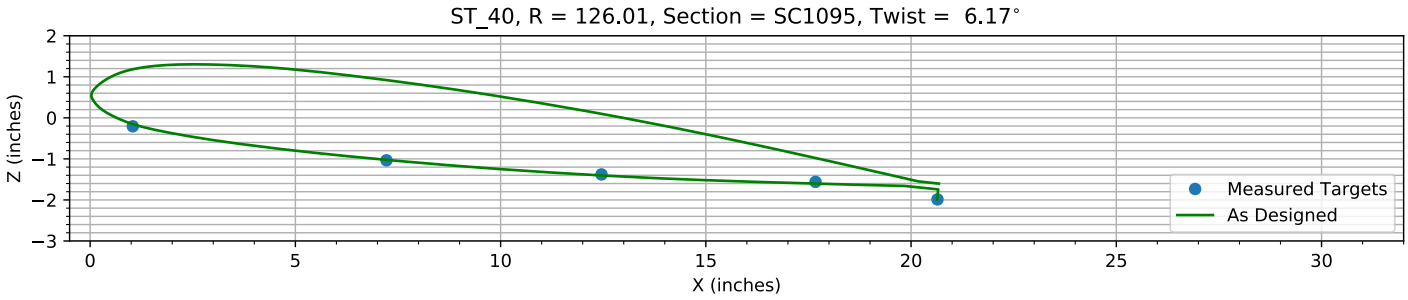

Figure 6-9. Target locations vs section profile at station 40.

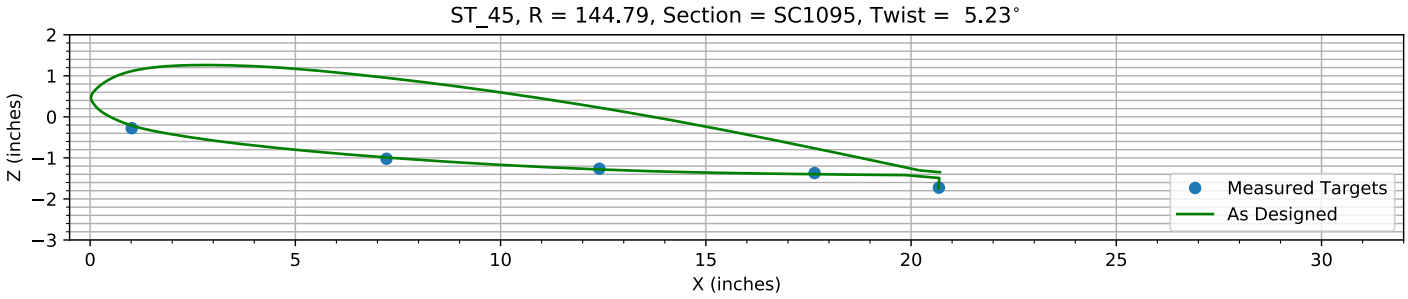

Figure 6-10. Target locations vs section profile at station 45.

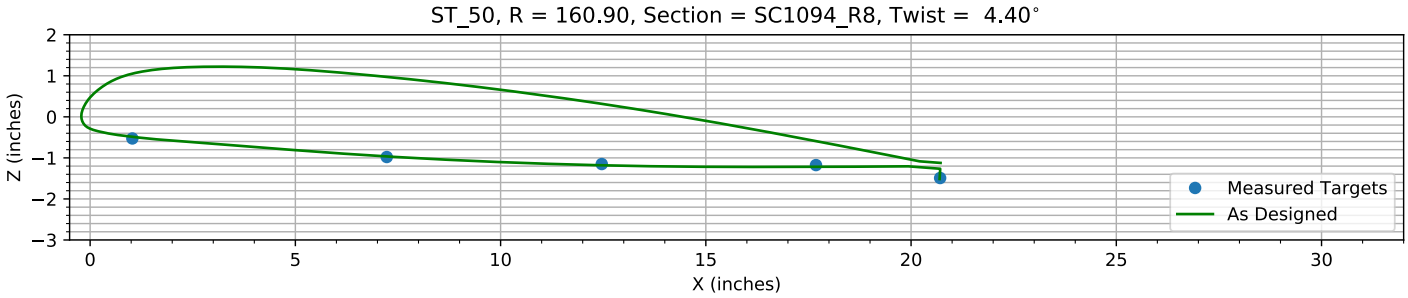

Figure 6-11. Target locations vs section profile at station 50.

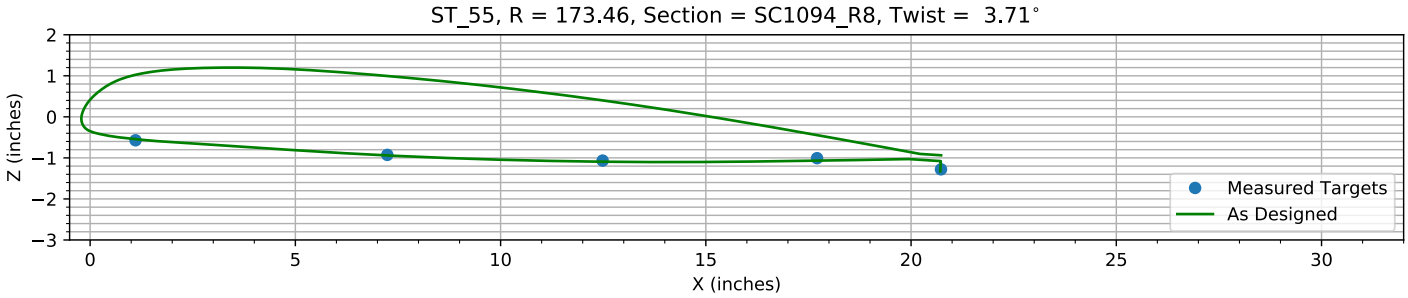

Figure 6-12. Target locations vs section profile at station 55.

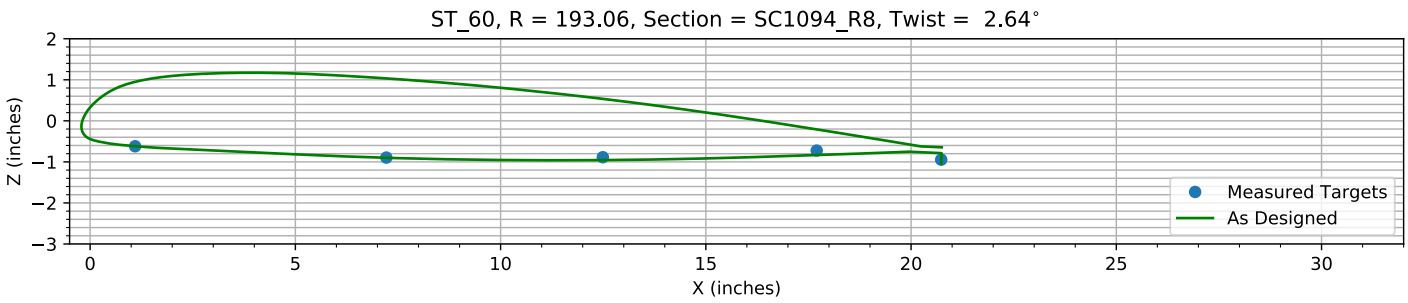

Figure 6-13. Target locations vs section profile at station 60.

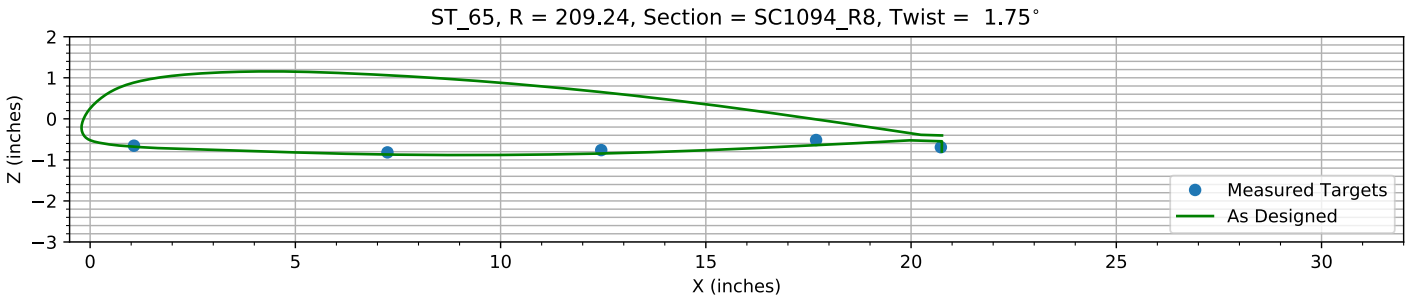

Figure 6-14. Target locations vs section profile at station 65.

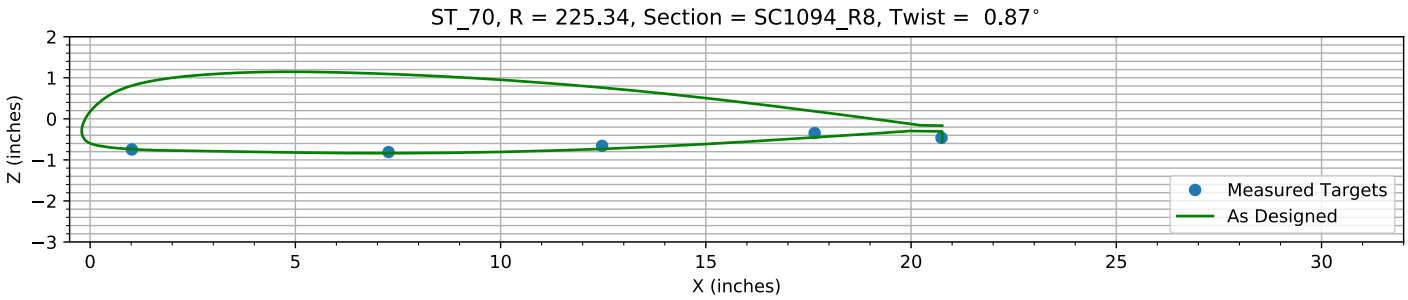

Figure 6-15. Target locations vs section profile at station 70.

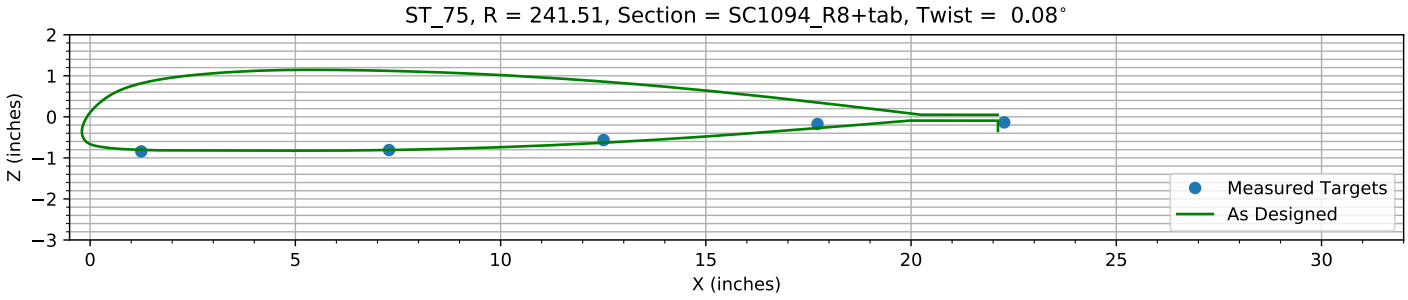

Figure 6-16. Target locations vs section profile at station 75.

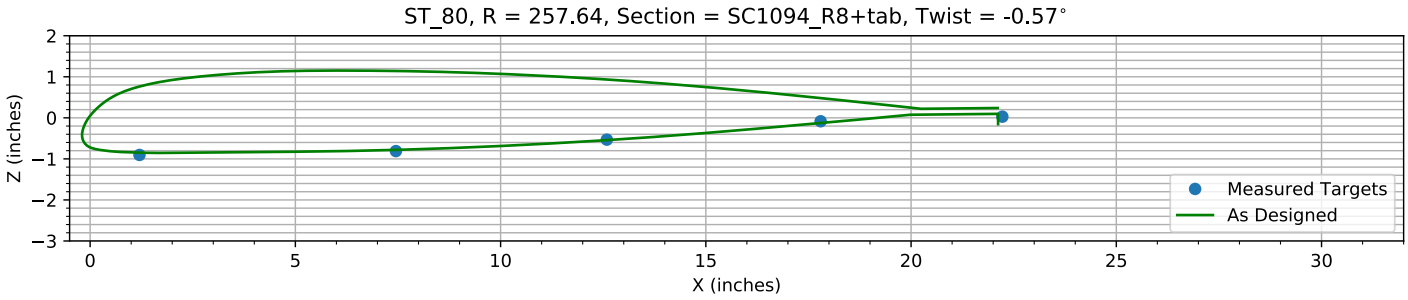

Figure 6-17. Target locations vs section profile at station 80.

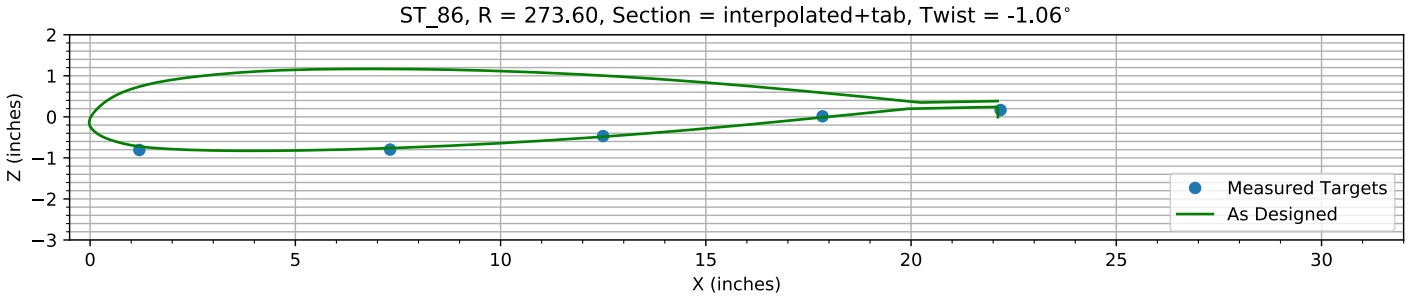

Figure 6-18. Target locations vs section profile at station 86.

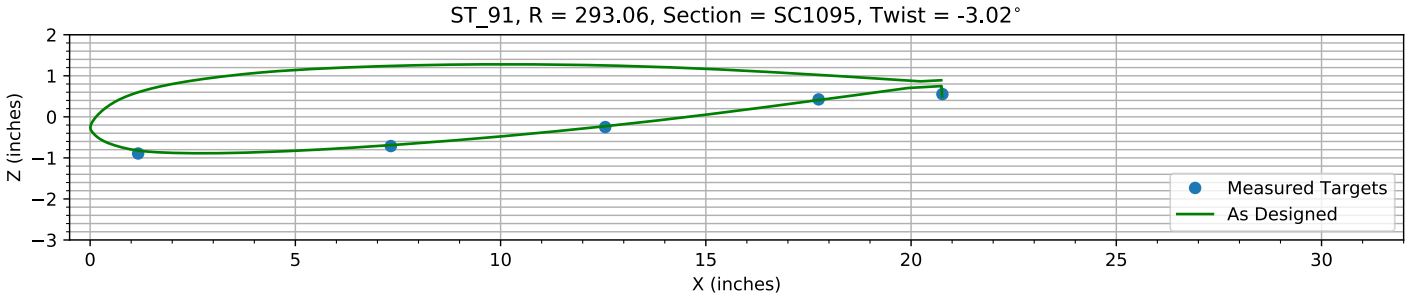

Figure 6-19. Target locations vs section profile at station 91.

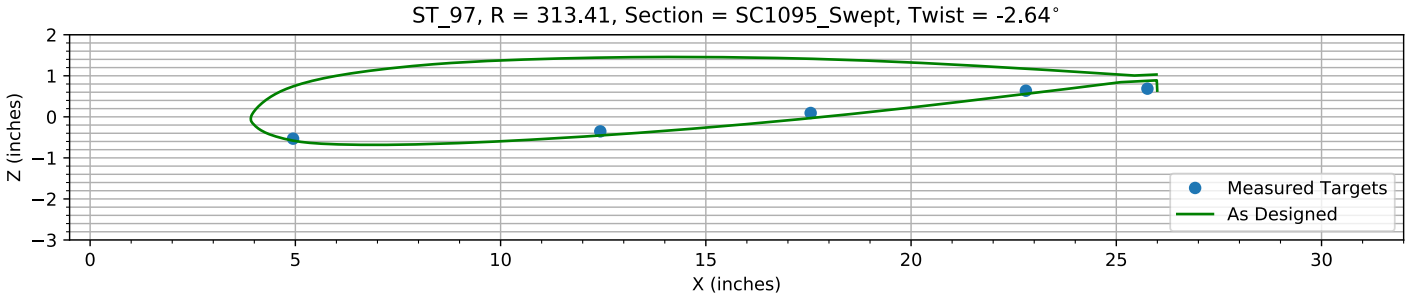

Figure 6-20. Target locations vs section profile at station 97.

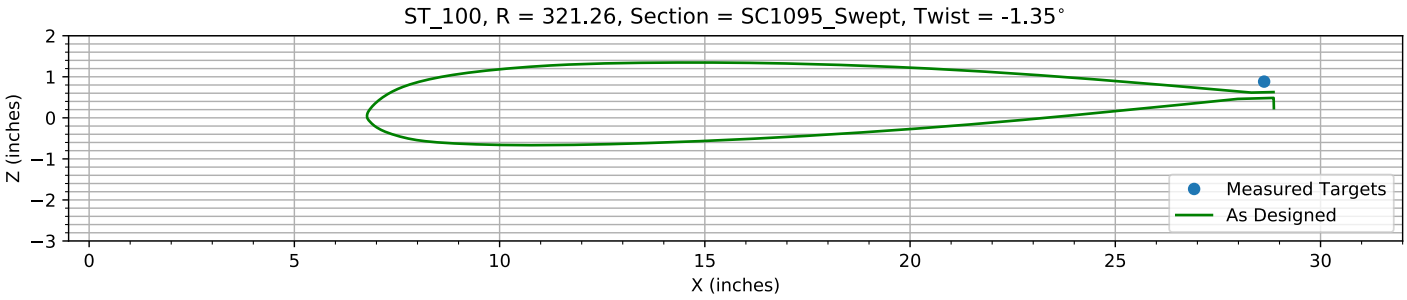

Figure 6-21. Target locations vs section profile at station 100.

Chapter 7: Flap and ΔZ Registration (15 rows)

The targets at the 15 spanwise stations nearest the root are used to determing the Z and flap offset.

The estimated Z error, -0.32422 inches, is within an allowed range of ±2.000 inches.

The estimated flap error is -0.11123°.

7.1: Target Location Errors After Flap Target Registration

Table 7-1. Measured(1) with flap registration vs as designed(2) in inches.

Name	X1	Y1	Z1	X2	Y2	Z2	dX	dY	dZ	dR
B1_R20_C05	0.98691	64.48	0.059064	0.98691	64.48	0.089418	0	0	-0.030354	0.030354
B1_R20_C36	7.1363	64.488	-1.1143	7.1363	64.488	-1.1283	0	0	0.013954	0.013954
B1_R20_C61	12.343	64.431	-1.7261	12.343	64.431	-1.7893	0	0	0.063197	0.063197
B1_R20_C86	17.559	64.416	-2.2127	17.559	64.416	-2.2715	0	0	0.058817	0.058817
B1_R20_C99	20.497	64.364	-2.7489	20.506	64.364	-2.821	-0.008818	0	0.072171	0.072708
B1_R25_C05	1.0691	80.484	-0.025565	1.0691	80.484	-6.412e-06	0	0	-0.025558	0.025558
B1_R25_C36	7.1836	80.445	-1.1381	7.1836	80.445	-1.1051	0	0	-0.033059	0.033059
B1_R25_C61	12.302	80.475	-1.6563	12.302	80.475	-1.6821	0	0	0.025799	0.025799
B1_R25_C86	17.555	80.455	-2.0854	17.555	80.455	-2.0949	0	0	0.0094949	0.0094949
B1_R25_C99	20.522	80.476	-2.6373	20.544	80.476	-2.6043	-0.022305	0	-0.032957	0.039795
B1_R30_C05	1.0294	96.548	-0.092278	1.0294	96.548	-0.044073	0	0	-0.048205	0.048205
B1_R30_C36	7.2155	96.574	-1.0934	7.2155	96.574	-1.0788	0	0	-0.014643	0.014643
B1_R30_C61	12.37	96.544	-1.5795	12.37	96.544	-1.5857	0	0	0.0061852	0.0061852
B1_R30_C86	17.629	96.508	-1.9247	17.629	96.508	-1.9236	0	0	-0.0010348	0.0010348
B1_R30_C99	20.576	96.44	-2.444	20.579	96.44	-2.3898	-0.0031386	0	-0.054219	0.05431
B1_R35_C05	1.0695	112.6	-0.13392	1.0695	112.6	-0.1152	0	0	-0.018716	0.018716
B1_R35_C36	7.2127	112.63	-1.0648	7.2127	112.63	-1.0485	0	0	-0.016282	0.016282
B1_R35_C61	12.382	112.62	-1.4736	12.382	112.62	-1.4842	0	0	0.010585	0.010585
B1_R35_C86	17.629	112.61	-1.7451	17.629	112.61	-1.7476	0	0	0.002481	0.002481
B1_R35_C99	20.632	112.59	-2.205	20.611	112.59	-2.1726	0.020713	0	-0.032429	0.03848
B1_R40_C05	1.04	126.02	-0.21486	1.04	126.02	-0.15363	0	0	-0.061237	0.061237
B1_R40_C36	7.2203	126.02	-1.0432	7.2203	126.02	-1.0244	0	0	-0.018768	0.018768
B1_R40_C61	12.458	126.01	-1.3873	12.458	126.01	-1.4034	0	0	0.016093	0.016093
B1_R40_C86	17.672	125.99	-1.5686	17.672	125.99	-1.6031	0	0	0.034463	0.034463
B1_R40_C99	20.643	126	-1.9962	20.635	126	-1.9923	0.0080542	0	-0.0039524	0.0089717
B1_R45_C05	1.0135	144.78	-0.28704	1.0135	144.78	-0.21235	0	0	-0.07469	0.07469
B1_R45_C36	7.2202	144.8	-1.0307	7.2202	144.8	-0.98983	0	0	-0.04087	0.04087
B1_R45_C61	12.406	144.78	-1.2748	12.406	144.78	-1.2816	0	0	0.0068622	0.0068622
B1_R45_C86	17.65	144.78	-1.3789	17.65	144.78	-1.3982	0	0	0.01936	0.01936
B1_R45_C99	20.678	144.8	-1.7343	20.666	144.8	-1.7392	0.012014	0	0.0048691	0.012963
B1_R50_C05	1.0287	160.95	-0.53685	1.0287	160.95	-0.48673	0	0	-0.050126	0.050126
B1_R50_C36	7.2269	160.92	-0.98901	7.2269	160.92	-0.96465	0	0	-0.024356	0.024356
B1_R50_C61	12.465	160.9	-1.1602	12.465	160.9	-1.1804	0	0	0.020189	0.020189
B1_R50_C86	17.684	160.88	-1.1856	17.684	160.88	-1.2179	0	0	0.032342	0.032342
B1_R50_C99	20.708	160.87	-1.5007	20.695	160.87	-1.5147	0.012883	0	0.013986	0.019015
B1_R55_C05	1.1061	173.51	-0.58237	1.1061	173.51	-0.5441	0	0	-0.038264	0.038264
B1_R55_C36	7.2397	173.48	-0.93782	7.2397	173.48	-0.94019	0	0	0.0023774	0.0023774
B1_R55_C61	12.486	173.43	-1.0769	12.486	173.43	-1.0933	0	0	0.016415	0.016415

Name	X1	Y1	Z1	X2	Y2	Z2	dX	dY	dZ	dR
B1_R55_C86	17.71	173.42	-1.0178	17.71	173.42	-1.0679	0	0	0.05008	0.05008
B1_R55_C99	20.729	173.44	-1.29	20.712	173.44	-1.3283	0.016396	0	0.03831	0.041671
B1_R60_C05	1.0965	193.03	-0.63157	1.0965	193.03	-0.61839	0	0	-0.013181	0.013181
B1_R60_C36	7.2164	193.06	-0.907	7.2164	193.06	-0.9005	0	0	-0.0065029	0.0065029
B1_R60_C61	12.491	193.08	-0.89837	12.491	193.08	-0.95634	0	0	0.057967	0.057967
B1_R60_C86	17.701	193.06	-0.73671	17.701	193.06	-0.83378	0	0	0.097078	0.097078
B1_R60_C99	20.734	193.04	-0.95774	20.734	193.04	-1.0375	-0.00062291	0	0.079745	0.079748
B1_R65_C05	1.0675	209.29	-0.66729	1.0675	209.29	-0.67916	0	0	0.011869	0.011869
B1_R65_C36	7.2431	209.27	-0.83004	7.2431	209.27	-0.86921	0	0	0.039171	0.039171
B1_R65_C61	12.451	209.23	-0.77463	12.451	209.23	-0.84493	0	0	0.0703	0.0703
B1_R65_C86	17.686	209.21	-0.52885	17.686	209.21	-0.64204	0	0	0.11319	0.11319
B1_R65_C99	20.726	209.18	-0.70441	20.748	209.18	-0.79781	-0.02268	0	0.093396	0.096111
B1_R70_C05	1.0168	225.38	-0.75966	1.0168	225.38	-0.73896	0	0	-0.020699	0.020699
B1_R70_C36	7.2704	225.35	-0.82303	7.2704	225.35	-0.83757	0	0	0.014544	0.014544
B1_R70_C61	12.473	225.31	-0.67189	12.473	225.31	-0.7329	0	0	0.06101	0.06101
B1_R70_C86	17.651	225.29	-0.36043	17.651	225.29	-0.45291	0	0	0.092482	0.092482
B1_R70_C99	20.742	225.36	-0.47621	20.759	225.36	-0.5574	-0.016899	0	0.081196	0.082936
B1_R75_C05	1.2452	241.53	-0.8571	1.2452	241.53	-0.80551	0	0	-0.051592	0.051592
B1_R75_C36	7.2823	241.52	-0.82404	7.2823	241.52	-0.80859	0	0	-0.015443	0.015443
B1_R75_C61	12.509	241.5	-0.58066	12.509	241.5	-0.63012	0	0	0.049457	0.049457
B1_R75_C86	17.72	241.48	-0.1892	17.72	241.48	-0.27442	0	0	0.085222	0.085222
B1_R80_C05	1.2021	257.63	-0.91974	1.2021	257.63	-0.84832	0	0	-0.071423	0.071423
B1_R80_C36	7.4495	257.64	-0.82564	7.4495	257.64	-0.78086	0	0	-0.044775	0.044775
B1_R80_C61	12.588	257.63	-0.54645	12.588	257.63	-0.5432	0	0	-0.0032518	0.0032518
B1_R80_C86	17.797	257.6	-0.099112	17.797	257.6	-0.127	0	0	0.027889	0.027889
B1_R86_C05	1.1993	273.59	-0.82446	1.1993	273.59	-0.72187	0	0	-0.10259	0.10259
B1_R86_C36	7.3084	273.59	-0.81387	7.3084	273.59	-0.76249	0	0	-0.051377	0.051377
B1_R86_C61	12.497	273.62	-0.48442	12.497	273.62	-0.48401	0	0	-0.00040947	0.00040947
B1_R86_C86	17.843	273.59	-0.0035596	17.843	273.59	-0.013558	0	0	0.009998	0.009998
B1_R91_C05	1.1698	292.99	-0.91	1.1698	292.99	-0.8212	0	0	-0.088796	0.088796
B1_R91_C36	7.3253	293.07	-0.72895	7.3253	293.07	-0.68933	0	0	-0.039625	0.039625
B1_R91_C61	12.549	293.07	-0.26694	12.549	293.07	-0.22896	0	0	-0.037982	0.037982
B1_R91_C86	17.748	293.05	0.40762	17.748	293.05	0.40791	0	0	-0.00029114	0.00029114
B1_R91_C99	20.763	293.13	0.53686	20.755	293.13	0.50147	0.0082181	0	0.035395	0.036337
B1_R97_C05	4.9441	313.41	-0.54995	4.9441	313.41	-0.57967	0	0	0.02972	0.02972
B1_R97_C36	12.428	313.46	-0.37227	12.428	313.46	-0.45586	0	0	0.083587	0.083587
B1_R97_C61	17.554	313.45	0.075562	17.554	313.45	-0.032999	0	0	0.10856	0.10856
B1_R97_C86	22.797	313.41	0.61874	22.797	313.41	0.55868	0	0	0.060056	0.060056
B1_R97_C99	25.758	313.32	0.66797	25.966	313.32	0.64241	-0.20783	0	0.025566	0.2094
HUB_LE	2.2651	30.004	-3.1759	2.19	30	-3.5	0.075139	0.0038814	0.32413	0.33274
HUB_TE	8.2617	29.995	-3.1757	8.19	30	-3.5	0.071732	-0.0053668	0.32431	0.33219
RMS Errors:							0.026746	0.00074517	0.070754	0.075644

7.2: Flap Registration Plots (15 rows)

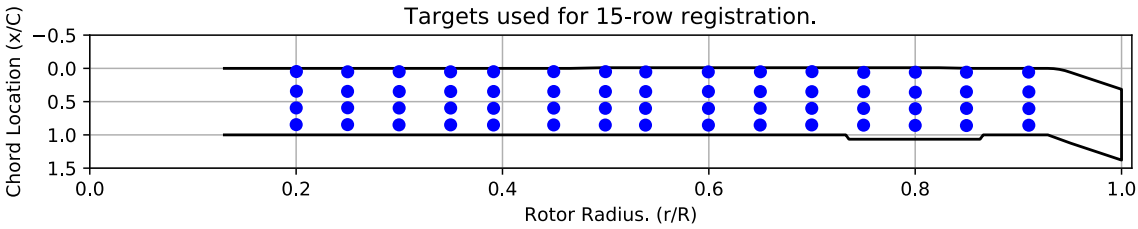

Figure 7-1. Targets used for 15 row root registration.

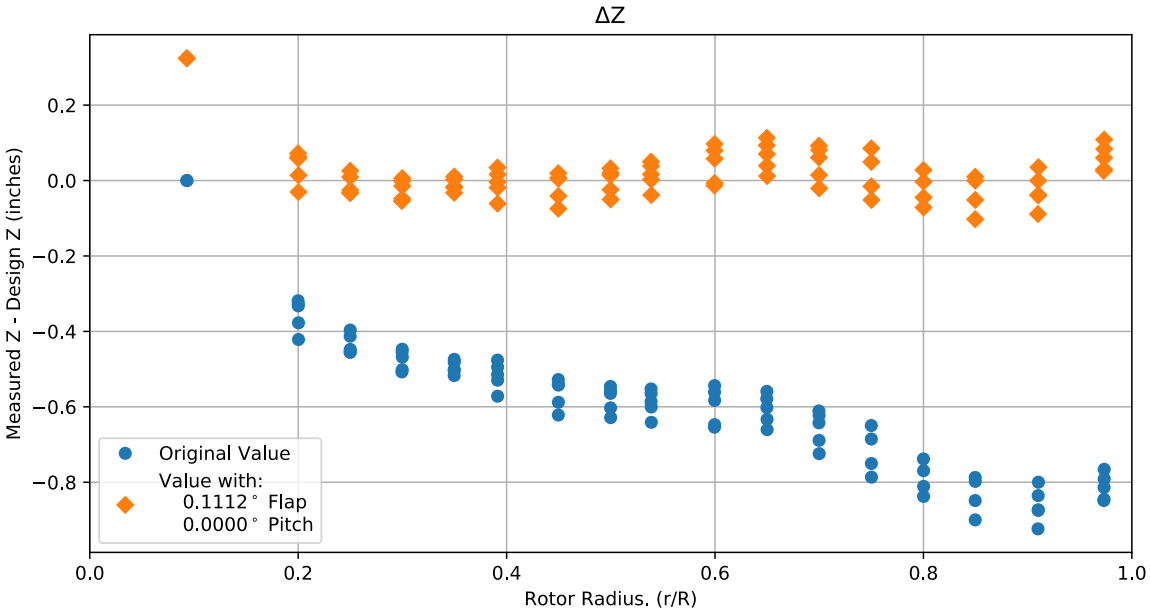

Figure 7-2. Flap target registration, ΔZ error vs rotor radius.

Note: the “as designed” geometry used for the swept tip may have some inaccuracies.

7.3: Estimated Bending and Twist at the Quarter Chord

The error bars shown represent the residual errors for fitting the measure target locations to the "as designed" geometry. These errors are generally much larger than those due to the VSTARS measurement errors. Therefore, the most likely source of these errors is the placement of the trailing-edge targets, differences between the "as designed" and "as built" geometries, and blade deformation during measurement. In the future, iterative adjustment of the "as designed" twist angle may be implemented to see if it reduces the fit error in delta twist. Note: The "as designed" geometry used for the swept tip may have some inaccuracies.

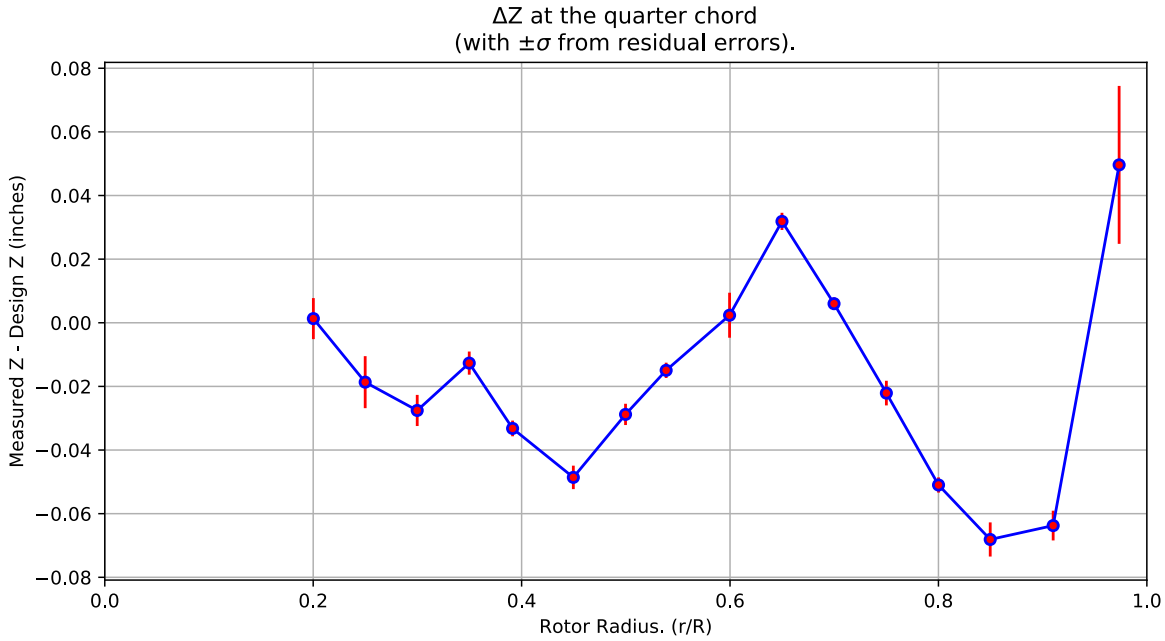

Figure 7-3. ΔZ error at the quarter chord vs rotor radius.

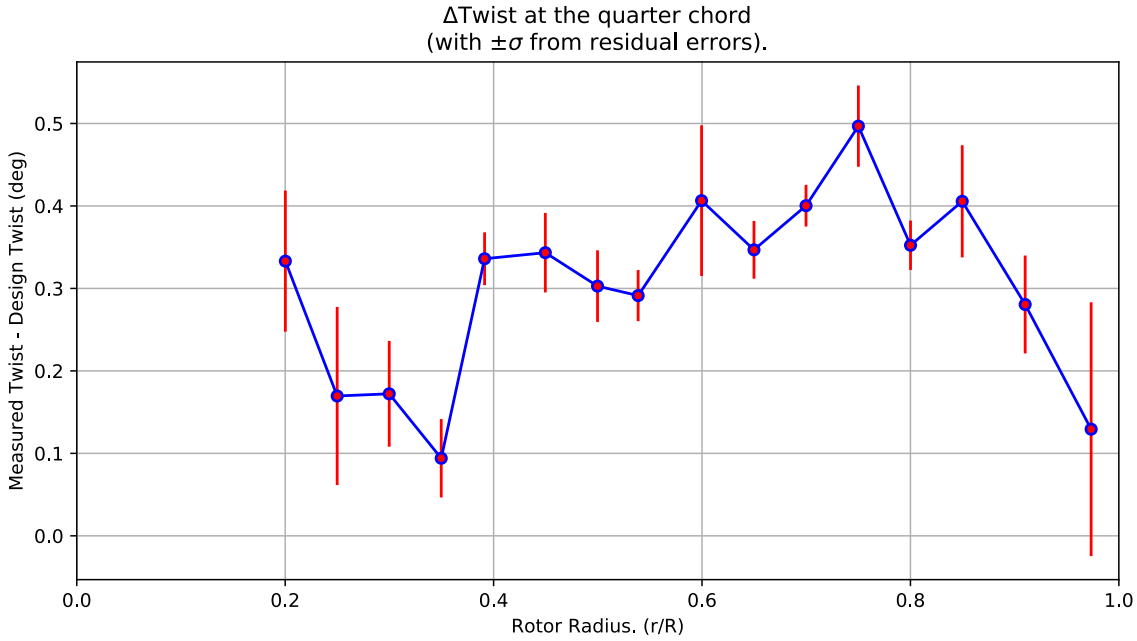

Figure 7-4. ΔTwist error at the quarter chord vs rotor radius.

Table 7-2. Quarter-chord bending and twist statistics.

r	r/R	dZ 1/4-chord	dT	sigma dZ meas	sigma dT meas	sigma dZ res	sigma dT res	n	t_conf
64.454	0.20017	0.001308	0.33312	6.1099e-10	4.6611e-09	0.006444	0.085534	4	4.3027
80.465	0.24989	-0.018666	0.16955	6.1328e-10	4.691e-09	0.0081734	0.10797	4	4.3027
96.544	0.29983	-0.027561	0.1722	6.1343e-10	4.6585e-09	0.0048913	0.064118	4	4.3027
112.62	0.34974	-0.012678	0.094043	6.1443e-10	4.6677e-09	0.0036365	0.047533	4	4.3027
126.01	0.39134	-0.033211	0.33601	6.1448e-10	4.6431e-09	0.0024643	0.032033	4	4.3027
144.78	0.44964	-0.048596	0.34335	6.1343e-10	4.6463e-09	0.0036855	0.048184	4	4.3027
160.91	0.49973	-0.028799	0.3028	6.1438e-10	4.6372e-09	0.0033438	0.043433	4	4.3027
173.46	0.5387	-0.014949	0.2913	6.1658e-10	4.6501e-09	0.0024054	0.031003	4	4.3027
193.06	0.59956	0.002372	0.40643	6.1603e-10	4.6475e-09	0.0070716	0.09133	4	4.3027
209.25	0.64985	0.031865	0.34681	6.1543e-10	4.6492e-09	0.0027036	0.03503	4	4.3027
225.33	0.6998	0.0060023	0.40033	6.1479e-10	4.6446e-09	0.0019477	0.025289	4	4.3027
241.51	0.75003	-0.022102	0.4968	6.2078e-10	4.6849e-09	0.0038711	0.049293	4	4.3027
257.63	0.80008	-0.050986	0.35232	6.2298e-10	4.66e-09	0.002388	0.029944	4	4.3027
273.6	0.84968	-0.068109	0.40564	6.2002e-10	4.6453e-09	0.0053665	0.067995	4	4.3027
293.05	0.91009	-0.063743	0.2805	6.1994e-10	4.6581e-09	0.004671	0.059366	4	4.3027
313.43	0.97339	0.049625	0.12931	8.6108e-10	4.3467e-09	0.02482	0.15389	4	4.3027

7.4: Section Plots

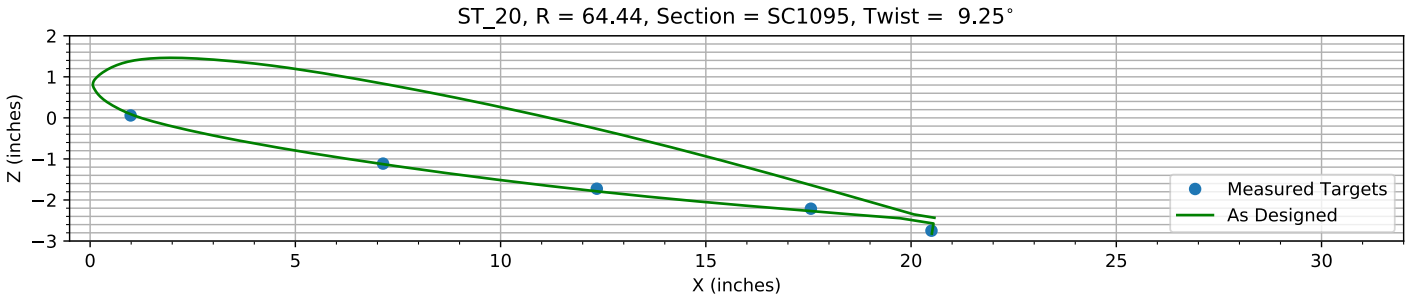

Figure 7-5. Target locations vs section profile at station 20.

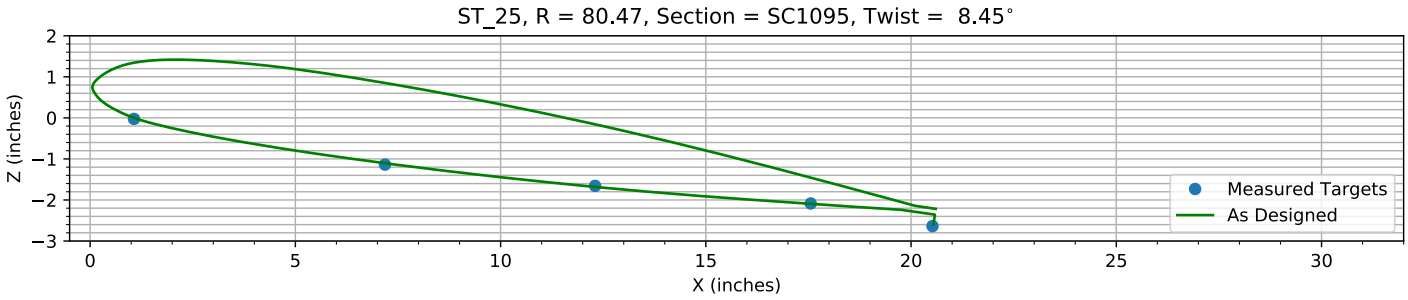

Figure 7-6. Target locations vs section profile at station 25.

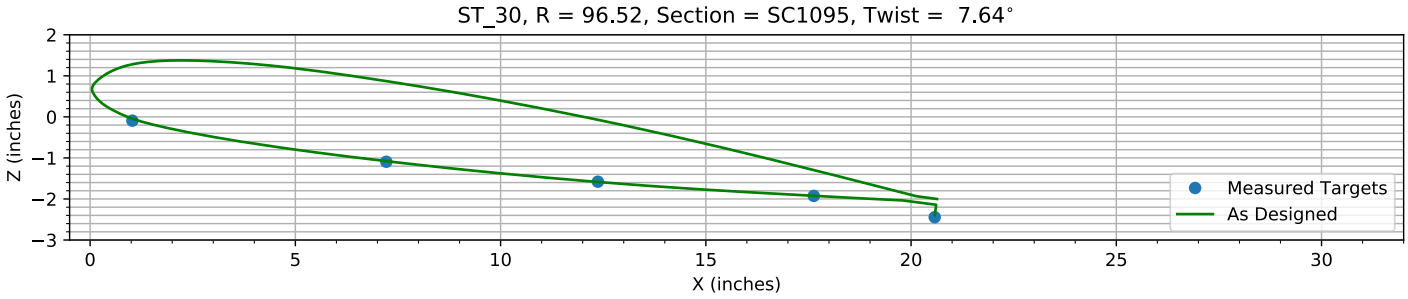

Figure 7-7. Target locations vs section profile at station 30.

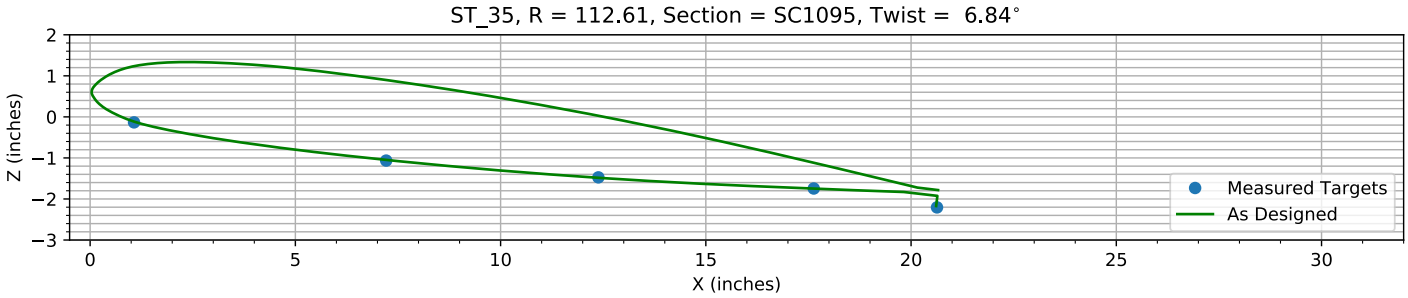

Figure 7-8. Target locations vs section profile at station 35.

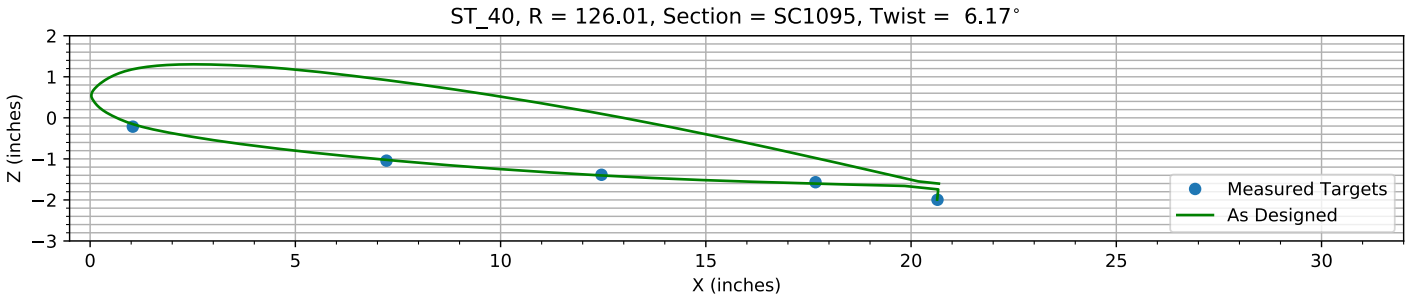

Figure 7-9. Target locations vs section profile at station 40.

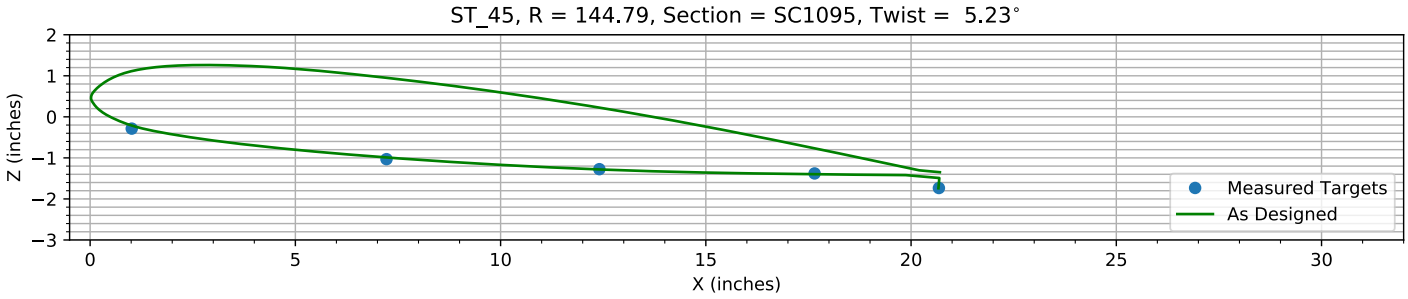

Figure 7-10. Target locations vs section profile at station 45.

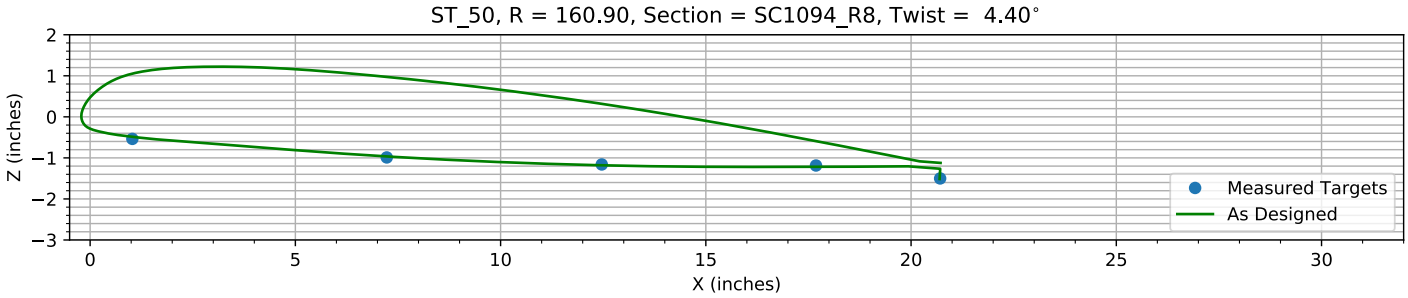

Figure 7-11. Target locations vs section profile at station 50.

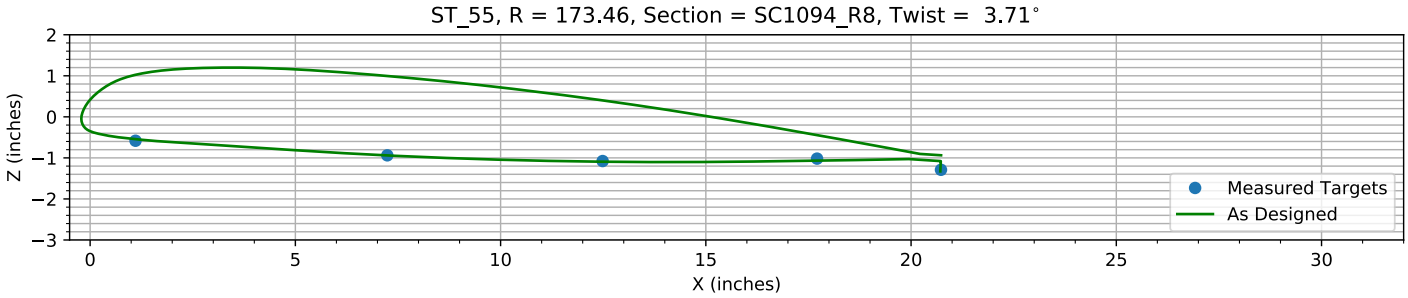

Figure 7-12. Target locations vs section profile at station 55.

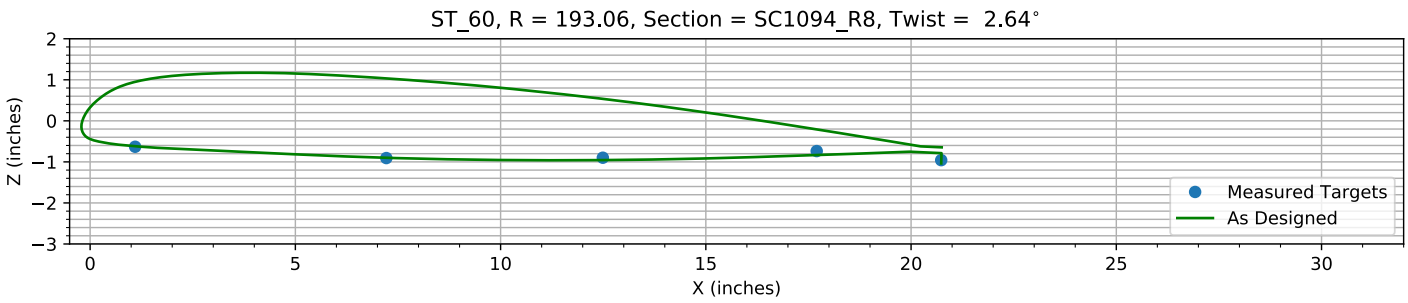

Figure 7-13. Target locations vs section profile at station 60.

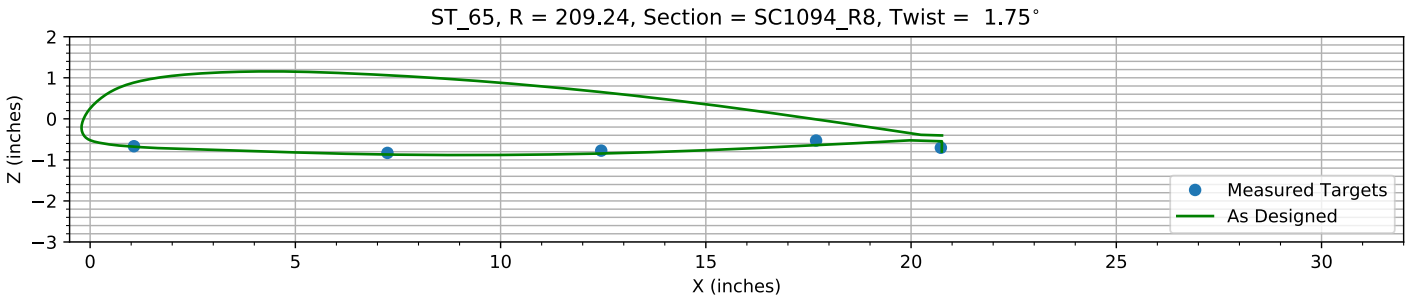

Figure 7-14. Target locations vs section profile at station 65.

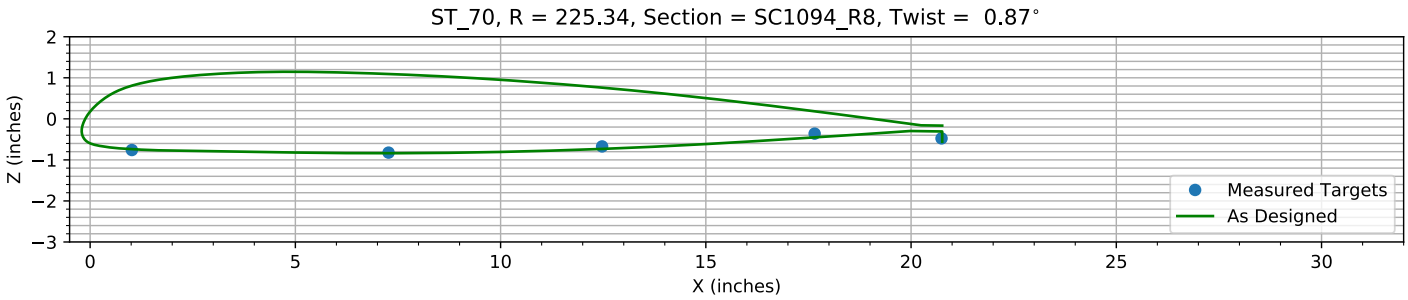

Figure 7-15. Target locations vs section profile at station 70.

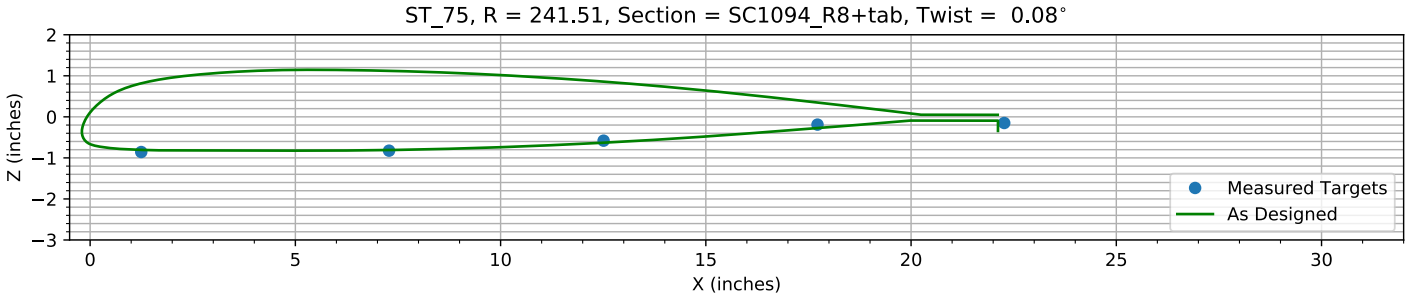

Figure 7-16. Target locations vs section profile at station 75.

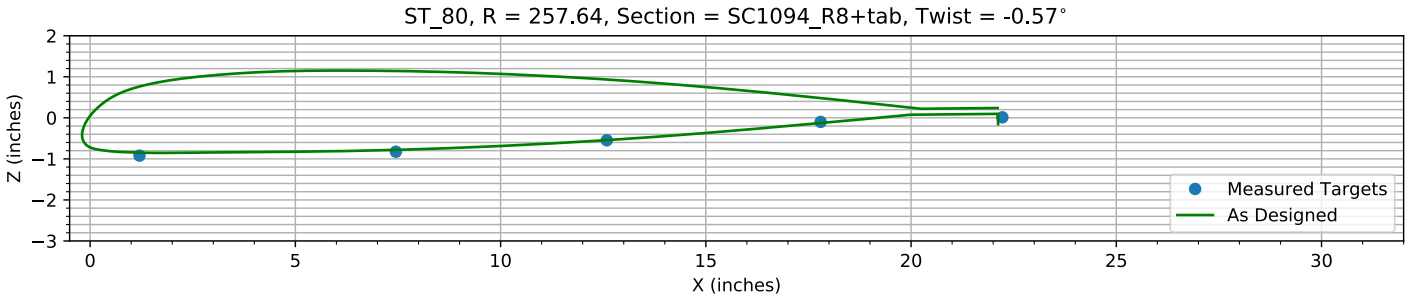

Figure 7-17. Target locations vs section profile at station 80.

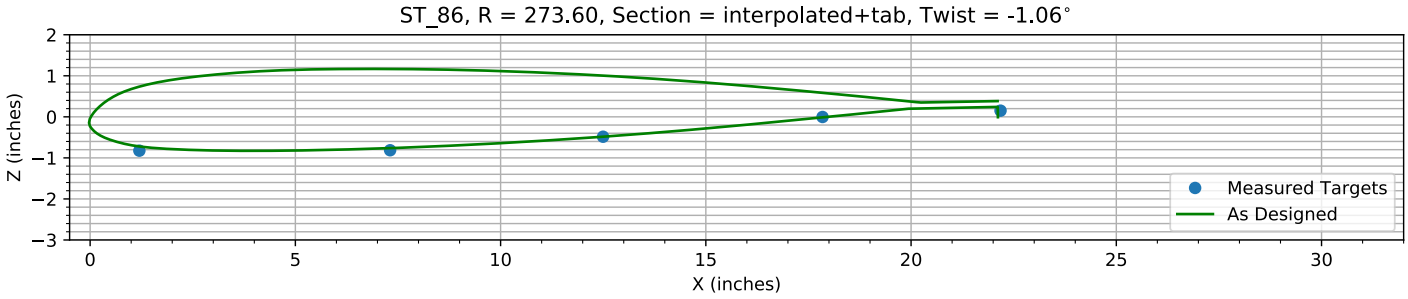

Figure 7-18. Target locations vs section profile at station 86.

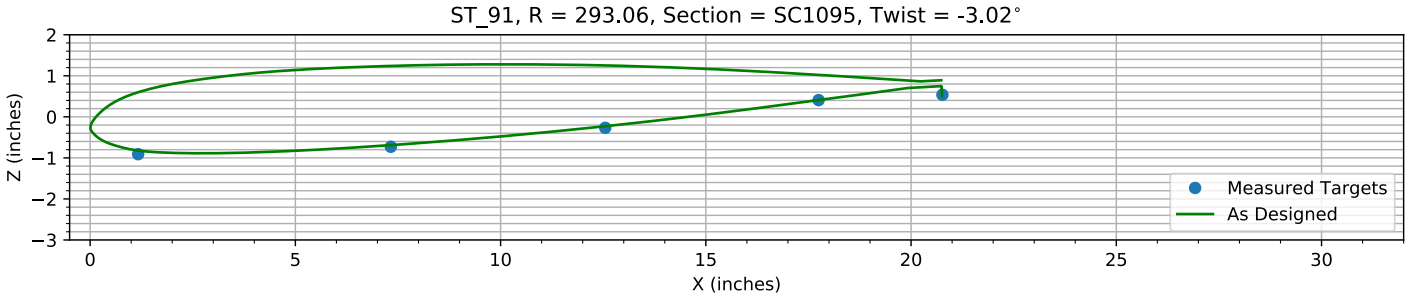

Figure 7-19. Target locations vs section profile at station 91.

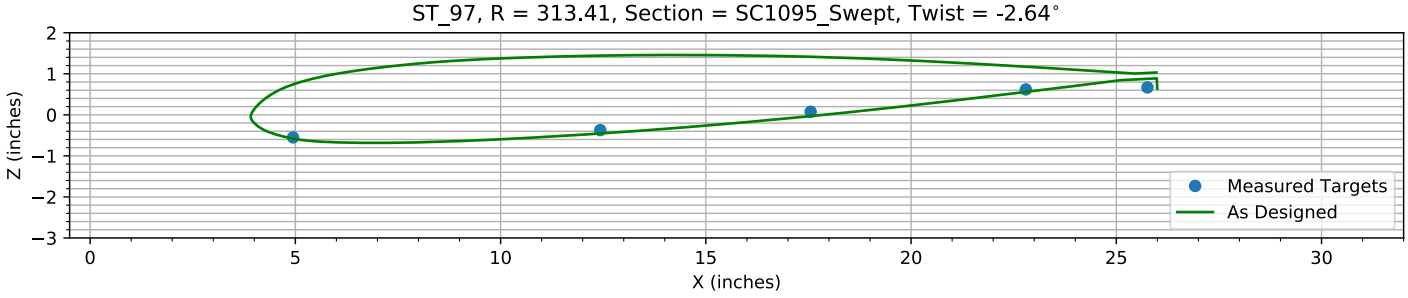

Figure 7-20. Target locations vs section profile at station 97.

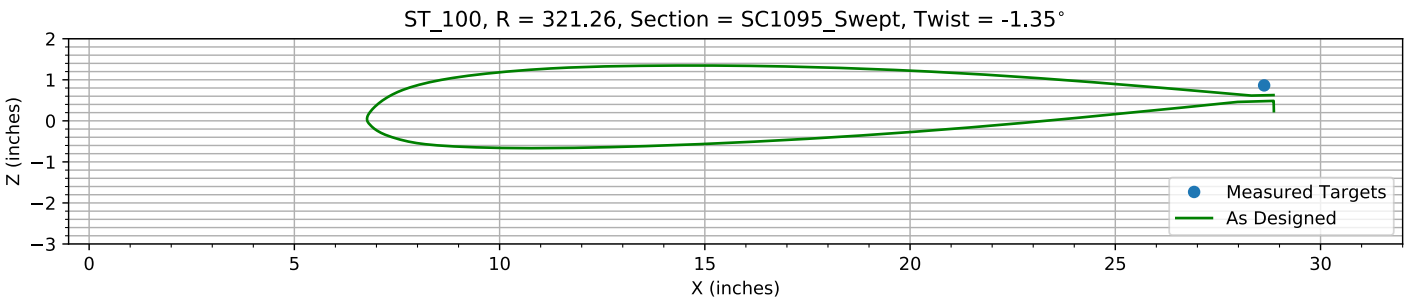

Figure 7-21. Target locations vs section profile at station 100.

Chapter 8: Pitch, Flap, and ΔZ Registration (6 rows)

The targets at the 6 spanwise stations nearest the root are used to determing the Z, flap, and pitch offset.

The estimated Z error, -0.32839 inches, is within an allowed range of ±2.000 inches.

The estimated flap error is -0.11842°.

The estimated pitch error is -0.083495°.

8.1: Target Location Errors After Target Registration

Table 8-1. Measured(1) with pitch and flap registration vs as designed(2) in inches.

Name	X1	Y1	Z1	X2	Y2	Z2	dX	dY	dZ	dR
B1_R20_C05	0.99212	64.479	0.073681	0.99212	64.479	0.087364	0	0	-0.013682	0.013682
B1_R20_C36	7.1398	64.488	-1.1087	7.1398	64.488	-1.1288	0	0	0.02012	0.02012
B1_R20_C61	12.346	64.43	-1.728	12.346	64.43	-1.7895	0	0	0.061547	0.061547
B1_R20_C86	17.561	64.416	-2.2222	17.561	64.416	-2.2716	0	0	0.049435	0.049435
B1_R20_C99	20.498	64.364	-2.7627	20.506	64.364	-2.821	-0.007727	0	0.058347	0.058857
B1_R25_C05	1.0742	80.484	-0.009059	1.0742	80.484	-0.0018135	0	0	-0.0072455	0.0072455
B1_R25_C36	7.1871	80.445	-1.1306	7.1871	80.445	-1.1055	0	0	-0.025014	0.025014
B1_R25_C61	12.304	80.475	-1.6561	12.304	80.475	-1.6823	0	0	0.026196	0.026196
B1_R25_C86	17.557	80.454	-2.0929	17.557	80.454	-2.0951	0	0	0.0021172	0.0021172
B1_R25_C99	20.523	80.476	-2.6491	20.544	80.476	-2.6043	-0.021048	0	-0.044795	0.049494
B1_R30_C05	1.0344	96.548	-0.073699	1.0344	96.548	-0.045828	0	0	-0.027871	0.027871
B1_R30_C36	7.219	96.574	-1.0839	7.219	96.574	-1.0792	0	0	-0.0046623	0.0046623
B1_R30_C61	12.372	96.544	-1.5774	12.372	96.544	-1.5859	0	0	0.008471	0.008471
B1_R30_C86	17.631	96.508	-1.9303	17.631	96.508	-1.9238	0	0	-0.0065218	0.0065218
B1_R30_C99	20.577	96.44	-2.4539	20.579	96.44	-2.3898	-0.0015976	0	-0.064133	0.064153
B1_R35_C05	1.0745	112.6	-0.11338	1.0745	112.6	-0.1168	0	0	0.003418	0.003418
B1_R35_C36	7.2162	112.63	-1.0532	7.2162	112.63	-1.0488	0	0	-0.0043279	0.0043279
B1_R35_C61	12.385	112.62	-1.4695	12.385	112.62	-1.4844	0	0	0.014841	0.014841
B1_R35_C86	17.632	112.61	-1.7487	17.632	112.61	-1.7477	0	0	-0.0010071	0.0010071
B1_R35_C99	20.634	112.59	-2.213	20.611	112.59	-2.1726	0.022606	0	-0.040398	0.046292
B1_R40_C05	1.0448	126.02	-0.1926	1.0448	126.02	-0.15518	0	0	-0.037418	0.037418
B1_R40_C36	7.2239	126.02	-1.0299	7.2239	126.02	-1.0247	0	0	-0.0051835	0.0051835
B1_R40_C61	12.461	126.01	-1.3817	12.461	126.01	-1.4035	0	0	0.021882	0.021882
B1_R40_C86	17.675	125.99	-1.5706	17.675	125.99	-1.6032	0	0	0.032568	0.032568
B1_R40_C99	20.646	126	-2.0025	20.635	126	-1.9923	0.010253	0	-0.010256	0.014502
B1_R45_C05	1.0183	144.78	-0.26239	1.0183	144.78	-0.21379	0	0	-0.048597	0.048597
B1_R45_C36	7.2238	144.8	-1.0151	7.2238	144.8	-0.9901	0	0	-0.024987	0.024987
B1_R45_C61	12.409	144.78	-1.2667	12.409	144.78	-1.2817	0	0	0.015046	0.015046
B1_R45_C86	17.653	144.78	-1.3784	17.653	144.78	-1.3983	0	0	0.019813	0.019813
B1_R45_C99	20.68	144.8	-1.7383	20.666	144.8	-1.7392	0.014598	0	0.0008755	0.014624
B1_R50_C05	1.033	160.95	-0.51019	1.033	160.95	-0.48724	0	0	-0.022953	0.022953
B1_R50_C36	7.2306	160.92	-0.97138	7.2306	160.92	-0.96487	0	0	-0.0065071	0.0065071
B1_R50_C61	12.468	160.9	-1.1503	12.468	160.9	-1.1805	0	0	0.030259	0.030259
B1_R50_C86	17.687	160.88	-1.1832	17.687	160.88	-1.2179	0	0	0.034718	0.034718
B1_R50_C99	20.711	160.87	-1.5027	20.695	160.87	-1.5147	0.015811	0	0.011965	0.019828
B1_R55_C05	1.1103	173.51	-0.55424	1.1103	173.51	-0.54455	0	0	-0.009696	0.009696

Name	X1	Y1	Z1	X2	Y2	Z2	dX	dY	dZ	dR
B1_R55_C36	7.2435	173.48	-0.91863	7.2435	173.48	-0.94038	0	0	0.021744	0.021744
B1_R55_C61	12.489	173.43	-1.0654	12.489	173.43	-1.0934	0	0	0.027987	0.027987
B1_R55_C86	17.713	173.42	-1.0139	17.713	173.42	-1.0679	0	0	0.053948	0.053948
B1_R55_C99	20.732	173.44	-1.2905	20.712	173.44	-1.3283	0.019633	0	0.037837	0.042627
B1_R60_C05	1.1007	193.03	-0.60098	1.1007	193.03	-0.61876	0	0	0.01777	0.01777
B1_R60_C36	7.2202	193.06	-0.88533	7.2202	193.06	-0.90061	0	0	0.015285	0.015285
B1_R60_C61	12.494	193.08	-0.88438	12.494	193.08	-0.95631	0	0	0.071929	0.071929
B1_R60_C86	17.705	193.06	-0.73031	17.705	193.06	-0.83365	0	0	0.10334	0.10334
B1_R60_C99	20.737	193.04	-0.95577	20.734	193.04	-1.0375	0.0031016	0	0.081725	0.081784
B1_R65_C05	1.0717	209.29	-0.63462	1.0717	209.29	-0.67945	0	0	0.044834	0.044834
B1_R65_C36	7.247	209.27	-0.80637	7.247	209.27	-0.86926	0	0	0.062896	0.062896
B1_R65_C61	12.455	209.22	-0.75855	12.455	209.22	-0.84483	0	0	0.086281	0.086281
B1_R65_C86	17.69	209.21	-0.52041	17.69	209.21	-0.64183	0	0	0.12142	0.12142
B1_R65_C99	20.73	209.18	-0.7004	20.748	209.18	-0.79781	-0.018583	0	0.097412	0.099169
B1_R70_C05	1.0208	225.38	-0.72489	1.0208	225.38	-0.73918	0	0	0.014291	0.014291
B1_R70_C36	7.2743	225.35	-0.79738	7.2743	225.35	-0.83757	0	0	0.040187	0.040187
B1_R70_C61	12.477	225.31	-0.65383	12.477	225.31	-0.73274	0	0	0.078911	0.078911
B1_R70_C86	17.655	225.29	-0.34992	17.655	225.29	-0.45262	0	0	0.1027	0.1027
B1_R70_C99	20.746	225.36	-0.47019	20.759	225.36	-0.55741	-0.012467	0	0.087218	0.088105
B1_R75_C05	1.2491	241.53	-0.82065	1.2491	241.53	-0.80566	0	0	-0.014989	0.014989
B1_R75_C36	7.2863	241.52	-0.79638	7.2863	241.52	-0.80853	0	0	0.012156	0.012156
B1_R75_C61	12.513	241.5	-0.56062	12.513	241.5	-0.6299	0	0	0.069271	0.069271
B1_R75_C86	17.725	241.48	-0.17676	17.725	241.48	-0.27404	0	0	0.097287	0.097287
B1_R80_C05	1.2059	257.63	-0.8812	1.2059	257.63	-0.84843	0	0	-0.032772	0.032772
B1_R80_C36	7.4534	257.64	-0.7962	7.4534	257.64	-0.78076	0	0	-0.01544	0.01544
B1_R80_C61	12.592	257.63	-0.5245	12.592	257.63	-0.54292	0	0	0.018419	0.018419
B1_R80_C86	17.802	257.6	-0.084758	17.802	257.6	-0.12656	0	0	0.041797	0.041797
B1_R86_C05	1.2033	273.59	-0.78391	1.2033	273.59	-0.72239	0	0	-0.061521	0.061521
B1_R86_C36	7.3124	273.59	-0.78223	7.3124	273.59	-0.76235	0	0	-0.019871	0.019871
B1_R86_C61	12.501	273.62	-0.46033	12.501	273.62	-0.4837	0	0	0.023369	0.023369
B1_R86_C86	17.848	273.59	0.012733	17.848	273.59	-0.013061	0	0	0.025794	0.025794
B1_R91_C05	1.1737	292.99	-0.86697	1.1737	292.99	-0.82171	0	0	-0.045265	0.045265
B1_R91_C36	7.3294	293.07	-0.69489	7.3294	293.07	-0.68904	0	0	-0.0058449	0.0058449
B1_R91_C61	12.554	293.07	-0.24049	12.554	293.07	-0.22847	0	0	-0.012023	0.012023
B1_R91_C86	17.753	293.05	0.4265	17.753	293.05	0.40867	0	0	0.017832	0.017832
B1_R91_C99	20.769	293.13	0.55135	20.755	293.13	0.50145	0.014138	0	0.049897	0.051862
B1_R97_C05	4.9485	313.41	-0.50987	4.9485	313.41	-0.58049	0	0	0.070628	0.070628
B1_R97_C36	12.433	313.46	-0.34308	12.433	313.46	-0.45554	0	0	0.11246	0.11246
B1_R97_C61	17.559	313.44	0.097277	17.559	313.44	-0.032463	0	0	0.12974	0.12974
B1_R97_C86	22.803	313.41	0.63281	22.803	313.41	0.55945	0	0	0.073354	0.073354
B1_R97_C99	25.764	313.32	0.67772	25.966	313.32	0.64243	-0.20153	0	0.03529	0.20459
HUB_LE	2.2656	30.004	-3.1674	2.19	30	-3.5	0.07562	0.0038321	0.33256	0.34107
HUB_TE	8.2622	29.995	-3.176	8.19	30	-3.5	0.072207	-0.0054161	0.324	0.33199
RMS Errors:							0.026199	0.00074646	0.071844	0.076476

8.2: Pitch and Flap Registration Plots (6 rows)

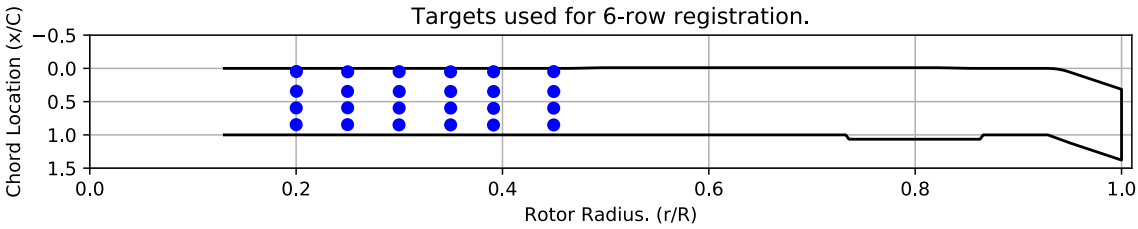

Figure 8-1. Targets used for 6 row root registration.

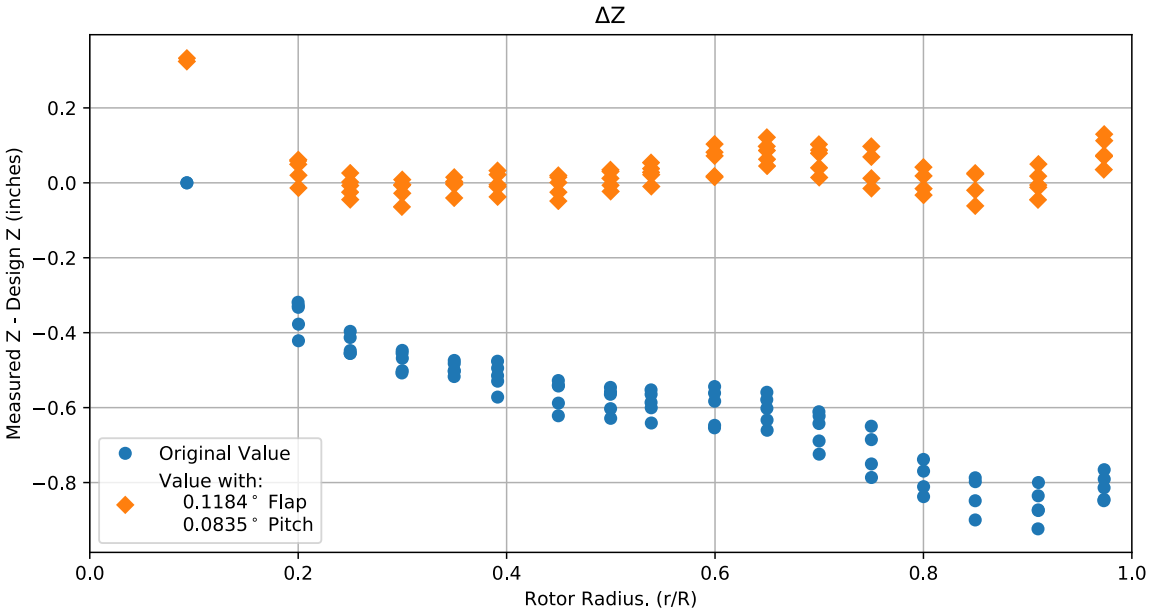

Figure 8-2. Pitch and flap target registration, ΔZ error vs rotor radius.

Note: the “as designed” geometry used for the swept tip may have some inaccuracies.

8.3: Estimated Bending and Twist at the Quarter Chord

The error bars shown represent the residual errors for fitting the measure target locations to the "as designed" geometry. These errors are generally much larger than those due to the VSTARS measurement errors. Therefore, the most likely source of these errors is the placement of the trailing-edge targets, differences between the "as designed" and "as built" geometries, and blade deformation during measurement. In the future, iterative adjustment of the "as designed" twist angle may be implemented to see if it reduces the fit error in delta twist. Note: The "as designed" geometry used for the swept tip may have some inaccuracies.

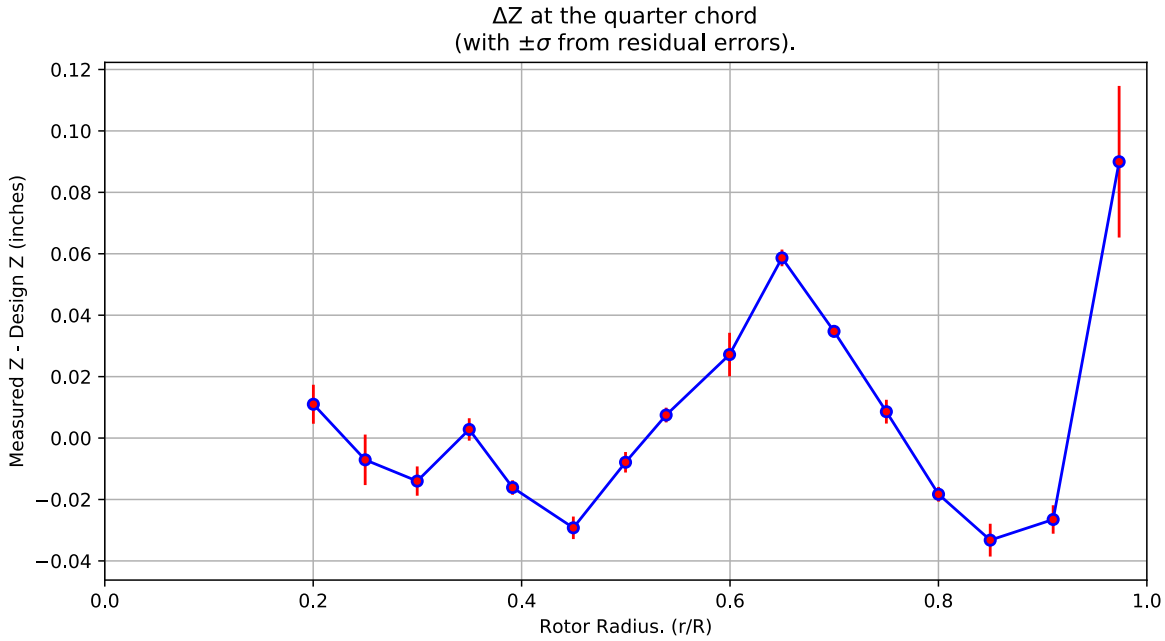

Figure 8-3. ΔZ error at the quarter chord vs rotor radius.

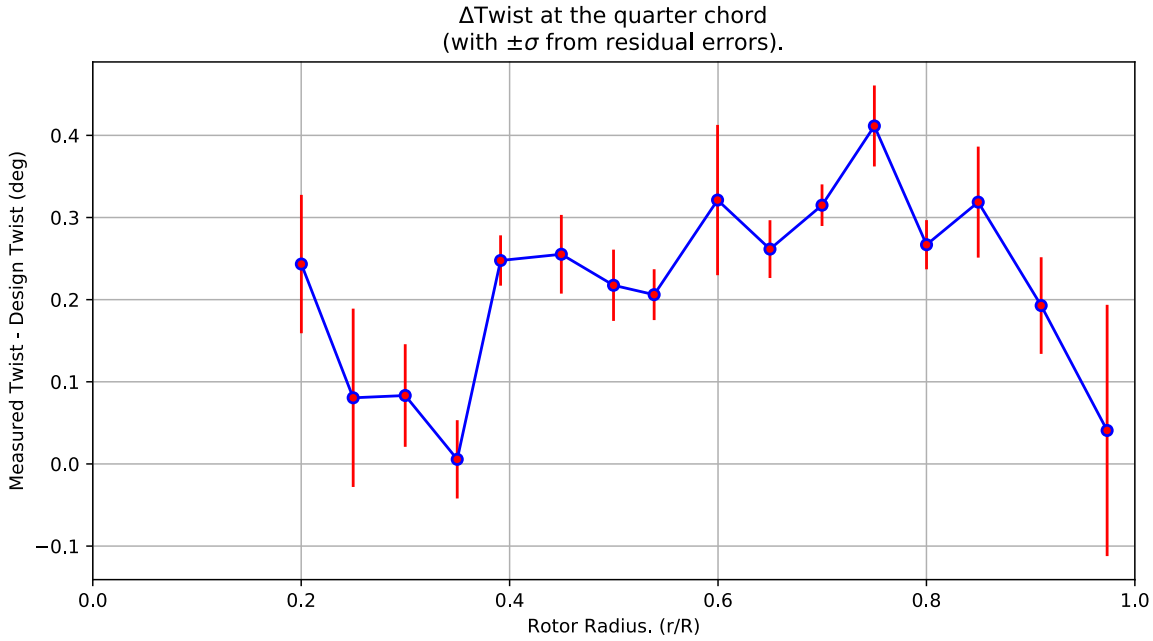

Figure 8-4. ΔTwist error at the quarter chord vs rotor radius.

Table 8-2. Quarter-chord bending and twist statistics.

r	r/R	dZ 1/4-chord	dT	sigma dZ meas	sigma dT meas	sigma dZ res	sigma dT res	n	t_conf
64.453	0.20017	0.011009	0.24334	6.1119e-10	4.6621e-09	0.0063505	0.084231	4	4.3027
80.464	0.24989	-0.007086	0.080512	6.1347e-10	4.6919e-09	0.0082239	0.10855	4	4.3027
96.543	0.29982	-0.014005	0.083297	6.1362e-10	4.6593e-09	0.0047681	0.062455	4	4.3027
112.62	0.34974	0.0028024	0.0055987	6.1462e-10	4.6684e-09	0.0036494	0.047664	4	4.3027
126.01	0.39134	-0.016106	0.24766	6.1468e-10	4.6437e-09	0.0023591	0.030641	4	4.3027
144.78	0.44963	-0.029221	0.25526	6.1363e-10	4.6468e-09	0.0036671	0.047904	4	4.3027
160.91	0.49973	-0.00788	0.21751	6.1456e-10	4.6376e-09	0.0033431	0.043387	4	4.3027
173.46	0.5387	0.0074937	0.20607	6.1677e-10	4.6504e-09	0.0024037	0.030955	4	4.3027
193.06	0.59956	0.027185	0.32125	6.1622e-10	4.6476e-09	0.0070895	0.091481	4	4.3027
209.25	0.64985	0.058654	0.26154	6.1562e-10	4.6492e-09	0.0027173	0.035176	4	4.3027
225.33	0.69979	0.03474	0.315	6.1498e-10	4.6445e-09	0.0019524	0.025325	4	4.3027
241.51	0.75003	0.0085912	0.41144	6.2097e-10	4.6848e-09	0.0038749	0.049296	4	4.3027
257.63	0.80008	-0.018301	0.26687	6.2317e-10	4.6597e-09	0.0023898	0.029939	4	4.3027
273.6	0.84968	-0.033237	0.31874	6.2021e-10	4.6451e-09	0.0053386	0.067577	4	4.3027
293.05	0.91008	-0.026511	0.19281	6.2014e-10	4.6577e-09	0.0046329	0.058823	4	4.3027
313.43	0.97339	0.089968	0.04076	8.6134e-10	4.3463e-09	0.024682	0.15295	4	4.3027

8.4: Section Plots

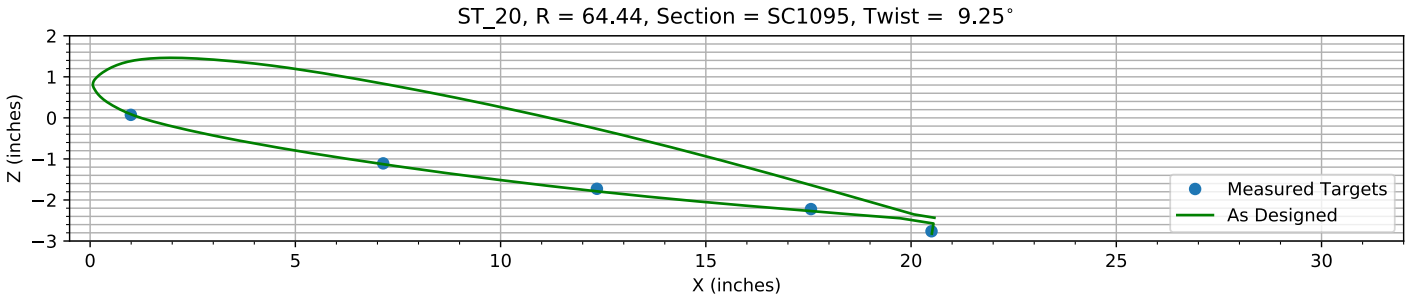

Figure 8-5. Target locations vs section profile at station 20.

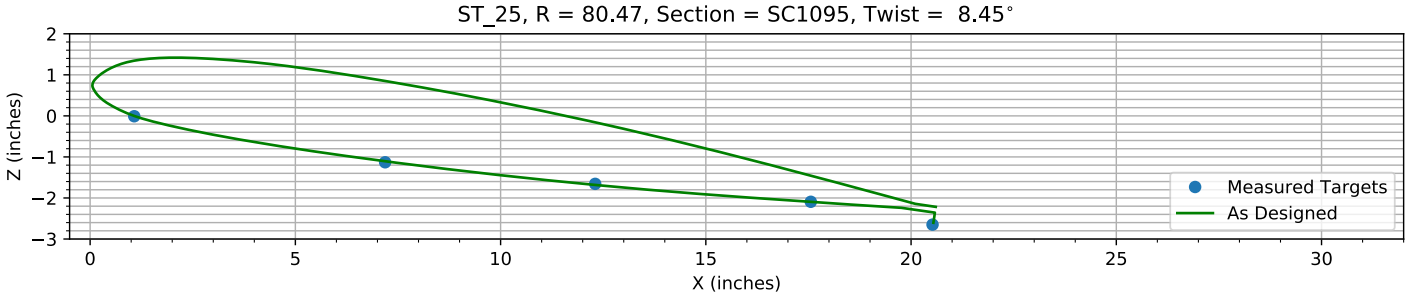

Figure 8-6. Target locations vs section profile at station 25.

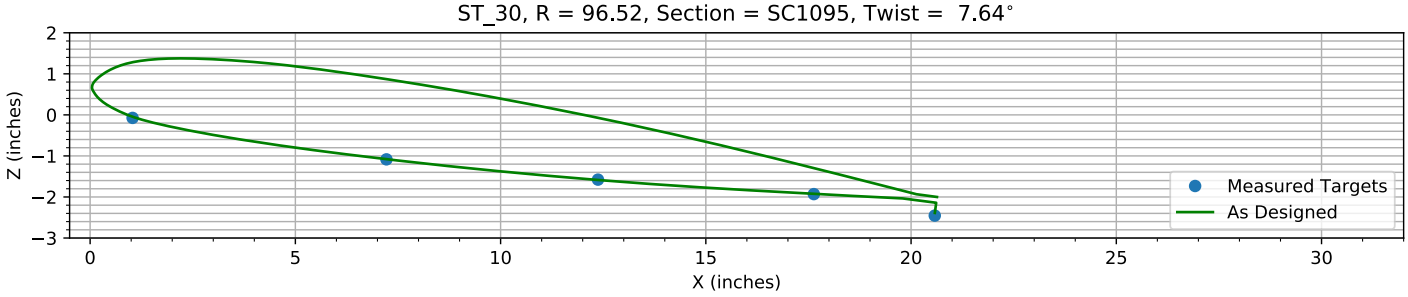

Figure 8-7. Target locations vs section profile at station 30.

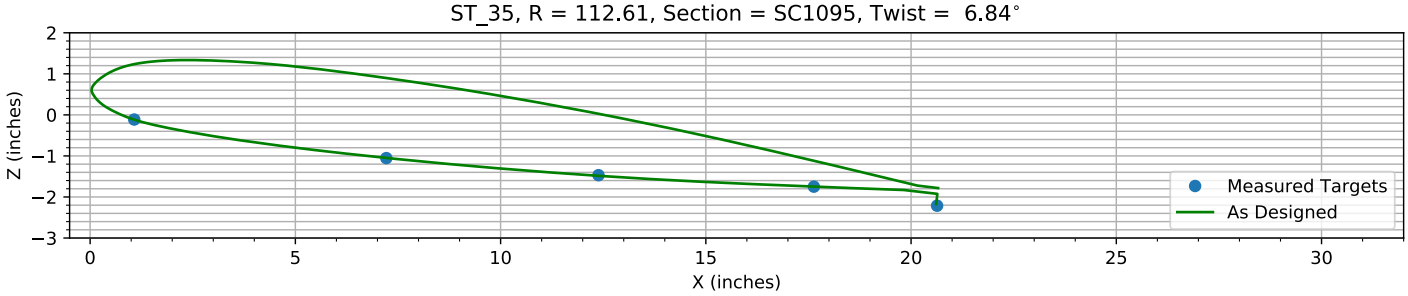

Figure 8-8. Target locations vs section profile at station 35.

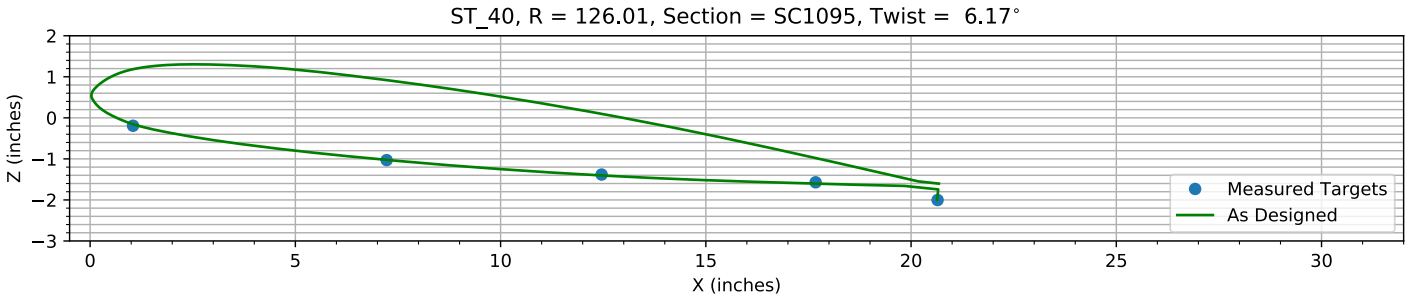

Figure 8-9. Target locations vs section profile at station 40.

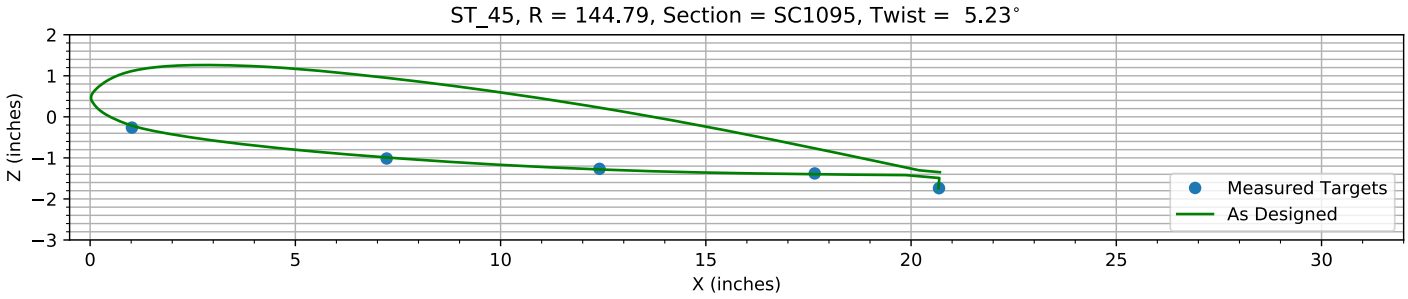

Figure 8-10. Target locations vs section profile at station 45.

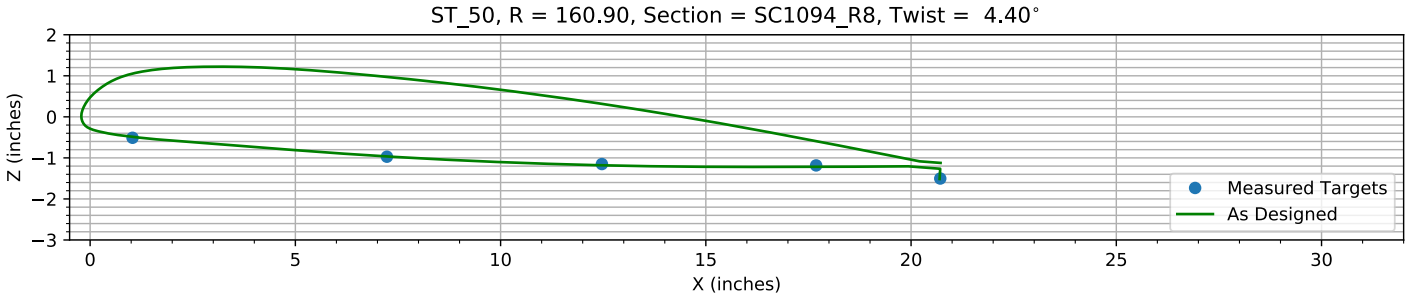

Figure 8-11. Target locations vs section profile at station 50.

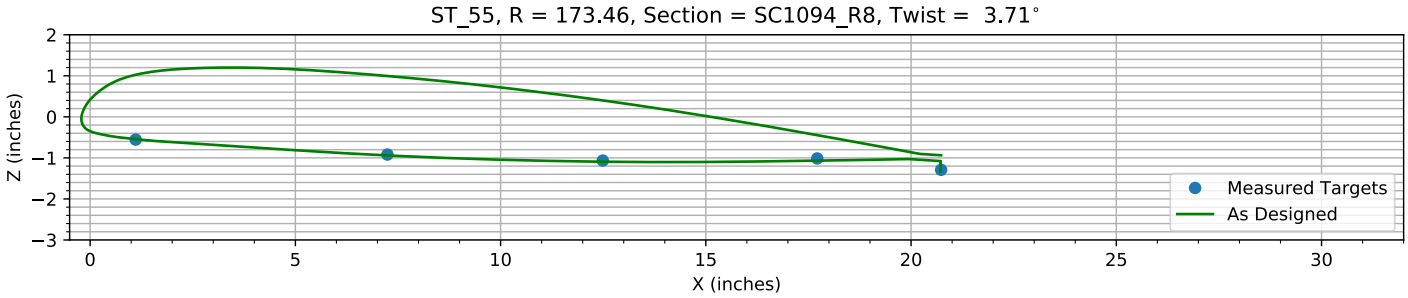

Figure 8-12. Target locations vs section profile at station 55.

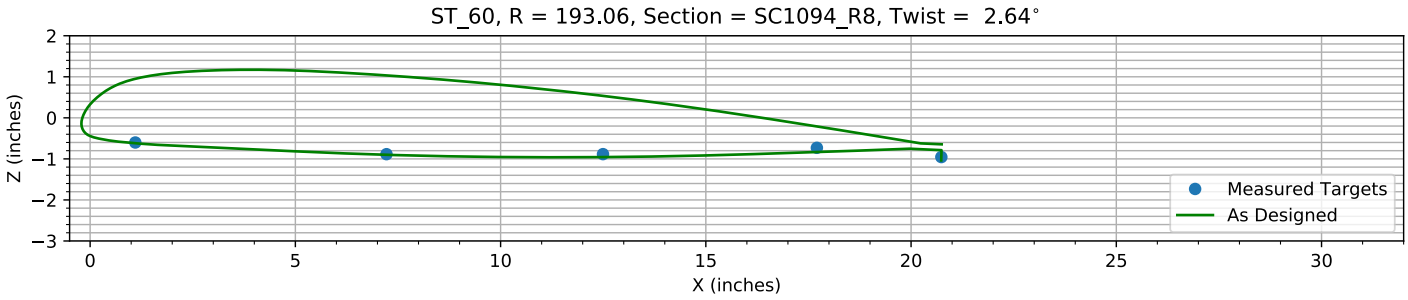

Figure 8-13. Target locations vs section profile at station 60.

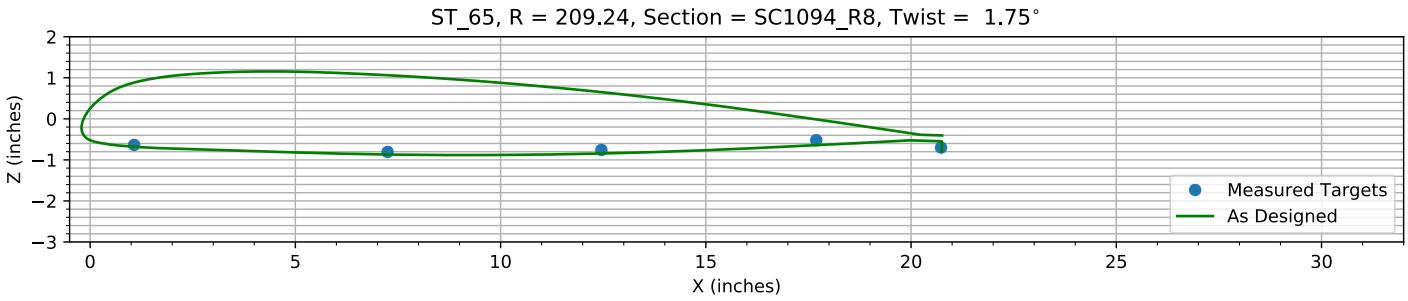

Figure 8-14. Target locations vs section profile at station 65.

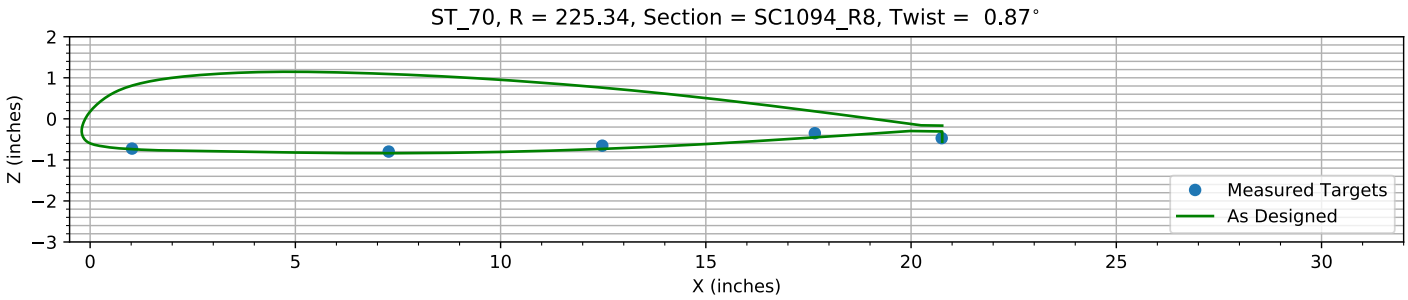

Figure 8-15. Target locations vs section profile at station 70.

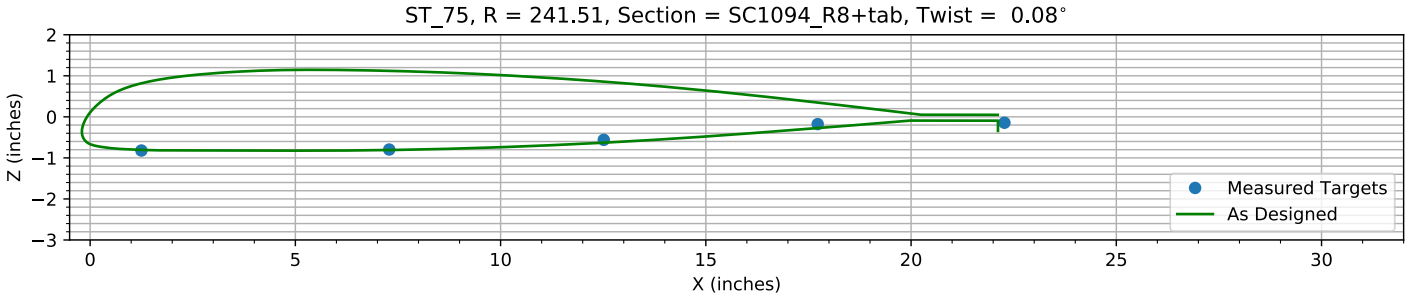

Figure 8-16. Target locations vs section profile at station 75.

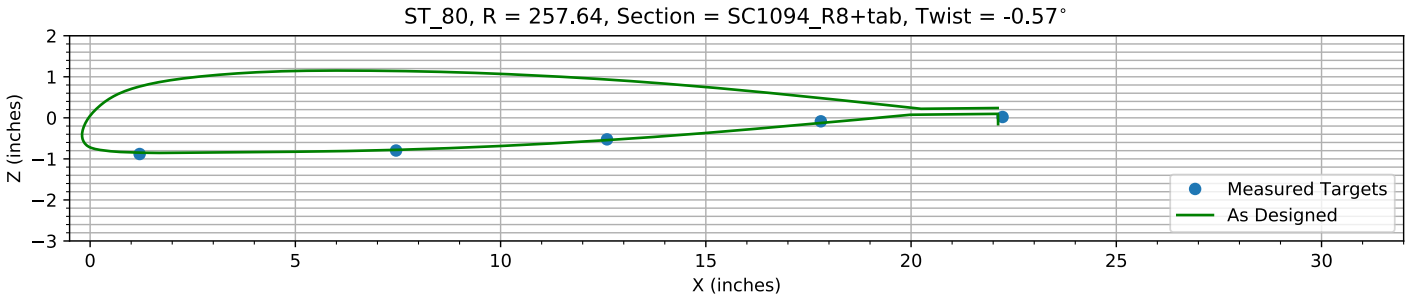

Figure 8-17. Target locations vs section profile at station 80.

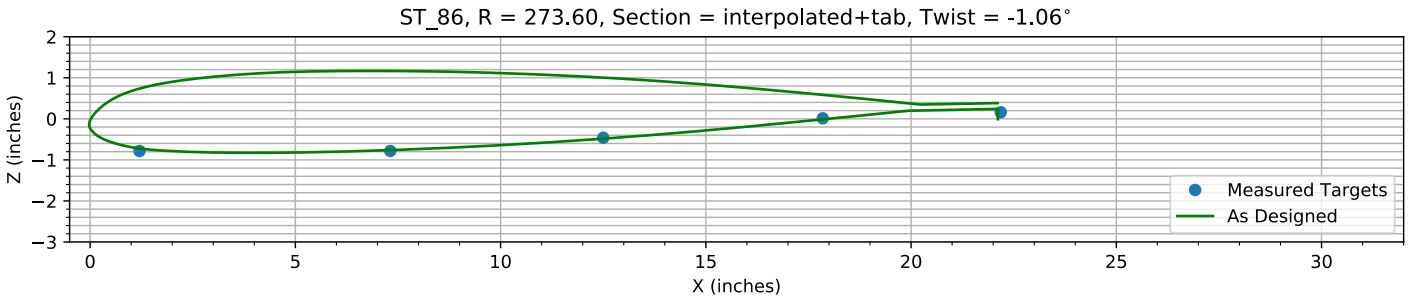

Figure 8-18. Target locations vs section profile at station 86.

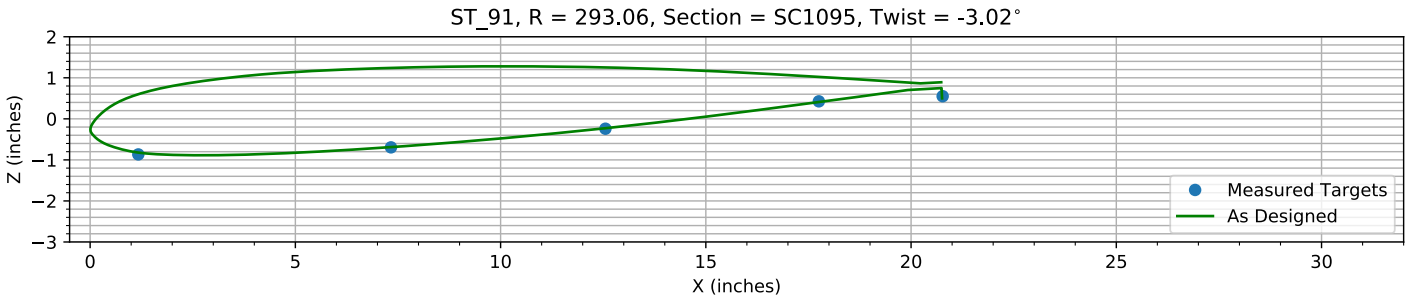

Figure 8-19. Target locations vs section profile at station 91.

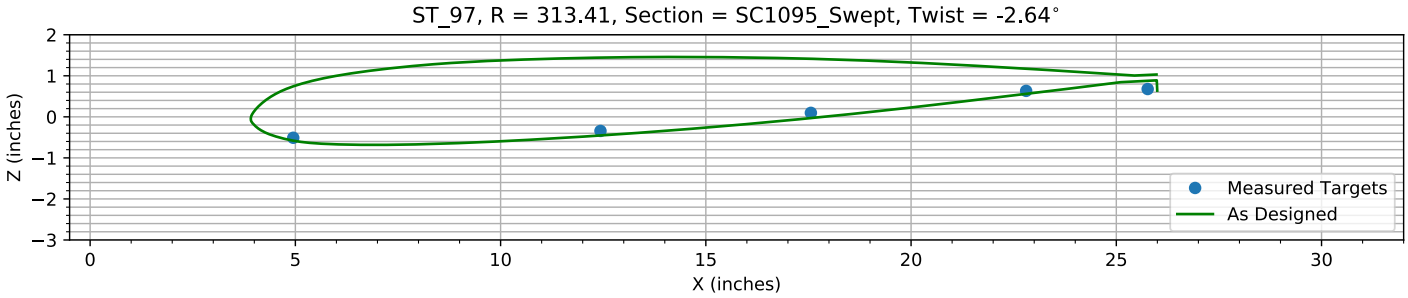

Figure 8-20. Target locations vs section profile at station 97.

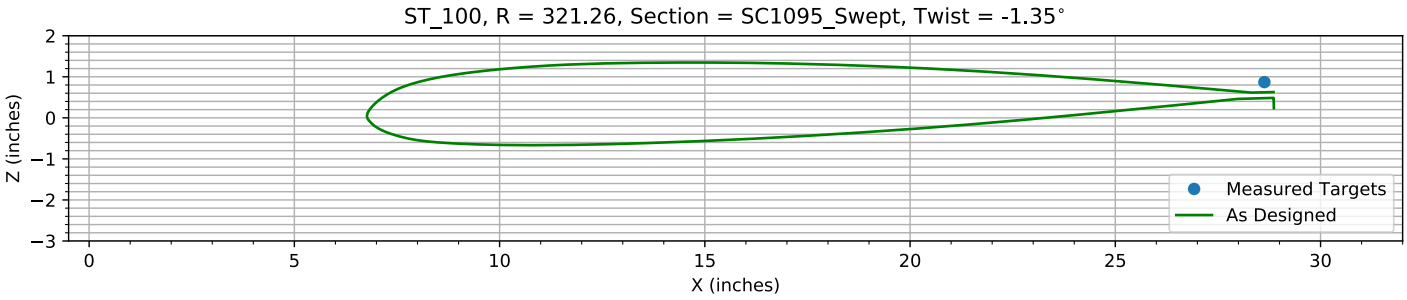

Figure 8-21. Target locations vs section profile at station 100.

Chapter 9: Pitch, Flap, and ΔZ Registration (15 rows)

The targets at the 15 spanwise stations nearest the root are used to determing the Z, flap, and pitch offset.

The estimated Z error, -0.33852 inches, is within an allowed range of ±2.000 inches.

The estimated flap error is -0.10811°.

The estimated pitch error is -0.11474°.

9.1: Target Location Errors After Target Registration

Table 9-1. Measured(1) with pitch and flap registration vs as designed(2) in inches.

Name	X1	Y1	Z1	X2	Y2	Z2	dX	dY	dZ	dR
B1_R20_C05	0.99407	64.48	0.079896	0.99407	64.48	0.086591	0	0	-0.0066951	0.0066951
B1_R20_C36	7.1411	64.488	-1.1058	7.1411	64.488	-1.129	0	0	0.023171	0.023171
B1_R20_C61	12.347	64.431	-1.728	12.347	64.431	-1.7897	0	0	0.061685	0.061685
B1_R20_C86	17.562	64.416	-2.225	17.562	64.416	-2.2717	0	0	0.046683	0.046683
B1_R20_C99	20.498	64.364	-2.7671	20.506	64.364	-2.821	-0.0073196	0	0.053946	0.05444
B1_R25_C05	1.0761	80.484	-0.0057685	1.0761	80.484	-0.002494	0	0	-0.0032745	0.0032745
B1_R25_C36	7.1884	80.445	-1.1306	7.1884	80.445	-1.1057	0	0	-0.02488	0.02488
B1_R25_C61	12.305	80.475	-1.659	12.305	80.475	-1.6824	0	0	0.02346	0.02346
B1_R25_C86	17.558	80.455	-2.0986	17.558	80.455	-2.0951	0	0	-0.0035246	0.0035246
B1_R25_C99	20.523	80.476	-2.6564	20.544	80.476	-2.6043	-0.020585	0	-0.05211	0.056028
B1_R30_C05	1.0362	96.548	-0.073277	1.0362	96.548	-0.046486	0	0	-0.02679	0.02679
B1_R30_C36	7.2204	96.574	-1.0868	7.2204	96.574	-1.0794	0	0	-0.0074647	0.0074647
B1_R30_C61	12.373	96.544	-1.5832	12.373	96.544	-1.586	0	0	0.0027947	0.0027947
B1_R30_C86	17.632	96.508	-1.9389	17.632	96.508	-1.9238	0	0	-0.015099	0.015099
B1_R30_C99	20.578	96.44	-2.4641	20.579	96.44	-2.3898	-0.0010335	0	-0.07435	0.074357
B1_R35_C05	1.0763	112.6	-0.11587	1.0763	112.6	-0.1174	0	0	0.0015287	0.0015287
B1_R35_C36	7.2176	112.63	-1.059	7.2176	112.63	-1.049	0	0	-0.010035	0.010035
B1_R35_C61	12.386	112.62	-1.4782	12.386	112.62	-1.4844	0	0	0.0062533	0.0062533
B1_R35_C86	17.633	112.61	-1.7602	17.633	112.61	-1.7477	0	0	-0.012491	0.012491
B1_R35_C99	20.634	112.59	-2.2262	20.611	112.59	-2.1726	0.023295	0	-0.053552	0.058399
B1_R40_C05	1.0466	126.02	-0.19749	1.0466	126.02	-0.15575	0	0	-0.041738	0.041738
B1_R40_C36	7.2253	126.02	-1.0382	7.2253	126.02	-1.0248	0	0	-0.013319	0.013319
B1_R40_C61	12.463	126.01	-1.3928	12.463	126.01	-1.4036	0	0	0.01083	0.01083
B1_R40_C86	17.676	125.99	-1.5845	17.676	125.99	-1.6032	0	0	0.018644	0.018644
B1_R40_C99	20.646	126	-2.0181	20.635	126	-1.9923	0.011053	0	-0.025829	0.028095
B1_R45_C05	1.02	144.78	-0.27064	1.02	144.78	-0.21433	0	0	-0.056309	0.056309
B1_R45_C36	7.2251	144.8	-1.0267	7.2251	144.8	-0.9902	0	0	-0.036523	0.036523
B1_R45_C61	12.41	144.78	-1.2812	12.41	144.78	-1.2818	0	0	0.00063305	0.00063305
B1_R45_C86	17.654	144.78	-1.3958	17.654	144.78	-1.3983	0	0	0.0025052	0.0025052
B1_R45_C99	20.681	144.8	-1.7573	20.666	144.8	-1.7392	0.015535	0	-0.018102	0.023854
B1_R50_C05	1.0346	160.95	-0.52135	1.0346	160.95	-0.48743	0	0	-0.033928	0.033928
B1_R50_C36	7.232	160.92	-0.98592	7.232	160.92	-0.96495	0	0	-0.020966	0.020966
B1_R50_C61	12.469	160.9	-1.1676	12.469	160.9	-1.1805	0	0	0.012893	0.012893
B1_R50_C86	17.688	160.88	-1.2034	17.688	160.88	-1.2179	0	0	0.014476	0.014476
B1_R50_C99	20.712	160.87	-1.5246	20.695	160.87	-1.5147	0.01687	0	-0.0099207	0.019571
B1_R55_C05	1.1119	173.51	-0.56771	1.1119	173.51	-0.54471	0	0	-0.022998	0.022998

Name	X1	Y1	Z1	X2	Y2	Z2	dX	dY	dZ	dR
B1_R55_C36	7.2449	173.48	-0.93544	7.2449	173.48	-0.94044	0	0	0.0050025	0.0050025
B1_R55_C61	12.49	173.43	-1.085	12.49	173.43	-1.0934	0	0	0.0083404	0.0083404
B1_R55_C86	17.715	173.42	-1.0364	17.715	173.42	-1.0678	0	0	0.031418	0.031418
B1_R55_C99	20.733	173.45	-1.3146	20.712	173.45	-1.3283	0.020803	0	0.013677	0.024897
B1_R60_C05	1.1022	193.03	-0.61796	1.1022	193.03	-0.61889	0	0	0.0009315	0.0009315
B1_R60_C36	7.2216	193.06	-0.90565	7.2216	193.06	-0.90065	0	0	-0.0049918	0.0049918
B1_R60_C61	12.496	193.08	-0.90758	12.496	193.08	-0.9563	0	0	0.048718	0.048718
B1_R60_C86	17.707	193.06	-0.75634	17.707	193.06	-0.83359	0	0	0.077251	0.077251
B1_R60_C99	20.739	193.05	-0.98345	20.734	193.05	-1.0375	0.0044476	0	0.054034	0.054217
B1_R65_C05	1.0732	209.29	-0.65451	1.0732	209.29	-0.67956	0	0	0.025058	0.025058
B1_R65_C36	7.2485	209.27	-0.82962	7.2485	209.27	-0.86928	0	0	0.039667	0.039667
B1_R65_C61	12.456	209.23	-0.78463	12.456	209.23	-0.8448	0	0	0.060164	0.060164
B1_R65_C86	17.692	209.21	-0.54934	17.692	209.21	-0.64174	0	0	0.092404	0.092404
B1_R65_C99	20.731	209.18	-0.73098	20.748	209.18	-0.79781	-0.017103	0	0.066822	0.068976
B1_R70_C05	1.0223	225.38	-0.74764	1.0223	225.38	-0.73927	0	0	-0.0083772	0.0083772
B1_R70_C36	7.2758	225.35	-0.82354	7.2758	225.35	-0.83757	0	0	0.014029	0.014029
B1_R70_C61	12.479	225.31	-0.68282	12.479	225.31	-0.73268	0	0	0.049862	0.049862
B1_R70_C86	17.657	225.29	-0.38172	17.657	225.29	-0.4525	0	0	0.070781	0.070781
B1_R70_C99	20.748	225.36	-0.50369	20.759	225.36	-0.5574	-0.010868	0	0.053707	0.054796
B1_R75_C05	1.2505	241.53	-0.84643	1.2505	241.53	-0.80571	0	0	-0.040718	0.040718
B1_R75_C36	7.2877	241.52	-0.82545	7.2877	241.52	-0.80851	0	0	-0.016937	0.016937
B1_R75_C61	12.515	241.5	-0.59254	12.515	241.5	-0.62981	0	0	0.037267	0.037267
B1_R75_C86	17.727	241.48	-0.21151	17.727	241.48	-0.2739	0	0	0.062386	0.062386
B1_R80_C05	1.2073	257.63	-0.90986	1.2073	257.63	-0.84847	0	0	-0.061388	0.061388
B1_R80_C36	7.4549	257.64	-0.82826	7.4549	257.64	-0.78072	0	0	-0.047542	0.047542
B1_R80_C61	12.594	257.63	-0.55937	12.594	257.63	-0.54282	0	0	-0.016548	0.016548
B1_R80_C86	17.804	257.6	-0.12246	17.804	257.6	-0.12639	0	0	0.0039311	0.0039311
B1_R86_C05	1.2047	273.59	-0.81544	1.2047	273.59	-0.72257	0	0	-0.09287	0.09287
B1_R86_C36	7.3138	273.59	-0.81708	7.3138	273.59	-0.7623	0	0	-0.054779	0.054779
B1_R86_C61	12.503	273.62	-0.49802	12.503	273.62	-0.48358	0	0	-0.014439	0.014439
B1_R86_C86	17.85	273.59	-0.027869	17.85	273.59	-0.012869	0	0	-0.015	0.015
B1_R91_C05	1.175	292.99	-0.90197	1.175	292.99	-0.82189	0	0	-0.080083	0.080083
B1_R91_C36	7.3309	293.07	-0.73326	7.3309	293.07	-0.68894	0	0	-0.044319	0.044319
B1_R91_C61	12.556	293.07	-0.28171	12.556	293.07	-0.22828	0	0	-0.05343	0.05343
B1_R91_C86	17.756	293.06	0.38244	17.756	293.06	0.40896	0	0	-0.02651	0.02651
B1_R91_C99	20.772	293.13	0.50564	20.755	293.13	0.50147	0.016271	0	0.004168	0.016796
B1_R97_C05	4.95	313.41	-0.5506	4.95	313.41	-0.58073	0	0	0.030132	0.030132
B1_R97_C36	12.435	313.46	-0.3879	12.435	313.46	-0.45545	0	0	0.067548	0.067548
B1_R97_C61	17.561	313.45	0.049662	17.561	313.45	-0.032311	0	0	0.081973	0.081973
B1_R97_C86	22.805	313.41	0.58234	22.805	313.41	0.55966	0	0	0.022676	0.022676
B1_R97_C99	25.766	313.32	0.62565	25.966	313.32	0.6424	-0.1996	0	-0.01675	0.2003
HUB_LE	2.2658	30.004	-3.1557	2.19	30	-3.5	0.075822	0.0038721	0.34428	0.35255
HUB_TE	8.2624	29.995	-3.1675	8.19	30	-3.5	0.072403	-0.0053761	0.33246	0.34029
RMS Errors:							0.026055	0.00074541	0.067054	0.071941

9.2: Pitch and Flap Registration Plots (15 rows)

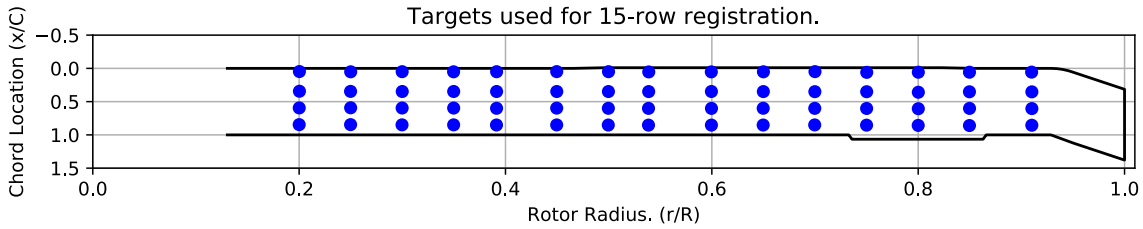

Figure 9-1. Targets used for 15 row root registration.

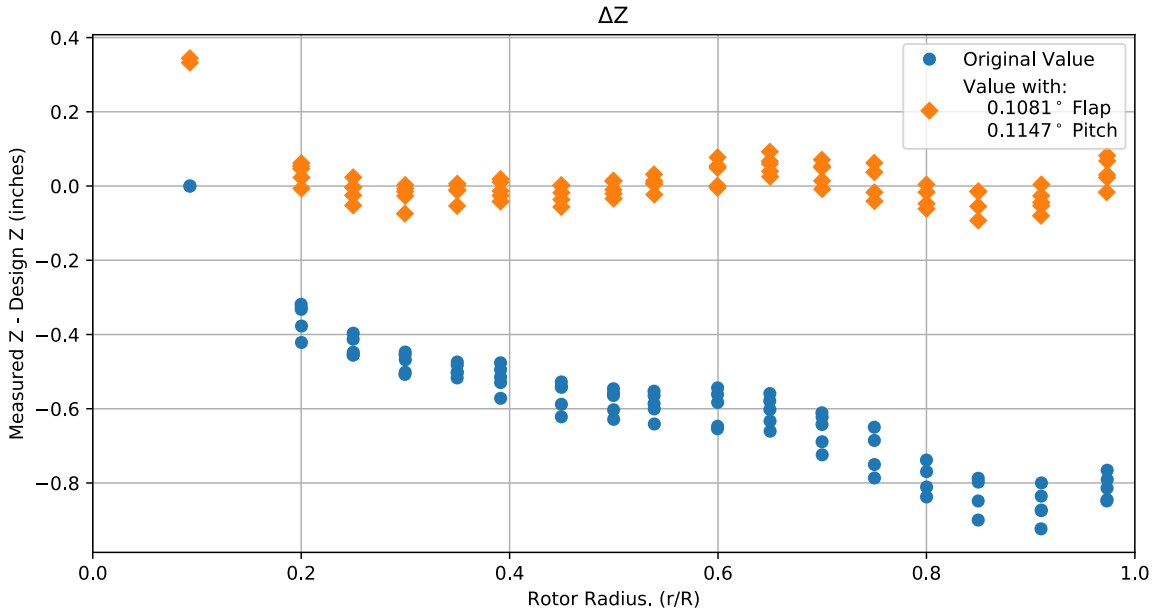

Figure 9-2. Pitch and flap target registration, ΔZ error vs rotor radius.

Note: the “as designed” geometry used for the swept tip may have some inaccuracies.

9.3: Estimated Bending and Twist at the Quarter Chord

The error bars shown represent the residual errors for fitting the measure target locations to the "as designed" geometry. These errors are generally much larger than those due to the VSTARS measurement errors. Therefore, the most likely source of these errors is the placement of the trailing-edge targets, differences between the "as designed" and "as built" geometries, and blade deformation during measurement. In the future, iterative adjustment of the "as designed" twist angle may be implemented to see if it reduces the fit error in delta twist. Note: The "as designed" geometry used for the swept tip may have some inaccuracies.

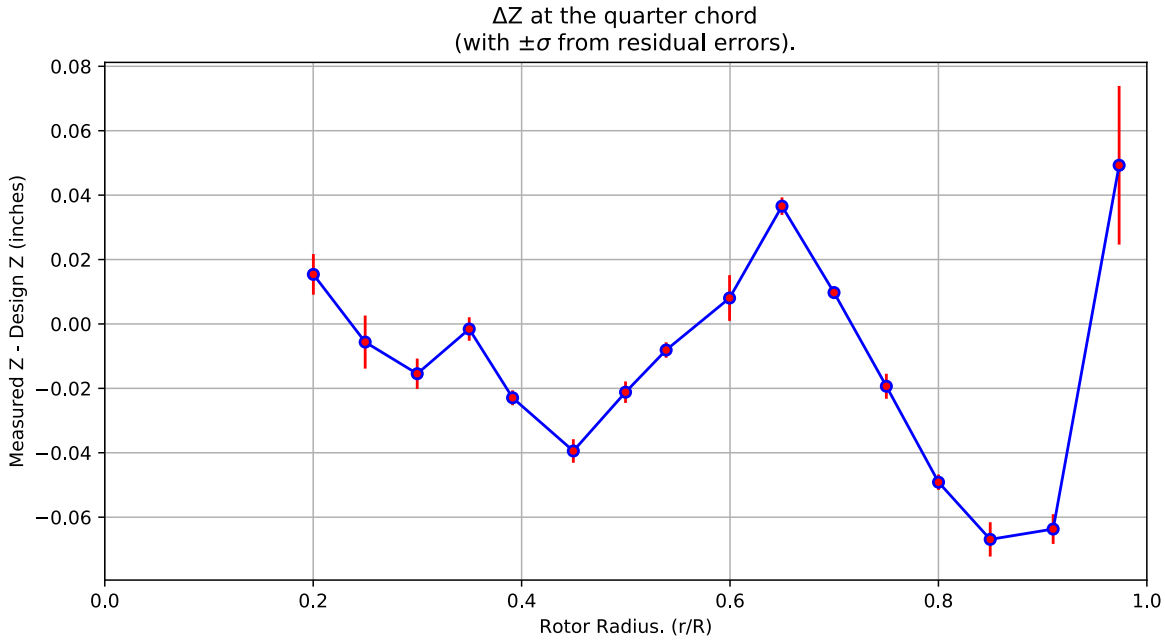

Figure 9-3. ΔZ error at the quarter chord vs rotor radius.

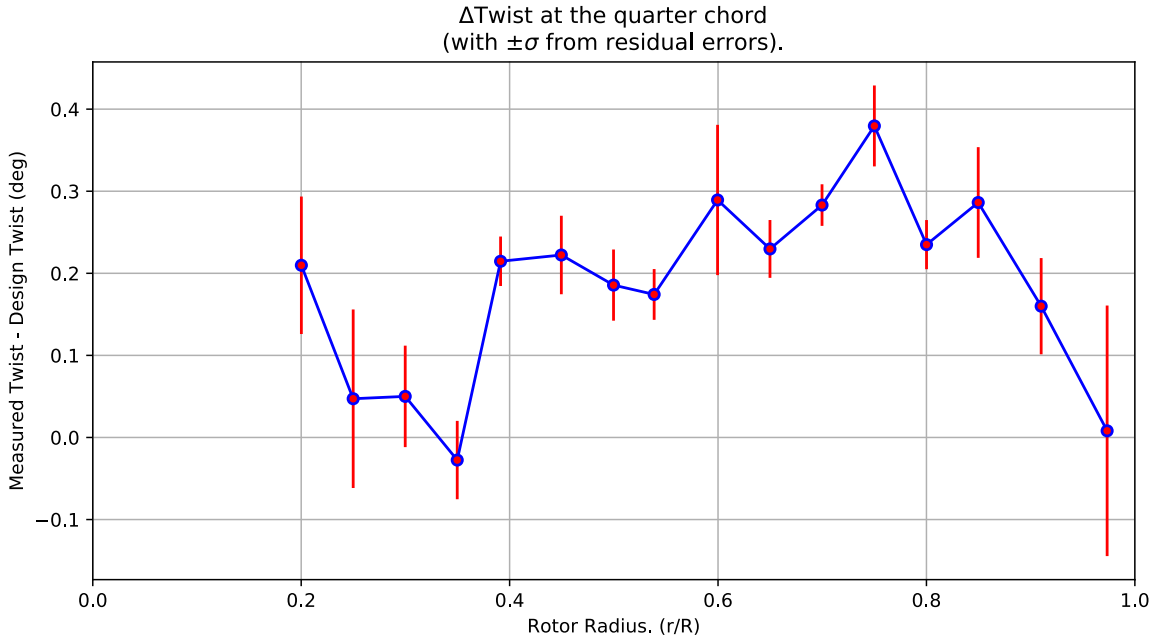

Figure 9-4. ΔTwist error at the quarter chord vs rotor radius.

Table 9-2. Quarter-chord bending and twist statistics.

r	r/R	dZ 1/4-chord	dT	sigma dZ meas	sigma dT meas	sigma dZ res	sigma dT res	n	t_conf
64.454	0.20017	0.015391	0.20977	6.1126e-10	4.6625e-09	0.0063162	0.083752	4	4.3027
80.465	0.24989	-0.0056302	0.047178	6.1355e-10	4.6922e-09	0.0082421	0.10876	4	4.3027
96.544	0.29983	-0.015461	0.050041	6.1369e-10	4.6595e-09	0.0047204	0.061812	4	4.3027
112.62	0.34974	-0.0015779	-0.027527	6.1469e-10	4.6686e-09	0.0036557	0.047732	4	4.3027
126.01	0.39134	-0.022927	0.21466	6.1475e-10	4.6439e-09	0.0023212	0.030139	4	4.3027
144.78	0.44964	-0.039446	0.2223	6.137e-10	4.647e-09	0.003662	0.047822	4	4.3027
160.91	0.49973	-0.021189	0.18563	6.1463e-10	4.6377e-09	0.0033428	0.04337	4	4.3027
173.46	0.5387	-0.0080934	0.17424	6.1684e-10	4.6505e-09	0.002402	0.030924	4	4.3027
193.06	0.59956	0.0080475	0.28934	6.1629e-10	4.6476e-09	0.0070971	0.091549	4	4.3027
209.25	0.64985	0.036574	0.22969	6.1569e-10	4.6492e-09	0.0027221	0.035226	4	4.3027
225.33	0.6998	0.0097402	0.28313	6.1505e-10	4.6445e-09	0.0019541	0.02534	4	4.3027
241.51	0.75003	-0.019343	0.37954	6.2104e-10	4.6847e-09	0.0038763	0.049297	4	4.3027
257.63	0.80008	-0.049145	0.23493	6.2324e-10	4.6596e-09	0.0023909	0.029943	4	4.3027
273.6	0.84968	-0.066893	0.28625	6.2028e-10	4.645e-09	0.005329	0.067433	4	4.3027
293.05	0.91009	-0.063687	0.15994	6.2021e-10	4.6575e-09	0.0046186	0.05862	4	4.3027
313.43	0.97339	0.049275	0.0081003	8.6143e-10	4.3461e-09	0.024635	0.15263	4	4.3027

9.4: Section Plots

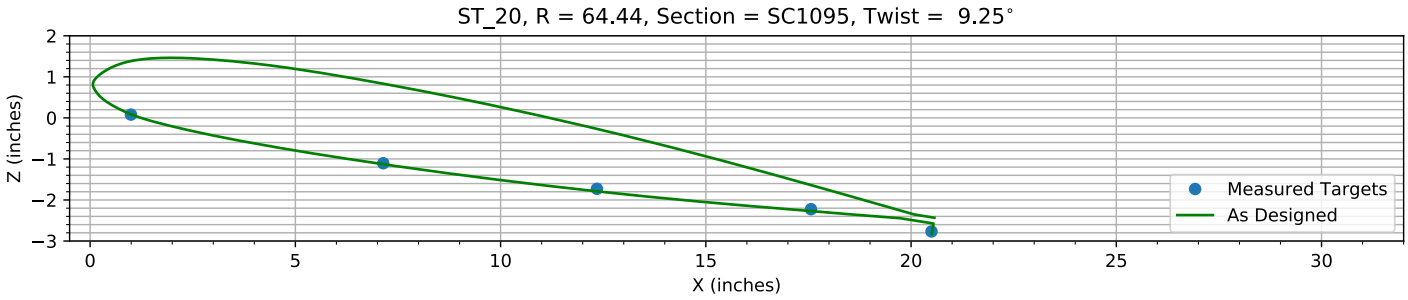

Figure 9-5. Target locations vs section profile at station 20.

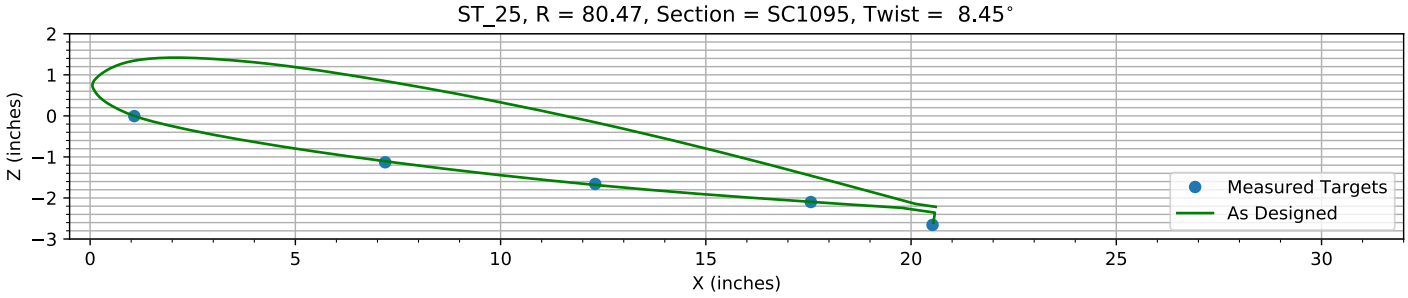

Figure 9-6. Target locations vs section profile at station 25.

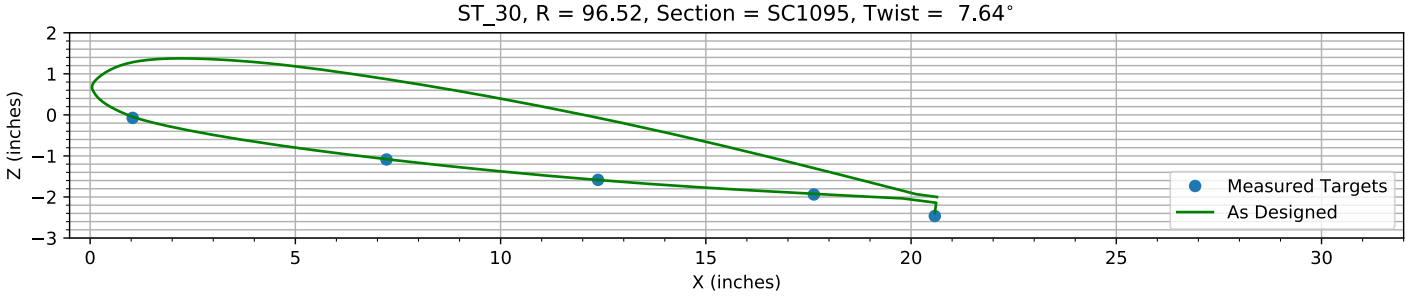

Figure 9-7. Target locations vs section profile at station 30.

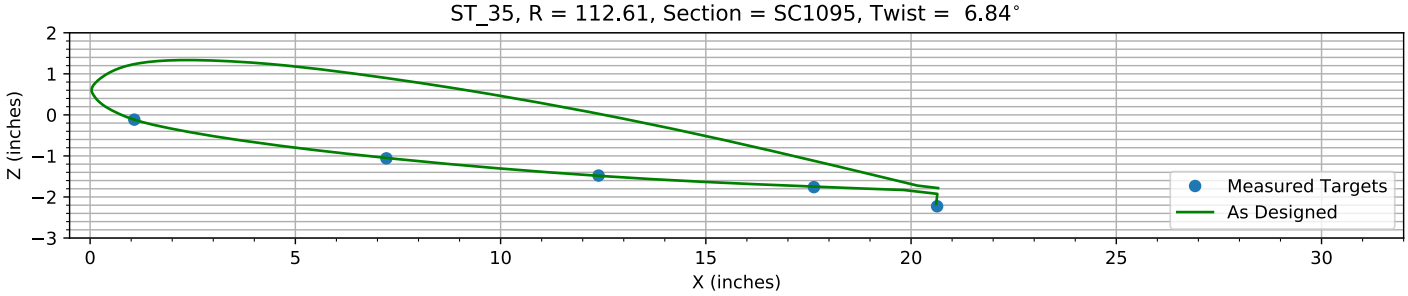

Figure 9-8. Target locations vs section profile at station 35.

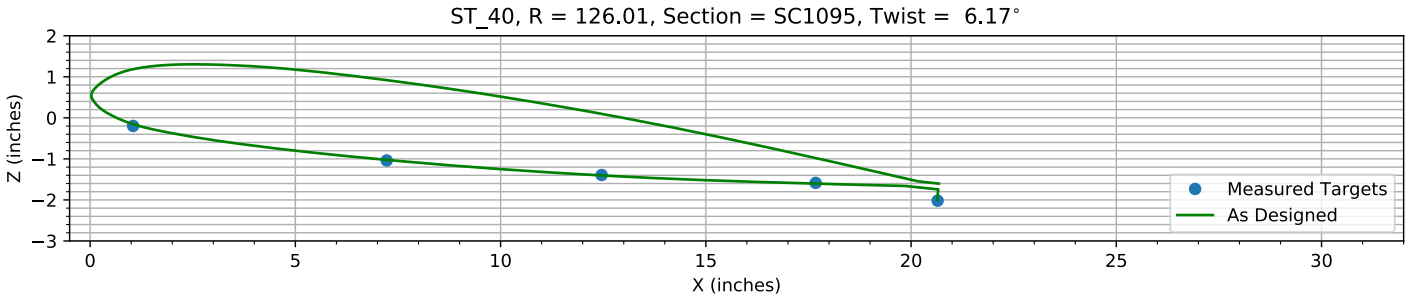

Figure 9-9. Target locations vs section profile at station 40.

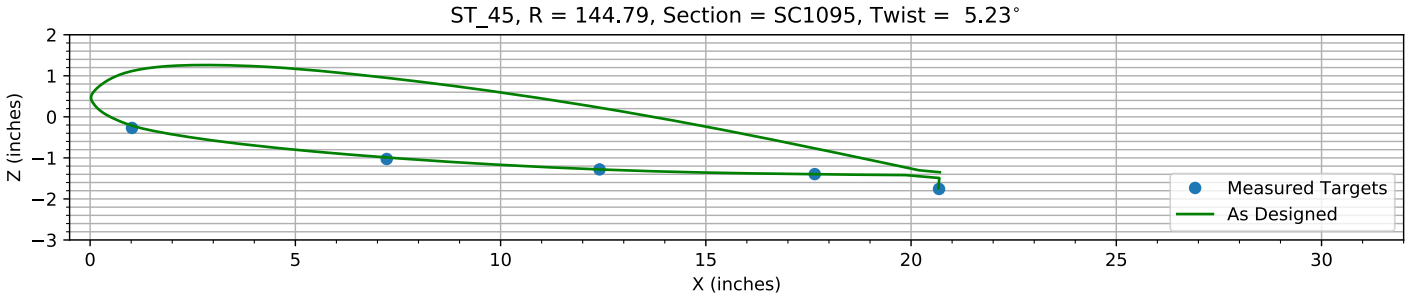

Figure 9-10. Target locations vs section profile at station 45.

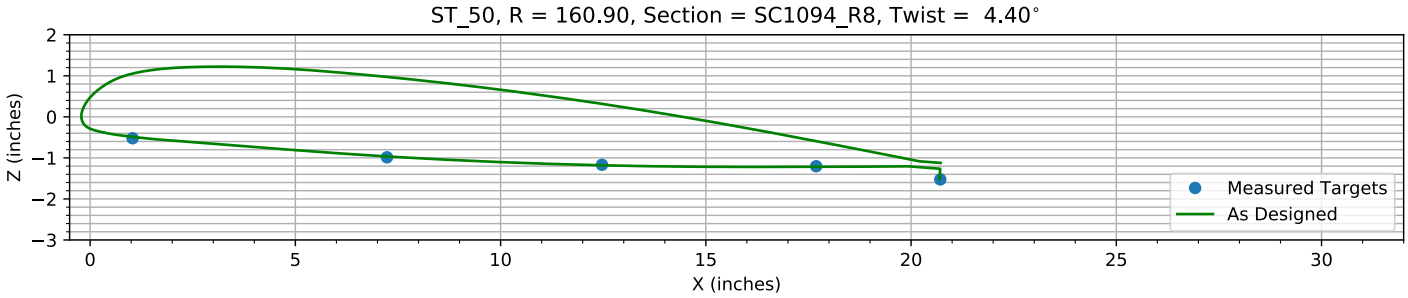

Figure 9-11. Target locations vs section profile at station 50.

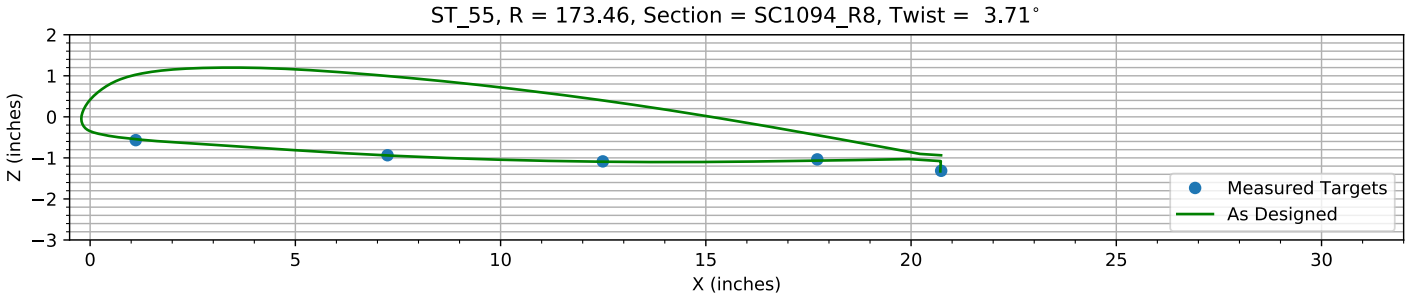

Figure 9-12. Target locations vs section profile at station 55.

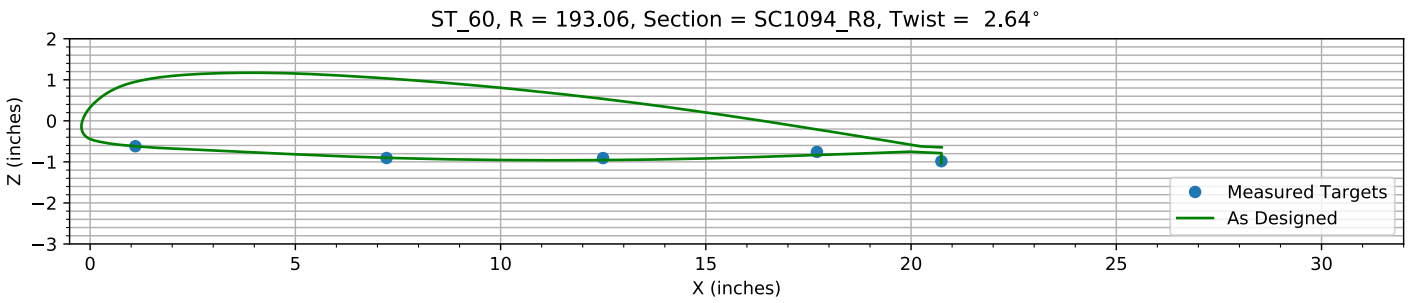

Figure 9-13. Target locations vs section profile at station 60.

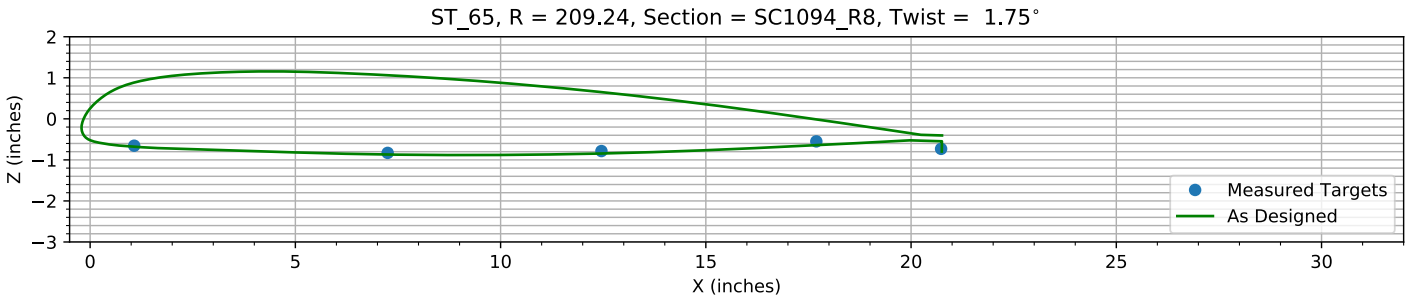

Figure 9-14. Target locations vs section profile at station 65.

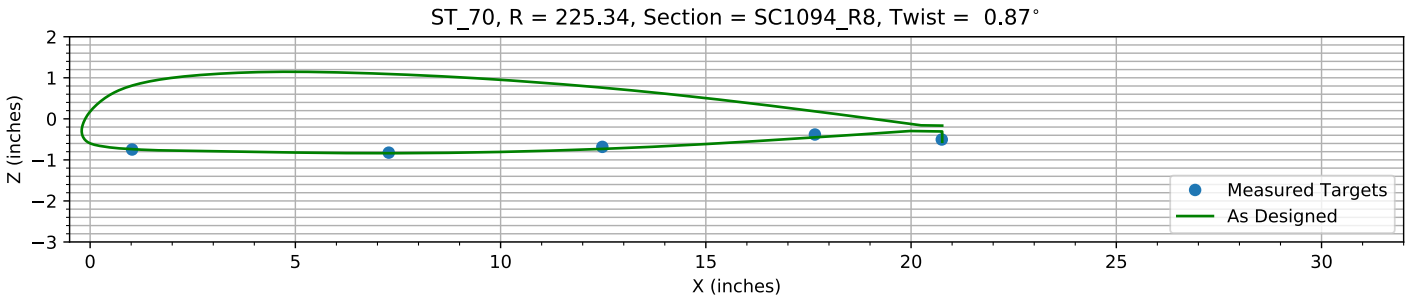

Figure 9-15. Target locations vs section profile at station 70.

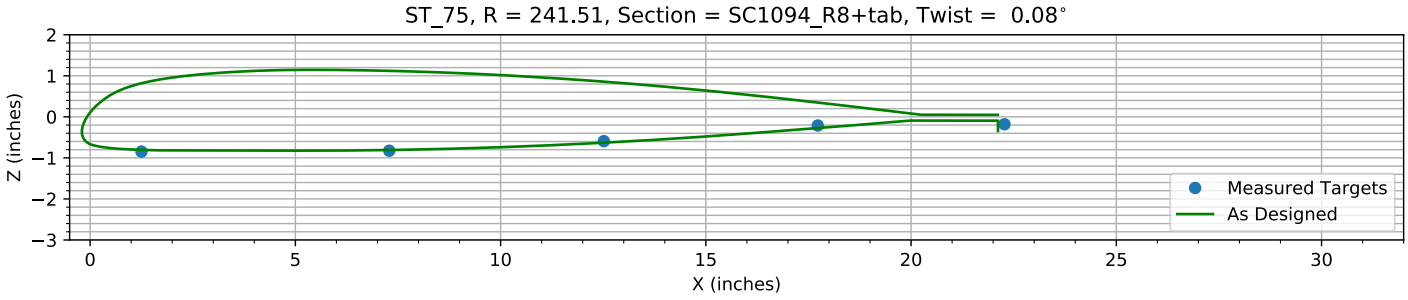

Figure 9-16. Target locations vs section profile at station 75.

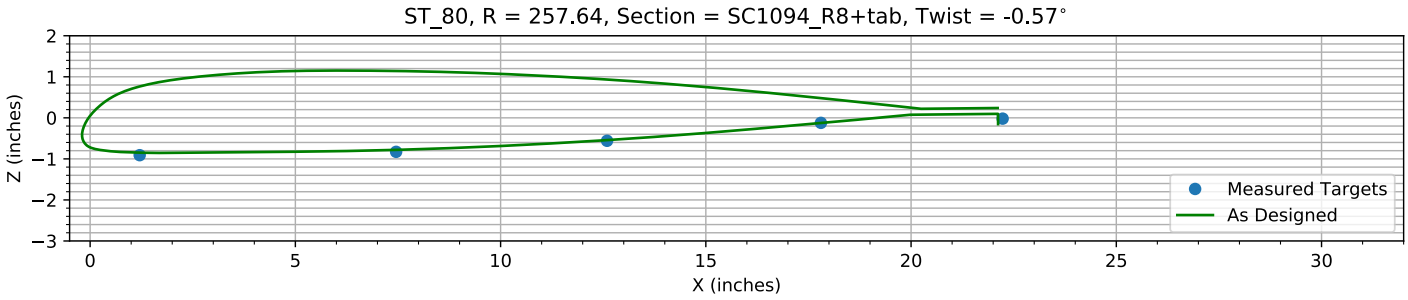

Figure 9-17. Target locations vs section profile at station 80.

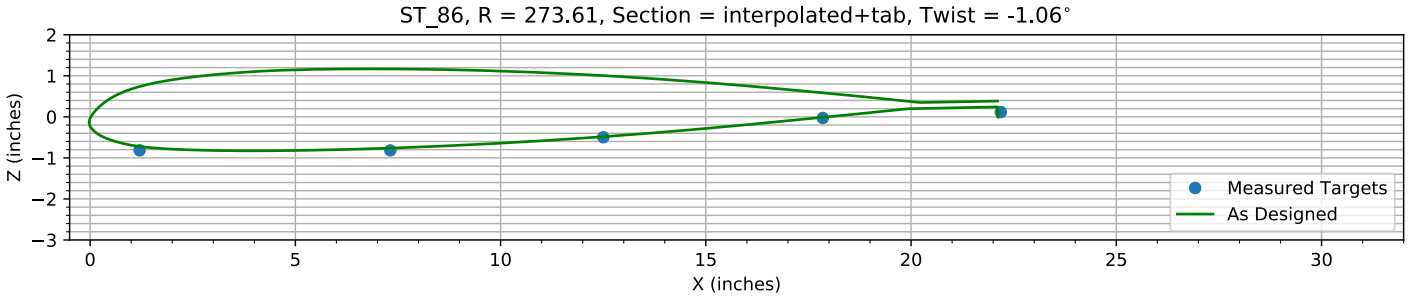

Figure 9-18. Target locations vs section profile at station 86.

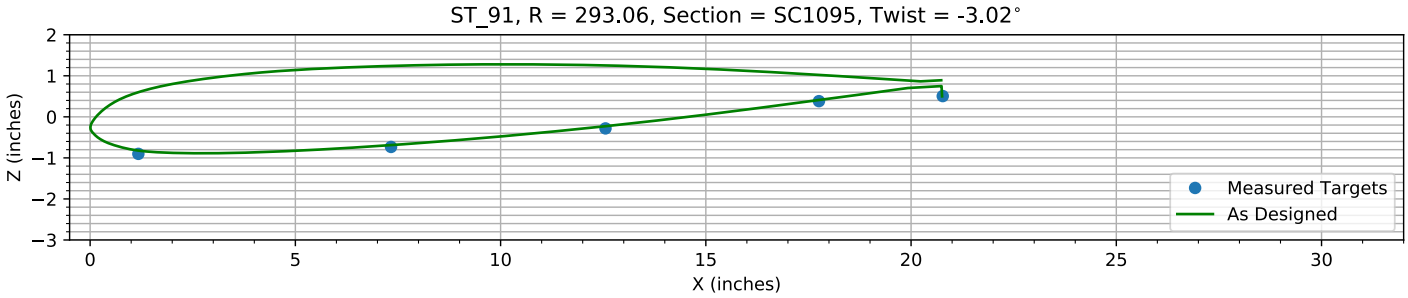

Figure 9-19. Target locations vs section profile at station 91.

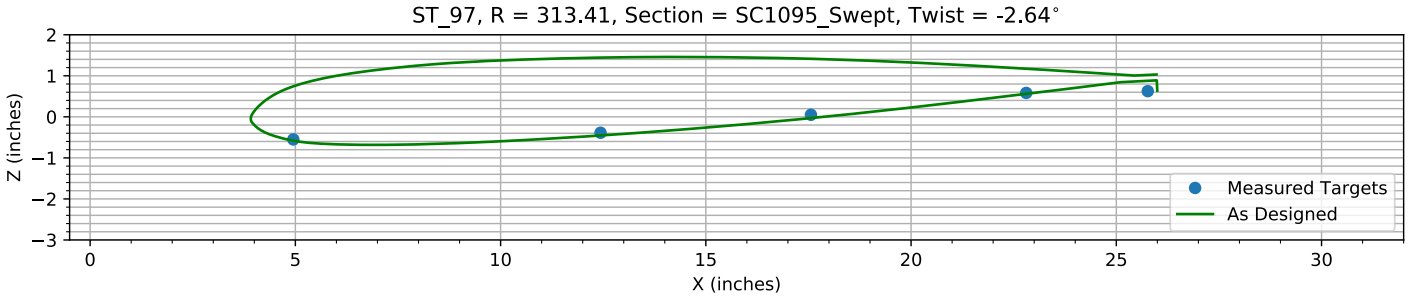

Figure 9-20. Target locations vs section profile at station 97.

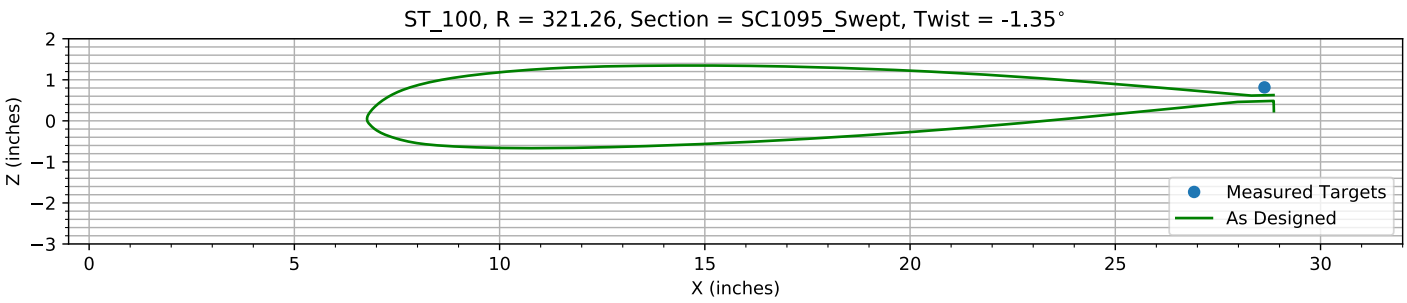

Figure 9-21. Target locations vs section profile at station 100.

I.2 Blade 2

The blade target registration report for Blade 2 is included here. It is based on the most recent V-STARS target location data for the vertically suspended blade. The condition of target 4 had degraded too much for the V-STARS system to measure it for this last measurement session, so its location was estimated based on its relative distance to nearby targets from previous V-STARS measurements.

Blade Target Registration

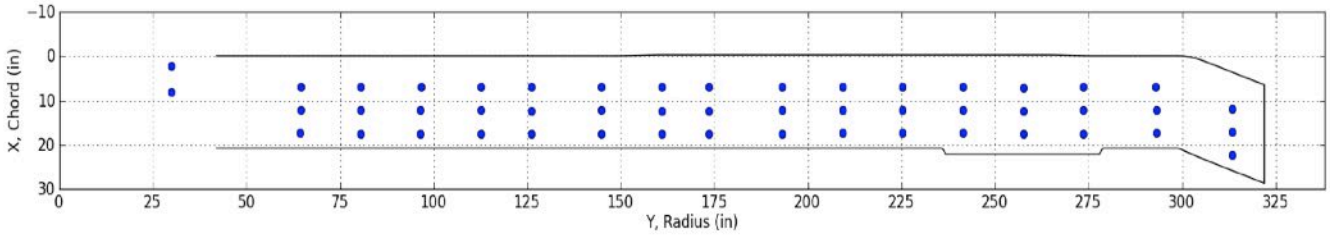

Registration Report for Blade Number 2

File: Blade 2 092512 vertical(1)_4.csv

Z reference allowed ±2.00 inches of travel

Aeromechanics Branch
Flight Vehicle Research and Technology Division
NASA Ames Research Center
Moffett Field, CA 94035

Chapter 1: VSTARS Target Location Data

Table 1-1. VSTARS target measurements (inches).

Name	Number	X	Y	Z	sigma X	sigma Y	sigma Z
B2_R20_C05		0.9746	62.789	-0.3295	0.0004	0.0004	0.0009
B2_R20_C36	1	7.0802	62.771	-1.5184	0.0006	0.0007	0.0019
B2_R20_C61	2	12.246	62.763	-2.1034	0.0005	0.0005	0.0013
B2_R20_C86	3	17.495	62.769	-2.583	0.0004	0.0004	0.0007
B2_R20_C99		20.43	62.731	-3.1713	0.0004	0.0004	0.0007
B2_R25_C05		0.9808	77.405	-0.4217	0.0004	0.0004	0.0009
B2_R25_C61	5	12.249	77.434	-2.08	0.0004	0.0004	0.0008
B2_R25_C86	6	17.466	77.441	-2.5364	0.0004	0.0004	0.0007
B2_R25_C99		20.421	77.407	-3.0824	0.0004	0.0004	0.0006
B2_R30_C05		0.9252	96.625	-0.5311	0.0004	0.0004	0.0008
B2_R30_C36	7	6.9991	96.593	-1.527	0.0004	0.0004	0.0006
B2_R30_C61	8	12.234	96.549	-2.02	0.0004	0.0004	0.0006
B2_R30_C86	9	17.432	96.543	-2.3645	0.0003	0.0004	0.0006
B2_R30_C99		20.444	96.534	-2.8971	0.0003	0.0003	0.0006
B2_R35_C05		1.0515	112.64	-0.6299	0.0003	0.0004	0.0006
B2_R35_C36	10	7.0801	112.65	-1.5387	0.0004	0.0004	0.0007
B2_R35_C61	11	12.353	112.67	-1.9552	0.0003	0.0004	0.0006
B2_R35_C86	12	17.533	112.65	-2.2158	0.0003	0.0004	0.0006
B2_R35_C99		20.512	112.62	-2.6949	0.0003	0.0004	0.0006
B2_R40_C05		1.0115	128.83	-0.7578	0.0004	0.0004	0.0007
B2_R40_C36	13	7.0966	128.78	-1.5409	0.0004	0.0004	0.0006
B2_R40_C61	14	12.339	128.77	-1.8782	0.0004	0.0004	0.0006
B2_R40_C86	15	17.558	128.69	-2.0676	0.0003	0.0004	0.0005
B2_R40_C99		20.522	128.7	-2.4998	0.0003	0.0004	0.0005
B2_R45_C05		0.9545	144.79	-0.8413	0.0003	0.0004	0.0007
B2_R45_C36	16	7.0633	144.77	-1.5688	0.0003	0.0004	0.0005
B2_R45_C61	17	12.264	144.8	-1.8122	0.0004	0.0004	0.0006
B2_R45_C86	18	17.564	144.8	-1.93	0.0003	0.0004	0.0005
B2_R45_C99		20.534	144.78	-2.3167	0.0003	0.0004	0.0005
B2_R50_C05		0.9062	160.82	-1.0984	0.0003	0.0004	0.0005
B2_R50_C36	19	7.1011	160.85	-1.5439	0.0006	0.0005	0.0007
B2_R50_C61	20	12.292	160.84	-1.7462	0.0003	0.0004	0.0005
B2_R50_C86	21	17.52	160.86	-1.7806	0.0003	0.0004	0.0005
B2_R50_C99		20.553	160.98	-2.1177	0.0003	0.0004	0.0005
B2_R55_C05		0.9358	178.75	-1.1974	0.0003	0.0004	0.0005
B2_R55_C36	22	7.0876	178.73	-1.5413	0.0003	0.0004	0.0005
B2_R55_C61	23	12.308	178.77	-1.6322	0.0003	0.0004	0.0005
B2_R55_C86	24	17.554	178.74	-1.5707	0.0003	0.0004	0.0005
B2_R55_C99		20.579	178.69	-1.8603	0.0003	0.0004	0.0005
B2_R60_C05		0.9129	193.08	-1.2546	0.0003	0.0004	0.0005
B2_R60_C36	25	7.0564	193.09	-1.5225	0.0003	0.0004	0.0005
B2_R60_C61	26	12.337	193.1	-1.5436	0.0003	0.0004	0.0005
B2_R60_C86	27	17.574	193.07	-1.4053	0.0004	0.0004	0.0005
B2_R60_C99		20.575	192.99	-1.6436	0.0003	0.0004	0.0005
B2_R65_C05		0.9539	209.13	-1.325	0.0003	0.0004	0.0005
B2_R65_C36	28	7.0695	209.18	-1.5051	0.0004	0.0005	0.0006
B2_R65_C61	29	12.302	209.19	-1.4626	0.0005	0.0006	0.0006
B2_R65_C86	30	17.564	209.23	-1.2256	0.0004	0.0005	0.0006
B2_R65_C99		20.555	209.18	-1.4271	0.0003	0.0004	0.0005
B2_R70_C05		0.8431	225.12	-1.4352	0.0004	0.0004	0.0005
B2_R70_C36	31	7.0371	225.25	-1.5171	0.0004	0.0004	0.0005

Name	Number	X	Y	Z	sigma X	sigma Y	sigma Z
B2_R70_C61	32	12.269	225.29	-1.3816	0.0004	0.0004	0.0005
B2_R70_C86	33	17.469	225.33	-1.0969	0.0004	0.0005	0.0006
B2_R70_C99		20.529	225.33	-1.226	0.0004	0.0004	0.0005
B2_R75_C05		0.9326	241.32	-1.5655	0.0004	0.0005	0.0006
B2_R75_C36	34	7.0444	241.34	-1.5278	0.0004	0.0005	0.0006
B2_R75_C61	35	12.262	241.37	-1.3217	0.0005	0.0007	0.0007
B2_R75_C86	36	17.516	241.36	-0.9595	0.0005	0.0008	0.0007
B2_R75_C105		22.015	241.36	-0.929	0.0004	0.0005	0.0005
B2_R80_C05		0.8442	257.59	-1.6716	0.0004	0.0005	0.0006
B2_R80_C36	37	6.9791	257.52	-1.5833	0.0004	0.0005	0.0006
B2_R80_C61	38	12.173	257.5	-1.3093	0.0006	0.0007	0.0008
B2_R80_C86	39	17.47	257.45	-0.9145	0.0005	0.0007	0.0007
B2_R80_C105		21.999	257.53	-0.7983	0.0004	0.0005	0.0006
B2_R86_C05		0.8896	276.23	-1.6024	0.0004	0.0005	0.0007
B2_R86_C36	40	7.0548	276.23	-1.6446	0.0004	0.0005	0.0007
B2_R86_C61	41	12.255	276.22	-1.2998	0.0005	0.0005	0.0008
B2_R86_C86	42	17.466	276.19	-0.8133	0.0005	0.0007	0.001
B2_R86_C105		21.889	276.19	-0.7478	0.0004	0.0005	0.0006
B2_R91_C05		0.8506	293.03	-1.7517	0.0005	0.0006	0.0007
B2_R91_C36	43	7.0182	293	-1.6295	0.0006	0.0006	0.0012
B2_R91_C61	44	12.239	293.05	-1.0778	0.0007	0.0009	0.0016
B2_R91_C86	45	17.424	292.99	-0.4695	0.0006	0.0007	0.001
B2_R91_C99		20.462	293	-0.3578	0.0004	0.0005	0.0007
B2_R97_C05		5.9976	313.04	-1.5685	0.0005	0.0007	0.0009
B2_R97_C36	46	12.143	313.11	-1.3599	0.0007	0.001	0.0018
B2_R97_C61	47	17.363	313.22	-0.8393	0.0007	0.0009	0.0009
B2_R97_C86	48	22.555	313.3	-0.2496	0.001	0.0012	0.0012
B2_R97_C99		25.52	313.28	-0.174	0.0005	0.0007	0.0007
Blade Tip		28.316	320.88	-0.441	0.0004	0.0005	0.0007
HUB_LE		2.1914	30	-3.5002	0.0004	0.0005	0.0008
HUB_TE		8.1886	30	-3.4998	0.0004	0.0005	0.0008
B2_R25_C36	4	7.0349	77.426	-1.5296	0.0004	0.0004	0.0005

Chapter 2: Bolt Hole Target Alignment

The measured X, Y, and Z locations of the bolt hole targets are compared to their "as designed" locations. X, Y, and Z translation errors, along with pitch and lag errors, are estimated, and compensating translations and rotations are then applied to all target measurements.

2.1: Bolt Hole Alignment Errors

Table 2-1. Measured(1) vs "as designed"(2) in inches.

Name	X1	Y1	Z1	X2	Y2	Z2	dX	dY	dZ	dR
HUB_LE	2.1914	30	-3.5002	2.19	30	-3.5	0.0014	0	-0.0002	0.0014142
HUB_TE	8.1886	30	-3.4998	8.19	30	-3.5	-0.0014	0	0.0002	0.0014142
RMS Errors:							0.0014	0	0.0002	0.0014142

Table 2-2. Initial alignment errors.

Alignment Error	Value
X Error	-8.8818e-16
Y Error	0
Z Error	0
Pitch Error	-0.0038215
Lag Error	0

2.2: Corrected Bolt Hole Alignment

Table 2-3. Measured(1) with alignment correction vs "as designed"(2) in inches.

Name	X1	Y1	Z1	X2	Y2	Z2	dX	dY	dZ	dR
HUB_LE	2.1914	30	-3.5002	2.19	30	-3.5	0.0014	0	-0.0002	0.0014142
HUB_TE	8.1886	30	-3.4998	8.19	30	-3.5	-0.0014	0	0.0002	0.0014142
RMS Errors:							0.0014	0	0.0002	0.0014142

Table 2-4. Errors after hole alignment correction.

Alignment Error	Value
X Error	-8.8818e-16
Y Error	0
Z Error	0
Pitch Error	-0.0038215
Lag Error	0

Chapter 3: Trailing-Edge Alignment

The measured X locations of the trailing-edge targets, excluding those on the tab and swept tip, are compared to the "as designed" locations. An estimated lag error, for rotation about the centroid of the two bolt hole targets, and an estimated centroid offset in the X direction that minimize the root-mean-square of the ΔX values with respect to the "as designed" trailing-edge X location, are determined and applied to all target measurements.

3.1: Trailing-Edge Alignment Errors

Table 3-1. Measured(1) vs "as designed"(2) in inches.

Name	X1	Y1	Z1	X2	Y2	Z2	dX	dY	dZ	dR
B2_R20_C05	0.9746	62.789	-0.3295	0.9746	62.789	0.10067	0	0	-0.43017	0.43017
B2_R20_C36	7.0802	62.771	-1.5184	7.0802	62.771	-1.1232	0	0	-0.39518	0.39518
B2_R20_C61	12.246	62.763	-2.1034	12.246	62.763	-1.7892	0	0	-0.31422	0.31422
B2_R20_C86	17.495	62.769	-2.583	17.495	62.769	-2.2843	0	0	-0.29868	0.29868
B2_R20_C99	20.43	62.731	-3.1713	20.502	62.731	-2.843	-0.071502	0	-0.32828	0.33597
B2_R25_C05	0.9808	77.405	-0.4217	0.9808	77.405	0.043826	0	0	-0.46553	0.46553
B2_R25_C36	7.0349	77.426	-1.5296	7.0349	77.426	-1.0908	0	0	-0.43879	0.43879
B2_R25_C61	12.249	77.434	-2.08	12.249	77.434	-1.6963	0	0	-0.3837	0.3837
B2_R25_C86	17.466	77.441	-2.5364	17.466	77.441	-2.1216	0	0	-0.4148	0.4148
B2_R25_C99	20.421	77.407	-3.0824	20.537	77.407	-2.6456	-0.11595	0	-0.43682	0.45194
B2_R30_C05	0.9252	96.625	-0.5311	0.9252	96.625	-0.0060188	0	0	-0.52508	0.52508
B2_R30_C36	6.9991	96.593	-1.527	6.9991	96.593	-1.0533	0	0	-0.47375	0.47375
B2_R30_C61	12.234	96.549	-2.02	12.234	96.549	-1.5746	0	0	-0.44543	0.44543
B2_R30_C86	17.432	96.543	-2.3645	17.432	96.543	-1.9126	0	0	-0.45188	0.45188
B2_R30_C99	20.444	96.534	-2.8971	20.579	96.534	-2.3885	-0.13485	0	-0.50858	0.52616
B2_R35_C05	1.0515	112.64	-0.6299	1.0515	112.64	-0.1095	0	0	-0.5204	0.5204
B2_R35_C36	7.0801	112.65	-1.5387	7.0801	112.65	-1.0348	0	0	-0.50387	0.50387
B2_R35_C61	12.353	112.67	-1.9552	12.353	112.67	-1.4819	0	0	-0.47332	0.47332
B2_R35_C86	17.533	112.65	-2.2158	17.533	112.65	-1.7433	0	0	-0.47248	0.47248
B2_R35_C99	20.512	112.62	-2.6949	20.611	112.62	-2.1722	-0.098974	0	-0.52271	0.532
B2_R40_C05	1.0115	128.83	-0.7578	1.0115	128.83	-0.15452	0	0	-0.60328	0.60328
B2_R40_C36	7.0966	128.78	-1.5409	7.0966	128.78	-1.0084	0	0	-0.53254	0.53254
B2_R40_C61	12.339	128.77	-1.8782	12.339	128.77	-1.3794	0	0	-0.49878	0.49878
B2_R40_C86	17.558	128.69	-2.0676	17.558	128.69	-1.5707	0	0	-0.49694	0.49694
B2_R40_C99	20.522	128.7	-2.4998	20.64	128.7	-1.956	-0.11769	0	-0.54384	0.55643
B2_R45_C05	0.9545	144.79	-0.8413	0.9545	144.79	-0.19342	0	0	-0.64788	0.64788
B2_R45_C36	7.0633	144.77	-1.5688	7.0633	144.77	-0.97806	0	0	-0.59074	0.59074
B2_R45_C61	12.264	144.8	-1.8122	12.264	144.8	-1.2759	0	0	-0.53632	0.53632
B2_R45_C86	17.564	144.8	-1.93	17.564	144.8	-1.397	0	0	-0.53304	0.53304
B2_R45_C99	20.534	144.78	-2.3167	20.666	144.78	-1.7395	-0.13235	0	-0.57719	0.59218
B2_R50_C05	0.9062	160.82	-1.0984	0.9062	160.82	-0.47164	0	0	-0.62676	0.62676
B2_R50_C36	7.1011	160.85	-1.5439	7.1011	160.85	-0.9572	0	0	-0.5867	0.5867
B2_R50_C61	12.292	160.84	-1.7462	12.292	160.84	-1.1767	0	0	-0.56952	0.56952
B2_R50_C86	17.52	160.86	-1.7806	17.52	160.86	-1.2187	0	0	-0.56193	0.56193
B2_R50_C99	20.553	160.98	-2.1177	20.695	160.98	-1.5132	-0.14235	0	-0.60455	0.62108
B2_R55_C05	0.9358	178.75	-1.1974	0.9358	178.75	-0.54709	0	0	-0.65031	0.65031
B2_R55_C36	7.0876	178.73	-1.5413	7.0876	178.73	-0.92312	0	0	-0.61818	0.61818
B2_R55_C61	12.308	178.77	-1.6322	12.308	178.77	-1.0549	0	0	-0.57734	0.57734
B2_R55_C86	17.554	178.74	-1.5707	17.554	178.74	-1.0076	0	0	-0.56311	0.56311
B2_R55_C99	20.579	178.69	-1.8603	20.719	178.69	-1.2505	-0.13994	0	-0.60978	0.62563
B2_R60_C05	0.9129	193.08	-1.2546	0.9129	193.08	-0.60255	0	0	-0.65205	0.65205
B2_R60_C36	7.0564	193.09	-1.5225	7.0564	193.09	-0.89573	0	0	-0.62677	0.62677
B2_R60_C61	12.337	193.1	-1.5436	12.337	193.1	-0.95722	0	0	-0.58638	0.58638
B2_R60_C86	17.574	193.07	-1.4053	17.574	193.07	-0.83807	0	0	-0.56723	0.56723

Name	X1	Y1	Z1	X2	Y2	Z2	dX	dY	dZ	dR
B2_R60_C99	20.575	192.99	-1.6436	20.734	192.99	-1.0383	-0.15977	0	-0.60526	0.62599
B2_R65_C05	0.9539	209.13	-1.325	0.9539	209.13	-0.67033	0	0	-0.65467	0.65467
B2_R65_C36	7.0695	209.18	-1.5051	7.0695	209.18	-0.86694	0	0	-0.63816	0.63816
B2_R65_C61	12.302	209.19	-1.4626	12.302	209.19	-0.84831	0	0	-0.61429	0.61429
B2_R65_C86	17.564	209.23	-1.2256	17.564	209.23	-0.64788	0	0	-0.57772	0.57772
B2_R65_C99	20.555	209.18	-1.4271	20.748	209.18	-0.79783	-0.19327	0	-0.62927	0.65829
B2_R70_C05	0.8431	225.12	-1.4352	0.8431	225.12	-0.72758	0	0	-0.70762	0.70762
B2_R70_C36	7.0371	225.25	-1.5171	7.0371	225.25	-0.83797	0	0	-0.67913	0.67913
B2_R70_C61	12.269	225.29	-1.3816	12.269	225.29	-0.74059	0	0	-0.64101	0.64101
B2_R70_C86	17.469	225.33	-1.0969	17.469	225.33	-0.4642	0	0	-0.6327	0.6327
B2_R70_C99	20.529	225.33	-1.226	20.759	225.33	-0.55775	-0.22962	0	-0.66825	0.7066
B2_R75_C05	0.9326	241.32	-1.5655	0.9326	241.32	-0.79191	0	0	-0.77359	0.77359
B2_R75_C36	7.0444	241.34	-1.5278	7.0444	241.34	-0.81237	0	0	-0.71543	0.71543
B2_R75_C61	12.262	241.37	-1.3217	12.262	241.37	-0.6434	0	0	-0.6783	0.6783
B2_R75_C86	17.516	241.36	-0.9595	17.516	241.36	-0.29171	0	0	-0.66779	0.66779
B2_R80_C05	0.8442	257.59	-1.6716	0.8442	257.59	-0.8366	0	0	-0.835	0.835
B2_R80_C36	6.9791	257.52	-1.5833	6.9791	257.52	-0.7931	0	0	-0.7902	0.7902
B2_R80_C61	12.173	257.5	-1.3093	12.173	257.5	-0.56969	0	0	-0.73961	0.73961
B2_R80_C86	17.47	257.45	-0.9145	17.47	257.45	-0.1576	0	0	-0.7569	0.7569
B2_R86_C05	0.8896	276.23	-1.6024	0.8896	276.23	-0.63927	0	0	-0.96313	0.96313
B2_R86_C36	7.0548	276.23	-1.6446	7.0548	276.23	-0.76645	0	0	-0.87815	0.87815
B2_R86_C61	12.255	276.22	-1.2998	12.255	276.22	-0.48608	0	0	-0.81372	0.81372
B2_R86_C86	17.466	276.19	-0.8133	17.466	276.19	-0.024826	0	0	-0.78847	0.78847
B2_R91_C05	0.8506	293.03	-1.7517	0.8506	293.03	-0.76322	0	0	-0.98848	0.98848
B2_R91_C36	7.0182	293	-1.6295	7.0182	293	-0.71033	0	0	-0.91917	0.91917
B2_R91_C61	12.239	293.05	-1.0778	12.239	293.05	-0.26177	0	0	-0.81603	0.81603
B2_R91_C86	17.424	292.99	-0.4695	17.424	292.99	0.36364	0	0	-0.83314	0.83314
B2_R91_C99	20.462	293	-0.3578	20.755	293	0.49781	-0.29325	0	-0.85561	0.90447
B2_R97_C05	5.9976	313.04	-1.5685	5.9976	313.04	-0.67898	0	0	-0.88952	0.88952
B2_R97_C36	12.143	313.11	-1.3599	12.143	313.11	-0.466	0	0	-0.8939	0.8939
B2_R97_C61	17.363	313.22	-0.8393	17.363	313.22	-0.040587	0	0	-0.79871	0.79871
B2_R97_C86	22.555	313.3	-0.2496	22.555	313.3	0.53701	0	0	-0.78661	0.78661
B2_R97_C99	25.52	313.28	-0.174	25.95	313.28	0.64397	-0.43056	0	-0.81797	0.92437
HUB_LE	2.1914	30	-3.5002	2.19	5.19	-3.5	0.0014	24.81	-0.0002	24.81
HUB_TE	8.1886	30	-3.4998	8.19	5.19	-3.5	-0.0014	24.81	0.0002	24.81
RMS Errors:							0.079932	3.9476	0.63174	3.9986

The estimated lag error is -0.046239°.

The estimated X error is 0.046814 inches.

3.2: Corrected Trailing-Edge Alignment

Table 3-2. Measured(1) with lag correction vs "as designed"(2) in inches.

Name	X1	Y1	Z1	X2	Y2	Z2	dX	dY	dZ	dR
B2_R20_C05	1.0479	62.792	-0.3295	1.0479	62.792	0.072059	0	0	-0.40156	0.40156
B2_R20_C36	7.1535	62.769	-1.5184	7.1535	62.769	-1.134	0	0	-0.38442	0.38442
B2_R20_C61	12.319	62.757	-2.1034	12.319	62.757	-1.7974	0	0	-0.30602	0.30602
B2_R20_C86	17.568	62.759	-2.583	17.568	62.759	-2.2906	0	0	-0.29244	0.29244
B2_R20_C99	20.503	62.719	-3.1713	20.502	62.719	-2.8432	0.001752	0	-0.32811	0.32812
B2_R25_C05	1.0659	77.408	-0.4217	1.0659	77.408	0.012254	0	0	-0.43395	0.43395
B2_R25_C36	7.12	77.425	-1.5296	7.12	77.425	-1.1022	0	0	-0.42735	0.42735
B2_R25_C61	12.334	77.428	-2.08	12.334	77.428	-1.7047	0	0	-0.37528	0.37528
B2_R25_C86	17.551	77.431	-2.5364	17.551	77.431	-2.1277	0	0	-0.40867	0.40867
B2_R25_C99	20.506	77.395	-3.0824	20.537	77.395	-2.6457	-0.030853	0	-0.43665	0.43774
B2_R30_C05	1.0258	96.629	-0.5311	1.0258	96.629	-0.043103	0	0	-0.488	0.488
B2_R30_C36	7.0997	96.592	-1.527	7.0997	96.592	-1.0652	0	0	-0.46177	0.46177
B2_R30_C61	12.334	96.543	-2.02	12.334	96.543	-1.5828	0	0	-0.43719	0.43719
B2_R30_C86	17.533	96.533	-2.3645	17.533	96.533	-1.9182	0	0	-0.44634	0.44634
B2_R30_C99	20.545	96.521	-2.8971	20.579	96.521	-2.3887	-0.034324	0	-0.50841	0.50957
B2_R35_C05	1.165	112.64	-0.6299	1.165	112.64	-0.14481	0	0	-0.48509	0.48509
B2_R35_C36	7.1936	112.65	-1.5387	7.1936	112.65	-1.0465	0	0	-0.49221	0.49221
B2_R35_C61	12.467	112.67	-1.9552	12.467	112.67	-1.4895	0	0	-0.46575	0.46575
B2_R35_C86	17.647	112.64	-2.2158	17.647	112.64	-1.748	0	0	-0.46784	0.46784
B2_R35_C99	20.626	112.61	-2.6949	20.611	112.61	-2.1724	0.014537	0	-0.52254	0.52274
B2_R40_C05	1.1381	128.83	-0.7578	1.1381	128.83	-0.19325	0	0	-0.56455	0.56455
B2_R40_C36	7.2231	128.77	-1.5409	7.2231	128.77	-1.0196	0	0	-0.52135	0.52135
B2_R40_C61	12.465	128.76	-1.8782	12.465	128.76	-1.3861	0	0	-0.49206	0.49206
B2_R40_C86	17.684	128.68	-2.0676	17.684	128.68	-1.574	0	0	-0.49356	0.49356
B2_R40_C99	20.649	128.68	-2.4998	20.64	128.68	-1.9561	0.0087906	0	-0.54368	0.54375
B2_R45_C05	1.094	144.79	-0.8413	1.094	144.79	-0.23634	0	0	-0.60496	0.60496
B2_R45_C36	7.2027	144.77	-1.5688	7.2027	144.77	-0.98859	0	0	-0.58021	0.58021
B2_R45_C61	12.404	144.79	-1.8122	12.404	144.79	-1.2814	0	0	-0.53078	0.53078
B2_R45_C86	17.704	144.79	-1.93	17.704	144.79	-1.3987	0	0	-0.53127	0.53127
B2_R45_C99	20.673	144.77	-2.3167	20.666	144.77	-1.7397	0.0071022	0	-0.57703	0.57707
B2_R50_C05	1.0586	160.82	-1.0984	1.0586	160.82	-0.48974	0	0	-0.60866	0.60866
B2_R50_C36	7.2535	160.85	-1.5439	7.2535	160.85	-0.9664	0	0	-0.5775	0.5775
B2_R50_C61	12.444	160.84	-1.7462	12.444	160.84	-1.1804	0	0	-0.56577	0.56577
B2_R50_C86	17.672	160.85	-1.7806	17.672	160.85	-1.2183	0	0	-0.56229	0.56229
B2_R50_C99	20.705	160.96	-2.1177	20.695	160.96	-1.5133	0.010174	0	-0.60436	0.60445
B2_R55_C05	1.1027	178.75	-1.1974	1.1027	178.75	-0.56393	0	0	-0.63347	0.63347
B2_R55_C36	7.2544	178.73	-1.5413	7.2544	178.73	-0.93034	0	0	-0.61096	0.61096
B2_R55_C61	12.475	178.76	-1.6322	12.475	178.76	-1.0561	0	0	-0.57612	0.57612
B2_R55_C86	17.721	178.73	-1.5707	17.721	178.73	-1.0043	0	0	-0.56637	0.56637
B2_R55_C99	20.746	178.68	-1.8603	20.719	178.68	-1.2507	0.026878	0	-0.6096	0.61019
B2_R60_C05	1.0913	193.09	-1.2546	1.0913	193.09	-0.61818	0	0	-0.63642	0.63642
B2_R60_C36	7.2348	193.09	-1.5225	7.2348	193.09	-0.90099	0	0	-0.62151	0.62151
B2_R60_C61	12.516	193.1	-1.5436	12.516	193.1	-0.95601	0	0	-0.58759	0.58759
B2_R60_C86	17.752	193.06	-1.4053	17.752	193.06	-0.83214	0	0	-0.57316	0.57316
B2_R60_C99	20.753	192.97	-1.6436	20.734	192.97	-1.0385	0.018585	0	-0.60508	0.60536
B2_R65_C05	1.1453	209.13	-1.325	1.1453	209.13	-0.68399	0	0	-0.64101	0.64101
B2_R65_C36	7.2609	209.18	-1.5051	7.2609	209.18	-0.86964	0	0	-0.63546	0.63546
B2_R65_C61	12.493	209.19	-1.4626	12.493	209.19	-0.84418	0	0	-0.61842	0.61842
B2_R65_C86	17.755	209.22	-1.2256	17.755	209.22	-0.63855	0	0	-0.58705	0.58705
B2_R65_C99	20.747	209.17	-1.4271	20.748	209.17	-0.79801	-0.0018487	0	-0.62909	0.62909
B2_R70_C05	1.0474	225.12	-1.4352	1.0474	225.12	-0.73966	0	0	-0.69554	0.69554

Name	X1	Y1	Z1	X2	Y2	Z2	dX	dY	dZ	dR
B2_R70_C36	7.2415	225.25	-1.5171	7.2415	225.25	-0.8378	0	0	-0.6793	0.6793
B2_R70_C61	12.473	225.28	-1.3816	12.473	225.28	-0.73313	0	0	-0.64847	0.64847
B2_R70_C86	17.674	225.32	-1.0969	17.674	225.32	-0.45106	0	0	-0.64584	0.64584
B2_R70_C99	20.734	225.32	-1.226	20.759	225.32	-0.55794	-0.02517	0	-0.66806	0.66853
B2_R75_C05	1.15	241.33	-1.5655	1.15	241.33	-0.8012	0	0	-0.7643	0.7643
B2_R75_C36	7.2618	241.34	-1.5278	7.2618	241.34	-0.80919	0	0	-0.71861	0.71861
B2_R75_C61	12.48	241.37	-1.3217	12.48	241.37	-0.63245	0	0	-0.68925	0.68925
B2_R75_C86	17.733	241.35	-0.9595	17.733	241.35	-0.27471	0	0	-0.68479	0.68479
B2_R80_C05	1.0747	257.6	-1.6716	1.0747	257.6	-0.84446	0	0	-0.82714	0.82714
B2_R80_C36	7.2095	257.52	-1.5833	7.2095	257.52	-0.78736	0	0	-0.79594	0.79594
B2_R80_C61	12.403	257.49	-1.3093	12.403	257.49	-0.5555	0	0	-0.7538	0.7538
B2_R80_C86	17.7	257.44	-0.9145	17.7	257.44	-0.13694	0	0	-0.77756	0.77756
B2_R86_C05	1.1351	276.23	-1.6024	1.1351	276.23	-0.69031	0	0	-0.91209	0.91209
B2_R86_C36	7.3003	276.22	-1.6446	7.3003	276.22	-0.7577	0	0	-0.8869	0.8869
B2_R86_C61	12.5	276.22	-1.2998	12.5	276.22	-0.46828	0	0	-0.83152	0.83152
B2_R86_C86	17.712	276.18	-0.8133	17.712	276.18	-0.00025692	0	0	-0.81304	0.81304
B2_R91_C05	1.1097	293.03	-1.7517	1.1097	293.03	-0.81282	0	0	-0.93888	0.93888
B2_R91_C36	7.2773	293	-1.6295	7.2773	293	-0.69294	0	0	-0.93656	0.93656
B2_R91_C61	12.499	293.04	-1.0778	12.499	293.04	-0.23465	0	0	-0.84315	0.84315
B2_R91_C86	17.683	292.98	-0.4695	17.683	292.98	0.39778	0	0	-0.86728	0.86728
B2_R91_C99	20.721	292.98	-0.3578	20.755	292.98	0.49746	-0.03421	0	-0.85526	0.85594
B2_R97_C05	6.2728	313.04	-1.5685	6.2728	313.04	-0.68445	0	0	-0.88405	0.88405
B2_R97_C36	12.419	313.11	-1.3599	12.419	313.11	-0.44754	0	0	-0.91236	0.91236
B2_R97_C61	17.638	313.21	-0.8393	17.638	313.21	-0.01307	0	0	-0.82623	0.82623
B2_R97_C86	22.831	313.29	-0.2496	22.831	313.29	0.57155	0	0	-0.82115	0.82115
B2_R97_C99	25.795	313.26	-0.174	25.944	313.26	0.64455	-0.1491	0	-0.81855	0.83202
HUB_LE	2.2382	30.002	-3.5002	2.19	5.19	-3.5	0.048215	24.812	-0.0002	24.812
HUB_TE	8.2354	29.998	-3.4998	8.19	5.19	-3.5	0.045413	24.808	0.0002	24.808
RMS Errors:							0.020148	3.9475	0.6297	3.9975

3.3: Trailing-Edge Registration Plots

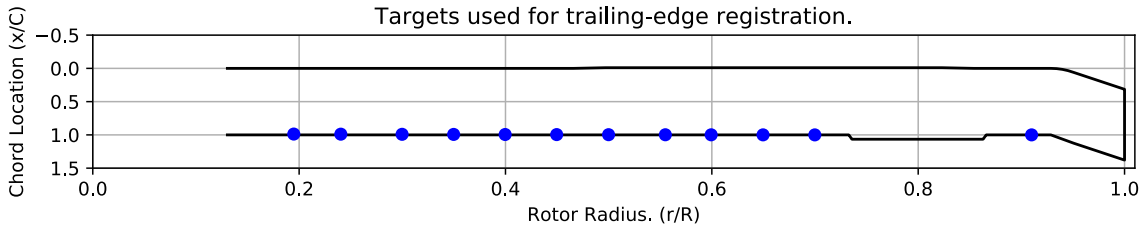

Figure 3-1. Targets used for trailing-edge alignment.

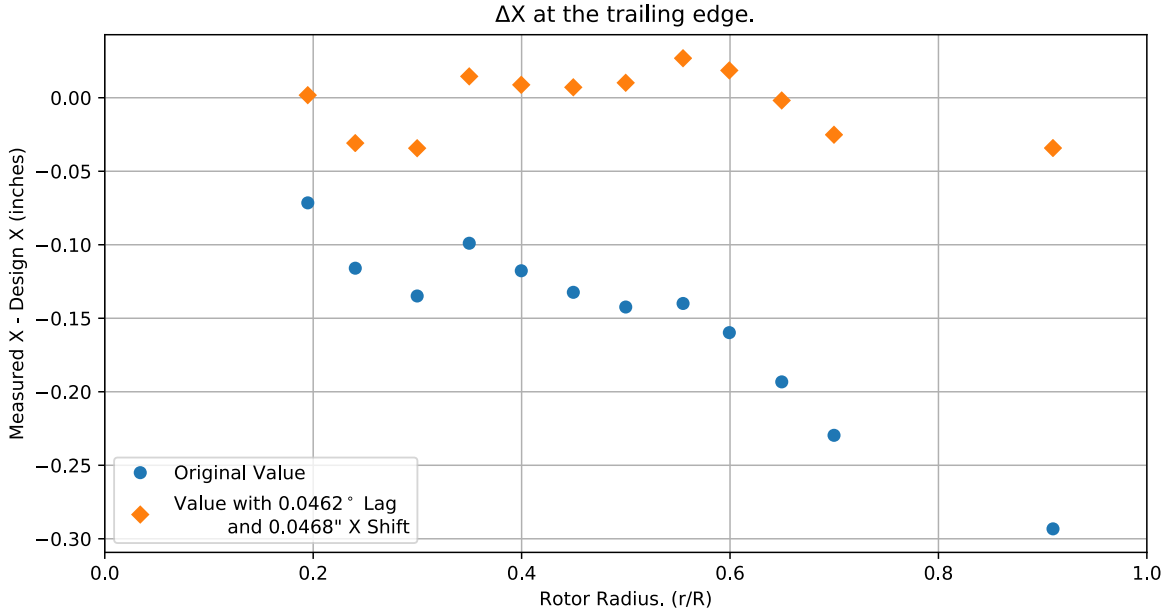

Figure 3-2. Trailing-edge ΔX error vs rotor radius.

Chapter 4: Flap Only Registration (6 rows)

The targets at the 6 spanwise stations nearest the root are used to determing the flap offset.

The estimated flap error is -0.30956°.

4.1: Target Location Errors After Flap Target Registration

Table 4-1. Measured(1) with flap registration vs "as designed"(2) in inches.

Name	X1	Y1	Z1	X2	Y2	Z2	dX	dY	dZ	dR
B2_R20_C05	1.0479	62.774	-0.15238	1.0479	62.774	0.072123	0	0	-0.2245	0.2245
B2_R20_C36	7.1535	62.758	-1.3414	7.1535	62.758	-1.134	0	0	-0.20738	0.20738
B2_R20_C61	12.319	62.749	-1.9264	12.319	62.749	-1.7974	0	0	-0.129	0.129
B2_R20_C86	17.568	62.754	-2.406	17.568	62.754	-2.2906	0	0	-0.1154	0.1154
B2_R20_C99	20.503	62.716	-2.9945	20.502	62.716	-2.8432	0.0017576	0	-0.15131	0.15132
B2_R25_C05	1.0659	77.391	-0.16561	1.0659	77.391	0.012317	0	0	-0.17792	0.17792
B2_R25_C36	7.12	77.414	-1.2734	7.12	77.414	-1.1022	0	0	-0.17113	0.17113
B2_R25_C61	12.334	77.42	-1.8238	12.334	77.42	-1.7048	0	0	-0.119	0.119
B2_R25_C86	17.551	77.425	-2.2802	17.551	77.425	-2.1278	0	0	-0.15235	0.15235
B2_R25_C99	20.506	77.392	-2.8263	20.537	77.392	-2.6458	-0.030846	0	-0.18055	0.18317
B2_R30_C05	1.0258	96.612	-0.17116	1.0258	96.612	-0.043041	0	0	-0.12812	0.12812
B2_R30_C36	7.0997	96.58	-1.1672	7.0997	96.58	-1.0652	0	0	-0.102	0.102
B2_R30_C61	12.334	96.534	-1.6605	12.334	96.534	-1.5829	0	0	-0.077632	0.077632
B2_R30_C86	17.533	96.526	-2.005	17.533	96.526	-1.9182	0	0	-0.086812	0.086812
B2_R30_C99	20.545	96.517	-2.5377	20.579	96.517	-2.3887	-0.034315	0	-0.14896	0.15287
B2_R35_C05	1.165	112.63	-0.18344	1.165	112.63	-0.14476	0	0	-0.038685	0.038685
B2_R35_C36	7.1936	112.64	-1.0922	7.1936	112.64	-1.0465	0	0	-0.045688	0.045688
B2_R35_C61	12.467	112.66	-1.5086	12.467	112.66	-1.4895	0	0	-0.019066	0.019066
B2_R35_C86	17.647	112.64	-1.7693	17.647	112.64	-1.748	0	0	-0.021267	0.021267
B2_R35_C99	20.626	112.61	-2.2486	20.611	112.61	-2.1724	0.014547	0	-0.076145	0.077523
B2_R40_C05	1.1381	128.82	-0.22385	1.1381	128.82	-0.19319	0	0	-0.030659	0.030659
B2_R40_C36	7.2231	128.76	-1.0073	7.2231	128.76	-1.0196	0	0	0.012308	0.012308
B2_R40_C61	12.465	128.75	-1.3446	12.465	128.75	-1.3862	0	0	0.04158	0.04158
B2_R40_C86	17.684	128.67	-1.5345	17.684	128.67	-1.5741	0	0	0.039679	0.039679
B2_R40_C99	20.649	128.68	-1.9666	20.64	128.68	-1.9562	0.0088022	0	-0.010424	0.013643
B2_R45_C05	1.094	144.77	-0.22115	1.094	144.77	-0.23629	0	0	0.015142	0.015142
B2_R45_C36	7.2027	144.76	-0.94875	7.2027	144.76	-0.98861	0	0	0.03986	0.03986
B2_R45_C61	12.404	144.78	-1.192	12.404	144.78	-1.2815	0	0	0.089472	0.089472
B2_R45_C86	17.704	144.78	-1.3098	17.704	144.78	-1.3988	0	0	0.088991	0.088991
B2_R45_C99	20.673	144.76	-1.6967	20.666	144.76	-1.7398	0.0071144	0	0.043129	0.043711
B2_R50_C05	1.0586	160.81	-0.39163	1.0586	160.81	-0.48968	0	0	0.098046	0.098046
B2_R50_C36	7.2535	160.83	-0.83699	7.2535	160.83	-0.96643	0	0	0.12944	0.12944
B2_R50_C61	12.444	160.82	-1.0393	12.444	160.82	-1.1805	0	0	0.14116	0.14116
B2_R50_C86	17.672	160.84	-1.0737	17.672	160.84	-1.2184	0	0	0.14479	0.14479
B2_R50_C99	20.705	160.95	-1.4102	20.695	160.95	-1.5135	0.010188	0	0.10333	0.10383
B2_R55_C05	1.1027	178.73	-0.39377	1.1027	178.73	-0.56388	0	0	0.17011	0.17011
B2_R55_C36	7.2544	178.72	-0.73775	7.2544	178.72	-0.93036	0	0	0.19261	0.19261
B2_R55_C61	12.475	178.75	-0.82849	12.475	178.75	-1.0562	0	0	0.22767	0.22767
B2_R55_C86	17.721	178.72	-0.76717	17.721	178.72	-1.0045	0	0	0.23731	0.23731
B2_R55_C99	20.746	178.67	-1.057	20.719	178.67	-1.2509	0.026891	0	0.19382	0.19567
B2_R60_C05	1.0913	193.07	-0.3735	1.0913	193.07	-0.61813	0	0	0.24463	0.24463
B2_R60_C36	7.2348	193.08	-0.64138	7.2348	193.08	-0.90102	0	0	0.25964	0.25964

Name	X1	Y1	Z1	X2	Y2	Z2	dX	dY	dZ	dR
B2_R60_C61	12.516	193.08	-0.66245	12.516	193.08	-0.9561	0	0	0.29365	0.29365
B2_R60_C86	17.752	193.04	-0.52437	17.752	193.04	-0.8323	0	0	0.30793	0.30793
B2_R60_C99	20.753	192.96	-0.7631	20.734	192.96	-1.0387	0.018597	0	0.27561	0.27623
B2_R65_C05	1.1453	209.12	-0.35721	1.1453	209.12	-0.68394	0	0	0.32673	0.32673
B2_R65_C36	7.2609	209.17	-0.53706	7.2609	209.17	-0.86967	0	0	0.33261	0.33261
B2_R65_C61	12.493	209.17	-0.49451	12.493	209.17	-0.84428	0	0	0.34977	0.34977
B2_R65_C86	17.755	209.2	-0.25736	17.755	209.2	-0.63873	0	0	0.38137	0.38137
B2_R65_C99	20.747	209.15	-0.45912	20.748	209.15	-0.79822	-0.0018381	0	0.3391	0.3391
B2_R70_C05	1.0474	225.11	-0.38101	1.0474	225.11	-0.7396	0	0	0.35859	0.35859
B2_R70_C36	7.2415	225.24	-0.46222	7.2415	225.24	-0.83782	0	0	0.37561	0.37561
B2_R70_C61	12.473	225.26	-0.32657	12.473	225.26	-0.73323	0	0	0.40666	0.40666
B2_R70_C86	17.674	225.31	-0.041629	17.674	225.31	-0.45125	0	0	0.40962	0.40962
B2_R70_C99	20.734	225.31	-0.17074	20.759	225.31	-0.55816	-0.025162	0	0.38742	0.38824
B2_R75_C05	1.15	241.31	-0.42377	1.15	241.31	-0.80116	0	0	0.37739	0.37739
B2_R75_C36	7.2618	241.32	-0.386	7.2618	241.32	-0.80921	0	0	0.4232	0.4232
B2_R75_C61	12.48	241.35	-0.17976	12.48	241.35	-0.63253	0	0	0.45277	0.45277
B2_R75_C86	17.733	241.33	0.18235	17.733	241.33	-0.27487	0	0	0.45721	0.45721
B2_R80_C05	1.0747	257.58	-0.44196	1.0747	257.58	-0.84443	0	0	0.40246	0.40246
B2_R80_C36	7.2095	257.51	-0.35408	7.2095	257.51	-0.78737	0	0	0.4333	0.4333
B2_R80_C61	12.403	257.48	-0.080221	12.403	257.48	-0.55557	0	0	0.47534	0.47534
B2_R80_C86	17.7	257.42	0.31427	17.7	257.42	-0.13708	0	0	0.45134	0.45134
B2_R86_C05	1.1351	276.22	-0.27207	1.1351	276.22	-0.69029	0	0	0.41822	0.41822
B2_R86_C36	7.3003	276.21	-0.31432	7.3003	276.21	-0.75771	0	0	0.44339	0.44339
B2_R86_C61	12.5	276.2	0.03044	12.5	276.2	-0.46832	0	0	0.49876	0.49876
B2_R86_C86	17.712	276.16	0.51674	17.712	276.16	-0.00034324	0	0	0.51708	0.51708
B2_R91_C05	1.1097	293.02	-0.3306	1.1097	293.02	-0.81273	0	0	0.48213	0.48213
B2_R91_C36	7.2773	292.99	-0.20858	7.2773	292.99	-0.69299	0	0	0.48441	0.48441
B2_R91_C61	12.499	293.03	0.34334	12.499	293.03	-0.23487	0	0	0.57822	0.57822
B2_R91_C86	17.683	292.96	0.95132	17.683	292.96	0.39732	0	0	0.554	0.554
B2_R91_C99	20.721	292.96	1.063	20.755	292.96	0.49688	-0.034229	0	0.56613	0.56717
B2_R97_C05	6.2728	313.03	-0.039294	6.2728	313.03	-0.68474	0	0	0.64545	0.64545
B2_R97_C36	12.419	313.09	0.16964	12.419	313.09	-0.44715	0	0	0.61678	0.61678
B2_R97_C61	17.638	313.19	0.69082	17.638	313.19	-0.012165	0	0	0.70298	0.70298
B2_R97_C86	22.831	313.27	1.2809	22.831	313.27	0.57312	0	0	0.70779	0.70779
B2_R97_C99	25.795	313.24	1.3564	25.936	313.24	0.64527	-0.14103	0	0.71111	0.72496
HUB_LE	2.2382	30.002	-3.5002	2.19	30	-3.5	0.048215	0.0023832	-0.00018713	0.048274
HUB_TE	8.2354	29.998	-3.4998	8.19	30	-3.5	0.045413	-0.0024587	0.00018672	0.04548
RMS Errors:							0.019399	0.00038525	0.3286	0.32917

4.2: Flap Registration Plots (6 rows)

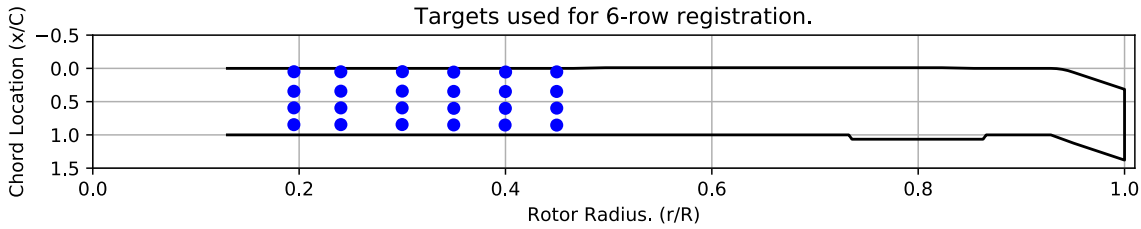

Figure 4-1. Targets used for 6 row root registration.

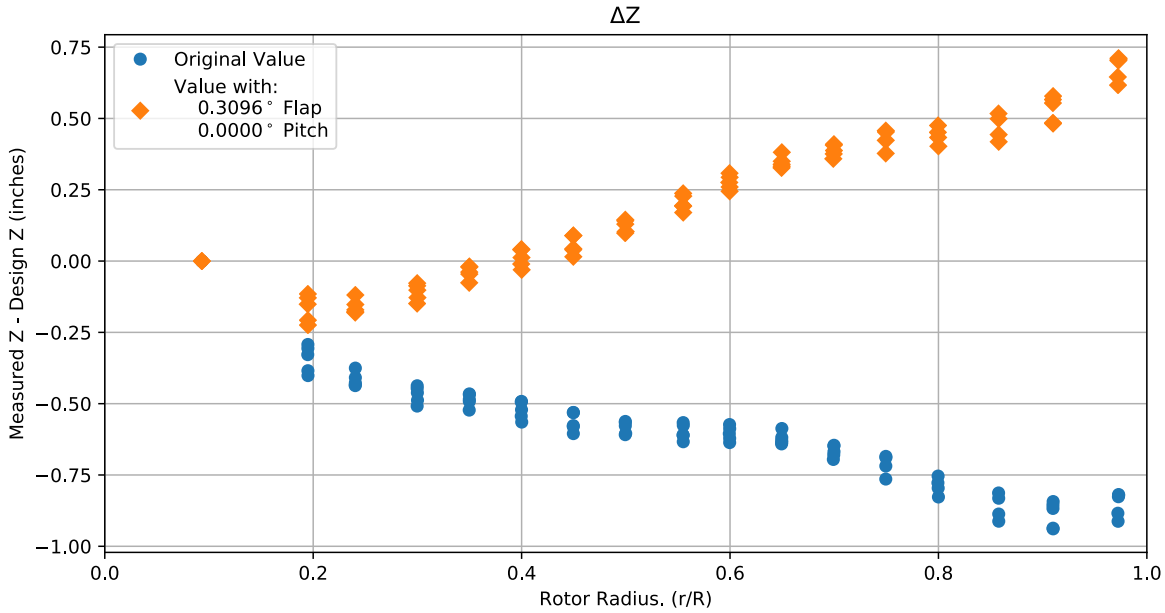

Figure 4-2. Flap target registration, ΔZ error vs rotor radius.

Note: the “as designed” geometry used for the swept tip may have some inaccuracies.

4.3: Estimated Bending and Twist at the Quarter Chord

The error bars shown represent the residual errors for fitting the measure target locations to the "as designed" geometry. These errors are generally much larger than those due to the VSTARS measurement errors. Therefore, the most likely source of these errors is the placement of the trailing-edge targets, differences between the "as designed" and "as built" geometries, and blade deformation during measurement. In the future, iterative adjustment of the "as designed" twist angle may be implemented to see if it reduces the fit error in delta twist. Note: The "as designed" geometry used for the swept tip may have some inaccuracies.

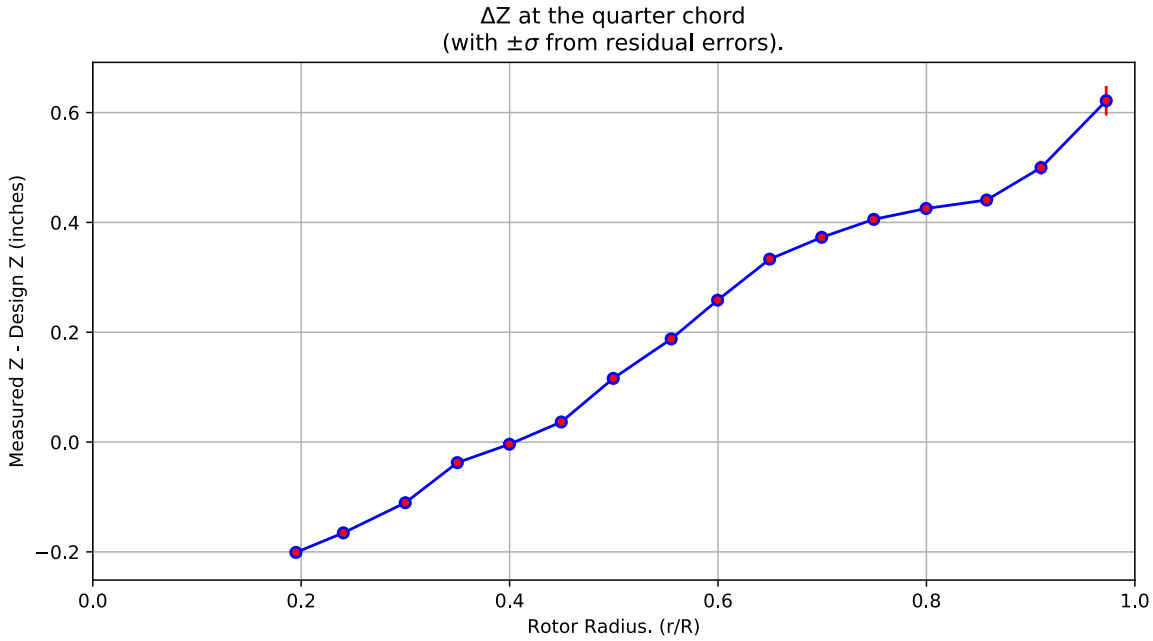

Figure 4-3. ΔZ error at the quarter chord vs rotor radius.

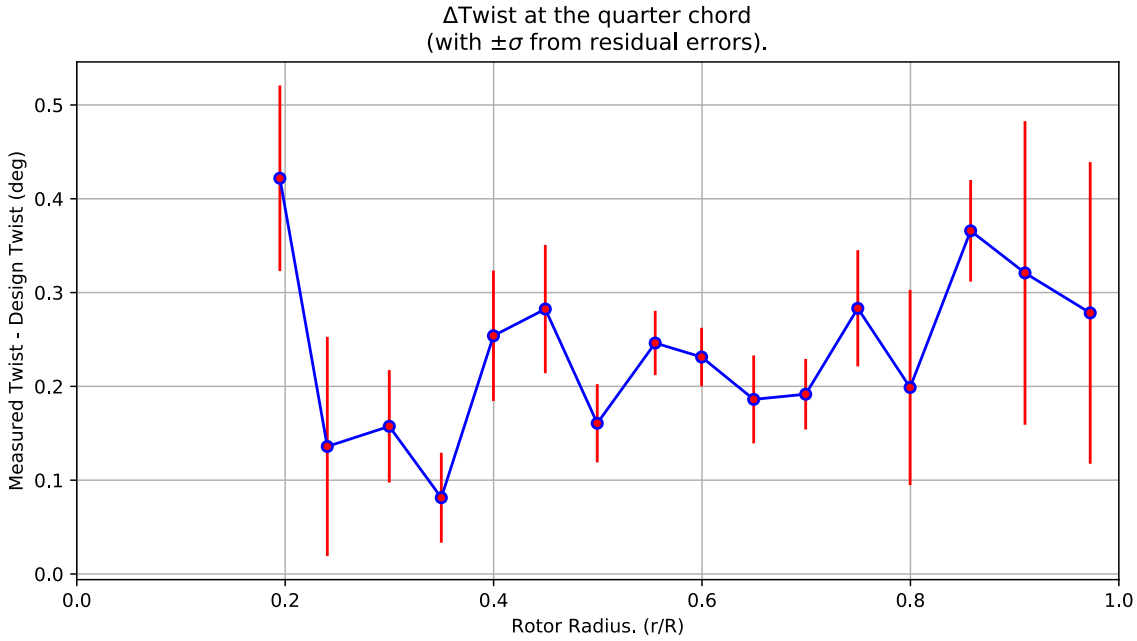

Figure 4-4. ΔTwist error at the quarter chord vs rotor radius.

Table 4-2. Quarter-chord bending and twist statistics.

r	r/R	dZ 1/4-chord	dT	sigma dZ meas	sigma dT meas	sigma dZ res	sigma dT res	n	t_conf
62.759	0.1949	-0.20097	0.42187	6.1248e-10	4.6781e-09	0.0074795	0.098915	4	4.3027
77.413	0.24041	-0.16537	0.13594	6.125e-10	4.6837e-09	0.0088291	0.11689	4	4.3027
96.563	0.29989	-0.11047	0.15739	6.1125e-10	4.6761e-09	0.0045065	0.059933	4	4.3027
112.64	0.34981	-0.037459	0.081299	6.1709e-10	4.6796e-09	0.0037059	0.047952	4	4.3027
128.75	0.39985	-0.0039389	0.25391	6.1691e-10	4.6655e-09	0.0053816	0.069482	4	4.3027
144.77	0.4496	0.036623	0.28242	6.1508e-10	4.6529e-09	0.005265	0.068386	4	4.3027
160.83	0.49946	0.11597	0.16067	6.1531e-10	4.6516e-09	0.0032171	0.04173	4	4.3027
178.73	0.55506	0.18781	0.24621	6.1664e-10	4.6485e-09	0.0026596	0.034256	4	4.3027
193.07	0.59959	0.25846	0.23128	6.1642e-10	4.6329e-09	0.0024262	0.031178	4	4.3027
209.16	0.64958	0.33309	0.18614	6.1792e-10	4.65e-09	0.0036595	0.046867	4	4.3027
225.23	0.69947	0.37284	0.19164	6.1509e-10	4.645e-09	0.0029014	0.037619	4	4.3027
241.33	0.74947	0.40557	0.28322	6.1793e-10	4.658e-09	0.004831	0.061976	4	4.3027
257.5	0.79968	0.42532	0.19882	6.1472e-10	4.6492e-09	0.0080024	0.10404	4	4.3027
276.2	0.85776	0.44081	0.36583	6.1831e-10	4.6603e-09	0.0042284	0.054175	4	4.3027
293	0.90994	0.49975	0.32091	6.1732e-10	4.6592e-09	0.012578	0.16186	4	4.3027
313.14	0.9725	0.62162	0.27829	9.2771e-10	4.6637e-09	0.026943	0.1608	4	4.3027

4.4: Section Plots

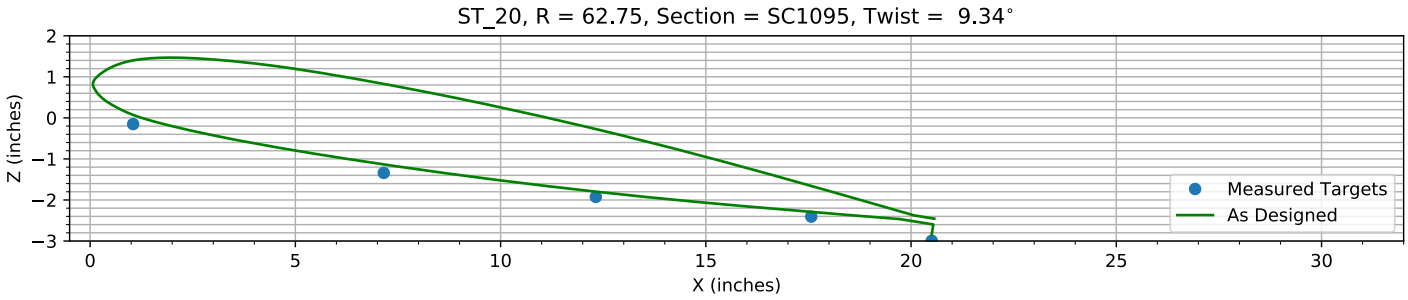

Figure 4-5. Target locations vs section profile at station 20.

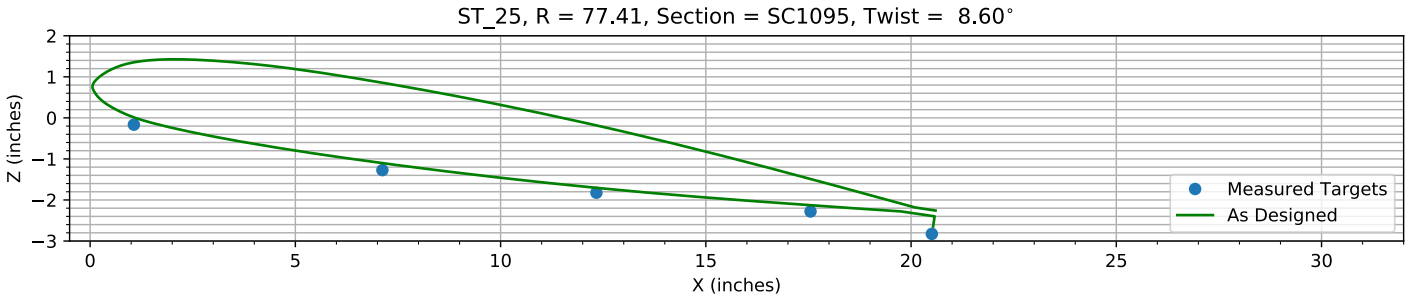

Figure 4-6. Target locations vs section profile at station 25.

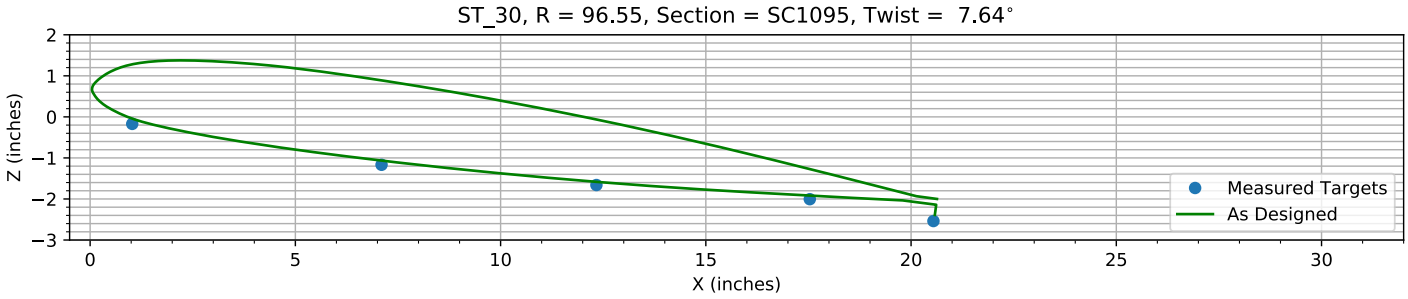

Figure 4-7. Target locations vs section profile at station 30.

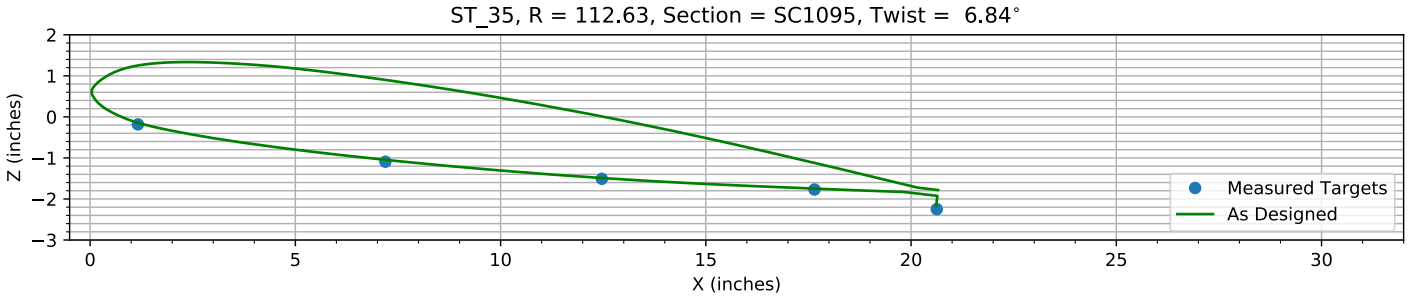

Figure 4-8. Target locations vs section profile at station 35.

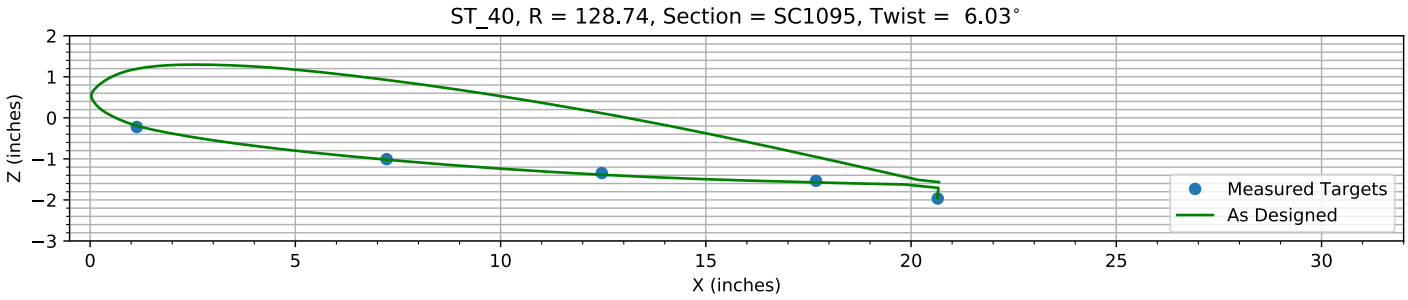

Figure 4-9. Target locations vs section profile at station 40.

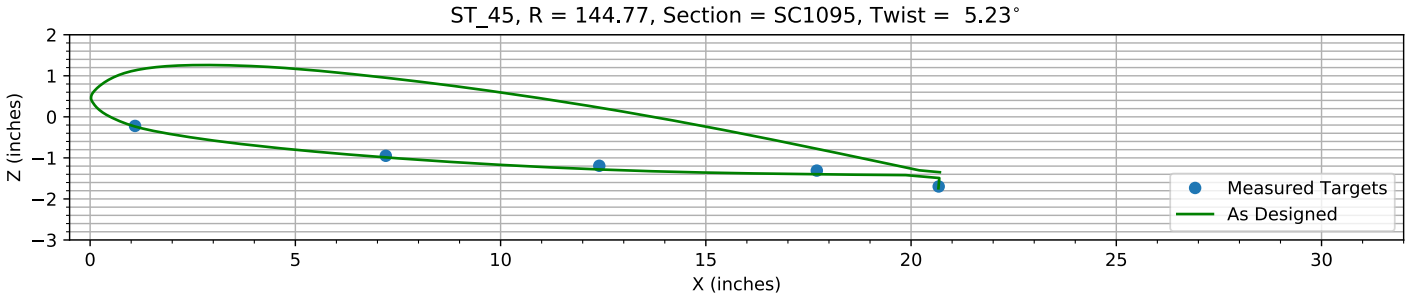

Figure 4-10. Target locations vs section profile at station 45.

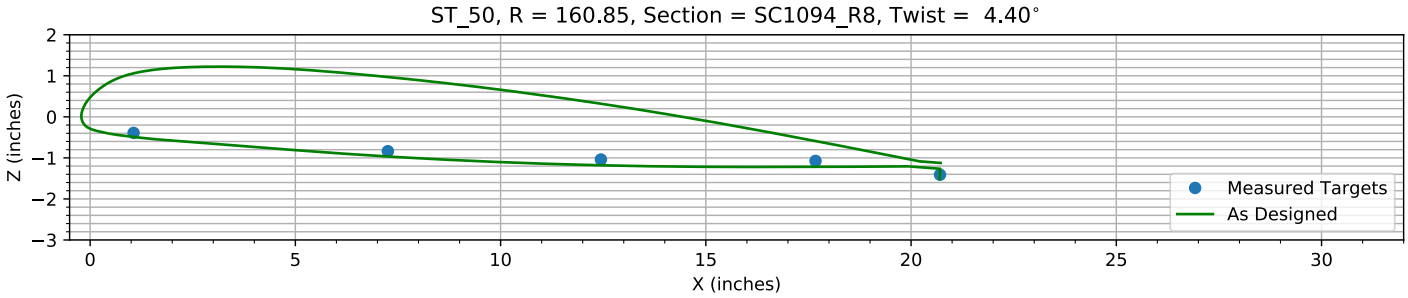

Figure 4-11. Target locations vs section profile at station 50.

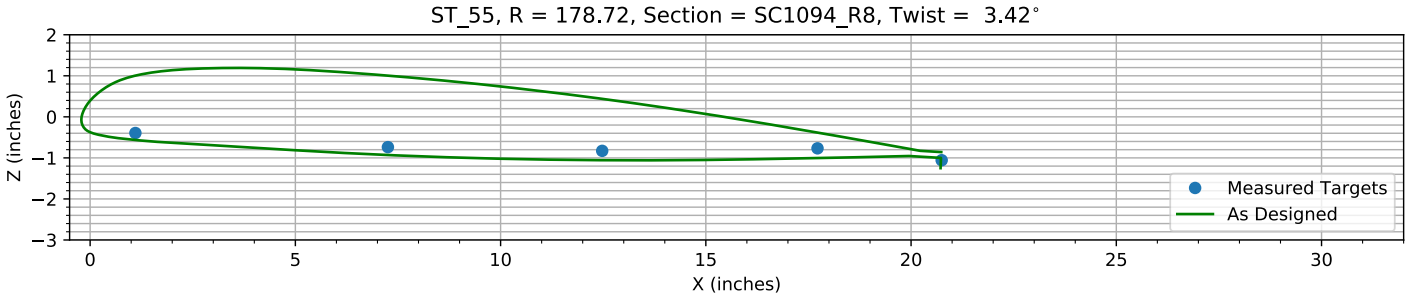

Figure 4-12. Target locations vs section profile at station 55.

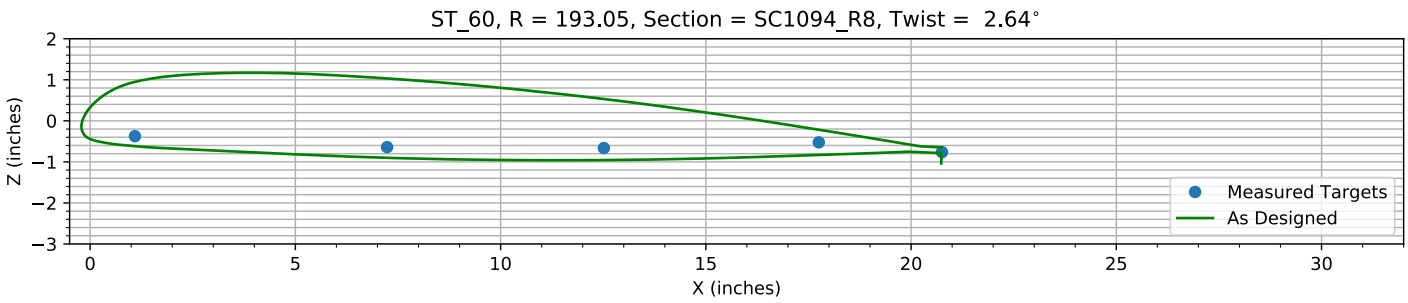

Figure 4-13. Target locations vs section profile at station 60.

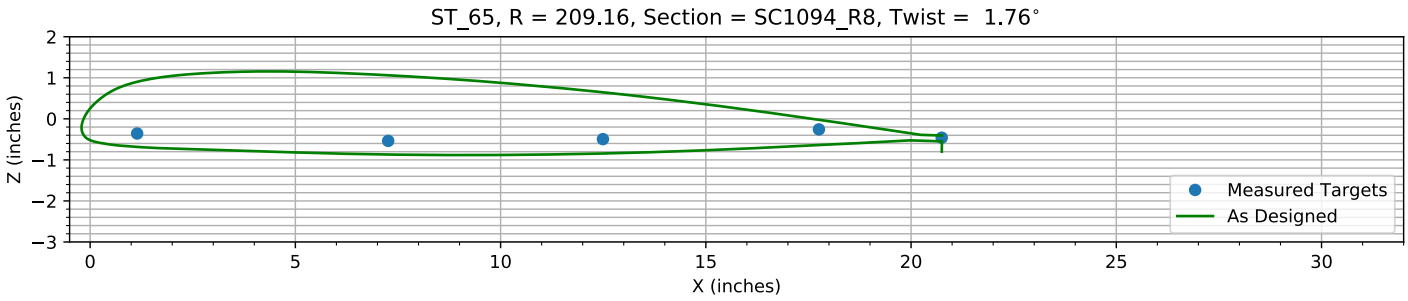

Figure 4-14. Target locations vs section profile at station 65.

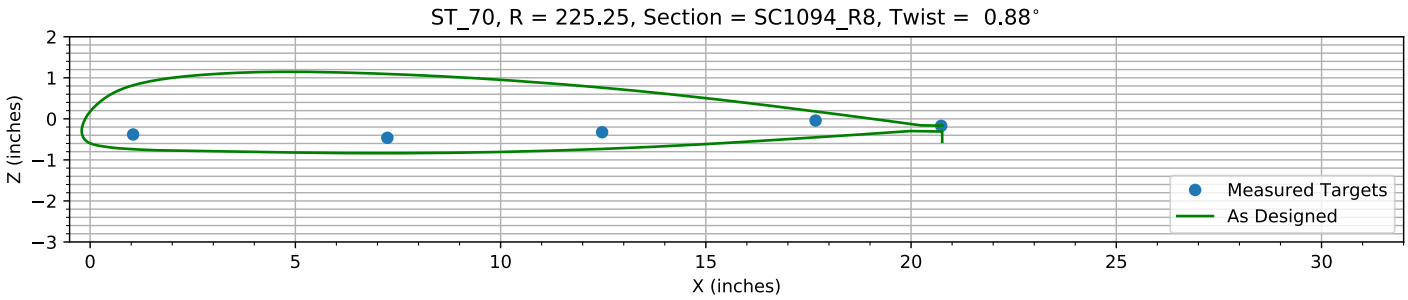

Figure 4-15. Target locations vs section profile at station 70.

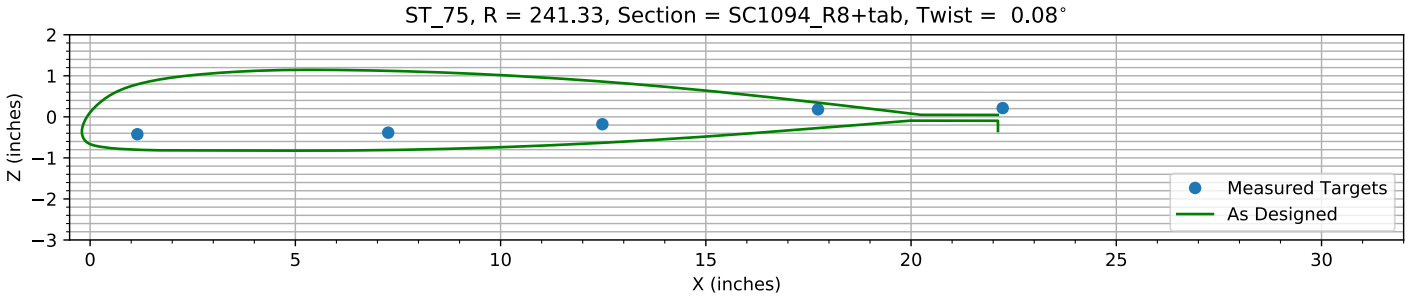

Figure 4-16. Target locations vs section profile at station 75.

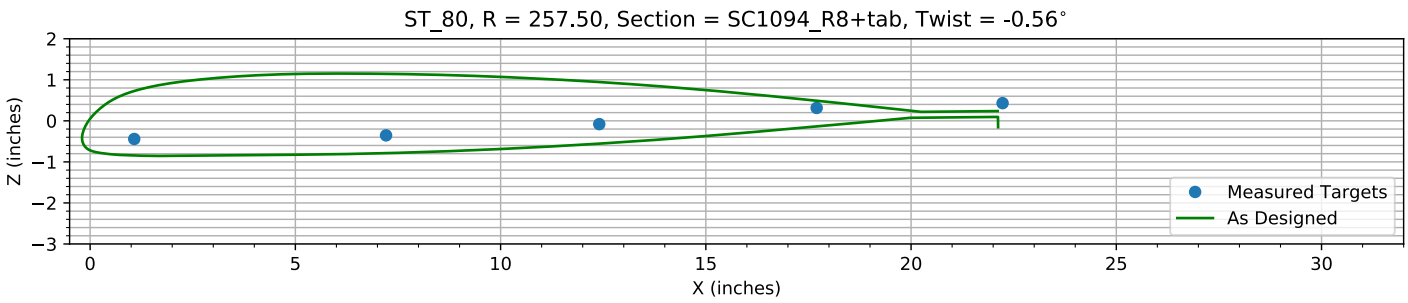

Figure 4-17. Target locations vs section profile at station 80.

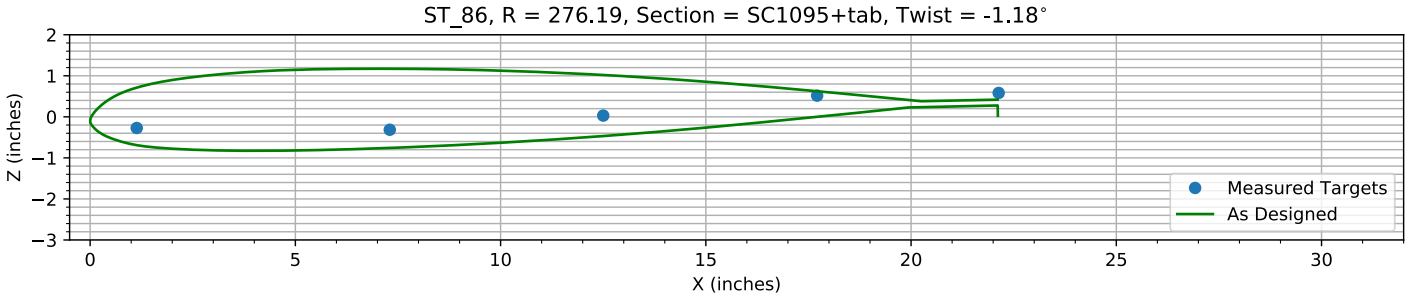

Figure 4-18. Target locations vs section profile at station 86.

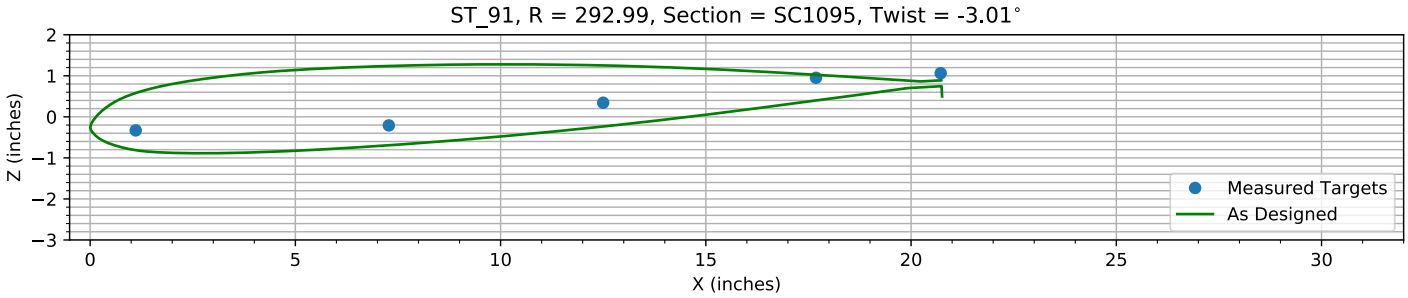

Figure 4-19. Target locations vs section profile at station 91.

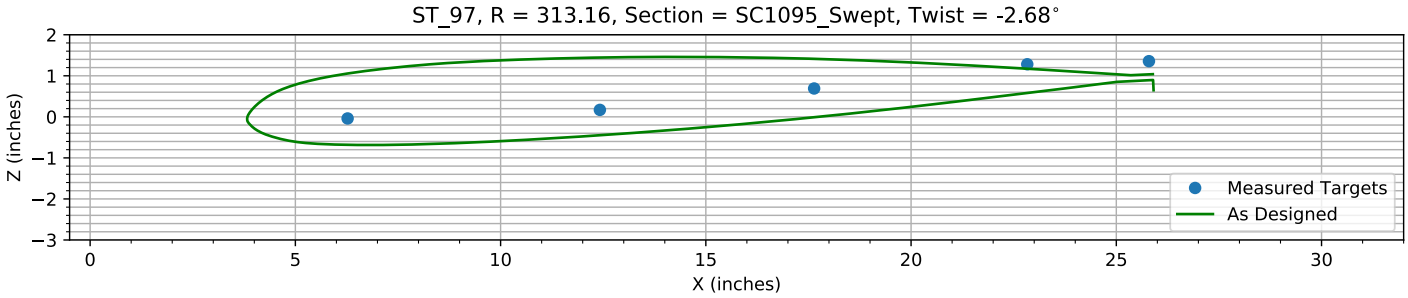

Figure 4-20. Target locations vs section profile at station 97.

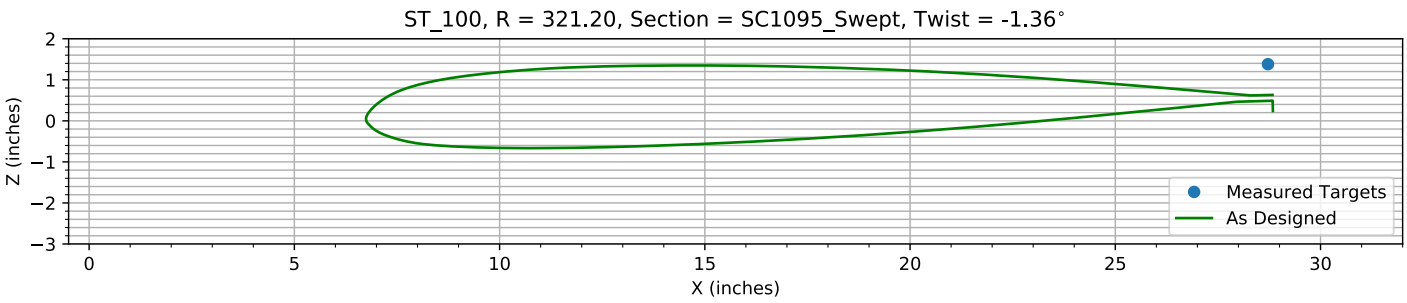

Figure 4-21. Target locations vs section profile at station 100.

Chapter 5: Flap Only Registration (15 rows)

The targets at the 15 spanwise stations nearest the root are used to determing the flap offset.

The estimated flap error is -0.22041°.

5.1: Target Location Errors After Flap Target Registration

Table 5-1. Measured(1) with flap registration vs "as designed"(2) in inches.

Name	X1	Y1	Z1	X2	Y2	Z2	dX	dY	dZ	dR
B2_R20_C05	1.0479	62.78	-0.20338	1.0479	62.78	0.072104	0	0	-0.27548	0.27548
B2_R20_C36	7.1535	62.761	-1.3924	7.1535	62.761	-1.134	0	0	-0.25836	0.25836
B2_R20_C61	12.319	62.752	-1.9774	12.319	62.752	-1.7974	0	0	-0.17998	0.17998
B2_R20_C86	17.568	62.756	-2.457	17.568	62.756	-2.2906	0	0	-0.16638	0.16638
B2_R20_C99	20.503	62.717	-3.0454	20.502	62.717	-2.8432	0.0017557	0	-0.20223	0.20224
B2_R25_C05	1.0659	77.396	-0.23935	1.0659	77.396	0.012298	0	0	-0.25165	0.25165
B2_R25_C36	7.12	77.417	-1.3472	7.12	77.417	-1.1022	0	0	-0.24491	0.24491
B2_R25_C61	12.334	77.423	-1.8976	12.334	77.423	-1.7048	0	0	-0.19281	0.19281
B2_R25_C86	17.551	77.427	-2.3539	17.551	77.427	-2.1278	0	0	-0.22617	0.22617
B2_R25_C99	20.506	77.393	-2.9001	20.537	77.393	-2.6458	-0.030848	0	-0.25431	0.25617
B2_R30_C05	1.0258	96.617	-0.27481	1.0258	96.617	-0.043059	0	0	-0.23175	0.23175
B2_R30_C36	7.0997	96.584	-1.2708	7.0997	96.584	-1.0652	0	0	-0.2056	0.2056
B2_R30_C61	12.334	96.537	-1.764	12.334	96.537	-1.5829	0	0	-0.18118	0.18118
B2_R30_C86	17.533	96.529	-2.1086	17.533	96.529	-1.9182	0	0	-0.19035	0.19035
B2_R30_C99	20.545	96.518	-2.6412	20.579	96.518	-2.3887	-0.034318	0	-0.25248	0.2548
B2_R35_C05	1.165	112.63	-0.31201	1.165	112.63	-0.14477	0	0	-0.16723	0.16723
B2_R35_C36	7.1936	112.64	-1.2208	7.1936	112.64	-1.0465	0	0	-0.17428	0.17428
B2_R35_C61	12.467	112.66	-1.6372	12.467	112.66	-1.4895	0	0	-0.1477	0.1477
B2_R35_C86	17.647	112.64	-1.8979	17.647	112.64	-1.748	0	0	-0.14987	0.14987
B2_R35_C99	20.626	112.61	-2.3771	20.611	112.61	-2.1724	0.014544	0	-0.2047	0.20522
B2_R40_C05	1.1381	128.82	-0.37762	1.1381	128.82	-0.19321	0	0	-0.1844	0.1844
B2_R40_C36	7.2231	128.77	-1.1609	7.2231	128.77	-1.0196	0	0	-0.14137	0.14137
B2_R40_C61	12.465	128.76	-1.4983	12.465	128.76	-1.3862	0	0	-0.1121	0.1121
B2_R40_C86	17.684	128.67	-1.688	17.684	128.67	-1.5741	0	0	-0.11389	0.11389
B2_R40_C99	20.649	128.68	-2.1202	20.64	128.68	-1.9562	0.0087984	0	-0.16399	0.16423
B2_R45_C05	1.094	144.78	-0.39973	1.094	144.78	-0.2363	0	0	-0.16343	0.16343
B2_R45_C36	7.2027	144.76	-1.1273	7.2027	144.76	-0.98861	0	0	-0.13871	0.13871
B2_R45_C61	12.404	144.79	-1.3706	12.404	144.79	-1.2815	0	0	-0.089151	0.089151
B2_R45_C86	17.704	144.78	-1.4884	17.704	144.78	-1.3988	0	0	-0.089636	0.089636
B2_R45_C99	20.673	144.76	-1.8752	20.666	144.76	-1.7397	0.0071104	0	-0.13547	0.13566
B2_R50_C05	1.0586	160.81	-0.59516	1.0586	160.81	-0.4897	0	0	-0.10547	0.10547
B2_R50_C36	7.2535	160.84	-1.0406	7.2535	160.84	-0.96642	0	0	-0.074146	0.074146
B2_R50_C61	12.444	160.83	-1.2429	12.444	160.83	-1.1805	0	0	-0.062421	0.062421
B2_R50_C86	17.672	160.84	-1.2772	17.672	160.84	-1.2184	0	0	-0.058839	0.058839
B2_R50_C99	20.705	160.96	-1.6139	20.695	160.96	-1.5134	0.010183	0	-0.10048	0.101
B2_R55_C05	1.1027	178.74	-0.6252	1.1027	178.74	-0.56389	0	0	-0.061302	0.061302
B2_R55_C36	7.2544	178.72	-0.96916	7.2544	178.72	-0.93035	0	0	-0.038802	0.038802
B2_R55_C61	12.475	178.75	-1.0599	12.475	178.75	-1.0561	0	0	-0.0038115	0.0038115
B2_R55_C86	17.721	178.72	-0.99857	17.721	178.72	-1.0044	0	0	0.0058618	0.0058618
B2_R55_C99	20.746	178.67	-1.2884	20.719	178.67	-1.2508	0.026887	0	-0.037557	0.046189
B2_R60_C05	1.0913	193.08	-0.62724	1.0913	193.08	-0.61814	0	0	-0.0090951	0.0090951
B2_R60_C36	7.2348	193.08	-0.89513	7.2348	193.08	-0.90101	0	0	0.0058831	0.0058831

Name	X1	Y1	Z1	X2	Y2	Z2	dX	dY	dZ	dR
B2_R60_C61	12.516	193.09	-0.9162	12.516	193.09	-0.95607	0	0	0.03987	0.03987
B2_R60_C86	17.752	193.05	-0.77806	17.752	193.05	-0.83225	0	0	0.054188	0.054188
B2_R60_C99	20.753	192.97	-1.0167	20.734	192.97	-1.0386	0.018593	0	0.02198	0.028789
B2_R65_C05	1.1453	209.12	-0.63591	1.1453	209.12	-0.68395	0	0	0.04804	0.04804
B2_R65_C36	7.2609	209.17	-0.81583	7.2609	209.17	-0.86966	0	0	0.053825	0.053825
B2_R65_C61	12.493	209.18	-0.7733	12.493	209.18	-0.84424	0	0	0.070944	0.070944
B2_R65_C86	17.755	209.21	-0.53619	17.755	209.21	-0.63867	0	0	0.10248	0.10248
B2_R65_C99	20.747	209.16	-0.73788	20.748	209.16	-0.79815	-0.0018416	0	0.060272	0.0603
B2_R70_C05	1.0474	225.11	-0.6846	1.0474	225.11	-0.73962	0	0	0.055025	0.055025
B2_R70_C36	7.2415	225.24	-0.766	7.2415	225.24	-0.83782	0	0	0.071812	0.071812
B2_R70_C61	12.473	225.27	-0.6304	12.473	225.27	-0.7332	0	0	0.1028	0.1028
B2_R70_C86	17.674	225.31	-0.34553	17.674	225.31	-0.45119	0	0	0.10566	0.10566
B2_R70_C99	20.734	225.31	-0.47464	20.759	225.31	-0.55809	-0.025165	0	0.083455	0.087166
B2_R75_C05	1.15	241.32	-0.75257	1.15	241.32	-0.80118	0	0	0.048607	0.048607
B2_R75_C36	7.2618	241.33	-0.71482	7.2618	241.33	-0.8092	0	0	0.094381	0.094381
B2_R75_C61	12.48	241.36	-0.50862	12.48	241.36	-0.6325	0	0	0.12389	0.12389
B2_R75_C86	17.733	241.34	-0.14648	17.733	241.34	-0.27481	0	0	0.12833	0.12833
B2_R80_C05	1.0747	257.59	-0.79608	1.0747	257.59	-0.84444	0	0	0.048361	0.048361
B2_R80_C36	7.2095	257.51	-0.70807	7.2095	257.51	-0.78737	0	0	0.079296	0.079296
B2_R80_C61	12.403	257.48	-0.43417	12.403	257.48	-0.55554	0	0	0.12137	0.12137
B2_R80_C86	17.7	257.43	-0.039595	17.7	257.43	-0.13703	0	0	0.097438	0.097438
B2_R86_C05	1.1351	276.22	-0.65518	1.1351	276.22	-0.6903	0	0	0.035112	0.035112
B2_R86_C36	7.3003	276.21	-0.69742	7.3003	276.21	-0.75771	0	0	0.060286	0.060286
B2_R86_C61	12.5	276.21	-0.35265	12.5	276.21	-0.46831	0	0	0.11566	0.11566
B2_R86_C86	17.712	276.17	0.13371	17.712	276.17	-0.00031487	0	0	0.13403	0.13403
B2_R91_C05	1.1097	293.02	-0.73985	1.1097	293.02	-0.81276	0	0	0.072909	0.072909
B2_R91_C36	7.2773	292.99	-0.61778	7.2773	292.99	-0.69298	0	0	0.075193	0.075193
B2_R91_C61	12.499	293.03	-0.065921	12.499	293.03	-0.2348	0	0	0.16888	0.16888
B2_R91_C86	17.683	292.97	0.54215	17.683	292.97	0.39747	0	0	0.14468	0.14468
B2_R91_C99	20.721	292.97	0.65384	20.755	292.97	0.49707	-0.034223	0	0.15678	0.16047
B2_R97_C05	6.2728	313.03	-0.47968	6.2728	313.03	-0.68464	0	0	0.20496	0.20496
B2_R97_C36	12.419	313.09	-0.27084	12.419	313.09	-0.44728	0	0	0.17644	0.17644
B2_R97_C61	17.638	313.2	0.25017	17.638	313.2	-0.012471	0	0	0.26264	0.26264
B2_R97_C86	22.831	313.27	0.84015	22.831	313.27	0.57262	0	0	0.26753	0.26753
B2_R97_C99	25.795	313.25	0.91566	25.939	313.25	0.64504	-0.14367	0	0.27063	0.3064
HUB_LE	2.2382	30.002	-3.5002	2.19	30	-3.5	0.048215	0.0023829	-0.00019083	0.048274
HUB_TE	8.2354	29.998	-3.4998	8.19	30	-3.5	0.045413	-0.0024585	0.00019054	0.04548
RMS Errors:							0.019642	0.0003852	0.14544	0.14677

5.2: Flap Registration Plots (15 rows)

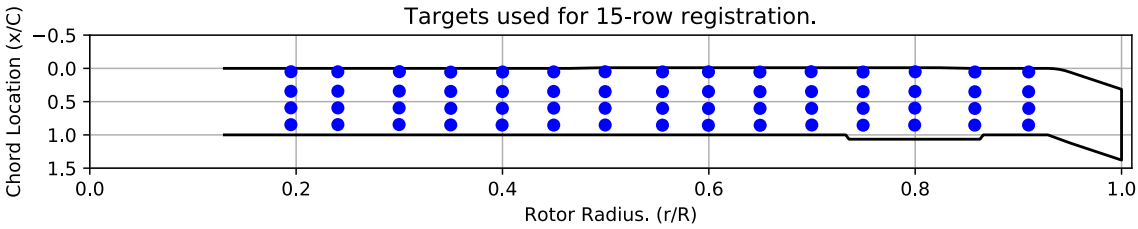

Figure 5-1. Targets used for 15 row root registration.

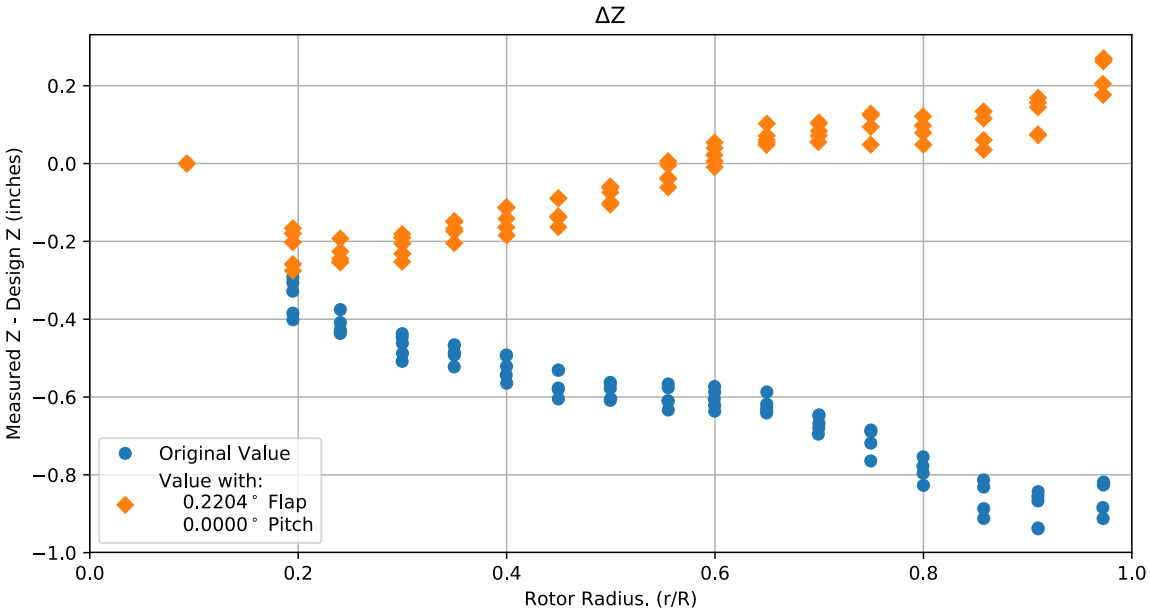

Figure 5-2. Flap target registration, ΔZ error vs rotor radius.

Note: the “as designed” geometry used for the swept tip may have some inaccuracies.

5.3: Estimated Bending and Twist at the Quarter Chord

The error bars shown represent the residual errors for fitting the measure target locations to the "as designed" geometry. These errors are generally much larger than those due to the VSTARS measurement errors. Therefore, the most likely source of these errors is the placement of the trailing-edge targets, differences between the "as designed" and "as built" geometries, and blade deformation during measurement. In the future, iterative adjustment of the "as designed" twist angle may be implemented to see if it reduces the fit error in delta twist. Note: The "as designed" geometry used for the swept tip may have some inaccuracies.

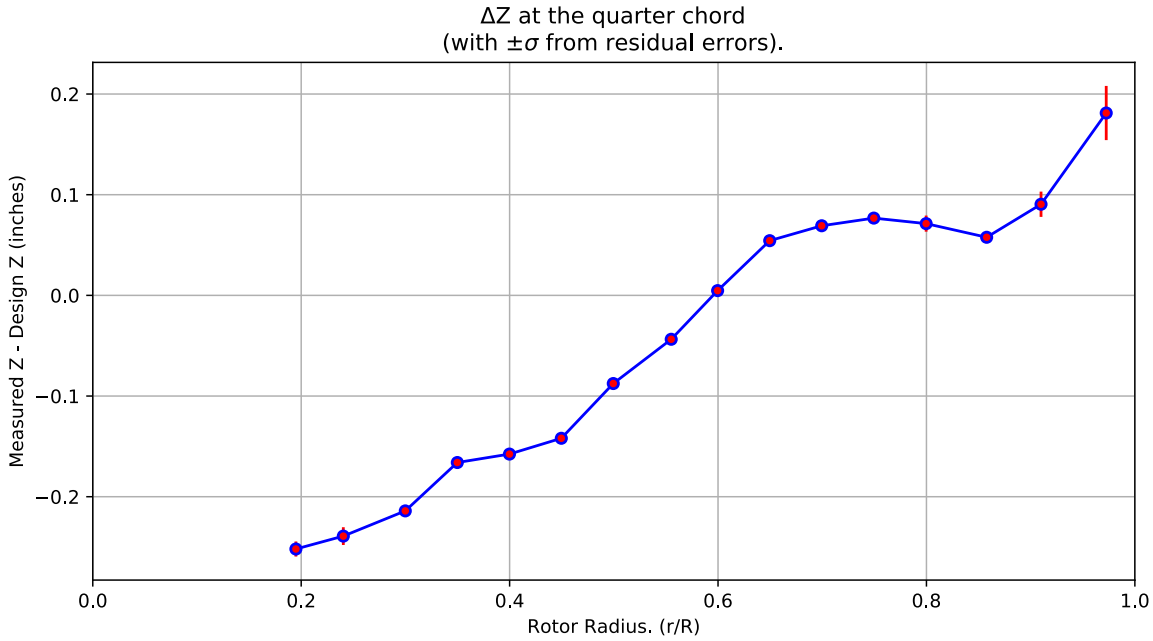

Figure 5-3. ΔZ error at the quarter chord vs rotor radius.

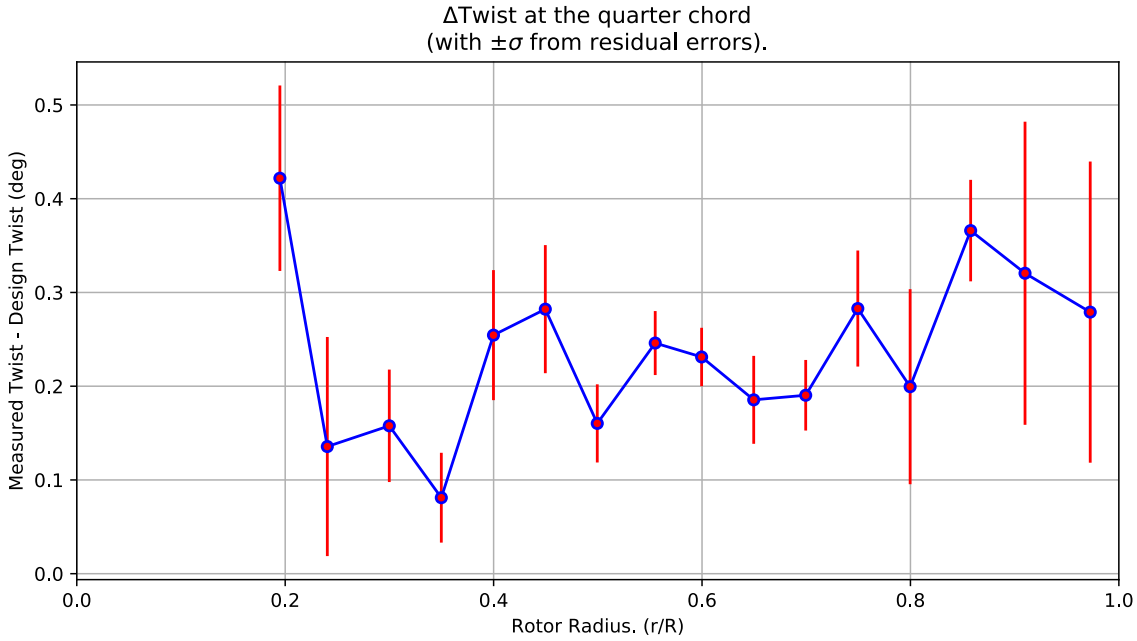

Figure 5-4. ΔTwist error at the quarter chord vs rotor radius.

Table 5-2. Quarter-chord bending and twist statistics.

r	r/R	dZ 1/4-chord	dT	sigma dZ meas	sigma dT meas	sigma dZ res	sigma dT res	n	t_conf
62.762	0.19491	-0.25195	0.42187	6.1248e-10	4.6781e-09	0.0074805	0.098927	4	4.3027
77.416	0.24042	-0.23913	0.13564	6.125e-10	4.6837e-09	0.0088275	0.11687	4	4.3027
96.566	0.2999	-0.21408	0.15775	6.1125e-10	4.6761e-09	0.0045104	0.059985	4	4.3027
112.64	0.34982	-0.16604	0.08106	6.1709e-10	4.6796e-09	0.0037027	0.047911	4	4.3027
128.76	0.39986	-0.15765	0.25448	6.1691e-10	4.6655e-09	0.0053721	0.06936	4	4.3027
144.78	0.44962	-0.14196	0.28219	6.1508e-10	4.6529e-09	0.00526	0.068321	4	4.3027
160.83	0.49947	-0.087577	0.16031	6.1531e-10	4.6516e-09	0.0032139	0.041687	4	4.3027
178.73	0.55508	-0.043614	0.24602	6.1664e-10	4.6485e-09	0.0026498	0.03413	4	4.3027
193.07	0.59961	0.0047229	0.23117	6.1642e-10	4.6329e-09	0.0024238	0.031147	4	4.3027
209.17	0.64959	0.054341	0.18545	6.1792e-10	4.65e-09	0.003662	0.046899	4	4.3027
225.24	0.69949	0.069144	0.19035	6.1509e-10	4.645e-09	0.0029036	0.037648	4	4.3027
241.33	0.74949	0.076754	0.28284	6.1793e-10	4.658e-09	0.0048254	0.061904	4	4.3027
257.5	0.79969	0.071274	0.19947	6.1472e-10	4.6492e-09	0.0080013	0.10402	4	4.3027
276.2	0.85778	0.057707	0.36599	6.1831e-10	4.6603e-09	0.0042257	0.05414	4	4.3027
293	0.90995	0.090511	0.32049	6.1732e-10	4.6592e-09	0.012563	0.16167	4	4.3027
313.15	0.97252	0.18114	0.27903	9.2771e-10	4.6637e-09	0.026915	0.16063	4	4.3027

5.4: Section Plots

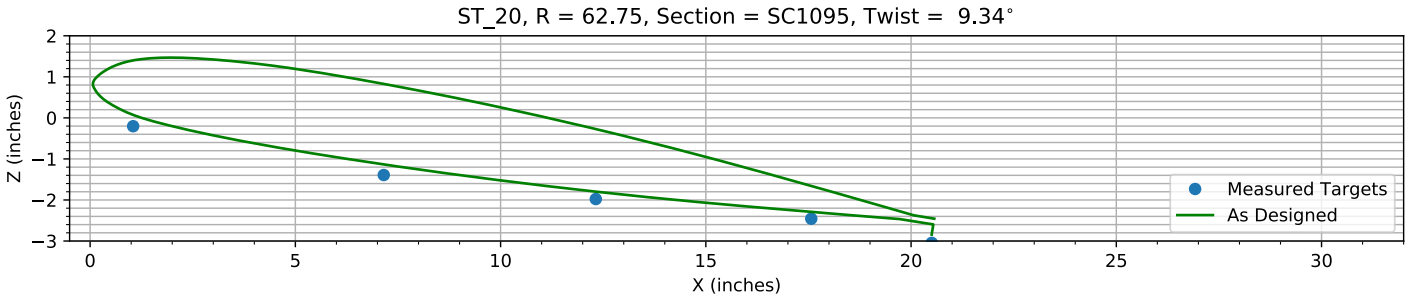

Figure 5-5. Target locations vs section profile at station 20.

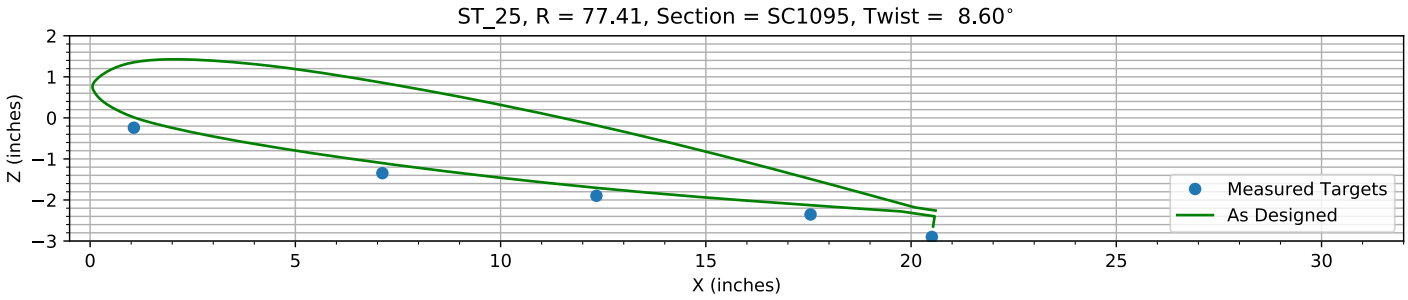

Figure 5-6. Target locations vs section profile at station 25.

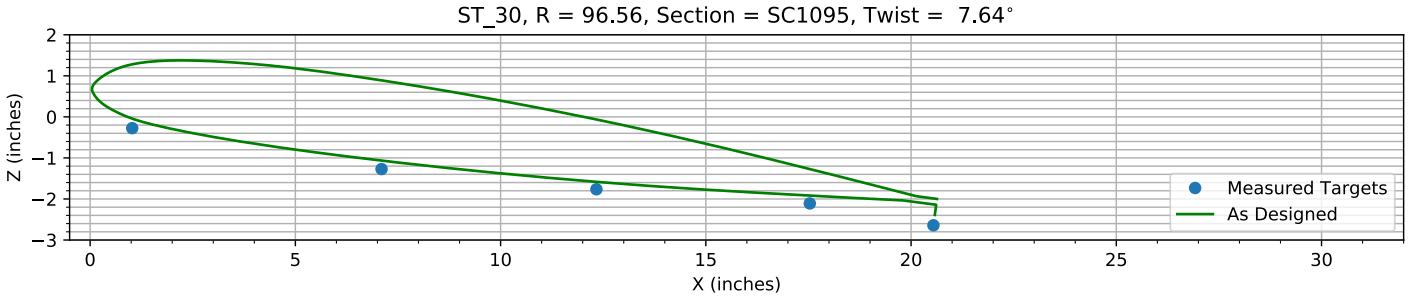

Figure 5-7. Target locations vs section profile at station 30.

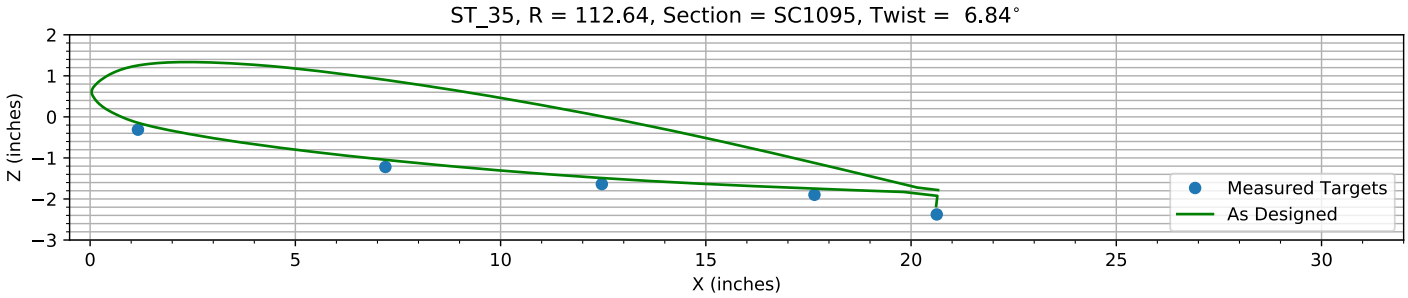

Figure 5-8. Target locations vs section profile at station 35.

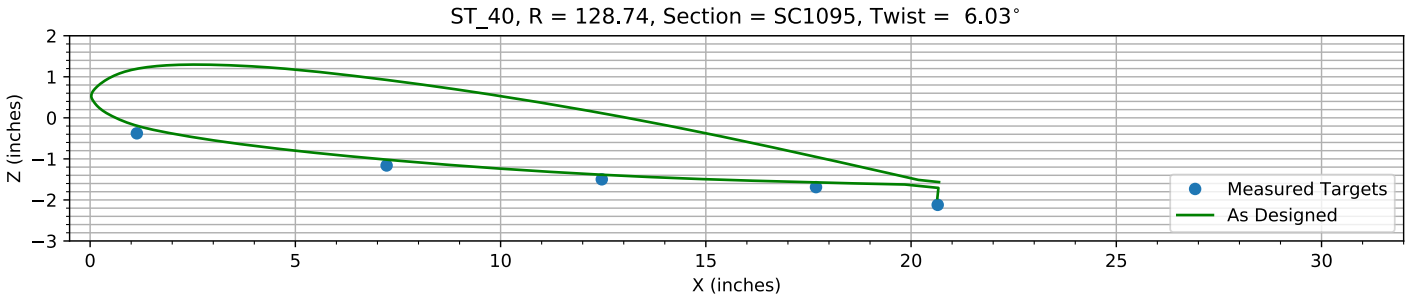

Figure 5-9. Target locations vs section profile at station 40.

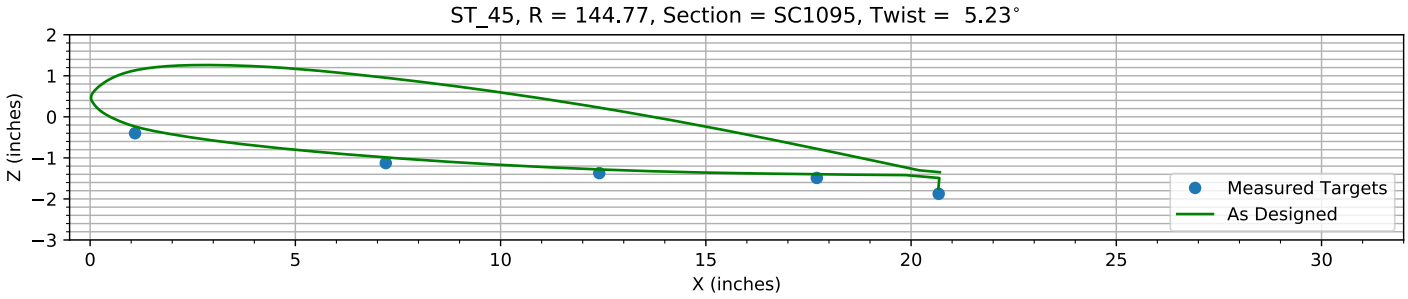

Figure 5-10. Target locations vs section profile at station 45.

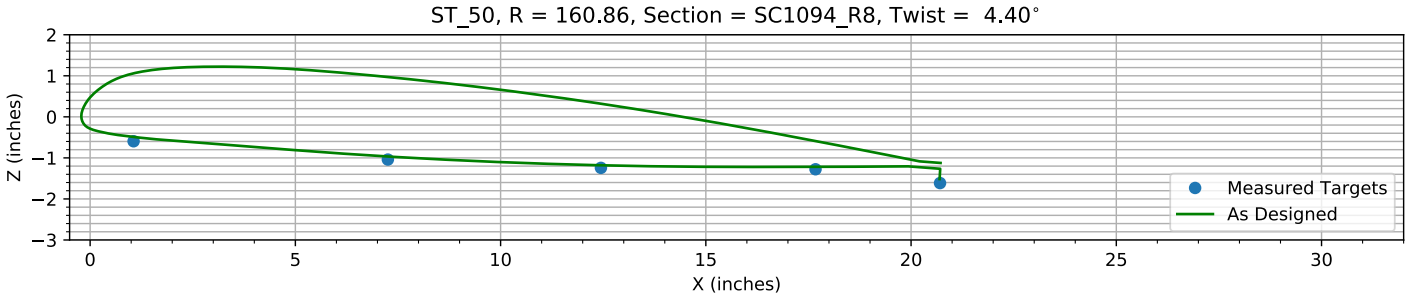

Figure 5-11. Target locations vs section profile at station 50.

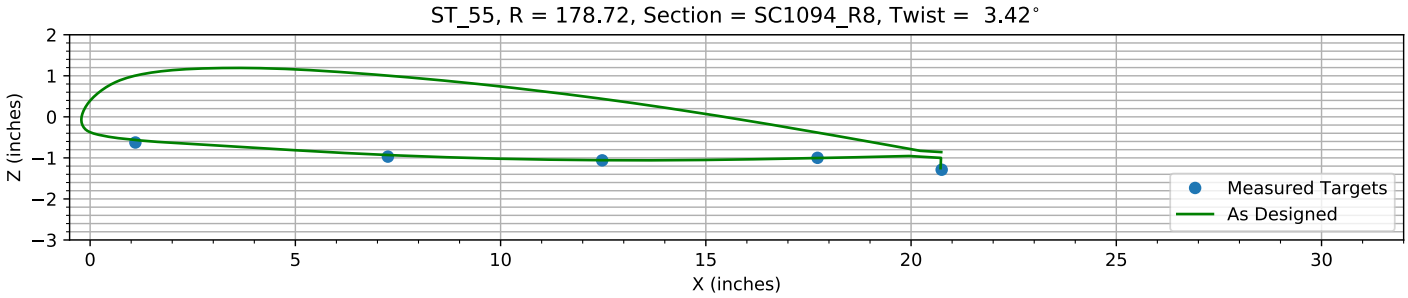

Figure 5-12. Target locations vs section profile at station 55.

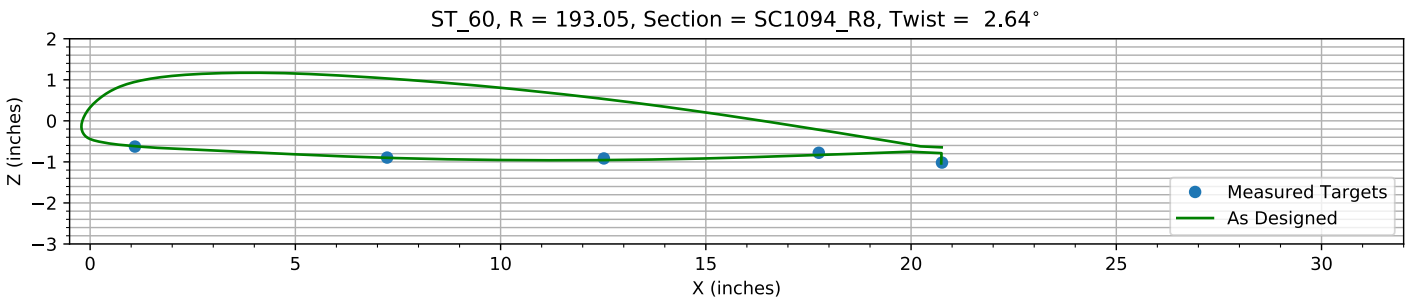

Figure 5-13. Target locations vs section profile at station 60.

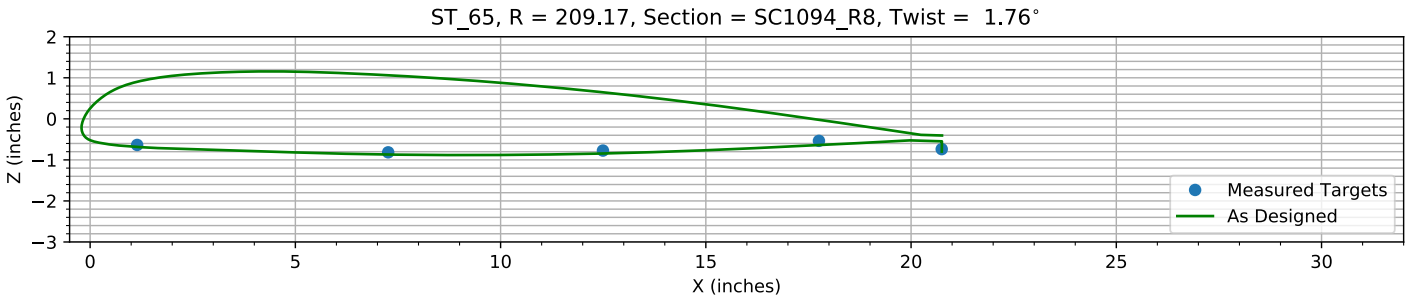

Figure 5-14. Target locations vs section profile at station 65.

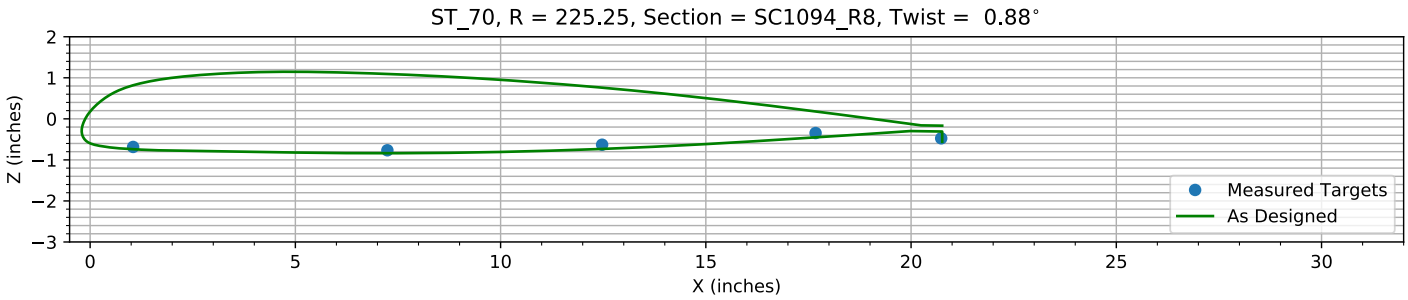

Figure 5-15. Target locations vs section profile at station 70.

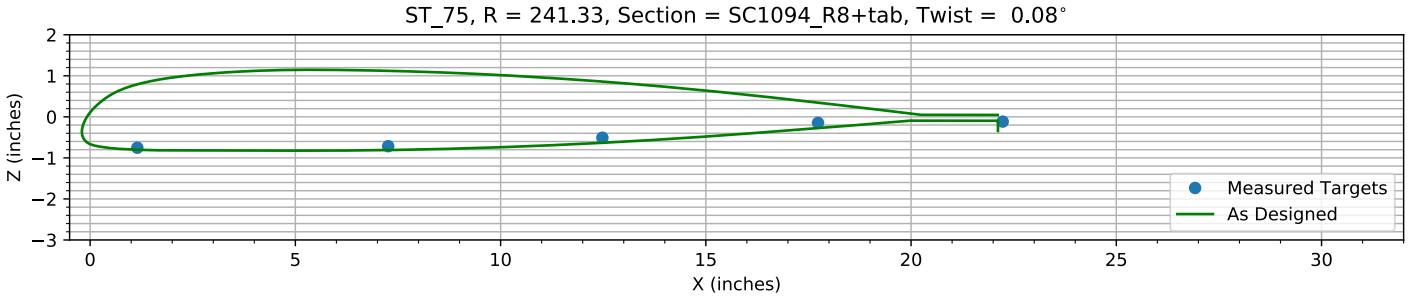

Figure 5-16. Target locations vs section profile at station 75.

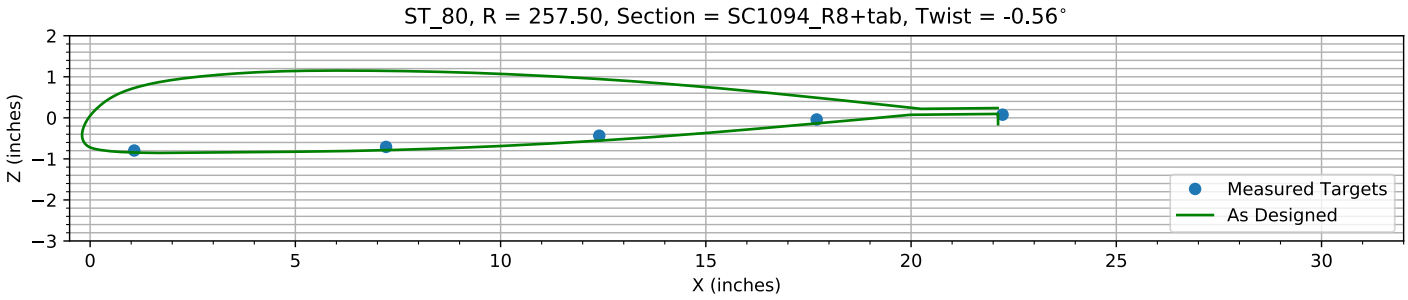

Figure 5-17. Target locations vs section profile at station 80.

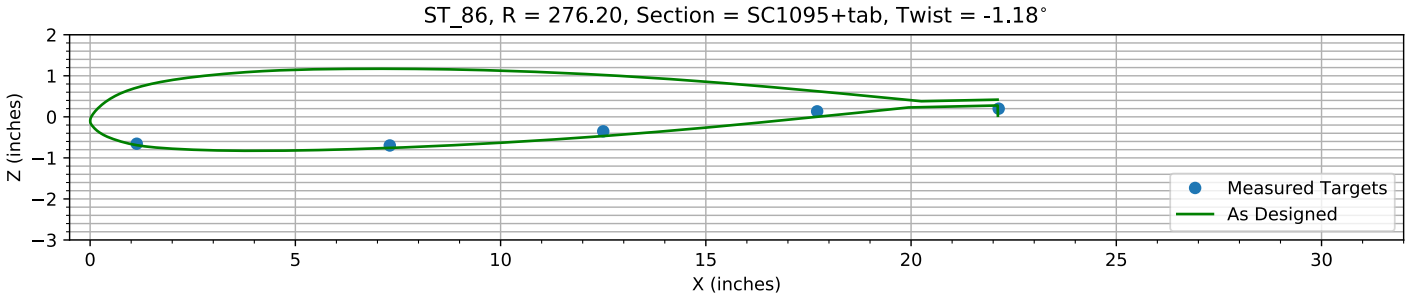

Figure 5-18. Target locations vs section profile at station 86.

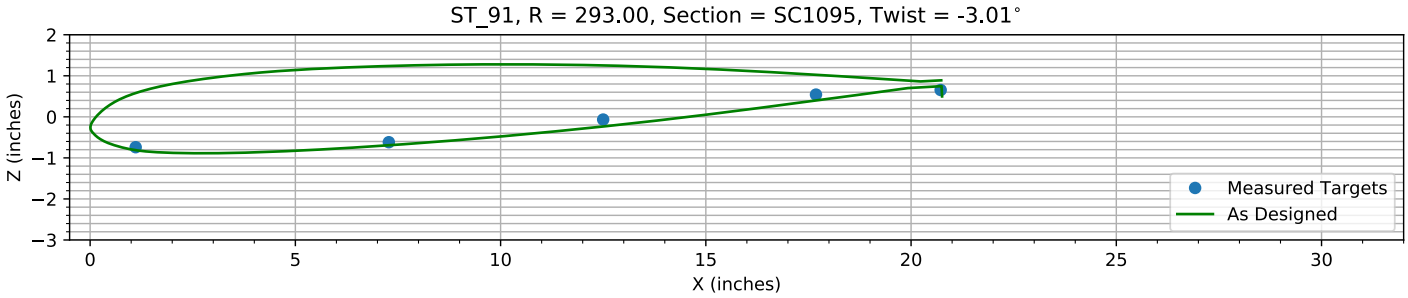

Figure 5-19. Target locations vs section profile at station 91.

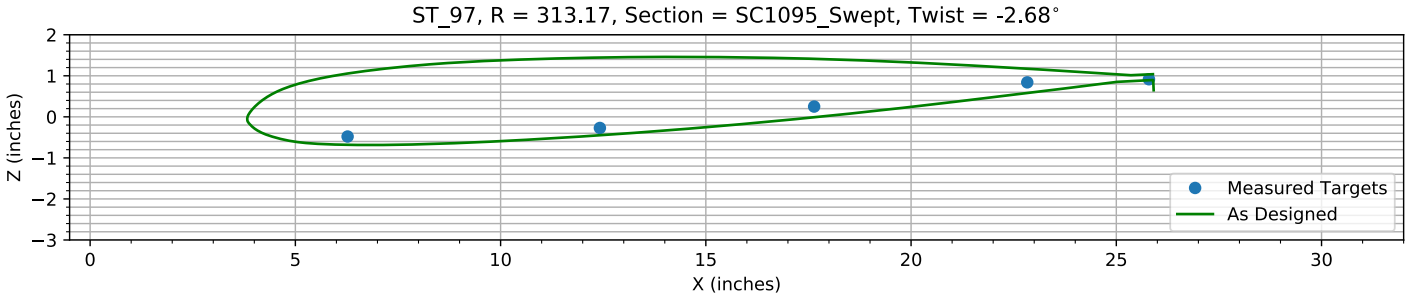

Figure 5-20. Target locations vs section profile at station 97.

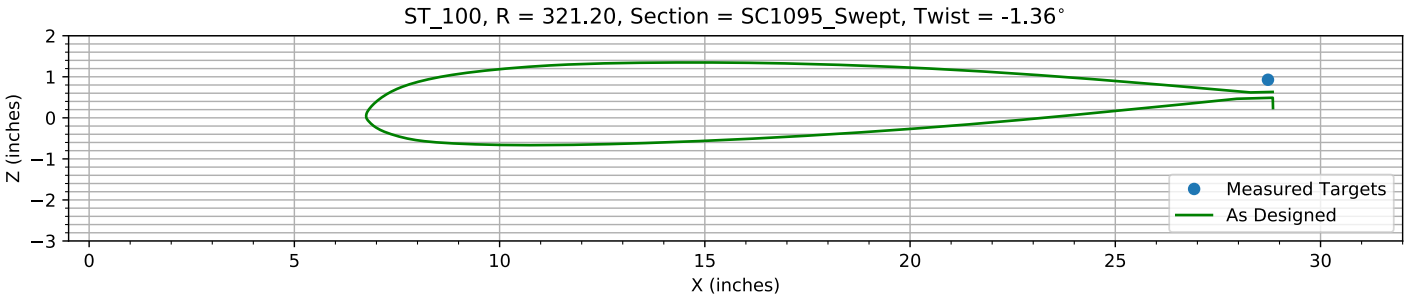

Figure 5-21. Target locations vs section profile at station 100.

Chapter 6: Flap and ΔZ Registration (6 rows)

The targets at the 6 spanwise stations nearest the root are used to determing the Z and flap offset.

The estimated Z error, -0.30715 inches, is within an allowed range of ±2.000 inches.

The estimated flap error is -0.12057°.

6.1: Target Location Errors After Flap Target Registration

Table 6-1. Measured(1) with flap registration vs as designed(2) in inches.

Name	X1	Y1	Z1	X2	Y2	Z2	dX	dY	dZ	dR
B2_R20_C05	1.0479	62.785	0.046645	1.0479	62.785	0.072086	0	0	-0.025441	0.025441
B2_R20_C36	7.1535	62.764	-1.1423	7.1535	62.764	-1.134	0	0	-0.0083082	0.0083082
B2_R20_C61	12.319	62.754	-1.7273	12.319	62.754	-1.7974	0	0	0.070082	0.070082
B2_R20_C86	17.568	62.757	-2.2069	17.568	62.757	-2.2906	0	0	0.083672	0.083672
B2_R20_C99	20.503	62.717	-2.7953	20.502	62.717	-2.8432	0.0017555	0	0.047905	0.047937
B2_R25_C05	1.0659	77.401	-0.014796	1.0659	77.401	0.01228	0	0	-0.027076	0.027076
B2_R25_C36	7.12	77.42	-1.1226	7.12	77.42	-1.1022	0	0	-0.020397	0.020397
B2_R25_C61	12.334	77.425	-1.6731	12.334	77.425	-1.7047	0	0	0.031688	0.031688
B2_R25_C86	17.551	77.429	-2.1294	17.551	77.429	-2.1278	0	0	-0.0016788	0.0016788
B2_R25_C99	20.506	77.393	-2.6755	20.537	77.393	-2.6458	-0.030849	0	-0.029749	0.042856
B2_R30_C05	1.0258	96.622	-0.083749	1.0258	96.622	-0.043077	0	0	-0.040672	0.040672
B2_R30_C36	7.0997	96.587	-1.0797	7.0997	96.587	-1.0652	0	0	-0.01449	0.01449
B2_R30_C61	12.334	96.539	-1.5728	12.334	96.539	-1.5828	0	0	0.010011	0.010011
B2_R30_C86	17.533	96.53	-1.9173	17.533	96.53	-1.9182	0	0	0.00084673	0.00084673
B2_R30_C99	20.545	96.519	-2.45	20.579	96.519	-2.3887	-0.034319	0	-0.061258	0.070216
B2_R35_C05	1.165	112.64	-0.14885	1.165	112.64	-0.14479	0	0	-0.004061	0.004061
B2_R35_C36	7.1936	112.64	-1.0576	7.1936	112.64	-1.0465	0	0	-0.01114	0.01114
B2_R35_C61	12.467	112.66	-1.4741	12.467	112.66	-1.4895	0	0	0.015386	0.015386
B2_R35_C86	17.647	112.64	-1.7347	17.647	112.64	-1.748	0	0	0.013249	0.013249
B2_R35_C99	20.626	112.61	-2.2139	20.611	112.61	-2.1724	0.014542	0	-0.04152	0.043992
B2_R40_C05	1.1381	128.83	-0.24268	1.1381	128.83	-0.19323	0	0	-0.049447	0.049447
B2_R40_C36	7.2231	128.77	-1.0259	7.2231	128.77	-1.0196	0	0	-0.0063394	0.0063394
B2_R40_C61	12.465	128.76	-1.3632	12.465	128.76	-1.3862	0	0	0.022944	0.022944
B2_R40_C86	17.684	128.68	-1.5528	17.684	128.68	-1.5741	0	0	0.021289	0.021289
B2_R40_C99	20.649	128.68	-1.985	20.64	128.68	-1.9562	0.0087956	0	-0.028824	0.030136
B2_R45_C05	1.094	144.78	-0.2926	1.094	144.78	-0.23632	0	0	-0.056277	0.056277
B2_R45_C36	7.2027	144.76	-1.0201	7.2027	144.76	-0.9886	0	0	-0.031541	0.031541
B2_R45_C61	12.404	144.79	-1.2635	12.404	144.79	-1.2814	0	0	0.017955	0.017955
B2_R45_C86	17.704	144.78	-1.3813	17.704	144.78	-1.3988	0	0	0.017471	0.017471
B2_R45_C99	20.673	144.76	-1.768	20.666	144.76	-1.7397	0.0071073	0	-0.028327	0.029205
B2_R50_C05	1.0586	160.81	-0.51596	1.0586	160.81	-0.48971	0	0	-0.026251	0.026251
B2_R50_C36	7.2535	160.84	-0.96141	7.2535	160.84	-0.96641	0	0	0.005003	0.005003
B2_R50_C61	12.444	160.83	-1.1637	12.444	160.83	-1.1805	0	0	0.01673	0.01673
B2_R50_C86	17.672	160.85	-1.1981	17.672	160.85	-1.2184	0	0	0.020269	0.020269
B2_R50_C99	20.705	160.96	-1.535	20.695	160.96	-1.5134	0.01018	0	-0.021569	0.02385
B2_R55_C05	1.1027	178.74	-0.57724	1.1027	178.74	-0.56391	0	0	-0.013325	0.013325
B2_R55_C36	7.2544	178.73	-0.92117	7.2544	178.73	-0.93035	0	0	0.0091778	0.0091778
B2_R55_C61	12.475	178.76	-1.012	12.475	178.76	-1.0561	0	0	0.044102	0.044102

Name	X1	Y1	Z1	X2	Y2	Z2	dX	dY	dZ	dR
B2_R55_C86	17.721	178.72	-0.95058	17.721	178.72	-1.0044	0	0	0.053814	0.053814
B2_R55_C99	20.746	178.67	-1.2403	20.719	178.67	-1.2508	0.026883	0	0.010482	0.028855
B2_R60_C05	1.0913	193.08	-0.60426	1.0913	193.08	-0.61816	0	0	0.013897	0.013897
B2_R60_C36	7.2348	193.08	-0.87216	7.2348	193.08	-0.901	0	0	0.028846	0.028846
B2_R60_C61	12.516	193.09	-0.89324	12.516	193.09	-0.95605	0	0	0.062805	0.062805
B2_R60_C86	17.752	193.05	-0.75503	17.752	193.05	-0.8322	0	0	0.077173	0.077173
B2_R60_C99	20.753	192.97	-0.9935	20.734	192.97	-1.0386	0.01859	0	0.045098	0.04878
B2_R65_C05	1.1453	209.13	-0.6409	1.1453	209.13	-0.68397	0	0	0.043072	0.043072
B2_R65_C36	7.2609	209.17	-0.8209	7.2609	209.17	-0.86965	0	0	0.048753	0.048753
B2_R65_C61	12.493	209.18	-0.77838	12.493	209.18	-0.84422	0	0	0.065838	0.065838
B2_R65_C86	17.755	209.21	-0.54132	17.755	209.21	-0.63862	0	0	0.097298	0.097298
B2_R65_C99	20.747	209.16	-0.74292	20.748	209.16	-0.79809	-0.0018445	0	0.055169	0.0552
B2_R70_C05	1.0474	225.12	-0.71745	1.0474	225.12	-0.73964	0	0	0.022193	0.022193
B2_R70_C36	7.2415	225.25	-0.79908	7.2415	225.25	-0.83781	0	0	0.038733	0.038733
B2_R70_C61	12.473	225.27	-0.66352	12.473	225.27	-0.73317	0	0	0.069653	0.069653
B2_R70_C86	17.674	225.32	-0.37872	17.674	225.32	-0.45113	0	0	0.072411	0.072411
B2_R70_C99	20.734	225.32	-0.50783	20.759	225.32	-0.55803	-0.025167	0	0.050198	0.056154
B2_R75_C05	1.15	241.32	-0.81365	1.15	241.32	-0.80119	0	0	-0.012462	0.012462
B2_R75_C36	7.2618	241.33	-0.77592	7.2618	241.33	-0.8092	0	0	0.033272	0.033272
B2_R75_C61	12.48	241.36	-0.56977	12.48	241.36	-0.63248	0	0	0.062714	0.062714
B2_R75_C86	17.733	241.34	-0.2076	17.733	241.34	-0.27477	0	0	0.067166	0.067166
B2_R80_C05	1.0747	257.59	-0.88551	1.0747	257.59	-0.84445	0	0	-0.041063	0.041063
B2_R80_C36	7.2095	257.51	-0.79737	7.2095	257.51	-0.78736	0	0	-0.010007	0.010007
B2_R80_C61	12.403	257.49	-0.52343	12.403	257.49	-0.55552	0	0	0.032098	0.032098
B2_R80_C86	17.7	257.43	-0.12875	17.7	257.43	-0.13699	0	0	0.0082475	0.0082475
B2_R86_C05	1.1351	276.23	-0.77709	1.1351	276.23	-0.6903	0	0	-0.086789	0.086789
B2_R86_C36	7.3003	276.22	-0.81931	7.3003	276.22	-0.7577	0	0	-0.061608	0.061608
B2_R86_C61	12.5	276.21	-0.47452	12.5	276.21	-0.46829	0	0	-0.0062315	0.0062315
B2_R86_C86	17.712	276.17	0.011899	17.712	276.17	-0.00028955	0	0	0.012189	0.012189
B2_R91_C05	1.1097	293.03	-0.89104	1.1097	293.03	-0.81279	0	0	-0.078248	0.078248
B2_R91_C36	7.2773	292.99	-0.76891	7.2773	292.99	-0.69296	0	0	-0.075946	0.075946
B2_R91_C61	12.499	293.04	-0.21712	12.499	293.04	-0.23473	0	0	0.017617	0.017617
B2_R91_C86	17.683	292.98	0.39106	17.683	292.98	0.3976	0	0	-0.0065461	0.0065461
B2_R91_C99	20.721	292.98	0.50276	20.755	292.98	0.49724	-0.034217	0	0.0055148	0.034659
B2_R97_C05	6.2728	313.04	-0.66573	6.2728	313.04	-0.68456	0	0	0.018827	0.018827
B2_R97_C36	12.419	313.1	-0.457	12.419	313.1	-0.4474	0	0	-0.0096035	0.0096035
B2_R97_C61	17.638	313.21	0.063828	17.638	313.21	-0.012737	0	0	0.076565	0.076565
B2_R97_C86	22.831	313.28	0.65368	22.831	313.28	0.57215	0	0	0.081538	0.081538
B2_R97_C99	25.795	313.26	0.72923	25.941	313.26	0.64482	-0.14608	0	0.084414	0.16872
HUB_LE	2.2382	30.002	-3.193	2.19	30	-3.5	0.048215	0.0017362	0.30695	0.31072
HUB_TE	8.2354	29.997	-3.1927	8.19	30	-3.5	0.045413	-0.0031045	0.30734	0.31069
RMS Errors:							0.019866	0.00040019	0.065285	0.068242

6.2: Flap Registration Plots (6 rows)

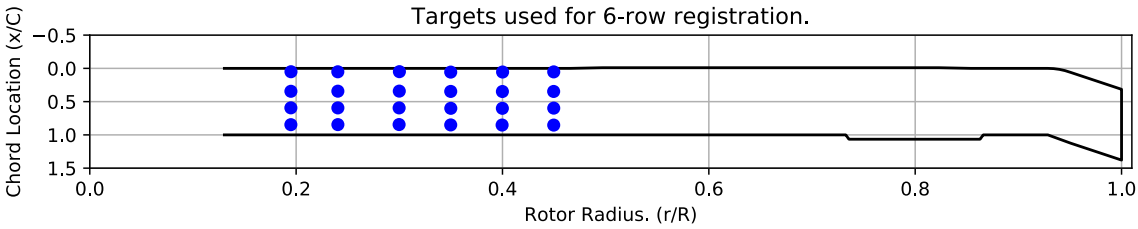

Figure 6-1. Targets used for 6 row root registration.

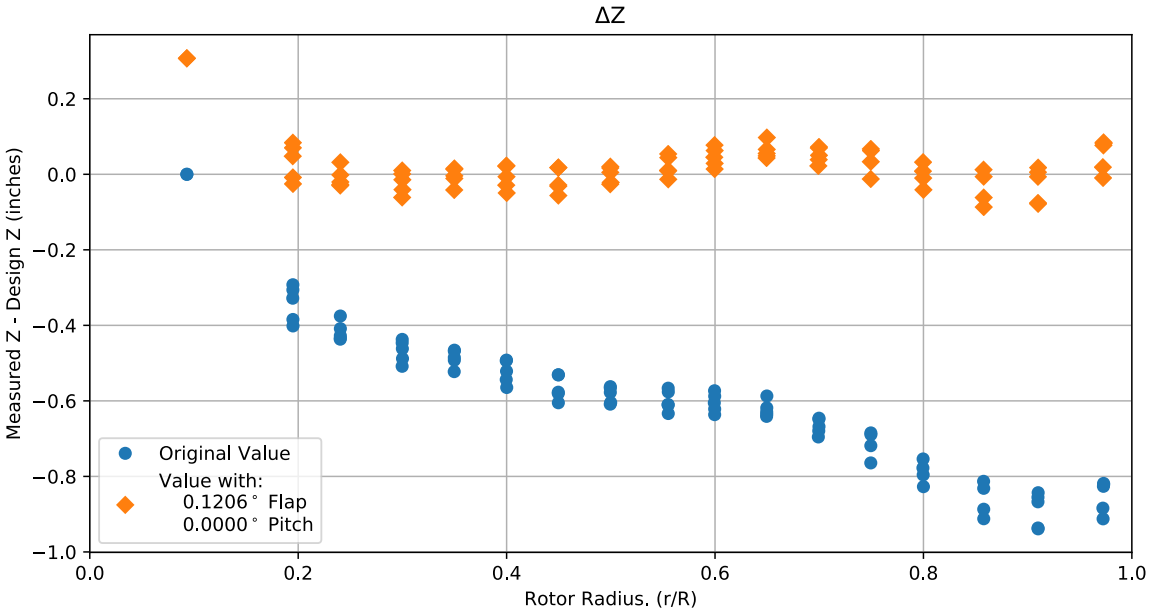

Figure 6-2. Flap target registration, ΔZ error vs rotor radius.

Note: the “as designed” geometry used for the swept tip may have some inaccuracies.

6.3: Estimated Bending and Twist at the Quarter Chord

The error bars shown represent the residual errors for fitting the measure target locations to the "as designed" geometry. These errors are generally much larger than those due to the VSTARS measurement errors. Therefore, the most likely source of these errors is the placement of the trailing-edge targets, differences between the "as designed" and "as built" geometries, and blade deformation during measurement. In the future, iterative adjustment of the "as designed" twist angle may be implemented to see if it reduces the fit error in delta twist. Note: The "as designed" geometry used for the swept tip may have some inaccuracies.

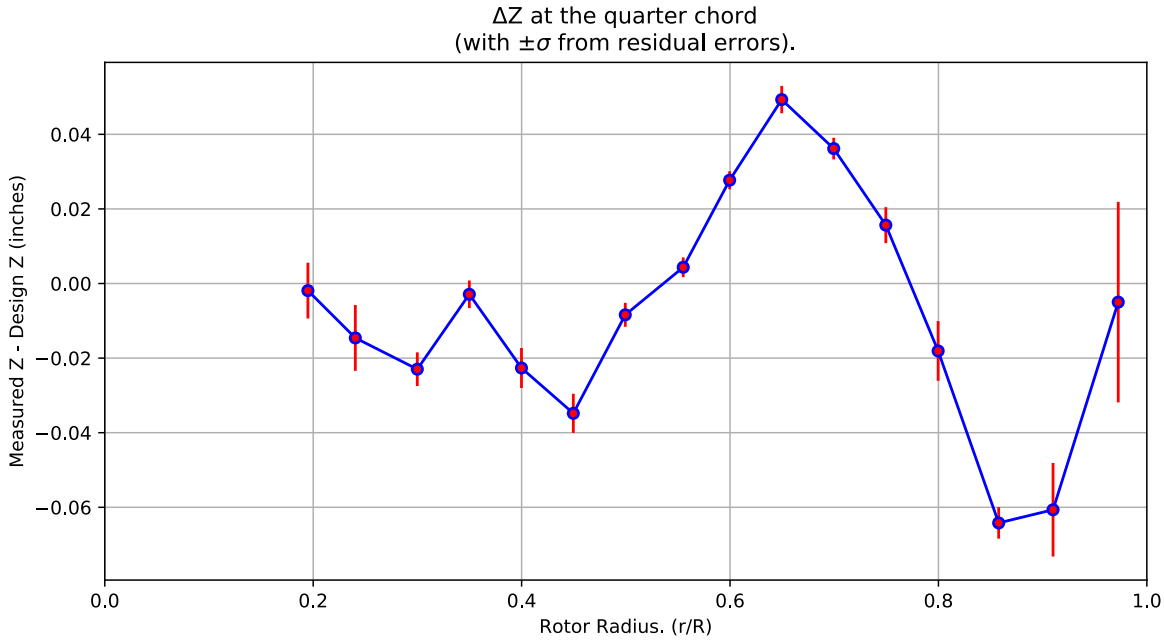

Figure 6-3. ΔZ error at the quarter chord vs rotor radius.

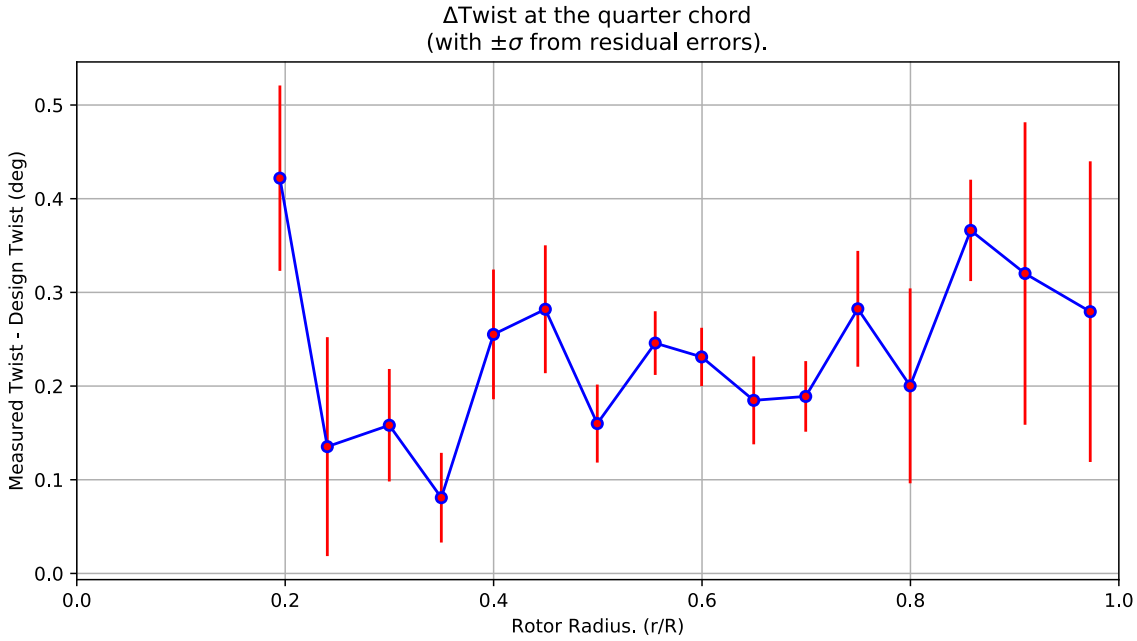

Figure 6-4. ΔTwist error at the quarter chord vs rotor radius.

Table 6-2. Quarter-chord bending and twist statistics.

r	r/R	dZ 1/4-chord	dT	sigma dZ meas	sigma dT meas	sigma dZ res	sigma dT res	n	t_conf
62.765	0.19492	-0.0019018	0.42192	6.1248e-10	4.6781e-09	0.0074814	0.09894	4	4.3027
77.419	0.24043	-0.01459	0.13535	6.125e-10	4.6837e-09	0.0088257	0.11684	4	4.3027
96.569	0.29991	-0.022972	0.1582	6.1125e-10	4.6761e-09	0.0045149	0.060045	4	4.3027
112.65	0.34983	-0.0028898	0.080851	6.1709e-10	4.6796e-09	0.0036991	0.047864	4	4.3027
128.76	0.39987	-0.022651	0.25517	6.1691e-10	4.6655e-09	0.0053617	0.069225	4	4.3027
144.78	0.44963	-0.034808	0.282	6.1508e-10	4.6529e-09	0.0052544	0.068249	4	4.3027
160.83	0.49948	-0.0083944	0.15996	6.1531e-10	4.6516e-09	0.0032104	0.041642	4	4.3027
178.74	0.55509	0.0043531	0.24588	6.1664e-10	4.6485e-09	0.0026389	0.03399	4	4.3027
193.08	0.59962	0.027696	0.23111	6.1642e-10	4.6329e-09	0.002421	0.031111	4	4.3027
209.17	0.64961	0.049315	0.18475	6.1792e-10	4.65e-09	0.0036647	0.046933	4	4.3027
225.24	0.6995	0.036174	0.18896	6.1509e-10	4.645e-09	0.0029063	0.037683	4	4.3027
241.34	0.7495	0.015654	0.28247	6.1793e-10	4.658e-09	0.0048192	0.061825	4	4.3027
257.51	0.79971	-0.018083	0.20023	6.1472e-10	4.6492e-09	0.0080001	0.10401	4	4.3027
276.21	0.85779	-0.06419	0.36618	6.1831e-10	4.6603e-09	0.0042227	0.054101	4	4.3027
293.01	0.90997	-0.060658	0.32014	6.1732e-10	4.6592e-09	0.012546	0.16145	4	4.3027
313.16	0.97253	-0.004989	0.27943	9.2771e-10	4.6637e-09	0.026888	0.16047	4	4.3027

6.4: Section Plots

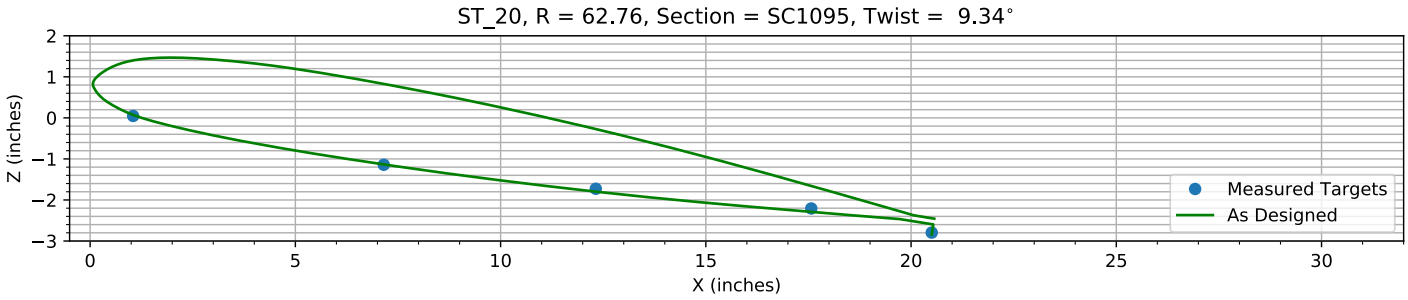

Figure 6-5. Target locations vs section profile at station 20.

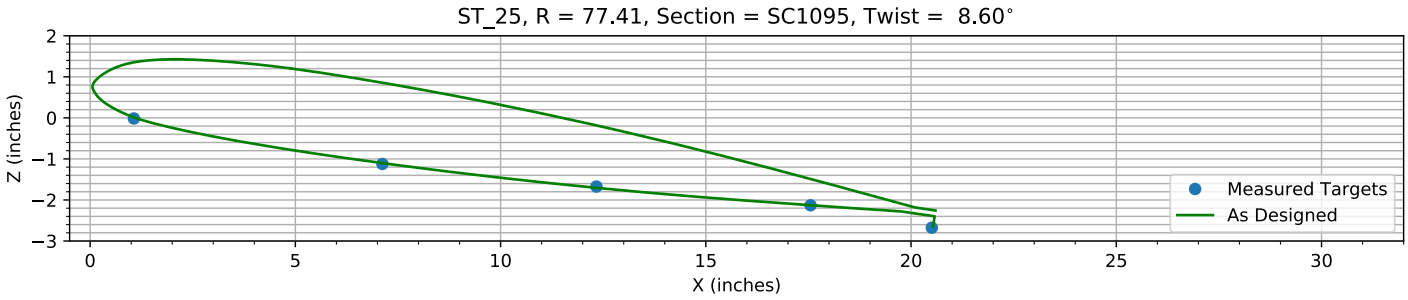

Figure 6-6. Target locations vs section profile at station 25.

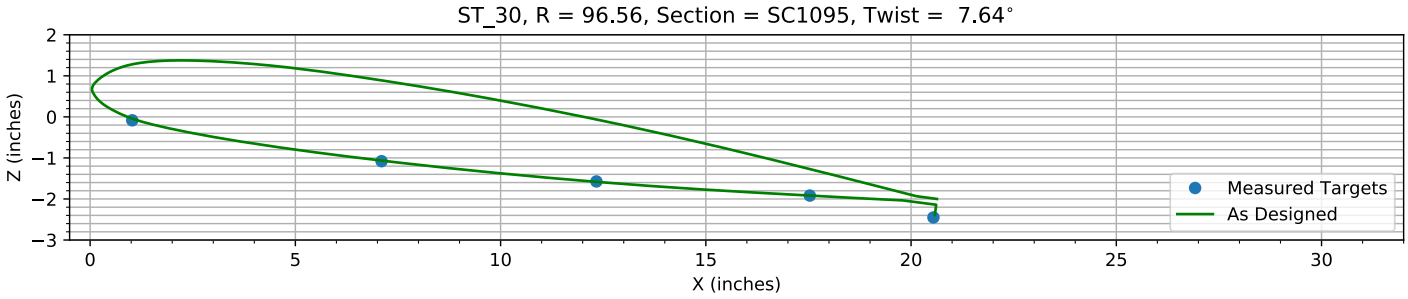

Figure 6-7. Target locations vs section profile at station 30.

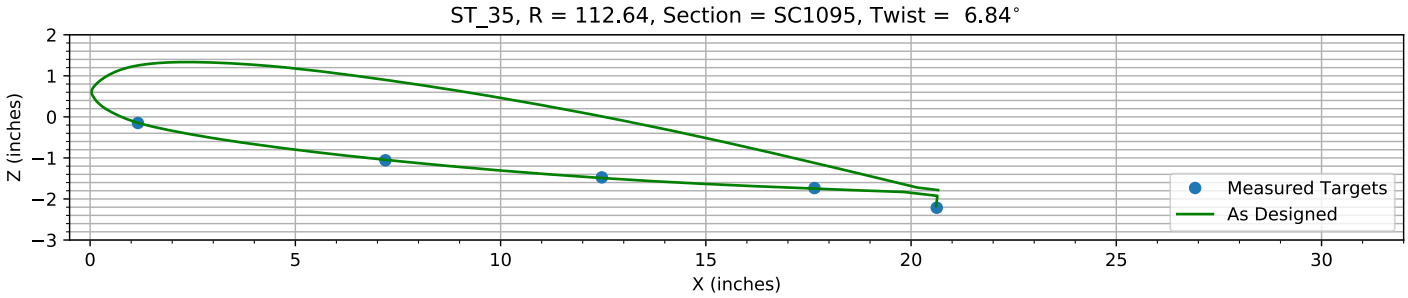

Figure 6-8. Target locations vs section profile at station 35.

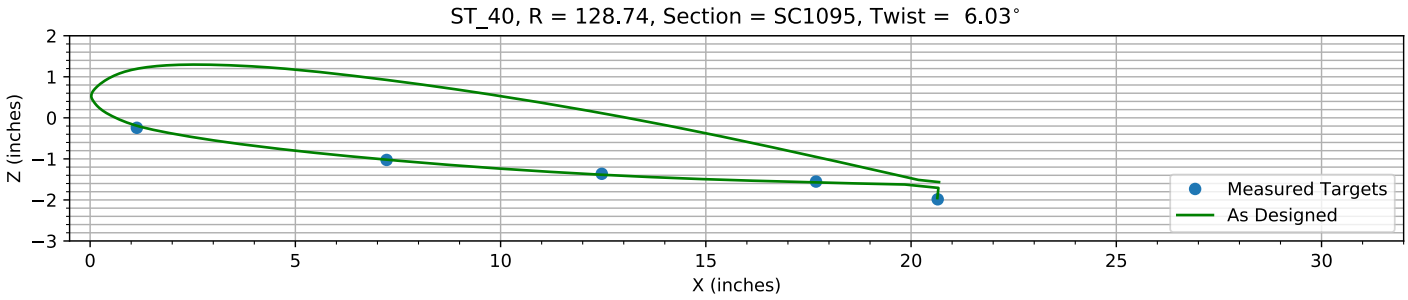

Figure 6-9. Target locations vs section profile at station 40.

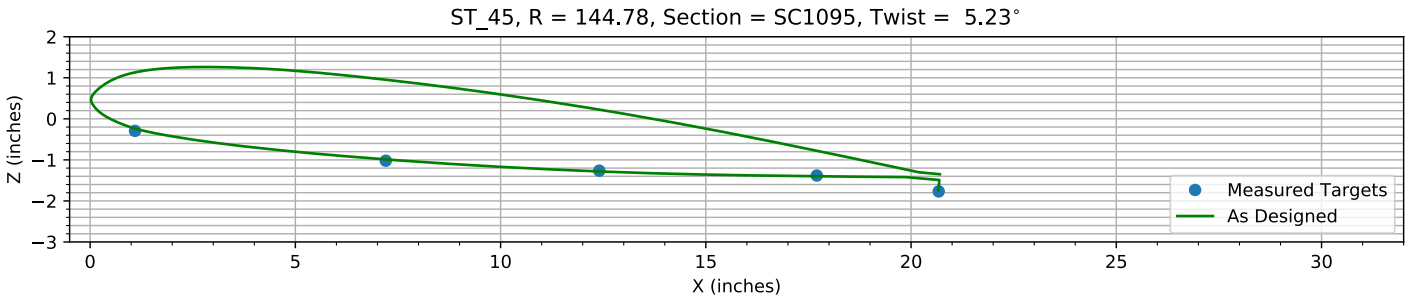

Figure 6-10. Target locations vs section profile at station 45.

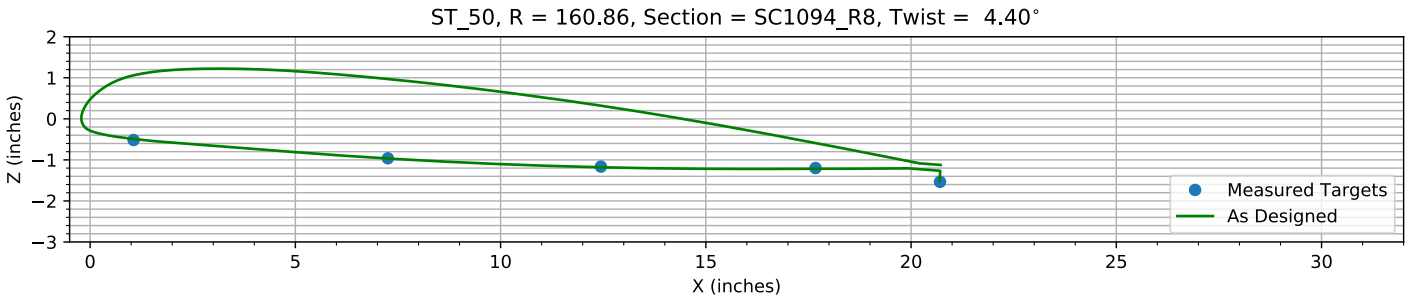

Figure 6-11. Target locations vs section profile at station 50.

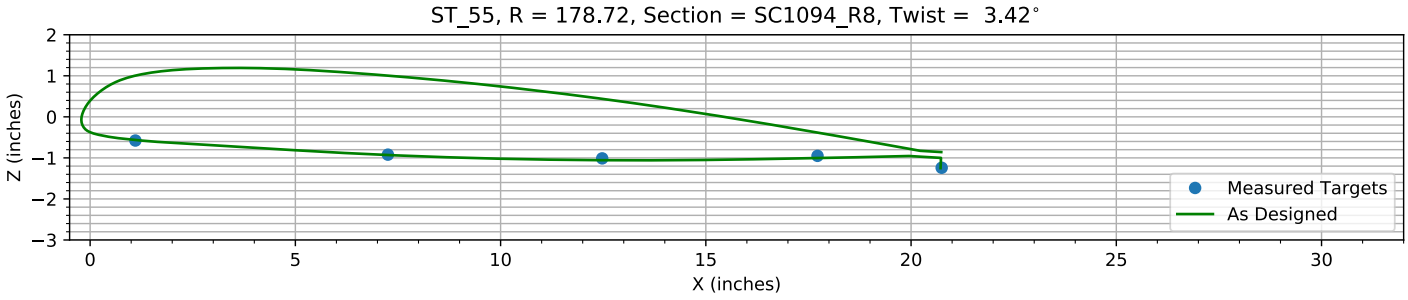

Figure 6-12. Target locations vs section profile at station 55.

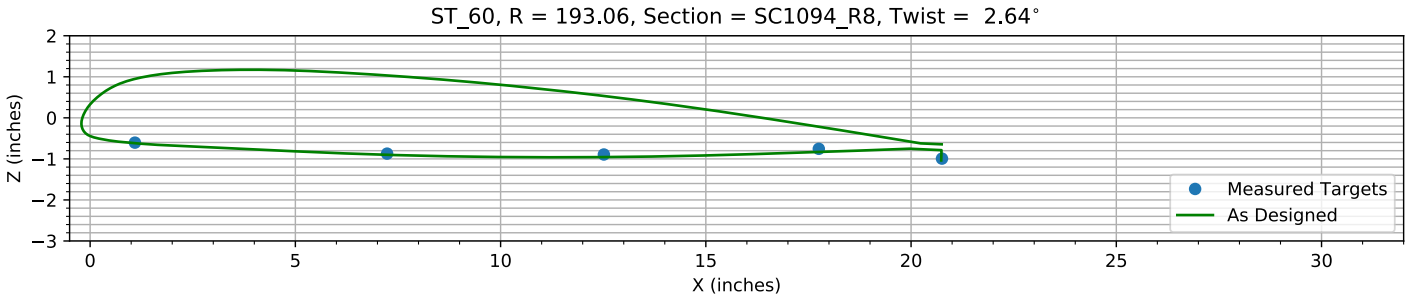

Figure 6-13. Target locations vs section profile at station 60.

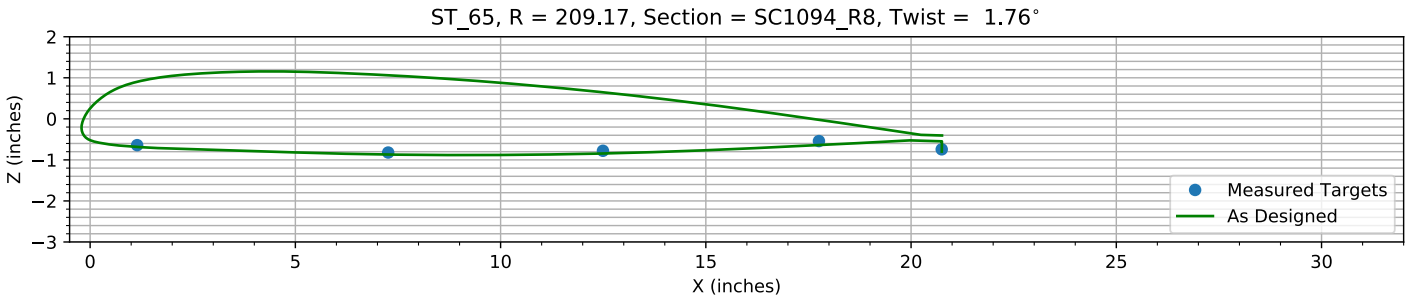

Figure 6-14. Target locations vs section profile at station 65.

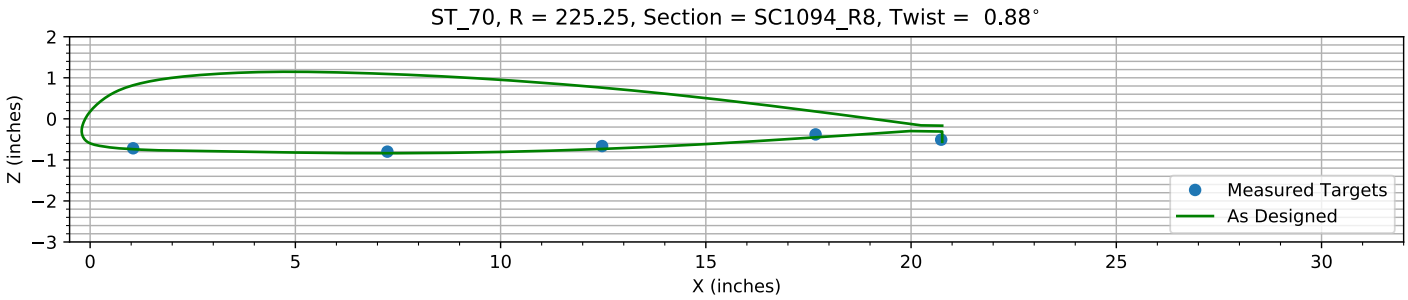

Figure 6-15. Target locations vs section profile at station 70.

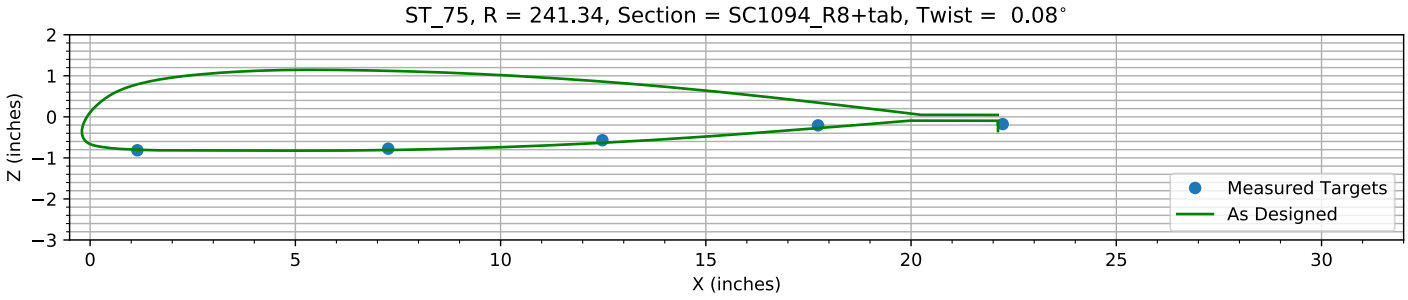

Figure 6-16. Target locations vs section profile at station 75.

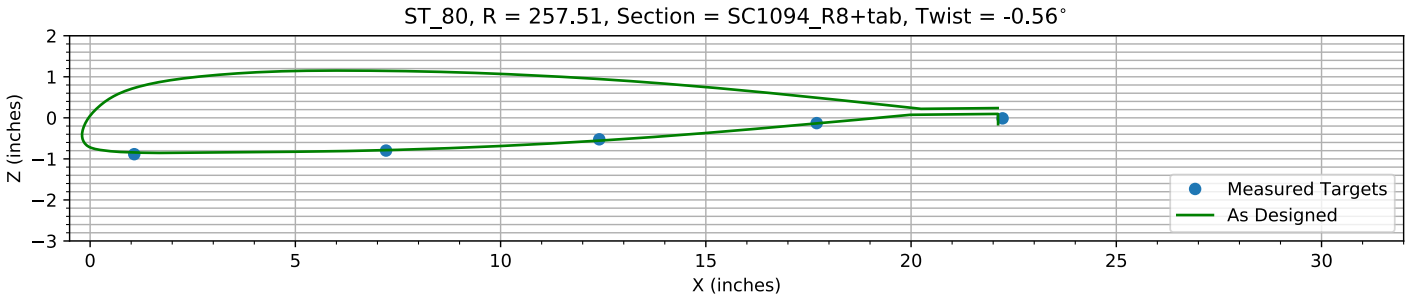

Figure 6-17. Target locations vs section profile at station 80.

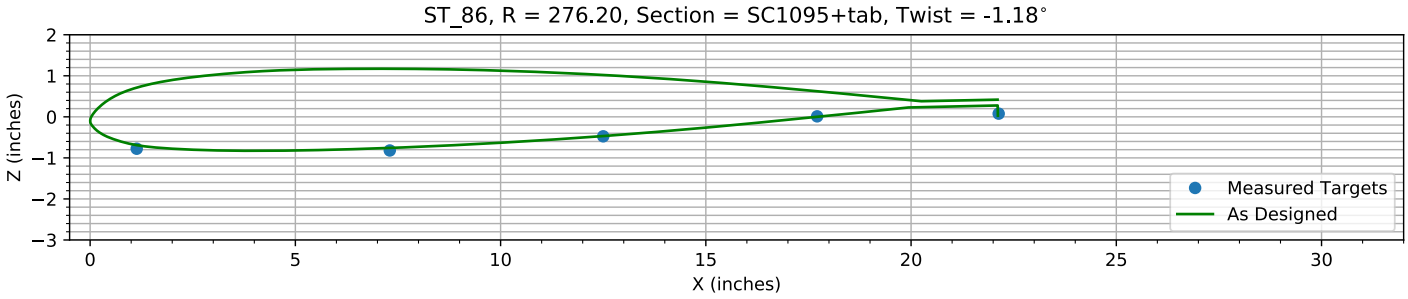

Figure 6-18. Target locations vs section profile at station 86.

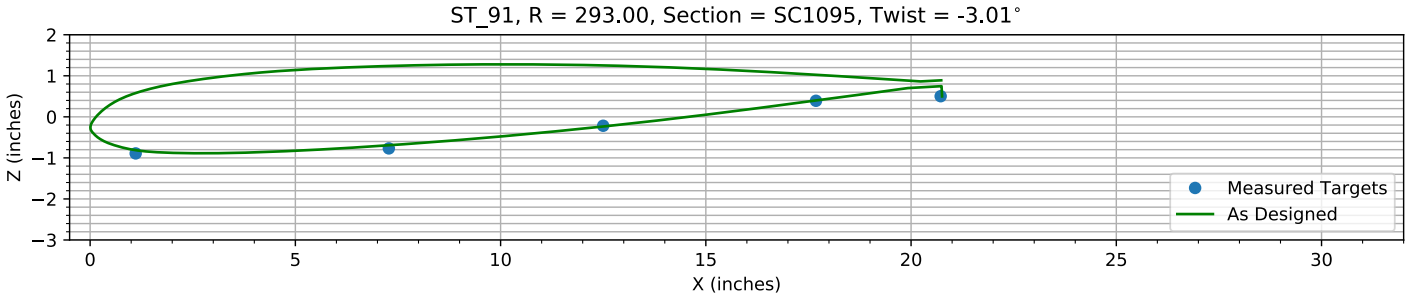

Figure 6-19. Target locations vs section profile at station 91.

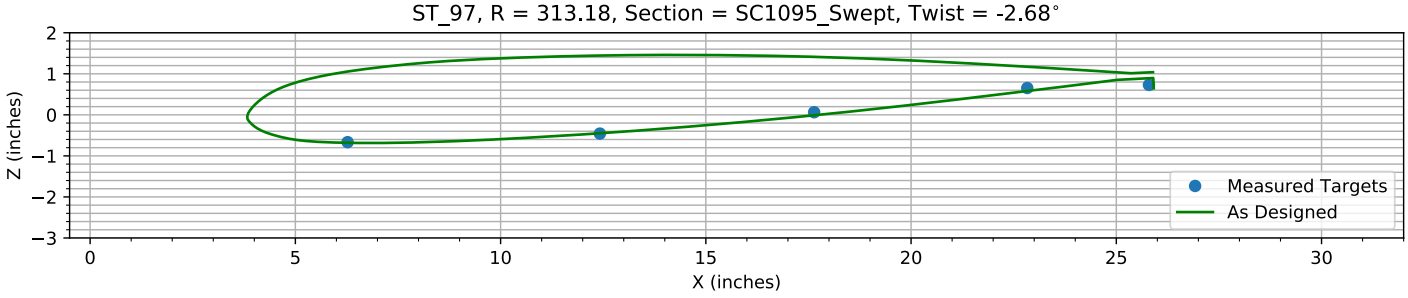

Figure 6-20. Target locations vs section profile at station 97.

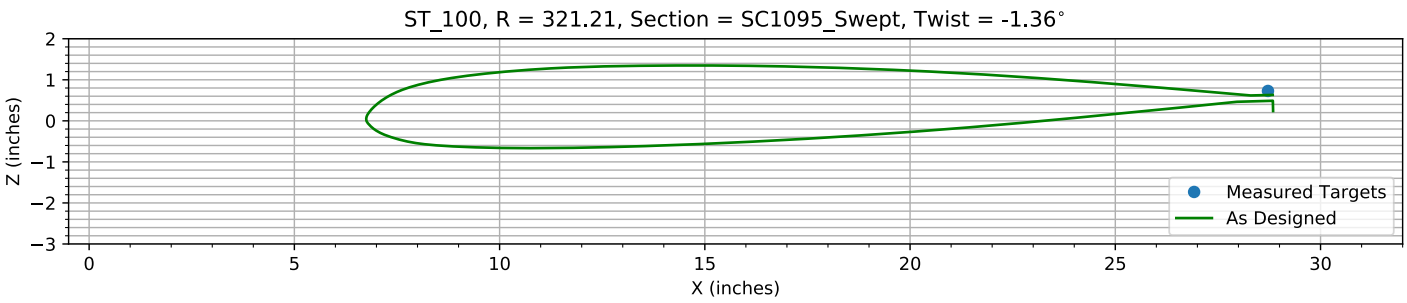

Figure 6-21. Target locations vs section profile at station 100.

Chapter 7: Flap and ΔZ Registration (15 rows)

The targets at the 15 spanwise stations nearest the root are used to determing the Z and flap offset.

The estimated Z error, -0.3093 inches, is within an allowed range of ±2.000 inches.

The estimated flap error is -0.11264°.

7.1: Target Location Errors After Flap Target Registration

Table 7-1. Measured(1) with flap registration vs as designed(2) in inches.

Name	X1	Y1	Z1	X2	Y2	Z2	dX	dY	dZ	dR
B2_R20_C05	1.0479	62.785	0.044259	1.0479	62.785	0.072084	0	0	-0.027825	0.027825
B2_R20_C36	7.1535	62.765	-1.1447	7.1535	62.765	-1.134	0	0	-0.010692	0.010692
B2_R20_C61	12.319	62.754	-1.7297	12.319	62.754	-1.7974	0	0	0.067699	0.067699
B2_R20_C86	17.568	62.757	-2.2093	17.568	62.757	-2.2906	0	0	0.081288	0.081288
B2_R20_C99	20.503	62.717	-2.7977	20.502	62.717	-2.8432	0.0017552	0	0.045528	0.045561
B2_R25_C05	1.0659	77.402	-0.019205	1.0659	77.402	0.012278	0	0	-0.031483	0.031483
B2_R25_C36	7.12	77.42	-1.127	7.12	77.42	-1.1022	0	0	-0.024808	0.024808
B2_R25_C61	12.334	77.425	-1.6775	12.334	77.425	-1.7047	0	0	0.027275	0.027275
B2_R25_C86	17.551	77.429	-2.1339	17.551	77.429	-2.1278	0	0	-0.0060928	0.0060928
B2_R25_C99	20.506	77.393	-2.6799	20.537	77.393	-2.6458	-0.030849	0	-0.034157	0.046026
B2_R30_C05	1.0258	96.622	-0.090817	1.0258	96.622	-0.043079	0	0	-0.047738	0.047738
B2_R30_C36	7.0997	96.587	-1.0868	7.0997	96.587	-1.0652	0	0	-0.021554	0.021554
B2_R30_C61	12.334	96.539	-1.5799	12.334	96.539	-1.5828	0	0	0.0029525	0.0029525
B2_R30_C86	17.533	96.53	-1.9244	17.533	96.53	-1.9182	0	0	-0.0062108	0.0062108
B2_R30_C99	20.545	96.519	-2.457	20.579	96.519	-2.3887	-0.03432	0	-0.068313	0.076449
B2_R35_C05	1.165	112.64	-0.15813	1.165	112.64	-0.14479	0	0	-0.013343	0.013343
B2_R35_C36	7.1936	112.64	-1.0669	7.1936	112.64	-1.0465	0	0	-0.020425	0.020425
B2_R35_C61	12.467	112.66	-1.4834	12.467	112.66	-1.4895	0	0	0.0060969	0.0060969
B2_R35_C86	17.647	112.64	-1.744	17.647	112.64	-1.748	0	0	0.0039618	0.0039618
B2_R35_C99	20.626	112.61	-2.2232	20.611	112.61	-2.1724	0.014541	0	-0.050802	0.052842
B2_R40_C05	1.1381	128.83	-0.2542	1.1381	128.83	-0.19323	0	0	-0.06097	0.06097
B2_R40_C36	7.2231	128.77	-1.0374	7.2231	128.77	-1.0196	0	0	-0.017856	0.017856
B2_R40_C61	12.465	128.76	-1.3747	12.465	128.76	-1.3862	0	0	0.011428	0.011428
B2_R40_C86	17.684	128.68	-1.5643	17.684	128.68	-1.5741	0	0	0.0097825	0.0097825
B2_R40_C99	20.649	128.68	-1.9965	20.64	128.68	-1.9562	0.0087953	0	-0.040331	0.041279
B2_R45_C05	1.094	144.78	-0.30633	1.094	144.78	-0.23632	0	0	-0.070008	0.070008
B2_R45_C36	7.2027	144.76	-1.0339	7.2027	144.76	-0.9886	0	0	-0.045271	0.045271
B2_R45_C61	12.404	144.79	-1.2772	12.404	144.79	-1.2814	0	0	0.0042201	0.0042201
B2_R45_C86	17.704	144.78	-1.395	17.704	144.78	-1.3988	0	0	0.0037359	0.0037359
B2_R45_C99	20.673	144.76	-1.7818	20.666	144.76	-1.7397	0.007107	0	-0.042059	0.042655
B2_R50_C05	1.0586	160.82	-0.53191	1.0586	160.82	-0.48971	0	0	-0.0422	0.0422
B2_R50_C36	7.2535	160.84	-0.97736	7.2535	160.84	-0.96641	0	0	-0.010952	0.010952
B2_R50_C61	12.444	160.83	-1.1797	12.444	160.83	-1.1805	0	0	0.0007749	0.0007749
B2_R50_C86	17.672	160.85	-1.2141	17.672	160.85	-1.2184	0	0	0.0043105	0.0043105
B2_R50_C99	20.705	160.96	-1.5509	20.695	160.96	-1.5134	0.010179	0	-0.037543	0.038899
B2_R55_C05	1.1027	178.74	-0.59567	1.1027	178.74	-0.56391	0	0	-0.031755	0.031755
B2_R55_C36	7.2544	178.73	-0.9396	7.2544	178.73	-0.93035	0	0	-0.0092525	0.0092525
B2_R55_C61	12.475	178.76	-1.0304	12.475	178.76	-1.0561	0	0	0.025667	0.025667

Name	X1	Y1	Z1	X2	Y2	Z2	dX	dY	dZ	dR
B2_R55_C86	17.721	178.72	-0.96901	17.721	178.72	-1.0044	0	0	0.035381	0.035381
B2_R55_C99	20.746	178.67	-1.2587	20.719	178.67	-1.2508	0.026883	0	-0.007944	0.028032
B2_R60_C05	1.0913	193.08	-0.62468	1.0913	193.08	-0.61816	0	0	-0.0065169	0.0065169
B2_R60_C36	7.2348	193.09	-0.89257	7.2348	193.09	-0.901	0	0	0.0084292	0.0084292
B2_R60_C61	12.516	193.09	-0.91366	12.516	193.09	-0.95605	0	0	0.042386	0.042386
B2_R60_C86	17.752	193.05	-0.77544	17.752	193.05	-0.8322	0	0	0.056757	0.056757
B2_R60_C99	20.753	192.97	-1.0139	20.734	192.97	-1.0386	0.01859	0	0.024693	0.030908
B2_R65_C05	1.1453	209.13	-0.66353	1.1453	209.13	-0.68397	0	0	0.020438	0.020438
B2_R65_C36	7.2609	209.17	-0.84354	7.2609	209.17	-0.86965	0	0	0.02611	0.02611
B2_R65_C61	12.493	209.18	-0.80102	12.493	209.18	-0.84422	0	0	0.043191	0.043191
B2_R65_C86	17.755	209.21	-0.56397	17.755	209.21	-0.63861	0	0	0.074645	0.074645
B2_R65_C99	20.747	209.16	-0.76556	20.748	209.16	-0.79809	-0.0018448	0	0.032523	0.032575
B2_R70_C05	1.0474	225.12	-0.74229	1.0474	225.12	-0.73964	0	0	-0.0026548	0.0026548
B2_R70_C36	7.2415	225.25	-0.82394	7.2415	225.25	-0.83781	0	0	0.013865	0.013865
B2_R70_C61	12.473	225.27	-0.68839	12.473	225.27	-0.73317	0	0	0.04478	0.04478
B2_R70_C86	17.674	225.32	-0.4036	17.674	225.32	-0.45113	0	0	0.047529	0.047529
B2_R70_C99	20.734	225.32	-0.53271	20.759	225.32	-0.55802	-0.025167	0	0.025316	0.035697
B2_R75_C05	1.15	241.32	-0.84074	1.15	241.32	-0.80119	0	0	-0.039552	0.039552
B2_R75_C36	7.2618	241.33	-0.80302	7.2618	241.33	-0.80919	0	0	0.0061786	0.0061786
B2_R75_C61	12.48	241.36	-0.59686	12.48	241.36	-0.63248	0	0	0.035615	0.035615
B2_R75_C86	17.733	241.34	-0.2347	17.733	241.34	-0.27476	0	0	0.040068	0.040068
B2_R80_C05	1.0747	257.59	-0.91485	1.0747	257.59	-0.84445	0	0	-0.070404	0.070404
B2_R80_C36	7.2095	257.51	-0.8267	7.2095	257.51	-0.78736	0	0	-0.03934	0.03934
B2_R80_C61	12.403	257.49	-0.55275	12.403	257.49	-0.55552	0	0	0.0027676	0.0027676
B2_R80_C86	17.7	257.43	-0.15807	17.7	257.43	-0.13699	0	0	-0.021076	0.021076
B2_R86_C05	1.1351	276.23	-0.80901	1.1351	276.23	-0.6903	0	0	-0.11871	0.11871
B2_R86_C36	7.3003	276.22	-0.85123	7.3003	276.22	-0.7577	0	0	-0.093528	0.093528
B2_R86_C61	12.5	276.21	-0.50644	12.5	276.21	-0.46829	0	0	-0.038152	0.038152
B2_R86_C86	17.712	276.18	-0.020015	17.712	276.18	-0.00028727	0	0	-0.019728	0.019728
B2_R91_C05	1.1097	293.03	-0.92528	1.1097	293.03	-0.81279	0	0	-0.11249	0.11249
B2_R91_C36	7.2773	293	-0.80315	7.2773	293	-0.69296	0	0	-0.11019	0.11019
B2_R91_C61	12.499	293.04	-0.25136	12.499	293.04	-0.23473	0	0	-0.016637	0.016637
B2_R91_C86	17.683	292.98	0.35682	17.683	292.98	0.39762	0	0	-0.040797	0.040797
B2_R91_C99	20.721	292.98	0.46852	20.755	292.98	0.49726	-0.034217	0	-0.02874	0.044685
B2_R97_C05	6.2728	313.04	-0.70274	6.2728	313.04	-0.68455	0	0	-0.018196	0.018196
B2_R97_C36	12.419	313.1	-0.49402	12.419	313.1	-0.44741	0	0	-0.046617	0.046617
B2_R97_C61	17.638	313.21	0.02679	17.638	313.21	-0.012761	0	0	0.039551	0.039551
B2_R97_C86	22.831	313.28	0.61664	22.831	313.28	0.5721	0	0	0.044531	0.044531
B2_R97_C99	25.795	313.26	0.69219	25.942	313.26	0.6448	-0.14629	0	0.047388	0.15378
HUB_LE	2.2382	30.002	-3.1909	2.19	30	-3.5	0.048215	0.0017745	0.3091	0.31284
HUB_TE	8.2354	29.997	-3.1905	8.19	30	-3.5	0.045413	-0.0030662	0.30949	0.31282
RMS Errors:							0.019886	0.00039858	0.064942	0.067919

7.2: Flap Registration Plots (15 rows)

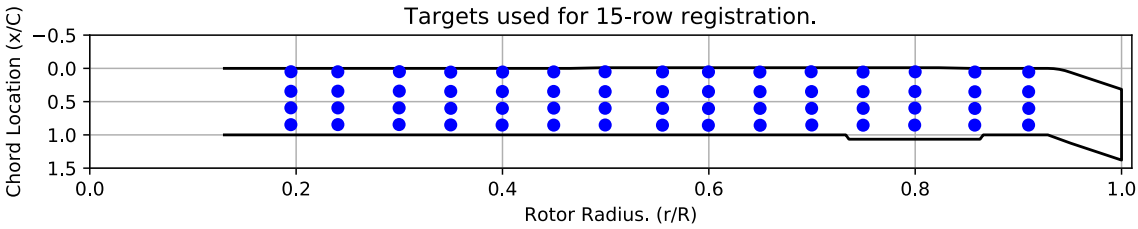

Figure 7-1. Targets used for 15 row root registration.

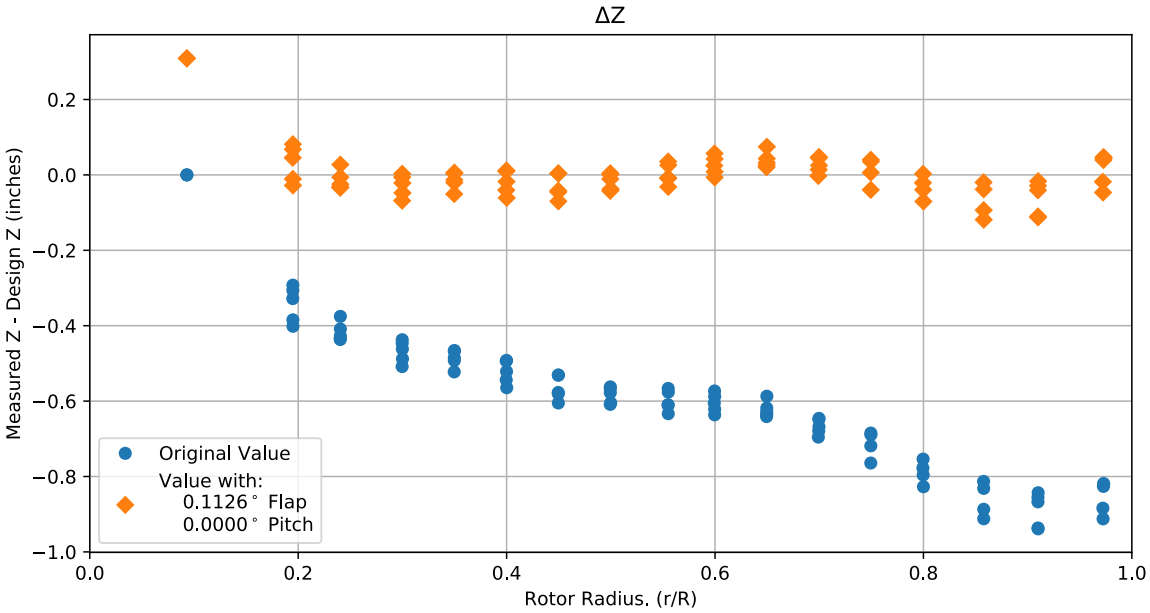

Figure 7-2. Flap target registration, ΔZ error vs rotor radius.

Note: the “as designed” geometry used for the swept tip may have some inaccuracies.

7.3: Estimated Bending and Twist at the Quarter Chord

The error bars shown represent the residual errors for fitting the measure target locations to the "as designed" geometry. These errors are generally much larger than those due to the VSTARS measurement errors. Therefore, the most likely source of these errors is the placement of the trailing-edge targets, differences between the "as designed" and "as built" geometries, and blade deformation during measurement. In the future, iterative adjustment of the "as designed" twist angle may be implemented to see if it reduces the fit error in delta twist. Note: The "as designed" geometry used for the swept tip may have some inaccuracies.

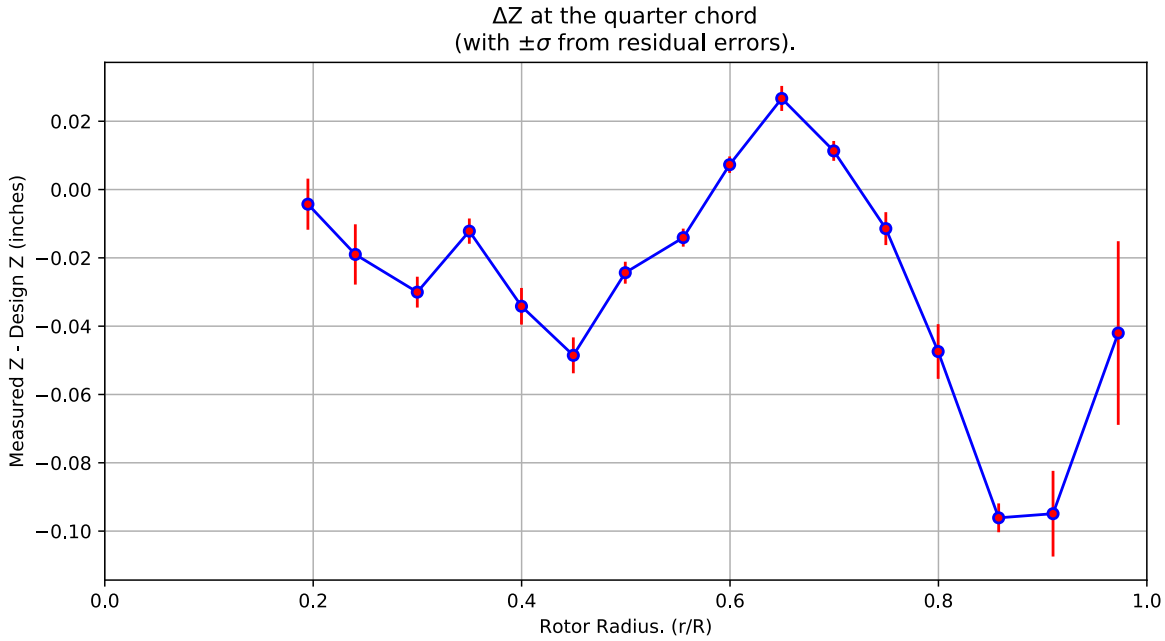

Figure 7-3. ΔZ error at the quarter chord vs rotor radius.

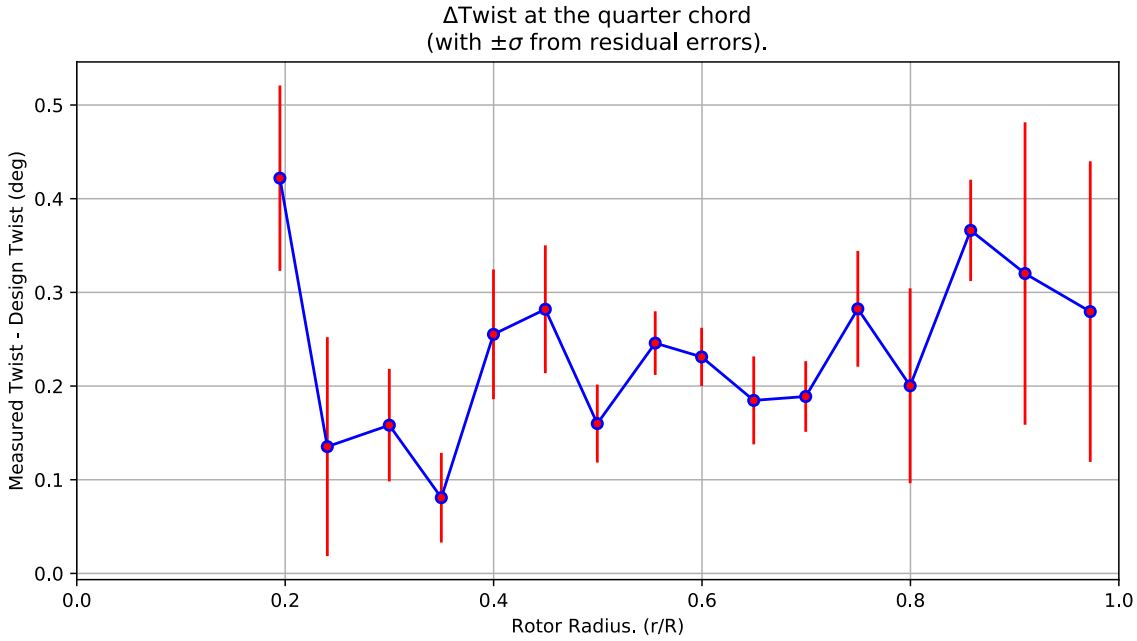

Figure 7-4. ΔTwist error at the quarter chord vs rotor radius.

Table 7-2. Quarter-chord bending and twist statistics.

r	r/R	dZ 1/4-chord	dT	sigma dZ meas	sigma dT meas	sigma dZ res	sigma dT res	n	t_conf
62.765	0.19492	-0.0042853	0.42192	6.1248e-10	4.6781e-09	0.0074815	0.098941	4	4.3027
77.419	0.24043	-0.018999	0.13533	6.125e-10	4.6837e-09	0.0088256	0.11684	4	4.3027
96.57	0.29991	-0.030036	0.15823	6.1125e-10	4.6761e-09	0.0045153	0.06005	4	4.3027
112.65	0.34983	-0.012174	0.080832	6.1709e-10	4.6796e-09	0.0036988	0.04786	4	4.3027
128.76	0.39987	-0.034171	0.25522	6.1691e-10	4.6655e-09	0.0053608	0.069215	4	4.3027
144.78	0.44963	-0.04854	0.28198	6.1508e-10	4.6529e-09	0.005254	0.068244	4	4.3027
160.83	0.49948	-0.024347	0.15993	6.1531e-10	4.6516e-09	0.0032101	0.041639	4	4.3027
178.74	0.55509	-0.014078	0.24586	6.1664e-10	4.6485e-09	0.002638	0.033979	4	4.3027
193.08	0.59962	0.0072803	0.2311	6.1642e-10	4.6329e-09	0.0024208	0.031108	4	4.3027
209.17	0.64961	0.026675	0.18469	6.1792e-10	4.65e-09	0.0036649	0.046936	4	4.3027
225.24	0.6995	0.011315	0.18884	6.1509e-10	4.645e-09	0.0029065	0.037686	4	4.3027
241.34	0.7495	-0.011438	0.28244	6.1793e-10	4.658e-09	0.0048188	0.061819	4	4.3027
257.51	0.79971	-0.047419	0.20029	6.1472e-10	4.6492e-09	0.008	0.10401	4	4.3027
276.21	0.85779	-0.096111	0.3662	6.1831e-10	4.6603e-09	0.0042224	0.054098	4	4.3027
293.01	0.90997	-0.094903	0.32011	6.1732e-10	4.6592e-09	0.012544	0.16143	4	4.3027
313.16	0.97254	-0.042012	0.27948	9.2771e-10	4.6637e-09	0.026885	0.16045	4	4.3027

7.4: Section Plots

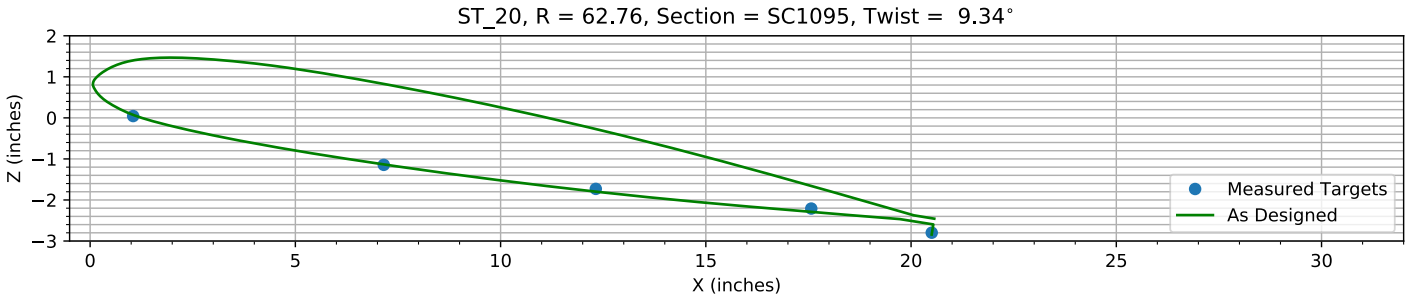

Figure 7-5. Target locations vs section profile at station 20.

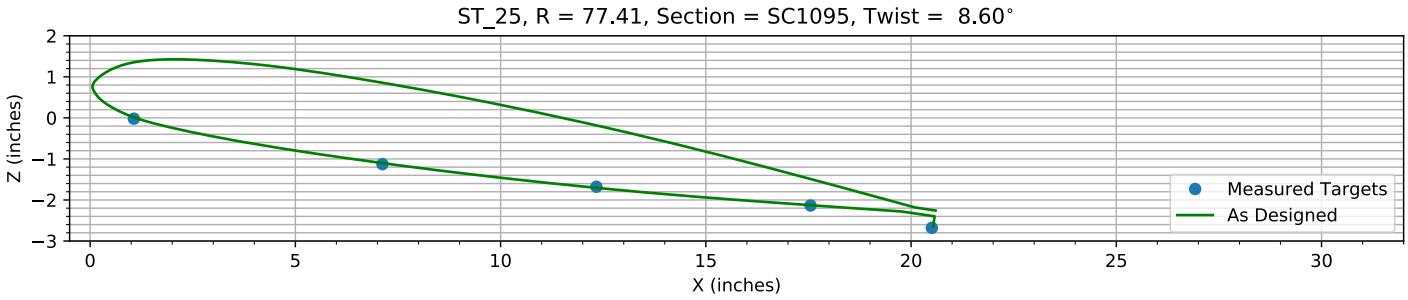

Figure 7-6. Target locations vs section profile at station 25.

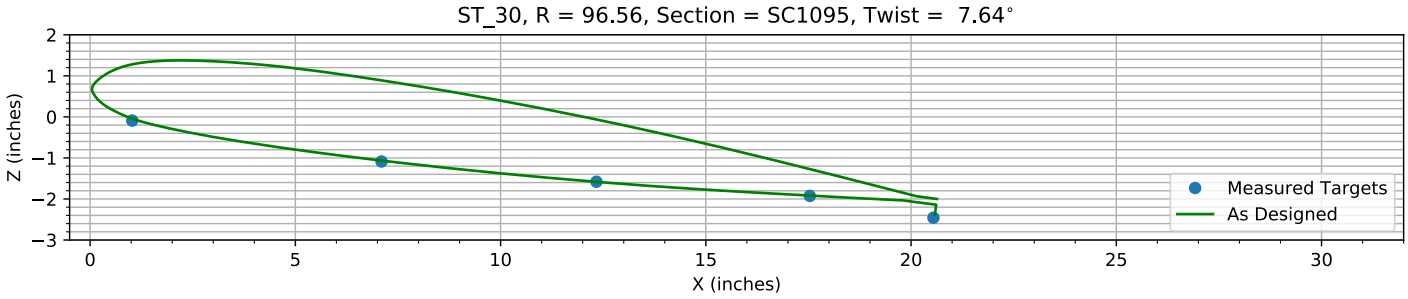

Figure 7-7. Target locations vs section profile at station 30.

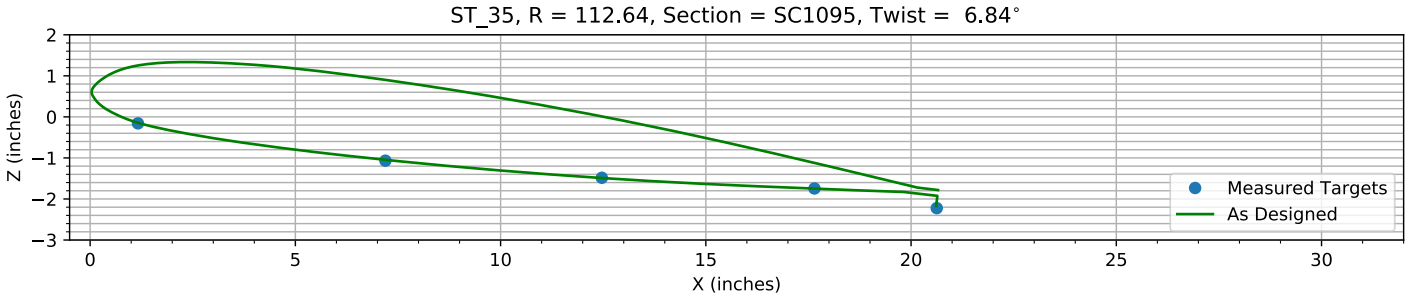

Figure 7-8. Target locations vs section profile at station 35.

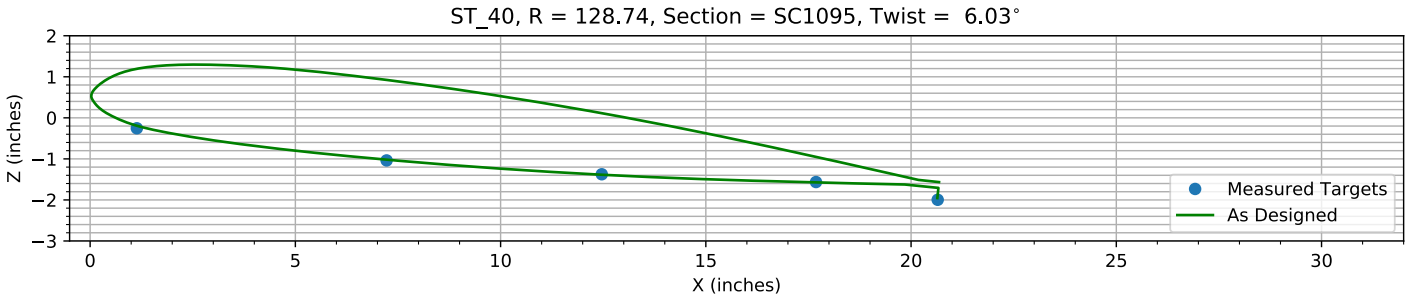

Figure 7-9. Target locations vs section profile at station 40.

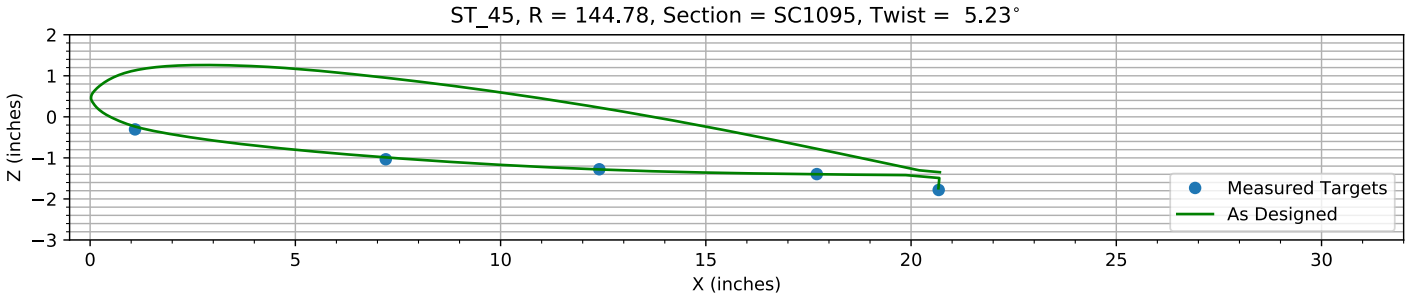

Figure 7-10. Target locations vs section profile at station 45.

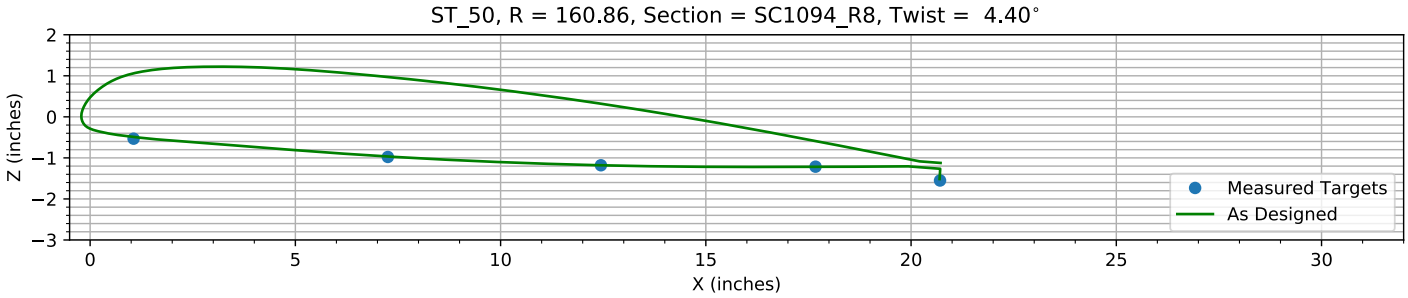

Figure 7-11. Target locations vs section profile at station 50.

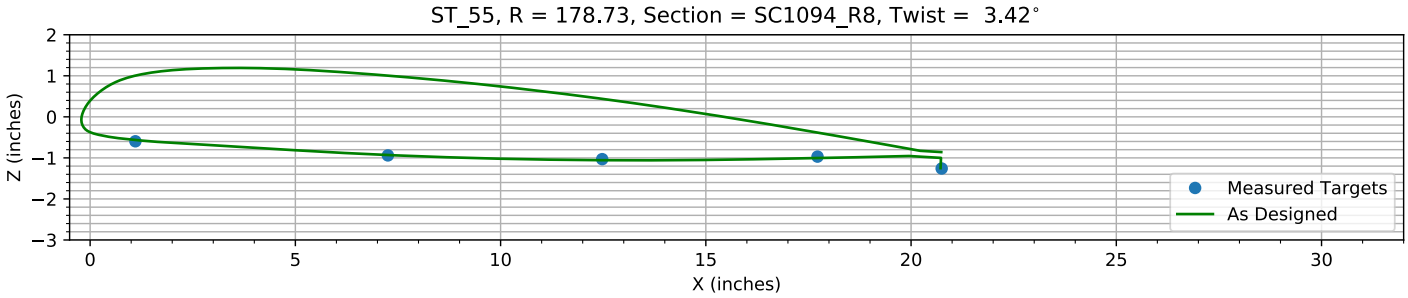

Figure 7-12. Target locations vs section profile at station 55.

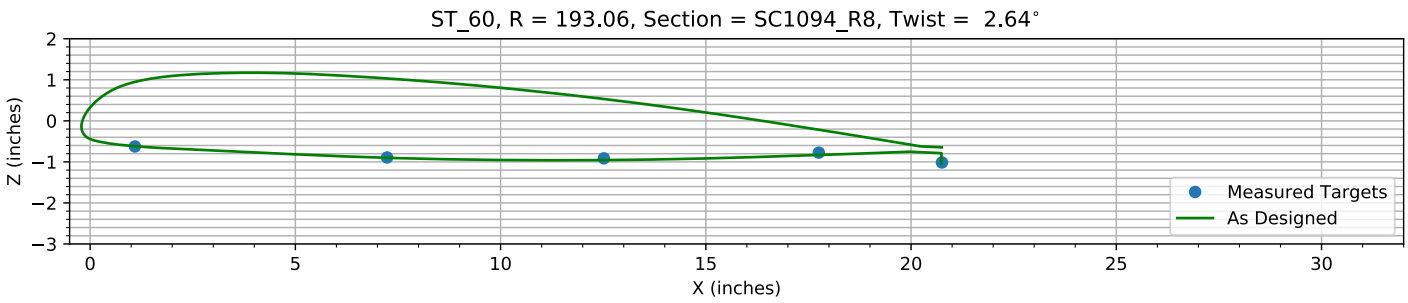

Figure 7-13. Target locations vs section profile at station 60.

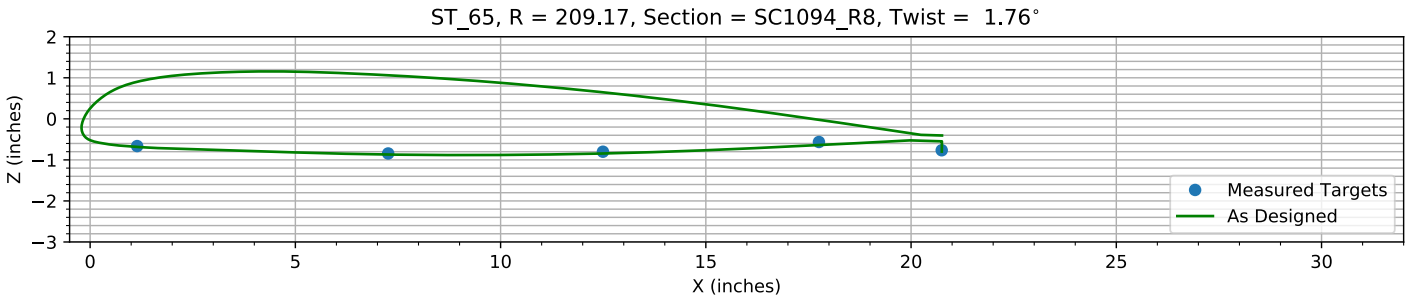

Figure 7-14. Target locations vs section profile at station 65.

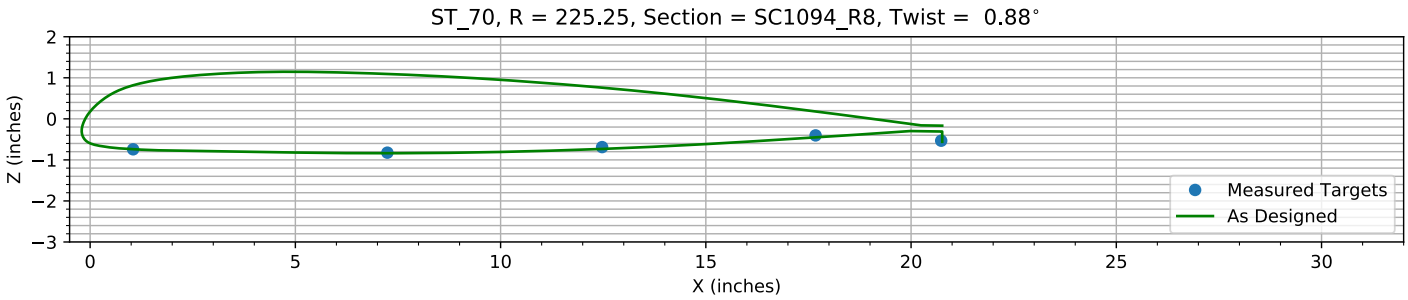

Figure 7-15. Target locations vs section profile at station 70.

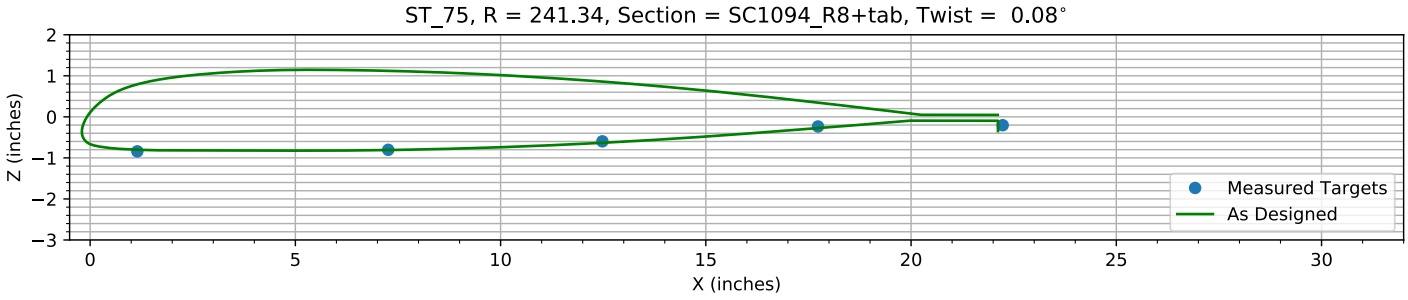

Figure 7-16. Target locations vs section profile at station 75.

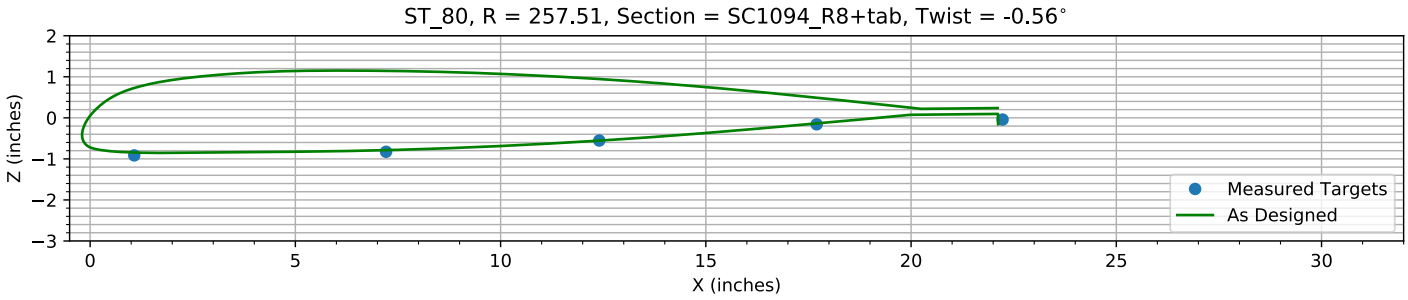

Figure 7-17. Target locations vs section profile at station 80.

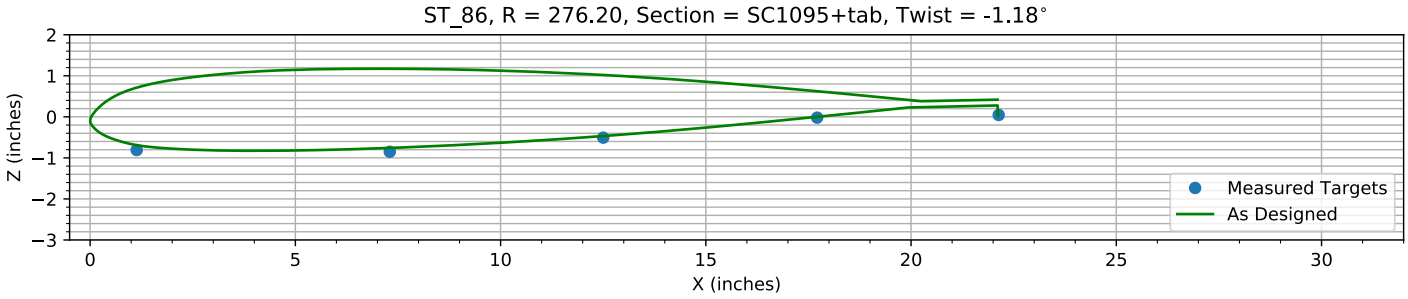

Figure 7-18. Target locations vs section profile at station 86.

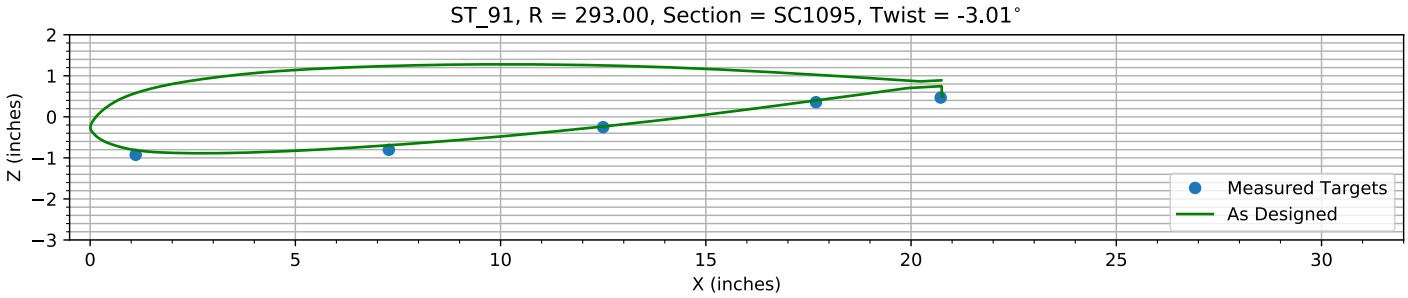

Figure 7-19. Target locations vs section profile at station 91.

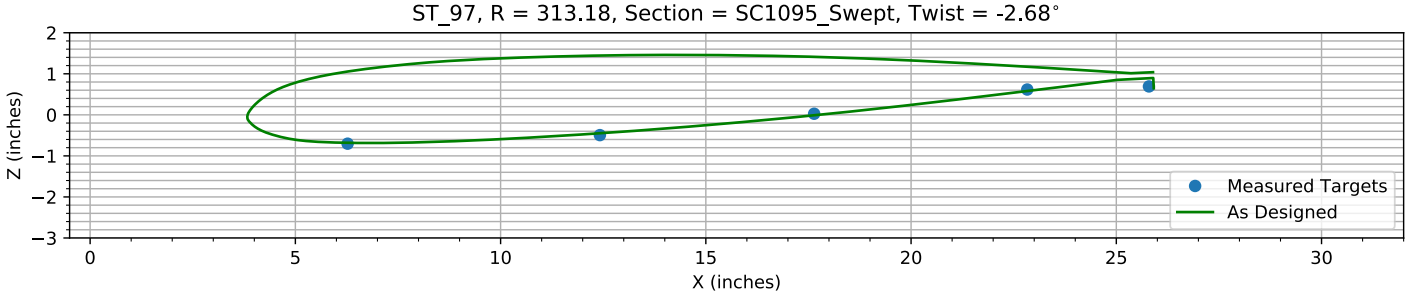

Figure 7-20. Target locations vs section profile at station 97.

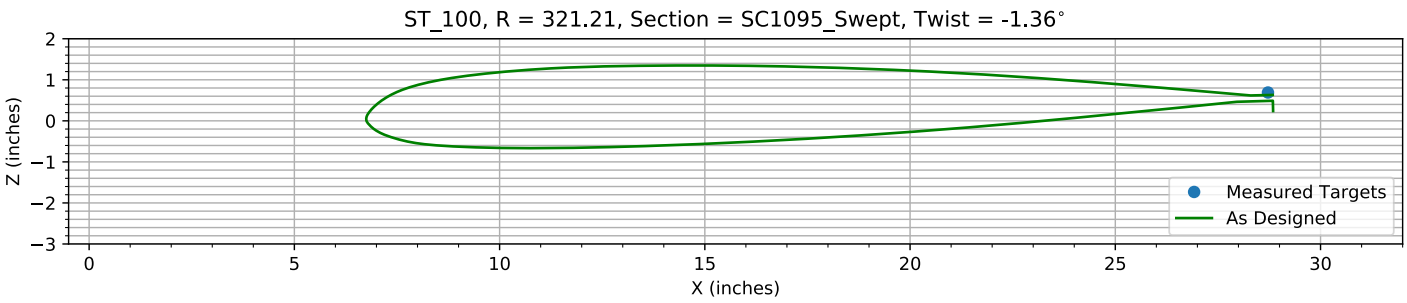

Figure 7-21. Target locations vs section profile at station 100.

Chapter 8: Pitch, Flap, and ΔZ Registration (6 rows)

The targets at the 6 spanwise stations nearest the root are used to determing the Z, flap, and pitch offset.

The estimated Z error, -0.31234 inches, is within an allowed range of ±2.000 inches.

The estimated flap error is -0.12197°.

The estimated pitch error is -0.071551°.

8.1: Target Location Errors After Target Registration

Table 8-1. Measured(1) with pitch and flap registration vs as designed(2) in inches.

Name	X1	Y1	Z1	X2	Y2	Z2	dX	dY	dZ	dR
B2_R20_C05	1.0523	62.784	0.057811	1.0523	62.784	0.070428	0	0	-0.012617	0.012617
B2_R20_C36	7.1564	62.764	-1.1388	7.1564	62.764	-1.1344	0	0	-0.0043323	0.0043323
B2_R20_C61	12.321	62.754	-1.7302	12.321	62.754	-1.7977	0	0	0.067421	0.067421
B2_R20_C86	17.57	62.757	-2.2164	17.57	62.757	-2.2907	0	0	0.074344	0.074344
B2_R20_C99	20.504	62.717	-2.8084	20.502	62.717	-2.8432	0.0026311	0	0.034777	0.034876
B2_R25_C05	1.0702	77.401	-0.003296	1.0702	77.401	0.010714	0	0	-0.014011	0.014011
B2_R25_C36	7.123	77.42	-1.1187	7.123	77.42	-1.1026	0	0	-0.016057	0.016057
B2_R25_C61	12.337	77.425	-1.6756	12.337	77.425	-1.705	0	0	0.029344	0.029344
B2_R25_C86	17.553	77.429	-2.1385	17.553	77.429	-2.1279	0	0	-0.010641	0.010641
B2_R25_C99	20.507	77.393	-2.6883	20.537	77.393	-2.6458	-0.029823	0	-0.042523	0.051939
B2_R30_C05	1.0301	96.622	-0.071731	1.0301	96.622	-0.044583	0	0	-0.027148	0.027148
B2_R30_C36	7.1027	96.587	-1.0753	7.1027	96.587	-1.0656	0	0	-0.0097029	0.0097029
B2_R30_C61	12.337	96.539	-1.5749	12.337	96.539	-1.583	0	0	0.0081032	0.0081032
B2_R30_C86	17.535	96.53	-1.9259	17.535	96.53	-1.9183	0	0	-0.0076422	0.0076422
B2_R30_C99	20.546	96.519	-2.4623	20.579	96.519	-2.3887	-0.033011	0	-0.073614	0.080677
B2_R35_C05	1.1692	112.64	-0.13662	1.1692	112.64	-0.14602	0	0	0.0094012	0.0094012
B2_R35_C36	7.1967	112.64	-1.0529	7.1967	112.64	-1.0468	0	0	-0.0061185	0.0061185
B2_R35_C61	12.469	112.66	-1.476	12.469	112.66	-1.4896	0	0	0.013674	0.013674
B2_R35_C86	17.649	112.64	-1.7431	17.649	112.64	-1.7481	0	0	0.0049912	0.0049912
B2_R35_C99	20.627	112.61	-2.226	20.611	112.61	-2.1724	0.016145	0	-0.053585	0.055965
B2_R40_C05	1.1422	128.83	-0.23001	1.1422	128.83	-0.1944	0	0	-0.035613	0.035613
B2_R40_C36	7.2262	128.77	-1.0208	7.2262	128.77	-1.0198	0	0	-0.0010022	0.0010022
B2_R40_C61	12.468	128.76	-1.3647	12.468	128.76	-1.3863	0	0	0.021597	0.021597
B2_R40_C86	17.687	128.68	-1.5608	17.687	128.68	-1.5741	0	0	0.01335	0.01335
B2_R40_C99	20.651	128.68	-1.9967	20.64	128.68	-1.9562	0.010685	0	-0.040528	0.041913
B2_R45_C05	1.098	144.78	-0.27949	1.098	144.78	-0.23746	0	0	-0.042035	0.042035
B2_R45_C36	7.2058	144.76	-1.0147	7.2058	144.76	-0.98883	0	0	-0.025832	0.025832
B2_R45_C61	12.407	144.79	-1.2645	12.407	144.79	-1.2816	0	0	0.01705	0.01705
B2_R45_C86	17.706	144.78	-1.3889	17.706	144.78	-1.3988	0	0	0.0098691	0.0098691
B2_R45_C99	20.675	144.76	-1.7794	20.666	144.76	-1.7397	0.0092682	0	-0.039668	0.040737
B2_R50_C05	1.0623	160.81	-0.50242	1.0623	160.81	-0.49015	0	0	-0.012271	0.012271
B2_R50_C36	7.2567	160.84	-0.9556	7.2567	160.84	-0.9666	0	0	0.011002	0.011002
B2_R50_C61	12.447	160.83	-1.1644	12.447	160.83	-1.1805	0	0	0.01612	0.01612
B2_R50_C86	17.675	160.85	-1.2053	17.675	160.85	-1.2184	0	0	0.013057	0.013057
B2_R50_C99	20.708	160.96	-1.546	20.695	160.96	-1.5134	0.012632	0	-0.032557	0.034921
B2_R55_C05	1.1063	178.74	-0.56331	1.1063	178.74	-0.56427	0	0	0.00095929	0.00095929

Name	X1	Y1	Z1	X2	Y2	Z2	dX	dY	dZ	dR
B2_R55_C36	7.2577	178.73	-0.91493	7.2577	178.73	-0.93049	0	0	0.015559	0.015559
B2_R55_C61	12.478	178.76	-1.0123	12.478	178.76	-1.0561	0	0	0.043842	0.043842
B2_R55_C86	17.724	178.72	-0.95741	17.724	178.72	-1.0043	0	0	0.046921	0.046921
B2_R55_C99	20.748	178.67	-1.2509	20.719	178.67	-1.2508	0.029704	0	-0.00012425	0.029704
B2_R60_C05	1.095	193.08	-0.58998	1.095	193.08	-0.61847	0	0	0.028497	0.028497
B2_R60_C36	7.2381	193.08	-0.86554	7.2381	193.08	-0.9011	0	0	0.035559	0.035559
B2_R60_C61	12.519	193.09	-0.89322	12.519	193.09	-0.95602	0	0	0.062799	0.062799
B2_R60_C86	17.756	193.05	-0.76155	17.756	193.05	-0.83209	0	0	0.070537	0.070537
B2_R60_C99	20.756	192.97	-1.0038	20.734	192.97	-1.0386	0.021719	0	0.034831	0.041048
B2_R65_C05	1.1489	209.13	-0.62629	1.1489	209.13	-0.68422	0	0	0.057931	0.057931
B2_R65_C36	7.2643	209.17	-0.81392	7.2643	209.17	-0.8697	0	0	0.055775	0.055775
B2_R65_C61	12.497	209.18	-0.77794	12.497	209.18	-0.84414	0	0	0.066198	0.066198
B2_R65_C86	17.759	209.21	-0.54745	17.759	209.21	-0.63844	0	0	0.090986	0.090986
B2_R65_C99	20.75	209.16	-0.75279	20.748	209.16	-0.79809	0.0015984	0	0.045304	0.045332
B2_R70_C05	1.0509	225.12	-0.70232	1.0509	225.12	-0.73983	0	0	0.037511	0.037511
B2_R70_C36	7.2449	225.25	-0.79168	7.2449	225.25	-0.8378	0	0	0.046119	0.046119
B2_R70_C61	12.477	225.27	-0.66266	12.477	225.27	-0.73303	0	0	0.070372	0.070372
B2_R70_C86	17.677	225.32	-0.38436	17.677	225.32	-0.45088	0	0	0.066523	0.066523
B2_R70_C99	20.737	225.32	-0.51729	20.759	225.32	-0.55803	-0.02143	0	0.040742	0.046034
B2_R75_C05	1.1533	241.32	-0.79826	1.1533	241.32	-0.80132	0	0	0.0030617	0.0030617
B2_R75_C36	7.2652	241.33	-0.76817	7.2652	241.33	-0.80914	0	0	0.040977	0.040977
B2_R75_C61	12.483	241.36	-0.56853	12.483	241.36	-0.63229	0	0	0.063761	0.063761
B2_R75_C86	17.737	241.34	-0.21292	17.737	241.34	-0.27444	0	0	0.061524	0.061524
B2_R80_C05	1.078	257.59	-0.86963	1.078	257.59	-0.84455	0	0	-0.025081	0.025081
B2_R80_C36	7.2129	257.51	-0.78916	7.2129	257.51	-0.78728	0	0	-0.0018803	0.0018803
B2_R80_C61	12.407	257.49	-0.5217	12.407	257.49	-0.55529	0	0	0.033598	0.033598
B2_R80_C86	17.705	257.43	-0.13363	17.705	257.43	-0.13662	0	0	0.002982	0.002982
B2_R86_C05	1.1385	276.23	-0.76083	1.1385	276.23	-0.6909	0	0	-0.069938	0.069938
B2_R86_C36	7.3037	276.22	-0.81075	7.3037	276.22	-0.75758	0	0	-0.053176	0.053176
B2_R86_C61	12.504	276.21	-0.47246	12.504	276.21	-0.46802	0	0	-0.0044415	0.0044415
B2_R86_C86	17.716	276.17	0.0074545	17.716	276.17	0.00015028	0	0	0.0073042	0.0073042
B2_R91_C05	1.113	293.03	-0.87434	1.113	293.03	-0.81329	0	0	-0.061045	0.061045
B2_R91_C36	7.2807	292.99	-0.75991	7.2807	292.99	-0.69272	0	0	-0.067188	0.067188
B2_R91_C61	12.503	293.04	-0.21464	12.503	293.04	-0.2343	0	0	0.019663	0.019663
B2_R91_C86	17.688	292.98	0.38706	17.688	292.98	0.39825	0	0	-0.01119	0.01119
B2_R91_C99	20.726	292.98	0.49496	20.755	292.98	0.49724	-0.029216	0	-0.0022763	0.029305
B2_R97_C05	6.2764	313.04	-0.65499	6.2764	313.04	-0.68461	0	0	0.029623	0.029623
B2_R97_C36	12.423	313.1	-0.45393	12.423	313.1	-0.44713	0	0	-0.0068033	0.0068033
B2_R97_C61	17.643	313.21	0.060377	17.643	313.21	-0.012286	0	0	0.072663	0.072663
B2_R97_C86	22.836	313.28	0.64375	22.836	313.28	0.57279	0	0	0.070964	0.070964
B2_R97_C99	25.801	313.26	0.7156	25.941	313.26	0.64482	-0.14076	0	0.070774	0.15755
HUB_LE	2.2386	30.002	-3.1842	2.19	30	-3.5	0.048607	0.0017177	0.31583	0.31956
HUB_TE	8.2358	29.997	-3.1913	8.19	30	-3.5	0.045801	-0.003123	0.30873	0.31213
RMS Errors:							0.01934	0.00040101	0.064189	0.067041

8.2: Pitch and Flap Registration Plots (6 rows)

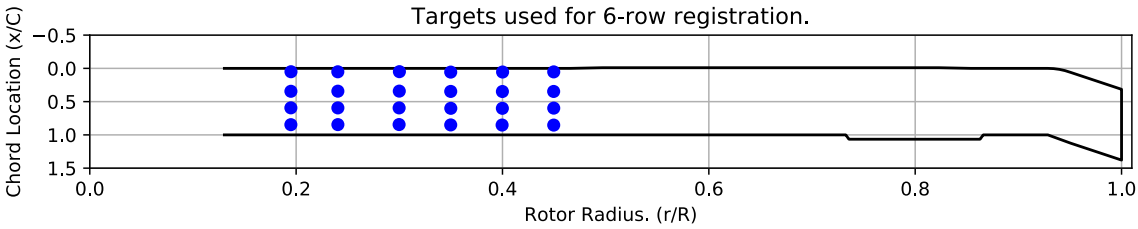

Figure 8-1. Targets used for 6 row root registration.

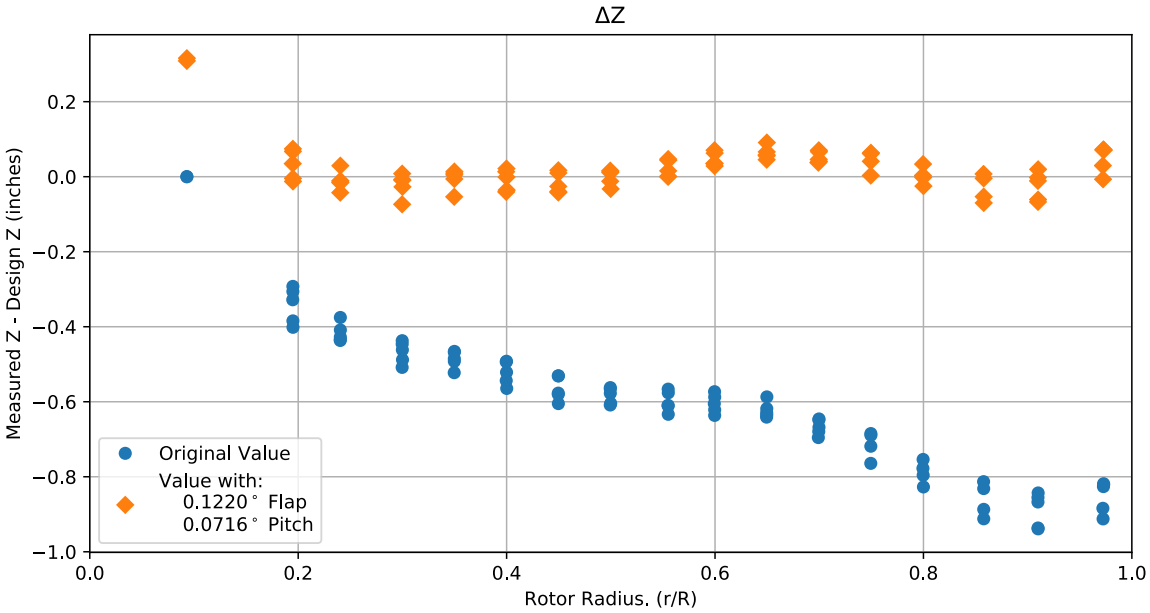

Figure 8-2. Pitch and flap target registration, ΔZ error vs rotor radius.

Note: the “as designed” geometry used for the swept tip may have some inaccuracies.

8.3: Estimated Bending and Twist at the Quarter Chord

The error bars shown represent the residual errors for fitting the measure target locations to the "as designed" geometry. These errors are generally much larger than those due to the VSTARS measurement errors. Therefore, the most likely source of these errors is the placement of the trailing-edge targets, differences between the "as designed" and "as built" geometries, and blade deformation during measurement. In the future, iterative adjustment of the "as designed" twist angle may be implemented to see if it reduces the fit error in delta twist. Note: The "as designed" geometry used for the swept tip may have some inaccuracies.

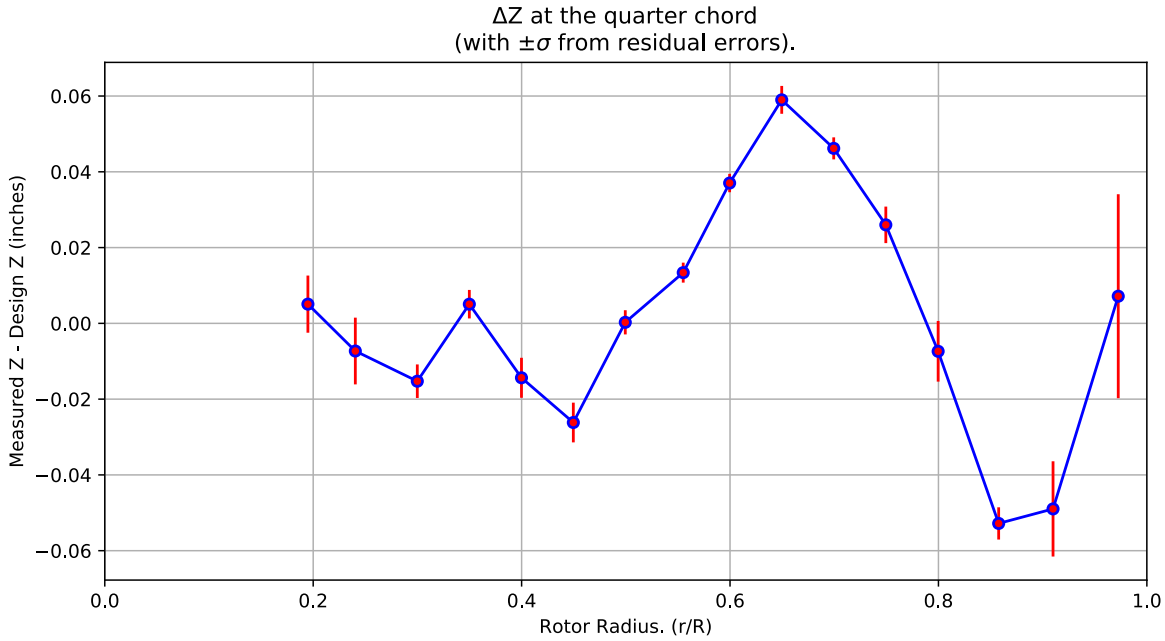

Figure 8-3. ΔZ error at the quarter chord vs rotor radius.

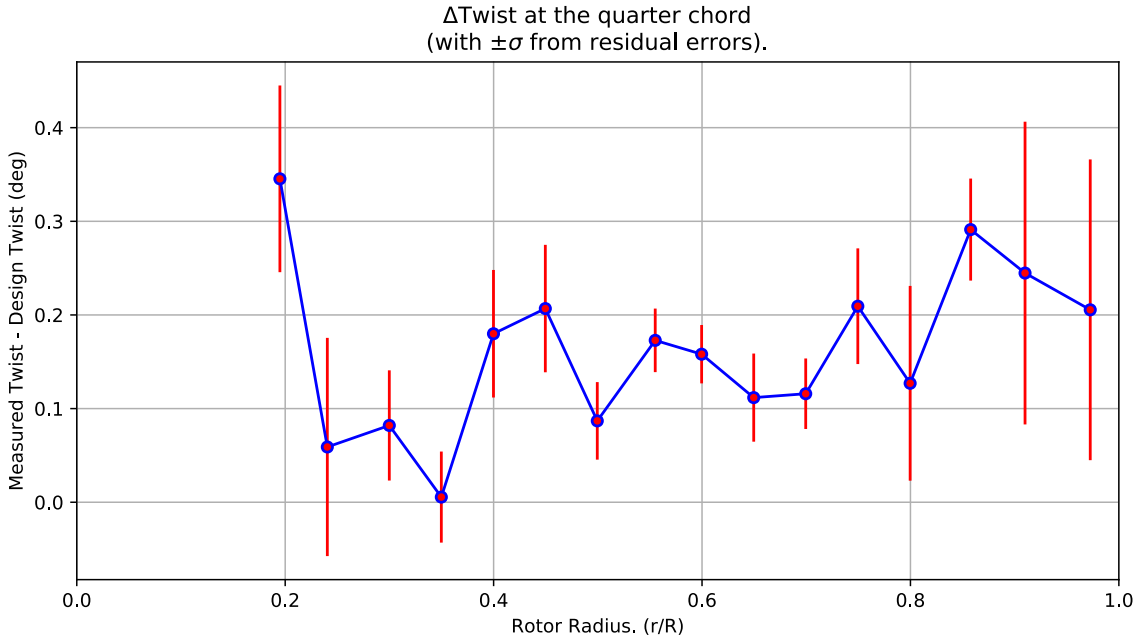

Figure 8-4. ΔTwist error at the quarter chord vs rotor radius.

Table 8-2. Quarter-chord bending and twist statistics.

r	r/R	dZ 1/4-chord	dT	sigma dZ meas	sigma dT meas	sigma dZ res	sigma dT res	n	t_conf
62.765	0.19492	0.0050734	0.34536	6.1265e-10	4.679e-09	0.0075433	0.099696	4	4.3027
77.419	0.24043	-0.007301	0.059004	6.1267e-10	4.6844e-09	0.0088071	0.11652	4	4.3027
96.569	0.2999	-0.015268	0.082007	6.1141e-10	4.6767e-09	0.004428	0.058849	4	4.3027
112.65	0.34983	0.0050616	0.0055021	6.1726e-10	4.6802e-09	0.0037606	0.048627	4	4.3027
128.76	0.39987	-0.014363	0.17994	6.1708e-10	4.666e-09	0.0052788	0.068108	4	4.3027
144.78	0.44963	-0.026171	0.20682	6.1524e-10	4.6533e-09	0.0052426	0.068048	4	4.3027
160.83	0.49948	0.00027424	0.086881	6.1547e-10	4.6519e-09	0.0031943	0.041404	4	4.3027
178.74	0.55509	0.013389	0.17287	6.1681e-10	4.6487e-09	0.0026363	0.033932	4	4.3027
193.08	0.59962	0.037037	0.15809	6.1658e-10	4.633e-09	0.002427	0.031165	4	4.3027
209.17	0.64961	0.058992	0.11172	6.1809e-10	4.65e-09	0.0036773	0.047058	4	4.3027
225.24	0.6995	0.046187	0.11588	6.1526e-10	4.6449e-09	0.0029061	0.03765	4	4.3027
241.34	0.7495	0.026001	0.20933	6.1809e-10	4.6578e-09	0.0048191	0.061773	4	4.3027
257.51	0.79971	-0.0073732	0.12701	6.1488e-10	4.649e-09	0.0080055	0.10399	4	4.3027
276.21	0.85779	-0.052807	0.29117	6.1848e-10	4.6601e-09	0.0042556	0.054479	4	4.3027
293.01	0.90997	-0.048974	0.24473	6.1749e-10	4.6588e-09	0.012572	0.16164	4	4.3027
313.16	0.97253	0.0071645	0.2055	9.2793e-10	4.6633e-09	0.026918	0.16058	4	4.3027

8.4: Section Plots

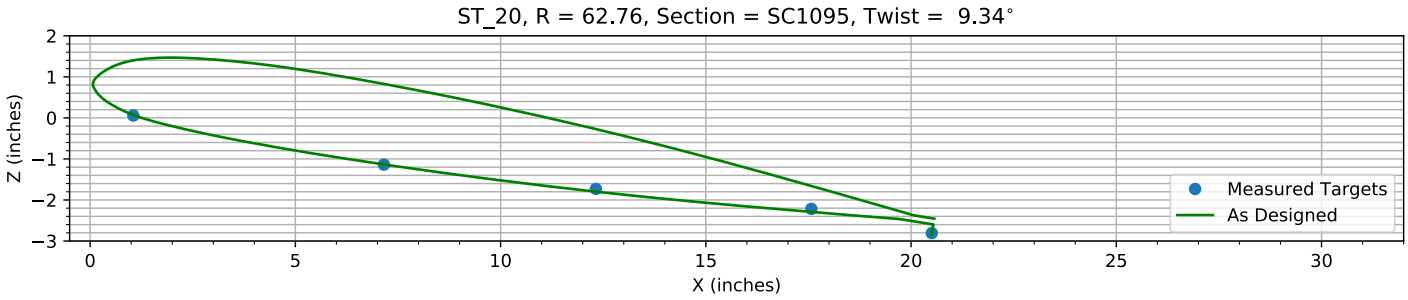

Figure 8-5. Target locations vs section profile at station 20.

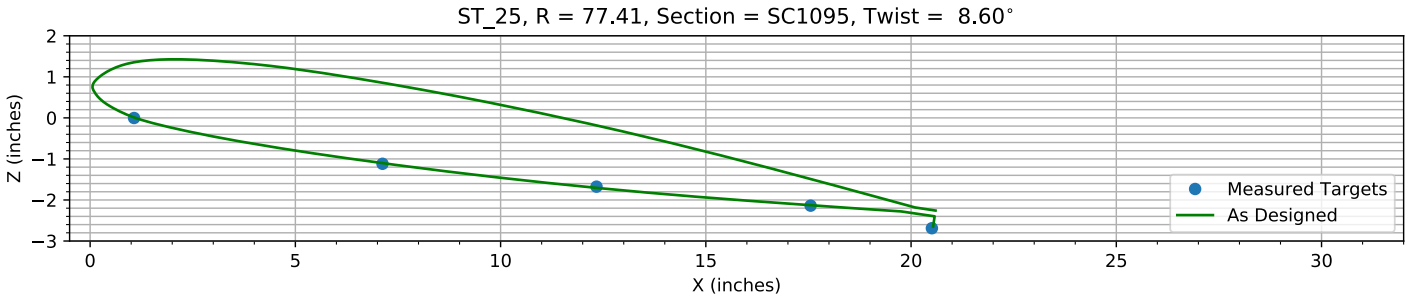

Figure 8-6. Target locations vs section profile at station 25.

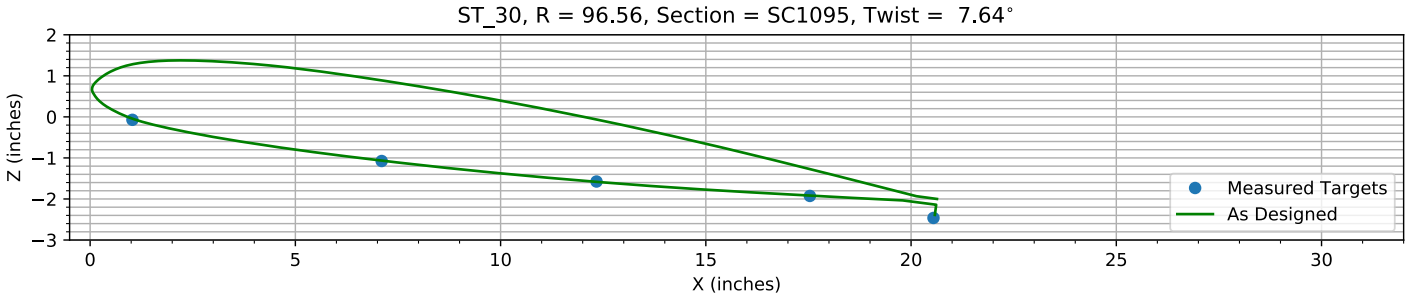

Figure 8-7. Target locations vs section profile at station 30.

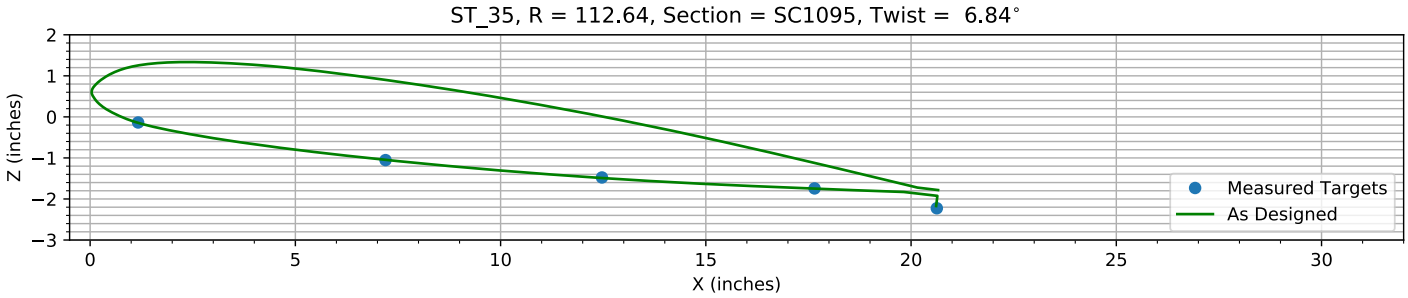

Figure 8-8. Target locations vs section profile at station 35.

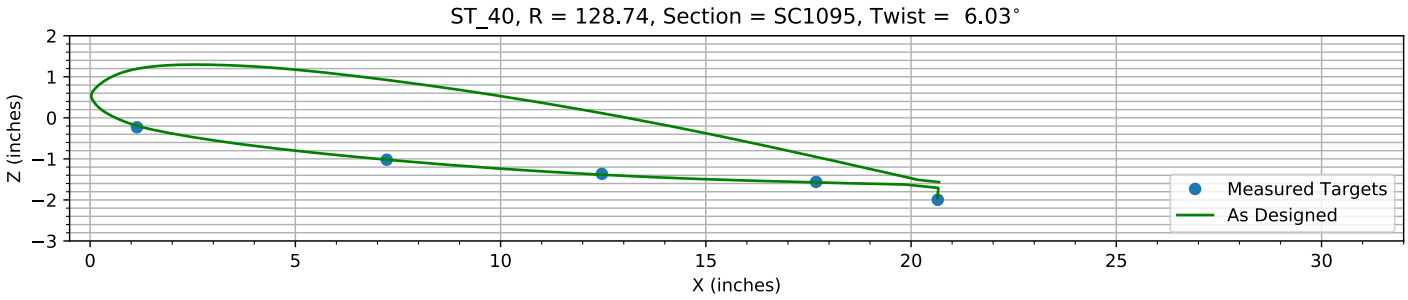

Figure 8-9. Target locations vs section profile at station 40.

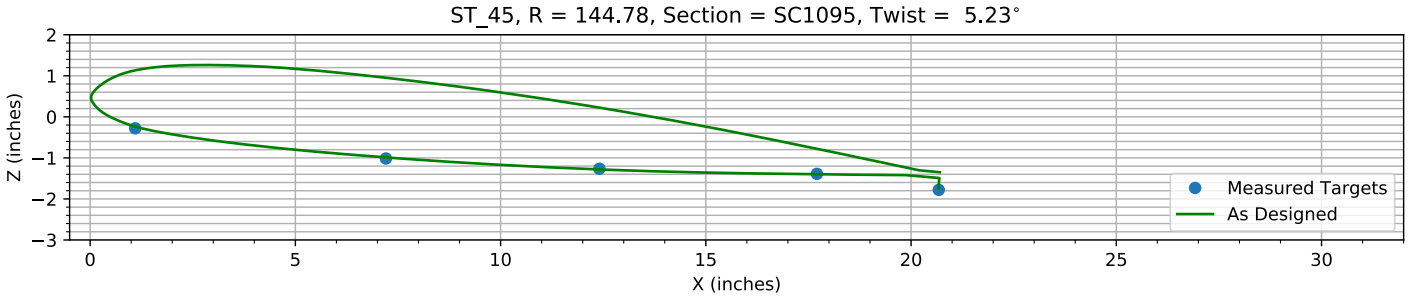

Figure 8-10. Target locations vs section profile at station 45.

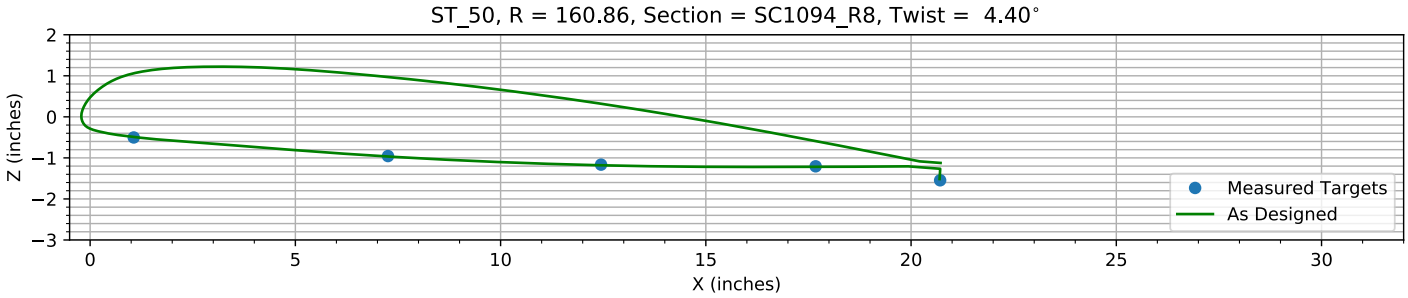

Figure 8-11. Target locations vs section profile at station 50.

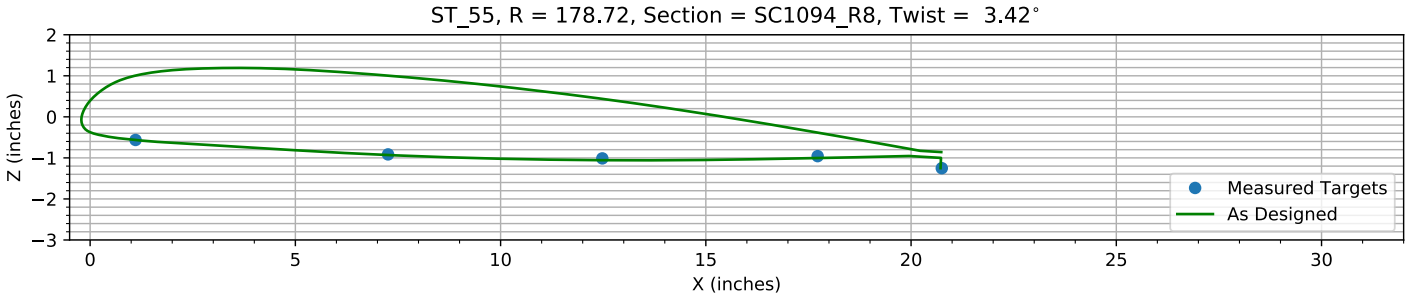

Figure 8-12. Target locations vs section profile at station 55.

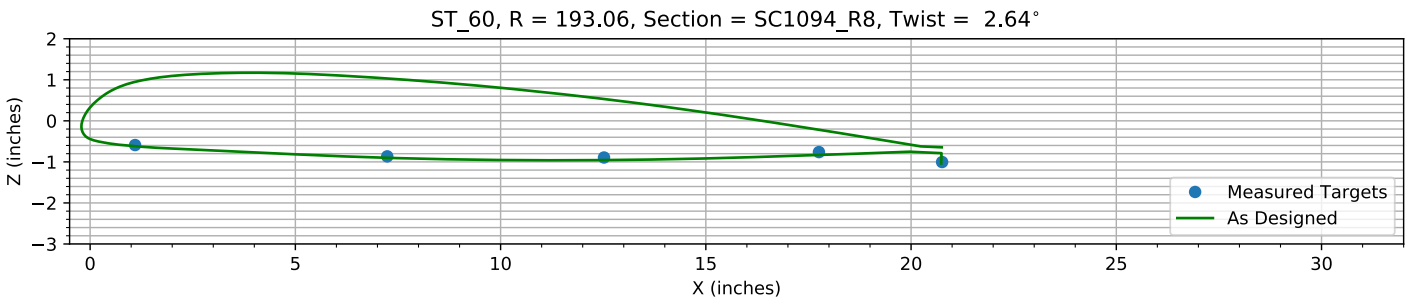

Figure 8-13. Target locations vs section profile at station 60.

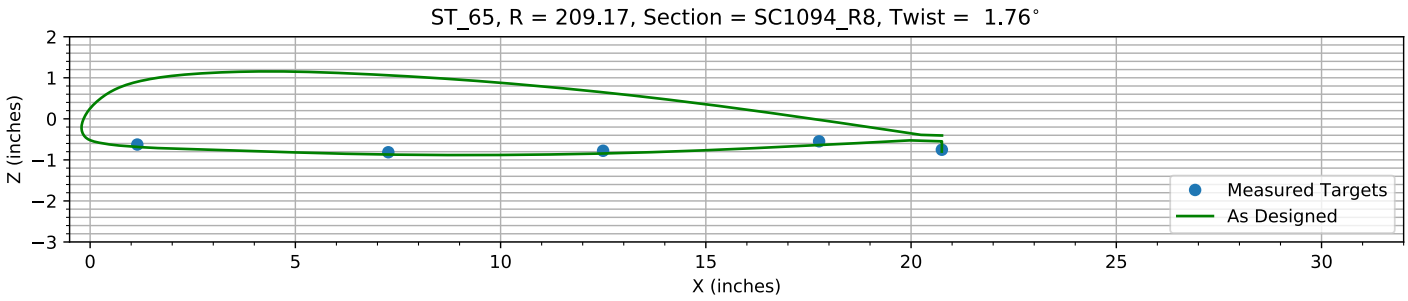

Figure 8-14. Target locations vs section profile at station 65.

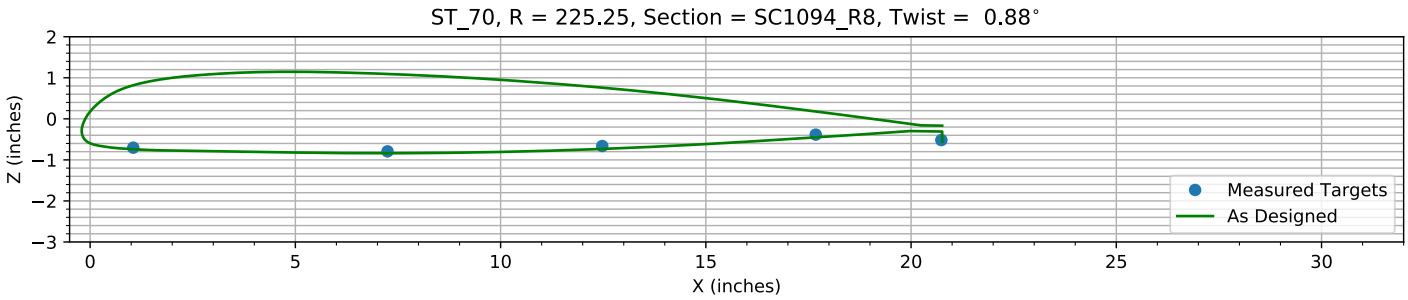

Figure 8-15. Target locations vs section profile at station 70.

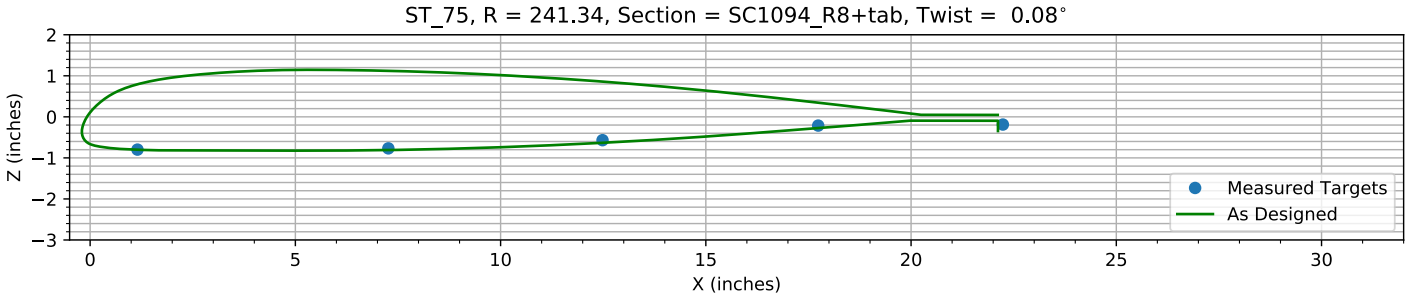

Figure 8-16. Target locations vs section profile at station 75.

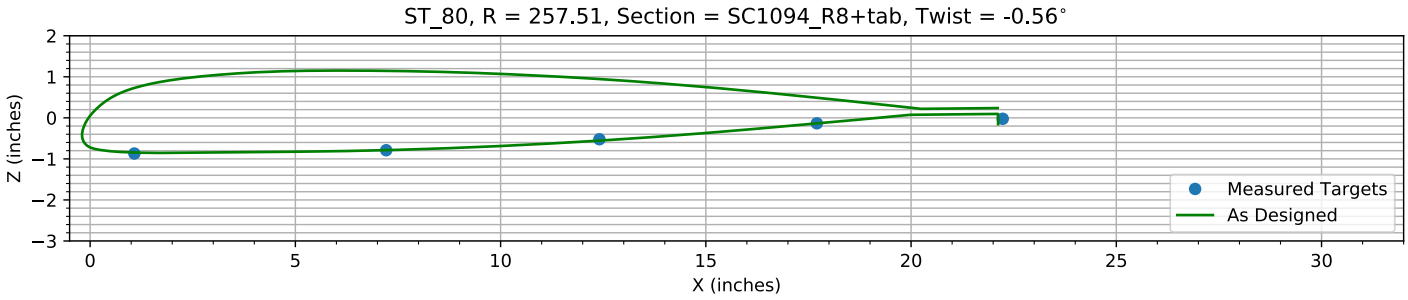

Figure 8-17. Target locations vs section profile at station 80.

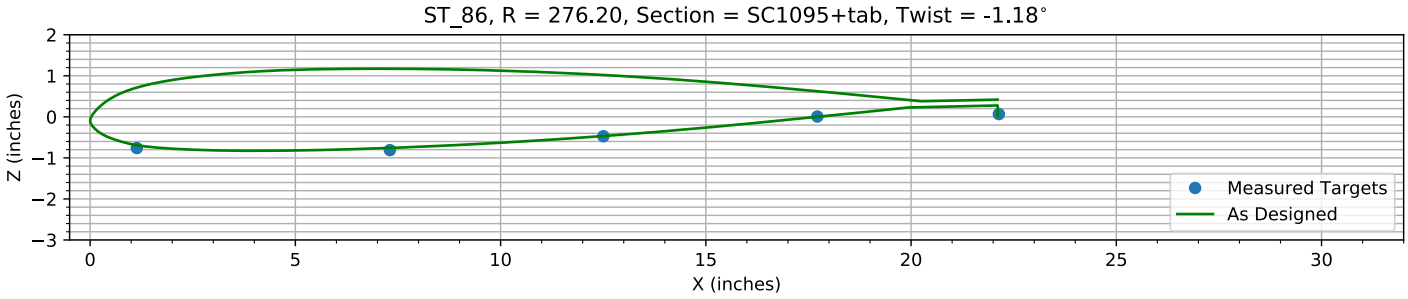

Figure 8-18. Target locations vs section profile at station 86.

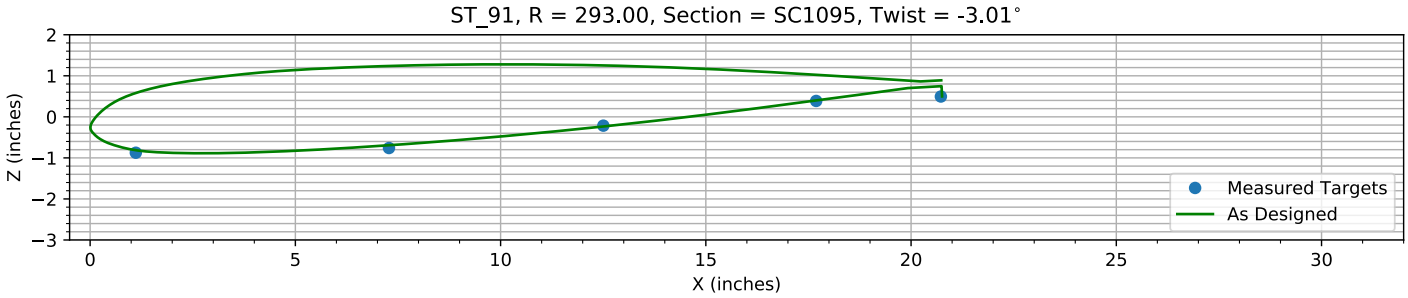

Figure 8-19. Target locations vs section profile at station 91.

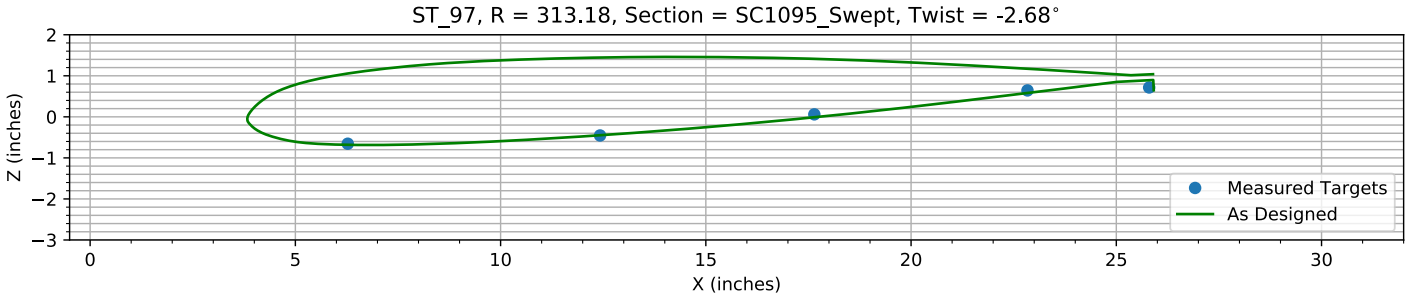

Figure 8-20. Target locations vs section profile at station 97.

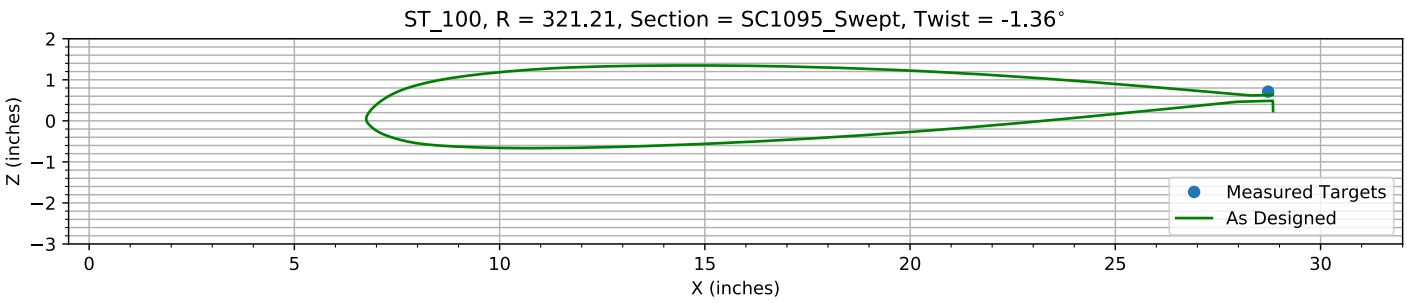

Figure 8-21. Target locations vs section profile at station 100.

Chapter 9: Pitch, Flap, and ΔZ Registration (15 rows)

The targets at the 15 spanwise stations nearest the root are used to determing the Z, flap, and pitch offset.

The estimated Z error, -0.32127 inches, is within an allowed range of ±2.000 inches.

The estimated flap error is -0.11065°.

The estimated pitch error is -0.090468°.

9.1: Target Location Errors After Target Registration

Table 9-1. Measured(1) with pitch and flap registration vs as designed(2) in inches.

Name	X1	Y1	Z1	X2	Y2	Z2	dX	dY	dZ	dR
B2_R20_C05	1.0535	62.785	0.061625	1.0535	62.785	0.069986	0	0	-0.0083603	0.0083603
B2_R20_C36	7.1572	62.765	-1.137	7.1572	62.765	-1.1345	0	0	-0.0024154	0.0024154
B2_R20_C61	12.322	62.754	-1.7301	12.322	62.754	-1.7977	0	0	0.067584	0.067584
B2_R20_C86	17.57	62.757	-2.218	17.57	62.757	-2.2908	0	0	0.072743	0.072743
B2_R20_C99	20.504	62.717	-2.811	20.502	62.717	-2.8432	0.0028622	0	0.03218	0.032307
B2_R25_C05	1.0714	77.402	-0.0023746	1.0714	77.402	0.010298	0	0	-0.012673	0.012673
B2_R25_C36	7.1237	77.42	-1.1198	7.1237	77.42	-1.1027	0	0	-0.017034	0.017034
B2_R25_C61	12.337	77.425	-1.6784	12.337	77.425	-1.705	0	0	0.026598	0.026598
B2_R25_C86	17.553	77.429	-2.1431	17.553	77.429	-2.1279	0	0	-0.015138	0.015138
B2_R25_C99	20.507	77.393	-2.6938	20.537	77.393	-2.6458	-0.029557	0	-0.048019	0.056387
B2_R30_C05	1.0312	96.622	-0.074592	1.0312	96.622	-0.044981	0	0	-0.02961	0.02961
B2_R30_C36	7.1035	96.587	-1.0802	7.1035	96.587	-1.0657	0	0	-0.01447	0.01447
B2_R30_C61	12.337	96.539	-1.5815	12.337	96.539	-1.5831	0	0	0.0015744	0.0015744
B2_R30_C86	17.535	96.531	-1.9342	17.535	96.531	-1.9183	0	0	-0.01591	0.01591
B2_R30_C99	20.546	96.519	-2.4716	20.579	96.519	-2.3887	-0.032677	0	-0.082901	0.089109
B2_R35_C05	1.1703	112.64	-0.14269	1.1703	112.64	-0.14634	0	0	0.0036555	0.0036555
B2_R35_C36	7.1975	112.64	-1.061	7.1975	112.64	-1.0469	0	0	-0.014099	0.014099
B2_R35_C61	12.47	112.66	-1.4858	12.47	112.66	-1.4897	0	0	0.0039085	0.0039085
B2_R35_C86	17.649	112.64	-1.7546	17.649	112.64	-1.7481	0	0	-0.006501	0.006501
B2_R35_C99	20.628	112.61	-2.2385	20.611	112.61	-2.1724	0.016552	0	-0.066077	0.068119
B2_R40_C05	1.1432	128.83	-0.23927	1.1432	128.83	-0.19471	0	0	-0.044564	0.044564
B2_R40_C36	7.227	128.77	-1.0321	7.227	128.77	-1.0199	0	0	-0.012188	0.012188
B2_R40_C61	12.468	128.76	-1.3777	12.468	128.76	-1.3863	0	0	0.0086459	0.0086459
B2_R40_C86	17.687	128.68	-1.5755	17.687	128.68	-1.5742	0	0	-0.0013284	0.0013284
B2_R40_C99	20.651	128.68	-2.0124	20.64	128.68	-1.9562	0.011163	0	-0.056202	0.0573
B2_R45_C05	1.099	144.78	-0.29189	1.099	144.78	-0.23775	0	0	-0.054133	0.054133
B2_R45_C36	7.2066	144.76	-1.0291	7.2066	144.76	-0.98889	0	0	-0.04018	0.04018
B2_R45_C61	12.407	144.79	-1.2806	12.407	144.79	-1.2816	0	0	0.00094588	0.00094588
B2_R45_C86	17.707	144.78	-1.4068	17.707	144.78	-1.3988	0	0	-0.0080052	0.0080052
B2_R45_C99	20.676	144.76	-1.7982	20.666	144.76	-1.7397	0.0098132	0	-0.058527	0.059344
B2_R50_C05	1.0633	160.82	-0.51797	1.0633	160.82	-0.49027	0	0	-0.027704	0.027704
B2_R50_C36	7.2575	160.84	-0.9732	7.2575	160.84	-0.96665	0	0	-0.0065494	0.0065494
B2_R50_C61	12.448	160.83	-1.1837	12.448	160.83	-1.1805	0	0	-0.0031768	0.0031768
B2_R50_C86	17.676	160.85	-1.2263	17.676	160.85	-1.2184	0	0	-0.0079907	0.0079907
B2_R50_C99	20.708	160.96	-1.568	20.695	160.96	-1.5134	0.013249	0	-0.054626	0.05621
B2_R55_C05	1.1073	178.74	-0.58242	1.1073	178.74	-0.56437	0	0	-0.01805	0.01805

Name	X1	Y1	Z1	X2	Y2	Z2	dX	dY	dZ	dR
B2_R55_C36	7.2585	178.73	-0.93606	7.2585	178.73	-0.93052	0	0	-0.0055388	0.0055388
B2_R55_C61	12.479	178.76	-1.0351	12.479	178.76	-1.0561	0	0	0.020981	0.020981
B2_R55_C86	17.725	178.72	-0.98199	17.725	178.72	-1.0043	0	0	0.022312	0.022312
B2_R55_C99	20.749	178.67	-1.2765	20.719	178.67	-1.2508	0.030413	0	-0.025706	0.039821
B2_R60_C05	1.0959	193.08	-0.61191	1.0959	193.08	-0.61855	0	0	0.0066469	0.0066469
B2_R60_C36	7.239	193.09	-0.8895	7.239	193.09	-0.90112	0	0	0.011622	0.011622
B2_R60_C61	12.52	193.09	-0.91893	12.52	193.09	-0.95601	0	0	0.037083	0.037083
B2_R60_C86	17.757	193.05	-0.78897	17.757	193.05	-0.83205	0	0	0.043075	0.043075
B2_R60_C99	20.757	192.97	-1.0322	20.734	192.97	-1.0386	0.022506	0	0.0064226	0.023404
B2_R65_C05	1.1498	209.13	-0.6514	1.1498	209.13	-0.68428	0	0	0.032878	0.032878
B2_R65_C36	7.2651	209.17	-0.84107	7.2651	209.17	-0.86971	0	0	0.02864	0.02864
B2_R65_C61	12.497	209.18	-0.80682	12.497	209.18	-0.84411	0	0	0.037298	0.037298
B2_R65_C86	17.76	209.21	-0.57807	17.76	209.21	-0.63838	0	0	0.060314	0.060314
B2_R65_C99	20.751	209.16	-0.78439	20.748	209.16	-0.79808	0.0024624	0	0.013699	0.013919
B2_R70_C05	1.0517	225.12	-0.73057	1.0517	225.12	-0.73989	0	0	0.009319	0.009319
B2_R70_C36	7.2457	225.25	-0.822	7.2457	225.25	-0.8378	0	0	0.015802	0.015802
B2_R70_C61	12.478	225.27	-0.69471	12.478	225.27	-0.73299	0	0	0.038286	0.038286
B2_R70_C86	17.678	225.32	-0.41813	17.678	225.32	-0.45081	0	0	0.032679	0.032679
B2_R70_C99	20.738	225.32	-0.55207	20.759	225.32	-0.55802	-0.020493	0	0.0059507	0.02134
B2_R75_C05	1.1542	241.32	-0.82974	1.1542	241.32	-0.80136	0	0	-0.028381	0.028381
B2_R75_C36	7.266	241.33	-0.80166	7.266	241.33	-0.80913	0	0	0.0074659	0.0074659
B2_R75_C61	12.484	241.36	-0.60375	12.484	241.36	-0.63223	0	0	0.028483	0.028483
B2_R75_C86	17.738	241.34	-0.24988	17.738	241.34	-0.27436	0	0	0.024479	0.024479
B2_R80_C05	1.0788	257.59	-0.9043	1.0788	257.59	-0.84457	0	0	-0.059721	0.059721
B2_R80_C36	7.2138	257.51	-0.82583	7.2138	257.51	-0.78725	0	0	-0.038579	0.038579
B2_R80_C61	12.408	257.49	-0.56008	12.408	257.49	-0.55523	0	0	-0.0048481	0.0048481
B2_R80_C86	17.706	257.43	-0.17376	17.706	257.43	-0.13652	0	0	-0.037242	0.037242
B2_R86_C05	1.1394	276.23	-0.7992	1.1394	276.23	-0.69104	0	0	-0.10816	0.10816
B2_R86_C36	7.3045	276.22	-0.85115	7.3045	276.22	-0.75755	0	0	-0.093607	0.093607
B2_R86_C61	12.505	276.21	-0.51458	12.505	276.21	-0.46795	0	0	-0.046627	0.046627
B2_R86_C86	17.717	276.18	-0.036375	17.717	276.18	0.00026329	0	0	-0.036638	0.036638
B2_R91_C05	1.1138	293.03	-0.91601	1.1138	293.03	-0.81342	0	0	-0.10259	0.10259
B2_R91_C36	7.2815	293	-0.80362	7.2815	293	-0.69266	0	0	-0.11095	0.11095
B2_R91_C61	12.504	293.04	-0.26008	12.504	293.04	-0.23419	0	0	-0.02589	0.02589
B2_R91_C86	17.69	292.98	0.33992	17.69	292.98	0.39843	0	0	-0.058506	0.058506
B2_R91_C99	20.727	292.98	0.44682	20.755	292.98	0.49726	-0.027965	0	-0.050439	0.057673
B2_R97_C05	6.2773	313.04	-0.70232	6.2773	313.04	-0.68462	0	0	-0.017706	0.017706
B2_R97_C36	12.424	313.1	-0.50331	12.424	313.1	-0.44708	0	0	-0.056226	0.056226
B2_R97_C61	17.644	313.21	0.009259	17.644	313.21	-0.012209	0	0	0.021468	0.021468
B2_R97_C86	22.837	313.28	0.5909	22.837	313.28	0.57288	0	0	0.018018	0.018018
B2_R97_C99	25.802	313.26	0.66178	25.942	313.26	0.6448	-0.13974	0	0.016979	0.14077
HUB_LE	2.2387	30.002	-3.1743	2.19	30	-3.5	0.048725	0.0017621	0.32573	0.32936
HUB_TE	8.2359	29.997	-3.1833	8.19	30	-3.5	0.045917	-0.0030785	0.31665	0.31998
RMS Errors:							0.019249	0.00039909	0.064956	0.067749

9.2: Pitch and Flap Registration Plots (15 rows)

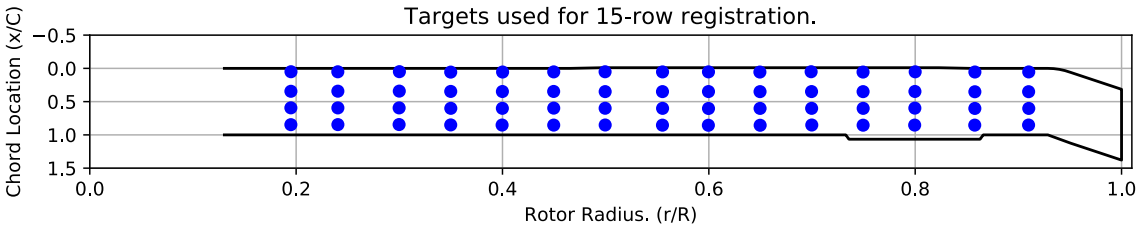

Figure 9-1. Targets used for 15 row root registration.

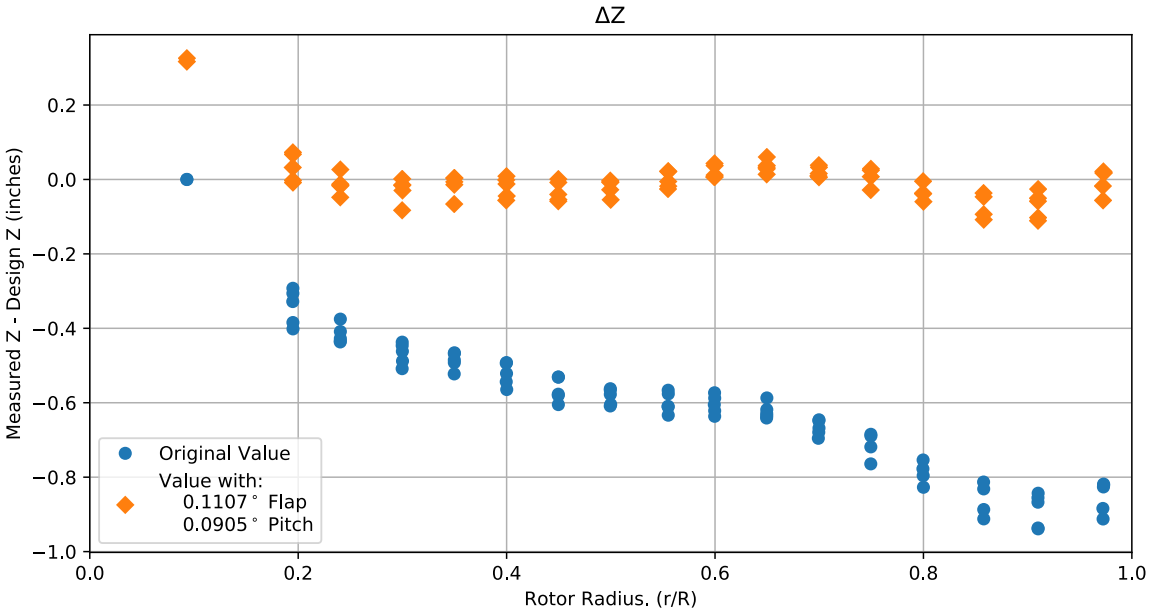

Figure 9-2. Pitch and flap target registration, ΔZ error vs rotor radius.

Note: the “as designed” geometry used for the swept tip may have some inaccuracies.

9.3: Estimated Bending and Twist at the Quarter Chord

The error bars shown represent the residual errors for fitting the measure target locations to the "as designed" geometry. These errors are generally much larger than those due to the VSTARS measurement errors. Therefore, the most likely source of these errors is the placement of the trailing-edge targets, differences between the "as designed" and "as built" geometries, and blade deformation during measurement. In the future, iterative adjustment of the "as designed" twist angle may be implemented to see if it reduces the fit error in delta twist. Note: The "as designed" geometry used for the swept tip may have some inaccuracies.

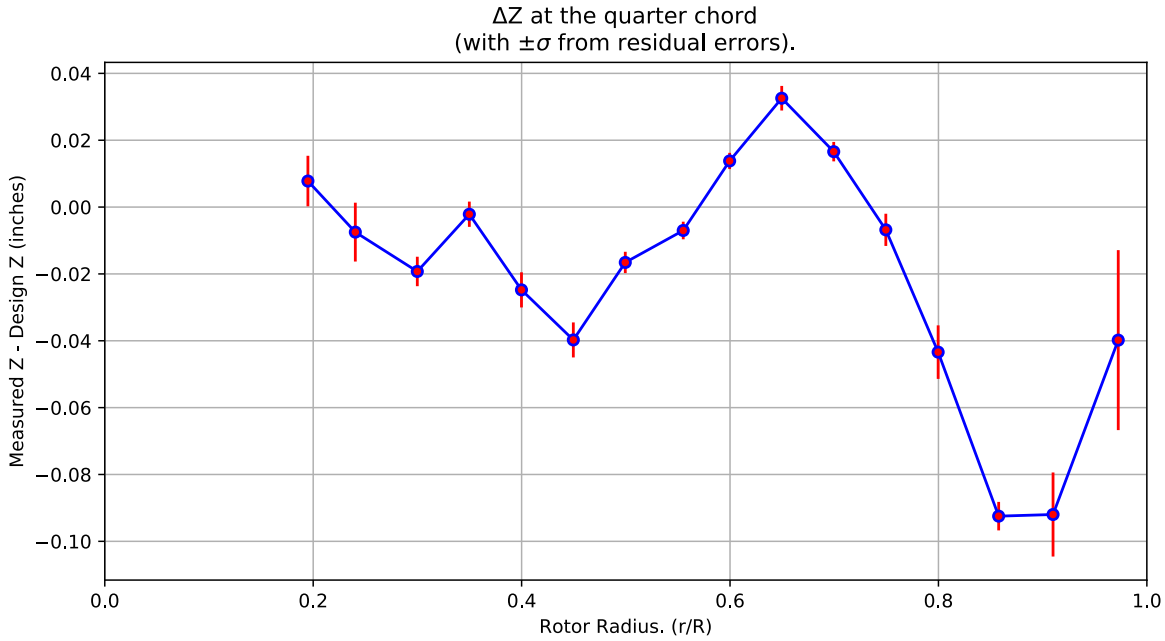

Figure 9-3. ΔZ error at the quarter chord vs rotor radius.

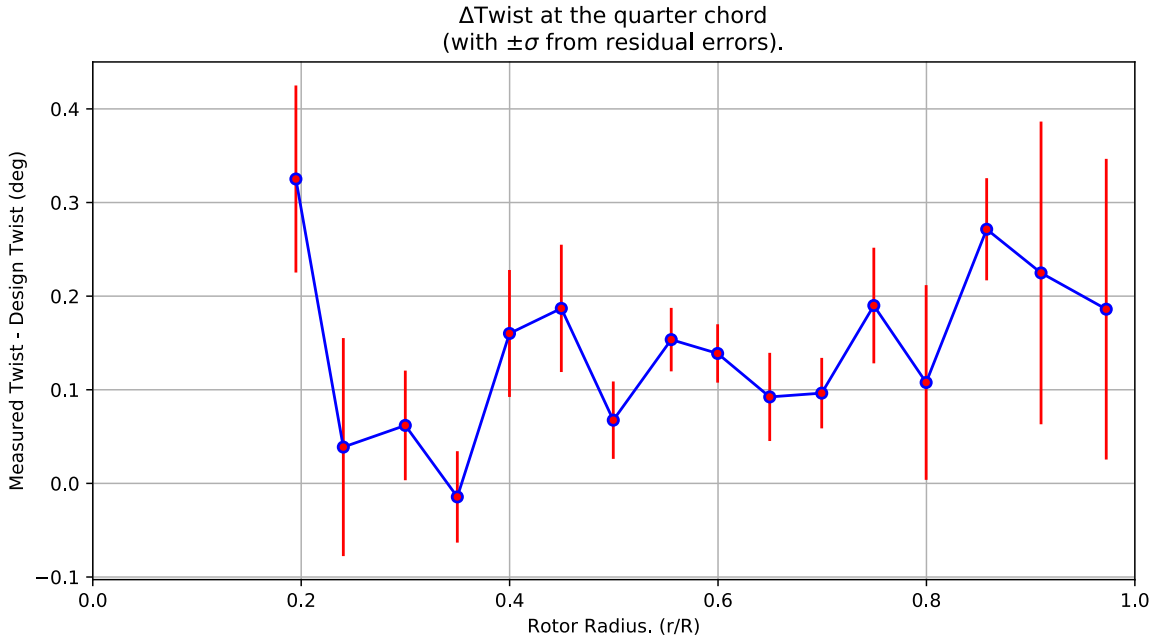

Figure 9-4. ΔTwist error at the quarter chord vs rotor radius.

Table 9-2. Quarter-chord bending and twist statistics.

r	r/R	dZ 1/4-chord	dT	sigma dZ meas	sigma dT meas	sigma dZ res	sigma dT res	n	t_conf
62.765	0.19492	0.007785	0.32511	6.1269e-10	4.6792e-09	0.0075602	0.099902	4	4.3027
77.419	0.24043	-0.007493	0.038777	6.1271e-10	4.6846e-09	0.0088023	0.11644	4	4.3027
96.57	0.29991	-0.019263	0.061914	6.1146e-10	4.6769e-09	0.004406	0.058546	4	4.3027
112.65	0.34983	-0.0021419	-0.014441	6.173e-10	4.6804e-09	0.0037767	0.048827	4	4.3027
128.76	0.39987	-0.024772	0.16014	6.1712e-10	4.6661e-09	0.0052559	0.067802	4	4.3027
144.78	0.44963	-0.039748	0.18694	6.1529e-10	4.6534e-09	0.0052391	0.067991	4	4.3027
160.83	0.49948	-0.016566	0.067524	6.1551e-10	4.652e-09	0.0031897	0.041336	4	4.3027
178.74	0.55509	-0.0070066	0.15356	6.1685e-10	4.6488e-09	0.0026344	0.033901	4	4.3027
193.08	0.59962	0.013796	0.13879	6.1663e-10	4.633e-09	0.0024282	0.031175	4	4.3027
209.17	0.64961	0.032565	0.092348	6.1813e-10	4.65e-09	0.0036808	0.047094	4	4.3027
225.24	0.6995	0.016579	0.096407	6.153e-10	4.6449e-09	0.0029064	0.037647	4	4.3027
241.34	0.7495	-0.0068109	0.18997	6.1813e-10	4.6578e-09	0.0048184	0.061752	4	4.3027
257.51	0.79971	-0.043395	0.10777	6.1492e-10	4.6489e-09	0.0080068	0.10399	4	4.3027
276.21	0.85779	-0.092466	0.27143	6.1852e-10	4.6601e-09	0.0042632	0.054564	4	4.3027
293.01	0.90997	-0.091974	0.22481	6.1753e-10	4.6587e-09	0.012576	0.16166	4	4.3027
313.16	0.97254	-0.039804	0.18606	9.2799e-10	4.6631e-09	0.026922	0.16059	4	4.3027

9.4: Section Plots

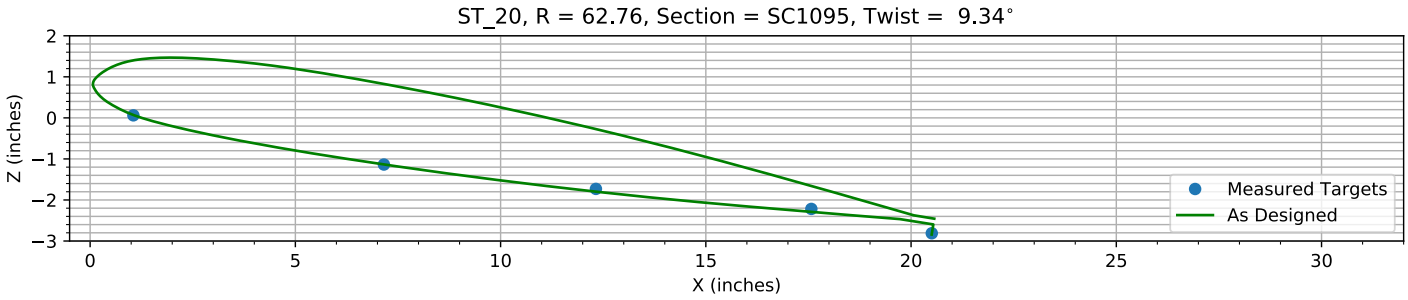

Figure 9-5. Target locations vs section profile at station 20.

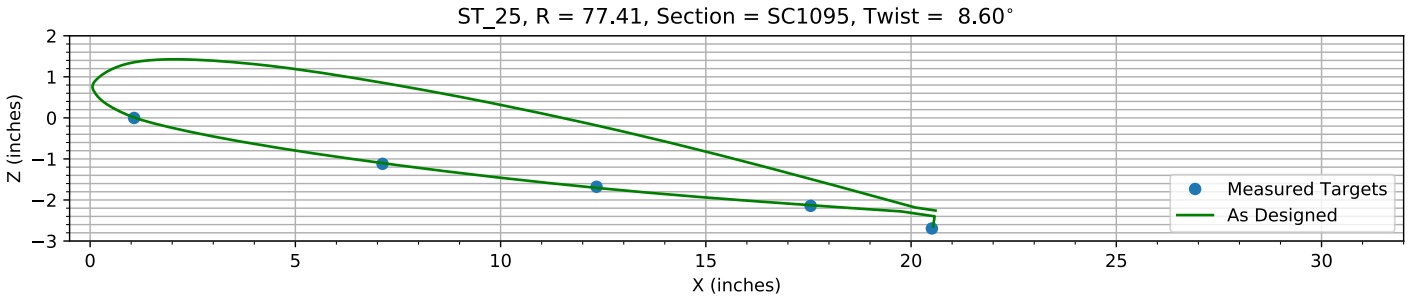

Figure 9-6. Target locations vs section profile at station 25.

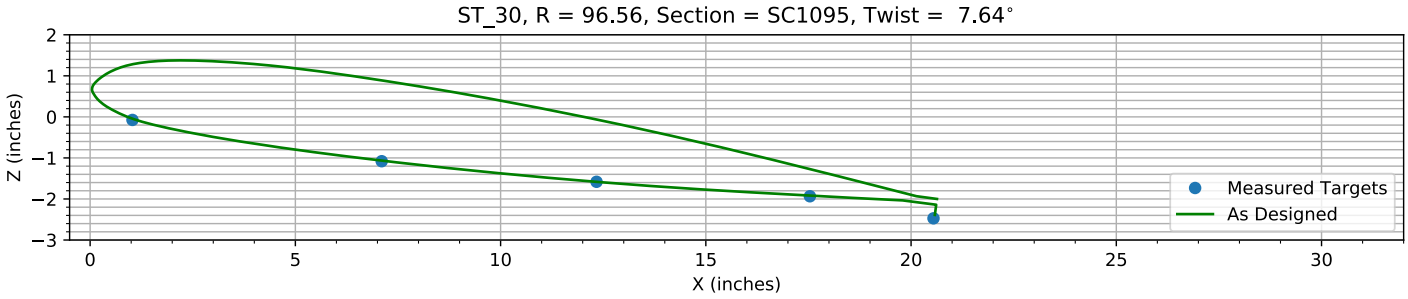

Figure 9-7. Target locations vs section profile at station 30.

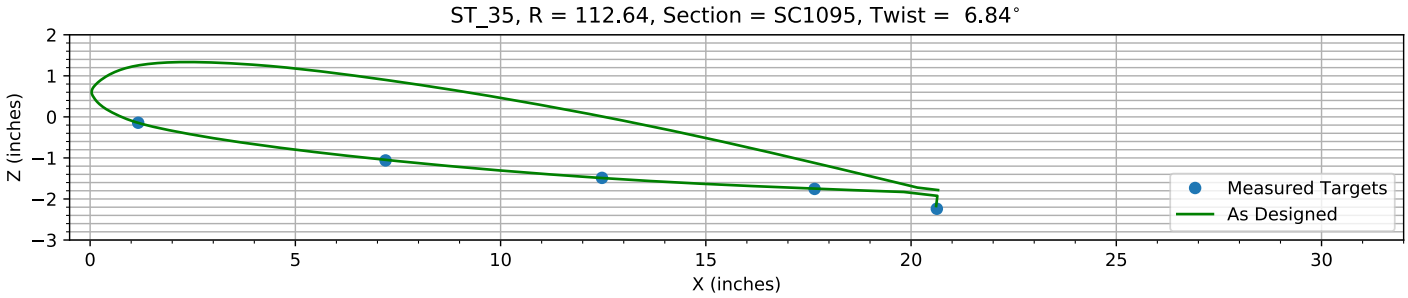

Figure 9-8. Target locations vs section profile at station 35.

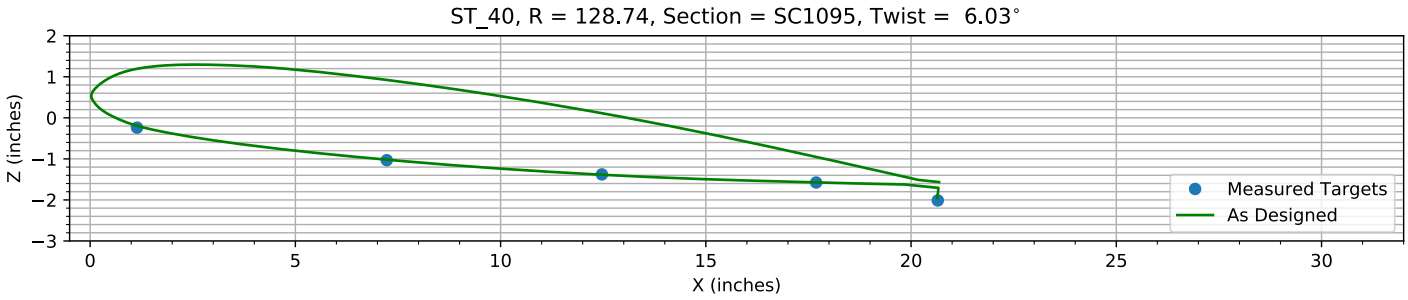

Figure 9-9. Target locations vs section profile at station 40.

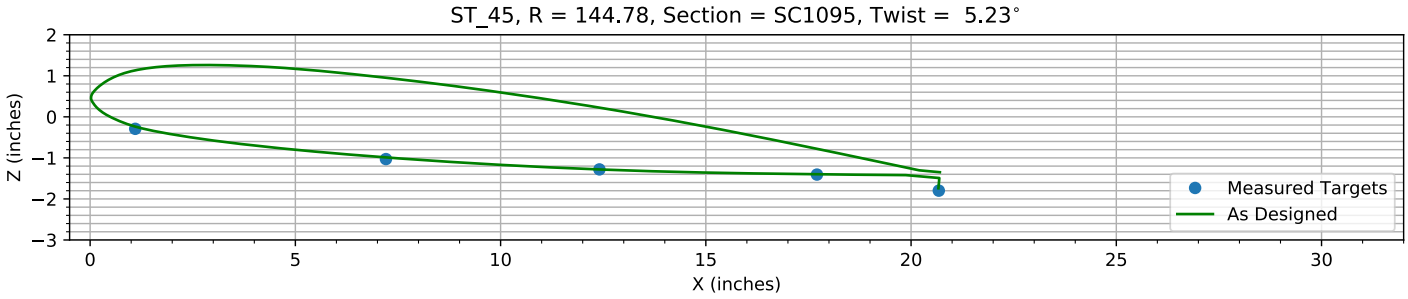

Figure 9-10. Target locations vs section profile at station 45.

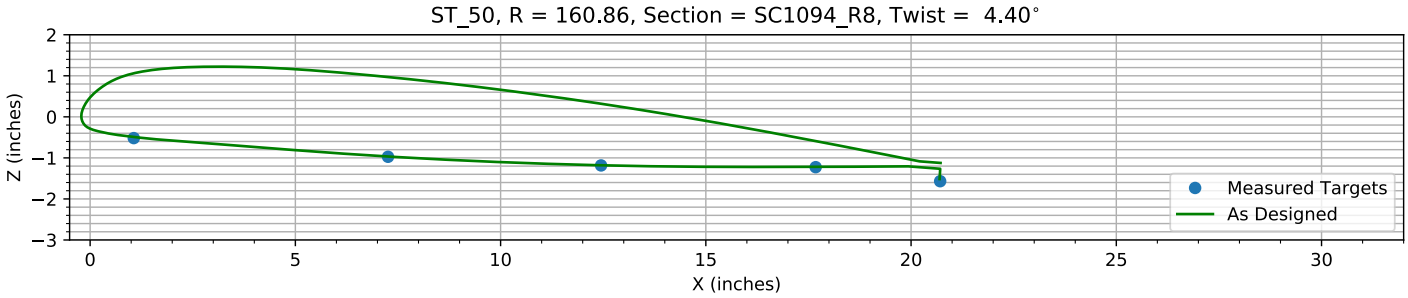

Figure 9-11. Target locations vs section profile at station 50.

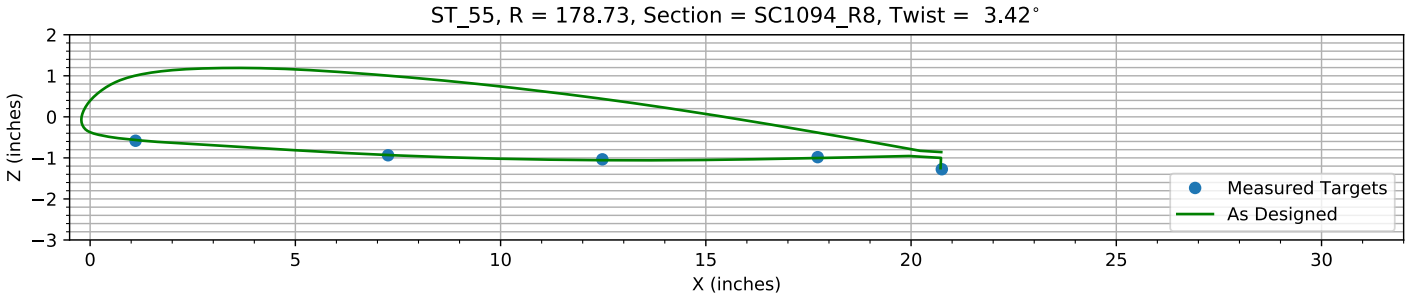

Figure 9-12. Target locations vs section profile at station 55.

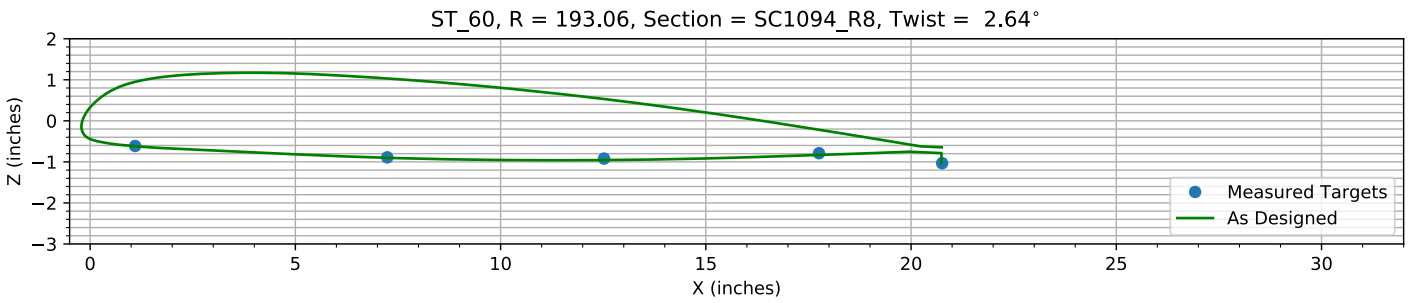

Figure 9-13. Target locations vs section profile at station 60.

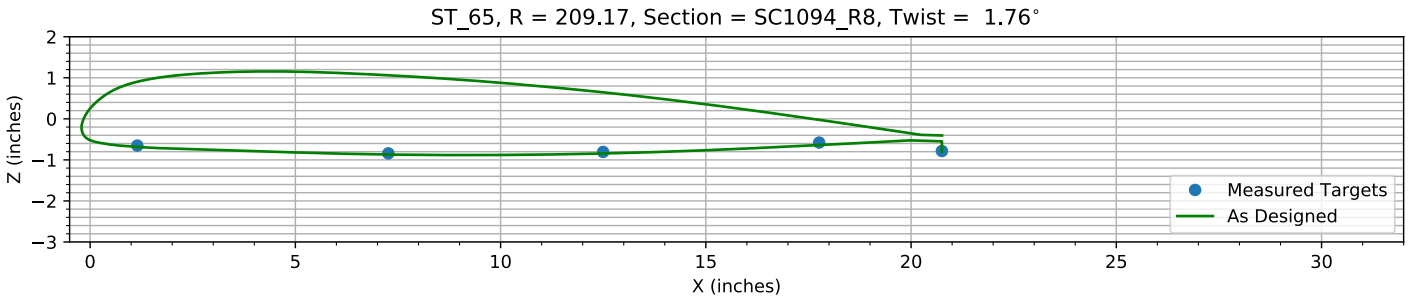

Figure 9-14. Target locations vs section profile at station 65.

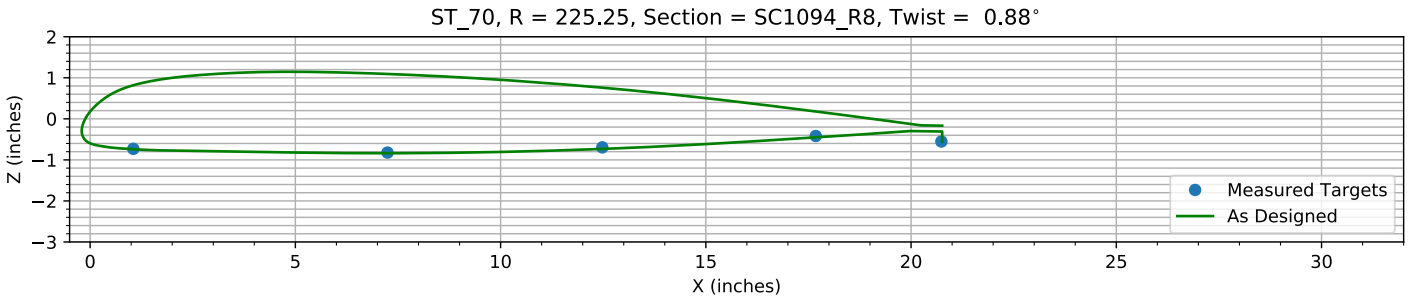

Figure 9-15. Target locations vs section profile at station 70.

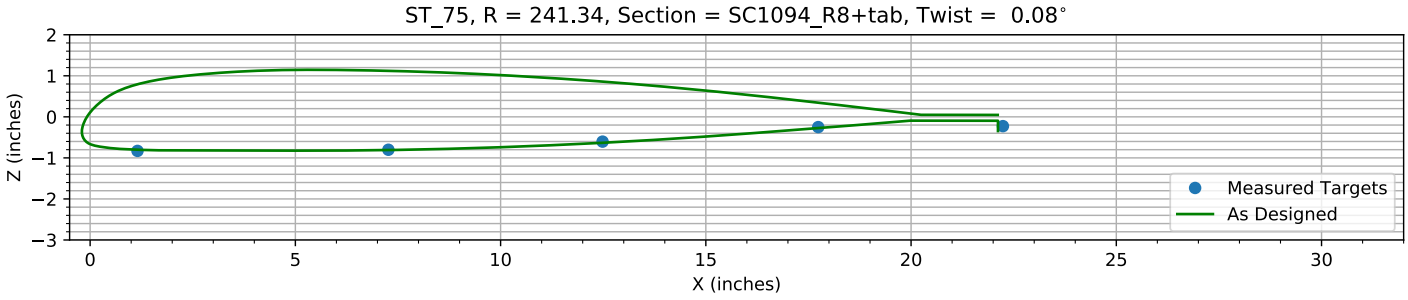

Figure 9-16. Target locations vs section profile at station 75.

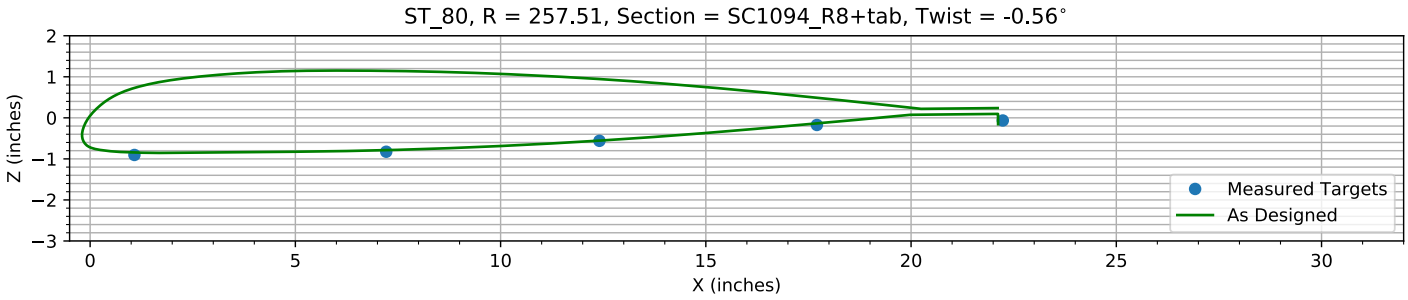

Figure 9-17. Target locations vs section profile at station 80.

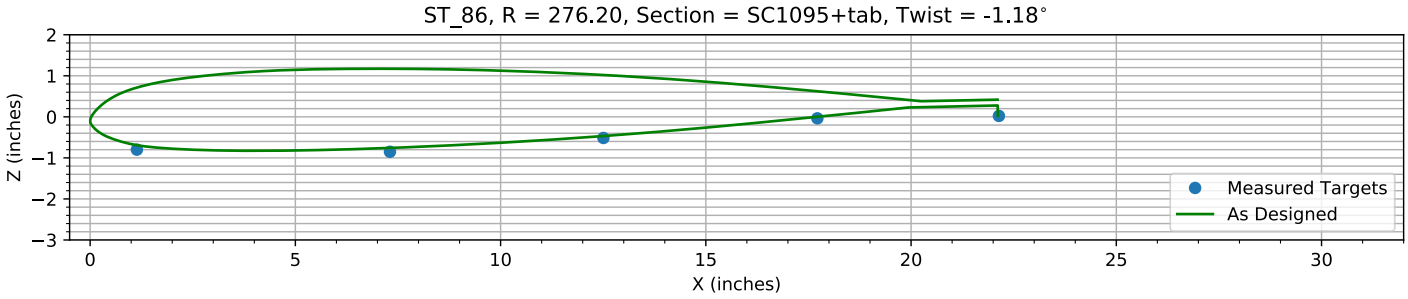

Figure 9-18. Target locations vs section profile at station 86.

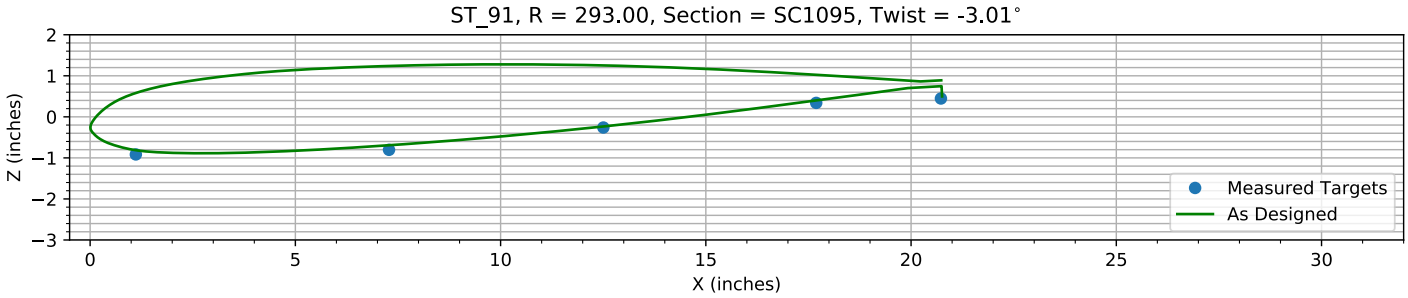

Figure 9-19. Target locations vs section profile at station 91.

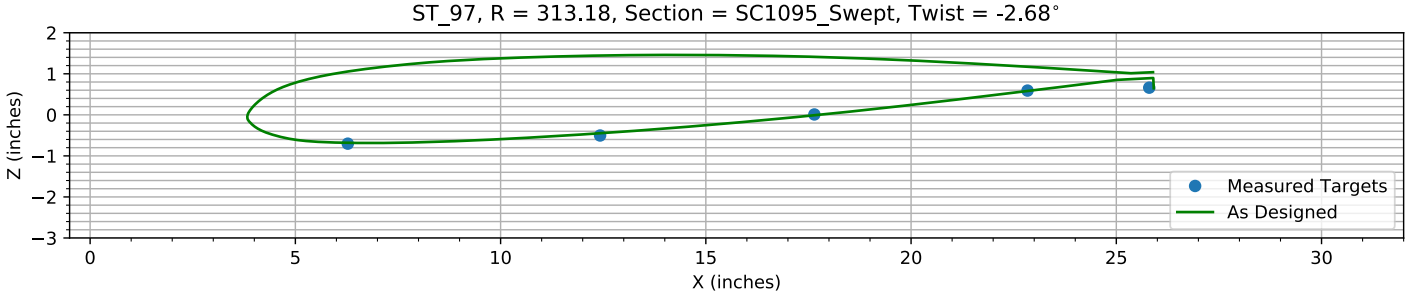

Figure 9-20. Target locations vs section profile at station 97.

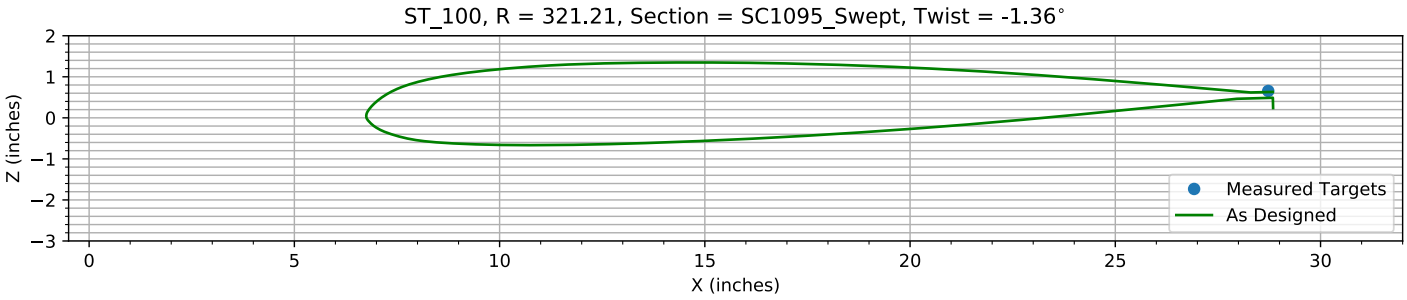

Figure 9-21. Target locations vs section profile at station 100.

I.3 Blade 3

The blade target registration report for Blade 3 is included here. It is based on the most recent V-STARS target location data for the vertically suspended blade. The condition of target 46 had degraded too much for the V-STARS system to measure it for this last measurement session, so its location was estimated based on its relative distance to nearby targets from previous V-STARS measurements.

Blade Target Registration

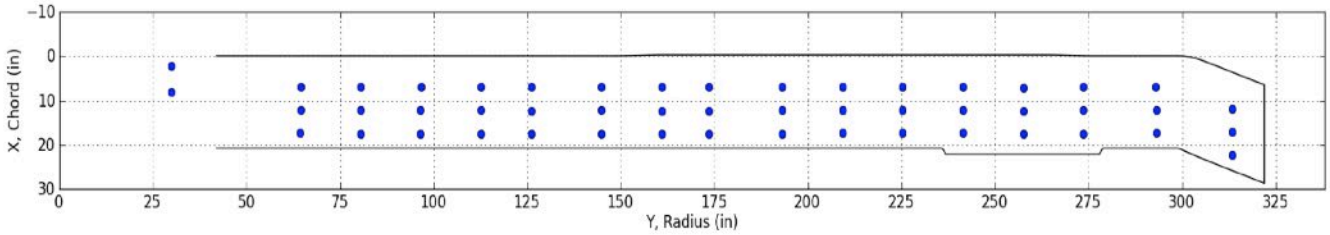

Registration Report for Blade Number 3

File: Blade 3 092012 vertical(1)_46.csv

Z reference allowed ±2.00 inches of travel

Aeromechanics Branch
Flight Vehicle Research and Technology Division
NASA Ames Research Center
Moffett Field, CA 94035

Chapter 1: VSTARS Target Location Data

Table 1-1. VSTARS target measurements (inches).

Name	Number	X	Y	Z	sigma X	sigma Y	sigma Z
B3_R20_C05		0.9669	62.377	-0.306	0.0004	0.0004	0.0009
B3_R20_C36	1	7.0301	62.393	-1.4704	0.0007	0.0007	0.0019
B3_R20_C61	2	11.133	62.383	-1.9356	0.0007	0.0007	0.0015
B3_R20_C86	3	17.47	62.435	-2.5362	0.0008	0.001	0.003
B3_R20_C99		20.442	62.388	-3.0697	0.0004	0.0004	0.0006
B3_R25_C05		0.9982	75.956	-0.4021	0.0004	0.0004	0.0009
B3_R25_C36	4	7.1212	75.916	-1.5025	0.0005	0.0005	0.0012
B3_R25_C61	5	12.424	75.859	-1.9338	0.0012	0.0016	0.0031
B3_R25_C86	6	17.59	75.921	-2.4916	0.0005	0.0005	0.0013
B3_R25_C99		20.505	75.876	-2.9838	0.0004	0.0003	0.0006
B3_R30_C05		0.973	96.436	-0.5339	0.0004	0.0004	0.0008
B3_R30_C36	7	7.0895	96.452	-1.5039	0.0005	0.0004	0.0008
B3_R30_C61	8	12.295	96.477	-1.9781	0.0004	0.0004	0.0007
B3_R30_C86	9	17.542	96.449	-2.3156	0.0004	0.0004	0.0006
B3_R30_C99		20.52	96.478	-2.791	0.0003	0.0003	0.0005
B3_R35_C05		0.9997	112.48	-0.6084	0.0004	0.0004	0.0007
B3_R35_C36	10	7.1035	112.48	-1.5029	0.0004	0.0004	0.0007
B3_R35_C61	11	12.348	112.45	-1.9082	0.0004	0.0004	0.0006
B3_R35_C86	12	17.569	112.47	-2.1561	0.0004	0.0004	0.0006
B3_R35_C99		20.567	112.5	-2.5752	0.0003	0.0003	0.0005
B3_R40_C05		1.0329	128.85	-0.7402	0.0004	0.0004	0.0007
B3_R40_C36	13	7.1642	128.82	-1.51	0.0004	0.0004	0.0006
B3_R40_C61	14	12.378	128.82	-1.8278	0.0004	0.0004	0.0006
B3_R40_C86	15	17.606	128.8	-1.9798	0.0004	0.0004	0.0007
B3_R40_C99		20.629	128.79	-2.3749	0.0003	0.0003	0.0005
B3_R45_C05		1.0628	144.74	-0.8491	0.0003	0.0004	0.0007
B3_R45_C36	16	7.1152	144.78	-1.5203	0.0004	0.0004	0.0006
B3_R45_C61	17	12.347	144.78	-1.7692	0.0005	0.0005	0.0006
B3_R45_C86	18	17.634	144.82	-1.8621	0.0004	0.0004	0.0006
B3_R45_C99		20.625	144.79	-2.1889	0.0003	0.0003	0.0005
B3_R50_C05		1.0126	161.01	-1.1009	0.0003	0.0003	0.0005
B3_R50_C36	19	7.1648	160.99	-1.5247	0.0005	0.0006	0.0009
B3_R50_C61	20	12.408	160.89	-1.7059	0.0005	0.0005	0.0006
B3_R50_C86	21	17.674	160.88	-1.7219	0.0004	0.0004	0.0006
B3_R50_C99		20.646	160.83	-2.0132	0.0003	0.0003	0.0005
B3_R55_C05		1.0558	178.95	-1.2047	0.0003	0.0004	0.0005
B3_R55_C36	22	7.1517	178.93	-1.5117	0.0003	0.0004	0.0005
B3_R55_C61	23	12.401	178.91	-1.5975	0.0003	0.0004	0.0005
B3_R55_C86	24	17.681	178.89	-1.5164	0.0003	0.0004	0.0005
B3_R55_C99		20.678	178.87	-1.7657	0.0003	0.0004	0.0005
B3_R60_C05		1.0081	193.11	-1.2615	0.0003	0.0004	0.0005
B3_R60_C36	25	7.225	193.1	-1.5041	0.0006	0.0006	0.0007
B3_R60_C61	26	12.423	193.05	-1.5009	0.0004	0.0005	0.0008
B3_R60_C86	27	17.647	193.01	-1.3553	0.0006	0.0006	0.0007
B3_R60_C99		20.689	192.97	-1.5536	0.0003	0.0004	0.0005
B3_R65_C05		1.0028	209.26	-1.326	0.0003	0.0004	0.0005
B3_R65_C36	28	7.1828	209.24	-1.4772	0.0004	0.0005	0.0009
B3_R65_C61	29	12.408	209.23	-1.4281	0.0004	0.0004	0.0007
B3_R65_C86	30	17.655	209.22	-1.1794	0.0003	0.0004	0.0005
B3_R65_C99		20.687	209.13	-1.3374	0.0003	0.0004	0.0005
B3_R70_C05		0.9912	221.86	-1.4044	0.0003	0.0004	0.0005

Name	Number	X	Y	Z	sigma X	sigma Y	sigma Z
B3_R70_C36	31	7.2278	221.87	-1.4741	0.0004	0.0004	0.0006
B3_R70_C61	32	12.43	221.86	-1.3579	0.0004	0.0004	0.0007
B3_R70_C86	33	17.674	221.88	-1.0274	0.0006	0.0007	0.0011
B3_R70_C99		20.666	221.76	-1.1725	0.0003	0.0004	0.0005
B3_R75_C05		1.0296	241.35	-1.5192	0.0004	0.0004	0.0005
B3_R75_C36	34	7.1799	241.36	-1.4618	0.0006	0.0007	0.0008
B3_R75_C61	35	12.435	241.35	-1.2305	0.0007	0.0007	0.0008
B3_R75_C86	36	17.662	241.34	-0.842	0.0006	0.0007	0.0007
B3_R75_C105		22.126	241.32	-0.8145	0.0003	0.0004	0.0005
B3_R80_C05		1.0922	257.59	-1.5876	0.0004	0.0004	0.0005
B3_R80_C36	37	7.2816	257.55	-1.4658	0.0004	0.0004	0.0005
B3_R80_C61	38	12.486	257.53	-1.1739	0.0004	0.0004	0.0006
B3_R80_C86	39	17.711	257.52	-0.7375	0.0005	0.0005	0.0007
B3_R80_C105		22.087	257.43	-0.6544	0.0003	0.0004	0.0005
B3_R86_C05		1.0486	276.28	-1.454	0.0004	0.0005	0.0007
B3_R86_C36	40	7.2735	276.23	-1.4855	0.0008	0.0011	0.001
B3_R86_C61	41	12.465	276.18	-1.1274	0.0005	0.0006	0.0007
B3_R86_C86	42	17.689	276.11	-0.6314	0.0006	0.0009	0.0009
B3_R86_C105		22.056	276	-0.5089	0.0004	0.0004	0.0005
B3_R91_C05		1.1279	295.54	-1.591	0.0004	0.0005	0.0007
B3_R91_C36	43	7.2485	295.51	-1.3968	0.001	0.001	0.0023
B3_R91_C61	44	12.487	295.52	-0.8705	0.0006	0.0006	0.0008
B3_R91_C86	45	17.599	295.53	-0.1631	0.0008	0.0007	0.0014
B3_R91_C99		20.628	295.46	0.0128	0.0004	0.0005	0.0006
B3_R97_C05		6.0244	313.3	-1.2677	0.0005	0.0006	0.0007
B3_R97_C61	47	17.455	313.28	-0.5553	0.0007	0.001	0.0009
B3_R97_C86	48	22.673	313.26	0.0422	0.0006	0.0011	0.001
B3_R97_C99		25.649	313.12	0.1378	0.0004	0.0006	0.0006
Blade Tip		28.448	320.67	0.1074	0.0004	0.0005	0.0006
HUB_LE		2.1907	30	-3.5044	0.0004	0.0005	0.0007
HUB_TE		8.1895	30	-3.4996	0.0004	0.0005	0.0007
B3_R97_C36	46	12.209	313.3	-0.98209	0.0006	0.0015	0.001

Chapter 2: Bolt Hole Target Alignment

The measured X, Y, and Z locations of the bolt hole targets are compared to their "as designed" locations. X, Y, and Z translation errors, along with pitch and lag errors, are estimated, and compensating translations and rotations are then applied to all target measurements.

2.1: Bolt Hole Alignment Errors

Table 2-1. Measured(1) vs "as designed"(2) in inches.

Name	X1	Y1	Z1	X2	Y2	Z2	dX	dY	dZ	dR
HUB_LE	2.1907	30	-3.5044	2.19	30	-3.5	0.0007	0	-0.0044	0.0044553
HUB_TE	8.1895	30	-3.4996	8.19	30	-3.5	-0.0005	0	0.0004	0.00064031
RMS Errors:							0.00060828	0	0.0031241	0.0031828

Table 2-2. Initial alignment errors.

Alignment Error	Value
X Error	0.0001
Y Error	0
Z Error	-0.002
Pitch Error	-0.045846
Lag Error	0

2.2: Corrected Bolt Hole Alignment

Table 2-3. Measured(1) with alignment correction vs "as designed"(2) in inches.

Name	X1	Y1	Z1	X2	Y2	Z2	dX	dY	dZ	dR
HUB_LE	2.1907	30	-3.5044	2.19	30	-3.5	0.0007	0	-0.0044	0.0044553
HUB_TE	8.1895	30	-3.4996	8.19	30	-3.5	-0.0005	0	0.0004	0.00064031
RMS Errors:							0.00060828	0	0.0031241	0.0031828

Table 2-4. Errors after hole alignment correction.

Alignment Error	Value
X Error	0.0001
Y Error	0
Z Error	-0.002
Pitch Error	-0.045846
Lag Error	0

Chapter 3: Trailing-Edge Alignment

The measured X locations of the trailing-edge targets, excluding those on the tab and swept tip, are compared to the "as designed" locations. An estimated lag error, for rotation about the centroid of the two bolt hole targets, and an estimated centroid offset in the X direction that minimize the root-mean-square of the ΔX values with respect to the "as designed" trailing-edge X location, are determined and applied to all target measurements.

3.1: Trailing-Edge Alignment Errors

Table 3-1. Measured(1) vs "as designed"(2) in inches.

Name	X1	Y1	Z1	X2	Y2	Z2	dX	dY	dZ	dR
B3_R20_C05	0.9669	62.377	-0.306	0.9669	62.377	0.10534	0	0	-0.41134	0.41134
B3_R20_C36	7.0301	62.393	-1.4704	7.0301	62.393	-1.1165	0	0	-0.3539	0.3539
B3_R20_C61	11.133	62.383	-1.9356	11.133	62.383	-1.6638	0	0	-0.2718	0.2718
B3_R20_C86	17.47	62.435	-2.5362	17.47	62.435	-2.2859	0	0	-0.25028	0.25028
B3_R20_C99	20.442	62.388	-3.0697	20.501	62.388	-2.8476	-0.059043	0	-0.22205	0.22977
B3_R25_C05	0.9982	75.956	-0.4021	0.9982	75.956	0.042505	0	0	-0.4446	0.4446
B3_R25_C36	7.1212	75.916	-1.5025	7.1212	75.916	-1.1051	0	0	-0.39736	0.39736
B3_R25_C61	12.424	75.859	-1.9338	12.424	75.859	-1.7236	0	0	-0.21019	0.21019
B3_R25_C86	17.59	75.921	-2.4916	17.59	75.921	-2.1471	0	0	-0.34446	0.34446
B3_R25_C99	20.505	75.876	-2.9838	20.533	75.876	-2.6662	-0.028785	0	-0.31763	0.31893
B3_R30_C05	0.973	96.436	-0.5339	0.973	96.436	-0.023415	0	0	-0.51048	0.51048
B3_R30_C36	7.0895	96.452	-1.5039	7.0895	96.452	-1.0643	0	0	-0.43961	0.43961
B3_R30_C61	12.295	96.477	-1.9781	12.295	96.477	-1.58	0	0	-0.39807	0.39807
B3_R30_C86	17.542	96.449	-2.3156	17.542	96.449	-1.9196	0	0	-0.39603	0.39603
B3_R30_C99	20.52	96.478	-2.791	20.579	96.478	-2.3893	-0.058437	0	-0.40174	0.40597
B3_R35_C05	0.9997	112.48	-0.6084	0.9997	112.48	-0.091517	0	0	-0.51688	0.51688
B3_R35_C36	7.1035	112.48	-1.5029	7.1035	112.48	-1.0375	0	0	-0.46536	0.46536
B3_R35_C61	12.348	112.45	-1.9082	12.348	112.45	-1.483	0	0	-0.42523	0.42523
B3_R35_C86	17.569	112.47	-2.1561	17.569	112.47	-1.7467	0	0	-0.40941	0.40941
B3_R35_C99	20.567	112.5	-2.5752	20.611	112.5	-2.1739	-0.043835	0	-0.40131	0.4037
B3_R40_C05	1.0329	128.85	-0.7402	1.0329	128.85	-0.16144	0	0	-0.57876	0.57876
B3_R40_C36	7.1642	128.82	-1.51	7.1642	128.82	-1.0143	0	0	-0.49574	0.49574
B3_R40_C61	12.378	128.82	-1.8278	12.378	128.82	-1.3812	0	0	-0.44657	0.44657
B3_R40_C86	17.606	128.8	-1.9798	17.606	128.8	-1.5707	0	0	-0.40907	0.40907
B3_R40_C99	20.629	128.79	-2.3749	20.64	128.79	-1.9547	-0.011446	0	-0.42018	0.42034
B3_R45_C05	1.0628	144.74	-0.8491	1.0628	144.74	-0.22712	0	0	-0.62198	0.62198
B3_R45_C36	7.1152	144.78	-1.5203	7.1152	144.78	-0.98206	0	0	-0.53824	0.53824
B3_R45_C61	12.347	144.78	-1.7692	12.347	144.78	-1.2793	0	0	-0.4899	0.4899
B3_R45_C86	17.634	144.82	-1.8621	17.634	144.82	-1.3976	0	0	-0.46451	0.46451
B3_R45_C99	20.625	144.79	-2.1889	20.666	144.79	-1.7394	-0.040764	0	-0.44948	0.45133
B3_R50_C05	1.0126	161.01	-1.1009	1.0126	161.01	-0.48505	0	0	-0.61585	0.61585
B3_R50_C36	7.1648	160.99	-1.5247	7.1648	160.99	-0.96077	0	0	-0.56393	0.56393
B3_R50_C61	12.408	160.89	-1.7059	12.408	160.89	-1.1792	0	0	-0.52667	0.52667
B3_R50_C86	17.674	160.88	-1.7219	17.674	160.88	-1.2179	0	0	-0.50397	0.50397
B3_R50_C99	20.646	160.83	-2.0132	20.695	160.83	-1.5153	-0.048944	0	-0.49791	0.50031
B3_R55_C05	1.0558	178.95	-1.2047	1.0558	178.95	-0.56002	0	0	-0.64468	0.64468
B3_R55_C36	7.1517	178.93	-1.5117	7.1517	178.93	-0.92552	0	0	-0.58618	0.58618
B3_R55_C61	12.401	178.91	-1.5975	12.401	178.91	-1.0546	0	0	-0.54293	0.54293
B3_R55_C86	17.681	178.89	-1.5164	17.681	178.89	-1.0032	0	0	-0.51322	0.51322
B3_R55_C99	20.678	178.87	-1.7657	20.719	178.87	-1.2479	-0.041155	0	-0.51784	0.51947
B3_R60_C05	1.0081	193.11	-1.2615	1.0081	193.11	-0.61107	0	0	-0.65043	0.65043
B3_R60_C36	7.225	193.1	-1.5041	7.225	193.1	-0.90068	0	0	-0.60342	0.60342
B3_R60_C61	12.423	193.05	-1.5009	12.423	193.05	-0.95706	0	0	-0.54384	0.54384
B3_R60_C86	17.647	193.01	-1.3553	17.647	193.01	-0.83622	0	0	-0.51908	0.51908

Name	X1	Y1	Z1	X2	Y2	Z2	dX	dY	dZ	dR
B3_R60_C99	20.689	192.97	-1.5536	20.734	192.97	-1.0386	-0.045453	0	-0.51501	0.51701
B3_R65_C05	1.0028	209.26	-1.326	1.0028	209.26	-0.67439	0	0	-0.65161	0.65161
B3_R65_C36	7.1828	209.24	-1.4772	7.1828	209.24	-0.86841	0	0	-0.60879	0.60879
B3_R65_C61	12.408	209.23	-1.4281	12.408	209.23	-0.84578	0	0	-0.58232	0.58232
B3_R65_C86	17.655	209.22	-1.1794	17.655	209.22	-0.64347	0	0	-0.53593	0.53593
B3_R65_C99	20.687	209.13	-1.3374	20.748	209.13	-0.79859	-0.06153	0	-0.53881	0.54231
B3_R70_C05	0.9912	221.86	-1.4044	0.9912	221.86	-0.72353	0	0	-0.68087	0.68087
B3_R70_C36	7.2278	221.87	-1.4741	7.2278	221.87	-0.8444	0	0	-0.6297	0.6297
B3_R70_C61	12.43	221.86	-1.3579	12.43	221.86	-0.75832	0	0	-0.59958	0.59958
B3_R70_C86	17.674	221.88	-1.0274	17.674	221.88	-0.49196	0	0	-0.53544	0.53544
B3_R70_C99	20.666	221.76	-1.1725	20.757	221.76	-0.61091	-0.091428	0	-0.56159	0.56898
B3_R75_C05	1.0296	241.35	-1.5192	1.0296	241.35	-0.79626	0	0	-0.72294	0.72294
B3_R75_C36	7.1799	241.36	-1.4618	7.1799	241.36	-0.81039	0	0	-0.65141	0.65141
B3_R75_C61	12.435	241.35	-1.2305	12.435	241.35	-0.63479	0	0	-0.59571	0.59571
B3_R75_C86	17.662	241.34	-0.842	17.662	241.34	-0.28033	0	0	-0.56167	0.56167
B3_R80_C05	1.0922	257.59	-1.5876	1.0922	257.59	-0.84497	0	0	-0.74263	0.74263
B3_R80_C36	7.2816	257.55	-1.4658	7.2816	257.55	-0.78542	0	0	-0.68038	0.68038
B3_R80_C61	12.486	257.53	-1.1739	12.486	257.53	-0.5502	0	0	-0.6237	0.6237
B3_R80_C86	17.711	257.52	-0.7375	17.711	257.52	-0.13538	0	0	-0.60212	0.60212
B3_R86_C05	1.0486	276.28	-1.454	1.0486	276.28	-0.67451	0	0	-0.77949	0.77949
B3_R86_C36	7.2735	276.23	-1.4855	7.2735	276.23	-0.7587	0	0	-0.7268	0.7268
B3_R86_C61	12.465	276.18	-1.1274	12.465	276.18	-0.47093	0	0	-0.65647	0.65647
B3_R86_C86	17.689	276.11	-0.6314	17.689	276.11	-0.002914	0	0	-0.62849	0.62849
B3_R91_C05	1.1279	295.54	-1.591	1.1279	295.54	-0.83341	0	0	-0.75759	0.75759
B3_R91_C36	7.2485	295.51	-1.3968	7.2485	295.51	-0.68585	0	0	-0.71095	0.71095
B3_R91_C61	12.487	295.52	-0.8705	12.487	295.52	-0.20338	0	0	-0.66712	0.66712
B3_R91_C86	17.599	295.53	-0.1631	17.599	295.53	0.44375	0	0	-0.60685	0.60685
B3_R91_C99	20.628	295.46	0.0128	20.753	295.46	0.56706	-0.12518	0	-0.55426	0.56823
B3_R97_C05	6.0244	313.3	-1.2677	6.0244	313.3	-0.67328	0	0	-0.59442	0.59442
B3_R97_C36	12.209	313.3	-0.98209	12.209	313.3	-0.46607	0	0	-0.51602	0.51602
B3_R97_C61	17.455	313.28	-0.5553	17.455	313.28	-0.034208	0	0	-0.52109	0.52109
B3_R97_C86	22.673	313.26	0.0422	22.673	313.26	0.55414	0	0	-0.51194	0.51194
B3_R97_C99	25.649	313.12	0.1378	25.892	313.12	0.64923	-0.24322	0	-0.51143	0.56632
HUB_LE	2.1907	30	-3.5044	2.19	5.19	-3.5	0.0007	24.81	-0.0044	24.81
HUB_TE	8.1895	30	-3.4996	8.19	5.19	-3.5	-0.0005	24.81	0.0004	24.81
RMS Errors:							0.036383	3.9476	0.53551	3.9839

The estimated lag error is -0.016792°.

The estimated X error is 0.015108 inches.

3.2: Corrected Trailing-Edge Alignment

Table 3-2. Measured(1) with lag correction vs "as designed"(2) in inches.

Name	X1	Y1	Z1	X2	Y2	Z2	dX	dY	dZ	dR
B3_R20_C05	0.9915	62.379	-0.306	0.9915	62.379	0.09543	0	0	-0.40143	0.40143
B3_R20_C36	7.0547	62.392	-1.4704	7.0547	62.392	-1.1201	0	0	-0.35025	0.35025
B3_R20_C61	11.157	62.381	-1.9356	11.157	62.381	-1.6667	0	0	-0.26891	0.26891
B3_R20_C86	17.495	62.431	-2.5362	17.495	62.431	-2.288	0	0	-0.24817	0.24817
B3_R20_C99	20.466	62.383	-3.0697	20.501	62.383	-2.8477	-0.034433	0	-0.22199	0.22465
B3_R25_C05	1.0268	75.957	-0.4021	1.0268	75.957	0.031784	0	0	-0.43388	0.43388
B3_R25_C36	7.1498	75.916	-1.5025	7.1498	75.916	-1.109	0	0	-0.3935	0.3935
B3_R25_C61	12.453	75.857	-1.9338	12.453	75.857	-1.7264	0	0	-0.2074	0.2074
B3_R25_C86	17.619	75.917	-2.4916	17.619	75.917	-2.1492	0	0	-0.34236	0.34236
B3_R25_C99	20.533	75.871	-2.9838	20.533	75.871	-2.6662	-0.00022302	0	-0.31757	0.31757
B3_R30_C05	1.0076	96.437	-0.5339	1.0076	96.437	-0.035995	0	0	-0.4979	0.4979
B3_R30_C36	7.1241	96.452	-1.5039	7.1241	96.452	-1.0683	0	0	-0.43557	0.43557
B3_R30_C61	12.33	96.475	-1.9781	12.33	96.475	-1.5829	0	0	-0.39523	0.39523
B3_R30_C86	17.576	96.445	-2.3156	17.576	96.445	-1.9215	0	0	-0.39412	0.39412
B3_R30_C99	20.555	96.474	-2.791	20.579	96.474	-2.3893	-0.023838	0	-0.40168	0.40239
B3_R35_C05	1.039	112.48	-0.6084	1.039	112.48	-0.10481	0	0	-0.50359	0.50359
B3_R35_C36	7.1428	112.48	-1.5029	7.1428	112.48	-1.0416	0	0	-0.46133	0.46133
B3_R35_C61	12.388	112.45	-1.9082	12.388	112.45	-1.4856	0	0	-0.42256	0.42256
B3_R35_C86	17.608	112.47	-2.1561	17.608	112.47	-1.7483	0	0	-0.4078	0.4078
B3_R35_C99	20.606	112.49	-2.5752	20.611	112.49	-2.1739	-0.0045421	0	-0.40125	0.40128
B3_R40_C05	1.077	128.85	-0.7402	1.077	128.85	-0.17522	0	0	-0.56498	0.56498
B3_R40_C36	7.2083	128.82	-1.51	7.2083	128.82	-1.0182	0	0	-0.49184	0.49184
B3_R40_C61	12.422	128.82	-1.8278	12.422	128.82	-1.3836	0	0	-0.4442	0.4442
B3_R40_C86	17.65	128.8	-1.9798	17.65	128.8	-1.5719	0	0	-0.40789	0.40789
B3_R40_C99	20.673	128.78	-2.3749	20.64	128.78	-1.9548	0.032621	0	-0.42012	0.42138
B3_R45_C05	1.1115	144.75	-0.8491	1.1115	144.75	-0.24116	0	0	-0.60794	0.60794
B3_R45_C36	7.1639	144.78	-1.5203	7.1639	144.78	-0.98568	0	0	-0.53462	0.53462
B3_R45_C61	12.396	144.77	-1.7692	12.396	144.77	-1.2812	0	0	-0.48796	0.48796
B3_R45_C86	17.683	144.81	-1.8621	17.683	144.81	-1.3982	0	0	-0.46389	0.46389
B3_R45_C99	20.674	144.78	-2.1889	20.666	144.78	-1.7395	0.00799	0	-0.44942	0.44949
B3_R50_C05	1.0661	161.01	-1.1009	1.0661	161.01	-0.49134	0	0	-0.60956	0.60956
B3_R50_C36	7.2183	160.99	-1.5247	7.2183	160.99	-0.96399	0	0	-0.56071	0.56071
B3_R50_C61	12.461	160.89	-1.7059	12.461	160.89	-1.1804	0	0	-0.52547	0.52547
B3_R50_C86	17.727	160.88	-1.7219	17.727	160.88	-1.2178	0	0	-0.50409	0.50409
B3_R50_C99	20.7	160.83	-2.0132	20.695	160.83	-1.5154	0.0045125	0	-0.49785	0.49787
B3_R55_C05	1.1146	178.95	-1.2047	1.1146	178.95	-0.56587	0	0	-0.63883	0.63883
B3_R55_C36	7.2105	178.93	-1.5117	7.2105	178.93	-0.92805	0	0	-0.58365	0.58365
B3_R55_C61	12.459	178.91	-1.5975	12.459	178.91	-1.0549	0	0	-0.54255	0.54255
B3_R55_C86	17.74	178.89	-1.5164	17.74	178.89	-1.002	0	0	-0.51437	0.51437
B3_R55_C99	20.736	178.86	-1.7657	20.719	178.86	-1.2479	0.017587	0	-0.51777	0.51807
B3_R60_C05	1.071	193.11	-1.2615	1.071	193.11	-0.61653	0	0	-0.64497	0.64497
B3_R60_C36	7.2879	193.1	-1.5041	7.2879	193.1	-0.90254	0	0	-0.60156	0.60156
B3_R60_C61	12.485	193.05	-1.5009	12.485	193.05	-0.95658	0	0	-0.54432	0.54432
B3_R60_C86	17.71	193.01	-1.3553	17.71	193.01	-0.83413	0	0	-0.52117	0.52117
B3_R60_C99	20.752	192.97	-1.5536	20.734	192.97	-1.0387	0.01742	0	-0.51494	0.51524
B3_R65_C05	1.0704	209.26	-1.326	1.0704	209.26	-0.67923	0	0	-0.64677	0.64677
B3_R65_C36	7.2504	209.24	-1.4772	7.2504	209.24	-0.86936	0	0	-0.60784	0.60784
B3_R65_C61	12.476	209.23	-1.4281	12.476	209.23	-0.84429	0	0	-0.58381	0.58381
B3_R65_C86	17.722	209.22	-1.1794	17.722	209.22	-0.64017	0	0	-0.53923	0.53923
B3_R65_C99	20.755	209.12	-1.3374	20.748	209.12	-0.79866	0.0060783	0	-0.53874	0.53878
B3_R70_C05	1.0625	221.86	-1.4044	1.0625	221.86	-0.7278	0	0	-0.6766	0.6766

Name	X1	Y1	Z1	X2	Y2	Z2	dX	dY	dZ	dR
B3_R70_C36	7.2991	221.87	-1.4741	7.2991	221.87	-0.84454	0	0	-0.62956	0.62956
B3_R70_C61	12.501	221.85	-1.3579	12.501	221.85	-0.75585	0	0	-0.60205	0.60205
B3_R70_C86	17.746	221.88	-1.0274	17.746	221.88	-0.48761	0	0	-0.53979	0.53979
B3_R70_C99	20.737	221.75	-1.1725	20.757	221.75	-0.61098	-0.02012	0	-0.56152	0.56188
B3_R75_C05	1.1066	241.35	-1.5192	1.1066	241.35	-0.7995	0	0	-0.7197	0.7197
B3_R75_C36	7.257	241.36	-1.4618	7.257	241.36	-0.80923	0	0	-0.65257	0.65257
B3_R75_C61	12.512	241.35	-1.2305	12.512	241.35	-0.63081	0	0	-0.59969	0.59969
B3_R75_C86	17.739	241.34	-0.842	17.739	241.34	-0.2743	0	0	-0.5677	0.5677
B3_R80_C05	1.174	257.59	-1.5876	1.174	257.59	-0.8474	0	0	-0.7402	0.7402
B3_R80_C36	7.3634	257.55	-1.4658	7.3634	257.55	-0.78326	0	0	-0.68254	0.68254
B3_R80_C61	12.568	257.53	-1.1739	12.568	257.53	-0.54494	0	0	-0.62896	0.62896
B3_R80_C86	17.793	257.51	-0.7375	17.793	257.51	-0.12804	0	0	-0.60946	0.60946
B3_R86_C05	1.1359	276.28	-1.454	1.1359	276.28	-0.69051	0	0	-0.76349	0.76349
B3_R86_C36	7.3608	276.23	-1.4855	7.3608	276.23	-0.75542	0	0	-0.73008	0.73008
B3_R86_C61	12.552	276.18	-1.1274	12.552	276.18	-0.4646	0	0	-0.6628	0.6628
B3_R86_C86	17.776	276.11	-0.6314	17.776	276.11	0.0058158	0	0	-0.63722	0.63722
B3_R91_C05	1.2208	295.54	-1.591	1.2208	295.54	-0.84553	0	0	-0.74547	0.74547
B3_R91_C36	7.3414	295.51	-1.3968	7.3414	295.51	-0.67895	0	0	-0.71785	0.71785
B3_R91_C61	12.58	295.52	-0.8705	12.58	295.52	-0.1932	0	0	-0.6773	0.6773
B3_R91_C86	17.692	295.52	-0.1631	17.692	295.52	0.45644	0	0	-0.61954	0.61954
B3_R91_C99	20.721	295.46	0.0128	20.753	295.46	0.56694	-0.032279	0	-0.55414	0.55508
B3_R97_C05	6.1225	313.3	-1.2677	6.1225	313.3	-0.67588	0	0	-0.59182	0.59182
B3_R97_C36	12.307	313.29	-0.98209	12.307	313.29	-0.45959	0	0	-0.5225	0.5225
B3_R97_C61	17.553	313.28	-0.5553	17.553	313.28	-0.024404	0	0	-0.5309	0.5309
B3_R97_C86	22.771	313.26	0.0422	22.771	313.26	0.56644	0	0	-0.52424	0.52424
B3_R97_C99	25.747	313.11	0.1378	25.89	313.11	0.64943	-0.14295	0	-0.51163	0.53122
HUB_LE	2.2058	30.001	-3.5044	2.19	5.19	-3.5	0.015808	24.811	-0.0044	24.811
HUB_TE	8.2046	29.999	-3.4996	8.19	5.19	-3.5	0.014608	24.809	0.0004	24.809
RMS Errors:							0.018112	3.9476	0.53462	3.9836

3.3: Trailing-Edge Registration Plots

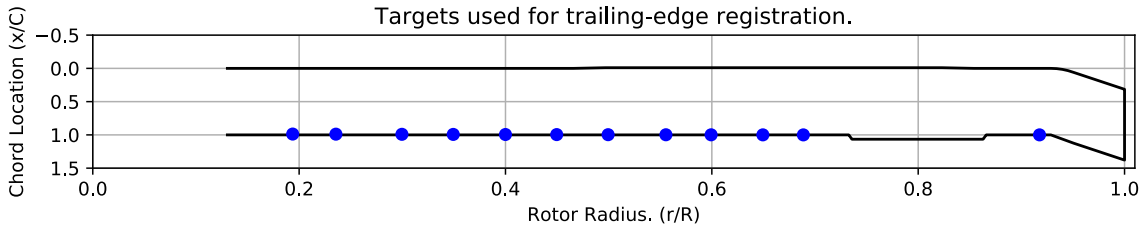

Figure 3-1. Targets used for trailing-edge alignment.

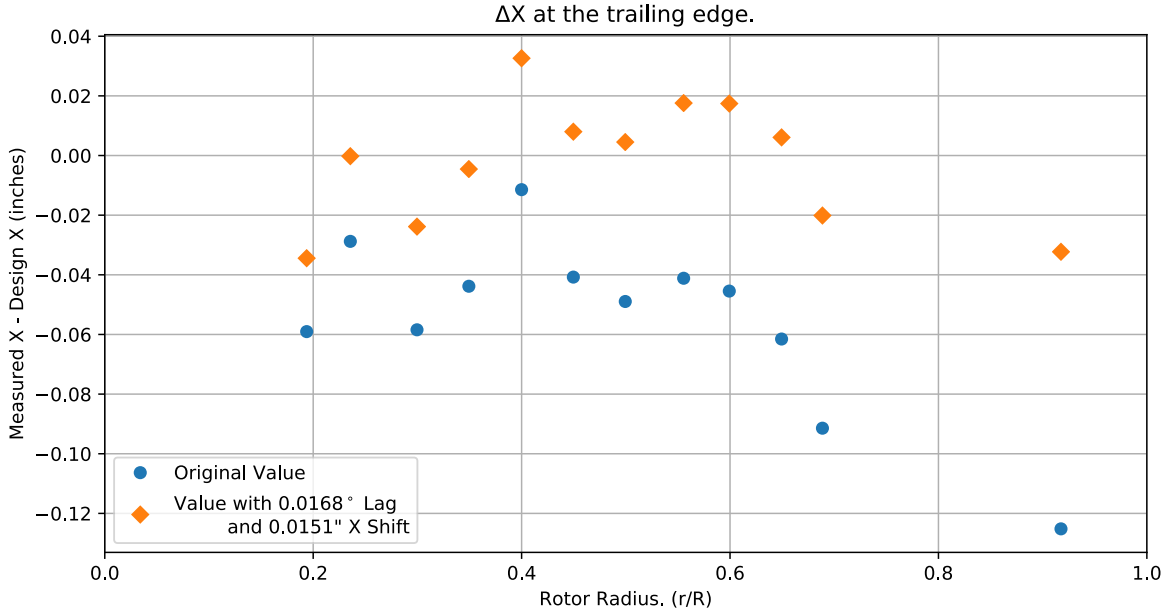

Figure 3-2. Trailing-edge ΔX error vs rotor radius.

Chapter 4: Flap Only Registration (6 rows)

The targets at the 6 spanwise stations nearest the root are used to determing the flap offset.

The estimated flap error is -0.28085°.

4.1: Target Location Errors After Flap Target Registration

Table 4-1. Measured(1) with flap registration vs "as designed"(2) in inches.

Name	X1	Y1	Z1	X2	Y2	Z2	dX	dY	dZ	dR
B3_R20_C05	0.9915	62.363	-0.14733	0.9915	62.363	0.09549	0	0	-0.24282	0.24282
B3_R20_C36	7.0547	62.382	-1.3116	7.0547	62.382	-1.1202	0	0	-0.19148	0.19148
B3_R20_C61	11.157	62.373	-1.7769	11.157	62.373	-1.6667	0	0	-0.11016	0.11016
B3_R20_C86	17.495	62.426	-2.3772	17.495	62.426	-2.2881	0	0	-0.08916	0.08916
B3_R20_C99	20.466	62.381	-2.911	20.501	62.381	-2.8477	-0.034427	0	-0.063232	0.071996
B3_R25_C05	1.0268	75.941	-0.17687	1.0268	75.941	0.031842	0	0	-0.20871	0.20871
B3_R25_C36	7.1498	75.905	-1.2775	7.1498	75.905	-1.109	0	0	-0.16844	0.16844
B3_R25_C61	12.453	75.848	-1.709	12.453	75.848	-1.7265	0	0	0.017411	0.017411
B3_R25_C86	17.619	75.912	-2.2665	17.619	75.912	-2.1493	0	0	-0.11724	0.11724
B3_R25_C99	20.533	75.868	-2.759	20.533	75.868	-2.6663	-0.00021582	0	-0.092686	0.092686
B3_R30_C05	1.0076	96.422	-0.20828	1.0076	96.422	-0.035939	0	0	-0.17234	0.17234
B3_R30_C36	7.1241	96.441	-1.1782	7.1241	96.441	-1.0683	0	0	-0.10985	0.10985
B3_R30_C61	12.33	96.466	-1.6523	12.33	96.466	-1.5829	0	0	-0.069358	0.069358
B3_R30_C86	17.576	96.438	-1.9899	17.576	96.438	-1.9216	0	0	-0.068367	0.068367
B3_R30_C99	20.555	96.47	-2.4652	20.579	96.47	-2.3894	-0.023829	0	-0.075794	0.079452
B3_R35_C05	1.039	112.46	-0.20415	1.039	112.46	-0.10475	0	0	-0.099398	0.099398
B3_R35_C36	7.1428	112.47	-1.0986	7.1428	112.47	-1.0416	0	0	-0.057033	0.057033
B3_R35_C61	12.388	112.44	-1.5041	12.388	112.44	-1.4857	0	0	-0.018376	0.018376
B3_R35_C86	17.608	112.46	-1.7519	17.608	112.46	-1.7484	0	0	-0.0034824	0.0034824
B3_R35_C99	20.606	112.49	-2.1709	20.611	112.49	-2.174	-0.0045316	0	0.0031667	0.0055284
B3_R40_C05	1.077	128.83	-0.25571	1.077	128.83	-0.17516	0	0	-0.080551	0.080551
B3_R40_C36	7.2083	128.81	-1.0256	7.2083	128.81	-1.0182	0	0	-0.0074686	0.0074686
B3_R40_C61	12.422	128.81	-1.3435	12.422	128.81	-1.3837	0	0	0.0402	0.0402
B3_R40_C86	17.65	128.79	-1.4956	17.65	128.79	-1.572	0	0	0.076455	0.076455
B3_R40_C99	20.673	128.78	-1.8907	20.64	128.78	-1.9549	0.032632	0	0.064168	0.071989
B3_R45_C05	1.1115	144.73	-0.28668	1.1115	144.73	-0.24111	0	0	-0.045573	0.045573
B3_R45_C36	7.1639	144.77	-0.9577	7.1639	144.77	-0.9857	0	0	0.028008	0.028008
B3_R45_C61	12.396	144.76	-1.2066	12.396	144.76	-1.2813	0	0	0.074667	0.074667
B3_R45_C86	17.683	144.8	-1.2993	17.683	144.8	-1.3983	0	0	0.098966	0.098966
B3_R45_C99	20.674	144.77	-1.6263	20.666	144.77	-1.7396	0.0080018	0	0.11329	0.11357
B3_R50_C05	1.0661	160.99	-0.45877	1.0661	160.99	-0.49129	0	0	0.032514	0.032514
B3_R50_C36	7.2183	160.98	-0.88265	7.2183	160.98	-0.96401	0	0	0.081365	0.081365
B3_R50_C61	12.461	160.88	-1.0643	12.461	160.88	-1.1805	0	0	0.11617	0.11617
B3_R50_C86	17.727	160.87	-1.0804	17.727	160.87	-1.2179	0	0	0.13754	0.13754
B3_R50_C99	20.7	160.82	-1.3719	20.695	160.82	-1.5155	0.0045254	0	0.14354	0.14361
B3_R55_C05	1.1146	178.94	-0.47463	1.1146	178.94	-0.56582	0	0	0.091193	0.091193
B3_R55_C36	7.2105	178.92	-0.78173	7.2105	178.92	-0.92808	0	0	0.14635	0.14635
B3_R55_C61	12.459	178.9	-0.8676	12.459	178.9	-1.055	0	0	0.18742	0.18742
B3_R55_C86	17.74	178.88	-0.78661	17.74	178.88	-1.0022	0	0	0.21555	0.21555
B3_R55_C99	20.736	178.85	-1.036	20.719	178.85	-1.2481	0.017599	0	0.21205	0.21278
B3_R60_C05	1.071	193.1	-0.46199	1.071	193.1	-0.61648	0	0	0.15449	0.15449
B3_R60_C36	7.2879	193.09	-0.70466	7.2879	193.09	-0.90256	0	0	0.1979	0.1979

Name	X1	Y1	Z1	X2	Y2	Z2	dX	dY	dZ	dR
B3_R60_C61	12.485	193.04	-0.70169	12.485	193.04	-0.95666	0	0	0.25497	0.25497
B3_R60_C86	17.71	193	-0.5563	17.71	193	-0.83428	0	0	0.27797	0.27797
B3_R60_C99	20.752	192.95	-0.75481	20.734	192.95	-1.0388	0.017432	0	0.28402	0.28455
B3_R65_C05	1.0704	209.25	-0.44735	1.0704	209.25	-0.67918	0	0	0.23182	0.23182
B3_R65_C36	7.2504	209.23	-0.59862	7.2504	209.23	-0.86939	0	0	0.27077	0.27077
B3_R65_C61	12.476	209.22	-0.54958	12.476	209.22	-0.84437	0	0	0.2948	0.2948
B3_R65_C86	17.722	209.2	-0.30095	17.722	209.2	-0.64033	0	0	0.33938	0.33938
B3_R65_C99	20.755	209.11	-0.45941	20.748	209.11	-0.79885	0.006088	0	0.33944	0.33949
B3_R70_C05	1.0625	221.85	-0.46397	1.0625	221.85	-0.72775	0	0	0.26378	0.26378
B3_R70_C36	7.2991	221.85	-0.53365	7.2991	221.85	-0.84457	0	0	0.31092	0.31092
B3_R70_C61	12.501	221.84	-0.41752	12.501	221.84	-0.75594	0	0	0.33842	0.33842
B3_R70_C86	17.746	221.86	-0.086906	17.746	221.86	-0.48778	0	0	0.40088	0.40088
B3_R70_C99	20.737	221.74	-0.23261	20.757	221.74	-0.61119	-0.020112	0	0.37857	0.37911
B3_R75_C05	1.1066	241.34	-0.48325	1.1066	241.34	-0.79946	0	0	0.31621	0.31621
B3_R75_C36	7.257	241.34	-0.42581	7.257	241.34	-0.80925	0	0	0.38344	0.38344
B3_R75_C61	12.512	241.34	-0.19455	12.512	241.34	-0.63089	0	0	0.43634	0.43634
B3_R75_C86	17.739	241.32	0.1939	17.739	241.32	-0.27445	0	0	0.46835	0.46835
B3_R80_C05	1.174	257.57	-0.47206	1.174	257.57	-0.84737	0	0	0.37531	0.37531
B3_R80_C36	7.3634	257.54	-0.35044	7.3634	257.54	-0.78327	0	0	0.43284	0.43284
B3_R80_C61	12.568	257.51	-0.058659	12.568	257.51	-0.54501	0	0	0.48635	0.48635
B3_R80_C86	17.793	257.5	0.37767	17.793	257.5	-0.12817	0	0	0.50583	0.50583
B3_R86_C05	1.1359	276.26	-0.24684	1.1359	276.26	-0.69049	0	0	0.44364	0.44364
B3_R86_C36	7.3608	276.22	-0.27858	7.3608	276.22	-0.75543	0	0	0.47685	0.47685
B3_R86_C61	12.552	276.16	0.079265	12.552	276.16	-0.46464	0	0	0.54391	0.54391
B3_R86_C86	17.776	276.09	0.57492	17.776	276.09	0.0057343	0	0	0.56918	0.56918
B3_R91_C05	1.2208	295.53	-0.28941	1.2208	295.53	-0.84544	0	0	0.55603	0.55603
B3_R91_C36	7.3414	295.5	-0.095361	7.3414	295.5	-0.679	0	0	0.58364	0.58364
B3_R91_C61	12.58	295.51	0.43098	12.58	295.51	-0.19342	0	0	0.6244	0.6244
B3_R91_C86	17.692	295.5	1.1384	17.692	295.5	0.45599	0	0	0.68238	0.68238
B3_R91_C99	20.721	295.44	1.314	20.753	295.44	0.56636	-0.0323	0	0.7476	0.7483
B3_R97_C05	6.1225	313.29	0.12094	6.1225	313.29	-0.67621	0	0	0.79716	0.79716
B3_R97_C36	12.307	313.28	0.4065	12.307	313.28	-0.45919	0	0	0.86569	0.86569
B3_R97_C61	17.553	313.26	0.8332	17.553	313.26	-0.023535	0	0	0.85673	0.85673
B3_R97_C86	22.771	313.24	1.4306	22.771	313.24	0.56788	0	0	0.86272	0.86272
B3_R97_C99	25.747	313.09	1.5255	25.882	313.09	0.65011	-0.1352	0	0.87539	0.88577
HUB_LE	2.2058	30.001	-3.5044	2.19	30	-3.5	0.015808	0.00089614	-0.0043957	0.016432
HUB_TE	8.2046	29.999	-3.4996	8.19	30	-3.5	0.014608	-0.00088544	0.00039566	0.01464
RMS Errors:							0.017343	0.00014174	0.35722	0.35765

4.2: Flap Registration Plots (6 rows)

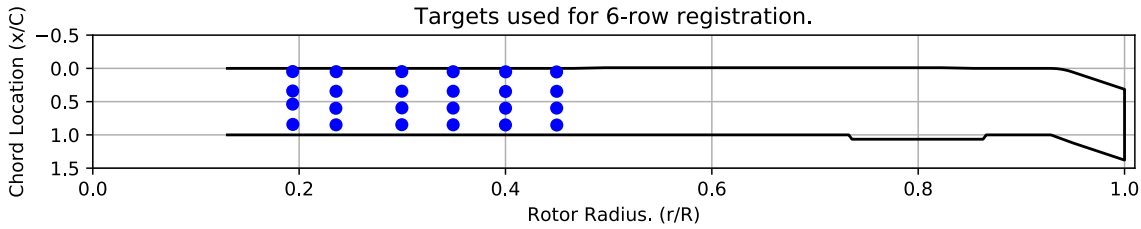

Figure 4-1. Targets used for 6 row root registration.

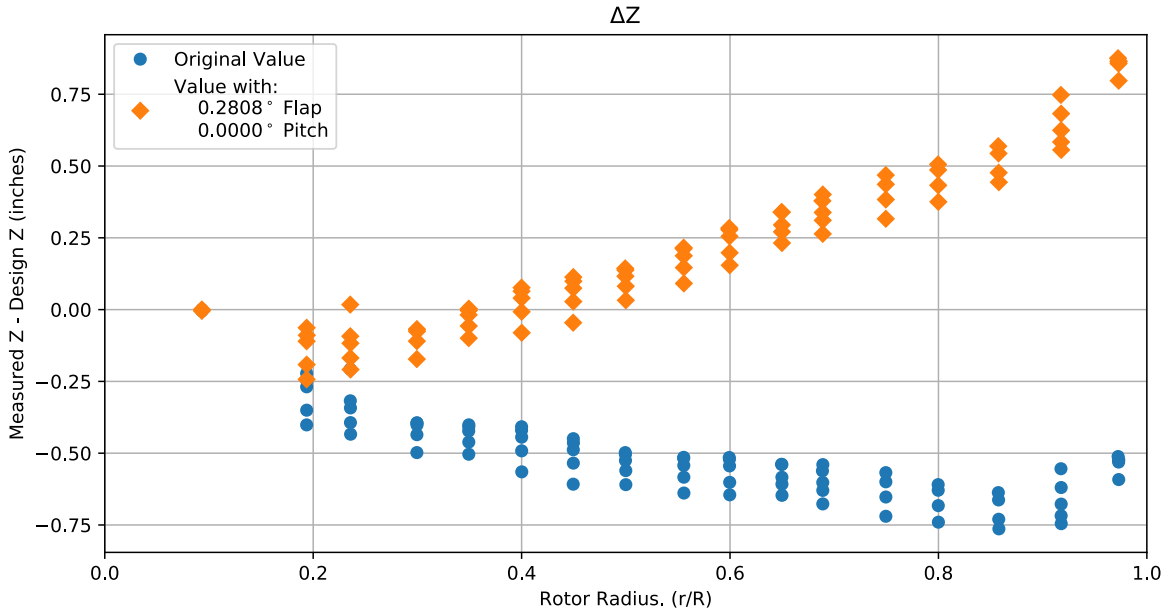

Figure 4-2. Flap target registration, ΔZ error vs rotor radius.

Note: the “as designed” geometry used for the swept tip may have some inaccuracies.

4.3: Estimated Bending and Twist at the Quarter Chord

The error bars shown represent the residual errors for fitting the measure target locations to the "as designed" geometry. These errors are generally much larger than those due to the VSTARS measurement errors. Therefore, the most likely source of these errors is the placement of the trailing-edge targets, differences between the "as designed" and "as built" geometries, and blade deformation during measurement. In the future, iterative adjustment of the "as designed" twist angle may be implemented to see if it reduces the fit error in delta twist. Note: The "as designed" geometry used for the swept tip may have some inaccuracies.

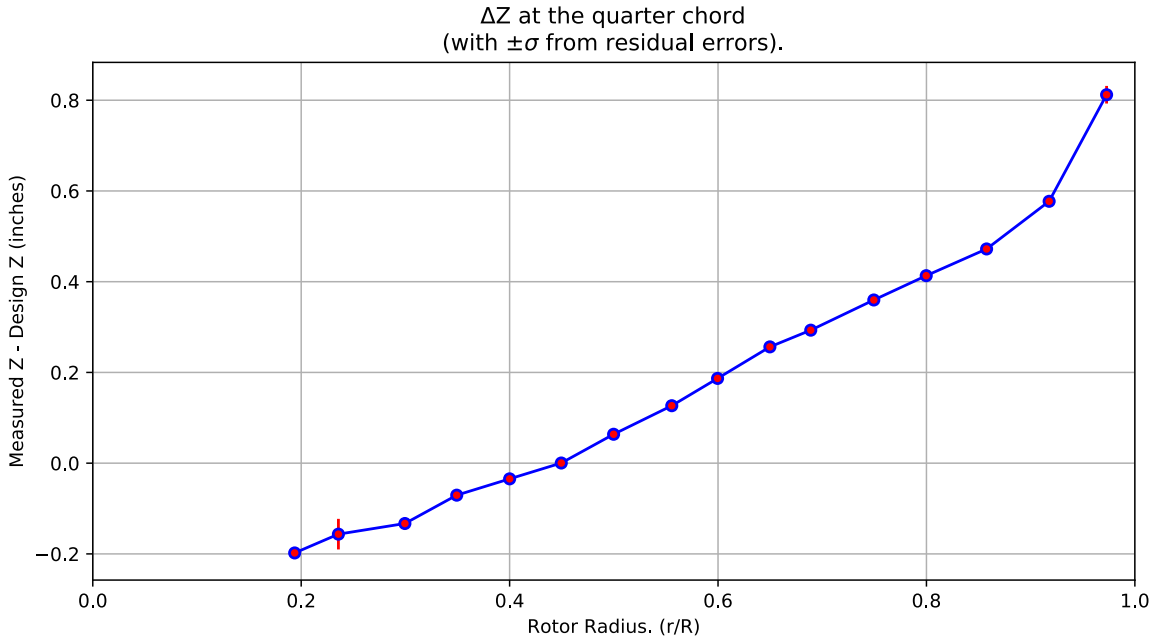

Figure 4-3. ΔZ error at the quarter chord vs rotor radius.

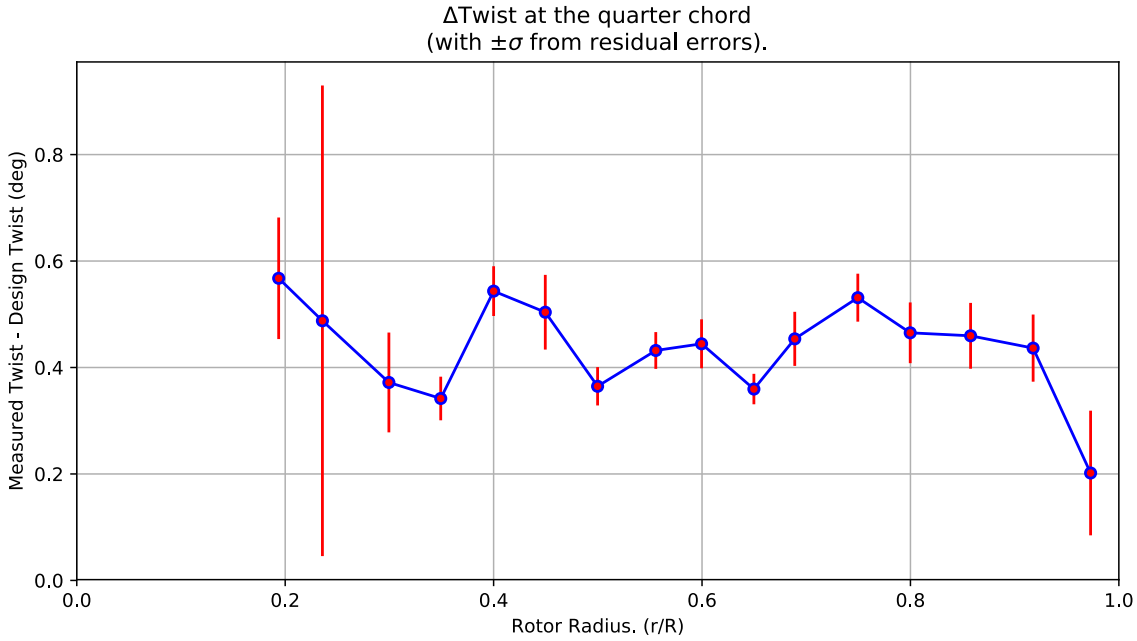

Figure 4-4. ΔTwist error at the quarter chord vs rotor radius.

Table 4-2. Quarter-chord bending and twist statistics.

r	r/R	dZ 1/4-chord	dT	sigma dZ meas	sigma dT meas	sigma dZ res	sigma dT res	n	t_conf
62.386	0.19375	-0.19788	0.56759	5.9982e-10	4.764e-09	0.0079414	0.11418	4	4.3027
75.902	0.23572	-0.15647	0.48776	6.1303e-10	4.6479e-09	0.033734	0.44206	4	4.3027
96.442	0.29951	-0.13302	0.37189	6.112e-10	4.6624e-09	0.0070689	0.093761	4	4.3027
112.46	0.34925	-0.070548	0.34178	6.1269e-10	4.6591e-09	0.0031141	0.040974	4	4.3027
128.81	0.40002	-0.034574	0.54349	6.1487e-10	4.6602e-09	0.0035897	0.046745	4	4.3027
144.77	0.44959	0.00033574	0.50385	6.1483e-10	4.6602e-09	0.0053875	0.070172	4	4.3027
160.93	0.49978	0.063709	0.36472	6.1513e-10	4.6359e-09	0.0027844	0.036025	4	4.3027
178.91	0.55561	0.12665	0.43198	6.1615e-10	4.6449e-09	0.0026772	0.034538	4	4.3027
193.06	0.59955	0.18682	0.44451	6.1648e-10	4.6443e-09	0.0035717	0.045999	4	4.3027
209.23	0.64977	0.25633	0.35951	6.1583e-10	4.6393e-09	0.0022173	0.028613	4	4.3027
221.85	0.68898	0.29315	0.45381	6.1659e-10	4.6327e-09	0.003957	0.050805	4	4.3027
241.34	0.74949	0.3597	0.53117	6.1708e-10	4.6417e-09	0.0035106	0.045058	4	4.3027
257.53	0.79978	0.41327	0.46516	6.208e-10	4.649e-09	0.0045151	0.057046	4	4.3027
276.18	0.85771	0.47217	0.45955	6.1971e-10	4.6444e-09	0.0048735	0.061825	4	4.3027
295.51	0.91773	0.57719	0.43642	6.2165e-10	4.6837e-09	0.0049749	0.063078	4	4.3027
313.27	0.97287	0.81212	0.20179	9.1724e-10	4.6385e-09	0.019413	0.1171	4	4.3027

4.4: Section Plots

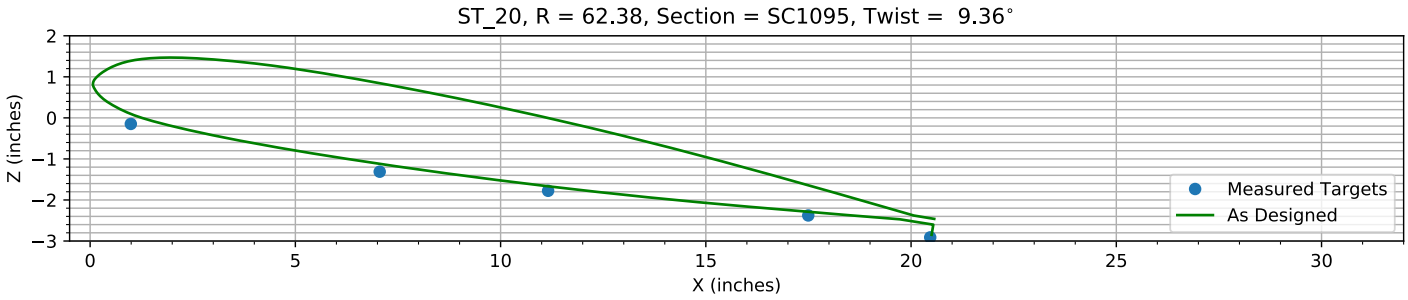

Figure 4-5. Target locations vs section profile at station 20.

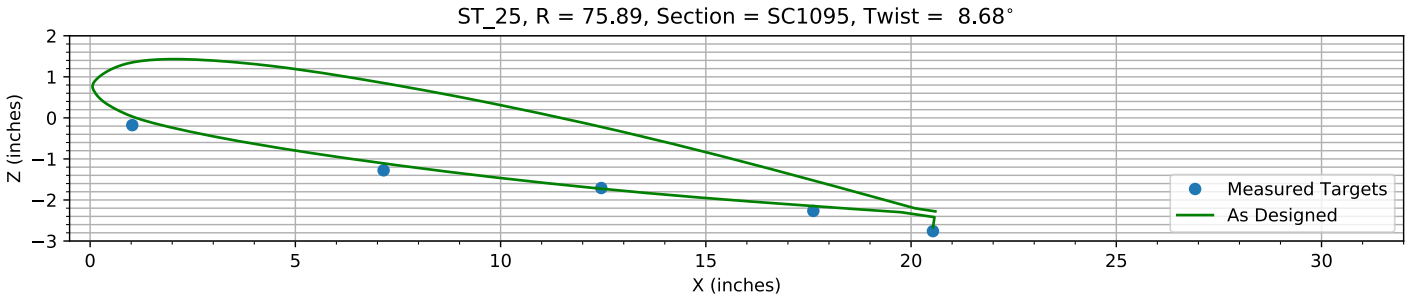

Figure 4-6. Target locations vs section profile at station 25.

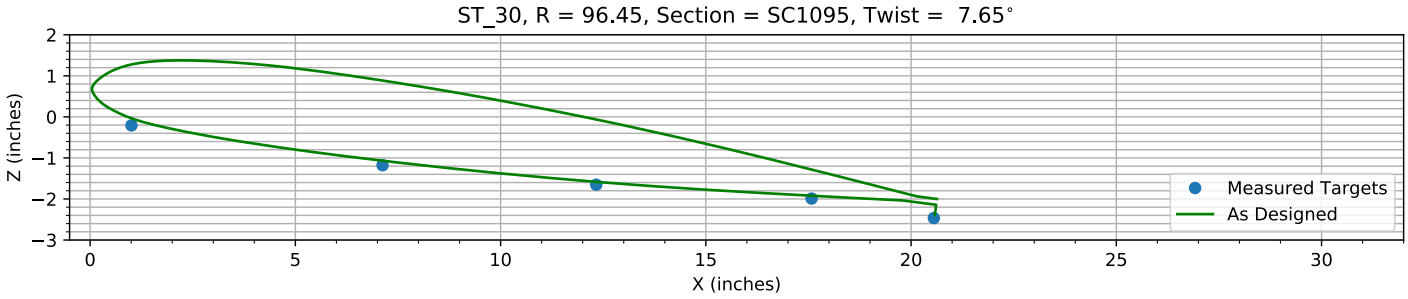

Figure 4-7. Target locations vs section profile at station 30.

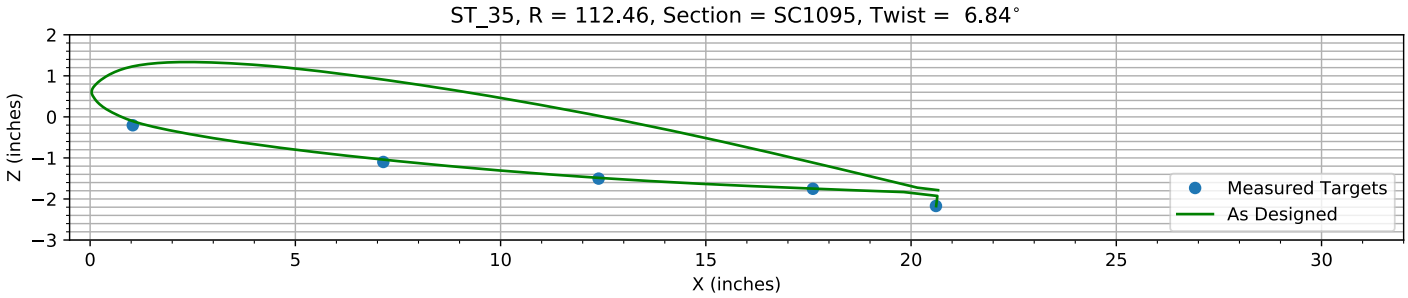

Figure 4-8. Target locations vs section profile at station 35.

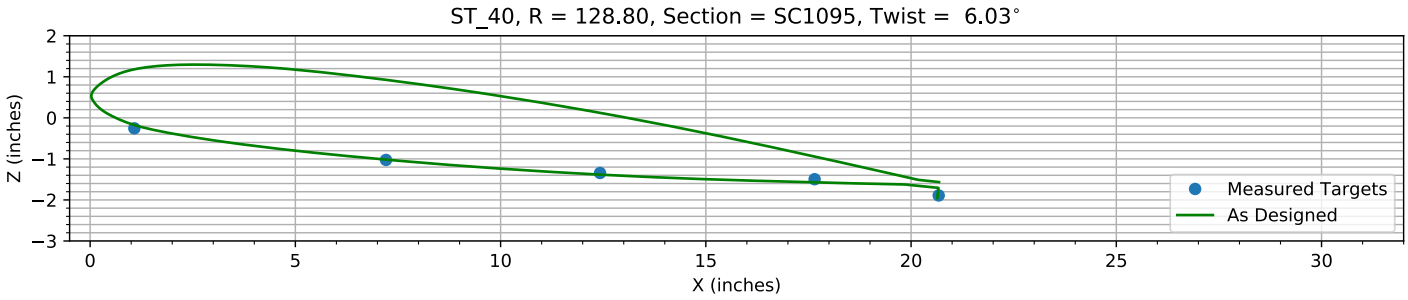

Figure 4-9. Target locations vs section profile at station 40.

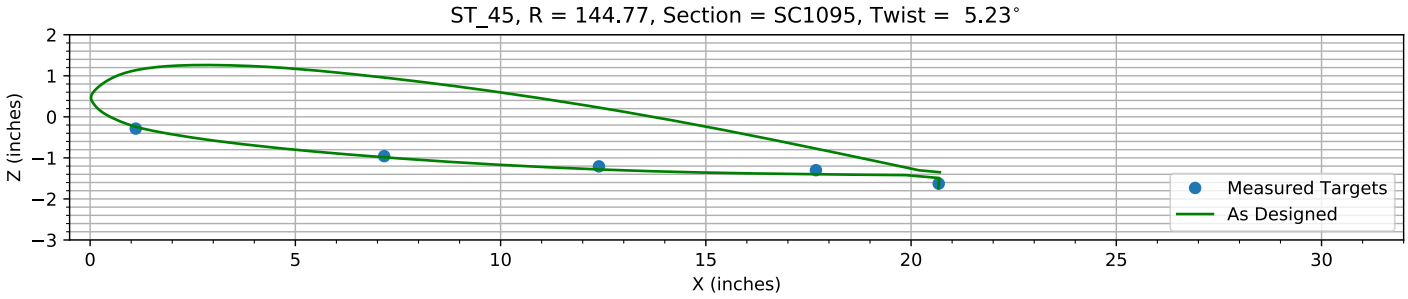

Figure 4-10. Target locations vs section profile at station 45.

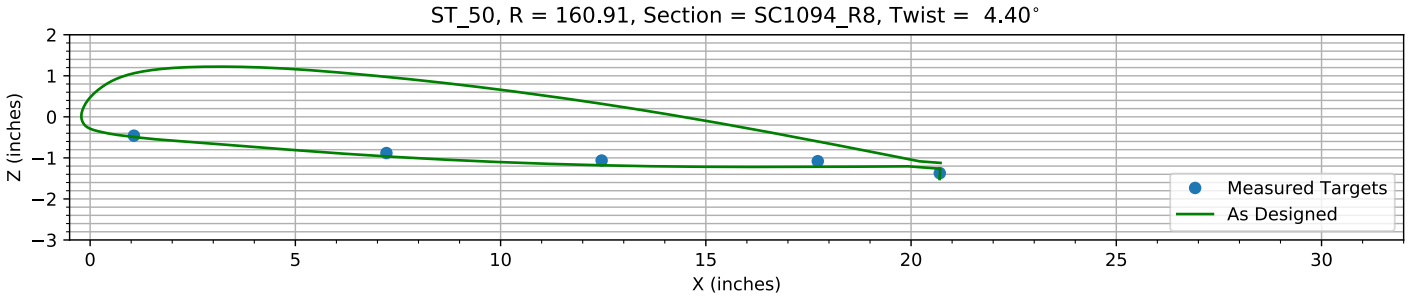

Figure 4-11. Target locations vs section profile at station 50.

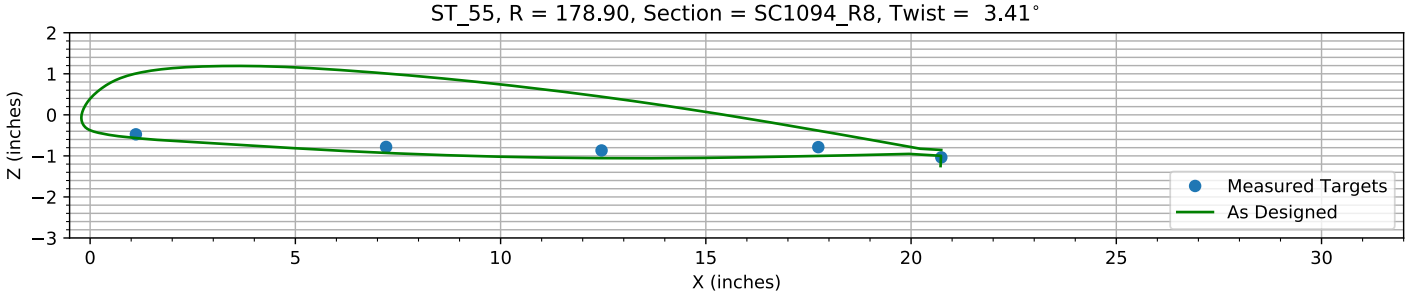

Figure 4-12. Target locations vs section profile at station 55.

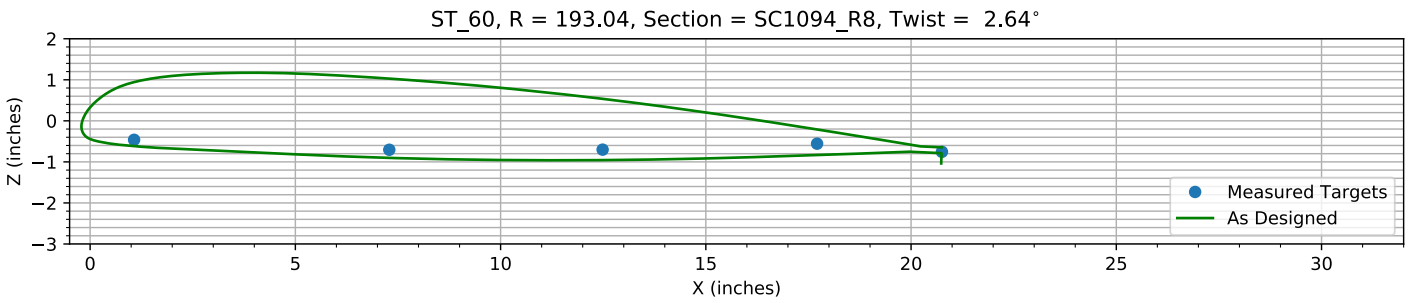

Figure 4-13. Target locations vs section profile at station 60.

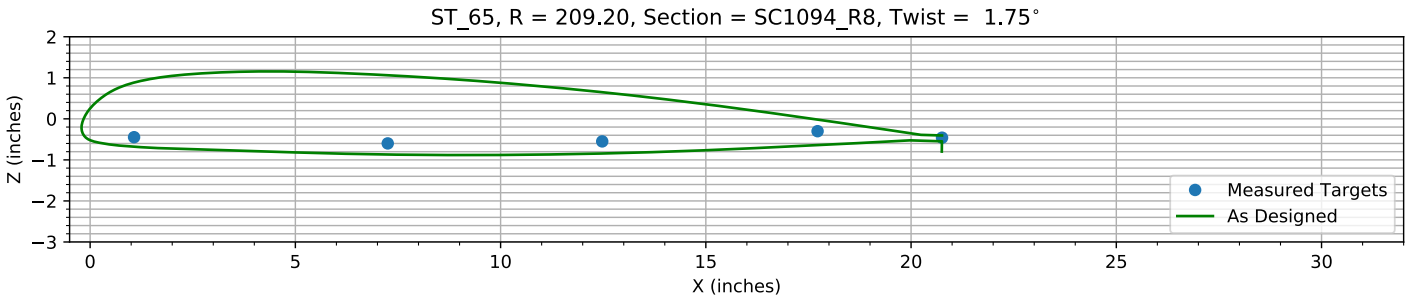

Figure 4-14. Target locations vs section profile at station 65.

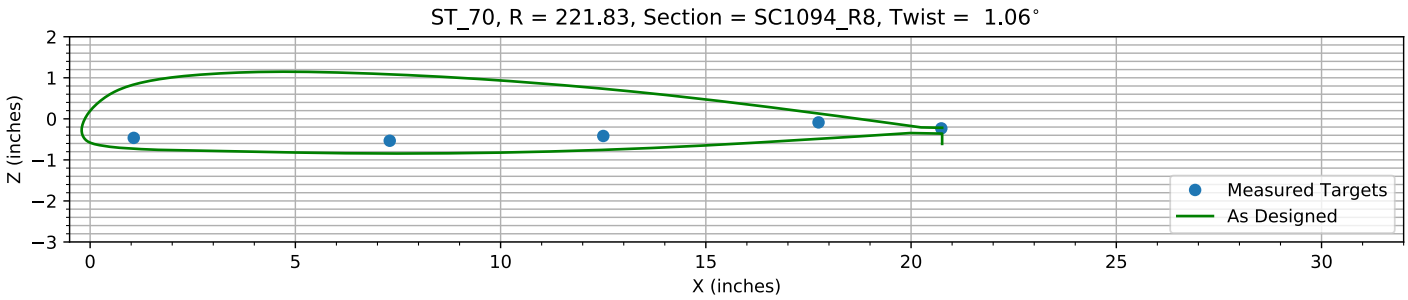

Figure 4-15. Target locations vs section profile at station 70.

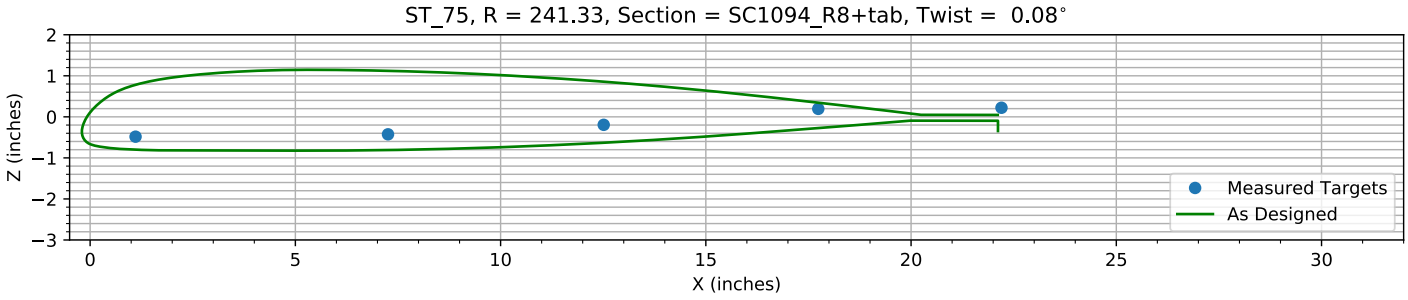

Figure 4-16. Target locations vs section profile at station 75.

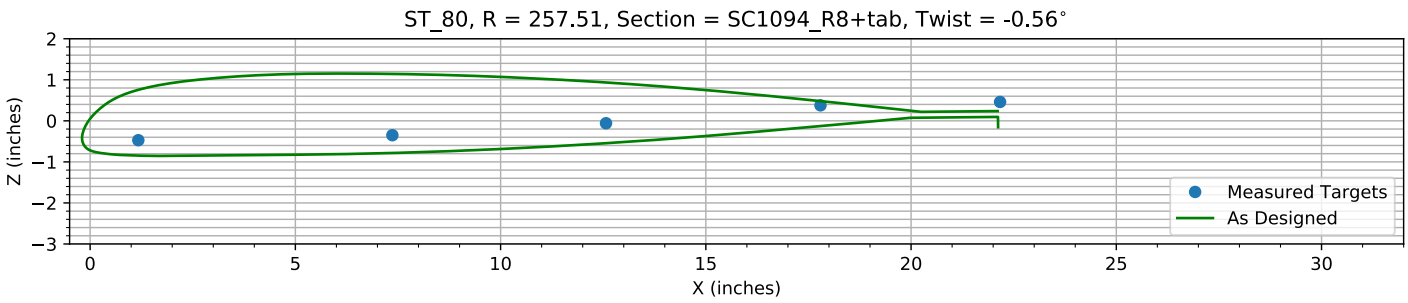

Figure 4-17. Target locations vs section profile at station 80.

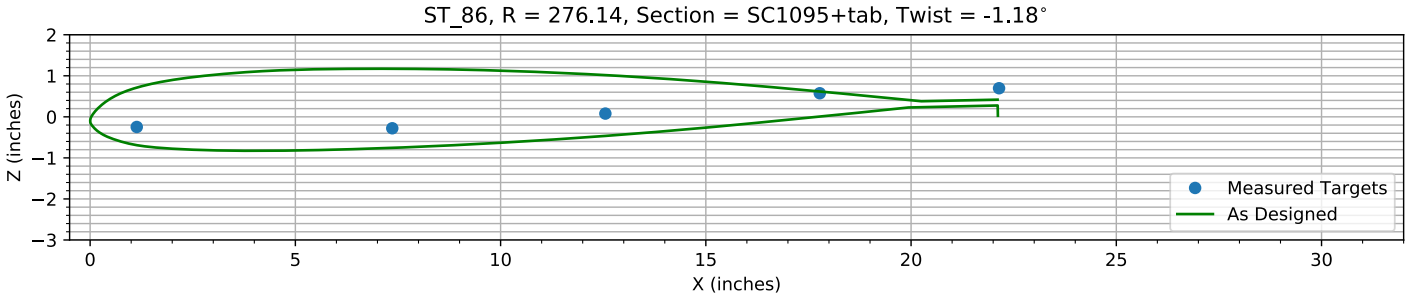

Figure 4-18. Target locations vs section profile at station 86.

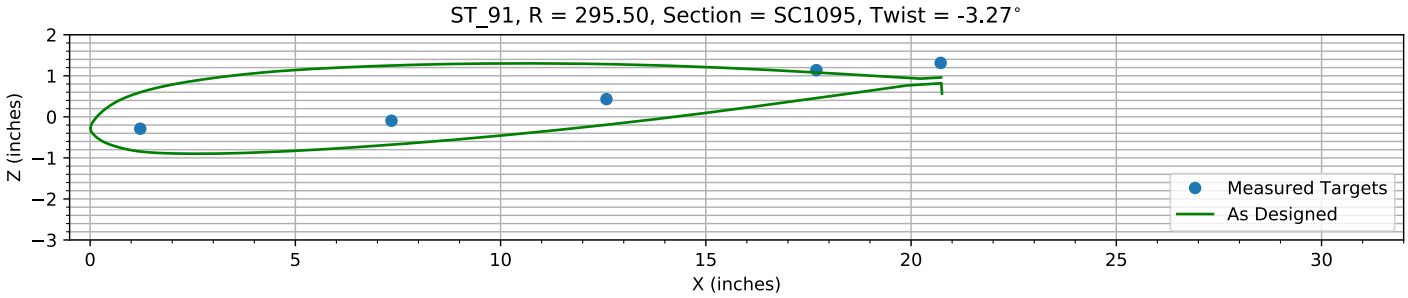

Figure 4-19. Target locations vs section profile at station 91.

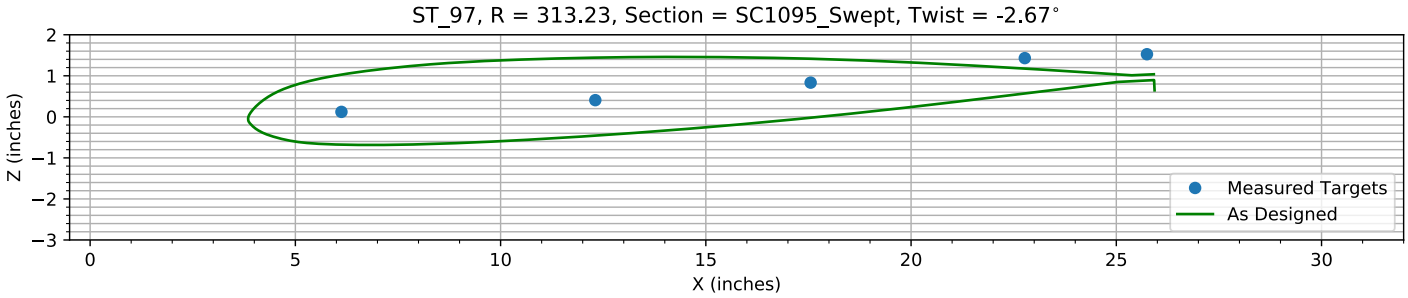

Figure 4-20. Target locations vs section profile at station 97.

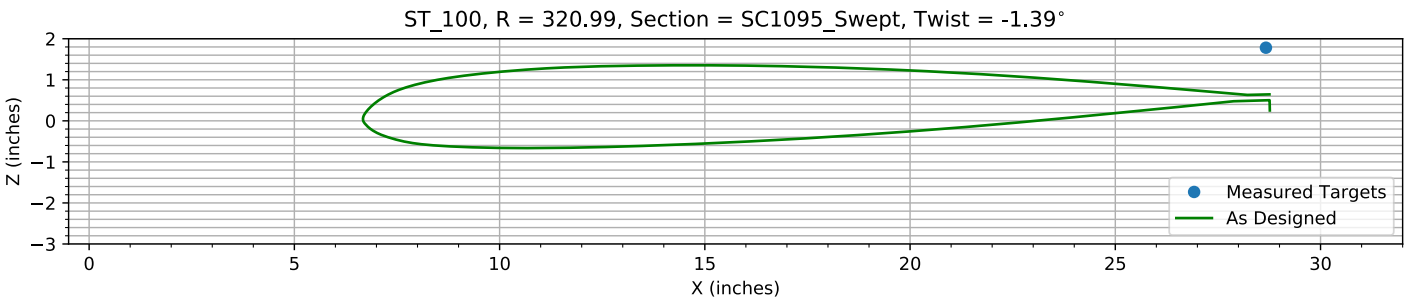

Figure 4-21. Target locations vs section profile at station 100.

Chapter 5: Flap Only Registration (15 rows)

The targets at the 15 spanwise stations nearest the root are used to determing the flap offset.

The estimated flap error is -0.19859°.

5.1: Target Location Errors After Flap Target Registration

Table 5-1. Measured(1) with flap registration vs "as designed"(2) in inches.

Name	X1	Y1	Z1	X2	Y2	Z2	dX	dY	dZ	dR
B3_R20_C05	0.9915	62.367	-0.1938	0.9915	62.367	0.095472	0	0	-0.28927	0.28927
B3_R20_C36	7.0547	62.385	-1.3581	7.0547	62.385	-1.1202	0	0	-0.23798	0.23798
B3_R20_C61	11.157	62.376	-1.8234	11.157	62.376	-1.6667	0	0	-0.15665	0.15665
B3_R20_C86	17.495	62.428	-2.4238	17.495	62.428	-2.2881	0	0	-0.13573	0.13573
B3_R20_C99	20.466	62.381	-2.9575	20.501	62.381	-2.8477	-0.034429	0	-0.10973	0.11501
B3_R25_C05	1.0268	75.946	-0.24283	1.0268	75.946	0.031824	0	0	-0.27466	0.27466
B3_R25_C36	7.1498	75.908	-1.3434	7.1498	75.908	-1.109	0	0	-0.23436	0.23436
B3_R25_C61	12.453	75.851	-1.7749	12.453	75.851	-1.7264	0	0	-0.048435	0.048435
B3_R25_C86	17.619	75.913	-2.3325	17.619	75.913	-2.1493	0	0	-0.18318	0.18318
B3_R25_C99	20.533	75.869	-2.8248	20.533	75.869	-2.6663	-0.0002182	0	-0.15856	0.15856
B3_R30_C05	1.0076	96.426	-0.30365	1.0076	96.426	-0.035956	0	0	-0.26769	0.26769
B3_R30_C36	7.1241	96.444	-1.2736	7.1241	96.444	-1.0683	0	0	-0.20525	0.20525
B3_R30_C61	12.33	96.469	-1.7477	12.33	96.469	-1.5829	0	0	-0.16481	0.16481
B3_R30_C86	17.576	96.44	-2.0853	17.576	96.44	-1.9215	0	0	-0.16378	0.16378
B3_R30_C99	20.555	96.471	-2.5606	20.579	96.471	-2.3894	-0.023832	0	-0.17125	0.1729
B3_R35_C05	1.039	112.47	-0.32255	1.039	112.47	-0.10477	0	0	-0.21778	0.21778
B3_R35_C36	7.1428	112.47	-1.217	7.1428	112.47	-1.0416	0	0	-0.17545	0.17545
B3_R35_C61	12.388	112.44	-1.6224	12.388	112.44	-1.4857	0	0	-0.13676	0.13676
B3_R35_C86	17.608	112.47	-1.8703	17.608	112.47	-1.7484	0	0	-0.12191	0.12191
B3_R35_C99	20.606	112.49	-2.2893	20.611	112.49	-2.174	-0.0045351	0	-0.11529	0.11538
B3_R40_C05	1.077	128.84	-0.39762	1.077	128.84	-0.17518	0	0	-0.22244	0.22244
B3_R40_C36	7.2083	128.81	-1.1675	7.2083	128.81	-1.0182	0	0	-0.14934	0.14934
B3_R40_C61	12.422	128.81	-1.4853	12.422	128.81	-1.3836	0	0	-0.10168	0.10168
B3_R40_C86	17.65	128.79	-1.6374	17.65	128.79	-1.572	0	0	-0.065412	0.065412
B3_R40_C99	20.673	128.78	-2.0325	20.64	128.78	-1.9548	0.032628	0	-0.077683	0.084257
B3_R45_C05	1.1115	144.74	-0.45141	1.1115	144.74	-0.24112	0	0	-0.21029	0.21029
B3_R45_C36	7.1639	144.77	-1.1225	7.1639	144.77	-0.9857	0	0	-0.13678	0.13678
B3_R45_C61	12.396	144.77	-1.3714	12.396	144.77	-1.2813	0	0	-0.090128	0.090128
B3_R45_C86	17.683	144.81	-1.4642	17.683	144.81	-1.3983	0	0	-0.065897	0.065897
B3_R45_C99	20.674	144.78	-1.7911	20.666	144.78	-1.7395	0.0079979	0	-0.051532	0.052149
B3_R50_C05	1.0661	161	-0.64685	1.0661	161	-0.4913	0	0	-0.15555	0.15555
B3_R50_C36	7.2183	160.98	-1.0707	7.2183	160.98	-0.964	0	0	-0.1067	0.1067
B3_R50_C61	12.461	160.88	-1.2522	12.461	160.88	-1.1805	0	0	-0.071767	0.071767
B3_R50_C86	17.727	160.87	-1.2683	17.727	160.87	-1.2179	0	0	-0.050397	0.050397
B3_R50_C99	20.7	160.82	-1.5598	20.695	160.82	-1.5154	0.0045211	0	-0.044326	0.044556
B3_R55_C05	1.1146	178.94	-0.68846	1.1146	178.94	-0.56584	0	0	-0.12263	0.12263
B3_R55_C36	7.2105	178.92	-0.99554	7.2105	178.92	-0.92807	0	0	-0.067468	0.067468
B3_R55_C61	12.459	178.9	-1.0814	12.459	178.9	-1.055	0	0	-0.026388	0.026388
B3_R55_C86	17.74	178.88	-1.0004	17.74	178.88	-1.0021	0	0	0.0017545	0.0017545
B3_R55_C99	20.736	178.86	-1.2498	20.719	178.86	-1.248	0.017595	0	-0.0017232	0.017679
B3_R60_C05	1.071	193.1	-0.69617	1.071	193.1	-0.6165	0	0	-0.079668	0.079668
B3_R60_C36	7.2879	193.09	-0.93882	7.2879	193.09	-0.90256	0	0	-0.036263	0.036263

Name	X1	Y1	Z1	X2	Y2	Z2	dX	dY	dZ	dR
B3_R60_C61	12.485	193.04	-0.93578	12.485	193.04	-0.95663	0	0	0.020851	0.020851
B3_R60_C86	17.71	193	-0.79033	17.71	193	-0.83423	0	0	0.043899	0.043899
B3_R60_C99	20.752	192.96	-0.98878	20.734	192.96	-1.0388	0.017428	0	0.049996	0.052947
B3_R65_C05	1.0704	209.25	-0.70471	1.0704	209.25	-0.67919	0	0	-0.025518	0.025518
B3_R65_C36	7.2504	209.24	-0.85596	7.2504	209.24	-0.86938	0	0	0.013423	0.013423
B3_R65_C61	12.476	209.22	-0.8069	12.476	209.22	-0.84435	0	0	0.037448	0.037448
B3_R65_C86	17.722	209.21	-0.55825	17.722	209.21	-0.64028	0	0	0.082028	0.082028
B3_R65_C99	20.755	209.12	-0.71657	20.748	209.12	-0.79879	0.0060848	0	0.082212	0.082437
B3_R70_C05	1.0625	221.85	-0.73942	1.0625	221.85	-0.72776	0	0	-0.011661	0.011661
B3_R70_C36	7.2991	221.86	-0.80911	7.2991	221.86	-0.84456	0	0	0.035451	0.035451
B3_R70_C61	12.501	221.84	-0.69296	12.501	221.84	-0.75591	0	0	0.06295	0.06295
B3_R70_C86	17.746	221.87	-0.36238	17.746	221.87	-0.48773	0	0	0.12535	0.12535
B3_R70_C99	20.737	221.74	-0.50791	20.757	221.74	-0.61112	-0.020115	0	0.10321	0.10516
B3_R75_C05	1.1066	241.34	-0.78668	1.1066	241.34	-0.79947	0	0	0.012792	0.012792
B3_R75_C36	7.257	241.35	-0.72926	7.257	241.35	-0.80924	0	0	0.079987	0.079987
B3_R75_C61	12.512	241.34	-0.49798	12.512	241.34	-0.63086	0	0	0.13288	0.13288
B3_R75_C86	17.739	241.33	-0.10952	17.739	241.33	-0.2744	0	0	0.16489	0.16489
B3_R80_C05	1.174	257.58	-0.7988	1.174	257.58	-0.84738	0	0	0.048576	0.048576
B3_R80_C36	7.3634	257.54	-0.67713	7.3634	257.54	-0.78327	0	0	0.10614	0.10614
B3_R80_C61	12.568	257.52	-0.38531	12.568	257.52	-0.54498	0	0	0.15967	0.15967
B3_R80_C86	17.793	257.5	0.051034	17.793	257.5	-0.12813	0	0	0.17916	0.17916
B3_R86_C05	1.1359	276.27	-0.60042	1.1359	276.27	-0.6905	0	0	0.090073	0.090073
B3_R86_C36	7.3608	276.22	-0.63209	7.3608	276.22	-0.75542	0	0	0.12334	0.12334
B3_R86_C61	12.552	276.17	-0.27417	12.552	276.17	-0.46463	0	0	0.19046	0.19046
B3_R86_C86	17.776	276.1	0.22159	17.776	276.1	0.0057611	0	0	0.21583	0.21583
B3_R91_C05	1.2208	295.53	-0.67065	1.2208	295.53	-0.84547	0	0	0.17482	0.17482
B3_R91_C36	7.3414	295.5	-0.47656	7.3414	295.5	-0.67898	0	0	0.20242	0.20242
B3_R91_C61	12.58	295.51	0.049776	12.58	295.51	-0.19335	0	0	0.24312	0.24312
B3_R91_C86	17.692	295.51	0.75717	17.692	295.51	0.45614	0	0	0.30104	0.30104
B3_R91_C99	20.721	295.45	0.93286	20.753	295.45	0.56655	-0.032293	0	0.3663	0.36773
B3_R97_C05	6.1225	313.29	-0.28579	6.1225	313.29	-0.6761	0	0	0.39031	0.39031
B3_R97_C36	12.307	313.28	-0.00022153	12.307	313.28	-0.45932	0	0	0.4591	0.4591
B3_R97_C61	17.553	313.26	0.4265	17.553	313.26	-0.023821	0	0	0.45033	0.45033
B3_R97_C86	22.771	313.24	1.0239	22.771	313.24	0.56741	0	0	0.45653	0.45653
B3_R97_C99	25.747	313.1	1.119	25.884	313.1	0.64989	-0.13772	0	0.46916	0.48895
HUB_LE	2.2058	30.001	-3.5044	2.19	30	-3.5	0.015808	0.00088982	-0.0043969	0.016432
HUB_TE	8.2046	29.999	-3.4996	8.19	30	-3.5	0.014608	-0.00088487	0.00039694	0.01464
RMS Errors:							0.017593	0.00014119	0.18084	0.18169

5.2: Flap Registration Plots (15 rows)

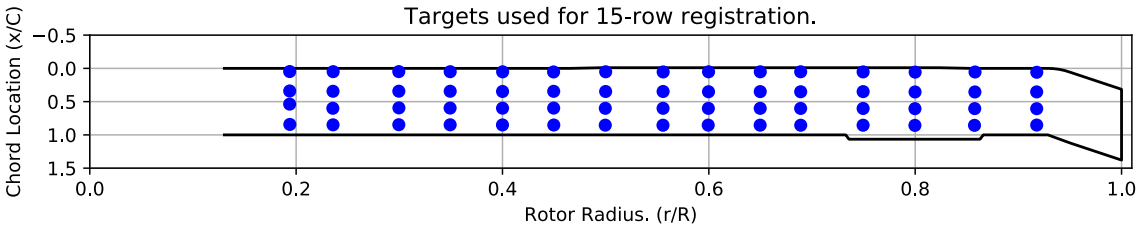

Figure 5-1. Targets used for 15 row root registration.

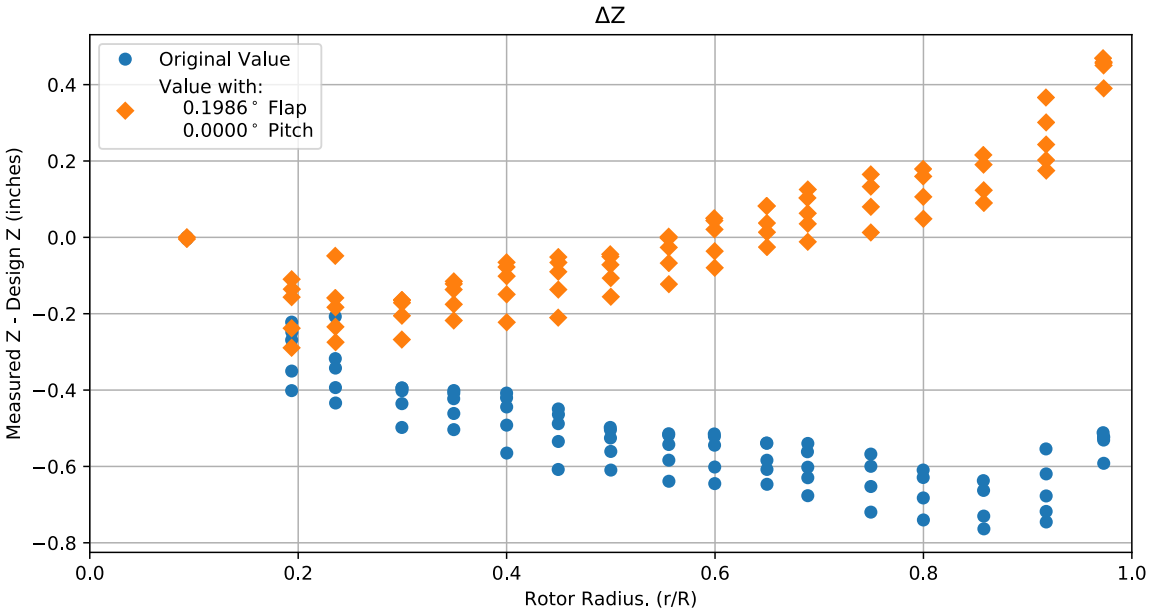

Figure 5-2. Flap target registration, ΔZ error vs rotor radius.

Note: the “as designed” geometry used for the swept tip may have some inaccuracies.

5.3: Estimated Bending and Twist at the Quarter Chord

The error bars shown represent the residual errors for fitting the measure target locations to the "as designed" geometry. These errors are generally much larger than those due to the VSTARS measurement errors. Therefore, the most likely source of these errors is the placement of the trailing-edge targets, differences between the "as designed" and "as built" geometries, and blade deformation during measurement. In the future, iterative adjustment of the "as designed" twist angle may be implemented to see if it reduces the fit error in delta twist. Note: The "as designed" geometry used for the swept tip may have some inaccuracies.

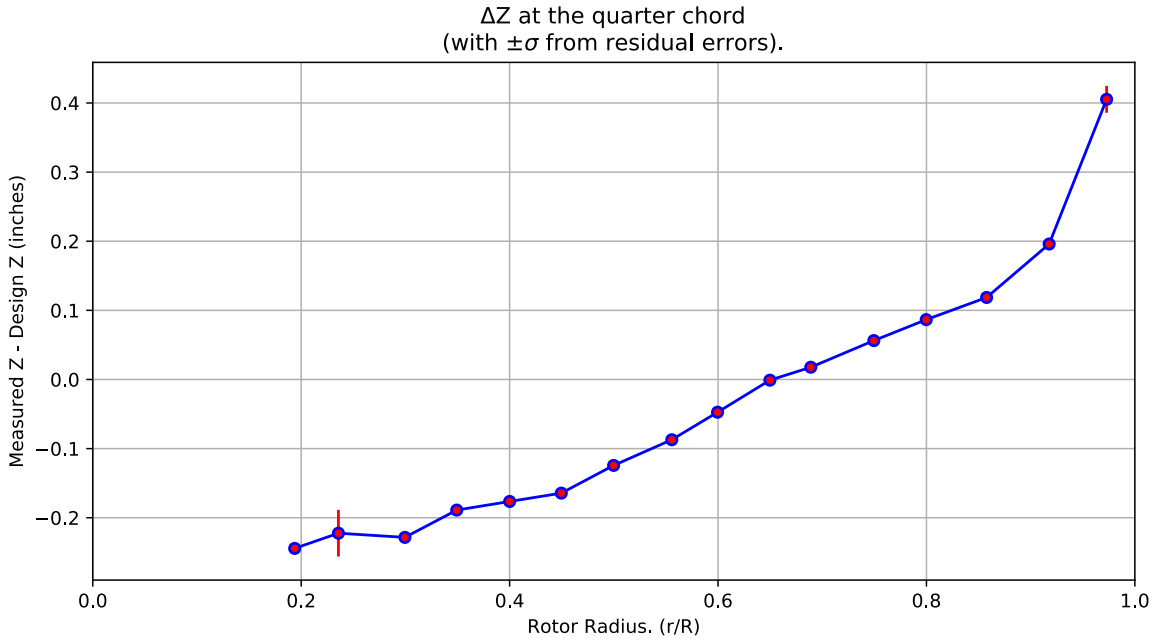

Figure 5-3. ΔZ error at the quarter chord vs rotor radius.

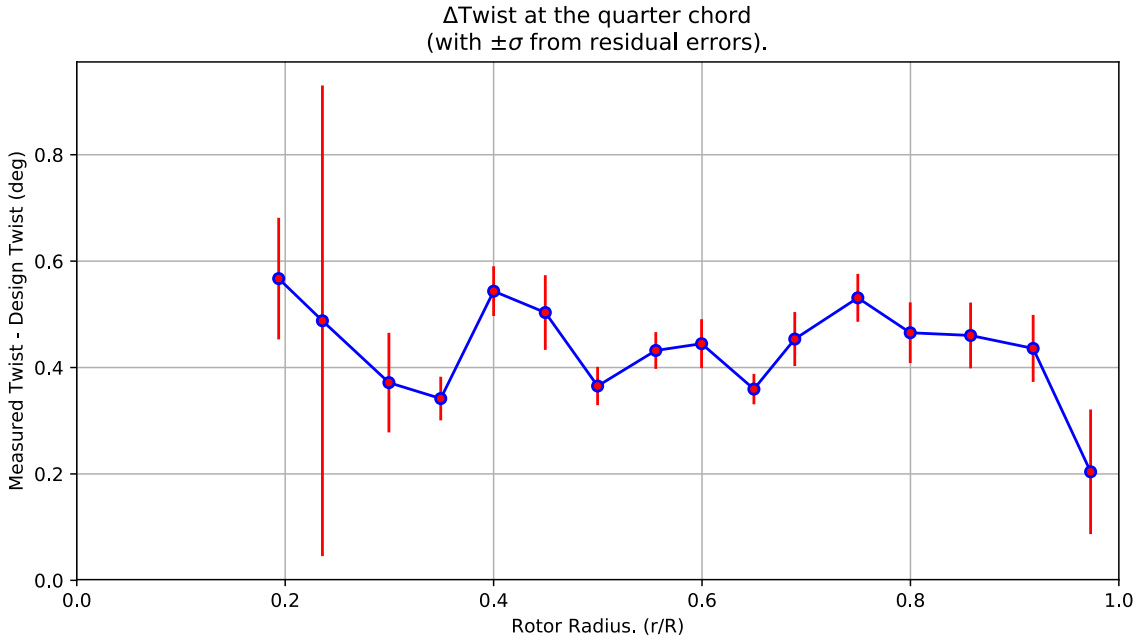

Figure 5-4. ΔTwist error at the quarter chord vs rotor radius.

Table 5-2. Quarter-chord bending and twist statistics.

r	r/R	dZ 1/4-chord	dT	sigma dZ meas	sigma dT meas	sigma dZ res	sigma dT res	n	t_conf
62.389	0.19375	-0.24436	0.56719	5.9982e-10	4.764e-09	0.0079481	0.11428	4	4.3027
75.905	0.23573	-0.22239	0.48787	6.1303e-10	4.6479e-09	0.033753	0.4423	4	4.3027
96.445	0.29952	-0.2284	0.37164	6.112e-10	4.6624e-09	0.0070583	0.09362	4	4.3027
112.46	0.34926	-0.18894	0.34168	6.1269e-10	4.6591e-09	0.0031186	0.041033	4	4.3027
128.81	0.40004	-0.17645	0.54354	6.1487e-10	4.6602e-09	0.0035896	0.046744	4	4.3027
144.77	0.4496	-0.16442	0.50338	6.1483e-10	4.6602e-09	0.0053871	0.070168	4	4.3027
160.93	0.49979	-0.12433	0.36523	6.1513e-10	4.6359e-09	0.0027847	0.03603	4	4.3027
178.91	0.55562	-0.087171	0.43205	6.1615e-10	4.6449e-09	0.002676	0.034522	4	4.3027
193.06	0.59956	-0.047333	0.44482	6.1648e-10	4.6443e-09	0.0035721	0.046004	4	4.3027
209.23	0.64978	-0.0010101	0.35948	6.1583e-10	4.6393e-09	0.0022175	0.028616	4	4.3027
221.86	0.68899	0.017701	0.45352	6.1659e-10	4.6327e-09	0.0039507	0.050724	4	4.3027
241.34	0.7495	0.056265	0.53102	6.1708e-10	4.6417e-09	0.0035084	0.045029	4	4.3027
257.54	0.7998	0.086554	0.46538	6.208e-10	4.649e-09	0.0045187	0.057091	4	4.3027
276.19	0.85773	0.11864	0.46028	6.1971e-10	4.6444e-09	0.0048734	0.061824	4	4.3027
295.51	0.91775	0.19597	0.43592	6.2165e-10	4.6837e-09	0.0049649	0.062951	4	4.3027
313.27	0.97289	0.40524	0.20404	9.1724e-10	4.6385e-09	0.019421	0.11715	4	4.3027

5.4: Section Plots

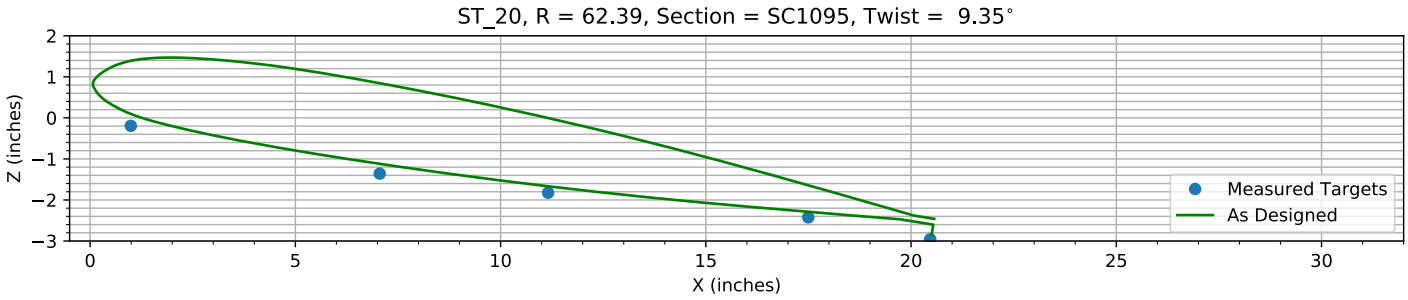

Figure 5-5. Target locations vs section profile at station 20.

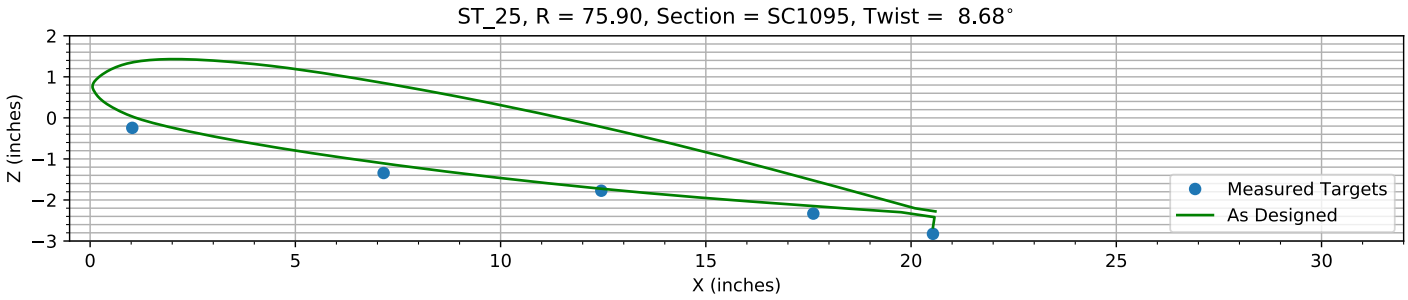

Figure 5-6. Target locations vs section profile at station 25.

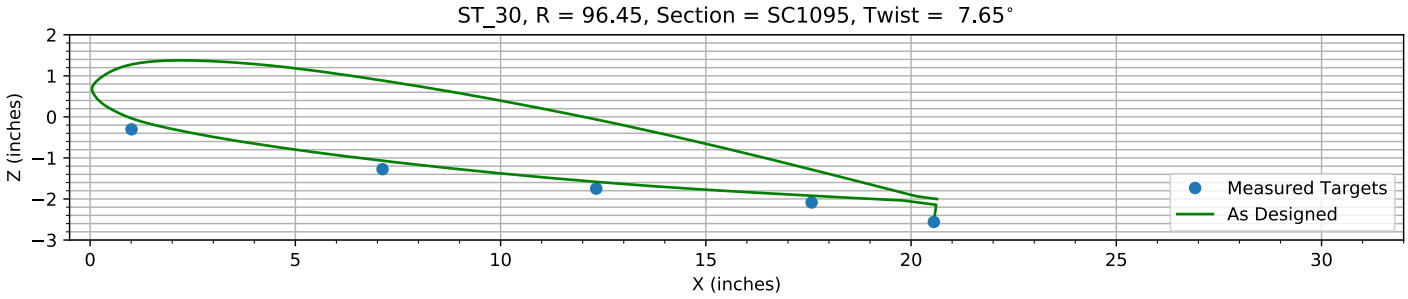

Figure 5-7. Target locations vs section profile at station 30.

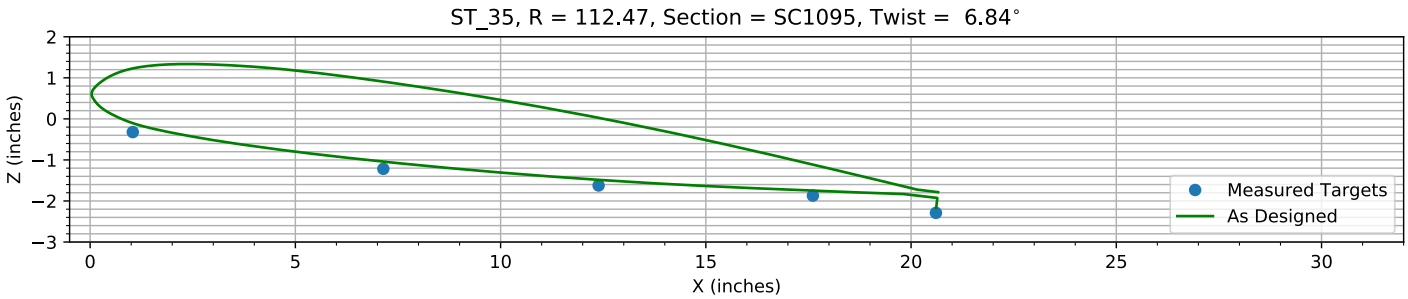

Figure 5-8. Target locations vs section profile at station 35.

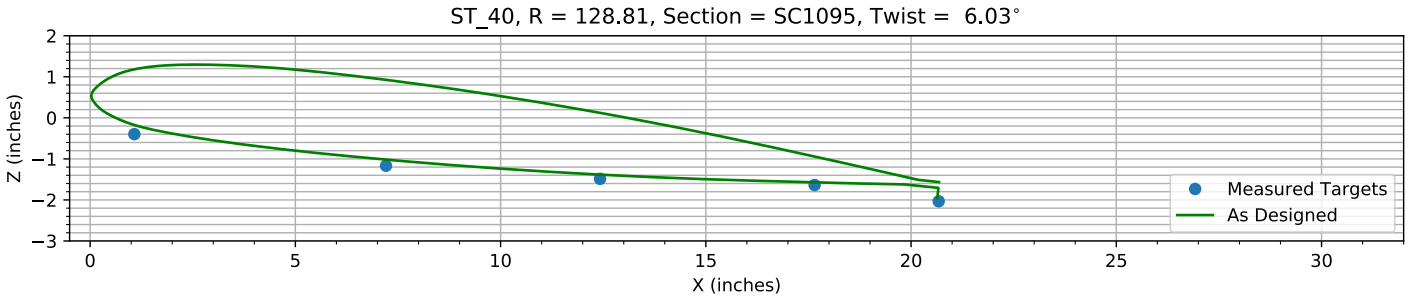

Figure 5-9. Target locations vs section profile at station 40.

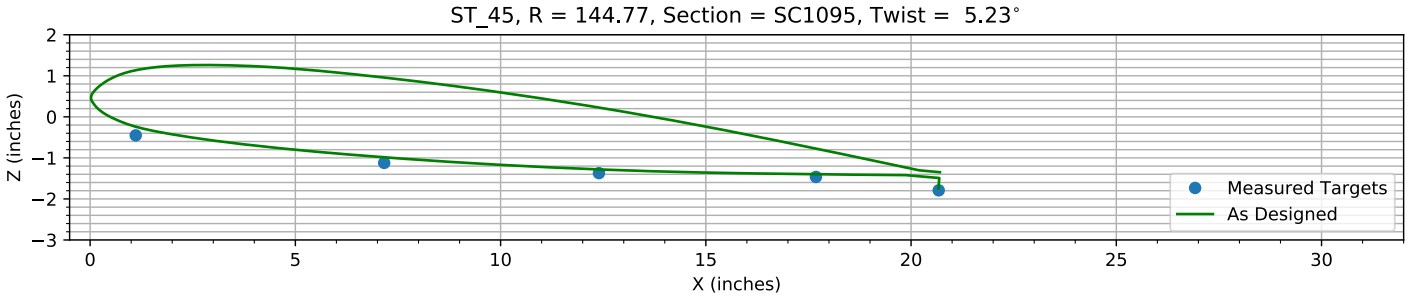

Figure 5-10. Target locations vs section profile at station 45.

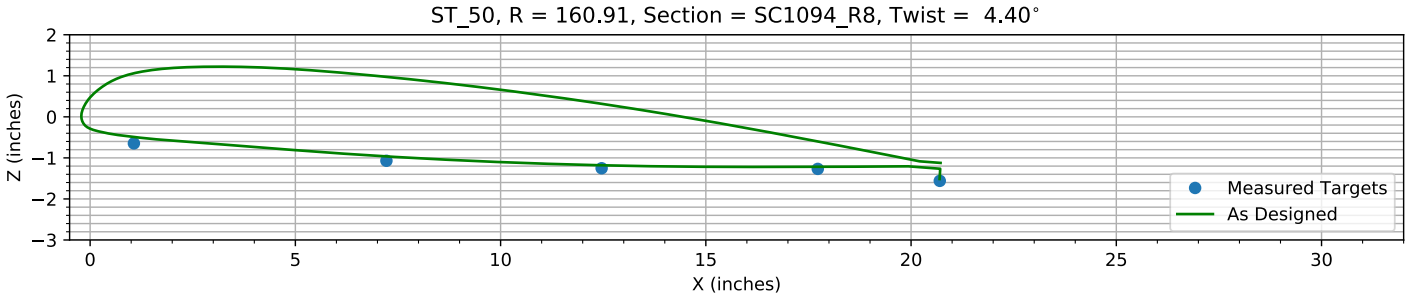

Figure 5-11. Target locations vs section profile at station 50.

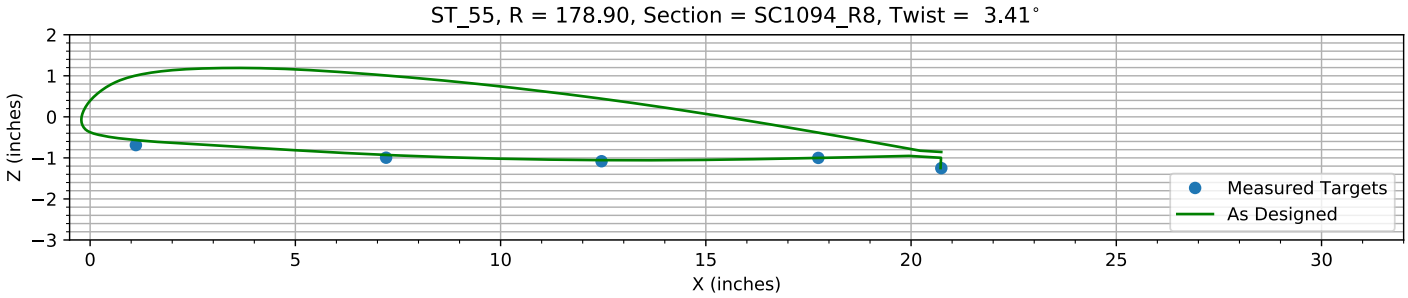

Figure 5-12. Target locations vs section profile at station 55.

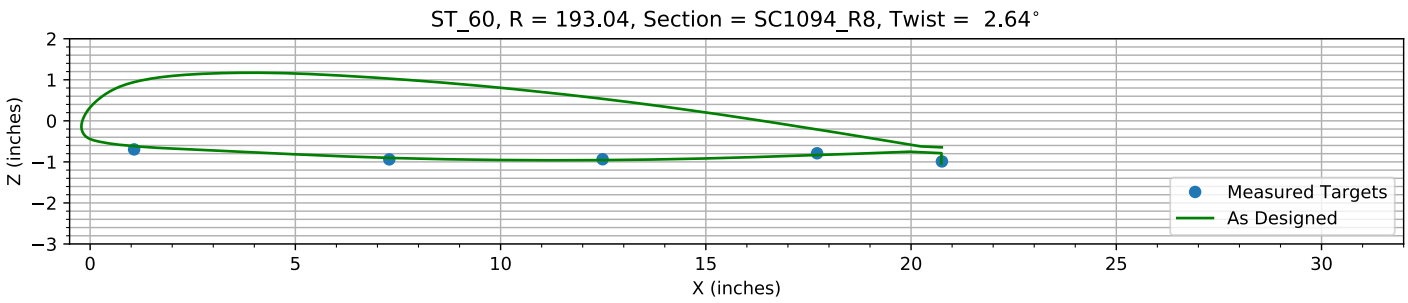

Figure 5-13. Target locations vs section profile at station 60.

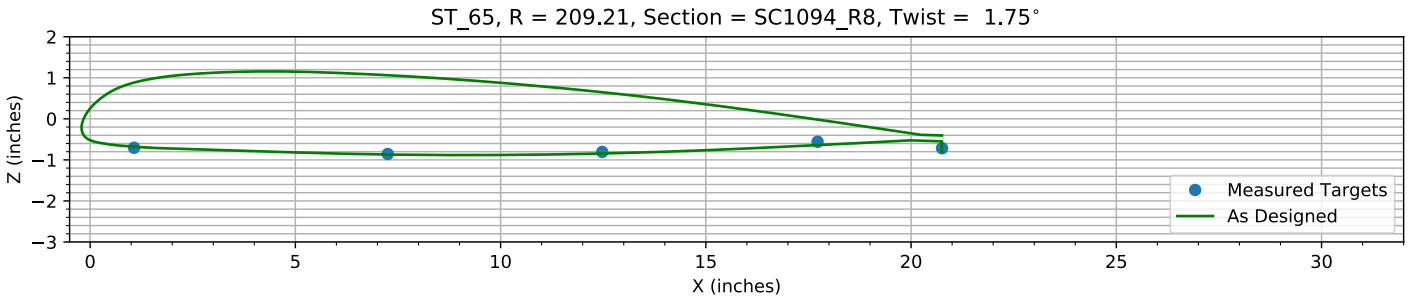

Figure 5-14. Target locations vs section profile at station 65.

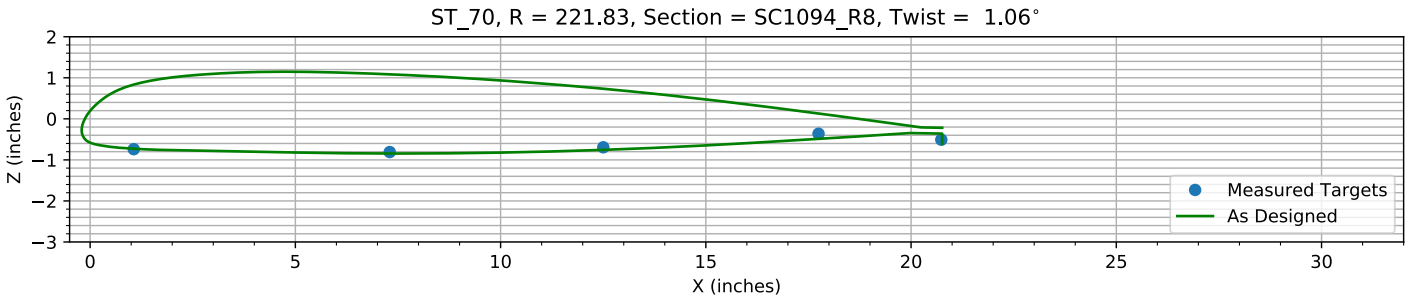

Figure 5-15. Target locations vs section profile at station 70.

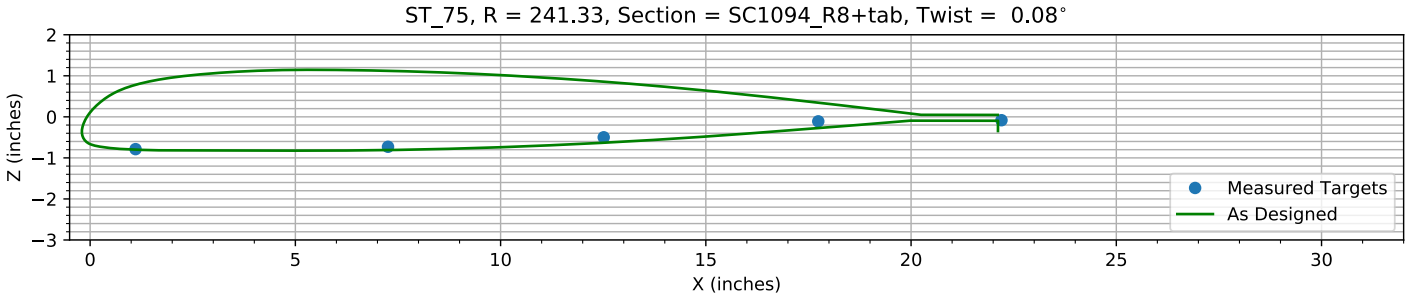

Figure 5-16. Target locations vs section profile at station 75.

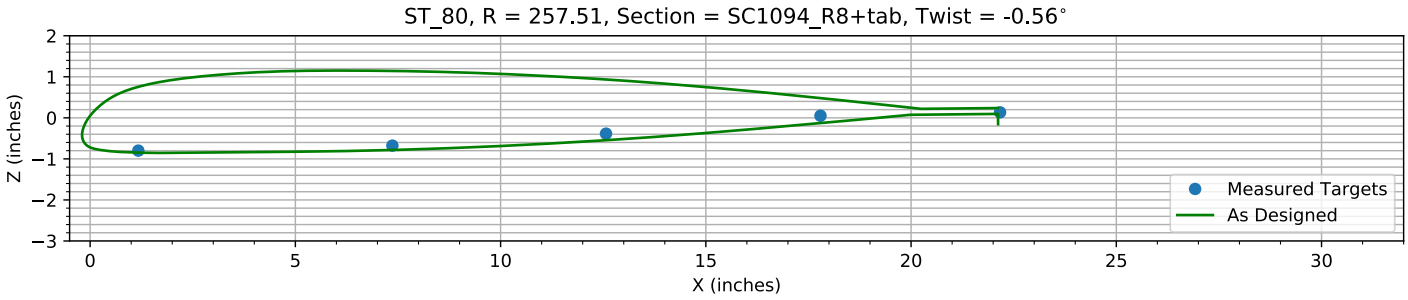

Figure 5-17. Target locations vs section profile at station 80.

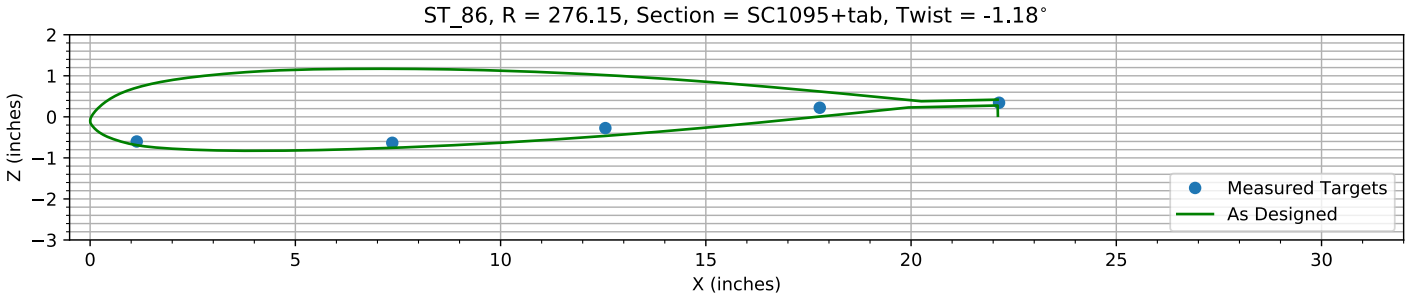

Figure 5-18. Target locations vs section profile at station 86.

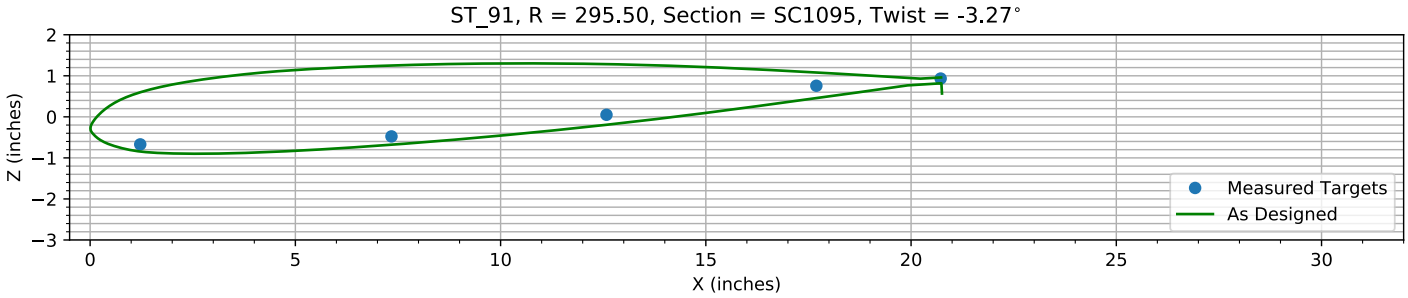

Figure 5-19. Target locations vs section profile at station 91.

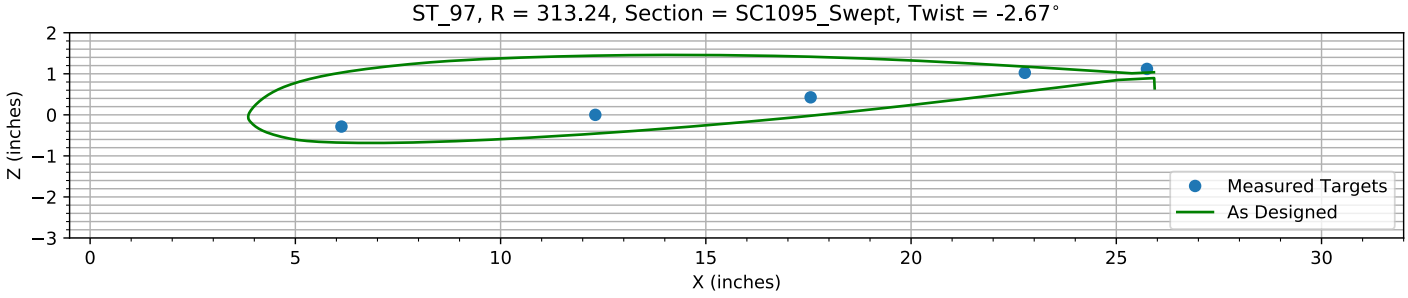

Figure 5-20. Target locations vs section profile at station 97.

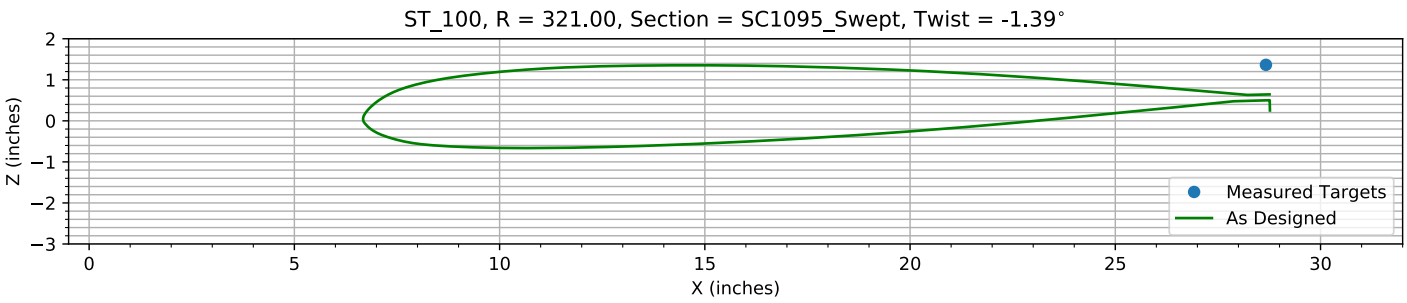

Figure 5-21. Target locations vs section profile at station 100.

Chapter 6: Flap and ΔZ Registration (6 rows)

The targets at the 6 spanwise stations nearest the root are used to determing the Z and flap offset.

The estimated Z error, -0.31312 inches, is within an allowed range of ±2.000 inches.

The estimated flap error is -0.094186°.

6.1: Target Location Errors After Flap Target Registration

Table 6-1. Measured(1) with flap registration vs as designed(2) in inches.

Name	X1	Y1	Z1	X2	Y2	Z2	dX	dY	dZ	dR
B3_R20_C05	0.9915	62.373	0.060345	0.9915	62.373	0.095451	0	0	-0.035107	0.035107
B3_R20_C36	7.0547	62.389	-1.104	7.0547	62.389	-1.1202	0	0	0.016124	0.016124
B3_R20_C61	11.157	62.378	-1.5692	11.157	62.378	-1.6667	0	0	0.09746	0.09746
B3_R20_C86	17.495	62.429	-2.1698	17.495	62.429	-2.288	0	0	0.11828	0.11828
B3_R20_C99	20.466	62.382	-2.7033	20.501	62.382	-2.8477	-0.03443	0	0.14438	0.14843
B3_R25_C05	1.0268	75.952	-0.013434	1.0268	75.952	0.031805	0	0	-0.045239	0.045239
B3_R25_C36	7.1498	75.912	-1.1139	7.1498	75.912	-1.109	0	0	-0.0048927	0.0048927
B3_R25_C61	12.453	75.854	-1.5453	12.453	75.854	-1.7264	0	0	0.18112	0.18112
B3_R25_C86	17.619	75.915	-2.103	17.619	75.915	-2.1493	0	0	0.046264	0.046264
B3_R25_C99	20.533	75.87	-2.5953	20.533	75.87	-2.6663	-0.00021969	0	0.070979	0.070979
B3_R30_C05	1.0076	96.431	-0.11157	1.0076	96.431	-0.035975	0	0	-0.075593	0.075593
B3_R30_C36	7.1241	96.448	-1.0815	7.1241	96.448	-1.0683	0	0	-0.013206	0.013206
B3_R30_C61	12.33	96.471	-1.5557	12.33	96.471	-1.5829	0	0	0.027184	0.027184
B3_R30_C86	17.576	96.442	-1.8933	17.576	96.442	-1.9215	0	0	0.028256	0.028256
B3_R30_C99	20.555	96.472	-2.3686	20.579	96.472	-2.3893	-0.023834	0	0.02074	0.031595
B3_R35_C05	1.039	112.47	-0.1597	1.039	112.47	-0.10479	0	0	-0.054912	0.054912
B3_R35_C36	7.1428	112.48	-1.0542	7.1428	112.48	-1.0416	0	0	-0.012612	0.012612
B3_R35_C61	12.388	112.45	-1.4595	12.388	112.45	-1.4857	0	0	0.026119	0.026119
B3_R35_C86	17.608	112.47	-1.7074	17.608	112.47	-1.7483	0	0	0.040925	0.040925
B3_R35_C99	20.606	112.49	-2.1265	20.611	112.49	-2.174	-0.004538	0	0.047505	0.047721
B3_R40_C05	1.077	128.84	-0.26459	1.077	128.84	-0.1752	0	0	-0.089394	0.089394
B3_R40_C36	7.2083	128.81	-1.0344	7.2083	128.81	-1.0182	0	0	-0.016272	0.016272
B3_R40_C61	12.422	128.81	-1.3522	12.422	128.81	-1.3836	0	0	0.031377	0.031377
B3_R40_C86	17.65	128.79	-1.5043	17.65	128.79	-1.5719	0	0	0.067672	0.067672
B3_R40_C99	20.673	128.78	-1.8994	20.64	128.78	-1.9548	0.032625	0	0.055422	0.064311
B3_R45_C05	1.1115	144.74	-0.34736	1.1115	144.74	-0.24114	0	0	-0.10621	0.10621
B3_R45_C36	7.1639	144.78	-1.0185	7.1639	144.78	-0.98569	0	0	-0.032805	0.032805
B3_R45_C61	12.396	144.77	-1.2674	12.396	144.77	-1.2813	0	0	0.013851	0.013851
B3_R45_C86	17.683	144.81	-1.3602	17.683	144.81	-1.3982	0	0	0.038001	0.038001
B3_R45_C99	20.674	144.78	-1.6871	20.666	144.78	-1.7395	0.0079943	0	0.052421	0.053027
B3_R50_C05	1.0661	161	-0.57242	1.0661	161	-0.49132	0	0	-0.081105	0.081105
B3_R50_C36	7.2183	160.99	-0.99625	7.2183	160.99	-0.964	0	0	-0.032254	0.032254
B3_R50_C61	12.461	160.89	-1.1776	12.461	160.89	-1.1805	0	0	0.0028434	0.0028434
B3_R50_C86	17.727	160.88	-1.1936	17.727	160.88	-1.2179	0	0	0.024218	0.024218
B3_R50_C99	20.7	160.82	-1.485	20.695	160.82	-1.5154	0.0045171	0	0.030381	0.030715
B3_R55_C05	1.1146	178.94	-0.64673	1.1146	178.94	-0.56585	0	0	-0.080879	0.080879
B3_R55_C36	7.2105	178.92	-0.95377	7.2105	178.92	-0.92806	0	0	-0.025705	0.025705
B3_R55_C61	12.459	178.91	-1.0396	12.459	178.91	-1.055	0	0	0.015383	0.015383

Name	X1	Y1	Z1	X2	Y2	Z2	dX	dY	dZ	dR
B3_R55_C86	17.74	178.89	-0.95853	17.74	178.89	-1.0021	0	0	0.043547	0.043547
B3_R55_C99	20.736	178.86	-1.2079	20.719	178.86	-1.248	0.017591	0	0.040111	0.043799
B3_R60_C05	1.071	193.11	-0.68025	1.071	193.11	-0.61652	0	0	-0.063729	0.063729
B3_R60_C36	7.2879	193.09	-0.92287	7.2879	193.09	-0.90255	0	0	-0.020323	0.020323
B3_R60_C61	12.485	193.05	-0.91975	12.485	193.05	-0.9566	0	0	0.036857	0.036857
B3_R60_C86	17.71	193	-0.77422	17.71	193	-0.83418	0	0	0.059962	0.059962
B3_R60_C99	20.752	192.96	-0.97259	20.734	192.96	-1.0387	0.017424	0	0.066129	0.068386
B3_R65_C05	1.0704	209.25	-0.71821	1.0704	209.25	-0.67921	0	0	-0.038998	0.038998
B3_R65_C36	7.2504	209.24	-0.86943	7.2504	209.24	-0.86937	0	0	-5.6407e-05	5.6407e-05
B3_R65_C61	12.476	209.23	-0.82035	12.476	209.23	-0.84432	0	0	0.02397	0.02397
B3_R65_C86	17.722	209.21	-0.57167	17.722	209.21	-0.64022	0	0	0.068552	0.068552
B3_R65_C99	20.755	209.12	-0.72983	20.748	209.12	-0.79872	0.0060816	0	0.068896	0.069164
B3_R70_C05	1.0625	221.86	-0.77589	1.0625	221.86	-0.72778	0	0	-0.048108	0.048108
B3_R70_C36	7.2991	221.86	-0.84558	7.2991	221.86	-0.84455	0	0	-0.0010284	0.0010284
B3_R70_C61	12.501	221.85	-0.7294	12.501	221.85	-0.75588	0	0	0.026474	0.026474
B3_R70_C86	17.746	221.87	-0.39886	17.746	221.87	-0.48767	0	0	0.088806	0.088806
B3_R70_C99	20.737	221.75	-0.54417	20.757	221.75	-0.61105	-0.020118	0	0.066883	0.069843
B3_R75_C05	1.1066	241.35	-0.85865	1.1066	241.35	-0.79949	0	0	-0.059166	0.059166
B3_R75_C36	7.257	241.35	-0.80124	7.257	241.35	-0.80924	0	0	0.007996	0.007996
B3_R75_C61	12.512	241.35	-0.56995	12.512	241.35	-0.63084	0	0	0.060884	0.060884
B3_R75_C86	17.739	241.34	-0.18147	17.739	241.34	-0.27435	0	0	0.092883	0.092883
B3_R80_C05	1.174	257.58	-0.90036	1.174	257.58	-0.84739	0	0	-0.052972	0.052972
B3_R80_C36	7.3634	257.55	-0.77862	7.3634	257.55	-0.78326	0	0	0.004642	0.004642
B3_R80_C61	12.568	257.52	-0.48676	12.568	257.52	-0.54496	0	0	0.058203	0.058203
B3_R80_C86	17.793	257.51	-0.050384	17.793	257.51	-0.12808	0	0	0.077698	0.077698
B3_R86_C05	1.1359	276.27	-0.73604	1.1359	276.27	-0.6905	0	0	-0.045534	0.045534
B3_R86_C36	7.3608	276.23	-0.76761	7.3608	276.23	-0.75542	0	0	-0.012194	0.012194
B3_R86_C61	12.552	276.17	-0.4096	12.552	276.17	-0.46461	0	0	0.055014	0.055014
B3_R86_C86	17.776	276.1	0.086284	17.776	276.1	0.0057891	0	0	0.080495	0.080495
B3_R91_C05	1.2208	295.54	-0.84137	1.2208	295.54	-0.8455	0	0	0.0041309	0.0041309
B3_R91_C36	7.3414	295.51	-0.64722	7.3414	295.51	-0.67896	0	0	0.031745	0.031745
B3_R91_C61	12.58	295.52	-0.1209	12.58	295.52	-0.19327	0	0	0.072372	0.072372
B3_R91_C86	17.692	295.52	0.5865	17.692	295.52	0.45629	0	0	0.13021	0.13021
B3_R91_C99	20.721	295.45	0.7623	20.753	295.45	0.56675	-0.032286	0	0.19554	0.19819
B3_R97_C05	6.1225	313.3	-0.48887	6.1225	313.3	-0.67599	0	0	0.18711	0.18711
B3_R97_C36	12.307	313.29	-0.20328	12.307	313.29	-0.45946	0	0	0.25618	0.25618
B3_R97_C61	17.553	313.27	0.22348	17.553	313.27	-0.024119	0	0	0.2476	0.2476
B3_R97_C86	22.771	313.25	0.82095	22.771	313.25	0.56691	0	0	0.25404	0.25404
B3_R97_C99	25.747	313.11	0.91632	25.887	313.11	0.64965	-0.14044	0	0.26667	0.30139
HUB_LE	2.2058	30	-3.1913	2.19	30	-3.5	0.015808	0.00036708	0.30872	0.30913
HUB_TE	8.2046	29.999	-3.1865	8.19	30	-3.5	0.014608	-0.0013989	0.31352	0.31387
RMS Errors:							0.017862	0.00016271	0.10003	0.10161

6.2: Flap Registration Plots (6 rows)

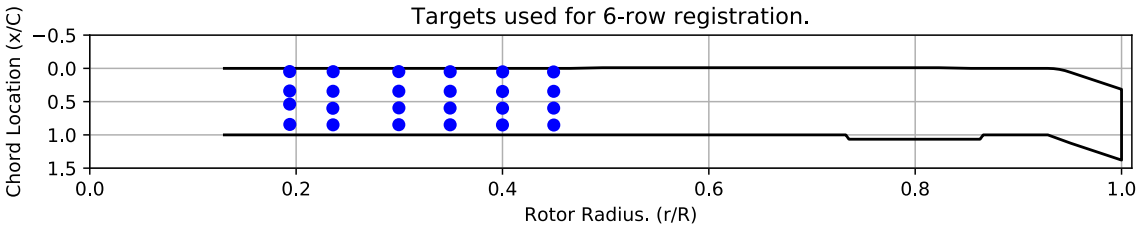

Figure 6-1. Targets used for 6 row root registration.

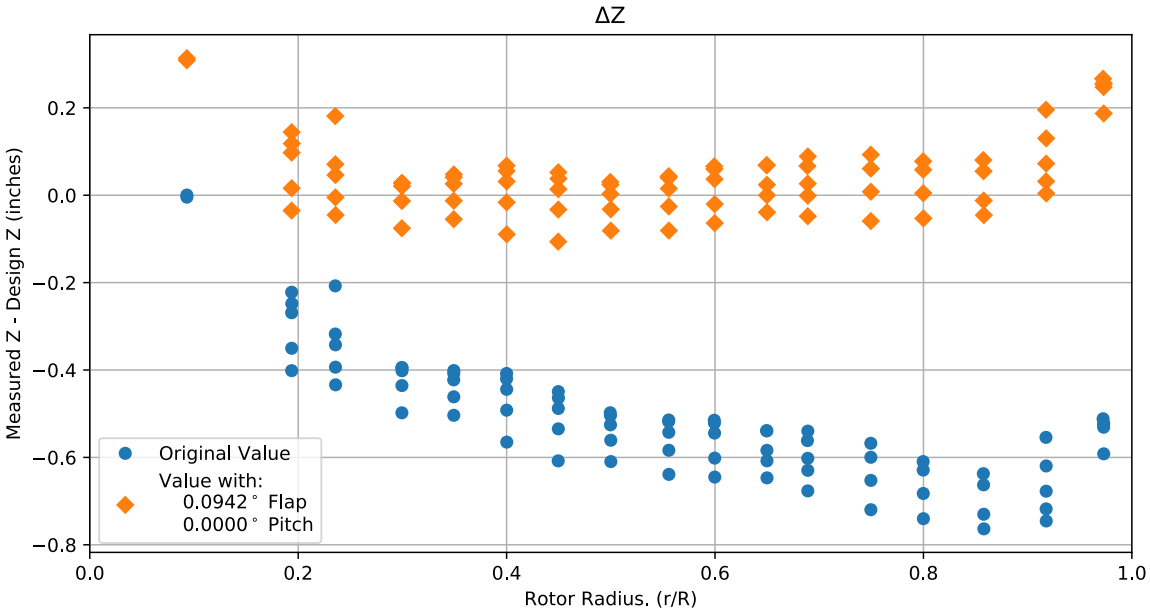

Figure 6-2. Flap target registration, ΔZ error vs rotor radius.

Note: the “as designed” geometry used for the swept tip may have some inaccuracies.

6.3: Estimated Bending and Twist at the Quarter Chord

The error bars shown represent the residual errors for fitting the measure target locations to the "as designed" geometry. These errors are generally much larger than those due to the VSTARS measurement errors. Therefore, the most likely source of these errors is the placement of the trailing-edge targets, differences between the "as designed" and "as built" geometries, and blade deformation during measurement. In the future, iterative adjustment of the "as designed" twist angle may be implemented to see if it reduces the fit error in delta twist. Note: The "as designed" geometry used for the swept tip may have some inaccuracies.

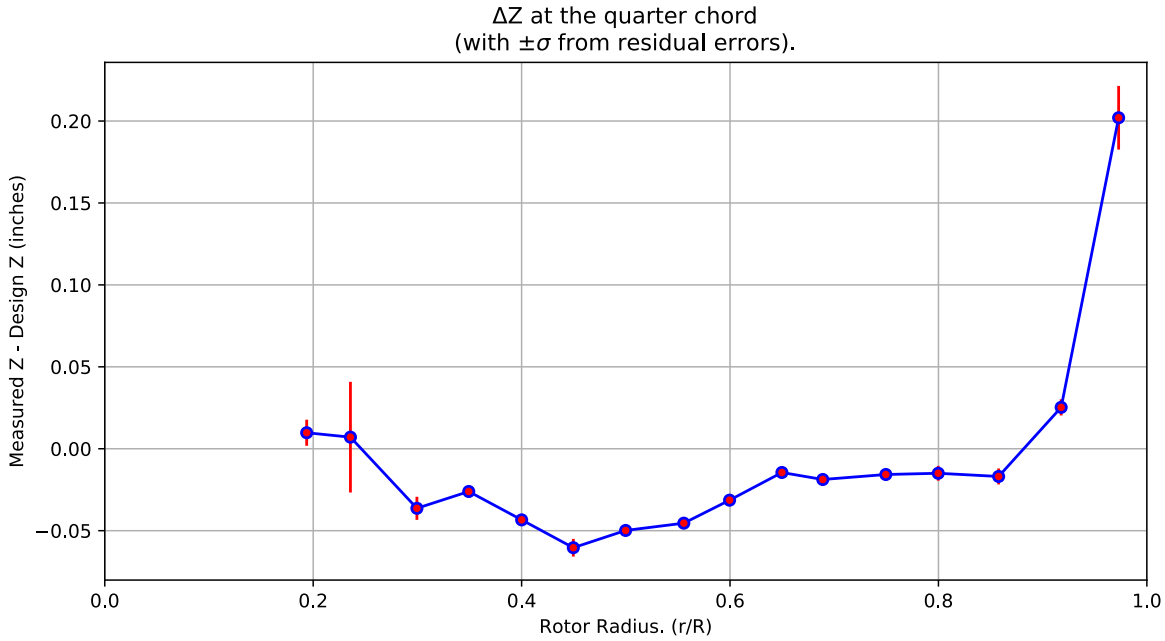

Figure 6-3. ΔZ error at the quarter chord vs rotor radius.

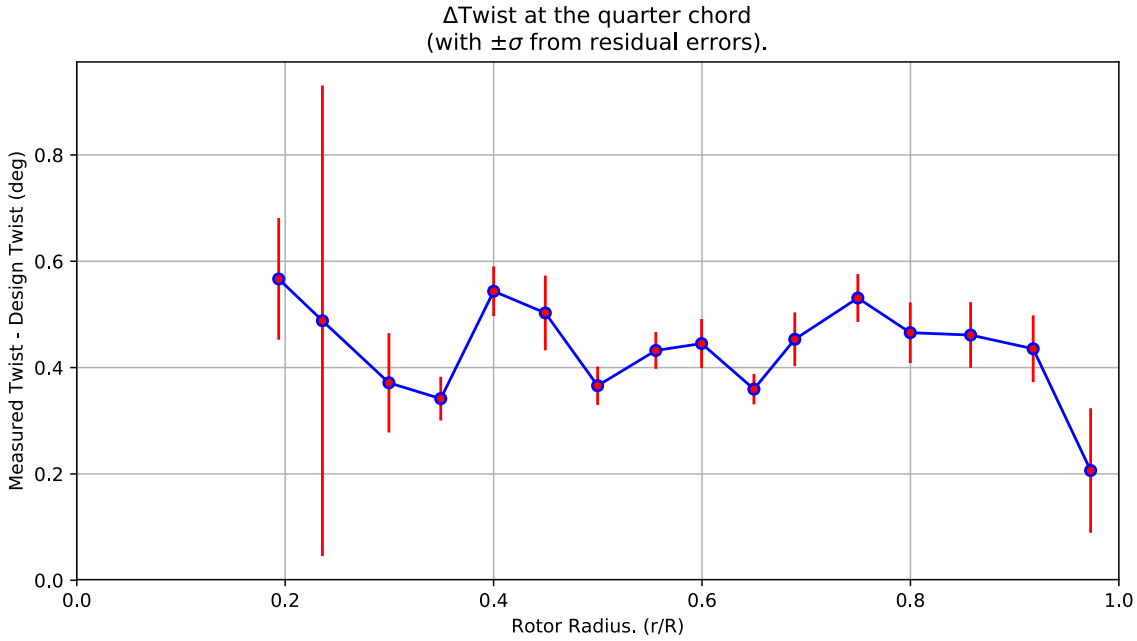

Figure 6-4. ΔTwist error at the quarter chord vs rotor radius.

Table 6-2. Quarter-chord bending and twist statistics.

r	r/R	dZ 1/4-chord	dT	sigma dZ meas	sigma dT meas	sigma dZ res	sigma dT res	n	t_conf
62.392	0.19376	0.0097759	0.56673	5.9982e-10	4.764e-09	0.0079567	0.1144	4	4.3027
75.908	0.23574	0.0070708	0.48806	6.1303e-10	4.6479e-09	0.033776	0.44261	4	4.3027
96.448	0.29953	-0.036338	0.37138	6.112e-10	4.6624e-09	0.007045	0.093445	4	4.3027
112.47	0.34927	-0.026082	0.34161	6.1269e-10	4.6591e-09	0.0031245	0.04111	4	4.3027
128.82	0.40005	-0.0434	0.54366	6.1487e-10	4.6602e-09	0.0035897	0.046746	4	4.3027
144.77	0.44961	-0.060394	0.50283	6.1483e-10	4.6602e-09	0.0053869	0.070165	4	4.3027
160.94	0.49981	-0.049856	0.36593	6.1513e-10	4.6359e-09	0.0027855	0.036039	4	4.3027
178.92	0.55564	-0.045413	0.43219	6.1615e-10	4.6449e-09	0.0026745	0.034503	4	4.3027
193.06	0.59958	-0.031381	0.44527	6.1648e-10	4.6443e-09	0.0035727	0.046011	4	4.3027
209.23	0.64979	-0.014489	0.35949	6.1583e-10	4.6393e-09	0.0022177	0.028619	4	4.3027
221.86	0.68901	-0.018762	0.45322	6.1659e-10	4.6327e-09	0.0039426	0.050621	4	4.3027
241.34	0.74952	-0.015711	0.53088	6.1708e-10	4.6417e-09	0.0035057	0.044995	4	4.3027
257.54	0.79981	-0.014964	0.46568	6.208e-10	4.649e-09	0.0045233	0.057149	4	4.3027
276.19	0.85774	-0.016911	0.46123	6.1971e-10	4.6444e-09	0.0048733	0.061823	4	4.3027
295.52	0.91776	0.025274	0.43542	6.2165e-10	4.6837e-09	0.004952	0.062788	4	4.3027
313.28	0.97291	0.20201	0.20645	9.1724e-10	4.6385e-09	0.019424	0.11717	4	4.3027

6.4: Section Plots

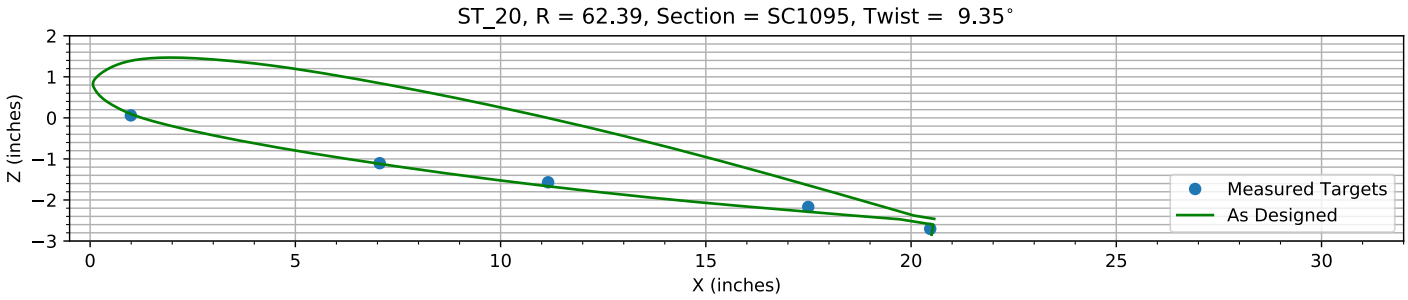

Figure 6-5. Target locations vs section profile at station 20.

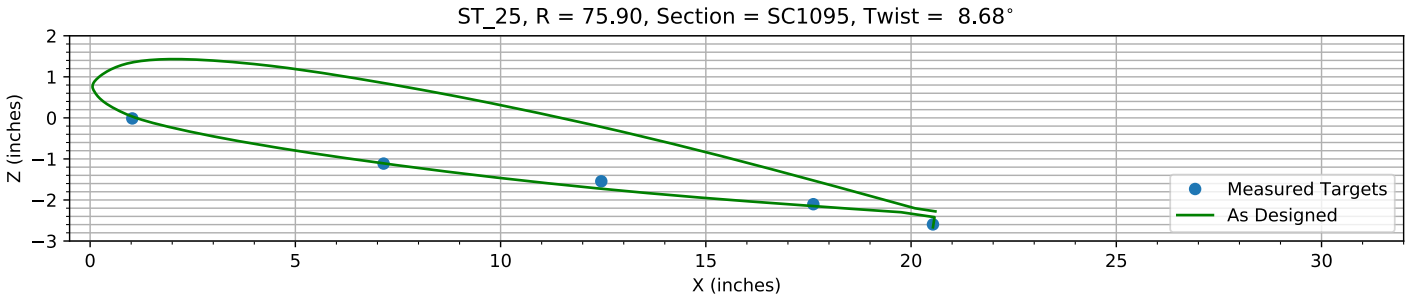

Figure 6-6. Target locations vs section profile at station 25.

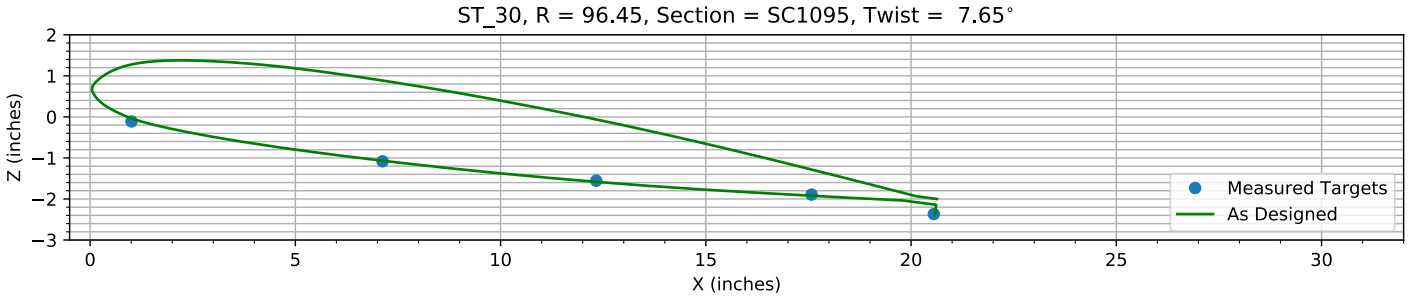

Figure 6-7. Target locations vs section profile at station 30.

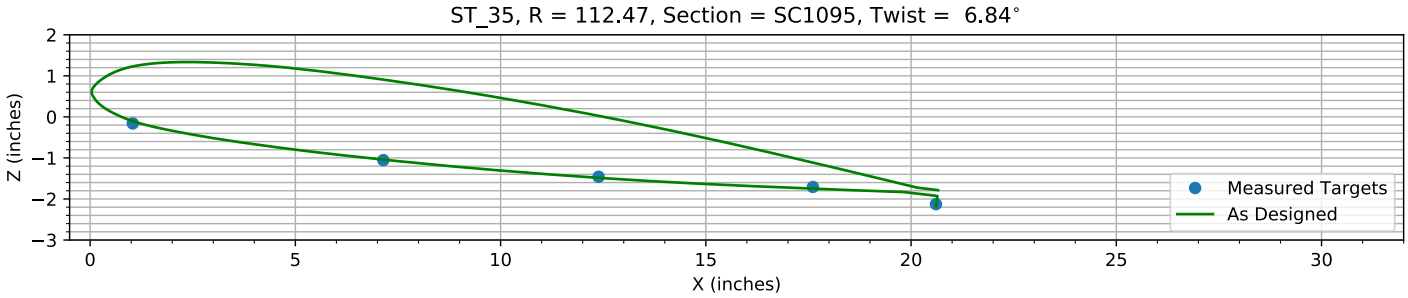

Figure 6-8. Target locations vs section profile at station 35.

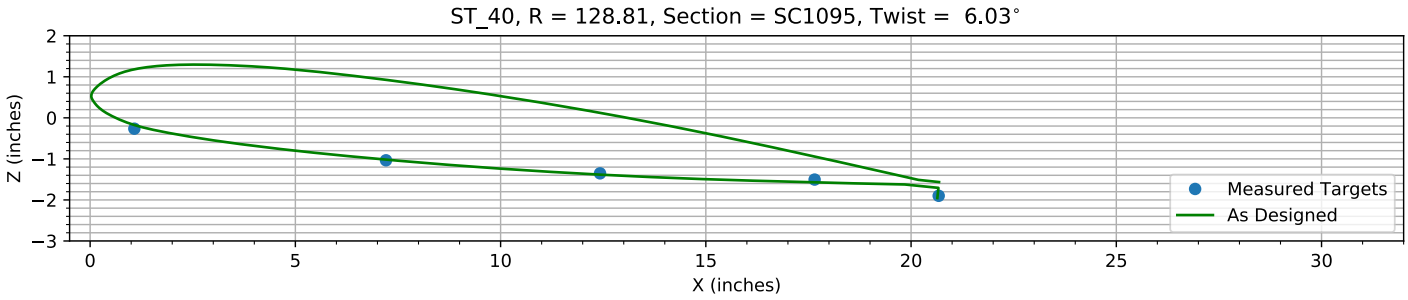

Figure 6-9. Target locations vs section profile at station 40.

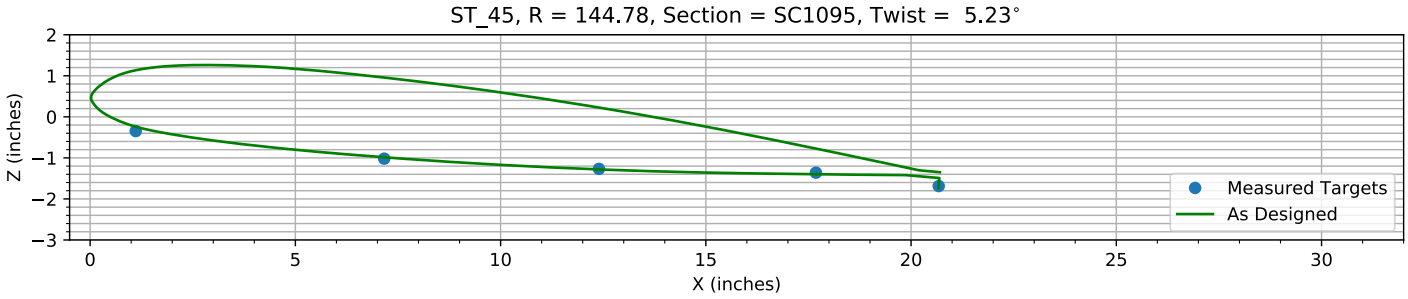

Figure 6-10. Target locations vs section profile at station 45.

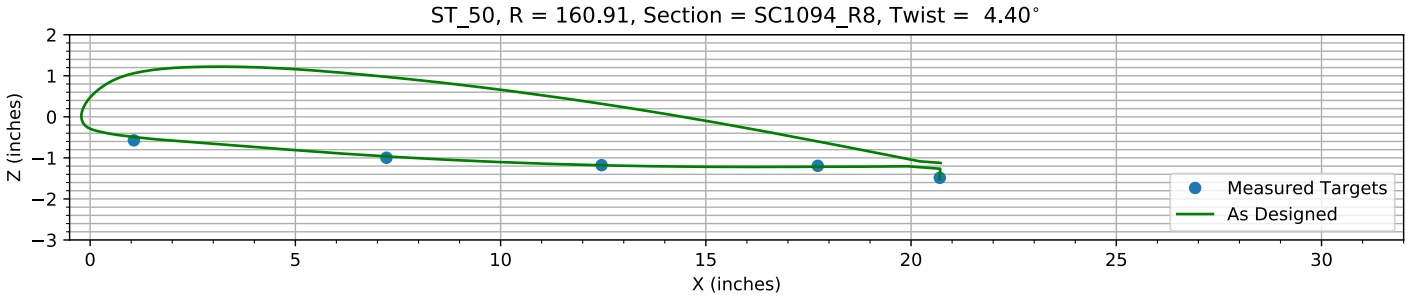

Figure 6-11. Target locations vs section profile at station 50.

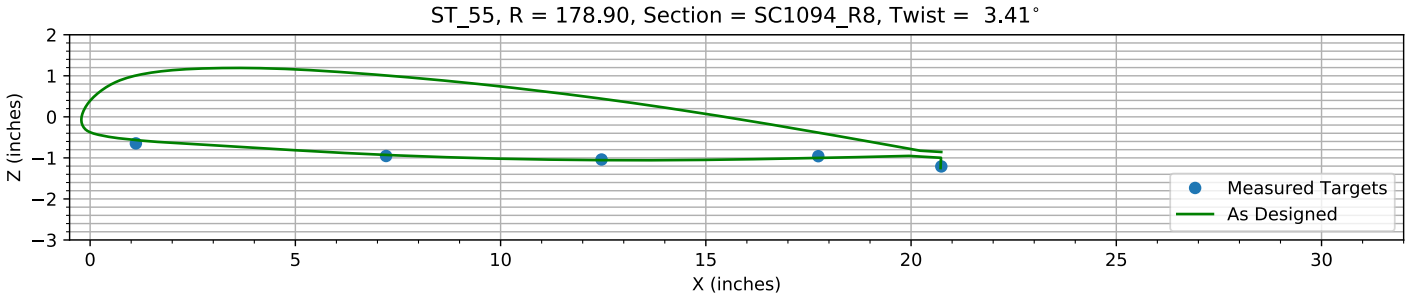

Figure 6-12. Target locations vs section profile at station 55.

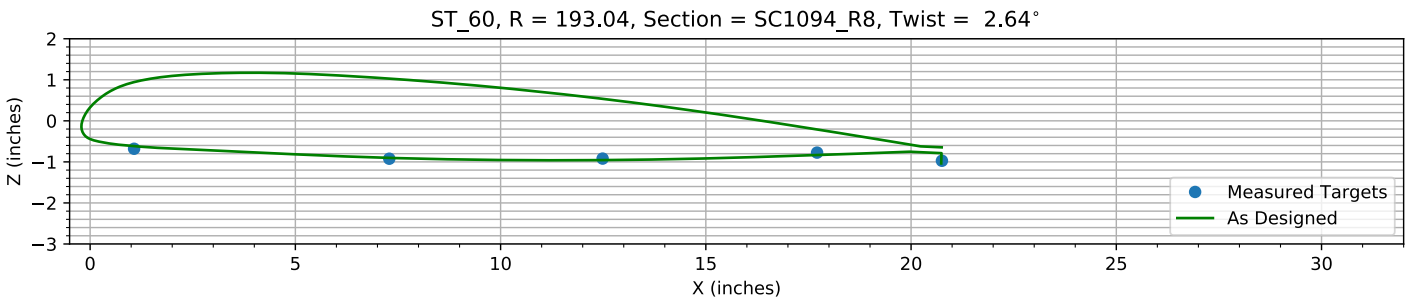

Figure 6-13. Target locations vs section profile at station 60.

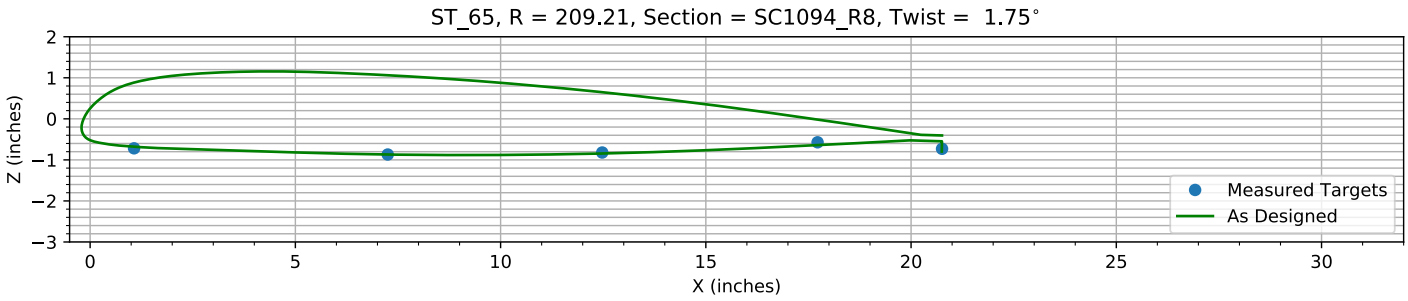

Figure 6-14. Target locations vs section profile at station 65.

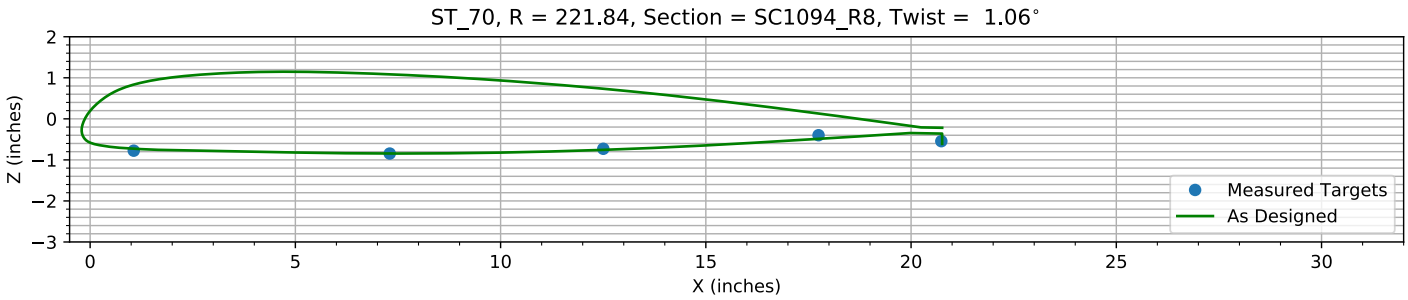

Figure 6-15. Target locations vs section profile at station 70.

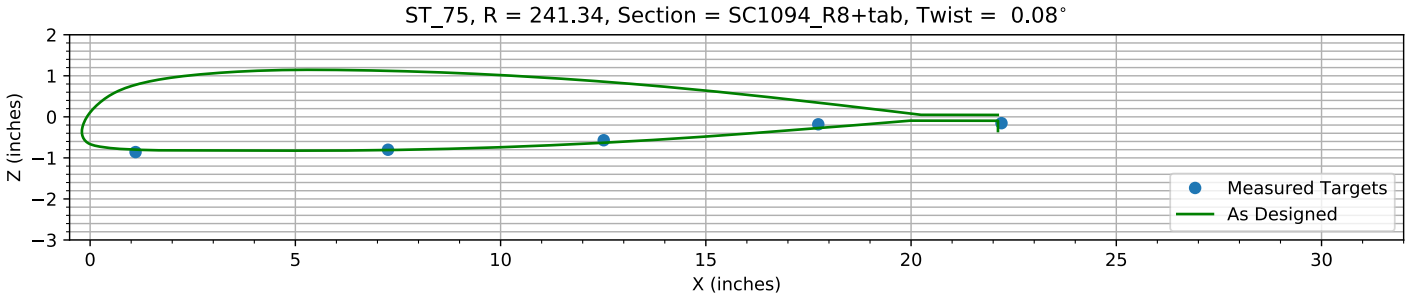

Figure 6-16. Target locations vs section profile at station 75.

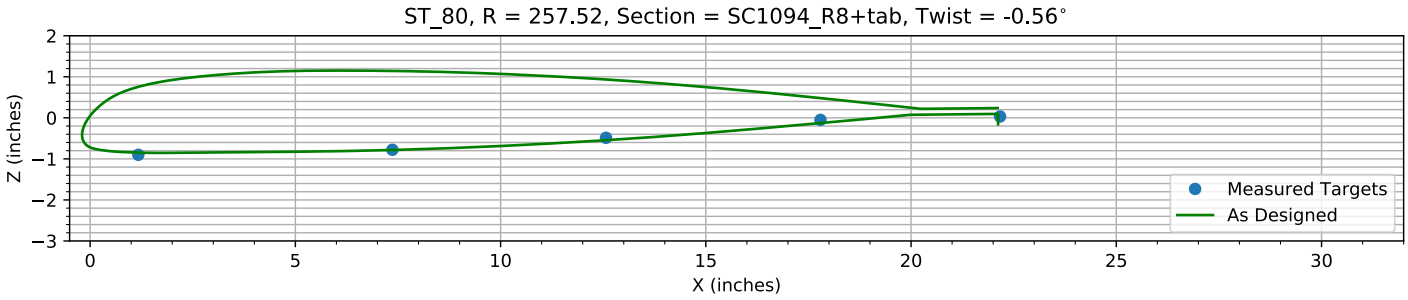

Figure 6-17. Target locations vs section profile at station 80.

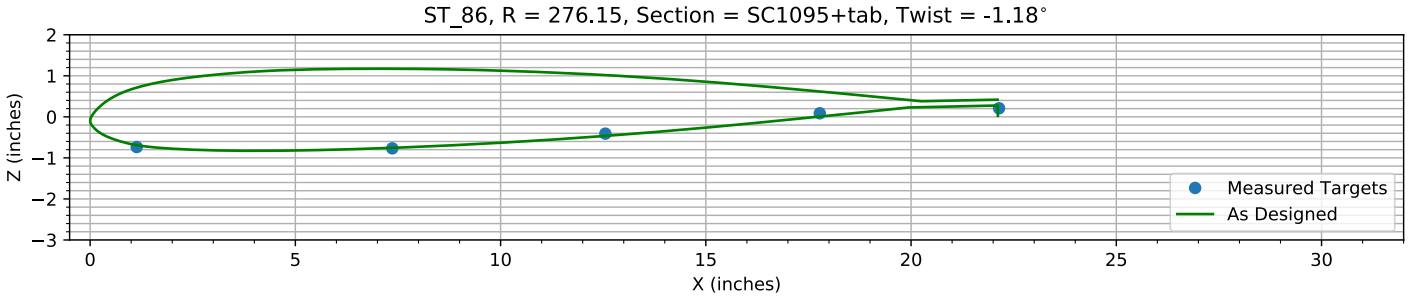

Figure 6-18. Target locations vs section profile at station 86.

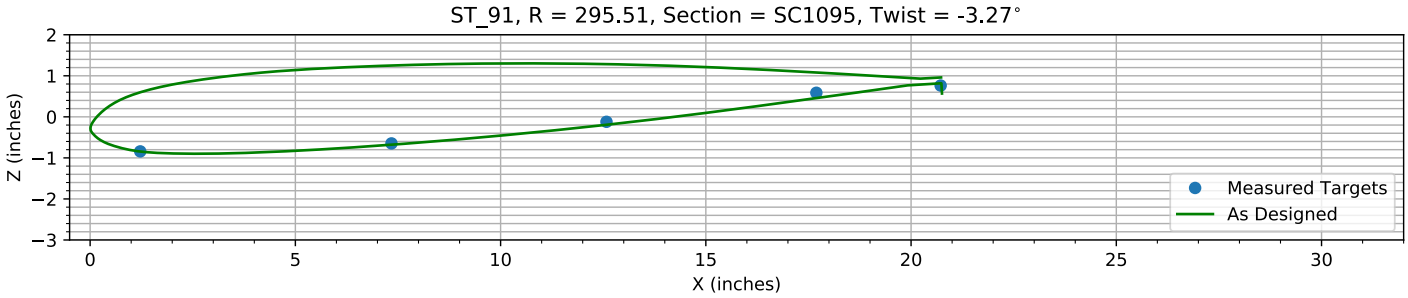

Figure 6-19. Target locations vs section profile at station 91.

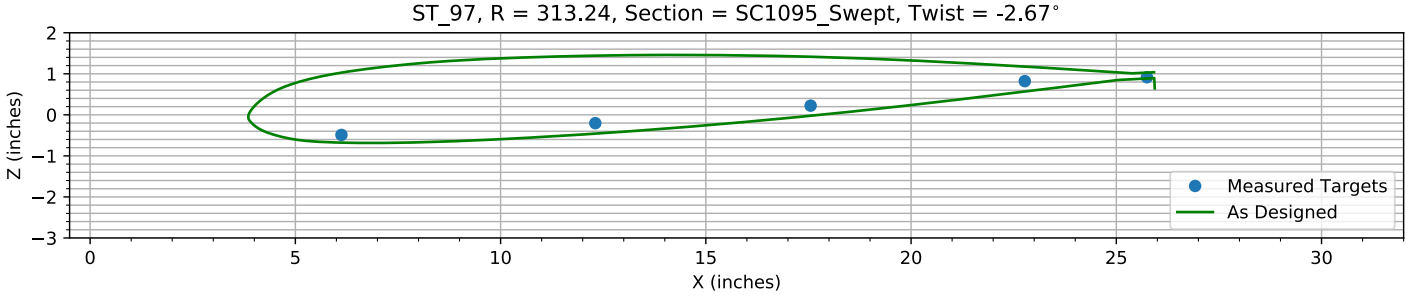

Figure 6-20. Target locations vs section profile at station 97.

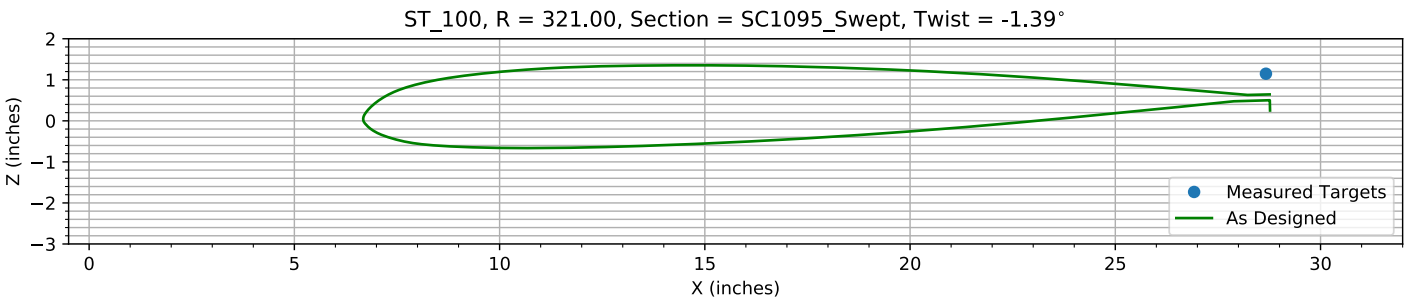

Figure 6-21. Target locations vs section profile at station 100.

Chapter 7: Flap and ΔZ Registration (15 rows)

The targets at the 15 spanwise stations nearest the root are used to determing the Z and flap offset.

The estimated Z error, -0.32869 inches, is within an allowed range of ±2.000 inches.

The estimated flap error is -0.091186°.

7.1: Target Location Errors After Flap Target Registration

Table 7-1. Measured(1) with flap registration vs as designed(2) in inches.

Name	X1	Y1	Z1	X2	Y2	Z2	dX	dY	dZ	dR
B3_R20_C05	0.9915	62.373	0.074212	0.9915	62.373	0.095451	0	0	-0.021238	0.021238
B3_R20_C36	7.0547	62.389	-1.0902	7.0547	62.389	-1.1202	0	0	0.029991	0.029991
B3_R20_C61	11.157	62.378	-1.5554	11.157	62.378	-1.6667	0	0	0.11133	0.11133
B3_R20_C86	17.495	62.429	-2.1559	17.495	62.429	-2.288	0	0	0.13215	0.13215
B3_R20_C99	20.466	62.382	-2.6895	20.501	62.382	-2.8477	-0.03443	0	0.15825	0.16195
B3_R25_C05	1.0268	75.952	-0.00027732	1.0268	75.952	0.031804	0	0	-0.032082	0.032082
B3_R25_C36	7.1498	75.912	-1.1007	7.1498	75.912	-1.109	0	0	0.0082659	0.0082659
B3_R25_C61	12.453	75.854	-1.5321	12.453	75.854	-1.7264	0	0	0.19428	0.19428
B3_R25_C86	17.619	75.915	-2.0898	17.619	75.915	-2.1493	0	0	0.059422	0.059422
B3_R25_C99	20.533	75.87	-2.5821	20.533	75.87	-2.6663	-0.00021974	0	0.08414	0.08414
B3_R30_C05	1.0076	96.432	-0.099484	1.0076	96.432	-0.035976	0	0	-0.063508	0.063508
B3_R30_C36	7.1241	96.448	-1.0695	7.1241	96.448	-1.0683	0	0	-0.0011226	0.0011226
B3_R30_C61	12.33	96.471	-1.5436	12.33	96.471	-1.5829	0	0	0.039266	0.039266
B3_R30_C86	17.576	96.442	-1.8812	17.576	96.442	-1.9215	0	0	0.040339	0.040339
B3_R30_C99	20.555	96.472	-2.3565	20.579	96.472	-2.3893	-0.023834	0	0.032822	0.040563
B3_R35_C05	1.039	112.47	-0.14845	1.039	112.47	-0.10479	0	0	-0.043667	0.043667
B3_R35_C36	7.1428	112.48	-1.0429	7.1428	112.48	-1.0416	0	0	-0.001368	0.001368
B3_R35_C61	12.388	112.45	-1.4483	12.388	112.45	-1.4857	0	0	0.037365	0.037365
B3_R35_C86	17.608	112.47	-1.6962	17.608	112.47	-1.7483	0	0	0.052169	0.052169
B3_R35_C99	20.606	112.49	-2.1152	20.611	112.49	-2.174	-0.0045381	0	0.058747	0.058922
B3_R40_C05	1.077	128.84	-0.2542	1.077	128.84	-0.1752	0	0	-0.079006	0.079006
B3_R40_C36	7.2083	128.81	-1.024	7.2083	128.81	-1.0182	0	0	-0.0058836	0.0058836
B3_R40_C61	12.422	128.81	-1.3419	12.422	128.81	-1.3836	0	0	0.041766	0.041766
B3_R40_C86	17.65	128.79	-1.4939	17.65	128.79	-1.5719	0	0	0.078061	0.078061
B3_R40_C99	20.673	128.78	-1.889	20.64	128.78	-1.9548	0.032625	0	0.065811	0.073454
B3_R45_C05	1.1115	144.74	-0.3378	1.1115	144.74	-0.24114	0	0	-0.096659	0.096659
B3_R45_C36	7.1639	144.78	-1.0089	7.1639	144.78	-0.98569	0	0	-0.023252	0.023252
B3_R45_C61	12.396	144.77	-1.2579	12.396	144.77	-1.2813	0	0	0.023404	0.023404
B3_R45_C86	17.683	144.81	-1.3507	17.683	144.81	-1.3982	0	0	0.047551	0.047551
B3_R45_C99	20.674	144.78	-1.6775	20.666	144.78	-1.7395	0.0079942	0	0.061973	0.062486
B3_R50_C05	1.0661	161	-0.56372	1.0661	161	-0.49132	0	0	-0.072401	0.072401
B3_R50_C36	7.2183	160.99	-0.98755	7.2183	160.99	-0.964	0	0	-0.02355	0.02355
B3_R50_C61	12.461	160.89	-1.1689	12.461	160.89	-1.1805	0	0	0.011552	0.011552
B3_R50_C86	17.727	160.88	-1.1849	17.727	160.88	-1.2178	0	0	0.032927	0.032927
B3_R50_C99	20.7	160.82	-1.4763	20.695	160.82	-1.5154	0.0045169	0	0.039093	0.039353
B3_R55_C05	1.1146	178.94	-0.63897	1.1146	178.94	-0.56585	0	0	-0.073114	0.073114
B3_R55_C36	7.2105	178.92	-0.946	7.2105	178.92	-0.92806	0	0	-0.01794	0.01794
B3_R55_C61	12.459	178.91	-1.0318	12.459	178.91	-1.055	0	0	0.023148	0.023148

Name	X1	Y1	Z1	X2	Y2	Z2	dX	dY	dZ	dR
B3_R55_C86	17.74	178.89	-0.95076	17.74	178.89	-1.0021	0	0	0.051313	0.051313
B3_R55_C99	20.736	178.86	-1.2001	20.719	178.86	-1.248	0.017591	0	0.047878	0.051008
B3_R60_C05	1.071	193.11	-0.67322	1.071	193.11	-0.61652	0	0	-0.056707	0.056707
B3_R60_C36	7.2879	193.09	-0.91585	7.2879	193.09	-0.90255	0	0	-0.0133	0.0133
B3_R60_C61	12.485	193.05	-0.91272	12.485	193.05	-0.9566	0	0	0.043882	0.043882
B3_R60_C86	17.71	193	-0.76719	17.71	193	-0.83418	0	0	0.066988	0.066988
B3_R60_C99	20.752	192.96	-0.96556	20.734	192.96	-1.0387	0.017424	0	0.073158	0.075204
B3_R65_C05	1.0704	209.25	-0.71203	1.0704	209.25	-0.67921	0	0	-0.032821	0.032821
B3_R65_C36	7.2504	209.24	-0.86325	7.2504	209.24	-0.86937	0	0	0.0061211	0.0061211
B3_R65_C61	12.476	209.23	-0.81417	12.476	209.23	-0.84432	0	0	0.030147	0.030147
B3_R65_C86	17.722	209.21	-0.56549	17.722	209.21	-0.64022	0	0	0.074729	0.074729
B3_R65_C99	20.755	209.12	-0.72364	20.748	209.12	-0.79872	0.0060815	0	0.075078	0.075324
B3_R70_C05	1.0625	221.86	-0.77037	1.0625	221.86	-0.72778	0	0	-0.042591	0.042591
B3_R70_C36	7.2991	221.86	-0.84006	7.2991	221.86	-0.84455	0	0	0.0044882	0.0044882
B3_R70_C61	12.501	221.85	-0.72388	12.501	221.85	-0.75588	0	0	0.031991	0.031991
B3_R70_C86	17.746	221.87	-0.39335	17.746	221.87	-0.48767	0	0	0.094321	0.094321
B3_R70_C99	20.737	221.75	-0.53864	20.757	221.75	-0.61105	-0.020118	0	0.072404	0.075147
B3_R75_C05	1.1066	241.35	-0.85416	1.1066	241.35	-0.79949	0	0	-0.054669	0.054669
B3_R75_C36	7.257	241.35	-0.79674	7.257	241.35	-0.80924	0	0	0.012492	0.012492
B3_R75_C61	12.512	241.35	-0.56546	12.512	241.35	-0.63084	0	0	0.06538	0.06538
B3_R75_C86	17.739	241.34	-0.17697	17.739	241.34	-0.27435	0	0	0.097379	0.097379
B3_R80_C05	1.174	257.58	-0.89671	1.174	257.58	-0.84739	0	0	-0.049325	0.049325
B3_R80_C36	7.3634	257.55	-0.77497	7.3634	257.55	-0.78326	0	0	0.0082902	0.0082902
B3_R80_C61	12.568	257.52	-0.48311	12.568	257.52	-0.54496	0	0	0.061852	0.061852
B3_R80_C86	17.793	257.51	-0.046734	17.793	257.51	-0.12808	0	0	0.081347	0.081347
B3_R86_C05	1.1359	276.27	-0.73337	1.1359	276.27	-0.6905	0	0	-0.042866	0.042866
B3_R86_C36	7.3608	276.23	-0.76494	7.3608	276.23	-0.75542	0	0	-0.0095239	0.0095239
B3_R86_C61	12.552	276.17	-0.40693	12.552	276.17	-0.46461	0	0	0.057687	0.057687
B3_R86_C86	17.776	276.1	0.088961	17.776	276.1	0.0057899	0	0	0.083171	0.083171
B3_R91_C05	1.2208	295.54	-0.83971	1.2208	295.54	-0.8455	0	0	0.0057908	0.0057908
B3_R91_C36	7.3414	295.51	-0.64556	7.3414	295.51	-0.67896	0	0	0.033405	0.033405
B3_R91_C61	12.58	295.52	-0.11924	12.58	295.52	-0.19327	0	0	0.07403	0.07403
B3_R91_C86	17.692	295.52	0.58816	17.692	295.52	0.4563	0	0	0.13186	0.13186
B3_R91_C99	20.721	295.45	0.76396	20.753	295.45	0.56676	-0.032285	0	0.1972	0.19983
B3_R97_C05	6.1225	313.3	-0.48814	6.1225	313.3	-0.67598	0	0	0.18784	0.18784
B3_R97_C36	12.307	313.29	-0.20255	12.307	313.29	-0.45946	0	0	0.25691	0.25691
B3_R97_C61	17.553	313.27	0.22421	17.553	313.27	-0.024127	0	0	0.24834	0.24834
B3_R97_C86	22.771	313.25	0.82168	22.771	313.25	0.5669	0	0	0.25479	0.25479
B3_R97_C99	25.747	313.11	0.91706	25.887	313.11	0.64964	-0.14051	0	0.26741	0.30208
HUB_LE	2.2058	30	-3.1757	2.19	30	-3.5	0.015808	0.00035848	0.32429	0.32467
HUB_TE	8.2046	29.999	-3.1709	8.19	30	-3.5	0.014608	-0.0014072	0.32908	0.32941
RMS Errors:							0.01787	0.00016338	0.10319	0.10473

7.2: Flap Registration Plots (15 rows)

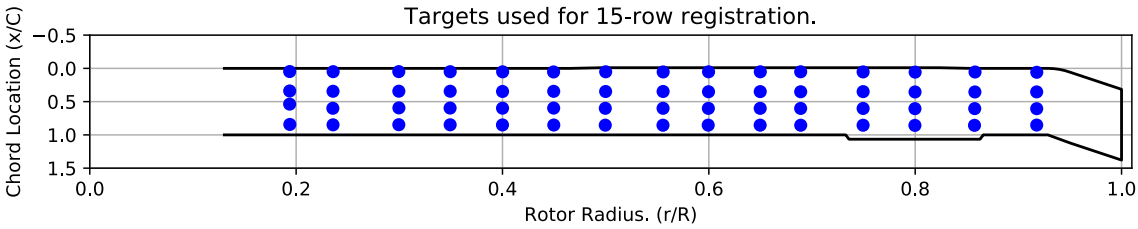

Figure 7-1. Targets used for 15 row root registration.

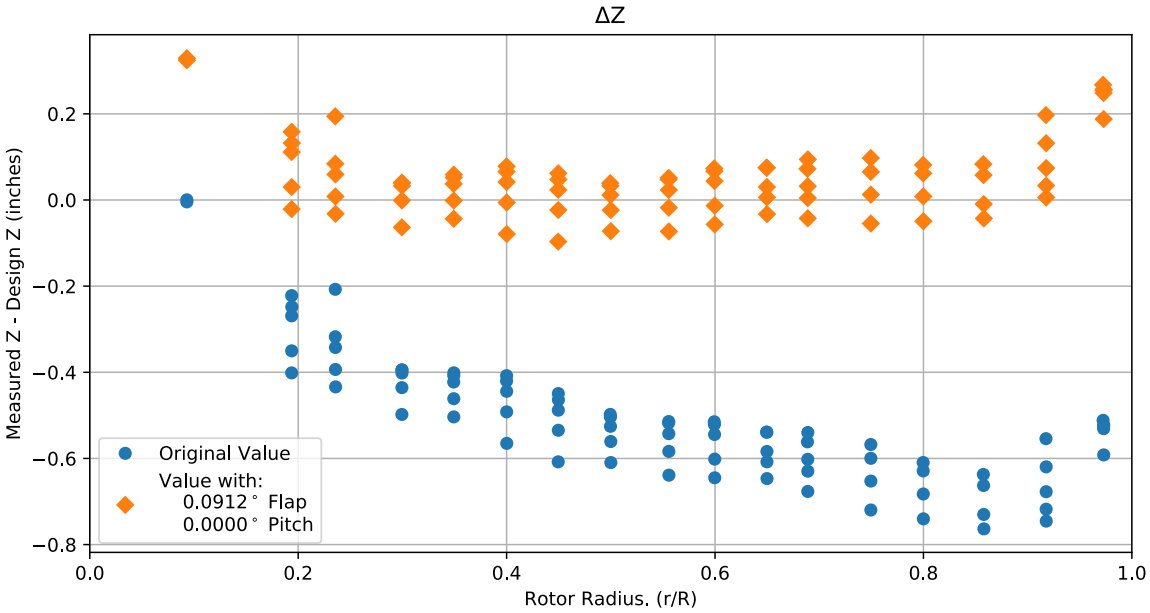

Figure 7-2. Flap target registration, ΔZ error vs rotor radius.

Note: the “as designed” geometry used for the swept tip may have some inaccuracies.

7.3: Estimated Bending and Twist at the Quarter Chord

The error bars shown represent the residual errors for fitting the measure target locations to the "as designed" geometry. These errors are generally much larger than those due to the VSTARS measurement errors. Therefore, the most likely source of these errors is the placement of the trailing-edge targets, differences between the "as designed" and "as built" geometries, and blade deformation during measurement. In the future, iterative adjustment of the "as designed" twist angle may be implemented to see if it reduces the fit error in delta twist. Note: The "as designed" geometry used for the swept tip may have some inaccuracies.

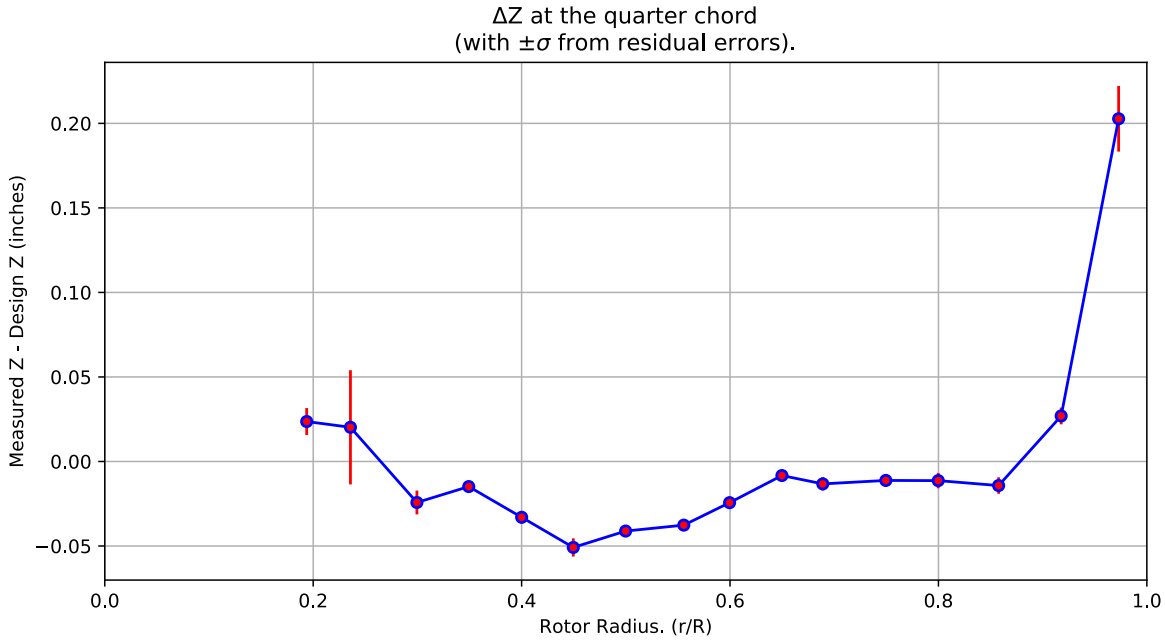

Figure 7-3. ΔZ error at the quarter chord vs rotor radius.

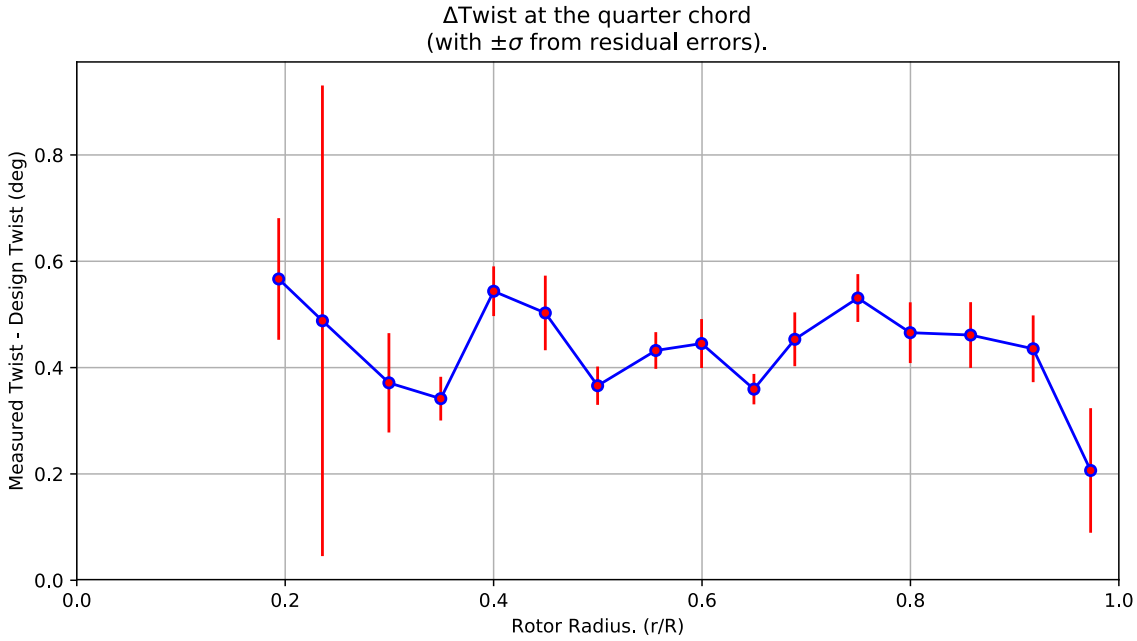

Figure 7-4. ΔTwist error at the quarter chord vs rotor radius.

Table 7-2. Quarter-chord bending and twist statistics.

r	r/R	dZ 1/4-chord	dT	sigma dZ meas	sigma dT meas	sigma dZ res	sigma dT res	n	t_conf
62.392	0.19376	0.023643	0.56672	5.9982e-10	4.764e-09	0.0079569	0.1144	4	4.3027
75.908	0.23574	0.020229	0.48806	6.1303e-10	4.6479e-09	0.033777	0.44262	4	4.3027
96.448	0.29953	-0.024255	0.37138	6.112e-10	4.6624e-09	0.0070446	0.09344	4	4.3027
112.47	0.34927	-0.014838	0.34161	6.1269e-10	4.6591e-09	0.0031247	0.041113	4	4.3027
128.82	0.40005	-0.033012	0.54366	6.1487e-10	4.6602e-09	0.0035897	0.046746	4	4.3027
144.77	0.44961	-0.05084	0.50281	6.1483e-10	4.6602e-09	0.0053869	0.070165	4	4.3027
160.94	0.49981	-0.041151	0.36595	6.1513e-10	4.6359e-09	0.0027855	0.03604	4	4.3027
178.92	0.55564	-0.037649	0.4322	6.1615e-10	4.6449e-09	0.0026745	0.034503	4	4.3027
193.06	0.59958	-0.024358	0.44528	6.1648e-10	4.6443e-09	0.0035727	0.046012	4	4.3027
209.23	0.64979	-0.0083119	0.35949	6.1583e-10	4.6393e-09	0.0022177	0.028619	4	4.3027
221.86	0.68901	-0.013245	0.45321	6.1659e-10	4.6327e-09	0.0039424	0.050618	4	4.3027
241.34	0.74952	-0.011214	0.53087	6.1708e-10	4.6417e-09	0.0035056	0.044994	4	4.3027
257.54	0.79981	-0.011316	0.46569	6.208e-10	4.649e-09	0.0045234	0.057151	4	4.3027
276.19	0.85775	-0.014241	0.46126	6.1971e-10	4.6444e-09	0.0048733	0.061823	4	4.3027
295.52	0.91777	0.026934	0.4354	6.2165e-10	4.6837e-09	0.0049516	0.062784	4	4.3027
313.28	0.97291	0.20273	0.20651	9.1724e-10	4.6385e-09	0.019424	0.11717	4	4.3027

7.4: Section Plots

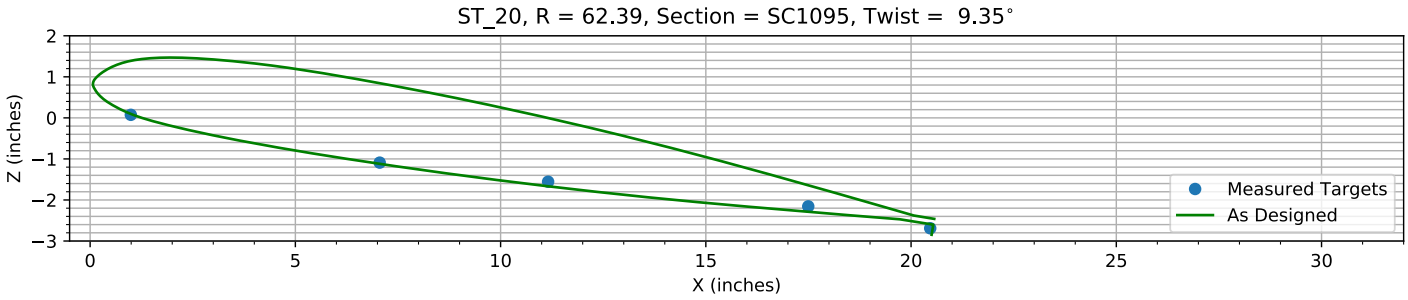

Figure 7-5. Target locations vs section profile at station 20.

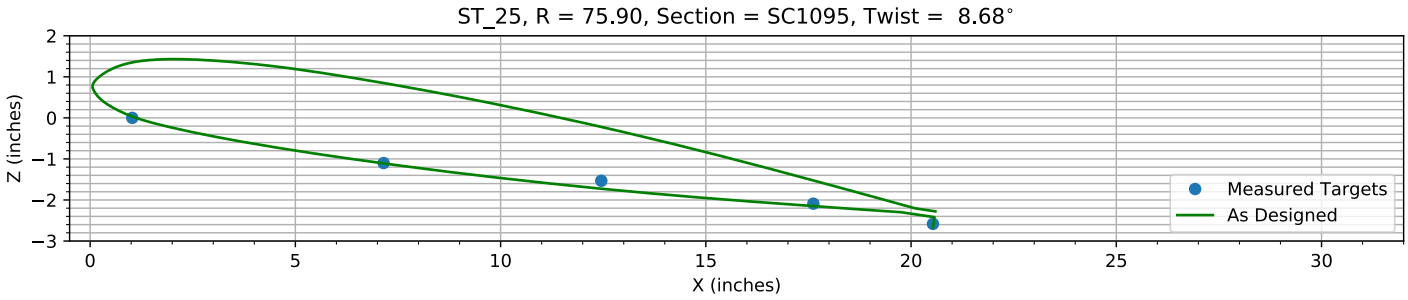

Figure 7-6. Target locations vs section profile at station 25.

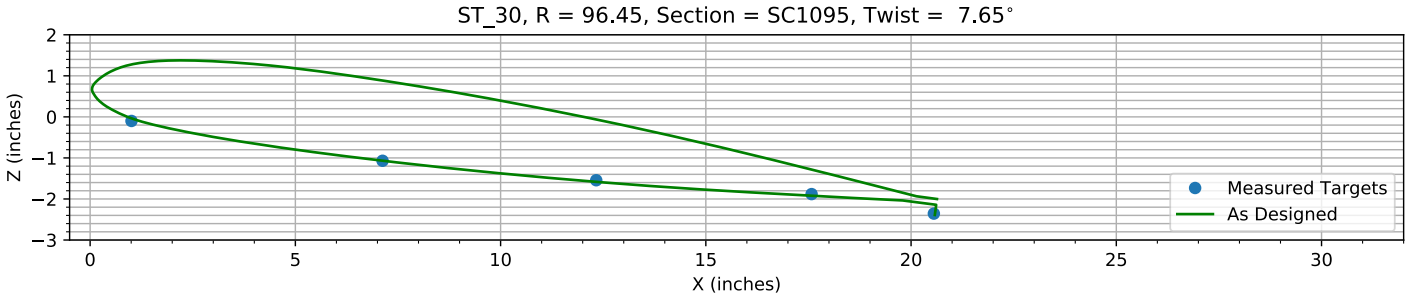

Figure 7-7. Target locations vs section profile at station 30.

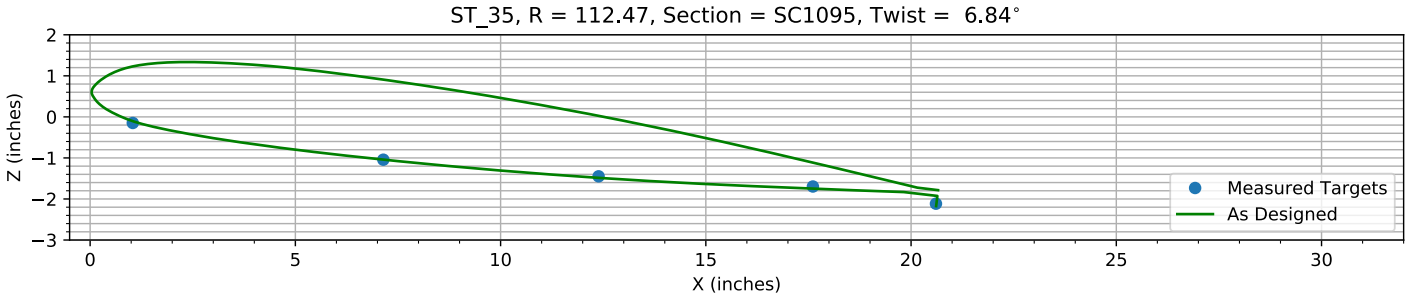

Figure 7-8. Target locations vs section profile at station 35.

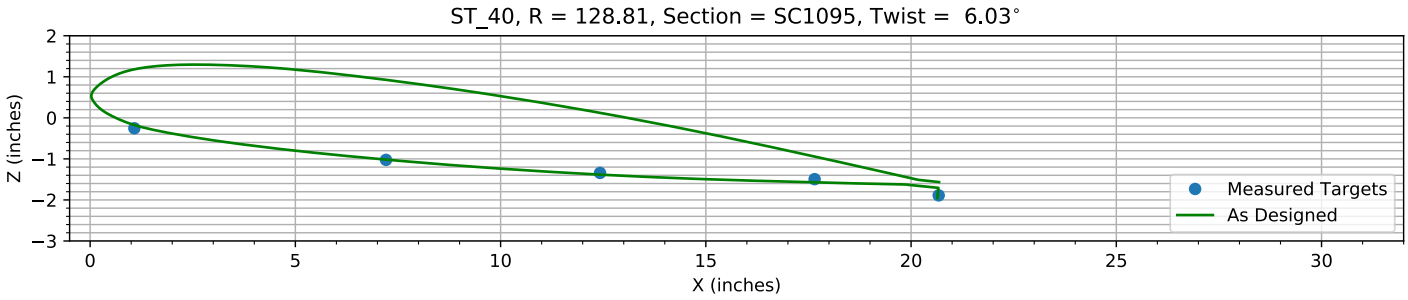

Figure 7-9. Target locations vs section profile at station 40.

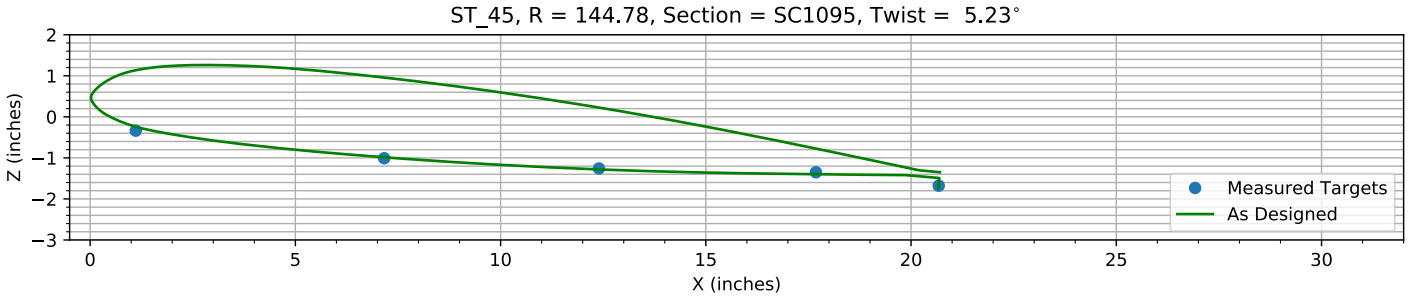

Figure 7-10. Target locations vs section profile at station 45.

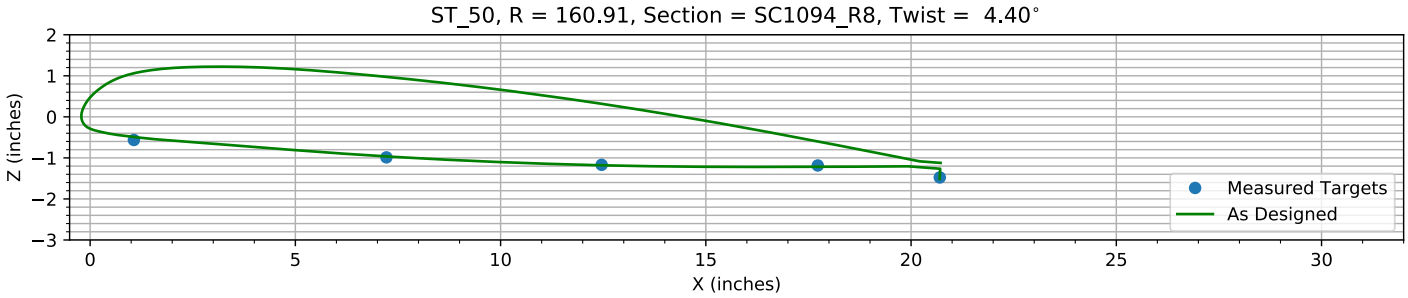

Figure 7-11. Target locations vs section profile at station 50.

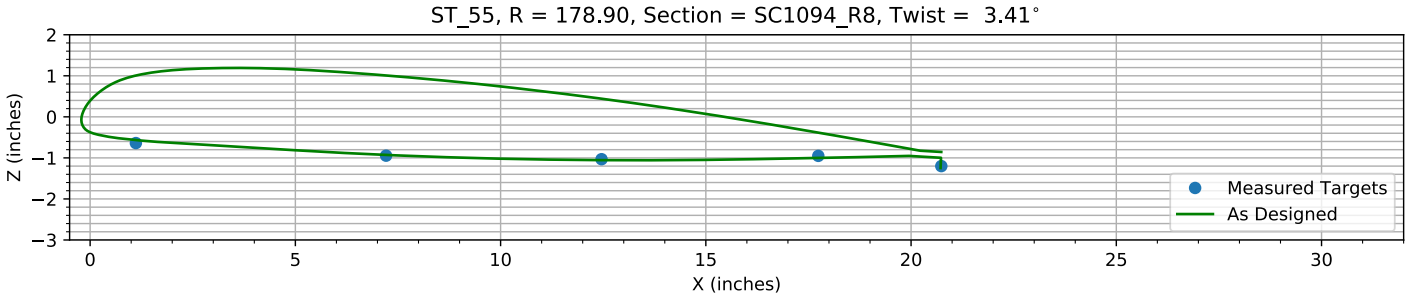

Figure 7-12. Target locations vs section profile at station 55.

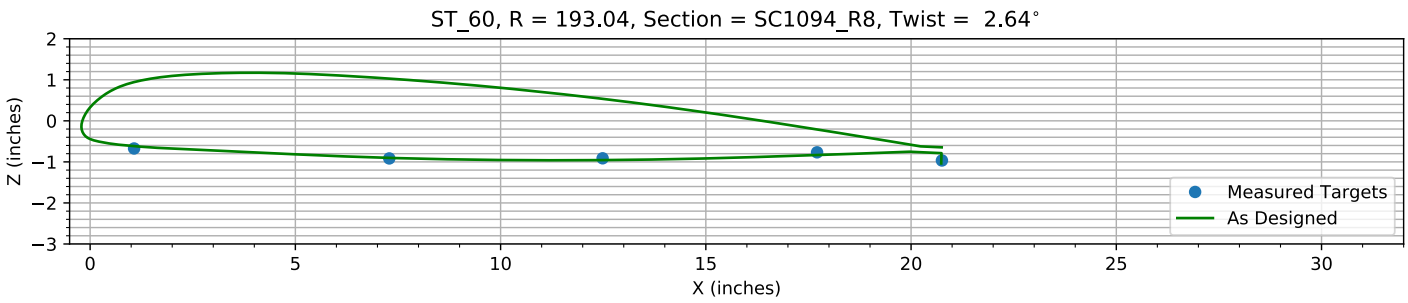

Figure 7-13. Target locations vs section profile at station 60.

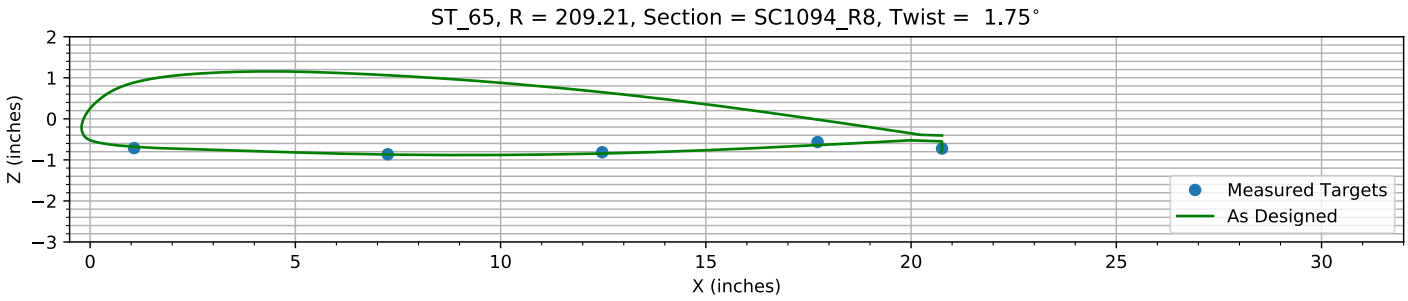

Figure 7-14. Target locations vs section profile at station 65.

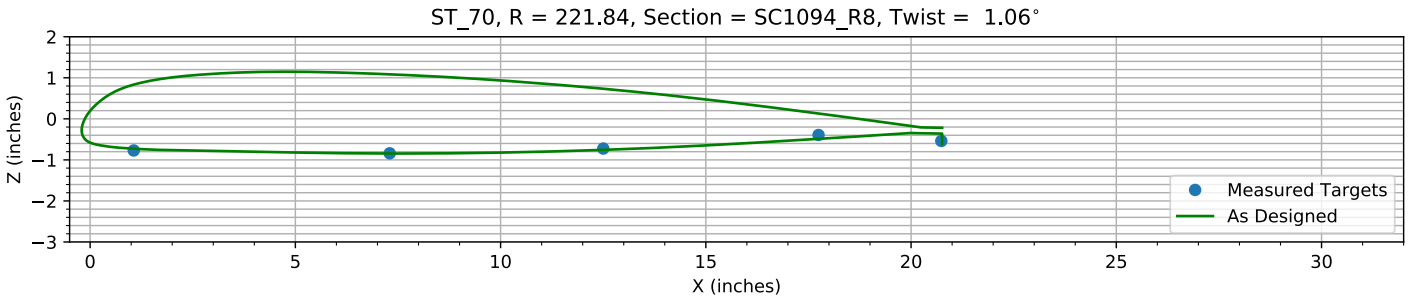

Figure 7-15. Target locations vs section profile at station 70.

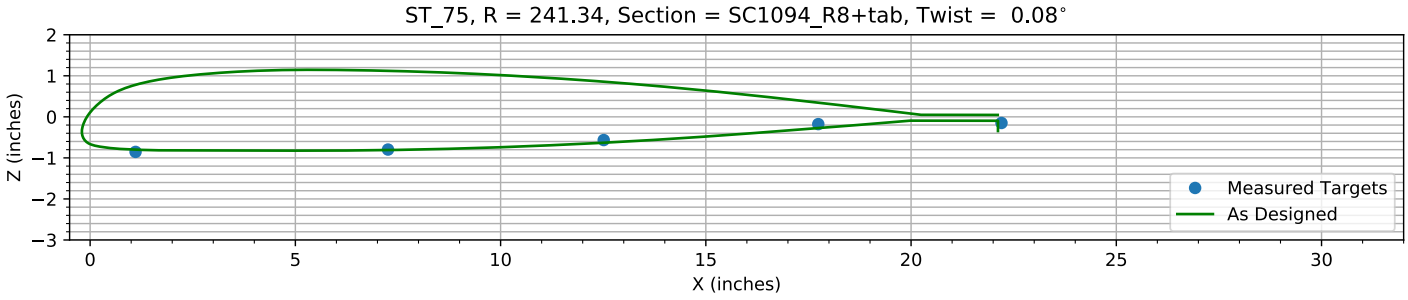

Figure 7-16. Target locations vs section profile at station 75.

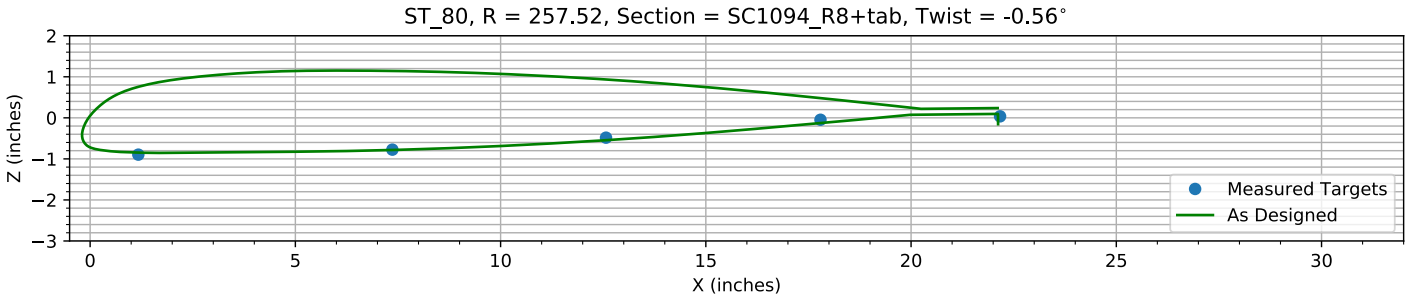

Figure 7-17. Target locations vs section profile at station 80.

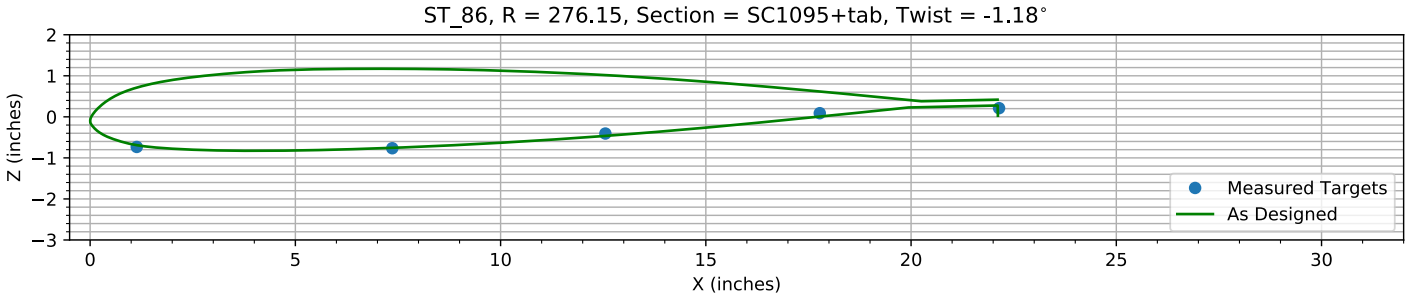

Figure 7-18. Target locations vs section profile at station 86.

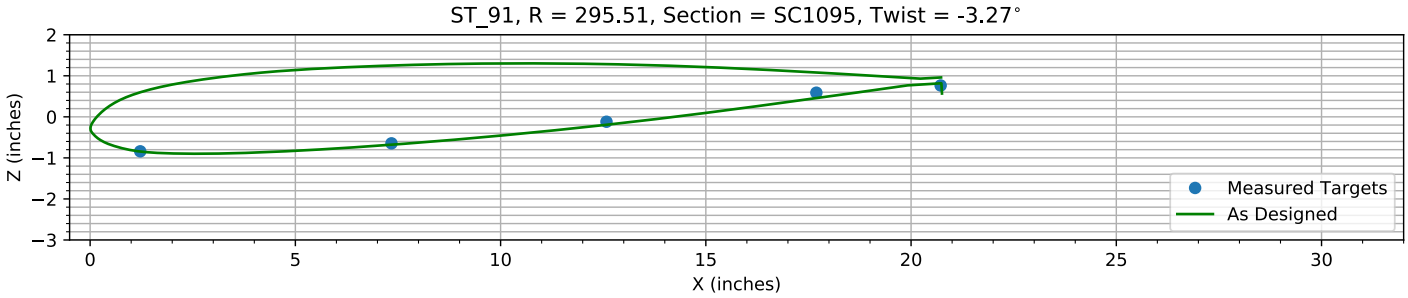

Figure 7-19. Target locations vs section profile at station 91.

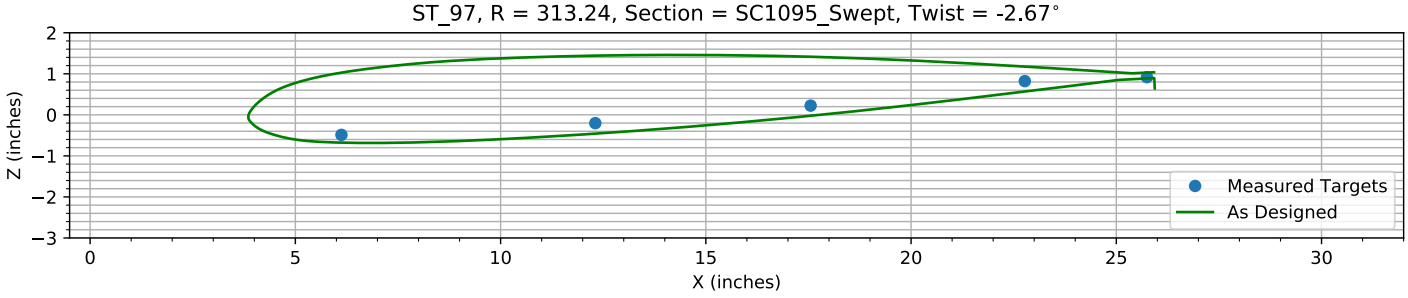

Figure 7-20. Target locations vs section profile at station 97.

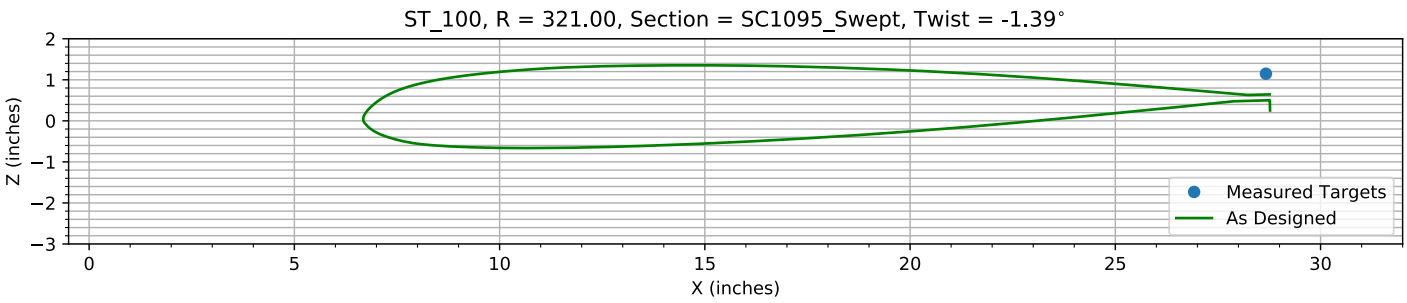

Figure 7-21. Target locations vs section profile at station 100.

Chapter 8: Pitch, Flap, and ΔZ Registration (6 rows)

The targets at the 6 spanwise stations nearest the root are used to determing the Z, flap, and pitch offset.

The estimated Z error, -0.32404 inches, is within an allowed range of ±2.000 inches.

The estimated flap error is -0.096021°.

The estimated pitch error is -0.1496°.

8.1: Target Location Errors After Target Registration

Table 8-1. Measured(1) with pitch and flap registration vs as designed(2) in inches.

Name	X1	Y1	Z1	X2	Y2	Z2	dX	dY	dZ	dR
B3_R20_C05	1.0008	62.373	0.083246	1.0008	62.373	0.091756	0	0	-0.0085103	0.0085103
B3_R20_C36	7.061	62.388	-1.097	7.061	62.388	-1.1211	0	0	0.024124	0.024124
B3_R20_C61	11.162	62.378	-1.5729	11.162	62.378	-1.6673	0	0	0.094417	0.094417
B3_R20_C86	17.498	62.429	-2.1899	17.498	62.429	-2.2883	0	0	0.098396	0.098396
B3_R20_C99	20.468	62.382	-2.7313	20.501	62.382	-2.8477	-0.03237	0	0.11644	0.12086
B3_R25_C05	1.0359	75.951	0.0098102	1.0359	75.951	0.028397	0	0	-0.018587	0.018587
B3_R25_C36	7.156	75.912	-1.1066	7.156	75.912	-1.1099	0	0	0.0032126	0.0032126
B3_R25_C61	12.458	75.853	-1.5519	12.458	75.853	-1.7269	0	0	0.17503	0.17503
B3_R25_C86	17.622	75.915	-2.1231	17.622	75.915	-2.1495	0	0	0.026456	0.026456
B3_R25_C99	20.535	75.87	-2.623	20.533	75.87	-2.6663	0.0021227	0	0.043299	0.043351
B3_R30_C05	1.0165	96.431	-0.087618	1.0165	96.431	-0.039108	0	0	-0.04851	0.04851
B3_R30_C36	7.1304	96.448	-1.0736	7.1304	96.448	-1.0691	0	0	-0.0044799	0.0044799
B3_R30_C61	12.335	96.471	-1.5613	12.335	96.471	-1.5833	0	0	0.021995	0.021995
B3_R30_C86	17.581	96.442	-1.9126	17.581	96.442	-1.9217	0	0	0.0091796	0.0091796
B3_R30_C99	20.558	96.472	-2.3957	20.579	96.472	-2.3893	-0.020898	0	-0.006337	0.021838
B3_R35_C05	1.0478	112.47	-0.13532	1.0478	112.47	-0.10769	0	0	-0.027624	0.027624
B3_R35_C36	7.1492	112.48	-1.0457	7.1492	112.48	-1.0422	0	0	-0.0035038	0.0035038
B3_R35_C61	12.393	112.45	-1.4648	12.393	112.45	-1.486	0	0	0.021236	0.021236
B3_R35_C86	17.613	112.47	-1.7263	17.613	112.47	-1.7485	0	0	0.022239	0.022239
B3_R35_C99	20.61	112.49	-2.1532	20.611	112.49	-2.174	-0.00096881	0	0.020806	0.020828
B3_R40_C05	1.0855	128.84	-0.23978	1.0855	128.84	-0.1778	0	0	-0.061985	0.061985
B3_R40_C36	7.2147	128.81	-1.0256	7.2147	128.81	-1.0187	0	0	-0.0068991	0.0068991
B3_R40_C61	12.428	128.81	-1.3571	12.428	128.81	-1.3839	0	0	0.026866	0.026866
B3_R40_C86	17.655	128.79	-1.5227	17.655	128.79	-1.5721	0	0	0.049346	0.049346
B3_R40_C99	20.677	128.78	-1.9257	20.64	128.78	-1.9548	0.036788	0	0.029071	0.046888
B3_R45_C05	1.1198	144.74	-0.32213	1.1198	144.74	-0.24348	0	0	-0.078645	0.078645
B3_R45_C36	7.1705	144.78	-1.0091	7.1705	144.78	-0.98617	0	0	-0.022892	0.022892
B3_R45_C61	12.402	144.77	-1.2716	12.402	144.77	-1.2815	0	0	0.0098502	0.0098502
B3_R45_C86	17.688	144.81	-1.3783	17.688	144.81	-1.3983	0	0	0.020035	0.020035
B3_R45_C99	20.679	144.78	-1.7129	20.666	144.78	-1.7395	0.012713	0	0.026579	0.029463
B3_R50_C05	1.0738	161	-0.54656	1.0738	161	-0.49222	0	0	-0.054336	0.054336
B3_R50_C36	7.2249	160.99	-0.98644	7.2249	160.99	-0.96439	0	0	-0.022052	0.022052
B3_R50_C61	12.467	160.89	-1.1815	12.467	160.89	-1.1806	0	0	-0.00090653	0.00090653
B3_R50_C86	17.733	160.88	-1.2113	17.733	160.88	-1.2178	0	0	0.0065642	0.0065642
B3_R50_C99	20.705	160.82	-1.5104	20.695	160.82	-1.5154	0.0097648	0	0.0049853	0.010964
B3_R55_C05	1.1221	178.94	-0.62042	1.1221	178.94	-0.56659	0	0	-0.053824	0.053824

Name	X1	Y1	Z1	X2	Y2	Z2	dX	dY	dZ	dR
B3_R55_C36	7.2171	178.92	-0.94337	7.2171	178.92	-0.92835	0	0	-0.015016	0.015016
B3_R55_C61	12.466	178.91	-1.0429	12.466	178.91	-1.055	0	0	0.012112	0.012112
B3_R55_C86	17.746	178.89	-0.97562	17.746	178.89	-1.0019	0	0	0.026321	0.026321
B3_R55_C99	20.742	178.86	-1.2328	20.719	178.86	-1.248	0.023564	0	0.015196	0.028039
B3_R60_C05	1.0784	193.11	-0.65336	1.0784	193.11	-0.61716	0	0	-0.036207	0.036207
B3_R60_C36	7.2947	193.09	-0.91222	7.2947	193.09	-0.90275	0	0	-0.0094708	0.0094708
B3_R60_C61	12.492	193.05	-0.92267	12.492	193.05	-0.95655	0	0	0.033881	0.033881
B3_R60_C86	17.717	193	-0.79078	17.717	193	-0.83394	0	0	0.043159	0.043159
B3_R60_C99	20.758	192.96	-0.99709	20.734	192.96	-1.0387	0.024012	0	0.041625	0.048055
B3_R65_C05	1.0778	209.25	-0.6908	1.0778	209.25	-0.67972	0	0	-0.011079	0.011079
B3_R65_C36	7.2573	209.24	-0.85816	7.2573	209.24	-0.86947	0	0	0.011308	0.011308
B3_R65_C61	12.483	209.23	-0.82272	12.483	209.23	-0.84415	0	0	0.021427	0.021427
B3_R65_C86	17.73	209.21	-0.58775	17.73	209.21	-0.63985	0	0	0.052099	0.052099
B3_R65_C99	20.762	209.12	-0.75382	20.748	209.12	-0.79872	0.013305	0	0.044902	0.046831
B3_R70_C05	1.0697	221.86	-0.74806	1.0697	221.86	-0.7282	0	0	-0.019857	0.019857
B3_R70_C36	7.3061	221.86	-0.83404	7.3061	221.86	-0.84457	0	0	0.01053	0.01053
B3_R70_C61	12.509	221.85	-0.73144	12.509	221.85	-0.75562	0	0	0.024175	0.024175
B3_R70_C86	17.754	221.87	-0.4146	17.754	221.87	-0.48717	0	0	0.072577	0.072577
B3_R70_C99	20.745	221.75	-0.56771	20.757	221.75	-0.61105	-0.012408	0	0.043339	0.045081
B3_R75_C05	1.1136	241.35	-0.83032	1.1136	241.35	-0.79977	0	0	-0.030542	0.030542
B3_R75_C36	7.264	241.35	-0.78896	7.264	241.35	-0.80913	0	0	0.020168	0.020168
B3_R75_C61	12.52	241.35	-0.5714	12.52	241.35	-0.63043	0	0	0.059034	0.059034
B3_R75_C86	17.748	241.34	-0.19656	17.748	241.34	-0.27367	0	0	0.07711	0.07711
B3_R80_C05	1.1809	257.58	-0.87168	1.1809	257.58	-0.84759	0	0	-0.024094	0.024094
B3_R80_C36	7.3705	257.55	-0.7661	7.3705	257.55	-0.78307	0	0	0.016973	0.016973
B3_R80_C61	12.576	257.52	-0.48783	12.576	257.52	-0.54446	0	0	0.056623	0.056623
B3_R80_C86	17.802	257.51	-0.065099	17.802	257.51	-0.12727	0	0	0.062172	0.062172
B3_R86_C05	1.1432	276.27	-0.70666	1.1432	276.27	-0.69173	0	0	-0.014932	0.014932
B3_R86_C36	7.3679	276.23	-0.75449	7.3679	276.23	-0.75515	0	0	0.00066035	0.00066035
B3_R86_C61	12.56	276.17	-0.41003	12.56	276.17	-0.46401	0	0	0.053981	0.053981
B3_R86_C86	17.785	276.1	0.072209	17.785	276.1	0.006728	0	0	0.065481	0.065481
B3_R91_C05	1.2278	295.54	-0.81159	1.2278	295.54	-0.84632	0	0	0.03473	0.03473
B3_R91_C36	7.3489	295.51	-0.63342	7.3489	295.51	-0.67841	0	0	0.044981	0.044981
B3_R91_C61	12.588	295.52	-0.12079	12.588	295.52	-0.19228	0	0	0.071496	0.071496
B3_R91_C86	17.703	295.52	0.57326	17.703	295.52	0.45776	0	0	0.1155	0.1155
B3_R91_C99	20.732	295.45	0.74115	20.753	295.45	0.56675	-0.021159	0	0.1744	0.17568
B3_R97_C05	6.1304	313.3	-0.47133	6.1304	313.3	-0.67618	0	0	0.20486	0.20486
B3_R97_C36	12.316	313.29	-0.20189	12.316	313.29	-0.45889	0	0	0.25701	0.25701
B3_R97_C61	17.563	313.27	0.21118	17.563	313.27	-0.023158	0	0	0.23433	0.23433
B3_R97_C86	22.782	313.25	0.79502	22.782	313.25	0.56829	0	0	0.22673	0.22673
B3_R97_C99	25.758	313.11	0.88261	25.887	313.11	0.64965	-0.12887	0	0.23296	0.26622
HUB_LE	2.2067	30	-3.1726	2.19	30	-3.5	0.016653	0.0003389	0.32743	0.32785
HUB_TE	8.2054	29.999	-3.1834	8.19	30	-3.5	0.015444	-0.0014272	0.31656	0.31694
RMS Errors:							0.016738	0.00016504	0.09203	0.09354

8.2: Pitch and Flap Registration Plots (6 rows)

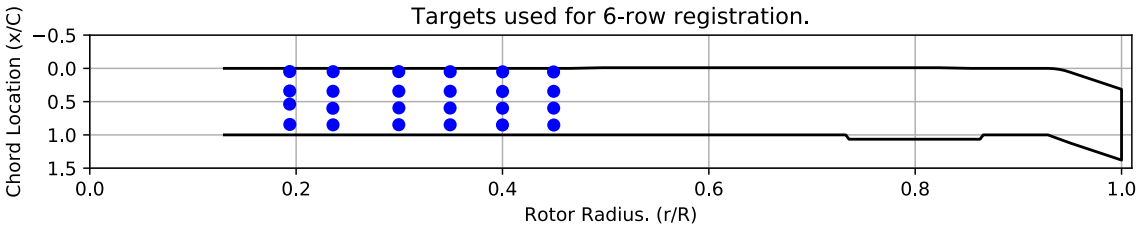

Figure 8-1. Targets used for 6 row root registration.

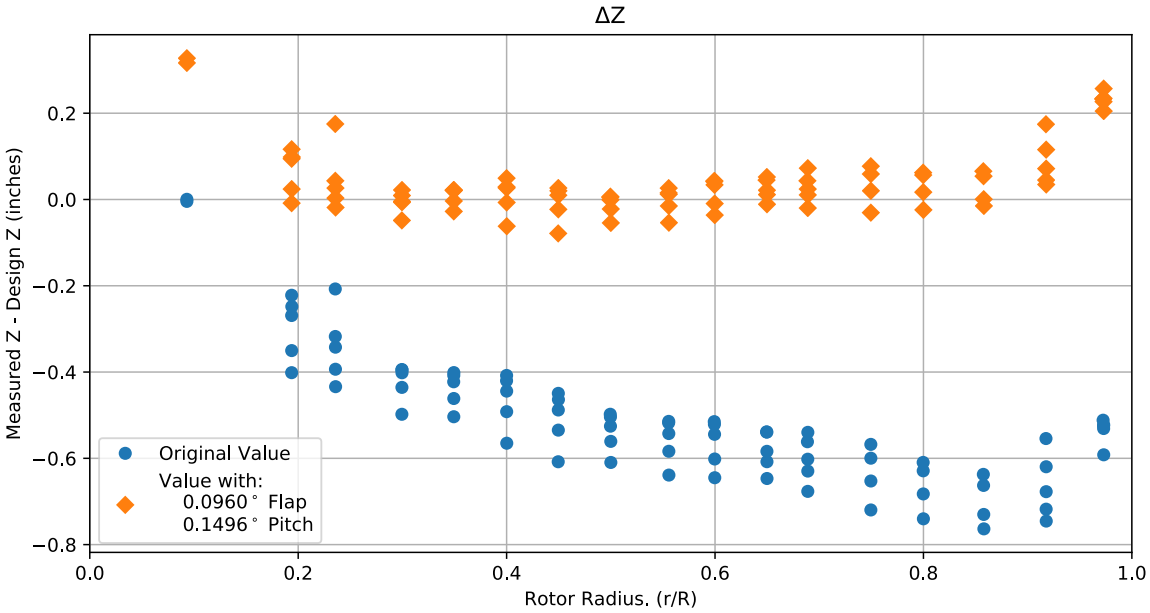

Figure 8-2. Pitch and flap target registration, ΔZ error vs rotor radius.

Note: the “as designed” geometry used for the swept tip may have some inaccuracies.

8.3: Estimated Bending and Twist at the Quarter Chord

The error bars shown represent the residual errors for fitting the measure target locations to the "as designed" geometry. These errors are generally much larger than those due to the VSTARS measurement errors. Therefore, the most likely source of these errors is the placement of the trailing-edge targets, differences between the "as designed" and "as built" geometries, and blade deformation during measurement. In the future, iterative adjustment of the "as designed" twist angle may be implemented to see if it reduces the fit error in delta twist. Note: The "as designed" geometry used for the swept tip may have some inaccuracies.

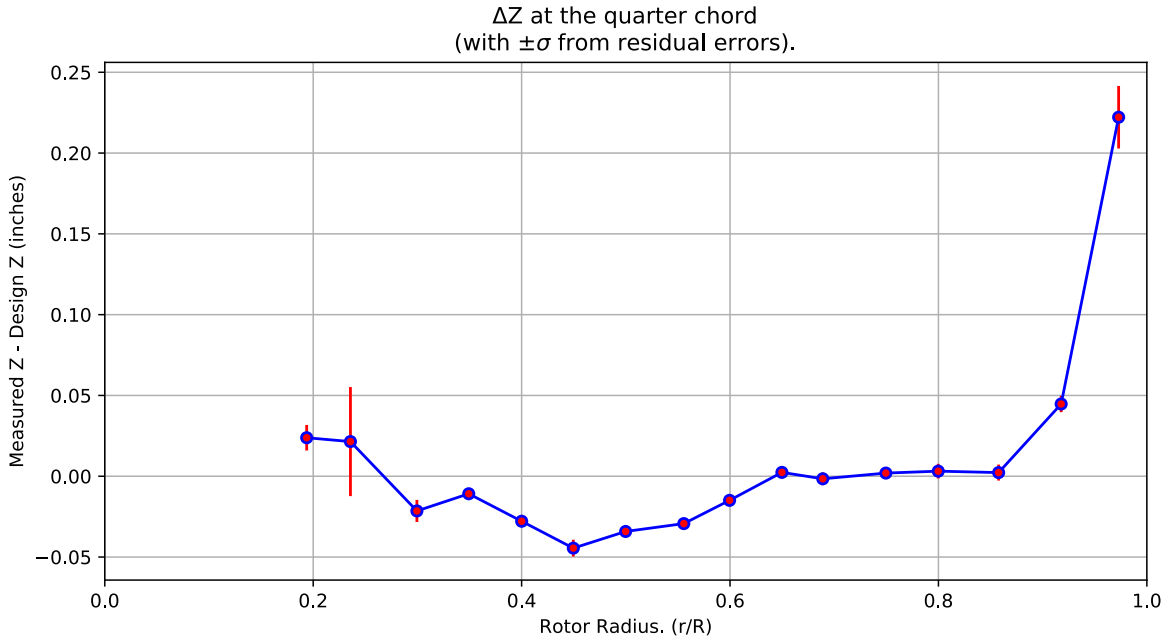

Figure 8-3. ΔZ error at the quarter chord vs rotor radius.

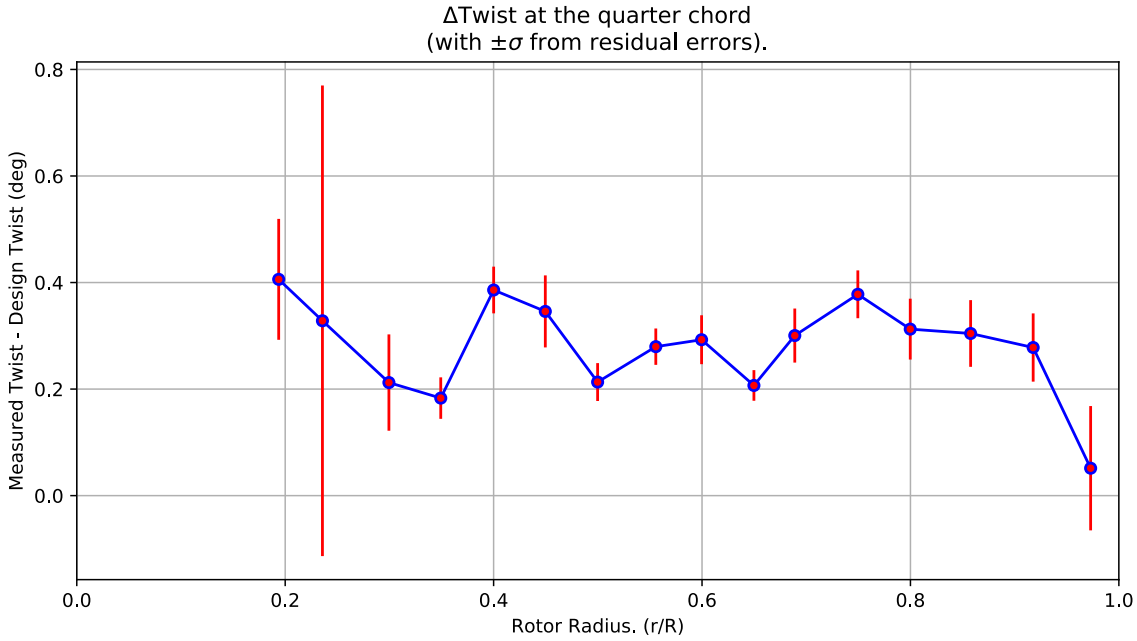

Figure 8-4. ΔTwist error at the quarter chord vs rotor radius.

Table 8-2. Quarter-chord bending and twist statistics.

r	r/R	dZ 1/4-chord	dT	sigma dZ meas	sigma dT meas	sigma dZ res	sigma dT res	n	t_conf
62.392	0.19376	0.023829	0.40598	6.0017e-10	4.7659e-09	0.0079054	0.1135	4	4.3027
75.908	0.23574	0.02145	0.3282	6.1338e-10	4.6496e-09	0.033754	0.44172	4	4.3027
96.448	0.29953	-0.021476	0.21223	6.1154e-10	4.6639e-09	0.0068261	0.090415	4	4.3027
112.47	0.34927	-0.010847	0.18308	6.1303e-10	4.6603e-09	0.0029635	0.038937	4	4.3027
128.81	0.40005	-0.027849	0.38598	6.1522e-10	4.6613e-09	0.0033713	0.043839	4	4.3027
144.77	0.44961	-0.044499	0.34579	6.1517e-10	4.6612e-09	0.0051988	0.067617	4	4.3027
160.94	0.49981	-0.034184	0.21319	6.1546e-10	4.6365e-09	0.002753	0.035568	4	4.3027
178.91	0.55564	-0.029308	0.27961	6.1648e-10	4.6453e-09	0.0026496	0.034131	4	4.3027
193.06	0.59958	-0.014917	0.29264	6.1681e-10	4.6445e-09	0.00357	0.045906	4	4.3027
209.23	0.64979	0.0023872	0.20681	6.1616e-10	4.6394e-09	0.0022322	0.02876	4	4.3027
221.86	0.68901	-0.0015822	0.30046	6.1693e-10	4.6326e-09	0.0039581	0.050738	4	4.3027
241.34	0.74952	0.001951	0.3779	6.1742e-10	4.6414e-09	0.0035043	0.044902	4	4.3027
257.54	0.79981	0.0031398	0.31255	6.2115e-10	4.6486e-09	0.0045281	0.057115	4	4.3027
276.19	0.85774	0.002264	0.30437	6.2006e-10	4.644e-09	0.0049437	0.062608	4	4.3027
295.52	0.91776	0.044712	0.27801	6.2202e-10	4.6828e-09	0.0050613	0.064056	4	4.3027
313.28	0.97291	0.22219	0.051452	9.1774e-10	4.6376e-09	0.019361	0.11667	4	4.3027

8.4: Section Plots

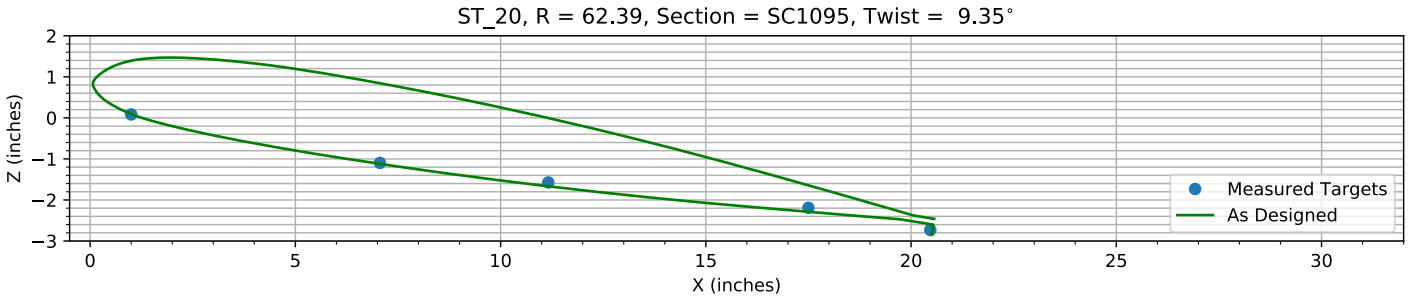

Figure 8-5. Target locations vs section profile at station 20.

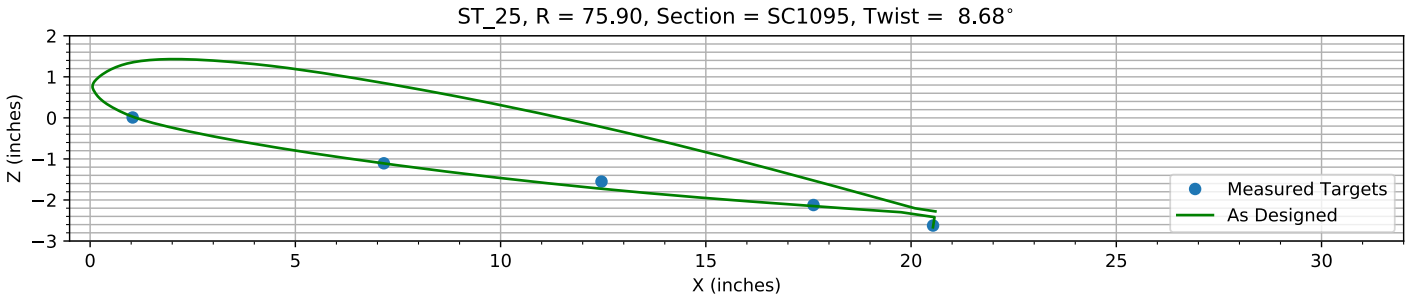

Figure 8-6. Target locations vs section profile at station 25.

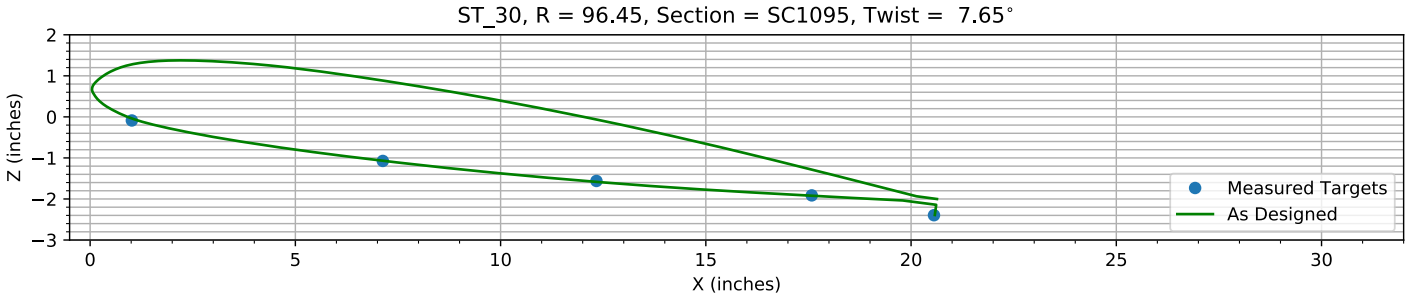

Figure 8-7. Target locations vs section profile at station 30.

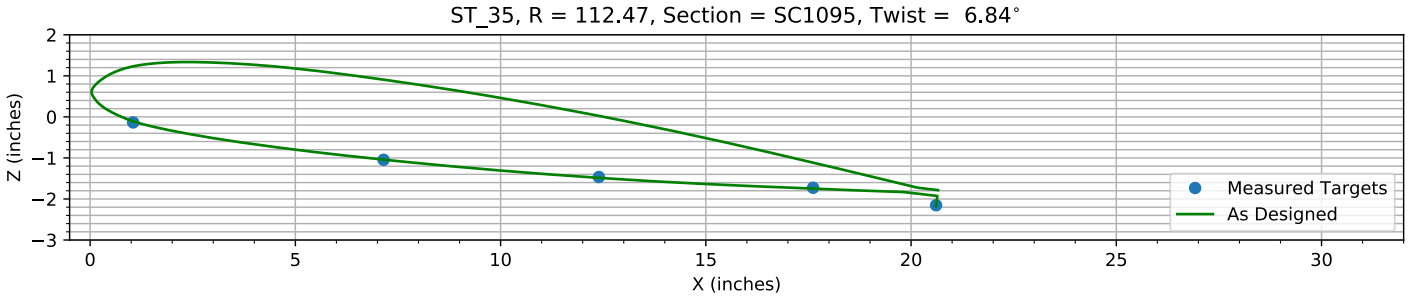

Figure 8-8. Target locations vs section profile at station 35.

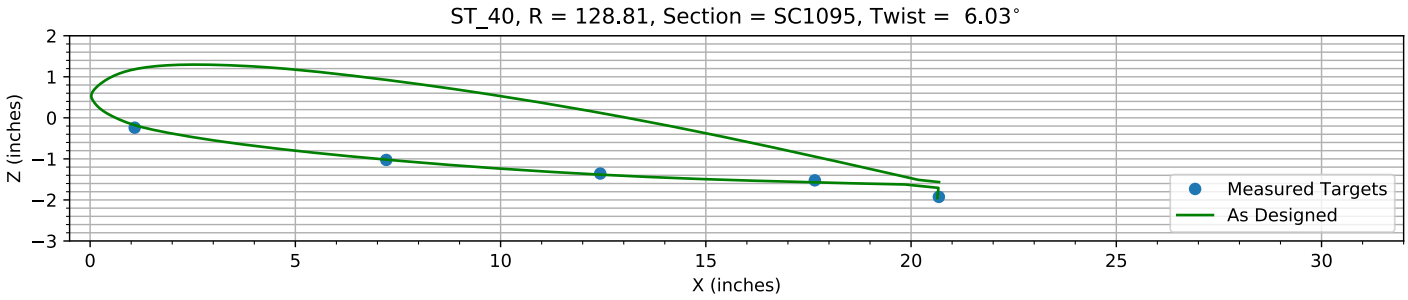

Figure 8-9. Target locations vs section profile at station 40.

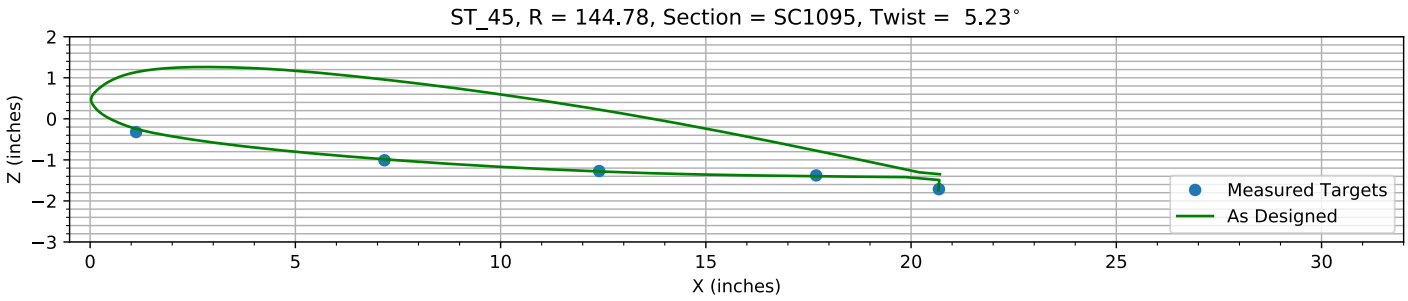

Figure 8-10. Target locations vs section profile at station 45.

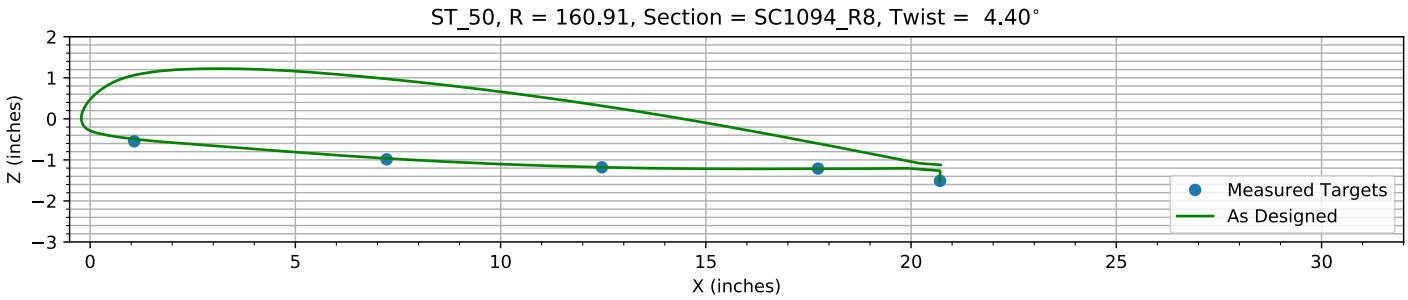

Figure 8-11. Target locations vs section profile at station 50.

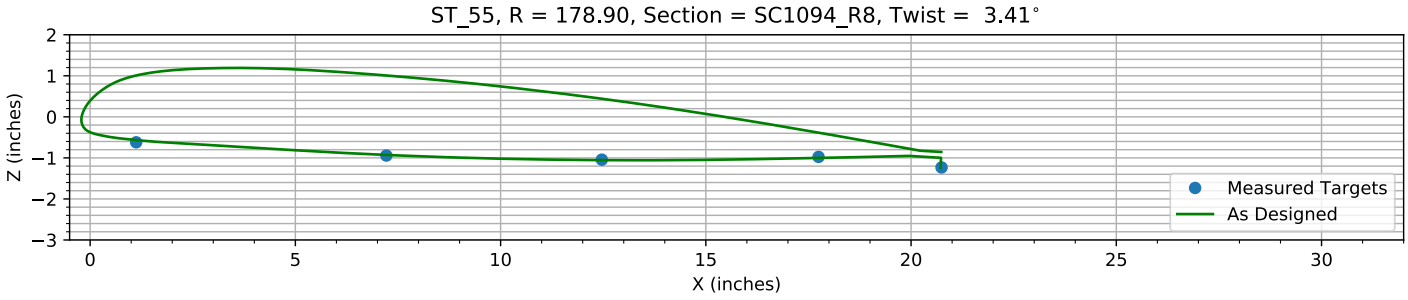

Figure 8-12. Target locations vs section profile at station 55.

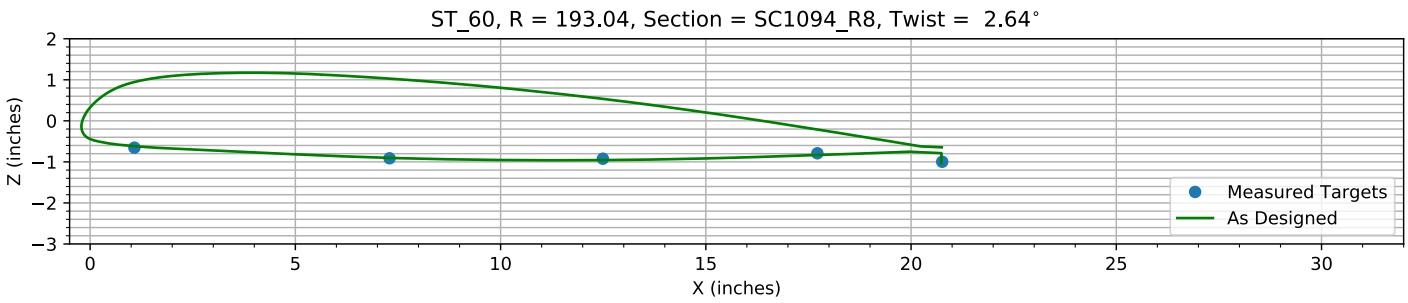

Figure 8-13. Target locations vs section profile at station 60.

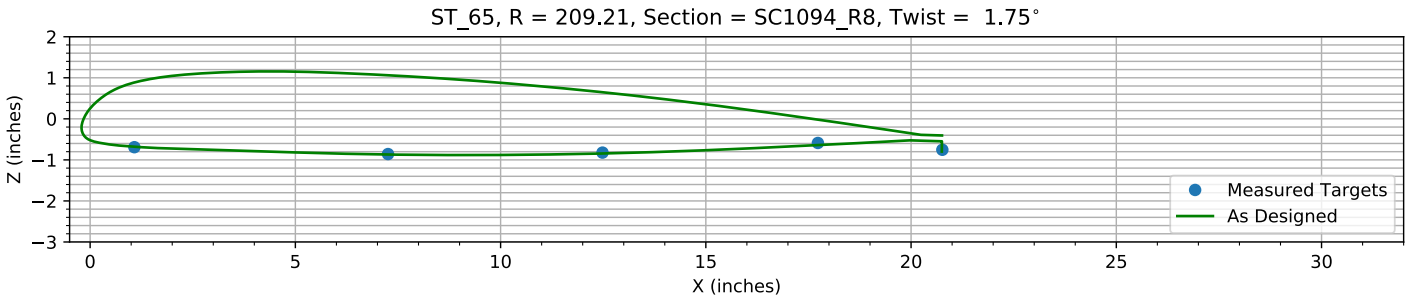

Figure 8-14. Target locations vs section profile at station 65.

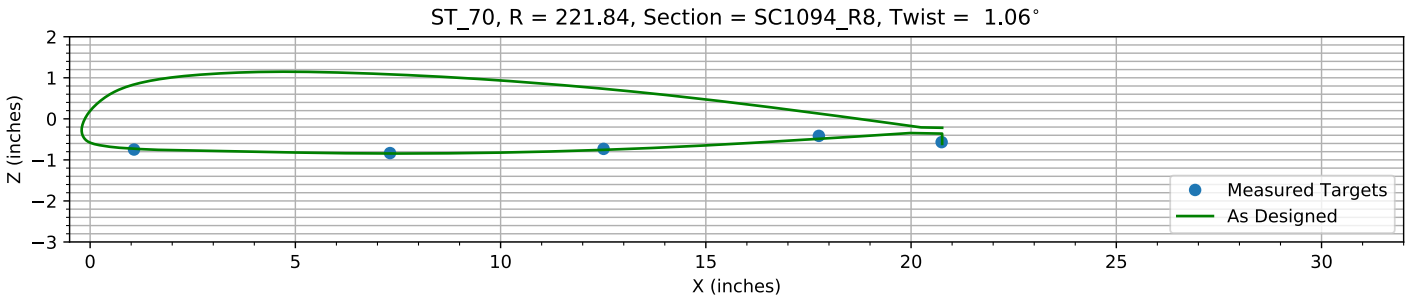

Figure 8-15. Target locations vs section profile at station 70.

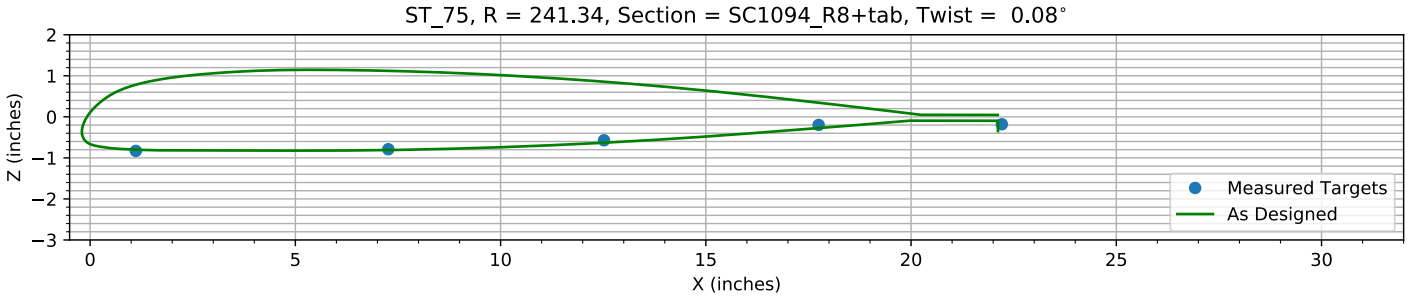

Figure 8-16. Target locations vs section profile at station 75.

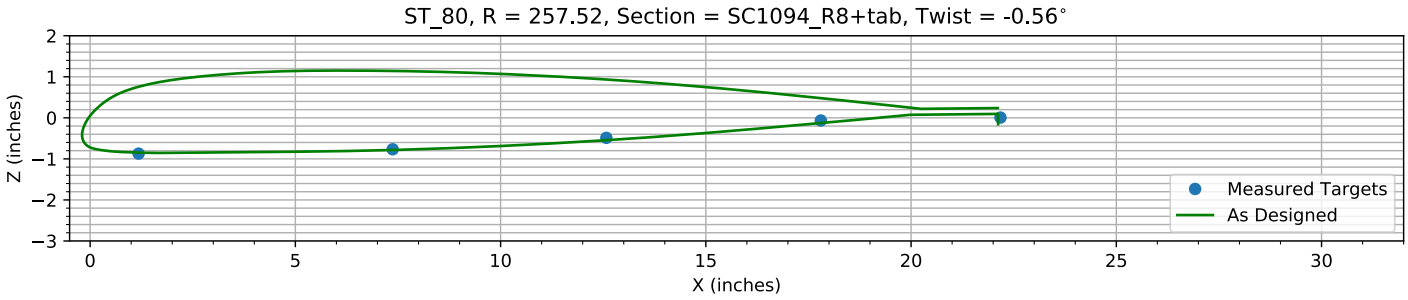

Figure 8-17. Target locations vs section profile at station 80.

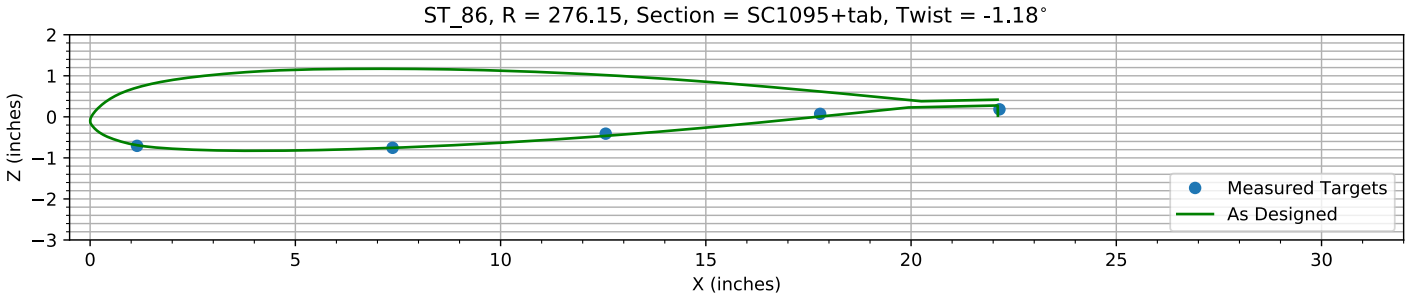

Figure 8-18. Target locations vs section profile at station 86.

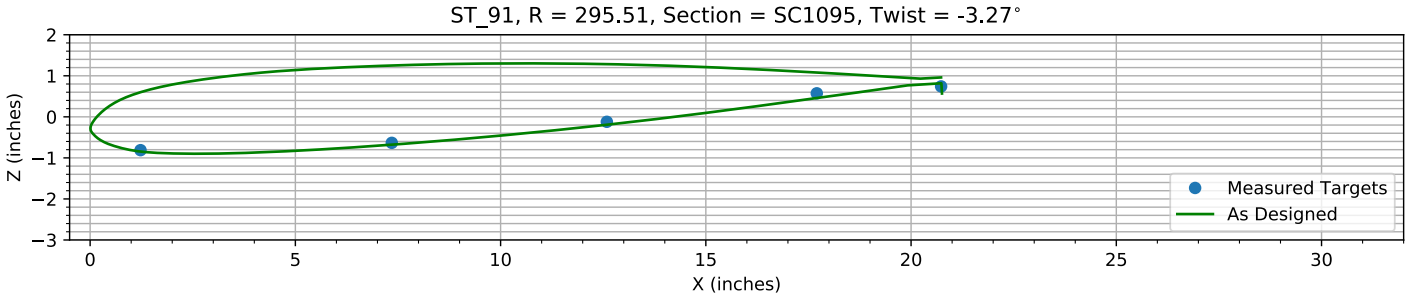

Figure 8-19. Target locations vs section profile at station 91.

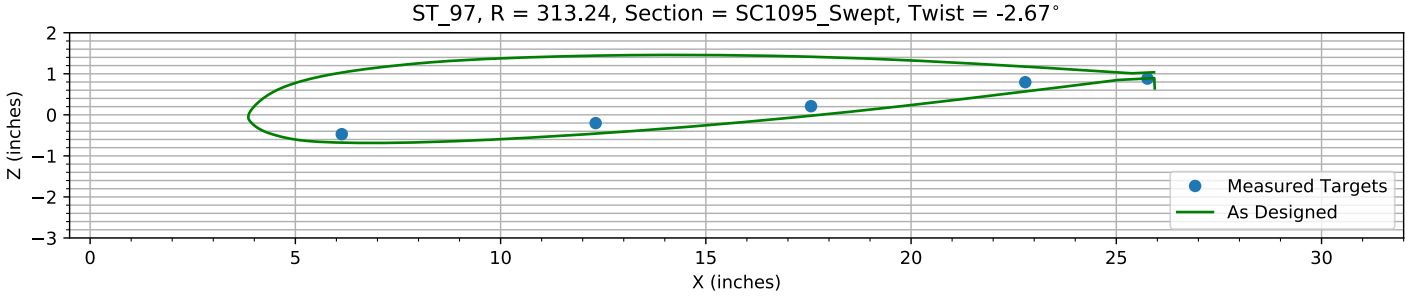

Figure 8-20. Target locations vs section profile at station 97.

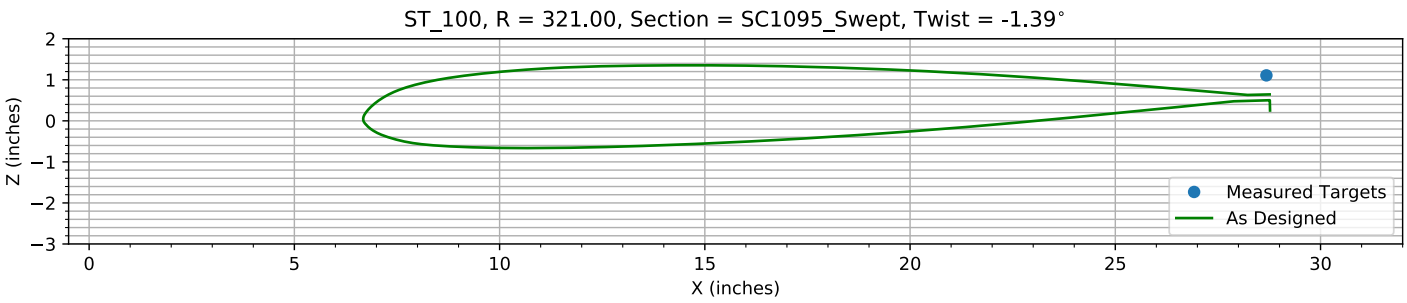

Figure 8-21. Target locations vs section profile at station 100.

Chapter 9: Pitch, Flap, and ΔZ Registration (15 rows)

The targets at the 15 spanwise stations nearest the root are used to determing the Z, flap, and pitch offset.

The estimated Z error, -0.35262 inches, is within an allowed range of ±2.000 inches.

The estimated flap error is -0.086276°.

The estimated pitch error is -0.18979°.

9.1: Target Location Errors After Target Registration

Table 9-1. Measured(1) with pitch and flap registration vs as designed(2) in inches.

Name	X1	Y1	Z1	X2	Y2	Z2	dX	dY	dZ	dR
B3_R20_C05	1.0034	62.373	0.10926	1.0034	62.373	0.090729	0	0	0.018534	0.018534
B3_R20_C36	7.0627	62.389	-1.0752	7.0627	62.389	-1.1213	0	0	0.046146	0.046146
B3_R20_C61	11.164	62.378	-1.554	11.164	62.378	-1.6675	0	0	0.11347	0.11347
B3_R20_C86	17.499	62.429	-2.1755	17.499	62.429	-2.2884	0	0	0.11291	0.11291
B3_R20_C99	20.469	62.382	-2.7189	20.501	62.382	-2.8477	-0.031759	0	0.1288	0.13266
B3_R25_C05	1.0385	75.952	0.033493	1.0385	75.952	0.027452	0	0	0.0060409	0.0060409
B3_R25_C36	7.1578	75.912	-1.0872	7.1578	75.912	-1.1101	0	0	0.022844	0.022844
B3_R25_C61	12.459	75.854	-1.5362	12.459	75.854	-1.7271	0	0	0.19086	0.19086
B3_R25_C86	17.623	75.915	-2.111	17.623	75.915	-2.1496	0	0	0.038582	0.038582
B3_R25_C99	20.536	75.87	-2.6129	20.533	75.87	-2.6662	0.0028028	0	0.053315	0.053389
B3_R30_C05	1.0189	96.432	-0.067404	1.0189	96.432	-0.039974	0	0	-0.027431	0.027431
B3_R30_C36	7.1322	96.448	-1.0576	7.1322	96.448	-1.0693	0	0	0.011646	0.011646
B3_R30_C61	12.336	96.472	-1.549	12.336	96.472	-1.5834	0	0	0.034375	0.034375
B3_R30_C86	17.582	96.443	-1.904	17.582	96.443	-1.9218	0	0	0.017831	0.017831
B3_R30_C99	20.559	96.472	-2.3892	20.579	96.472	-2.3893	-0.02007	0	0.00015834	0.020071
B3_R35_C05	1.0502	112.47	-0.11785	1.0502	112.47	-0.10848	0	0	-0.0093768	0.0093768
B3_R35_C36	7.151	112.48	-1.0326	7.151	112.48	-1.0424	0	0	0.0098591	0.0098591
B3_R35_C61	12.394	112.45	-1.4553	12.394	112.45	-1.4861	0	0	0.030843	0.030843
B3_R35_C86	17.614	112.47	-1.7204	17.614	112.47	-1.7486	0	0	0.028131	0.028131
B3_R35_C99	20.611	112.49	-2.1494	20.611	112.49	-2.174	2.0111e-05	0	0.02454	0.02454
B3_R40_C05	1.0878	128.84	-0.22513	1.0878	128.84	-0.17849	0	0	-0.046638	0.046638
B3_R40_C36	7.2165	128.81	-1.0153	7.2165	128.81	-1.0189	0	0	0.0036142	0.0036142
B3_R40_C61	12.43	128.81	-1.3504	12.43	128.81	-1.384	0	0	0.033646	0.033646
B3_R40_C86	17.657	128.79	-1.5197	17.657	128.79	-1.5721	0	0	0.052416	0.052416
B3_R40_C99	20.678	128.78	-1.9248	20.64	128.78	-1.9548	0.037927	0	0.029986	0.048349
B3_R45_C05	1.1221	144.74	-0.3102	1.1221	144.74	-0.24412	0	0	-0.06608	0.06608
B3_R45_C36	7.1722	144.78	-1.0014	7.1722	144.78	-0.98631	0	0	-0.015087	0.015087
B3_R45_C61	12.404	144.77	-1.2676	12.404	144.77	-1.2816	0	0	0.013915	0.013915
B3_R45_C86	17.69	144.81	-1.378	17.69	144.81	-1.3983	0	0	0.020339	0.020339
B3_R45_C99	20.68	144.78	-1.7147	20.666	144.78	-1.7395	0.013993	0	0.024772	0.028451
B3_R50_C05	1.0759	161	-0.53737	1.0759	161	-0.49247	0	0	-0.044898	0.044898
B3_R50_C36	7.2267	160.99	-0.98157	7.2267	160.99	-0.9645	0	0	-0.017067	0.017067
B3_R50_C61	12.469	160.89	-1.1803	12.469	160.89	-1.1806	0	0	0.00034503	0.00034503
B3_R50_C86	17.735	160.88	-1.2137	17.735	160.88	-1.2178	0	0	0.0040798	0.0040798
B3_R50_C99	20.706	160.82	-1.515	20.695	160.82	-1.5154	0.011177	0	0.00043001	0.011186
B3_R55_C05	1.1241	178.94	-0.61431	1.1241	178.94	-0.56679	0	0	-0.047517	0.047517

Name	X1	Y1	Z1	X2	Y2	Z2	dX	dY	dZ	dR
B3_R55_C36	7.2189	178.92	-0.94153	7.2189	178.92	-0.92843	0	0	-0.013107	0.013107
B3_R55_C61	12.468	178.91	-1.0447	12.468	178.91	-1.055	0	0	0.010272	0.010272
B3_R55_C86	17.748	178.89	-0.98117	17.748	178.89	-1.0019	0	0	0.020733	0.020733
B3_R55_C99	20.744	178.86	-1.2404	20.719	178.86	-1.248	0.025161	0	0.0075462	0.026268
B3_R60_C05	1.0804	193.11	-0.64964	1.0804	193.11	-0.61733	0	0	-0.032306	0.032306
B3_R60_C36	7.2965	193.09	-0.91285	7.2965	193.09	-0.9028	0	0	-0.01005	0.01005
B3_R60_C61	12.494	193.05	-0.92694	12.494	193.05	-0.95653	0	0	0.029593	0.029593
B3_R60_C86	17.719	193	-0.79871	17.719	193	-0.83387	0	0	0.035161	0.035161
B3_R60_C99	20.76	192.96	-1.0071	20.734	192.96	-1.0387	0.025767	0	0.031565	0.040747
B3_R65_C05	1.0797	209.25	-0.68982	1.0797	209.25	-0.67987	0	0	-0.0099569	0.0099569
B3_R65_C36	7.2592	209.24	-0.86151	7.2592	209.24	-0.8695	0	0	0.0079814	0.0079814
B3_R65_C61	12.485	209.23	-0.82974	12.485	209.23	-0.8441	0	0	0.014364	0.014364
B3_R65_C86	17.732	209.21	-0.59844	17.732	209.21	-0.63974	0	0	0.041299	0.041299
B3_R65_C99	20.764	209.12	-0.76663	20.748	209.12	-0.79872	0.015221	0	0.03209	0.035517
B3_R70_C05	1.0716	221.86	-0.74922	1.0716	221.86	-0.72832	0	0	-0.0209	0.0209
B3_R70_C36	7.308	221.86	-0.83957	7.308	221.86	-0.84457	0	0	0.0050002	0.0050002
B3_R70_C61	12.511	221.85	-0.74062	12.511	221.85	-0.75554	0	0	0.014922	0.014922
B3_R70_C86	17.756	221.87	-0.42746	17.756	221.87	-0.48704	0	0	0.059575	0.059575
B3_R70_C99	20.747	221.75	-0.58265	20.757	221.75	-0.61105	-0.010369	0	0.028391	0.030225
B3_R75_C05	1.1155	241.35	-0.83482	1.1155	241.35	-0.79985	0	0	-0.034966	0.034966
B3_R75_C36	7.2659	241.35	-0.79778	7.2659	241.35	-0.8091	0	0	0.011321	0.011321
B3_R75_C61	12.522	241.35	-0.5839	12.522	241.35	-0.63032	0	0	0.04642	0.04642
B3_R75_C86	17.75	241.34	-0.21273	17.75	241.34	-0.27349	0	0	0.060755	0.060755
B3_R80_C05	1.1827	257.58	-0.87899	1.1827	257.58	-0.84764	0	0	-0.031352	0.031352
B3_R80_C36	7.3724	257.55	-0.77775	7.3724	257.55	-0.78302	0	0	0.0052754	0.0052754
B3_R80_C61	12.578	257.52	-0.50313	12.578	257.52	-0.54432	0	0	0.041192	0.041192
B3_R80_C86	17.804	257.51	-0.084058	17.804	257.51	-0.12705	0	0	0.042996	0.042996
B3_R86_C05	1.1451	276.27	-0.71712	1.1451	276.27	-0.69204	0	0	-0.025078	0.025078
B3_R86_C36	7.3698	276.23	-0.76931	7.3698	276.23	-0.75508	0	0	-0.014233	0.014233
B3_R86_C61	12.563	276.17	-0.42849	12.563	276.17	-0.46385	0	0	0.035363	0.035363
B3_R86_C86	17.788	276.1	0.050099	17.788	276.1	0.0069773	0	0	0.043122	0.043122
B3_R91_C05	1.2297	295.54	-0.82539	1.2297	295.54	-0.84654	0	0	0.021149	0.021149
B3_R91_C36	7.3509	295.51	-0.65151	7.3509	295.51	-0.67826	0	0	0.026745	0.026745
B3_R91_C61	12.591	295.52	-0.14255	12.591	295.52	-0.19202	0	0	0.049463	0.049463
B3_R91_C86	17.706	295.52	0.54791	17.706	295.52	0.45816	0	0	0.089751	0.089751
B3_R91_C99	20.735	295.45	0.71368	20.753	295.45	0.56677	-0.018242	0	0.14691	0.14804
B3_R97_C05	6.1325	313.3	-0.49159	6.1325	313.3	-0.67622	0	0	0.18464	0.18464
B3_R97_C36	12.318	313.29	-0.22648	12.318	313.29	-0.45876	0	0	0.23227	0.23227
B3_R97_C61	17.565	313.27	0.1829	17.565	313.27	-0.022937	0	0	0.20584	0.20584
B3_R97_C86	22.785	313.25	0.76309	22.785	313.25	0.5686	0	0	0.19448	0.19448
B3_R97_C99	25.761	313.11	0.84861	25.887	313.11	0.64963	-0.12612	0	0.19898	0.23558
HUB_LE	2.207	30	-3.1419	2.19	30	-3.5	0.016978	0.00035022	0.35811	0.35851
HUB_TE	8.2058	29.999	-3.157	8.19	30	-3.5	0.01576	-0.0014151	0.34303	0.3434
RMS Errors:							0.016532	0.00016401	0.088884	0.090409

9.2: Pitch and Flap Registration Plots (15 rows)

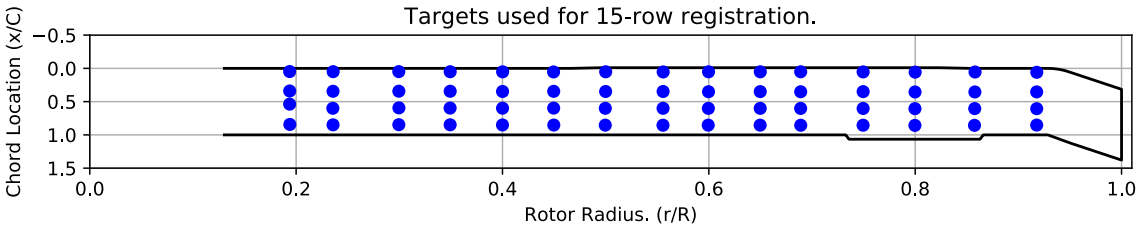

Figure 9-1. Targets used for 15 row root registration.

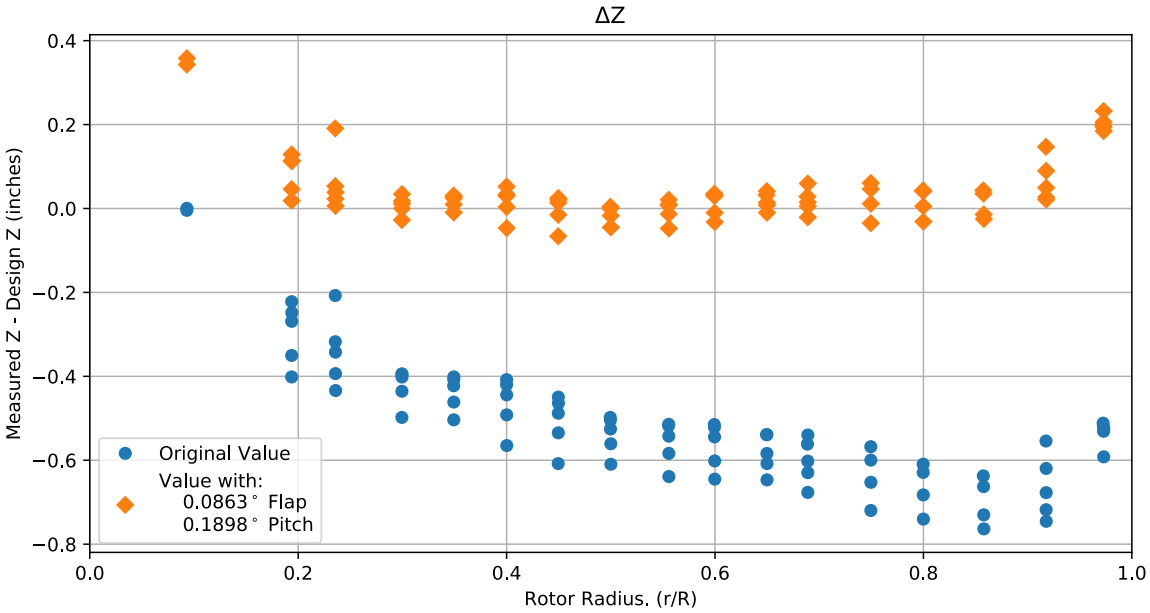

Figure 9-2. Pitch and flap target registration, ΔZ error vs rotor radius.

Note: the “as designed” geometry used for the swept tip may have some inaccuracies.

9.3: Estimated Bending and Twist at the Quarter Chord

The error bars shown represent the residual errors for fitting the measure target locations to the "as designed" geometry. These errors are generally much larger than those due to the VSTARS measurement errors. Therefore, the most likely source of these errors is the placement of the trailing-edge targets, differences between the "as designed" and "as built" geometries, and blade deformation during measurement. In the future, iterative adjustment of the "as designed" twist angle may be implemented to see if it reduces the fit error in delta twist. Note: The "as designed" geometry used for the swept tip may have some inaccuracies.

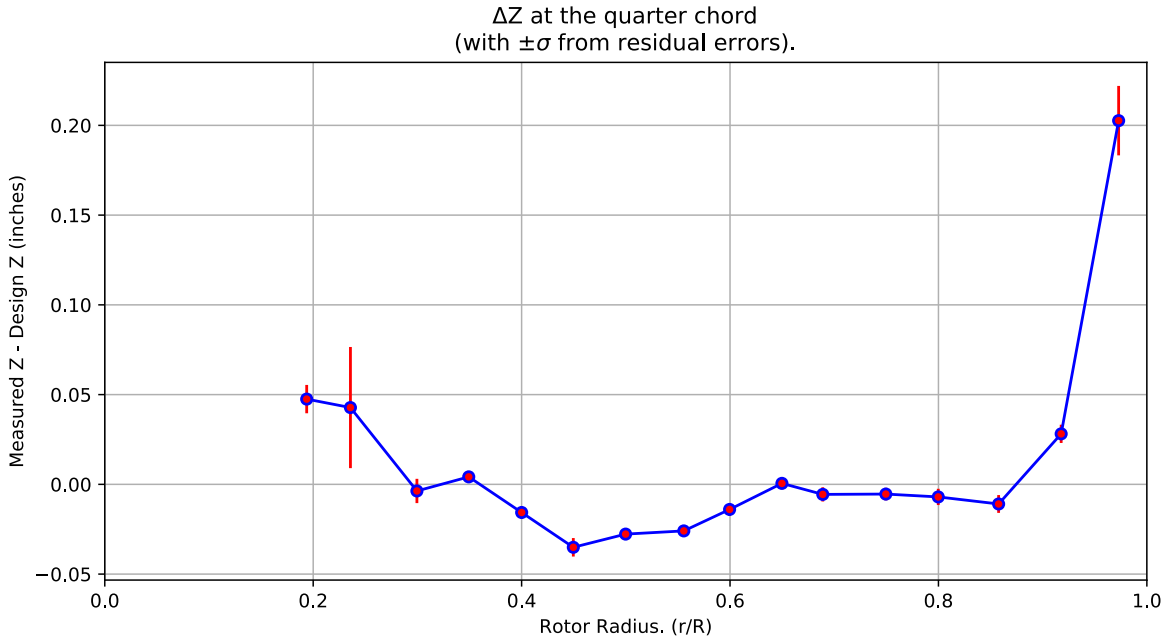

Figure 9-3. ΔZ error at the quarter chord vs rotor radius.

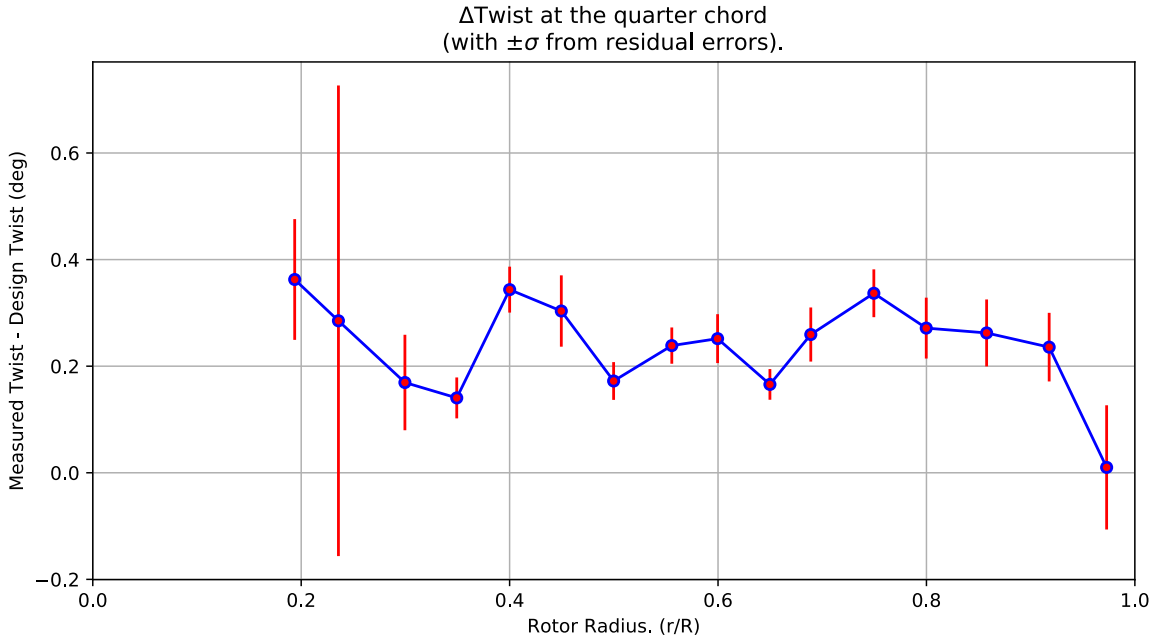

Figure 9-4. ΔTwist error at the quarter chord vs rotor radius.

Table 9-2. Quarter-chord bending and twist statistics.

r	r/R	dZ 1/4-chord	dT	sigma dZ meas	sigma dT meas	sigma dZ res	sigma dT res	n	t_conf
62.392	0.19377	0.047496	0.36265	6.0026e-10	4.7664e-09	0.0078941	0.11329	4	4.3027
75.908	0.23574	0.042782	0.28517	6.1348e-10	4.65e-09	0.03375	0.44151	4	4.3027
96.449	0.29953	-0.003686	0.16937	6.1163e-10	4.6643e-09	0.0067649	0.08957	4	4.3027
112.47	0.34927	0.0041693	0.14046	6.1313e-10	4.6607e-09	0.0029235	0.038396	4	4.3027
128.82	0.40005	-0.015676	0.34364	6.1531e-10	4.6616e-09	0.003314	0.043077	4	4.3027
144.77	0.44961	-0.035072	0.3035	6.1527e-10	4.6614e-09	0.0051476	0.066924	4	4.3027
160.94	0.49981	-0.027719	0.1722	6.1555e-10	4.6366e-09	0.0027442	0.035439	4	4.3027
178.92	0.55564	-0.025936	0.23862	6.1657e-10	4.6454e-09	0.0026426	0.034026	4	4.3027
193.06	0.59958	-0.01398	0.25168	6.169e-10	4.6446e-09	0.0035693	0.045878	4	4.3027
209.23	0.6498	0.00054822	0.1658	6.1626e-10	4.6394e-09	0.0022362	0.028799	4	4.3027
221.86	0.68901	-0.0055943	0.25939	6.1702e-10	4.6326e-09	0.0039615	0.05076	4	4.3027
241.35	0.74952	-0.0054134	0.3368	6.1751e-10	4.6413e-09	0.0035035	0.044873	4	4.3027
257.54	0.79981	-0.0070026	0.27146	6.2124e-10	4.6484e-09	0.0045297	0.05711	4	4.3027
276.19	0.85775	-0.010934	0.26237	6.2015e-10	4.6439e-09	0.0049622	0.062813	4	4.3027
295.52	0.91777	0.028143	0.23572	6.2211e-10	4.6826e-09	0.0050887	0.064371	4	4.3027
313.28	0.97291	0.20263	0.010095	9.1787e-10	4.6374e-09	0.019345	0.11655	4	4.3027

9.4: Section Plots

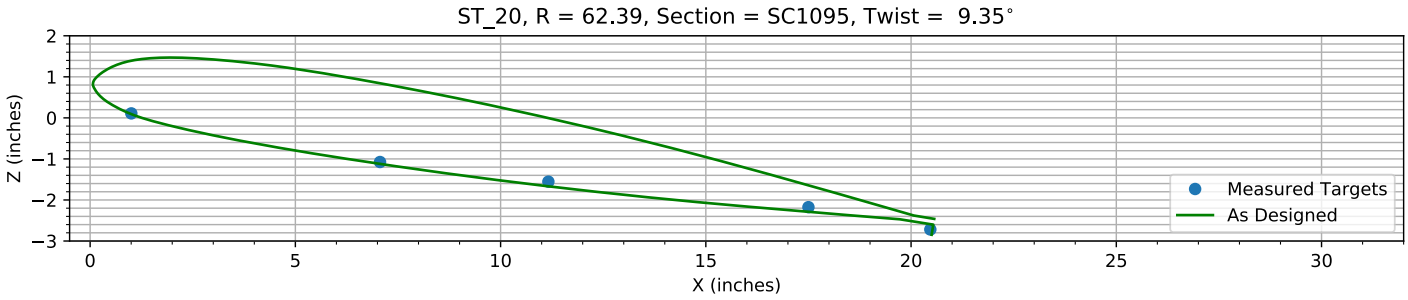

Figure 9-5. Target locations vs section profile at station 20.

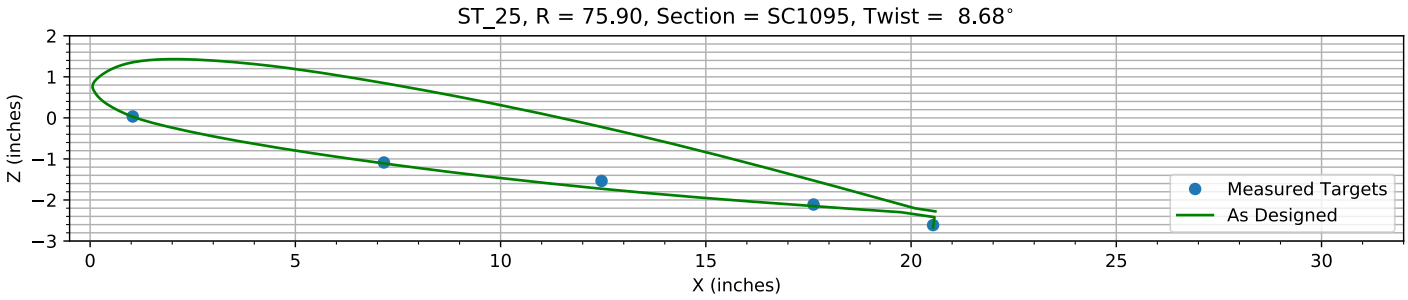

Figure 9-6. Target locations vs section profile at station 25.

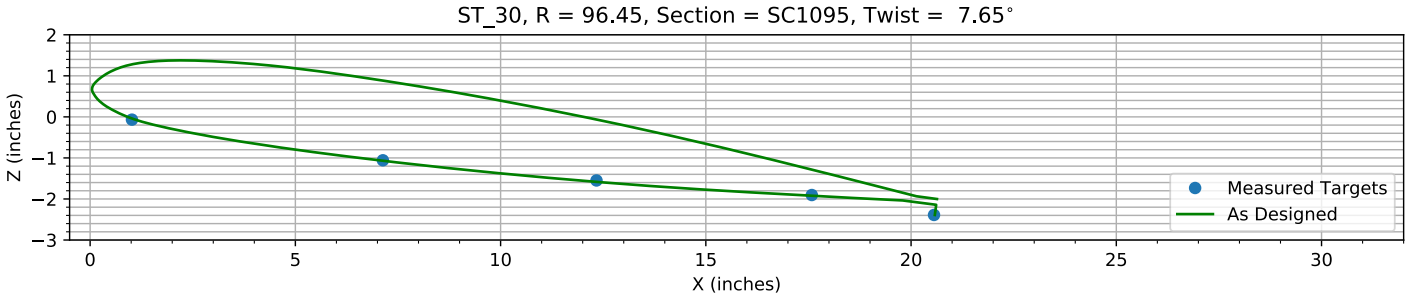

Figure 9-7. Target locations vs section profile at station 30.

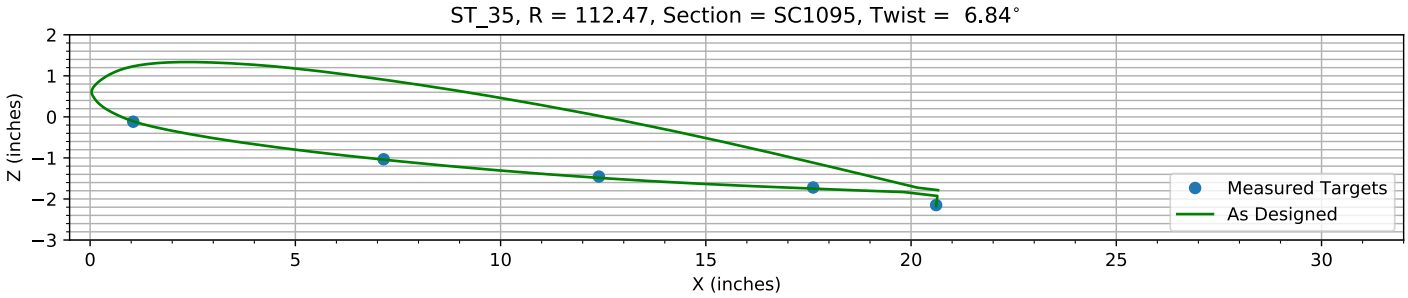

Figure 9-8. Target locations vs section profile at station 35.

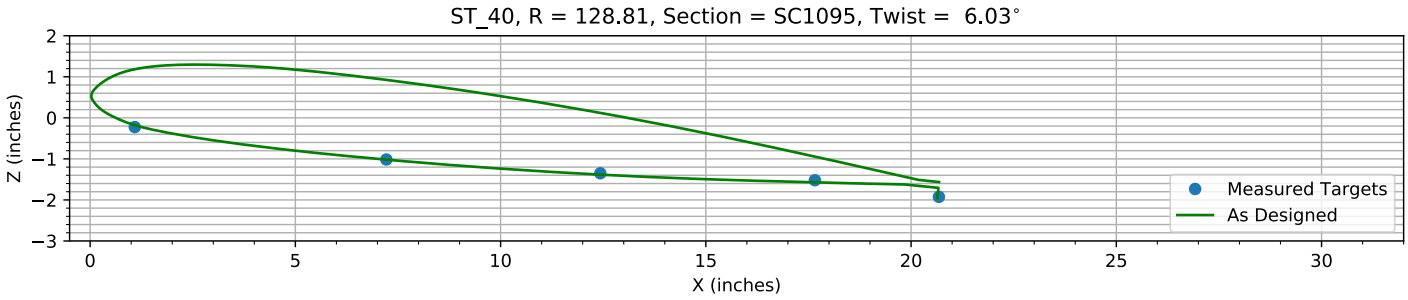

Figure 9-9. Target locations vs section profile at station 40.

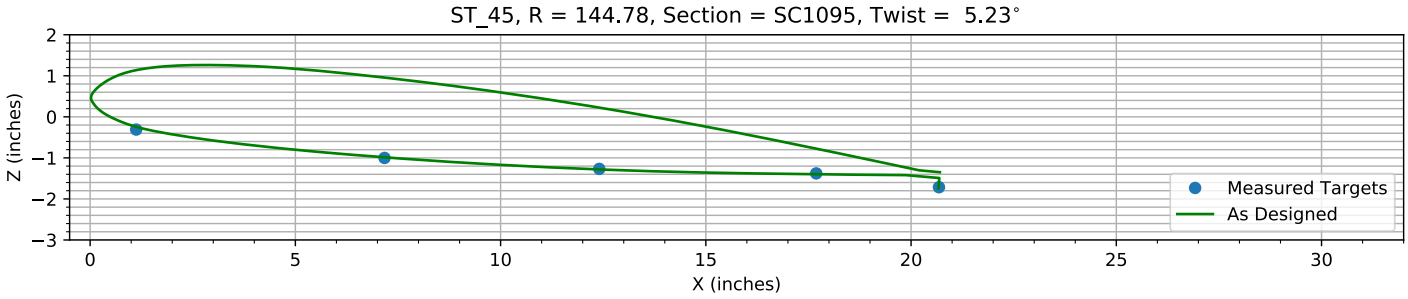

Figure 9-10. Target locations vs section profile at station 45.

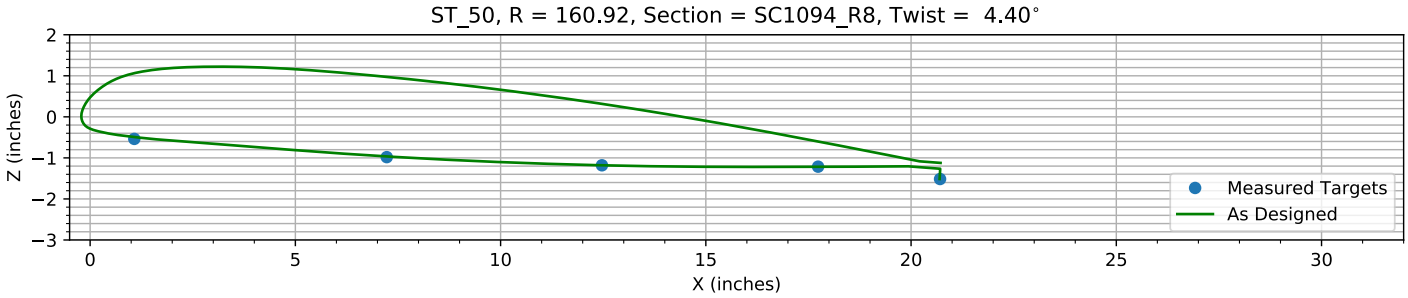

Figure 9-11. Target locations vs section profile at station 50.

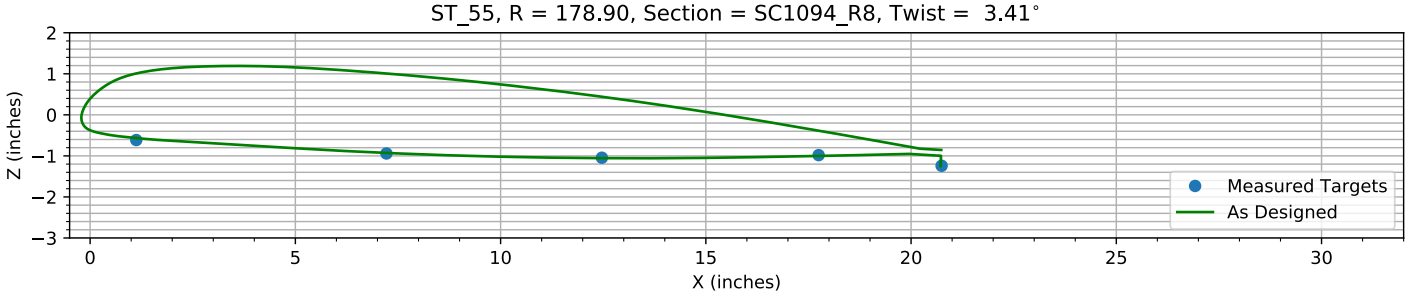

Figure 9-12. Target locations vs section profile at station 55.

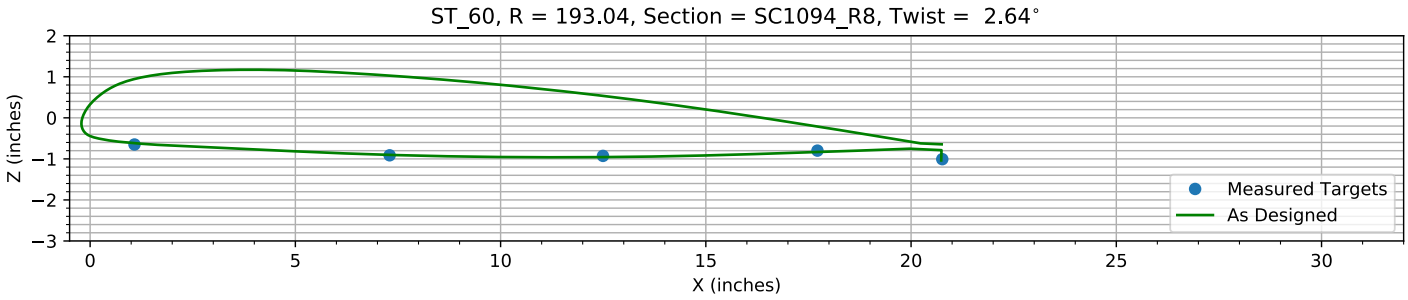

Figure 9-13. Target locations vs section profile at station 60.

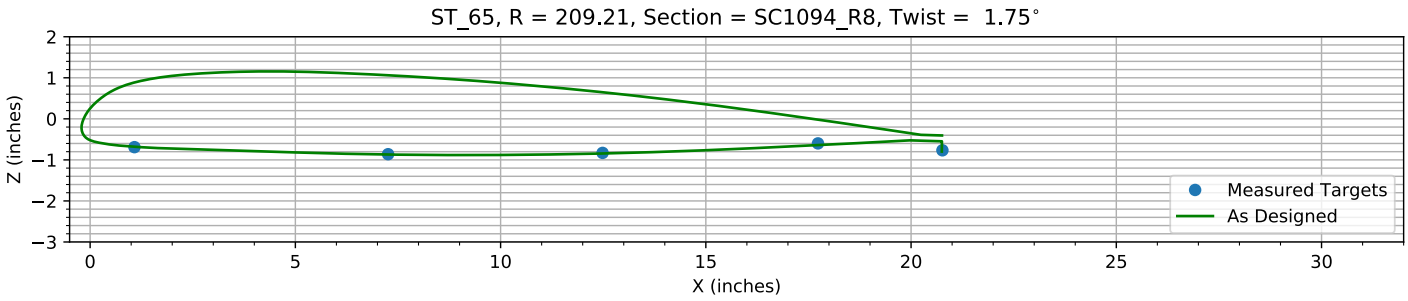

Figure 9-14. Target locations vs section profile at station 65.

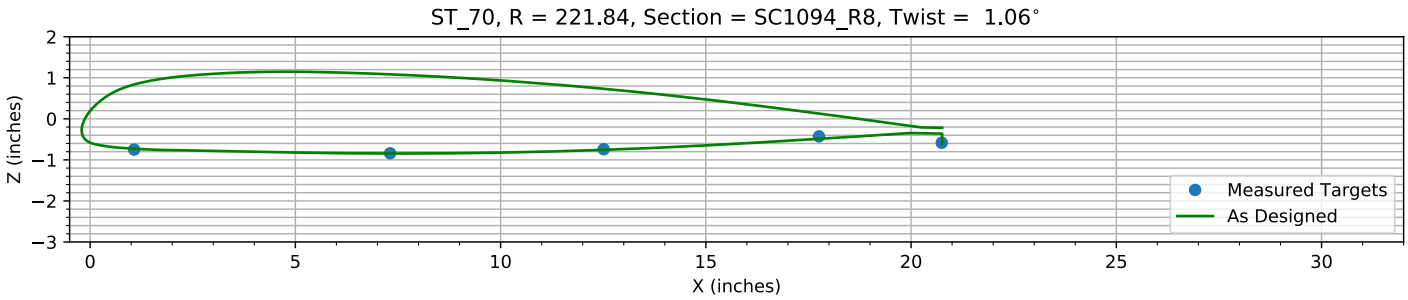

Figure 9-15. Target locations vs section profile at station 70.

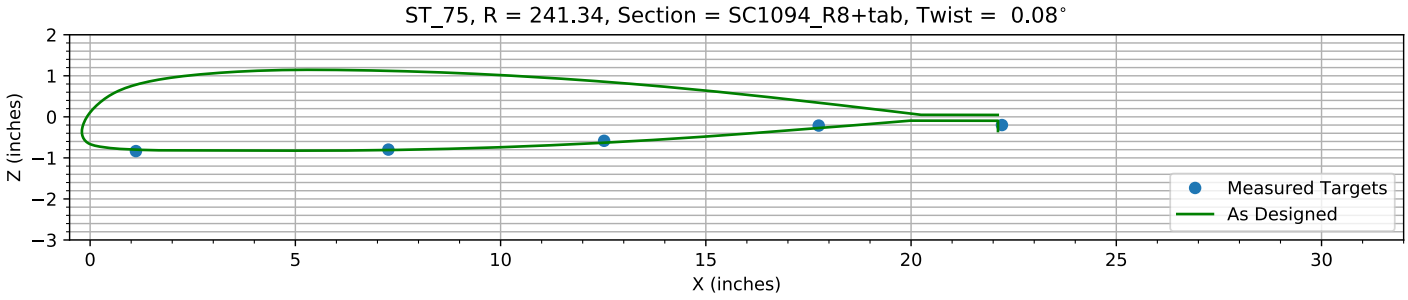

Figure 9-16. Target locations vs section profile at station 75.

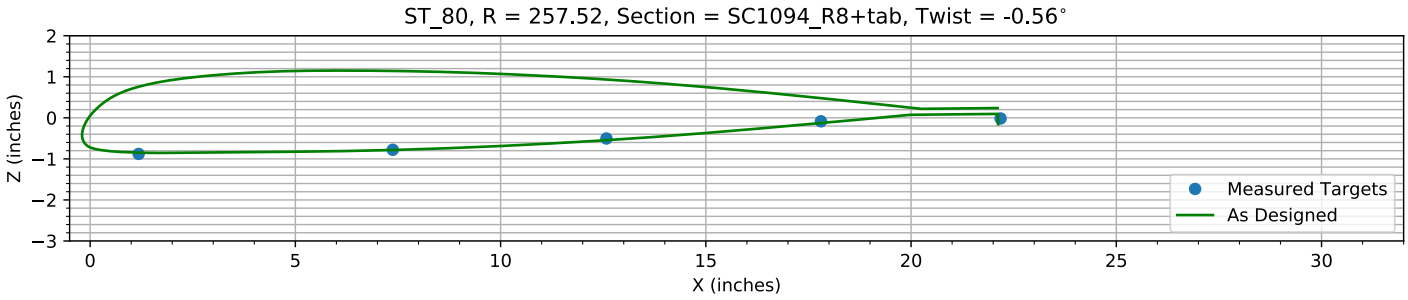

Figure 9-17. Target locations vs section profile at station 80.

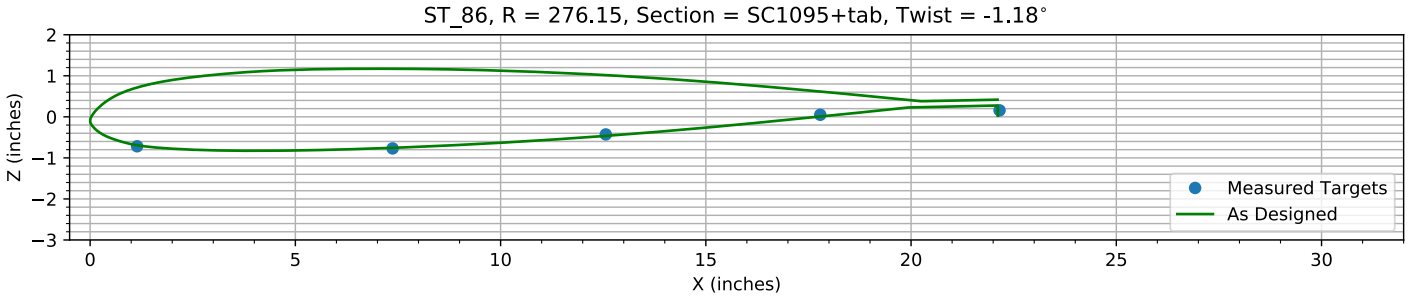

Figure 9-18. Target locations vs section profile at station 86.

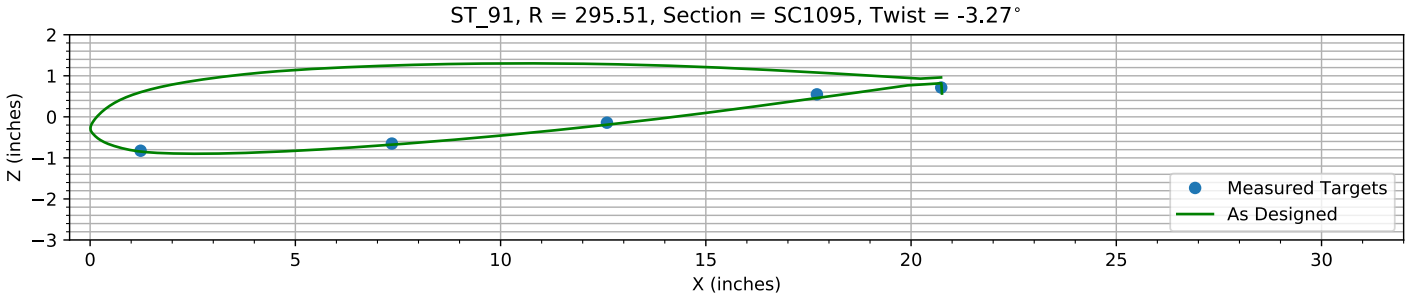

Figure 9-19. Target locations vs section profile at station 91.

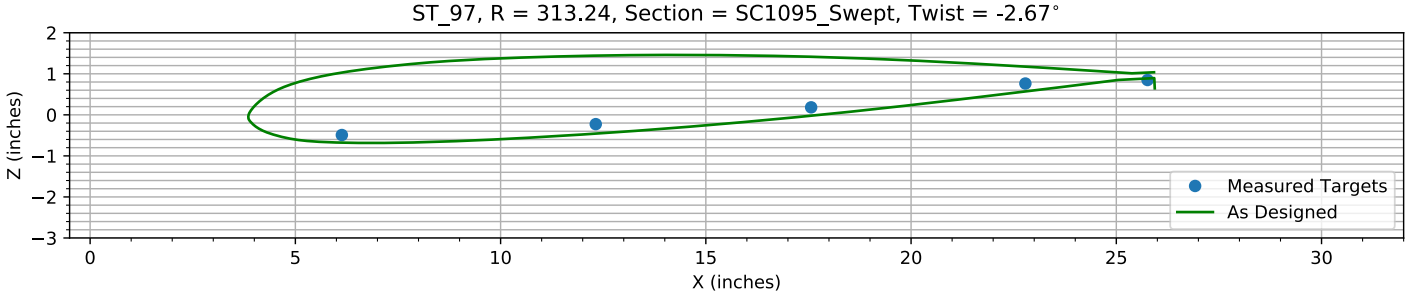

Figure 9-20. Target locations vs section profile at station 97.

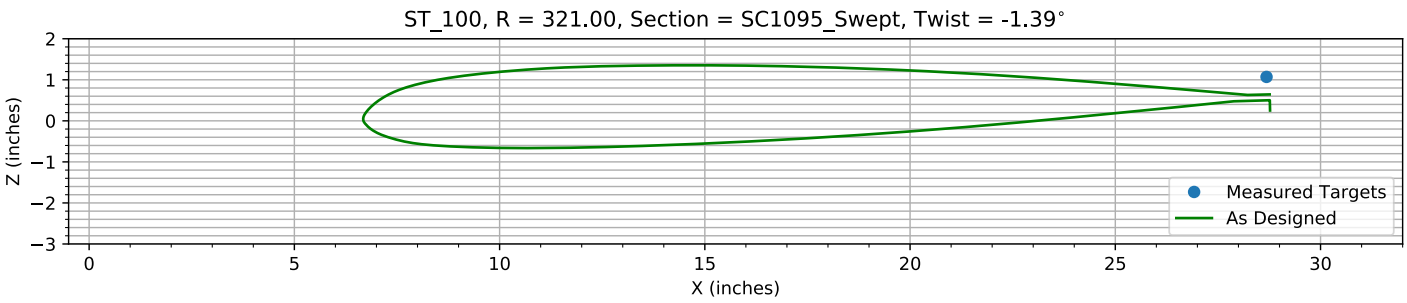

Figure 9-21. Target locations vs section profile at station 100.

I.4 Blade 4

The blade target registration report for Blade 4 is included here. It is based on the most recent V-STARS target location data for the vertically suspended blade. The condition of targets 4, 12 and 15 had degraded too much for the V-STARS system to measure them for this last measurement session, so their locations were estimated based on their relative distance to nearby targets from previous V-STARS measurements.

Blade Target

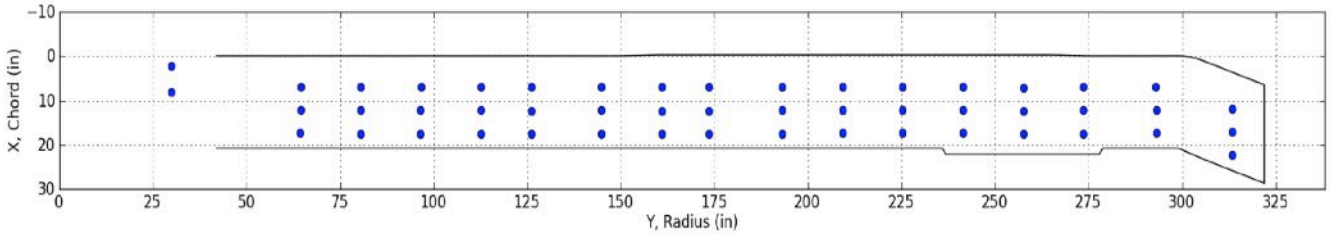

Registration

Registration Report for Blade Number 4

File: Blade 4 091812 vertical(1)_4_12_15.csv

Z reference allowed ±2.00 inches of travel

Aeromechanics Branch
Flight Vehicle Research and Technology Division
NASA Ames Research Center
Moffett Field, CA 94035

Chapter 1: VSTARS Target Location Data

Table 1-1. VSTARS target measurements (inches).

Name	Number	X	Y	Z	sigma X	sigma Y	sigma Z
B4_R20_C05		1.0519	64.451	-0.1436	0.0004	0.0004	0.0009
B4_R20_C36	1	7.1239	64.417	-1.2871	0.0005	0.0005	0.0012
B4_R20_C61	2	12.297	64.414	-1.888	0.0004	0.0004	0.0009
B4_R20_C86	3	17.518	64.42	-2.3708	0.0005	0.0005	0.0008
B4_R20_C99		20.49	64.384	-2.9317	0.0003	0.0003	0.0005
B4_R25_C05		1.0153	80.581	-0.1364	0.0004	0.0003	0.0008
B4_R25_C61	5	12.339	80.565	-1.7801	0.0003	0.0003	0.0007
B4_R25_C86	6	17.576	80.571	-2.1811	0.0004	0.0004	0.001
B4_R25_C99		20.529	80.573	-2.7497	0.0003	0.0003	0.0005
B4_R30_C05		1.0416	96.654	-0.1378	0.0003	0.0003	0.0007
B4_R30_C36	7	7.1207	96.655	-1.1202	0.0004	0.0003	0.0006
B4_R30_C61	8	12.366	96.628	-1.6056	0.0004	0.0004	0.0008
B4_R30_C86	9	17.611	96.626	-1.9415	0.0003	0.0003	0.0008
B4_R30_C99		20.565	96.571	-2.4726	0.0003	0.0003	0.0005
B4_R35_C05		1.0702	112.71	-0.1269	0.0003	0.0003	0.0007
B4_R35_C36	10	7.1656	112.76	-1.0091	0.0004	0.0004	0.0008
B4_R35_C61	11	12.382	112.73	-1.397	0.0004	0.0004	0.0009
B4_R35_C99		20.645	112.76	-2.1464	0.0003	0.0003	0.0005
B4_R40_C05		1.1313	128.84	-0.1282	0.0003	0.0003	0.0006
B4_R40_C36	13	7.2177	128.84	-0.9052	0.0005	0.0004	0.0006
B4_R40_C61	14	12.465	128.86	-1.247	0.0003	0.0004	0.0008
B4_R40_C99		20.676	128.86	-1.8538	0.0003	0.0003	0.0005
B4_R45_C05		1.0568	144.91	-0.1055	0.0003	0.0003	0.0007
B4_R45_C36	16	7.1603	144.88	-0.8036	0.0006	0.0005	0.0007
B4_R45_C61	17	12.392	144.88	-1.0742	0.0004	0.0004	0.0007
B4_R45_C86	18	17.651	144.89	-1.1853	0.0006	0.0005	0.0006
B4_R45_C99		20.674	144.89	-1.5586	0.0003	0.0003	0.0004
B4_R50_C05		1.0872	161.09	-0.2537	0.0003	0.0003	0.0005
B4_R50_C36	19	7.18	161.05	-0.708	0.0004	0.0004	0.0011
B4_R50_C61	20	12.453	161.02	-0.8784	0.0005	0.0005	0.0006
B4_R50_C86	21	17.692	161.01	-0.9059	0.0004	0.0004	0.0005
B4_R50_C99		20.684	161.04	-1.2363	0.0003	0.0003	0.0004
B4_R55_C05		1.1165	179.04	-0.22	0.0003	0.0003	0.0005
B4_R55_C36	22	7.233	179.03	-0.5178	0.0009	0.0006	0.0008
B4_R55_C61	23	12.474	179.03	-0.6399	0.0004	0.0004	0.0008
B4_R55_C86	24	17.708	179.01	-0.5675	0.0004	0.0003	0.0005
B4_R55_C99		20.714	178.98	-0.8478	0.0003	0.0003	0.0004
B4_R60_C05		1.1105	193.23	-0.178	0.0003	0.0003	0.0005
B4_R60_C36	25	7.2079	193.23	-0.4124	0.0004	0.0004	0.0008
B4_R60_C61	26	12.452	193.21	-0.4436	0.0003	0.0004	0.0006
B4_R60_C86	27	17.709	193.22	-0.3039	0.0008	0.0008	0.0017
B4_R60_C99		20.739	193.18	-0.5135	0.0003	0.0003	0.0004
B4_R65_C05		1.1286	209.28	-0.1284	0.0003	0.0003	0.0005
B4_R65_C36	28	7.2558	209.31	-0.2671	0.0004	0.0005	0.0006
B4_R65_C61	29	12.53	209.31	-0.2022	0.0004	0.0004	0.0005
B4_R65_C86	30	17.721	209.31	0.0307	0.0005	0.0005	0.0012
B4_R65_C99		20.749	209.25	-0.1427	0.0003	0.0003	0.0004
B4_R70_C05		1.1235	225.33	-0.1027	0.0003	0.0004	0.0005
B4_R70_C36	31	7.2754	225.36	-0.1355	0.0004	0.0004	0.0007
B4_R70_C61	32	12.519	225.35	0.0234	0.0003	0.0004	0.0006
B4_R70_C86	33	17.723	225.37	0.3541	0.0004	0.0004	0.0006

Name	Number	X	Y	Z	sigma X	sigma Y	sigma Z
B4_R70_C99		20.762	225.39	0.2386	0.0003	0.0004	0.0005
B4_R75_C05		1.0977	241.48	-0.0699	0.0003	0.0004	0.0005
B4_R75_C36	34	7.2718	241.49	-0.0355	0.0004	0.0004	0.0007
B4_R75_C61	35	12.499	241.48	0.2536	0.0004	0.0004	0.0007
B4_R75_C86	36	17.708	241.49	0.6869	0.0005	0.0005	0.0008
B4_R75_C105		22.191	241.44	0.7502	0.0003	0.0004	0.0005
B4_R80_C05		1.0868	257.61	-0.0357	0.0003	0.0004	0.0005
B4_R80_C36	37	7.2563	257.64	0.0921	0.0003	0.0004	0.0006
B4_R80_C61	38	12.479	257.65	0.4012	0.0004	0.0004	0.0008
B4_R80_C86	39	17.684	257.67	0.9044	0.0005	0.0006	0.0009
B4_R80_C105		22.191	257.57	0.9853	0.0003	0.0004	0.0005
B4_R86_C05		1.1607	276.32	0.216	0.0004	0.0004	0.0006
B4_R86_C36	40	7.308	276.32	0.2263	0.0005	0.0006	0.001
B4_R86_C61	41	12.506	276.32	0.6009	0.0004	0.0005	0.0006
B4_R86_C86	42	17.716	276.31	1.124	0.0004	0.0004	0.0006
B4_R86_C105		22.149	276.3	1.2798	0.0003	0.0004	0.0005
B4_R91_C05		1.1306	293	0.2544	0.0004	0.0005	0.0007
B4_R91_C36	43	7.2508	293.04	0.4204	0.0004	0.0006	0.0009
B4_R91_C61	44	12.467	293.05	0.9838	0.0004	0.0005	0.0007
B4_R91_C86	45	17.668	293.05	1.6768	0.0004	0.0005	0.0007
B4_R91_C99		20.689	293.04	1.8373	0.0004	0.0005	0.0006
B4_R97_C05		6.1818	313.21	0.7032	0.0004	0.0006	0.0008
B4_R97_C36	46	12.334	313.19	0.9127	0.0008	0.0015	0.0018
B4_R97_C61	47	17.508	313.26	1.5392	0.0008	0.0014	0.0016
B4_R97_C86	48	22.71	313.24	2.096	0.0006	0.001	0.0011
B4_R97_C99		25.752	313.26	2.2373	0.0004	0.0005	0.0006
Blade Tip		28.478	320.73	2.2145	0.0004	0.0005	0.0006
HUB_LE		2.1925	30	-3.4999	0.0004	0.0004	0.0006
HUB_TE		8.1875	30	-3.5002	0.0004	0.0004	0.0006
B4_R25_C36	4	7.095	80.573	-1.1935	0.0003	0.0003	0.0004
B4_R35_C86	12	17.63	112.74	-1.6462	0.0004	0.0003	0.0005
B4_R40_C86	15	17.684	128.81	-1.4025	0.0004	0.0004	0.0005

Chapter 2: Bolt Hole Target Alignment

The measured X, Y, and Z locations of the bolt hole targets are compared to their "as designed" locations. X, Y, and Z translation errors, along with pitch and lag errors, are estimated, and compensating translations and rotations are then applied to all target measurements.

2.1: Bolt Hole Alignment Errors

Table 2-1. Measured(1) vs "as designed"(2) in inches.

Name	X1	Y1	Z1	X2	Y2	Z2	dX	dY	dZ	dR
HUB_LE	2.1925	30	-3.4999	2.19	30	-3.5	0.0025	0	0.0001	0.002502
HUB_TE	8.1875	30	-3.5002	8.19	30	-3.5	-0.0025	0	-0.0002	0.002508
RMS Errors:							0.0025	0	0.00015811	0.002505

Table 2-2. Initial alignment errors.

Alignment Error	Value
X Error	-8.8818e-16
Y Error	0
Z Error	-5e-05
Pitch Error	0.0028672
Lag Error	0

2.2: Corrected Bolt Hole Alignment

Table 2-3. Measured(1) with alignment correction vs "as designed"(2) in inches.

Name	X1	Y1	Z1	X2	Y2	Z2	dX	dY	dZ	dR
HUB_LE	2.1925	30	-3.4999	2.19	30	-3.5	0.0025	0	0.0001	0.002502
HUB_TE	8.1875	30	-3.5002	8.19	30	-3.5	-0.0025	0	-0.0002	0.002508
RMS Errors:							0.0025	0	0.00015811	0.002505

Table 2-4. Errors after hole alignment correction.

Alignment Error	Value
X Error	-8.8818e-16
Y Error	0
Z Error	-5e-05
Pitch Error	0.0028672
Lag Error	0

Chapter 3: Trailing-Edge Alignment

The measured X locations of the trailing-edge targets, excluding those on the tab and swept tip, are compared to the "as designed" locations. An estimated lag error, for rotation about the centroid of the two bolt hole targets, and an estimated centroid offset in the X direction that minimize the root-mean-square of the ΔX values with respect to the "as designed" trailing-edge X location, are determined and applied to all target measurements.

3.1: Trailing-Edge Alignment Errors

Table 3-1. Measured(1) vs "as designed"(2) in inches.

Name	X1	Y1	Z1	X2	Y2	Z2	dX	dY	dZ	dR
B4_R20_C05	1.0519	64.451	-0.1436	1.0519	64.451	0.064481	0	0	-0.20808	0.20808
B4_R20_C36	7.1239	64.417	-1.2871	7.1239	64.417	-1.1266	0	0	-0.1605	0.1605
B4_R20_C61	12.297	64.414	-1.888	12.297	64.414	-1.7842	0	0	-0.10377	0.10377
B4_R20_C86	17.518	64.42	-2.3708	17.518	64.42	-2.268	0	0	-0.10275	0.10275
B4_R20_C99	20.49	64.384	-2.9317	20.506	64.384	-2.8208	-0.015319	0	-0.11094	0.11199
B4_R25_C05	1.0153	80.581	-0.1364	1.0153	80.581	0.019112	0	0	-0.15551	0.15551
B4_R25_C36	7.095	80.573	-1.1935	7.095	80.573	-1.0932	0	0	-0.10022	0.10022
B4_R25_C61	12.339	80.565	-1.7801	12.339	80.565	-1.685	0	0	-0.095057	0.095057
B4_R25_C86	17.576	80.571	-2.1811	17.576	80.571	-2.0951	0	0	-0.086006	0.086006
B4_R25_C99	20.529	80.573	-2.7497	20.544	80.573	-2.603	-0.015524	0	-0.14667	0.14749
B4_R30_C05	1.0416	96.654	-0.1378	1.0416	96.654	-0.04876	0	0	-0.08904	0.08904
B4_R30_C36	7.1207	96.655	-1.1202	7.1207	96.655	-1.0676	0	0	-0.05263	0.05263
B4_R30_C61	12.366	96.628	-1.6056	12.366	96.628	-1.5848	0	0	-0.020762	0.020762
B4_R30_C86	17.611	96.626	-1.9415	17.611	96.626	-1.9214	0	0	-0.020146	0.020146
B4_R30_C99	20.565	96.571	-2.4726	20.579	96.571	-2.388	-0.013729	0	-0.08458	0.085687
B4_R35_C05	1.0702	112.71	-0.1269	1.0702	112.71	-0.11581	0	0	-0.011087	0.011087
B4_R35_C36	7.1656	112.76	-1.0091	7.1656	112.76	-1.0434	0	0	0.034308	0.034308
B4_R35_C61	12.382	112.73	-1.397	12.382	112.73	-1.4835	0	0	0.08649	0.08649
B4_R35_C86	17.63	112.74	-1.6462	17.63	112.74	-1.7462	0	0	0.10004	0.10004
B4_R35_C99	20.645	112.76	-2.1464	20.611	112.76	-2.1704	0.03357	0	0.023971	0.04125
B4_R40_C05	1.1313	128.84	-0.1282	1.1313	128.84	-0.19133	0	0	0.063132	0.063132
B4_R40_C36	7.2177	128.84	-0.9052	7.2177	128.84	-1.0189	0	0	0.11375	0.11375
B4_R40_C61	12.465	128.86	-1.247	12.465	128.86	-1.3855	0	0	0.13849	0.13849
B4_R40_C86	17.684	128.81	-1.4025	17.684	128.81	-1.5726	0	0	0.17008	0.17008
B4_R40_C99	20.676	128.86	-1.8538	20.64	128.86	-1.9538	0.035336	0	0.099985	0.10605
B4_R45_C05	1.0568	144.91	-0.1055	1.0568	144.91	-0.22592	0	0	0.12042	0.12042
B4_R45_C36	7.1603	144.88	-0.8036	7.1603	144.88	-0.98524	0	0	0.18164	0.18164
B4_R45_C61	12.392	144.88	-1.0742	12.392	144.88	-1.2804	0	0	0.20619	0.20619
B4_R45_C86	17.651	144.89	-1.1853	17.651	144.89	-1.3969	0	0	0.21163	0.21163
B4_R45_C99	20.674	144.89	-1.5586	20.666	144.89	-1.738	0.0079811	0	0.17944	0.17962
B4_R50_C05	1.0872	161.09	-0.2537	1.0872	161.09	-0.49412	0	0	0.24042	0.24042
B4_R50_C36	7.18	161.05	-0.708	7.18	161.05	-0.96157	0	0	0.25357	0.25357
B4_R50_C61	12.453	161.02	-0.8784	12.453	161.02	-1.1793	0	0	0.30093	0.30093
B4_R50_C86	17.692	161.01	-0.9059	17.692	161.01	-1.2163	0	0	0.3104	0.3104
B4_R50_C99	20.684	161.04	-1.2363	20.695	161.04	-1.5122	-0.011049	0	0.27586	0.27608
B4_R55_C05	1.1165	179.04	-0.22	1.1165	179.04	-0.56641	0	0	0.34641	0.34641
B4_R55_C36	7.233	179.03	-0.5178	7.233	179.03	-0.92883	0	0	0.41103	0.41103
B4_R55_C61	12.474	179.03	-0.6399	12.474	179.03	-1.0542	0	0	0.41431	0.41431
B4_R55_C86	17.708	179.01	-0.5675	17.708	179.01	-1.0013	0	0	0.4338	0.4338
B4_R55_C99	20.714	178.98	-0.8478	20.719	178.98	-1.2462	-0.0052895	0	0.39838	0.39841
B4_R60_C05	1.1105	193.23	-0.178	1.1105	193.23	-0.62039	0	0	0.44239	0.44239
B4_R60_C36	7.2079	193.23	-0.4124	7.2079	193.23	-0.89993	0	0	0.48753	0.48753
B4_R60_C61	12.452	193.21	-0.4436	12.452	193.21	-0.95575	0	0	0.51215	0.51215
B4_R60_C86	17.709	193.22	-0.3039	17.709	193.22	-0.8316	0	0	0.5277	0.5277

Name	X1	Y1	Z1	X2	Y2	Z2	dX	dY	dZ	dR
B4_R60_C99	20.739	193.18	-0.5135	20.734	193.18	-1.0355	0.0043375	0	0.52195	0.52197
B4_R65_C05	1.1286	209.28	-0.1284	1.1286	209.28	-0.6834	0	0	0.555	0.555
B4_R65_C36	7.2558	209.31	-0.2671	7.2558	209.31	-0.86931	0	0	0.60221	0.60221
B4_R65_C61	12.53	209.31	-0.2022	12.53	209.31	-0.84248	0	0	0.64028	0.64028
B4_R65_C86	17.721	209.31	0.0307	17.721	209.31	-0.6391	0	0	0.6698	0.6698
B4_R65_C99	20.749	209.25	-0.1427	20.749	209.25	-0.79681	0.00067921	0	0.65411	0.65411
B4_R70_C05	1.1235	225.33	-0.1027	1.1235	225.33	-0.7447	0	0	0.642	0.642
B4_R70_C36	7.2754	225.36	-0.1355	7.2754	225.36	-0.83753	0	0	0.70203	0.70203
B4_R70_C61	12.519	225.35	0.0234	12.519	225.35	-0.73082	0	0	0.75422	0.75422
B4_R70_C86	17.723	225.37	0.3541	17.723	225.37	-0.44732	0	0	0.80142	0.80142
B4_R70_C99	20.762	225.39	0.2386	20.759	225.39	-0.55687	0.0028446	0	0.79547	0.79548
B4_R75_C05	1.0977	241.48	-0.0699	1.0977	241.48	-0.79954	0	0	0.72964	0.72964
B4_R75_C36	7.2718	241.49	-0.0355	7.2718	241.49	-0.80879	0	0	0.77329	0.77329
B4_R75_C61	12.499	241.48	0.2536	12.499	241.48	-0.63075	0	0	0.88435	0.88435
B4_R75_C86	17.708	241.49	0.6869	17.708	241.49	-0.27534	0	0	0.96224	0.96224
B4_R80_C05	1.0868	257.61	-0.0357	1.0868	257.61	-0.84486	0	0	0.80916	0.80916
B4_R80_C36	7.2563	257.64	0.0921	7.2563	257.64	-0.78597	0	0	0.87807	0.87807
B4_R80_C61	12.479	257.65	0.4012	12.479	257.65	-0.55011	0	0	0.95131	0.95131
B4_R80_C86	17.684	257.67	0.9044	17.684	257.67	-0.13663	0	0	1.041	1.041
B4_R86_C05	1.1607	276.32	0.216	1.1607	276.32	-0.6947	0	0	0.9107	0.9107
B4_R86_C36	7.308	276.32	0.2263	7.308	276.32	-0.75733	0	0	0.98363	0.98363
B4_R86_C61	12.506	276.32	0.6009	12.506	276.32	-0.4676	0	0	1.0685	1.0685
B4_R86_C86	17.716	276.31	1.124	17.716	276.31	0.00080386	0	0	1.1232	1.1232
B4_R91_C05	1.1306	293	0.2544	1.1306	293	-0.81575	0	0	1.0701	1.0701
B4_R91_C36	7.2508	293.04	0.4204	7.2508	293.04	-0.69463	0	0	1.115	1.115
B4_R91_C61	12.467	293.05	0.9838	12.467	293.05	-0.23783	0	0	1.2216	1.2216
B4_R91_C86	17.668	293.05	1.6768	17.668	293.05	0.3971	0	0	1.2797	1.2797
B4_R91_C99	20.689	293.04	1.8373	20.755	293.04	0.49892	-0.066515	0	1.3384	1.34
B4_R97_C05	6.1818	313.21	0.7032	6.1818	313.21	-0.67942	0	0	1.3826	1.3826
B4_R97_C36	12.334	313.19	0.9127	12.334	313.19	-0.45536	0	0	1.3681	1.3681
B4_R97_C61	17.508	313.26	1.5392	17.508	313.26	-0.028143	0	0	1.5673	1.5673
B4_R97_C86	22.71	313.24	2.096	22.71	313.24	0.55999	0	0	1.536	1.536
B4_R97_C99	25.752	313.26	2.2373	25.942	313.26	0.64474	-0.19002	0	1.5926	1.6039
HUB_LE	2.1925	30	-3.4999	2.19	5.19	-3.5	0.0025	24.81	0.0001	24.81
HUB_TE	8.1875	30	-3.5002	8.19	5.19	-3.5	-0.0025	24.81	-0.0002	24.81
RMS Errors:							0.023553	3.9476	0.67971	4.0057

The estimated lag error is -0.0057803°.

The estimated X error is -0.011162 inches.

3.2: Corrected Trailing-Edge Alignment

Table 3-2. Measured(1) with lag correction vs "as designed"(2) in inches.

Name	X1	Y1	Z1	X2	Y2	Z2	dX	dY	dZ	dR
B4_R20_C05	1.0442	64.452	-0.1436	1.0442	64.452	0.067337	0	0	-0.21094	0.21094
B4_R20_C36	7.1162	64.417	-1.2871	7.1162	64.417	-1.1255	0	0	-0.16162	0.16162
B4_R20_C61	12.289	64.413	-1.888	12.289	64.413	-1.7834	0	0	-0.10461	0.10461
B4_R20_C86	17.51	64.419	-2.3708	17.51	64.419	-2.2674	0	0	-0.10337	0.10337
B4_R20_C99	20.483	64.383	-2.9317	20.506	64.383	-2.8208	-0.023008	0	-0.11092	0.11328
B4_R25_C05	1.0092	80.581	-0.1364	1.0092	80.581	0.02134	0	0	-0.15774	0.15774
B4_R25_C36	7.089	80.573	-1.1935	7.089	80.573	-1.0924	0	0	-0.10101	0.10101
B4_R25_C61	12.333	80.564	-1.7801	12.333	80.564	-1.6845	0	0	-0.095632	0.095632
B4_R25_C86	17.57	80.569	-2.1811	17.57	80.569	-2.0947	0	0	-0.086405	0.086405
B4_R25_C99	20.523	80.571	-2.7497	20.544	80.571	-2.6031	-0.02158	0	-0.14665	0.14823
B4_R30_C05	1.0372	96.654	-0.1378	1.0372	96.654	-0.0472	0	0	-0.0906	0.0906
B4_R30_C36	7.1163	96.655	-1.1202	7.1163	96.655	-1.0671	0	0	-0.053148	0.053148
B4_R30_C61	12.361	96.627	-1.6056	12.361	96.627	-1.5845	0	0	-0.021119	0.021119
B4_R30_C86	17.606	96.625	-1.9415	17.606	96.625	-1.9211	0	0	-0.020372	0.020372
B4_R30_C99	20.561	96.569	-2.4726	20.579	96.569	-2.388	-0.018172	0	-0.084559	0.086489
B4_R35_C05	1.0674	112.71	-0.1269	1.0674	112.71	-0.1149	0	0	-0.012	0.012
B4_R35_C36	7.1628	112.76	-1.0091	7.1628	112.76	-1.0431	0	0	0.03402	0.03402
B4_R35_C61	12.379	112.73	-1.397	12.379	112.73	-1.4833	0	0	0.086305	0.086305
B4_R35_C86	17.627	112.74	-1.6462	17.627	112.74	-1.7461	0	0	0.099937	0.099937
B4_R35_C99	20.642	112.76	-2.1464	20.611	112.76	-2.1704	0.03076	0	0.023992	0.03901
B4_R40_C05	1.1301	128.84	-0.1282	1.1301	128.84	-0.19099	0	0	0.062791	0.062791
B4_R40_C36	7.2165	128.84	-0.9052	7.2165	128.84	-1.0188	0	0	0.11364	0.11364
B4_R40_C61	12.463	128.86	-1.247	12.463	128.86	-1.3854	0	0	0.13843	0.13843
B4_R40_C86	17.682	128.81	-1.4025	17.682	128.81	-1.5726	0	0	0.17006	0.17006
B4_R40_C99	20.674	128.86	-1.8538	20.64	128.86	-1.9538	0.03415	0	0.10001	0.10568
B4_R45_C05	1.0572	144.91	-0.1055	1.0572	144.91	-0.22605	0	0	0.12055	0.12055
B4_R45_C36	7.1607	144.88	-0.8036	7.1607	144.88	-0.98527	0	0	0.18167	0.18167
B4_R45_C61	12.392	144.88	-1.0742	12.392	144.88	-1.2804	0	0	0.20621	0.20621
B4_R45_C86	17.651	144.89	-1.1853	17.651	144.89	-1.397	0	0	0.21165	0.21165
B4_R45_C99	20.674	144.89	-1.5586	20.666	144.89	-1.7381	0.0084121	0	0.17946	0.17966
B4_R50_C05	1.0893	161.09	-0.2537	1.0893	161.09	-0.49437	0	0	0.24067	0.24067
B4_R50_C36	7.1821	161.05	-0.708	7.1821	161.05	-0.9617	0	0	0.2537	0.2537
B4_R50_C61	12.455	161.02	-0.8784	12.455	161.02	-1.1794	0	0	0.30098	0.30098
B4_R50_C86	17.694	161.01	-0.9059	17.694	161.01	-1.2163	0	0	0.31041	0.31041
B4_R50_C99	20.686	161.04	-1.2363	20.695	161.04	-1.5122	-0.0089885	0	0.27588	0.27603
B4_R55_C05	1.1204	179.04	-0.22	1.1204	179.04	-0.56679	0	0	0.34679	0.34679
B4_R55_C36	7.2369	179.03	-0.5178	7.2369	179.03	-0.92899	0	0	0.41119	0.41119
B4_R55_C61	12.478	179.03	-0.6399	12.478	179.03	-1.0542	0	0	0.41433	0.41433
B4_R55_C86	17.712	179	-0.5675	17.712	179	-1.0012	0	0	0.43374	0.43374
B4_R55_C99	20.718	178.98	-0.8478	20.719	178.98	-1.2462	-0.0014194	0	0.3984	0.39841
B4_R60_C05	1.1158	193.23	-0.178	1.1158	193.23	-0.62084	0	0	0.44284	0.44284
B4_R60_C36	7.2132	193.23	-0.4124	7.2132	193.23	-0.90009	0	0	0.48769	0.48769
B4_R60_C61	12.457	193.21	-0.4436	12.457	193.21	-0.95571	0	0	0.51211	0.51211
B4_R60_C86	17.714	193.22	-0.3039	17.714	193.22	-0.83143	0	0	0.52753	0.52753
B4_R60_C99	20.744	193.18	-0.5135	20.734	193.18	-1.0355	0.0096399	0	0.52198	0.52207
B4_R65_C05	1.1355	209.28	-0.1284	1.1355	209.28	-0.68388	0	0	0.55548	0.55548
B4_R65_C36	7.2627	209.31	-0.2671	7.2627	209.31	-0.8694	0	0	0.6023	0.6023
B4_R65_C61	12.537	209.31	-0.2022	12.537	209.31	-0.84231	0	0	0.64011	0.64011
B4_R65_C86	17.728	209.31	0.0307	17.728	209.31	-0.63877	0	0	0.66947	0.66947
B4_R65_C99	20.756	209.25	-0.1427	20.749	209.25	-0.79684	0.0076021	0	0.65414	0.65418
B4_R70_C05	1.132	225.33	-0.1027	1.132	225.33	-0.74516	0	0	0.64246	0.64246

Name	X1	Y1	Z1	X2	Y2	Z2	dX	dY	dZ	dR
B4_R70_C36	7.2839	225.36	-0.1355	7.2839	225.36	-0.83752	0	0	0.70202	0.70202
B4_R70_C61	12.527	225.35	0.0234	12.527	225.35	-0.73049	0	0	0.75389	0.75389
B4_R70_C86	17.732	225.37	0.3541	17.732	225.37	-0.44678	0	0	0.80088	0.80088
B4_R70_C99	20.77	225.39	0.2386	20.759	225.39	-0.55689	0.011396	0	0.79549	0.79558
B4_R75_C05	1.1079	241.48	-0.0699	1.1079	241.48	-0.79996	0	0	0.73006	0.73006
B4_R75_C36	7.282	241.49	-0.0355	7.282	241.49	-0.80864	0	0	0.77314	0.77314
B4_R75_C61	12.509	241.48	0.2536	12.509	241.48	-0.63021	0	0	0.88381	0.88381
B4_R75_C86	17.718	241.48	0.6869	17.718	241.48	-0.27455	0	0	0.96145	0.96145
B4_R80_C05	1.0986	257.61	-0.0357	1.0986	257.61	-0.84522	0	0	0.80952	0.80952
B4_R80_C36	7.2681	257.64	0.0921	7.2681	257.64	-0.78566	0	0	0.87776	0.87776
B4_R80_C61	12.491	257.65	0.4012	12.491	257.65	-0.54935	0	0	0.95055	0.95055
B4_R80_C86	17.696	257.67	0.9044	17.696	257.67	-0.13558	0	0	1.04	1.04
B4_R86_C05	1.1744	276.32	0.216	1.1744	276.32	-0.69696	0	0	0.91296	0.91296
B4_R86_C36	7.3217	276.32	0.2263	7.3217	276.32	-0.75681	0	0	0.98311	0.98311
B4_R86_C61	12.519	276.32	0.6009	12.519	276.32	-0.46661	0	0	1.0675	1.0675
B4_R86_C86	17.73	276.31	1.124	17.73	276.31	0.0021714	0	0	1.1218	1.1218
B4_R91_C05	1.146	293	0.2544	1.146	293	-0.81795	0	0	1.0723	1.0723
B4_R91_C36	7.2662	293.04	0.4204	7.2662	293.04	-0.69355	0	0	1.114	1.114
B4_R91_C61	12.483	293.05	0.9838	12.483	293.05	-0.23623	0	0	1.22	1.22
B4_R91_C86	17.683	293.05	1.6768	17.683	293.05	0.39912	0	0	1.2777	1.2777
B4_R91_C99	20.704	293.03	1.8373	20.755	293.03	0.49887	-0.051142	0	1.3384	1.3394
B4_R97_C05	6.1992	313.21	0.7032	6.1992	313.21	-0.67978	0	0	1.383	1.383
B4_R97_C36	12.351	313.19	0.9127	12.351	313.19	-0.4542	0	0	1.3669	1.3669
B4_R97_C61	17.525	313.26	1.5392	17.525	313.26	-0.026375	0	0	1.5656	1.5656
B4_R97_C86	22.727	313.24	2.096	22.727	313.24	0.56223	0	0	1.5338	1.5338
B4_R97_C99	25.77	313.26	2.2373	25.942	313.26	0.64481	-0.17185	0	1.5925	1.6017
HUB_LE	2.1813	30	-3.4999	2.19	5.19	-3.5	-0.0086618	24.81	0.0001	24.81
HUB_TE	8.1763	30	-3.5002	8.19	5.19	-3.5	-0.013662	24.81	-0.0002	24.81
RMS Errors:							0.02143	3.9476	0.67947	4.0057

3.3: Trailing-Edge Registration Plots

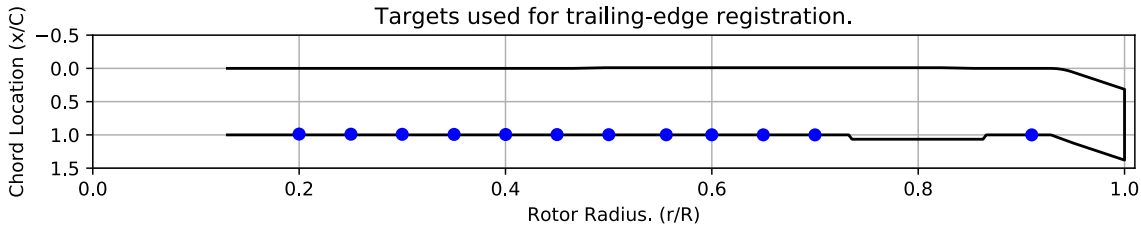

Figure 3-1. Targets used for trailing-edge alignment.

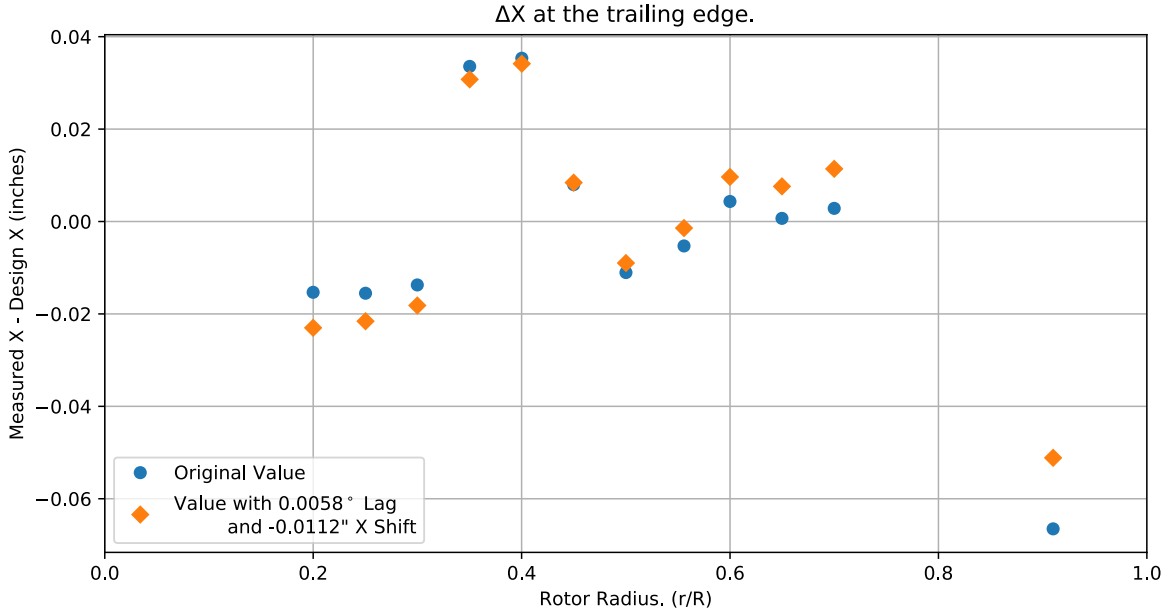

Figure 3-2. Trailing-edge ΔX error vs rotor radius.

Chapter 4: Flap Only Registration (6 rows)

The targets at the 6 spanwise stations nearest the root are used to determing the flap offset.

The estimated flap error is 0.040128°.

4.1: Target Location Errors After Flap Target Registration

Table 4-1. Measured(1) with flap registration vs "as designed"(2) in inches.

Name	X1	Y1	Z1	X2	Y2	Z2	dX	dY	dZ	dR
B4_R20_C05	1.0442	64.454	-0.16773	1.0442	64.454	0.067329	0	0	-0.23506	0.23506
B4_R20_C36	7.1162	64.418	-1.3112	7.1162	64.418	-1.1255	0	0	-0.18573	0.18573
B4_R20_C61	12.289	64.414	-1.9121	12.289	64.414	-1.7834	0	0	-0.12872	0.12872
B4_R20_C86	17.51	64.42	-2.3949	17.51	64.42	-2.2674	0	0	-0.12749	0.12749
B4_R20_C99	20.483	64.383	-2.9558	20.506	64.383	-2.8208	-0.023009	0	-0.135	0.13695
B4_R25_C05	1.0092	80.584	-0.17183	1.0092	80.584	0.021331	0	0	-0.19316	0.19316
B4_R25_C36	7.089	80.574	-1.2289	7.089	80.574	-1.0924	0	0	-0.13643	0.13643
B4_R25_C61	12.333	80.565	-1.8155	12.333	80.565	-1.6845	0	0	-0.13105	0.13105
B4_R25_C86	17.57	80.57	-2.2165	17.57	80.57	-2.0947	0	0	-0.12183	0.12183
B4_R25_C99	20.523	80.572	-2.7851	20.544	80.572	-2.603	-0.021581	0	-0.18207	0.18335
B4_R30_C05	1.0372	96.656	-0.18448	1.0372	96.656	-0.047208	0	0	-0.13727	0.13727
B4_R30_C36	7.1163	96.656	-1.1669	7.1163	96.656	-1.067	0	0	-0.099833	0.099833
B4_R30_C61	12.361	96.629	-1.6523	12.361	96.629	-1.5845	0	0	-0.067792	0.067792
B4_R30_C86	17.606	96.626	-1.9882	17.606	96.626	-1.9211	0	0	-0.067045	0.067045
B4_R30_C99	20.561	96.57	-2.5192	20.579	96.57	-2.388	-0.018174	0	-0.13119	0.13244
B4_R35_C05	1.0674	112.71	-0.18483	1.0674	112.71	-0.11491	0	0	-0.069917	0.069917
B4_R35_C36	7.1628	112.76	-1.0671	7.1628	112.76	-1.0431	0	0	-0.023947	0.023947
B4_R35_C61	12.379	112.73	-1.4549	12.379	112.73	-1.4833	0	0	0.028356	0.028356
B4_R35_C86	17.627	112.74	-1.7041	17.627	112.74	-1.7461	0	0	0.041974	0.041974
B4_R35_C99	20.642	112.76	-2.2044	20.611	112.76	-2.1704	0.030758	0	-0.03398	0.045834
B4_R40_C05	1.1301	128.84	-0.19743	1.1301	128.84	-0.191	0	0	-0.0064266	0.0064266
B4_R40_C36	7.2165	128.84	-0.97443	7.2165	128.84	-1.0188	0	0	0.044414	0.044414
B4_R40_C61	12.463	128.86	-1.3162	12.463	128.86	-1.3854	0	0	0.069182	0.069182
B4_R40_C86	17.682	128.81	-1.4717	17.682	128.81	-1.5725	0	0	0.10084	0.10084
B4_R40_C99	20.674	128.86	-1.923	20.64	128.86	-1.9538	0.034148	0	0.030755	0.045956
B4_R45_C05	1.0572	144.91	-0.18598	1.0572	144.91	-0.22606	0	0	0.040081	0.040081
B4_R45_C36	7.1607	144.88	-0.88406	7.1607	144.88	-0.98527	0	0	0.10121	0.10121
B4_R45_C61	12.392	144.88	-1.1547	12.392	144.88	-1.2804	0	0	0.12575	0.12575
B4_R45_C86	17.651	144.89	-1.2658	17.651	144.89	-1.3969	0	0	0.13117	0.13117
B4_R45_C99	20.674	144.89	-1.6391	20.666	144.89	-1.738	0.0084101	0	0.098981	0.099338
B4_R50_C05	1.0893	161.09	-0.34551	1.0893	161.09	-0.49438	0	0	0.14887	0.14887
B4_R50_C36	7.1821	161.05	-0.79978	7.1821	161.05	-0.96169	0	0	0.16191	0.16191
B4_R50_C61	12.455	161.02	-0.97016	12.455	161.02	-1.1794	0	0	0.20921	0.20921
B4_R50_C86	17.694	161.02	-0.99766	17.694	161.02	-1.2163	0	0	0.21863	0.21863
B4_R50_C99	20.686	161.04	-1.3281	20.695	161.04	-1.5122	-0.0089908	0	0.18408	0.1843
B4_R55_C05	1.1204	179.04	-0.32438	1.1204	179.04	-0.5668	0	0	0.24242	0.24242
B4_R55_C36	7.2369	179.03	-0.62217	7.2369	179.03	-0.92899	0	0	0.30682	0.30682
B4_R55_C61	12.478	179.03	-0.74427	12.478	179.03	-1.0542	0	0	0.30994	0.30994
B4_R55_C86	17.712	179.01	-0.67186	17.712	179.01	-1.0012	0	0	0.32935	0.32935
B4_R55_C99	20.718	178.98	-0.95214	20.719	178.98	-1.2462	-0.0014216	0	0.29404	0.29404
B4_R60_C05	1.1158	193.23	-0.29232	1.1158	193.23	-0.62084	0	0	0.32852	0.32852
B4_R60_C36	7.2132	193.23	-0.52672	7.2132	193.23	-0.90008	0	0	0.37336	0.37336

Name	X1	Y1	Z1	X2	Y2	Z2	dX	dY	dZ	dR
B4_R60_C61	12.457	193.21	-0.55791	12.457	193.21	-0.9557	0	0	0.39779	0.39779
B4_R60_C86	17.714	193.23	-0.41822	17.714	193.23	-0.83141	0	0	0.41319	0.41319
B4_R60_C99	20.744	193.18	-0.62779	20.734	193.18	-1.0354	0.0096379	0	0.40766	0.40778
B4_R65_C05	1.1355	209.28	-0.25396	1.1355	209.28	-0.68389	0	0	0.42993	0.42993
B4_R65_C36	7.2627	209.31	-0.39268	7.2627	209.31	-0.8694	0	0	0.47671	0.47671
B4_R65_C61	12.537	209.31	-0.32778	12.537	209.31	-0.8423	0	0	0.51452	0.51452
B4_R65_C86	17.728	209.31	-0.094883	17.728	209.31	-0.63874	0	0	0.54386	0.54386
B4_R65_C99	20.756	209.25	-0.26824	20.749	209.25	-0.7968	0.0076004	0	0.52856	0.52862
B4_R70_C05	1.132	225.33	-0.2395	1.132	225.33	-0.74517	0	0	0.50567	0.50567
B4_R70_C36	7.2839	225.36	-0.27233	7.2839	225.36	-0.83752	0	0	0.56519	0.56519
B4_R70_C61	12.527	225.36	-0.11342	12.527	225.36	-0.73048	0	0	0.61706	0.61706
B4_R70_C86	17.732	225.37	0.21727	17.732	225.37	-0.44675	0	0	0.66402	0.66402
B4_R70_C99	20.77	225.39	0.10175	20.759	225.39	-0.55686	0.011395	0	0.65861	0.65871
B4_R75_C05	1.1079	241.48	-0.21801	1.1079	241.48	-0.79997	0	0	0.58195	0.58195
B4_R75_C36	7.282	241.49	-0.18362	7.282	241.49	-0.80863	0	0	0.62501	0.62501
B4_R75_C61	12.509	241.49	0.10548	12.509	241.49	-0.6302	0	0	0.73568	0.73568
B4_R75_C86	17.718	241.49	0.53878	17.718	241.49	-0.27453	0	0	0.81331	0.81331
B4_R80_C05	1.0986	257.61	-0.19511	1.0986	257.61	-0.84523	0	0	0.65012	0.65012
B4_R80_C36	7.2681	257.64	-0.067329	7.2681	257.64	-0.78566	0	0	0.71833	0.71833
B4_R80_C61	12.491	257.65	0.24176	12.491	257.65	-0.54934	0	0	0.7911	0.7911
B4_R80_C86	17.696	257.67	0.74495	17.696	257.67	-0.13556	0	0	0.88051	0.88051
B4_R86_C05	1.1744	276.33	0.043484	1.1744	276.33	-0.69696	0	0	0.74044	0.74044
B4_R86_C36	7.3217	276.33	0.053784	7.3217	276.33	-0.75681	0	0	0.8106	0.8106
B4_R86_C61	12.519	276.32	0.42839	12.519	276.32	-0.4666	0	0	0.89498	0.89498
B4_R86_C86	17.73	276.31	0.95149	17.73	276.31	0.0021865	0	0	0.94931	0.94931
B4_R91_C05	1.146	293.01	0.070201	1.146	293.01	-0.81796	0	0	0.88816	0.88816
B4_R91_C36	7.2662	293.05	0.23617	7.2662	293.05	-0.69354	0	0	0.92972	0.92972
B4_R91_C61	12.483	293.05	0.79957	12.483	293.05	-0.23619	0	0	1.0358	1.0358
B4_R91_C86	17.683	293.05	1.4926	17.683	293.05	0.3992	0	0	1.0934	1.0934
B4_R91_C99	20.704	293.04	1.6531	20.755	293.04	0.49898	-0.051138	0	1.1541	1.1552
B4_R97_C05	6.1992	313.21	0.50485	6.1992	313.21	-0.67971	0	0	1.1846	1.1846
B4_R97_C36	12.351	313.19	0.71436	12.351	313.19	-0.45427	0	0	1.1686	1.1686
B4_R97_C61	17.525	313.26	1.3408	17.525	313.26	-0.026542	0	0	1.3674	1.3674
B4_R97_C86	22.727	313.25	1.8976	22.727	313.25	0.56196	0	0	1.3357	1.3357
B4_R97_C99	25.77	313.26	2.0389	25.943	313.26	0.64468	-0.17329	0	1.3942	1.405
HUB_LE	2.1813	30	-3.4999	2.19	30	-3.5	-0.0086618	0.0003036	9.9787e-05	0.0086677
HUB_TE	8.1763	30	-3.5002	8.19	30	-3.5	-0.013662	-0.00030142	-0.00019979	0.013667
RMS Errors:							0.021576	4.8133e-05	0.56971	0.57012

4.2: Flap Registration Plots (6 rows)

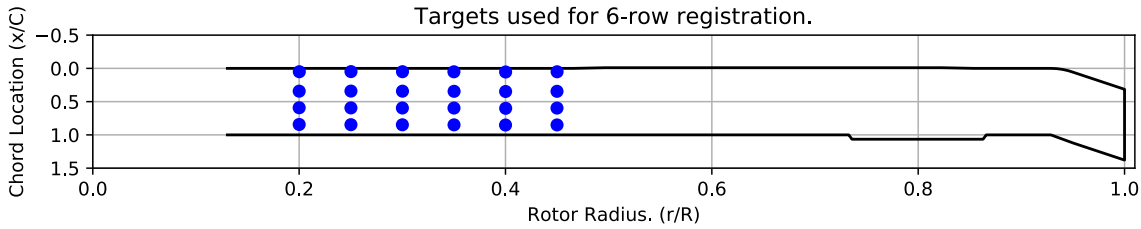

Figure 4-1. Targets used for 6 row root registration.

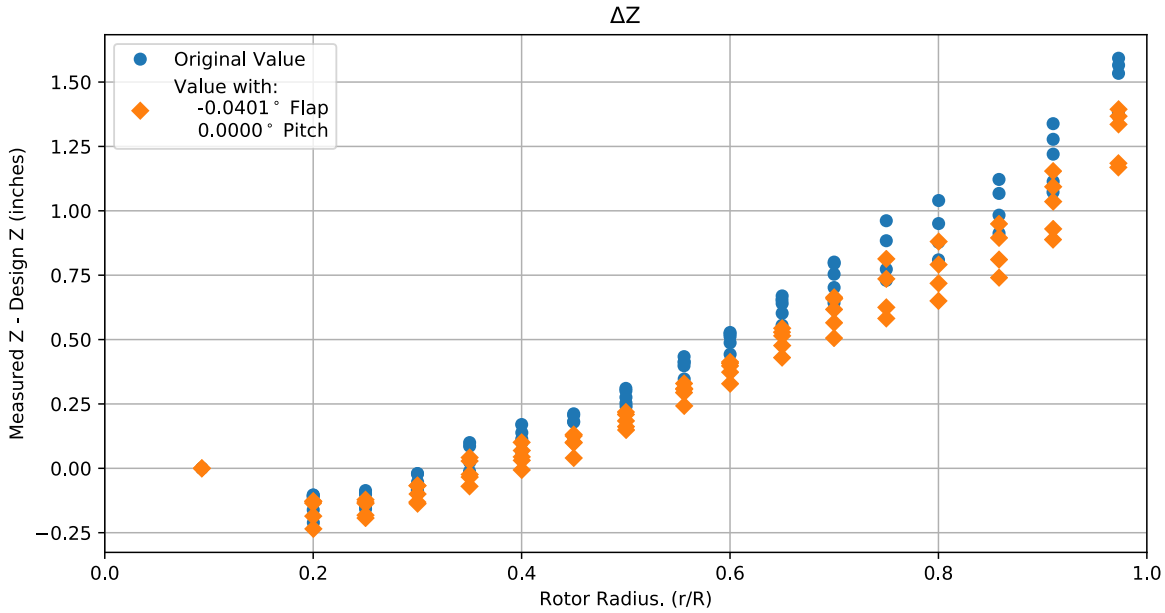

Figure 4-2. Flap target registration, ΔZ error vs rotor radius.

Note: the “as designed” geometry used for the swept tip may have some inaccuracies.

4.3: Estimated Bending and Twist at the Quarter Chord

The error bars shown represent the residual errors for fitting the measure target locations to the "as designed" geometry. These errors are generally much larger than those due to the VSTARS measurement errors. Therefore, the most likely source of these errors is the placement of the trailing-edge targets, differences between the "as designed" and "as built" geometries, and blade deformation during measurement. In the future, iterative adjustment of the "as designed" twist angle may be implemented to see if it reduces the fit error in delta twist. Note: The "as designed" geometry used for the swept tip may have some inaccuracies.

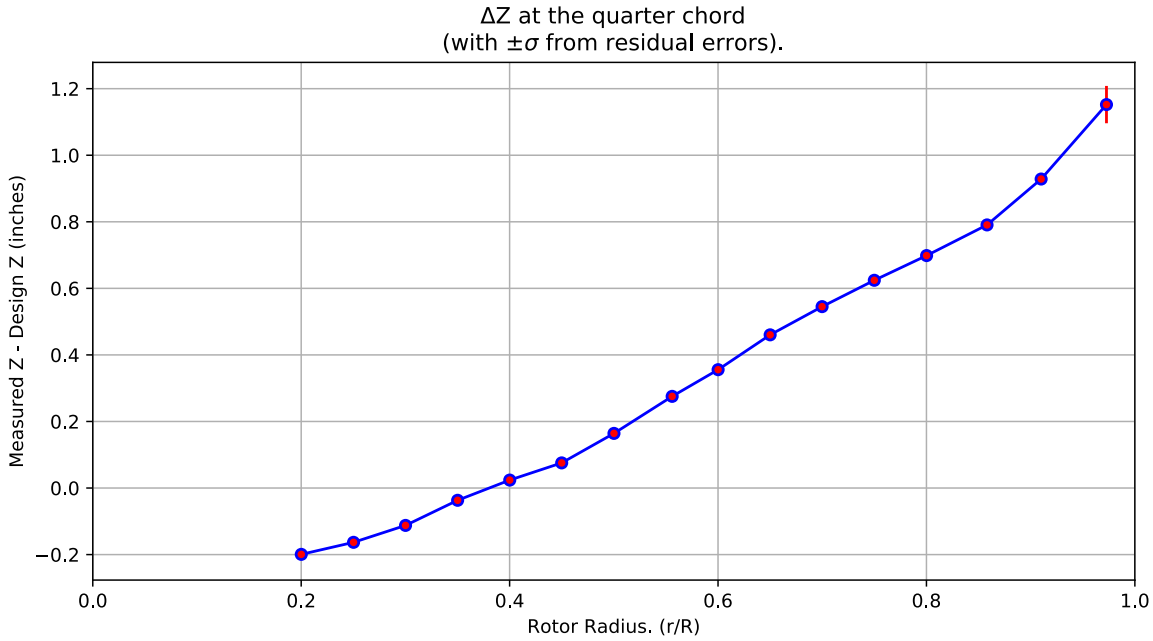

Figure 4-3. ΔZ error at the quarter chord vs rotor radius.

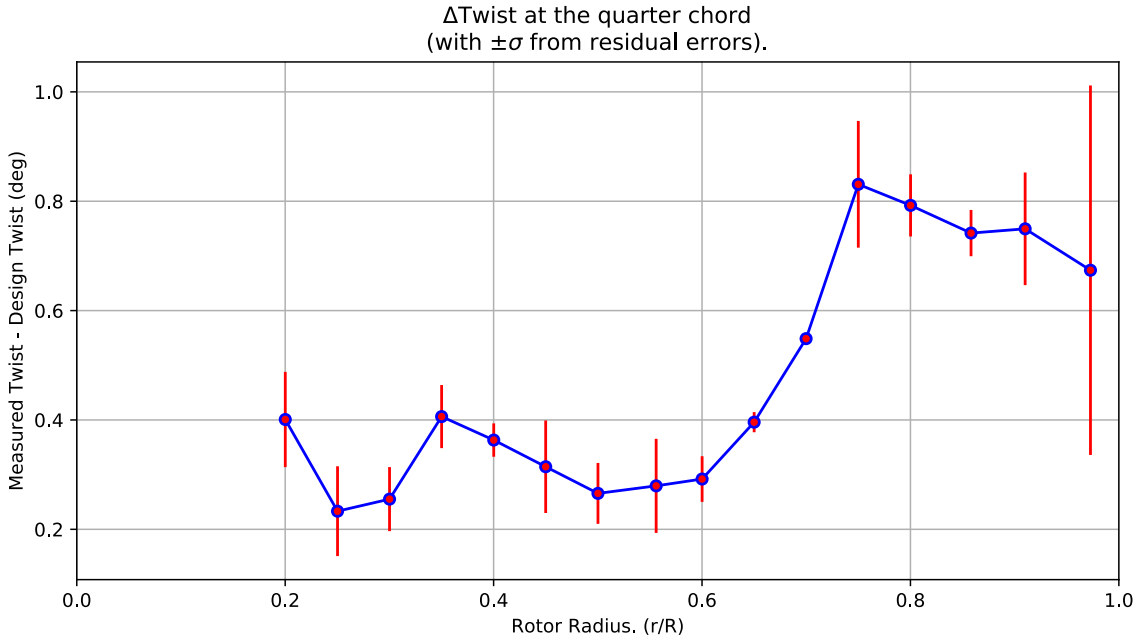

Figure 4-4. ΔTwist error at the quarter chord vs rotor radius.

Table 4-2. Quarter-chord bending and twist statistics.

r	r/R	dZ 1/4-chord	dT	sigma dZ meas	sigma dT meas	sigma dZ res	sigma dT res	n	t_conf
64.427	0.20008	-0.19933	0.40085	6.1154e-10	4.6917e-09	0.0065385	0.087121	4	4.3027
80.573	0.25023	-0.16316	0.23316	6.1073e-10	4.6617e-09	0.0061782	0.082124	4	4.3027
96.642	0.30013	-0.11232	0.25522	6.1204e-10	4.6595e-09	0.0044365	0.058564	4	4.3027
112.74	0.35011	-0.036856	0.40617	6.136e-10	4.664e-09	0.0043996	0.057692	4	4.3027
128.84	0.40013	0.023899	0.36323	6.166e-10	4.6634e-09	0.0023605	0.030508	4	4.3027
144.89	0.44997	0.075539	0.31445	6.1345e-10	4.6542e-09	0.0064603	0.084598	4	4.3027
161.04	0.50014	0.16418	0.26571	6.1506e-10	4.648e-09	0.0042917	0.055693	4	4.3027
179.03	0.55598	0.27544	0.27948	6.1682e-10	4.6539e-09	0.0066772	0.086033	4	4.3027
193.23	0.60008	0.35562	0.29196	6.1618e-10	4.6521e-09	0.0032295	0.04172	4	4.3027
209.3	0.65001	0.46032	0.39595	6.1805e-10	4.6503e-09	0.0014379	0.018405	4	4.3027
225.36	0.69986	0.54509	0.54868	6.1822e-10	4.6507e-09	0.00055129	0.0070517	4	4.3027
241.49	0.74996	0.62424	0.83095	6.1746e-10	4.6486e-09	0.0090306	0.11587	4	4.3027
257.64	0.80013	0.69849	0.79239	6.1687e-10	4.6524e-09	0.0044148	0.056851	4	4.3027
276.32	0.85814	0.79062	0.74174	6.1975e-10	4.6655e-09	0.0033214	0.042316	4	4.3027
293.04	0.91006	0.92848	0.74954	6.1789e-10	4.6687e-09	0.0080099	0.10301	4	4.3027
313.23	0.97276	1.1522	0.67384	9.2317e-10	4.6745e-09	0.056087	0.33784	4	4.3027

4.4: Section Plots

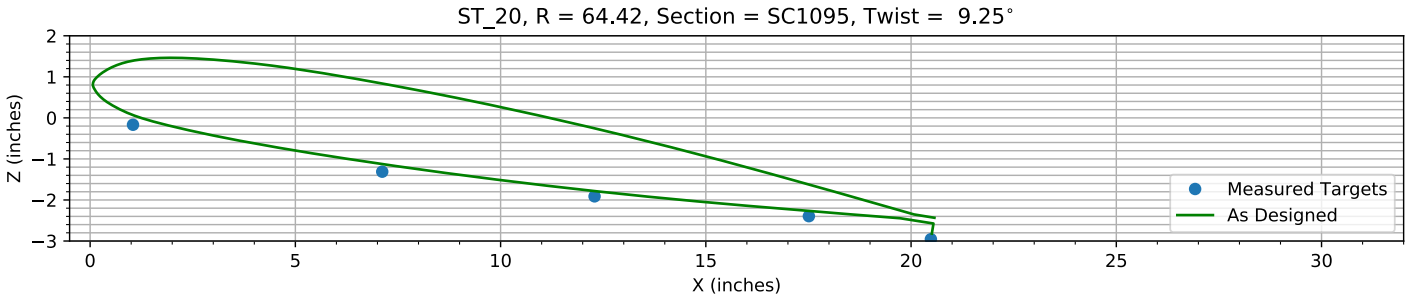

Figure 4-5. Target locations vs section profile at station 20.

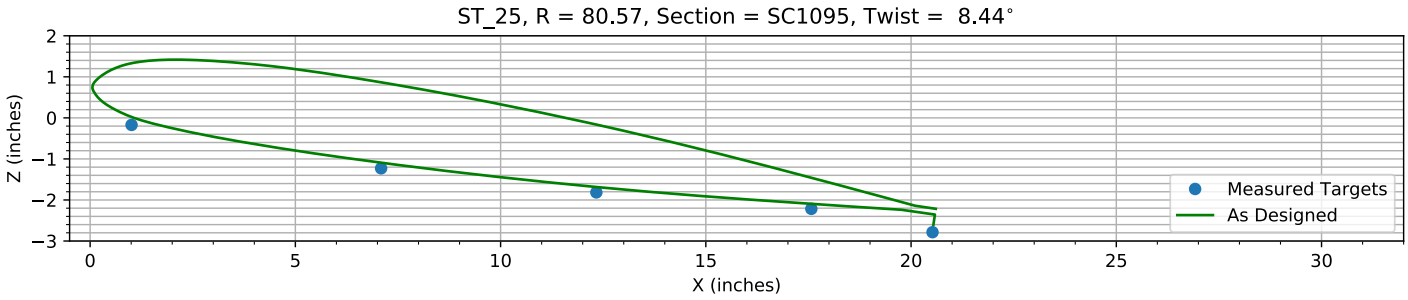

Figure 4-6. Target locations vs section profile at station 25.

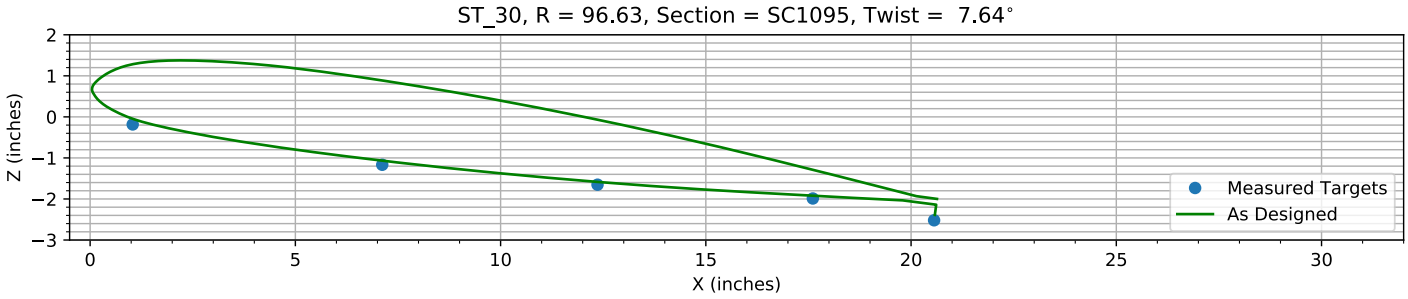

Figure 4-7. Target locations vs section profile at station 30.

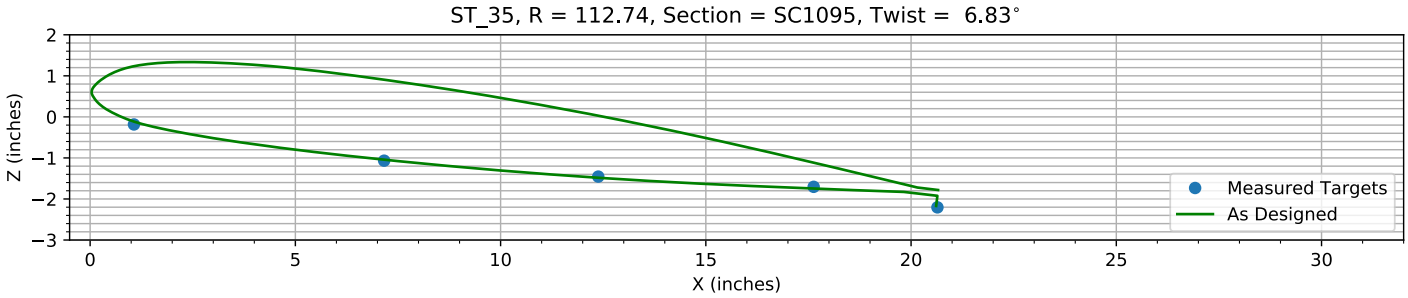

Figure 4-8. Target locations vs section profile at station 35.

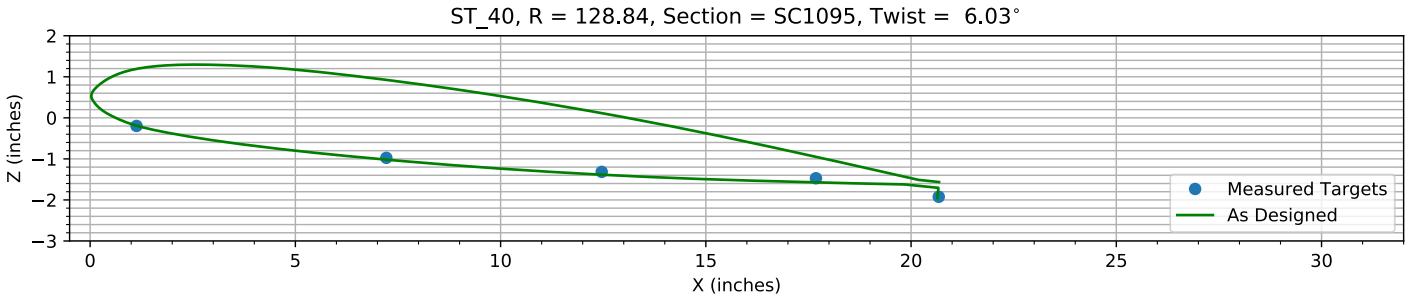

Figure 4-9. Target locations vs section profile at station 40.

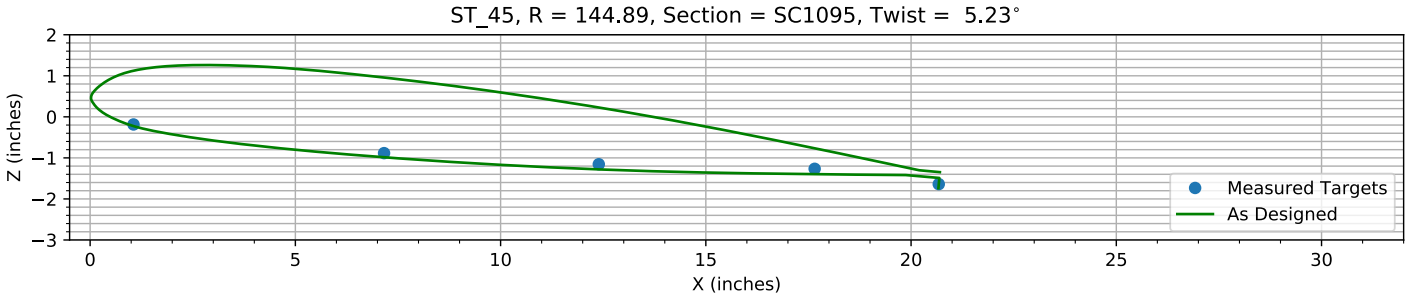

Figure 4-10. Target locations vs section profile at station 45.

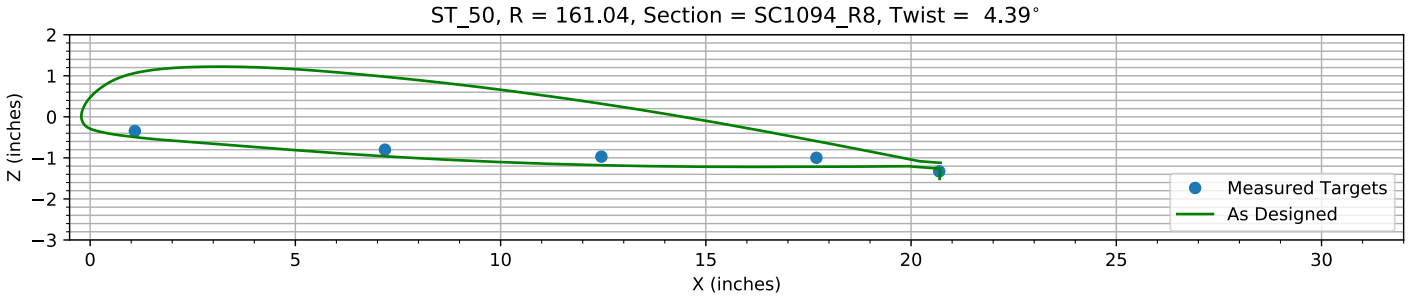

Figure 4-11. Target locations vs section profile at station 50.

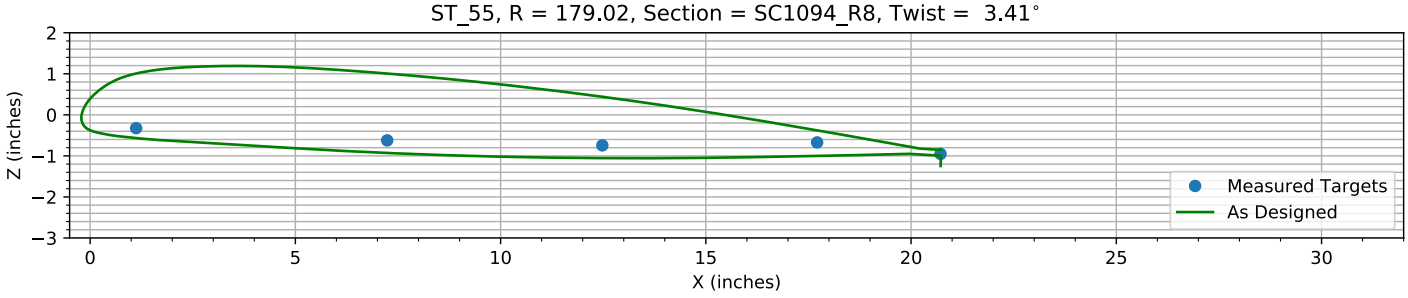

Figure 4-12. Target locations vs section profile at station 55.

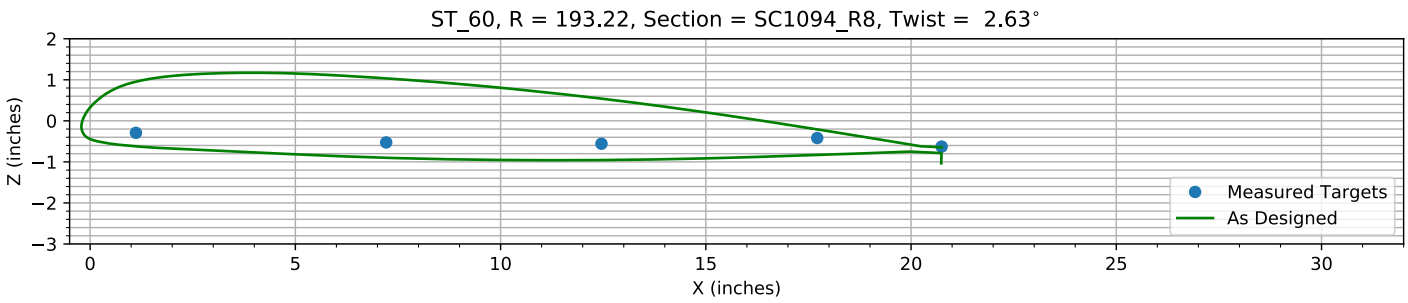

Figure 4-13. Target locations vs section profile at station 60.

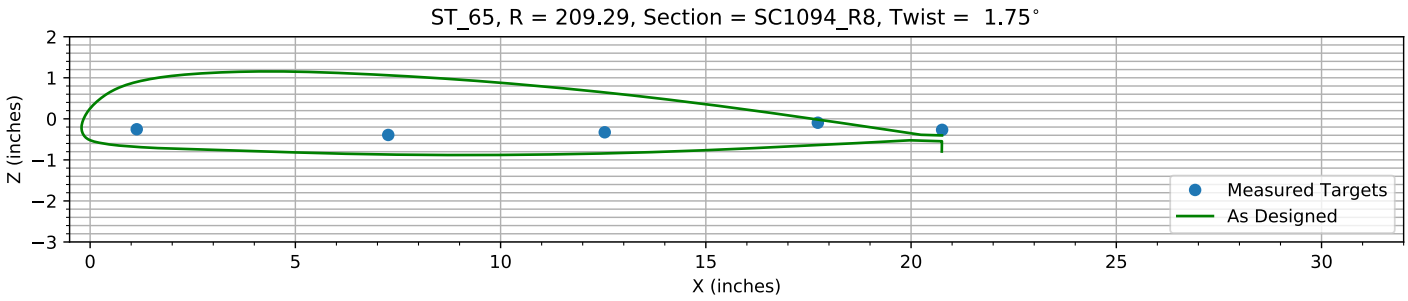

Figure 4-14. Target locations vs section profile at station 65.

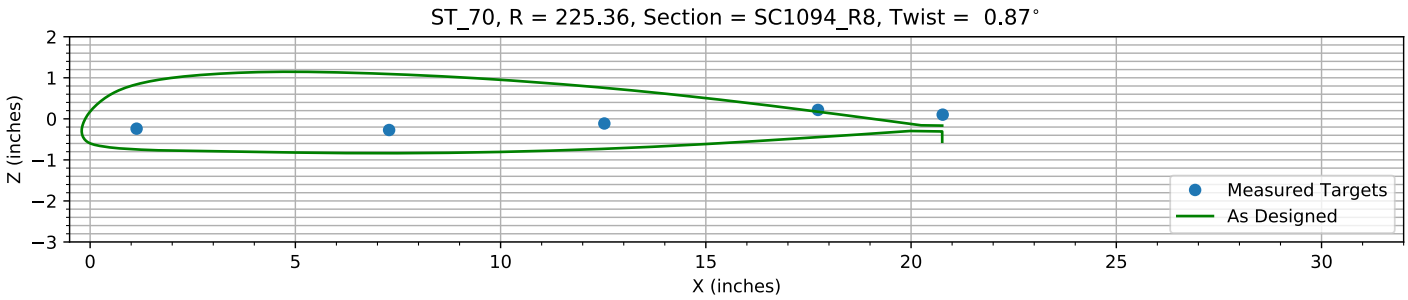

Figure 4-15. Target locations vs section profile at station 70.

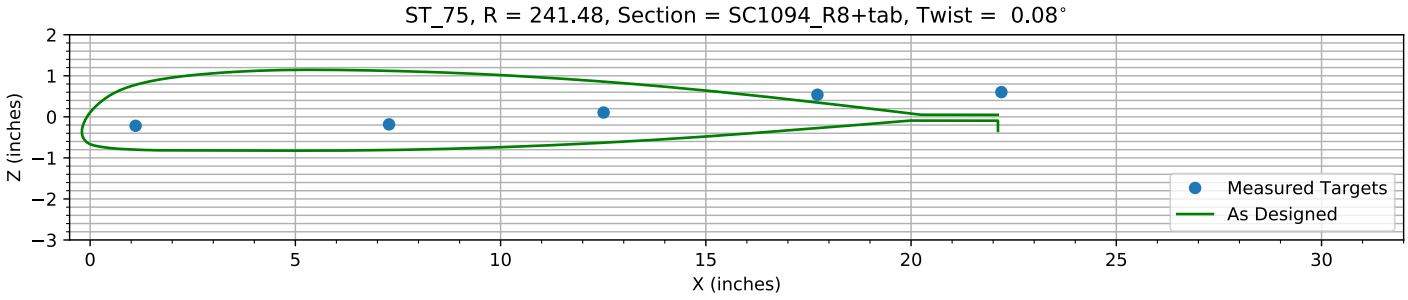

Figure 4-16. Target locations vs section profile at station 75.

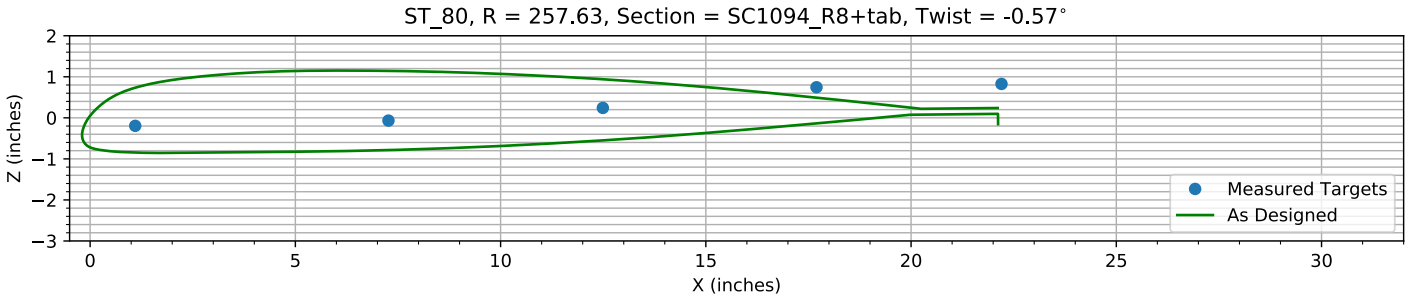

Figure 4-17. Target locations vs section profile at station 80.

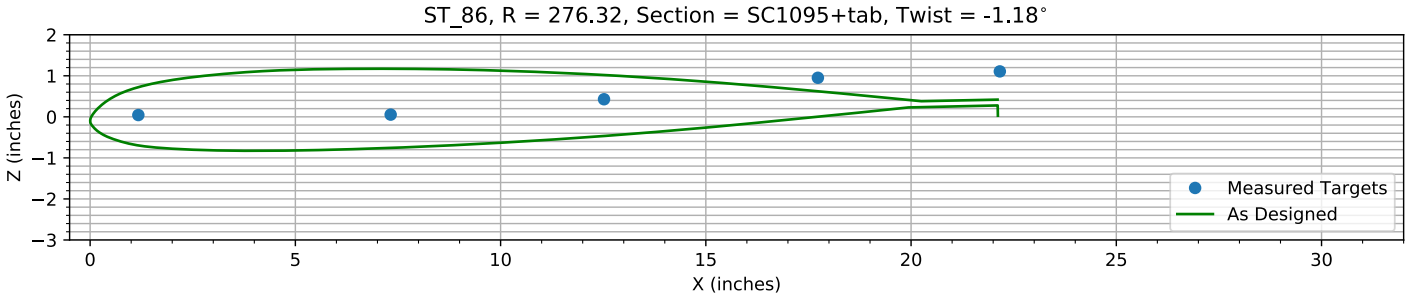

Figure 4-18. Target locations vs section profile at station 86.

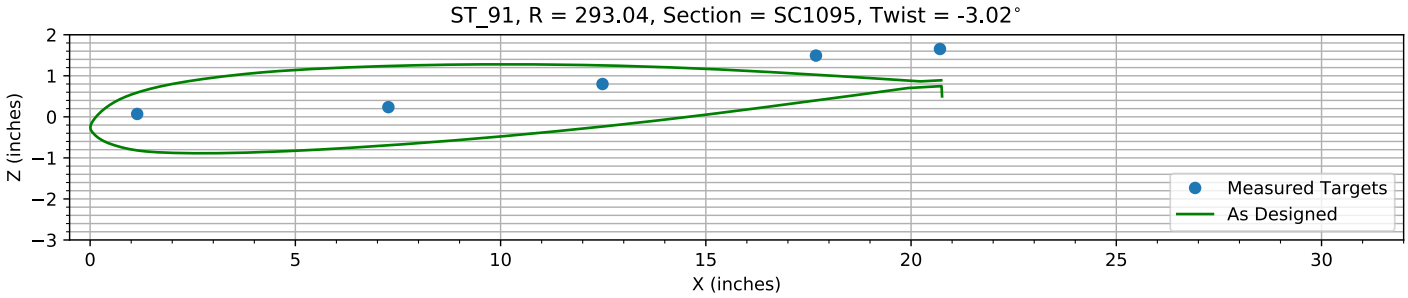

Figure 4-19. Target locations vs section profile at station 91.

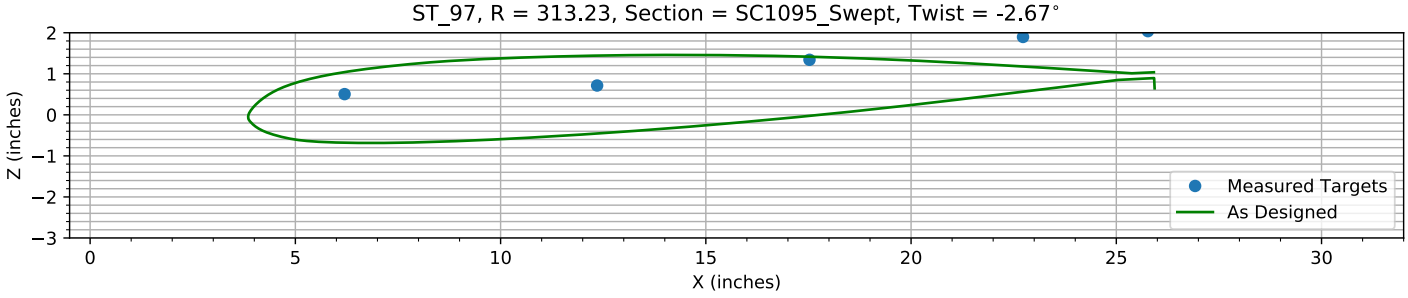

Figure 4-20. Target locations vs section profile at station 97.

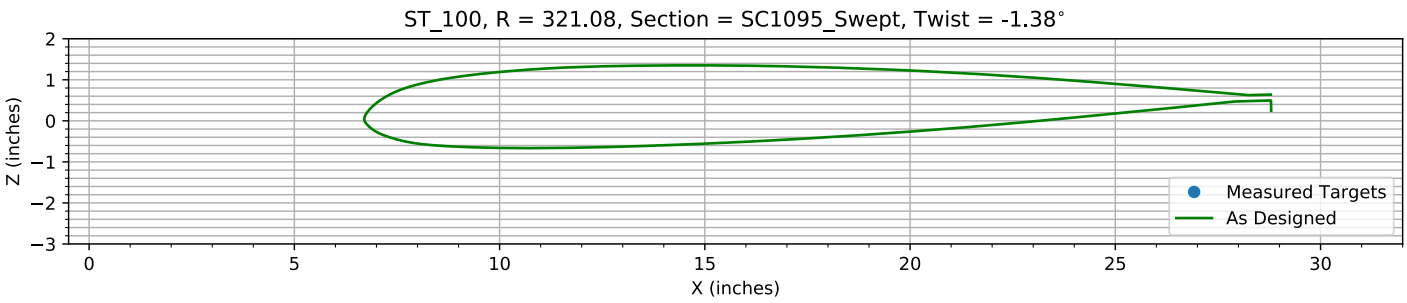

Figure 4-21. Target locations vs section profile at station 100.

Chapter 5: Flap Only Registration (15 rows)

The targets at the 15 spanwise stations nearest the root are used to determing the flap offset.

The estimated flap error is 0.18829°.

5.1: Target Location Errors After Flap Target Registration

Table 5-1. Measured(1) with flap registration vs "as designed"(2) in inches.

Name	X1	Y1	Z1	X2	Y2	Z2	dX	dY	dZ	dR
B4_R20_C05	1.0442	64.463	-0.25684	1.0442	64.463	0.067297	0	0	-0.32413	0.32413
B4_R20_C36	7.1162	64.424	-1.4002	7.1162	64.424	-1.1255	0	0	-0.27475	0.27475
B4_R20_C61	12.289	64.418	-2.0011	12.289	64.418	-1.7834	0	0	-0.21775	0.21775
B4_R20_C86	17.51	64.423	-2.4839	17.51	64.423	-2.2674	0	0	-0.21653	0.21653
B4_R20_C99	20.483	64.384	-3.0447	20.506	64.384	-2.8208	-0.023012	0	-0.22393	0.22511
B4_R25_C05	1.0092	80.592	-0.30264	1.0092	80.592	0.0213	0	0	-0.32394	0.32394
B4_R25_C36	7.089	80.58	-1.3597	7.089	80.58	-1.0924	0	0	-0.26723	0.26723
B4_R25_C61	12.333	80.57	-1.9463	12.333	80.57	-1.6844	0	0	-0.26184	0.26184
B4_R25_C86	17.57	80.574	-2.3473	17.57	80.574	-2.0947	0	0	-0.25264	0.25264
B4_R25_C99	20.523	80.573	-2.9159	20.544	80.573	-2.603	-0.021585	0	-0.31287	0.31362
B4_R30_C05	1.0372	96.665	-0.35686	1.0372	96.665	-0.047238	0	0	-0.30962	0.30962
B4_R30_C36	7.1163	96.662	-1.3393	7.1163	96.662	-1.067	0	0	-0.27222	0.27222
B4_R30_C61	12.361	96.633	-1.8246	12.361	96.633	-1.5844	0	0	-0.24012	0.24012
B4_R30_C86	17.606	96.63	-2.1605	17.606	96.63	-1.9211	0	0	-0.23938	0.23938
B4_R30_C99	20.561	96.572	-2.6914	20.579	96.572	-2.388	-0.018178	0	-0.30337	0.30391
B4_R35_C05	1.0674	112.72	-0.39871	1.0674	112.72	-0.11494	0	0	-0.28378	0.28378
B4_R35_C36	7.1628	112.77	-1.2811	7.1628	112.77	-1.0431	0	0	-0.23798	0.23798
B4_R35_C61	12.379	112.73	-1.6689	12.379	112.73	-1.4833	0	0	-0.18561	0.18561
B4_R35_C86	17.627	112.75	-1.9181	17.627	112.75	-1.7461	0	0	-0.17204	0.17204
B4_R35_C99	20.642	112.76	-2.4184	20.611	112.76	-2.1703	0.030752	0	-0.24803	0.24993
B4_R40_C05	1.1301	128.85	-0.45304	1.1301	128.85	-0.19103	0	0	-0.26201	0.26201
B4_R40_C36	7.2165	128.85	-1.23	7.2165	128.85	-1.0188	0	0	-0.2112	0.2112
B4_R40_C61	12.463	128.87	-1.5719	12.463	128.87	-1.3854	0	0	-0.1865	0.1865
B4_R40_C86	17.682	128.82	-1.7272	17.682	128.82	-1.5725	0	0	-0.15474	0.15474
B4_R40_C99	20.674	128.86	-2.1787	20.64	128.86	-1.9537	0.034141	0	-0.22494	0.22751
B4_R45_C05	1.0572	144.92	-0.48313	1.0572	144.92	-0.22609	0	0	-0.25704	0.25704
B4_R45_C36	7.1607	144.89	-1.1811	7.1607	144.89	-0.98526	0	0	-0.19588	0.19588
B4_R45_C61	12.392	144.89	-1.4517	12.392	144.89	-1.2804	0	0	-0.17137	0.17137
B4_R45_C86	17.651	144.9	-1.5629	17.651	144.9	-1.3969	0	0	-0.166	0.166
B4_R45_C99	20.674	144.89	-1.9362	20.666	144.89	-1.738	0.0084034	0	-0.19817	0.19835
B4_R50_C05	1.0893	161.1	-0.68451	1.0893	161.1	-0.49441	0	0	-0.1901	0.1901
B4_R50_C36	7.1821	161.06	-1.1387	7.1821	161.06	-0.96168	0	0	-0.17699	0.17699
B4_R50_C61	12.455	161.03	-1.309	12.455	161.03	-1.1793	0	0	-0.12965	0.12965
B4_R50_C86	17.694	161.02	-1.3365	17.694	161.02	-1.2162	0	0	-0.12024	0.12024
B4_R50_C99	20.686	161.05	-1.6669	20.695	161.05	-1.5121	-0.0089983	0	-0.15486	0.15512
B4_R55_C05	1.1204	179.05	-0.7098	1.1204	179.05	-0.56683	0	0	-0.14297	0.14297
B4_R55_C36	7.2369	179.03	-1.0076	7.2369	179.03	-0.92897	0	0	-0.078577	0.078577
B4_R55_C61	12.478	179.04	-1.1297	12.478	179.04	-1.0542	0	0	-0.075487	0.075487
B4_R55_C86	17.712	179.01	-1.0572	17.712	179.01	-1.0011	0	0	-0.056048	0.056048
B4_R55_C99	20.718	178.99	-1.3374	20.719	178.99	-1.2461	-0.0014288	0	-0.091312	0.091323
B4_R60_C05	1.1158	193.24	-0.71444	1.1158	193.24	-0.62087	0	0	-0.093562	0.093562
B4_R60_C36	7.2132	193.24	-0.94882	7.2132	193.24	-0.90007	0	0	-0.048753	0.048753

Name	X1	Y1	Z1	X2	Y2	Z2	dX	dY	dZ	dR
B4_R60_C61	12.457	193.22	-0.97996	12.457	193.22	-0.95565	0	0	-0.024315	0.024315
B4_R60_C86	17.714	193.23	-0.84031	17.714	193.23	-0.83132	0	0	-0.0089883	0.0089883
B4_R60_C99	20.744	193.19	-1.0498	20.734	193.19	-1.0353	0.0096311	0	-0.01442	0.017341
B4_R65_C05	1.1355	209.29	-0.71758	1.1355	209.29	-0.68392	0	0	-0.033657	0.033657
B4_R65_C36	7.2627	209.32	-0.85638	7.2627	209.32	-0.86938	0	0	0.013005	0.013005
B4_R65_C61	12.537	209.32	-0.79146	12.537	209.32	-0.84225	0	0	0.050787	0.050787
B4_R65_C86	17.728	209.32	-0.55858	17.728	209.32	-0.63864	0	0	0.080065	0.080065
B4_R65_C99	20.756	209.26	-0.73177	20.749	209.26	-0.79669	0.0075945	0	0.06492	0.065362
B4_R70_C05	1.132	225.34	-0.74463	1.132	225.34	-0.7452	0	0	0.00057764	0.00057764
B4_R70_C36	7.2839	225.37	-0.77753	7.2839	225.37	-0.8375	0	0	0.059977	0.059977
B4_R70_C61	12.527	225.36	-0.6186	12.527	225.36	-0.73042	0	0	0.11182	0.11182
B4_R70_C86	17.732	225.38	-0.28794	17.732	225.38	-0.44664	0	0	0.1587	0.1587
B4_R70_C99	20.77	225.4	-0.40352	20.759	225.4	-0.55673	0.01139	0	0.1532	0.15363
B4_R75_C05	1.1079	241.49	-0.7649	1.1079	241.49	-0.79999	0	0	0.035093	0.035093
B4_R75_C36	7.282	241.5	-0.73053	7.282	241.5	-0.80862	0	0	0.078088	0.078088
B4_R75_C61	12.509	241.5	-0.44141	12.509	241.5	-0.63015	0	0	0.18874	0.18874
B4_R75_C86	17.718	241.5	-0.0081114	17.718	241.5	-0.27443	0	0	0.26632	0.26632
B4_R80_C05	1.0986	257.62	-0.78369	1.0986	257.62	-0.84525	0	0	0.061554	0.061554
B4_R80_C36	7.2681	257.65	-0.65599	7.2681	257.65	-0.78565	0	0	0.12966	0.12966
B4_R80_C61	12.491	257.66	-0.34693	12.491	257.66	-0.5493	0	0	0.20237	0.20237
B4_R80_C86	17.696	257.68	0.15621	17.696	257.68	-0.13548	0	0	0.29169	0.29169
B4_R86_C05	1.1744	276.33	-0.5935	1.1744	276.33	-0.69697	0	0	0.10347	0.10347
B4_R86_C36	7.3217	276.33	-0.5832	7.3217	276.33	-0.75681	0	0	0.17361	0.17361
B4_R86_C61	12.519	276.33	-0.20858	12.519	276.33	-0.46657	0	0	0.25799	0.25799
B4_R86_C86	17.73	276.32	0.31454	17.73	276.32	0.0022376	0	0	0.3123	0.3123
B4_R91_C05	1.146	293.02	-0.60991	1.146	293.02	-0.81802	0	0	0.20811	0.20811
B4_R91_C36	7.2662	293.06	-0.44405	7.2662	293.06	-0.69351	0	0	0.24946	0.24946
B4_R91_C61	12.483	293.06	0.11933	12.483	293.06	-0.23605	0	0	0.35538	0.35538
B4_R91_C86	17.683	293.06	0.81234	17.683	293.06	0.39947	0	0	0.41287	0.41287
B4_R91_C99	20.704	293.05	0.97288	20.755	293.05	0.49933	-0.051127	0	0.47355	0.4763
B4_R97_C05	6.1992	313.22	-0.22751	6.1992	313.22	-0.67951	0	0	0.45201	0.45201
B4_R97_C36	12.351	313.2	-0.017955	12.351	313.2	-0.45451	0	0	0.43655	0.43655
B4_R97_C61	17.525	313.27	0.60832	17.525	313.27	-0.027105	0	0	0.63542	0.63542
B4_R97_C86	22.727	313.26	1.1652	22.727	313.26	0.56106	0	0	0.60411	0.60411
B4_R97_C99	25.77	313.27	1.3064	25.948	313.27	0.64423	-0.17817	0	0.66219	0.68574
HUB_LE	2.1813	30	-3.4999	2.19	30	-3.5	-0.0086618	0.00030386	9.9002e-05	0.0086677
HUB_TE	8.1763	30	-3.5002	8.19	30	-3.5	-0.013662	-0.00030193	-0.00019901	0.013667
RMS Errors:							0.022074	4.8195e-05	0.24511	0.24611

5.2: Flap Registration Plots (15 rows)

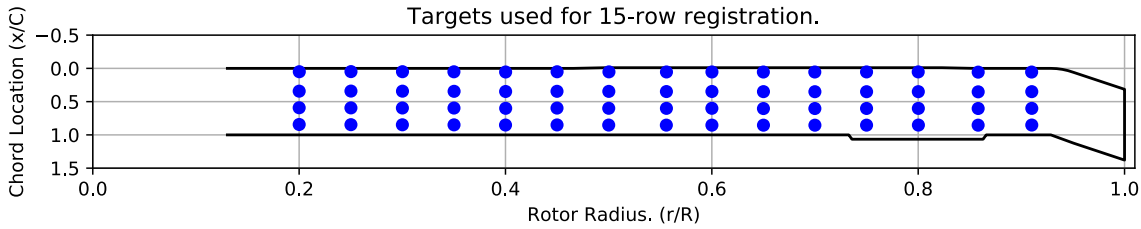

Figure 5-1. Targets used for 15 row root registration.

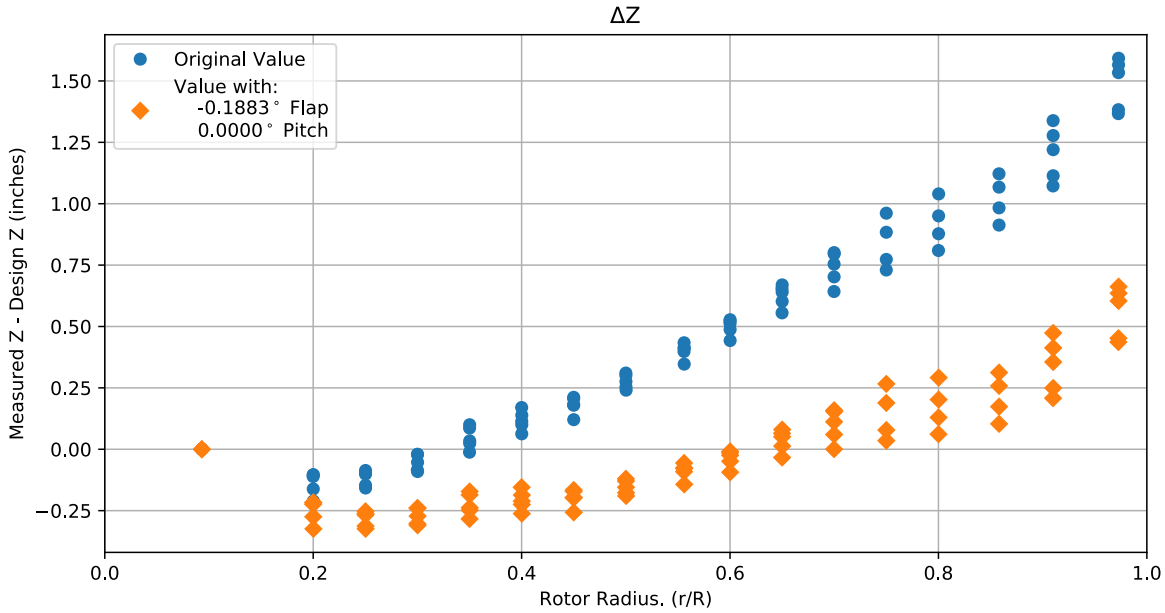

Figure 5-2. Flap target registration, ΔZ error vs rotor radius.

Note: the “as designed” geometry used for the swept tip may have some inaccuracies.

5.3: Estimated Bending and Twist at the Quarter Chord

The error bars shown represent the residual errors for fitting the measure target locations to the "as designed" geometry. These errors are generally much larger than those due to the VSTARS measurement errors. Therefore, the most likely source of these errors is the placement of the trailing-edge targets, differences between the "as designed" and "as built" geometries, and blade deformation during measurement. In the future, iterative adjustment of the "as designed" twist angle may be implemented to see if it reduces the fit error in delta twist. Note: The "as designed" geometry used for the swept tip may have some inaccuracies.

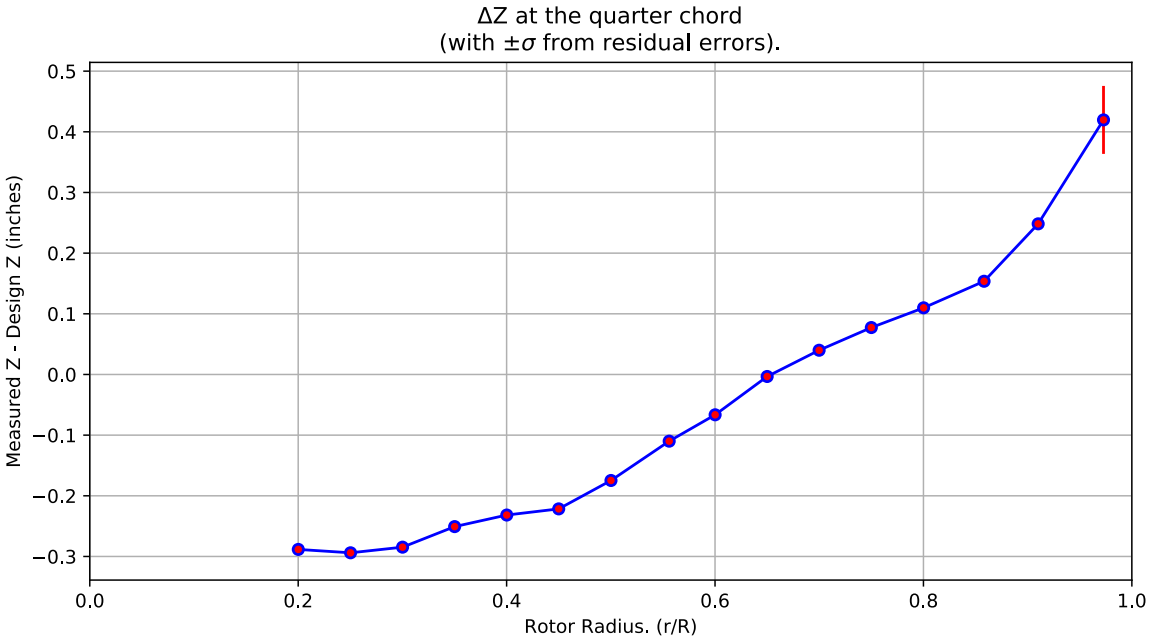

Figure 5-3. ΔZ error at the quarter chord vs rotor radius.

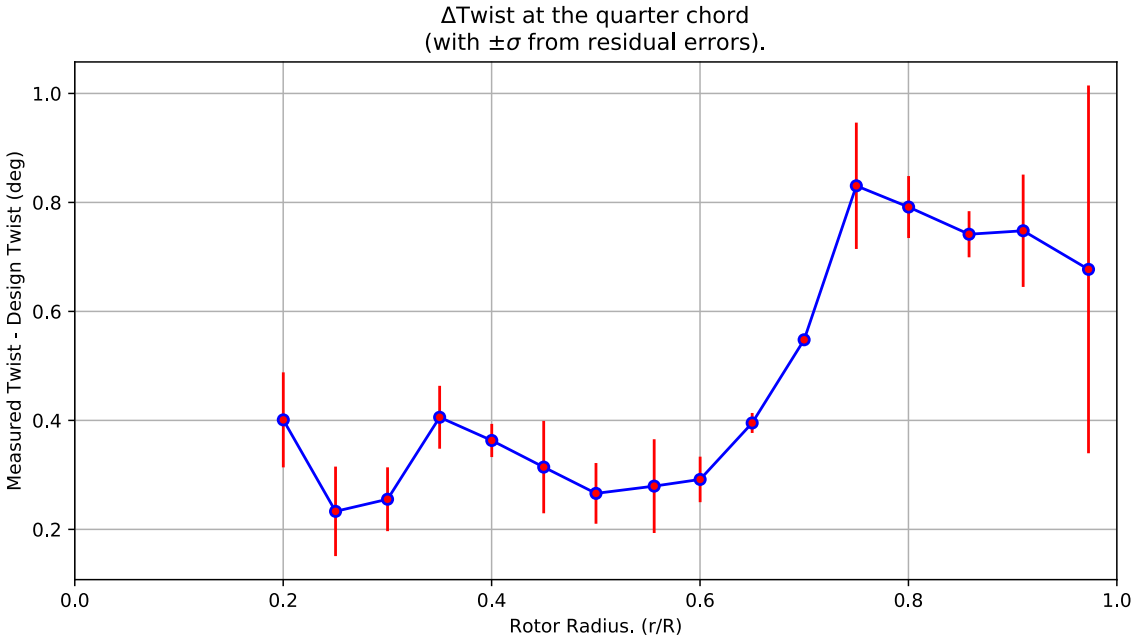

Figure 5-4. ΔTwist error at the quarter chord vs rotor radius.

Table 5-2. Quarter-chord bending and twist statistics.

r	r/R	dZ 1/4-chord	dT	sigma dZ meas	sigma dT meas	sigma dZ res	sigma dT res	n	t_conf
64.432	0.2001	-0.28838	0.40096	6.1154e-10	4.6917e-09	0.0065443	0.087198	4	4.3027
80.579	0.25024	-0.29395	0.23309	6.1073e-10	4.6617e-09	0.0061776	0.082116	4	4.3027
96.647	0.30015	-0.28467	0.25531	6.1204e-10	4.6595e-09	0.0044355	0.058552	4	4.3027
112.74	0.35013	-0.25079	0.40574	6.136e-10	4.664e-09	0.0044008	0.057708	4	4.3027
128.85	0.40015	-0.23171	0.36316	6.166e-10	4.6634e-09	0.0023556	0.030444	4	4.3027
144.9	0.44999	-0.22157	0.31428	6.1345e-10	4.6542e-09	0.0064718	0.084749	4	4.3027
161.05	0.50016	-0.17475	0.26606	6.1506e-10	4.648e-09	0.0042932	0.055713	4	4.3027
179.03	0.556	-0.10995	0.27938	6.1682e-10	4.6539e-09	0.0066773	0.086034	4	4.3027
193.23	0.6001	-0.066483	0.29168	6.1618e-10	4.6521e-09	0.0032345	0.041785	4	4.3027
209.31	0.65004	-0.0033291	0.39528	6.1805e-10	4.6503e-09	0.0014326	0.018338	4	4.3027
225.36	0.69989	0.039935	0.54795	6.1822e-10	4.6507e-09	0.0005542	0.007089	4	4.3027
241.5	0.74999	0.077344	0.83052	6.1746e-10	4.6486e-09	0.0090347	0.11593	4	4.3027
257.65	0.80016	0.10986	0.79153	6.1687e-10	4.6524e-09	0.0044157	0.056863	4	4.3027
276.33	0.85817	0.15364	0.74163	6.1975e-10	4.6655e-09	0.0033216	0.042319	4	4.3027
293.05	0.91009	0.2483	0.74801	6.1789e-10	4.6687e-09	0.0080152	0.10308	4	4.3027
313.24	0.97279	0.41961	0.67716	9.2317e-10	4.6745e-09	0.056024	0.33746	4	4.3027

5.4: Section Plots

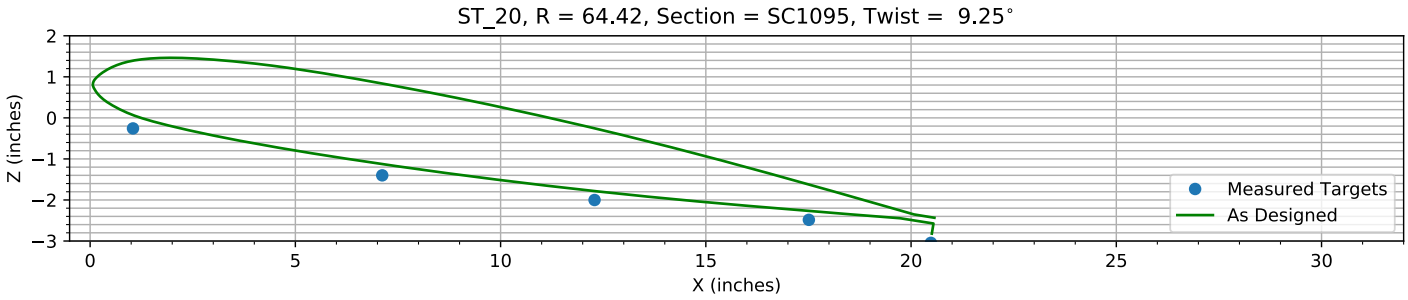

Figure 5-5. Target locations vs section profile at station 20.

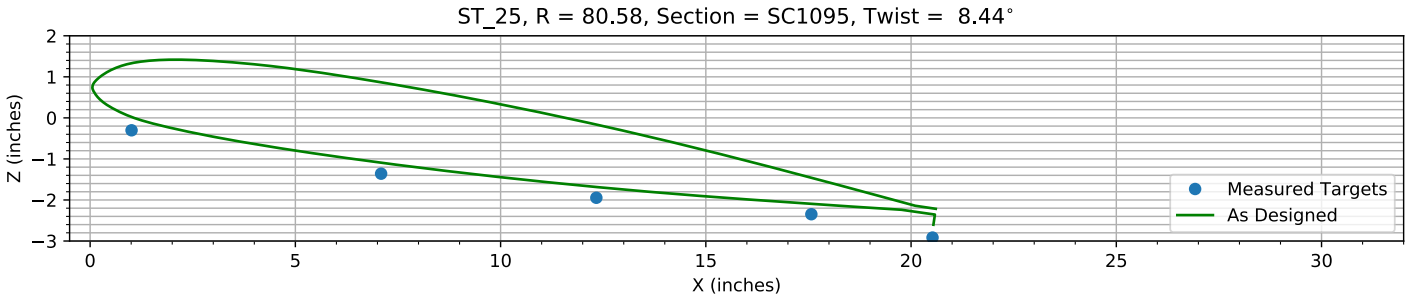

Figure 5-6. Target locations vs section profile at station 25.

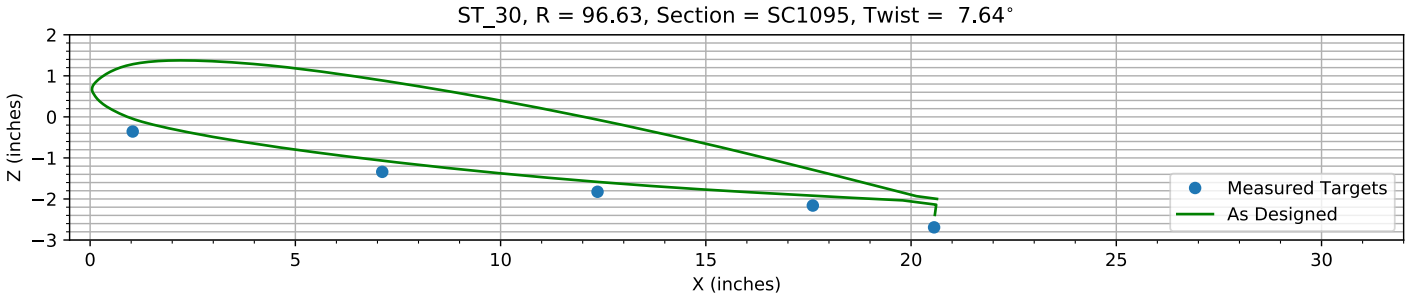

Figure 5-7. Target locations vs section profile at station 30.

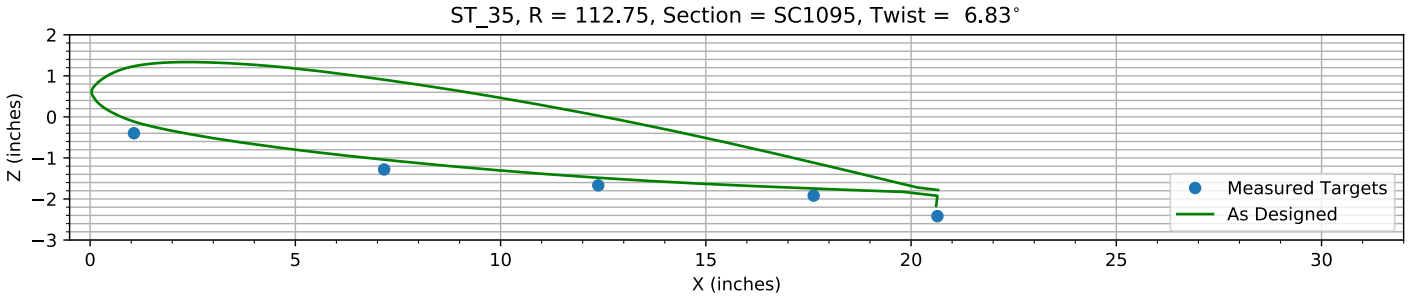

Figure 5-8. Target locations vs section profile at station 35.

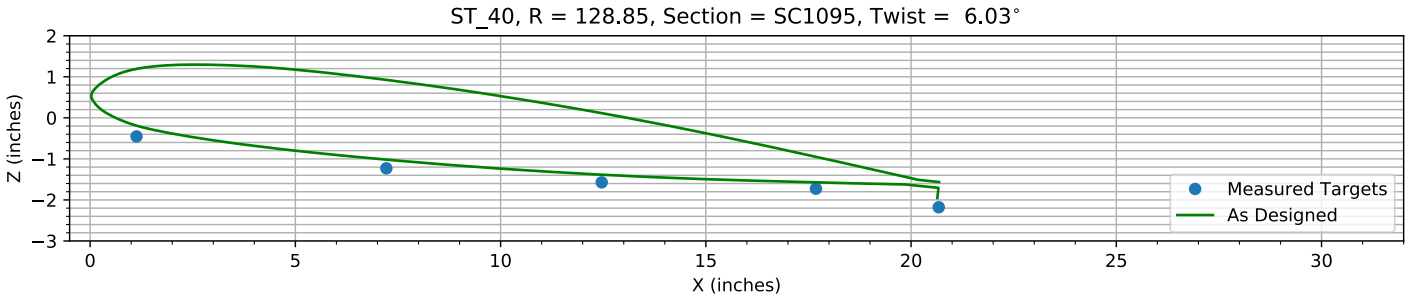

Figure 5-9. Target locations vs section profile at station 40.

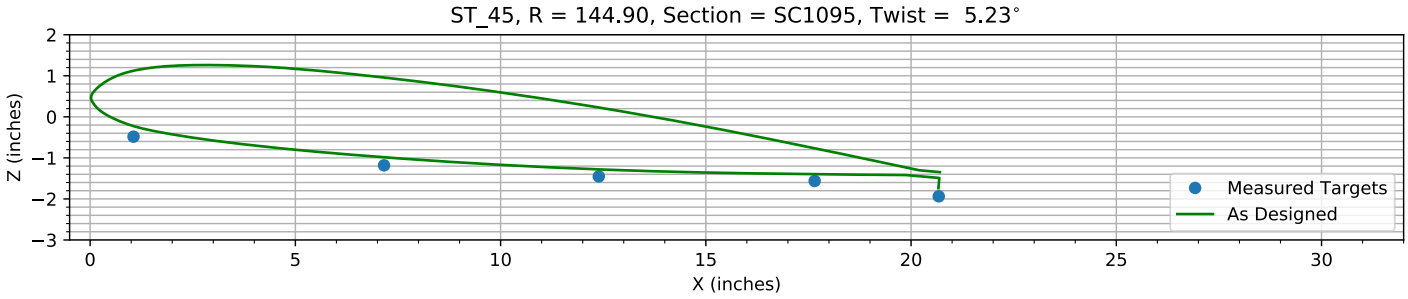

Figure 5-10. Target locations vs section profile at station 45.

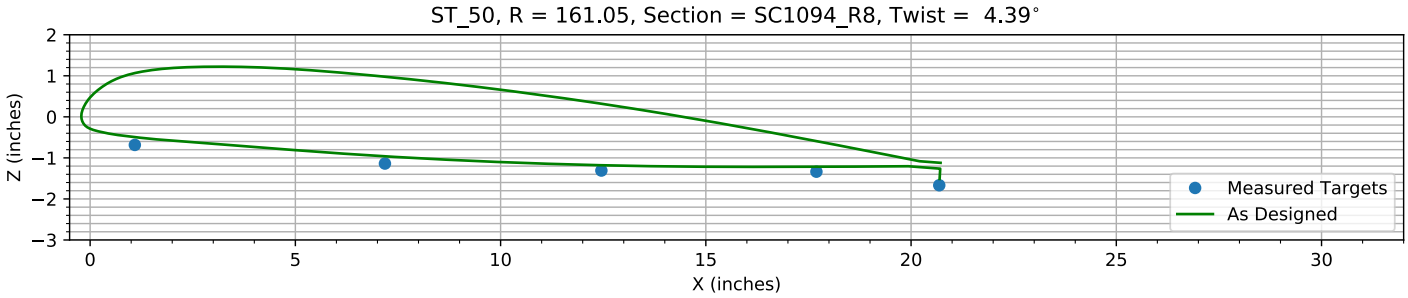

Figure 5-11. Target locations vs section profile at station 50.

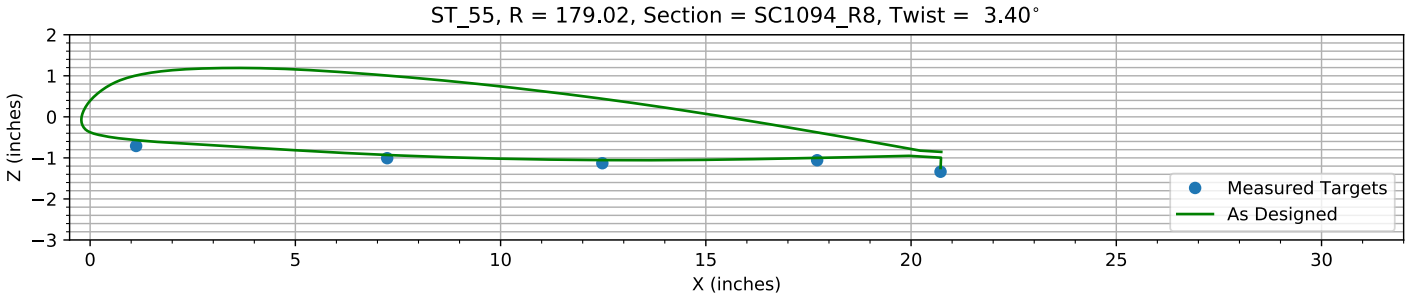

Figure 5-12. Target locations vs section profile at station 55.

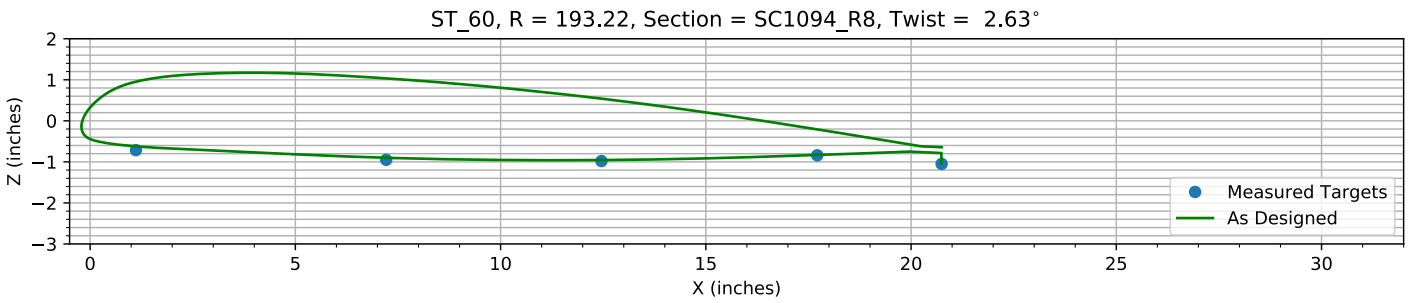

Figure 5-13. Target locations vs section profile at station 60.

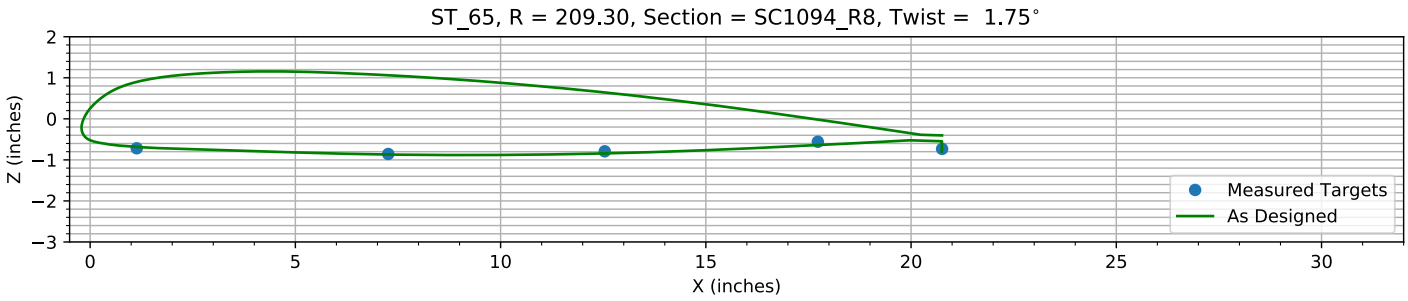

Figure 5-14. Target locations vs section profile at station 65.

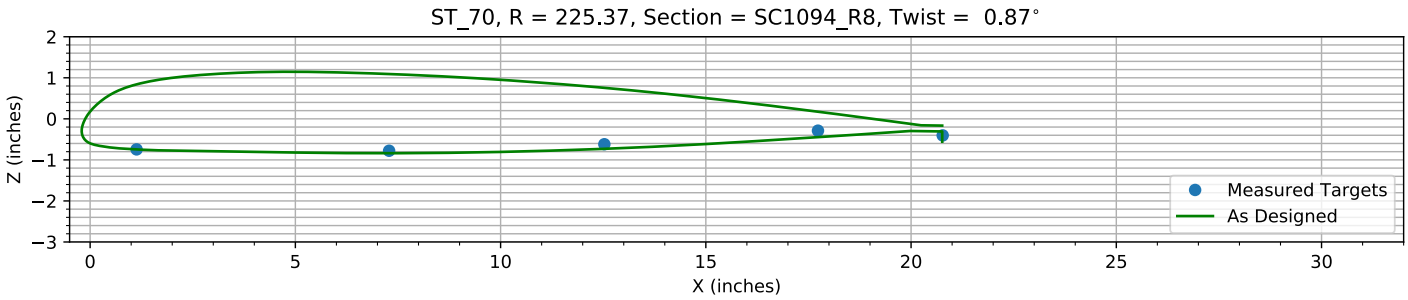

Figure 5-15. Target locations vs section profile at station 70.

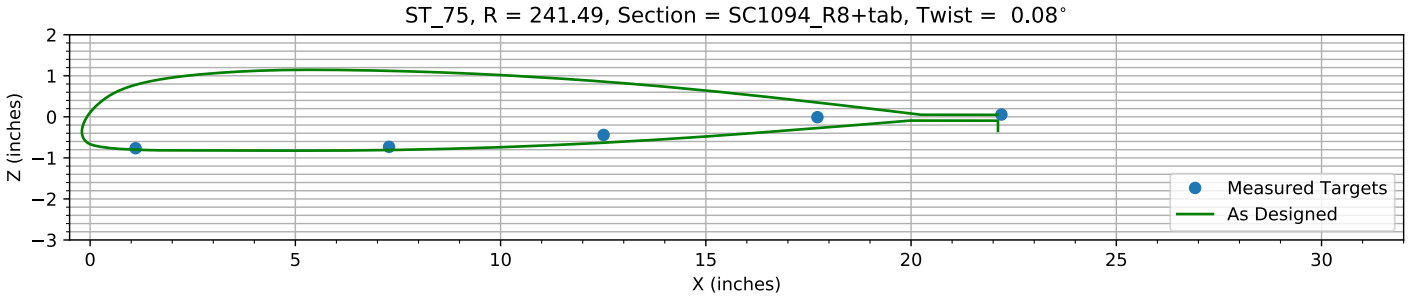

Figure 5-16. Target locations vs section profile at station 75.

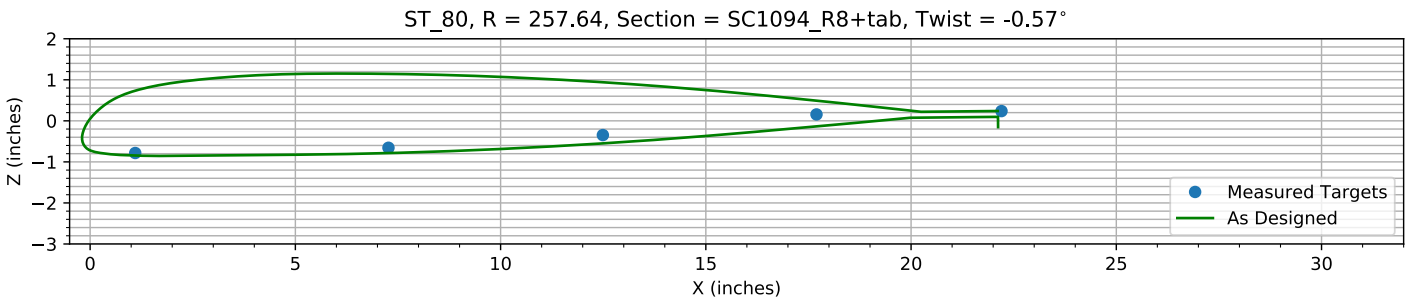

Figure 5-17. Target locations vs section profile at station 80.

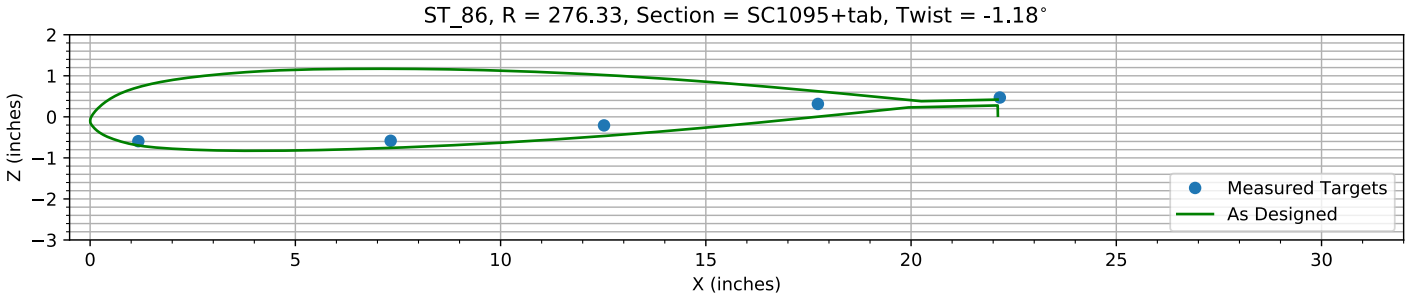

Figure 5-18. Target locations vs section profile at station 86.

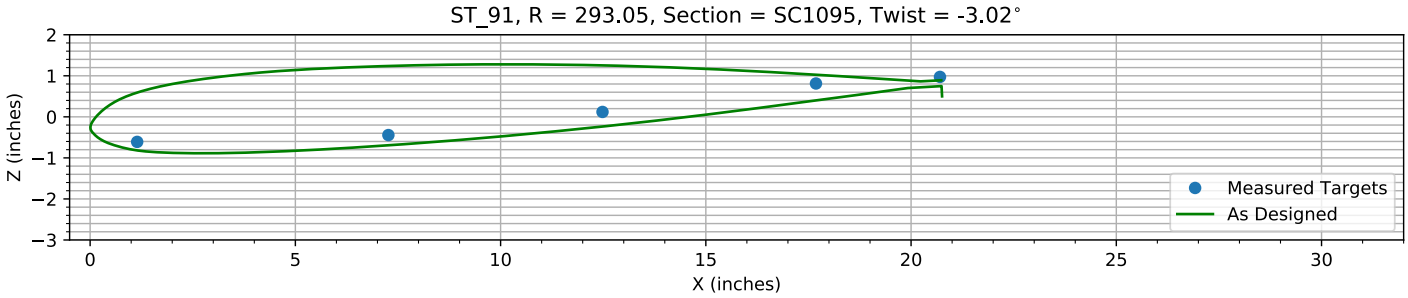

Figure 5-19. Target locations vs section profile at station 91.

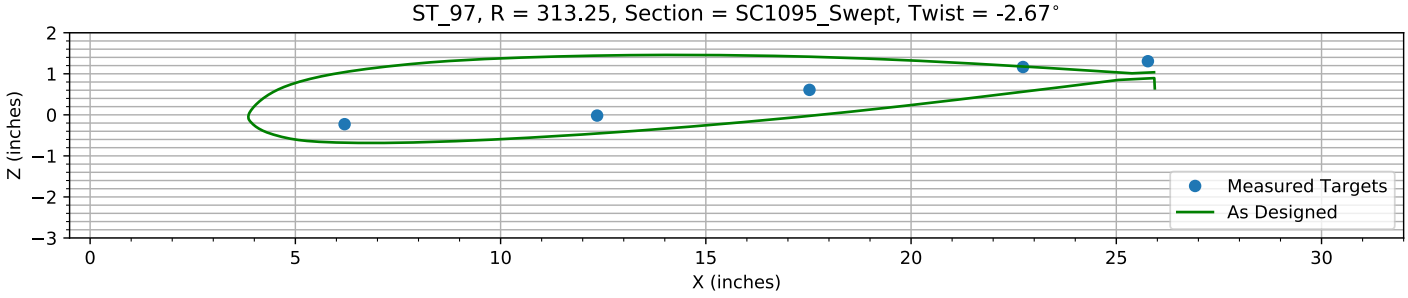

Figure 5-20. Target locations vs section profile at station 97.

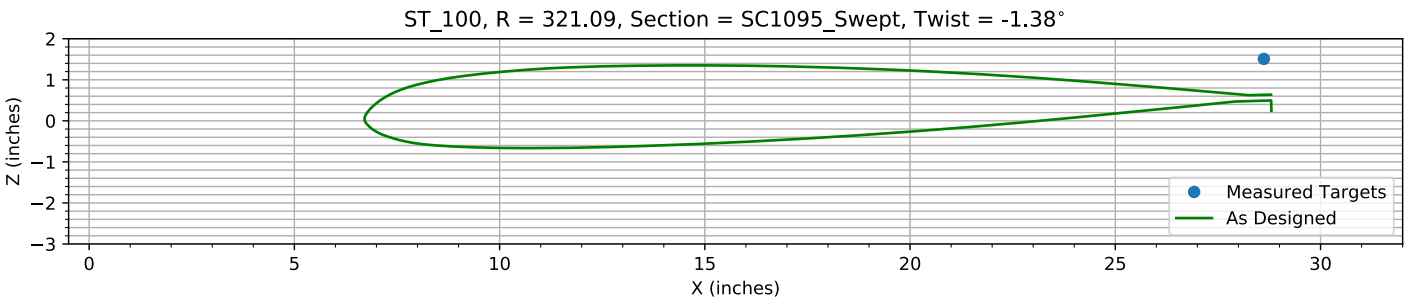

Figure 5-21. Target locations vs section profile at station 100.

Chapter 6: Flap and ΔZ Registration (6 rows)

The targets at the 6 spanwise stations nearest the root are used to determing the Z and flap offset.

The estimated Z error, -0.28444 inches, is within an allowed range of ±2.000 inches.

The estimated flap error is 0.22959°.

6.1: Target Location Errors After Flap Target Registration

Table 6-1. Measured(1) with flap registration vs as designed(2) in inches.

Name	X1	Y1	Z1	X2	Y2	Z2	dX	dY	dZ	dR
B4_R20_C05	1.0442	64.466	0.0027561	1.0442	64.466	0.067285	0	0	-0.064529	0.064529
B4_R20_C36	7.1162	64.427	-1.1406	7.1162	64.427	-1.1255	0	0	-0.015131	0.015131
B4_R20_C61	12.289	64.421	-1.7415	12.289	64.421	-1.7833	0	0	0.041864	0.041864
B4_R20_C86	17.51	64.425	-2.2243	17.51	64.425	-2.2674	0	0	0.043075	0.043075
B4_R20_C99	20.483	64.386	-2.785	20.506	64.386	-2.8207	-0.023016	0	0.035697	0.042473
B4_R25_C05	1.0092	80.595	-0.054676	1.0092	80.595	0.021287	0	0	-0.075963	0.075963
B4_R25_C36	7.089	80.583	-1.1117	7.089	80.583	-1.0924	0	0	-0.019263	0.019263
B4_R25_C61	12.333	80.572	-1.6983	12.333	80.572	-1.6844	0	0	-0.013876	0.013876
B4_R25_C86	17.57	80.575	-2.0993	17.57	80.575	-2.0946	0	0	-0.0046829	0.0046829
B4_R25_C99	20.523	80.575	-2.6679	20.544	80.575	-2.603	-0.021588	0	-0.064914	0.06841
B4_R30_C05	1.0372	96.668	-0.12048	1.0372	96.668	-0.047251	0	0	-0.07323	0.07323
B4_R30_C36	7.1163	96.665	-1.1029	7.1163	96.665	-1.067	0	0	-0.035841	0.035841
B4_R30_C61	12.361	96.636	-1.5882	12.361	96.636	-1.5844	0	0	-0.0037344	0.0037344
B4_R30_C86	17.606	96.632	-1.924	17.606	96.632	-1.9211	0	0	-0.0029963	0.0029963
B4_R30_C99	20.561	96.574	-2.4549	20.579	96.574	-2.388	-0.018182	0	-0.066944	0.069369
B4_R35_C05	1.0674	112.72	-0.17391	1.0674	112.72	-0.11495	0	0	-0.058957	0.058957
B4_R35_C36	7.1628	112.77	-1.0563	7.1628	112.77	-1.0431	0	0	-0.013218	0.013218
B4_R35_C61	12.379	112.74	-1.4441	12.379	112.74	-1.4832	0	0	0.039168	0.039168
B4_R35_C86	17.627	112.75	-1.6933	17.627	112.75	-1.746	0	0	0.052724	0.052724
B4_R35_C99	20.642	112.76	-2.1936	20.611	112.76	-2.1703	0.030749	0	-0.023278	0.038566
B4_R40_C05	1.1301	128.86	-0.23986	1.1301	128.86	-0.19104	0	0	-0.048821	0.048821
B4_R40_C36	7.2165	128.85	-1.0169	7.2165	128.85	-1.0188	0	0	0.0019707	0.0019707
B4_R40_C61	12.463	128.87	-1.3587	12.463	128.87	-1.3854	0	0	0.026645	0.026645
B4_R40_C86	17.682	128.82	-1.514	17.682	128.82	-1.5725	0	0	0.058438	0.058438
B4_R40_C99	20.674	128.86	-1.9655	20.64	128.86	-1.9537	0.034138	0	-0.011793	0.036118
B4_R45_C05	1.0572	144.92	-0.28153	1.0572	144.92	-0.2261	0	0	-0.055431	0.055431
B4_R45_C36	7.1607	144.89	-0.97952	7.1607	144.89	-0.98525	0	0	0.0057334	0.0057334
B4_R45_C61	12.392	144.89	-1.2501	12.392	144.89	-1.2804	0	0	0.030234	0.030234
B4_R45_C86	17.651	144.9	-1.3613	17.651	144.9	-1.3968	0	0	0.03558	0.03558
B4_R45_C99	20.674	144.89	-1.7345	20.666	144.89	-1.738	0.0084001	0	0.0034141	0.0090673
B4_R50_C05	1.0893	161.1	-0.49457	1.0893	161.1	-0.49442	0	0	-0.00015636	0.00015636
B4_R50_C36	7.1821	161.06	-0.94871	7.1821	161.06	-0.96167	0	0	0.012967	0.012967
B4_R50_C61	12.455	161.03	-1.119	12.455	161.03	-1.1793	0	0	0.060309	0.060309
B4_R50_C86	17.694	161.02	-1.1465	17.694	161.02	-1.2162	0	0	0.069712	0.069712
B4_R50_C99	20.686	161.05	-1.477	20.695	161.05	-1.512	-0.0090018	0	0.035072	0.036209
B4_R55_C05	1.1204	179.05	-0.5328	1.1204	179.05	-0.56684	0	0	0.034037	0.034037
B4_R55_C36	7.2369	179.04	-0.83055	7.2369	179.04	-0.92897	0	0	0.09842	0.09842
B4_R55_C61	12.478	179.04	-0.95266	12.478	179.04	-1.0542	0	0	0.10149	0.10149

Name	X1	Y1	Z1	X2	Y2	Z2	dX	dY	dZ	dR
B4_R55_C86	17.712	179.02	-0.88016	17.712	179.02	-1.0011	0	0	0.12094	0.12094
B4_R55_C99	20.718	178.99	-1.1604	20.719	178.99	-1.246	-0.001432	0	0.085685	0.085697
B4_R60_C05	1.1158	193.25	-0.54768	1.1158	193.25	-0.62089	0	0	0.073211	0.073211
B4_R60_C36	7.2132	193.24	-0.78206	7.2132	193.24	-0.90006	0	0	0.11801	0.11801
B4_R60_C61	12.457	193.22	-0.81319	12.457	193.22	-0.95563	0	0	0.14244	0.14244
B4_R60_C86	17.714	193.24	-0.67354	17.714	193.24	-0.83128	0	0	0.15774	0.15774
B4_R60_C99	20.744	193.19	-0.88297	20.734	193.19	-1.0353	0.0096282	0	0.15234	0.15264
B4_R65_C05	1.1355	209.29	-0.56239	1.1355	209.29	-0.68393	0	0	0.12155	0.12155
B4_R65_C36	7.2627	209.32	-0.70121	7.2627	209.32	-0.86938	0	0	0.16817	0.16817
B4_R65_C61	12.537	209.32	-0.63628	12.537	209.32	-0.84222	0	0	0.20594	0.20594
B4_R65_C86	17.728	209.32	-0.40341	17.728	209.32	-0.6386	0	0	0.2352	0.2352
B4_R65_C99	20.756	209.26	-0.57655	20.749	209.26	-0.79664	0.0075921	0	0.22009	0.22022
B4_R70_C05	1.132	225.35	-0.601	1.132	225.35	-0.74522	0	0	0.14421	0.14421
B4_R70_C36	7.2839	225.38	-0.63393	7.2839	225.38	-0.8375	0	0	0.20357	0.20357
B4_R70_C61	12.527	225.37	-0.47499	12.527	225.37	-0.7304	0	0	0.25541	0.25541
B4_R70_C86	17.732	225.38	-0.14434	17.732	225.38	-0.4466	0	0	0.30226	0.30226
B4_R70_C99	20.77	225.41	-0.25995	20.759	225.41	-0.55668	0.011388	0	0.29673	0.29695
B4_R75_C05	1.1079	241.49	-0.63292	1.1079	241.49	-0.8	0	0	0.16708	0.16708
B4_R75_C36	7.282	241.51	-0.59856	7.282	241.51	-0.80862	0	0	0.21006	0.21006
B4_R75_C61	12.509	241.5	-0.30943	12.509	241.5	-0.63013	0	0	0.3207	0.3207
B4_R75_C86	17.718	241.5	0.12386	17.718	241.5	-0.2744	0	0	0.39826	0.39826
B4_R80_C05	1.0986	257.62	-0.66333	1.0986	257.62	-0.84525	0	0	0.18192	0.18192
B4_R80_C36	7.2681	257.65	-0.53566	7.2681	257.65	-0.78565	0	0	0.24999	0.24999
B4_R80_C61	12.491	257.66	-0.2266	12.491	257.66	-0.54928	0	0	0.32268	0.32268
B4_R80_C86	17.696	257.68	0.27652	17.696	257.68	-0.13545	0	0	0.41197	0.41197
B4_R86_C05	1.1744	276.34	-0.48663	1.1744	276.34	-0.69698	0	0	0.21034	0.21034
B4_R86_C36	7.3217	276.34	-0.47633	7.3217	276.34	-0.7568	0	0	0.28047	0.28047
B4_R86_C61	12.519	276.33	-0.10172	12.519	276.33	-0.46656	0	0	0.36485	0.36485
B4_R86_C86	17.73	276.33	0.42141	17.73	276.33	0.0022558	0	0	0.41916	0.41916
B4_R91_C05	1.146	293.02	-0.51507	1.146	293.02	-0.81804	0	0	0.30297	0.30297
B4_R91_C36	7.2662	293.06	-0.34924	7.2662	293.06	-0.6935	0	0	0.34426	0.34426
B4_R91_C61	12.483	293.07	0.21413	12.483	293.07	-0.236	0	0	0.45014	0.45014
B4_R91_C86	17.683	293.07	0.90715	17.683	293.07	0.39956	0	0	0.50758	0.50758
B4_R91_C99	20.704	293.05	1.0677	20.755	293.05	0.49945	-0.051123	0	0.56825	0.57054
B4_R97_C05	6.1992	313.22	-0.14723	6.1992	313.22	-0.67944	0	0	0.53221	0.53221
B4_R97_C36	12.351	313.21	0.062332	12.351	313.21	-0.45459	0	0	0.51693	0.51693
B4_R97_C61	17.525	313.28	0.68855	17.525	313.28	-0.027309	0	0	0.71586	0.71586
B4_R97_C86	22.727	313.26	1.2454	22.727	313.26	0.56075	0	0	0.68466	0.68466
B4_R97_C99	25.77	313.28	1.3867	25.95	313.28	0.64406	-0.17983	0	0.74259	0.76405
HUB_LE	2.1813	30.001	-3.2155	2.19	30	-3.5	-0.0086618	0.0014437	0.28453	0.28467
HUB_TE	8.1763	30.001	-3.2158	8.19	30	-3.5	-0.013662	0.00083768	0.28424	0.28456
RMS Errors:							0.022243	0.00018779	0.25311	0.25409

6.2: Flap Registration Plots (6 rows)

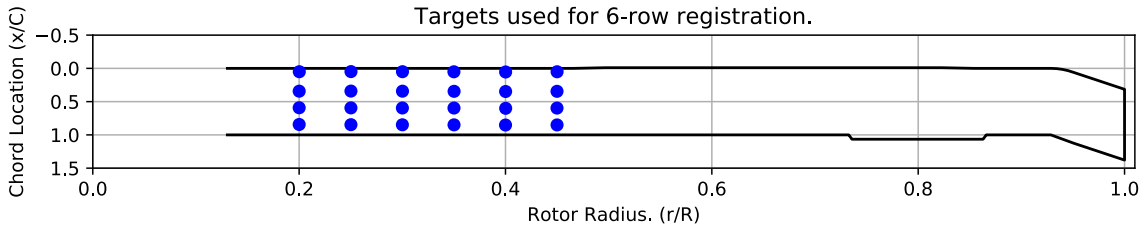

Figure 6-1. Targets used for 6 row root registration.

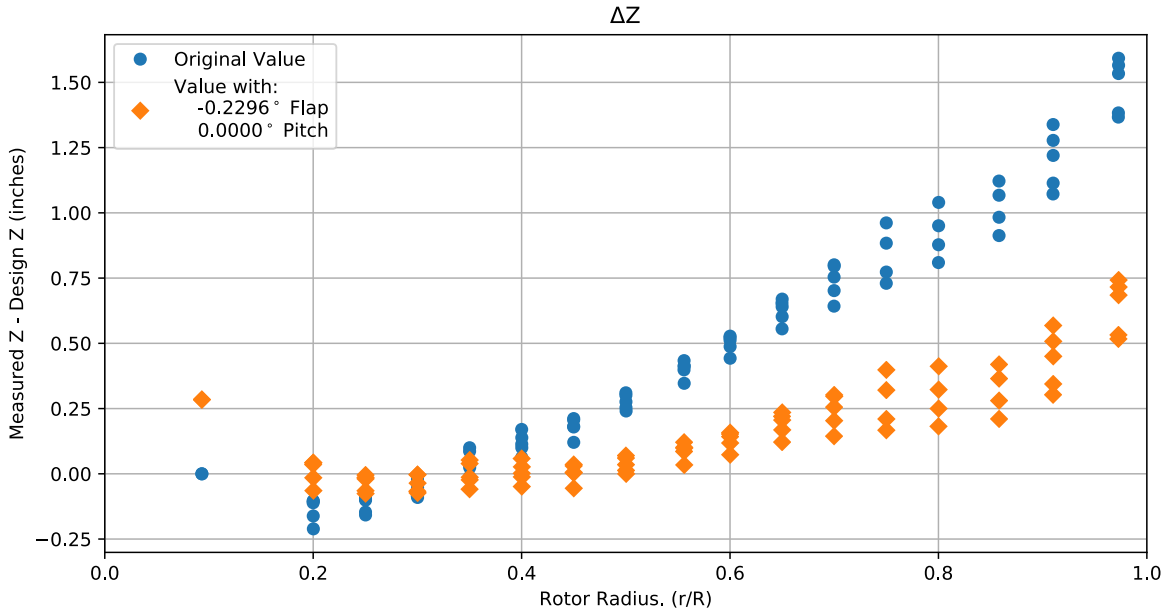

Figure 6-2. Flap target registration, ΔZ error vs rotor radius.

Note: the “as designed” geometry used for the swept tip may have some inaccuracies.

6.3: Estimated Bending and Twist at the Quarter Chord

The error bars shown represent the residual errors for fitting the measure target locations to the "as designed" geometry. These errors are generally much larger than those due to the VSTARS measurement errors. Therefore, the most likely source of these errors is the placement of the trailing-edge targets, differences between the "as designed" and "as built" geometries, and blade deformation during measurement. In the future, iterative adjustment of the "as designed" twist angle may be implemented to see if it reduces the fit error in delta twist. Note: The "as designed" geometry used for the swept tip may have some inaccuracies.

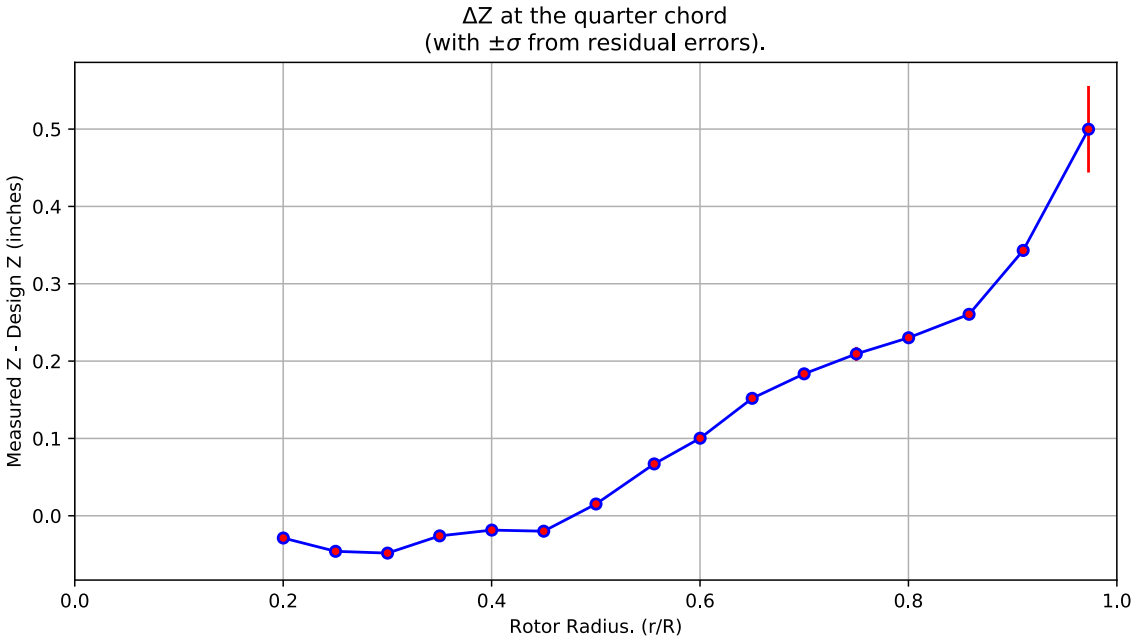

Figure 6-3. ΔZ error at the quarter chord vs rotor radius.

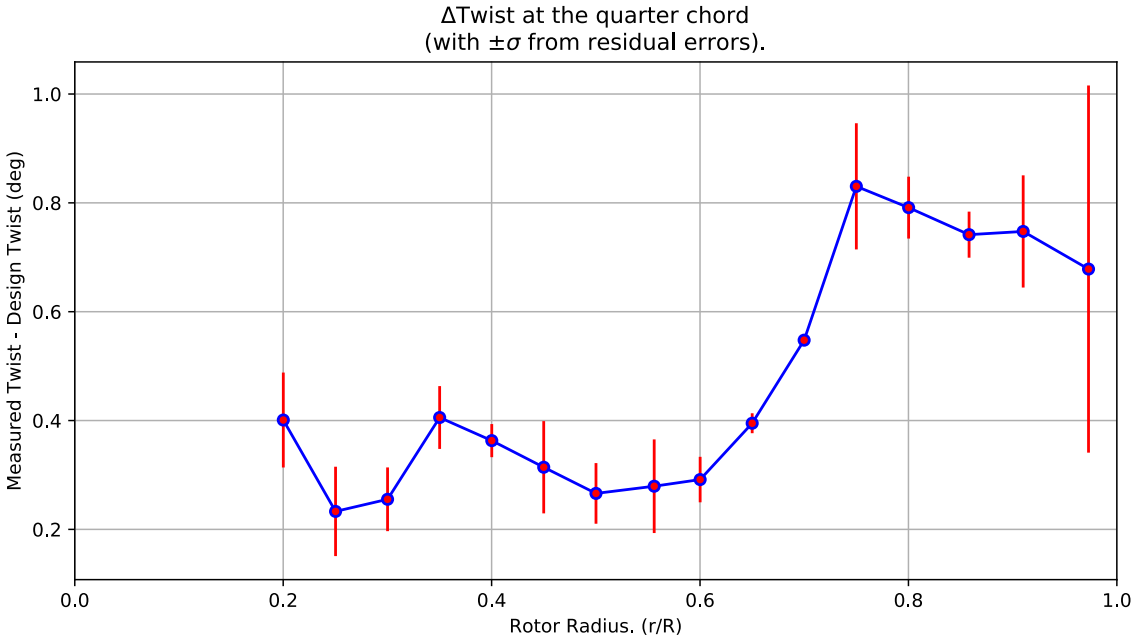

Figure 6-4. ΔTwist error at the quarter chord vs rotor radius.

Table 6-2. Quarter-chord bending and twist statistics.

r	r/R	dZ 1/4-chord	dT	sigma dZ meas	sigma dT meas	sigma dZ res	sigma dT res	n	t_conf
64.434	0.20011	-0.028771	0.40095	6.1154e-10	4.6917e-09	0.0065459	0.087219	4	4.3027
80.581	0.25025	-0.045976	0.23302	6.1073e-10	4.6617e-09	0.0061775	0.082115	4	4.3027
96.65	0.30016	-0.04829	0.25529	6.1204e-10	4.6595e-09	0.0044353	0.058549	4	4.3027
112.74	0.35014	-0.025999	0.40557	6.136e-10	4.664e-09	0.0044012	0.057713	4	4.3027
128.85	0.40015	-0.018535	0.36309	6.166e-10	4.6634e-09	0.0023543	0.030427	4	4.3027
144.9	0.45	-0.019963	0.31419	6.1345e-10	4.6542e-09	0.0064751	0.084792	4	4.3027
161.05	0.50017	0.015203	0.2661	6.1506e-10	4.648e-09	0.0042936	0.055718	4	4.3027
179.04	0.55601	0.067045	0.27931	6.1682e-10	4.6539e-09	0.0066774	0.086035	4	4.3027
193.24	0.60011	0.10028	0.29155	6.1618e-10	4.6521e-09	0.003236	0.041804	4	4.3027
209.32	0.65005	0.15185	0.39504	6.1805e-10	4.6503e-09	0.0014312	0.01832	4	4.3027
225.37	0.6999	0.18355	0.54769	6.1822e-10	4.6507e-09	0.00055509	0.0071004	4	4.3027
241.5	0.75	0.20932	0.83036	6.1746e-10	4.6486e-09	0.0090357	0.11594	4	4.3027
257.65	0.80017	0.2302	0.79125	6.1687e-10	4.6524e-09	0.0044159	0.056866	4	4.3027
276.33	0.85818	0.26051	0.74157	6.1975e-10	4.6655e-09	0.0033216	0.04232	4	4.3027
293.05	0.9101	0.34312	0.74749	6.1789e-10	4.6687e-09	0.0080166	0.1031	4	4.3027
313.24	0.9728	0.49981	0.67834	9.2317e-10	4.6745e-09	0.056008	0.33736	4	4.3027

6.4: Section Plots

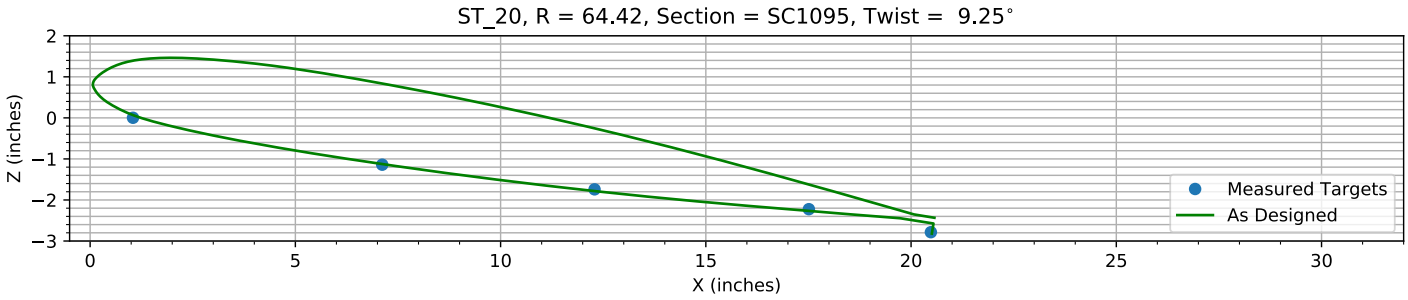

Figure 6-5. Target locations vs section profile at station 20.

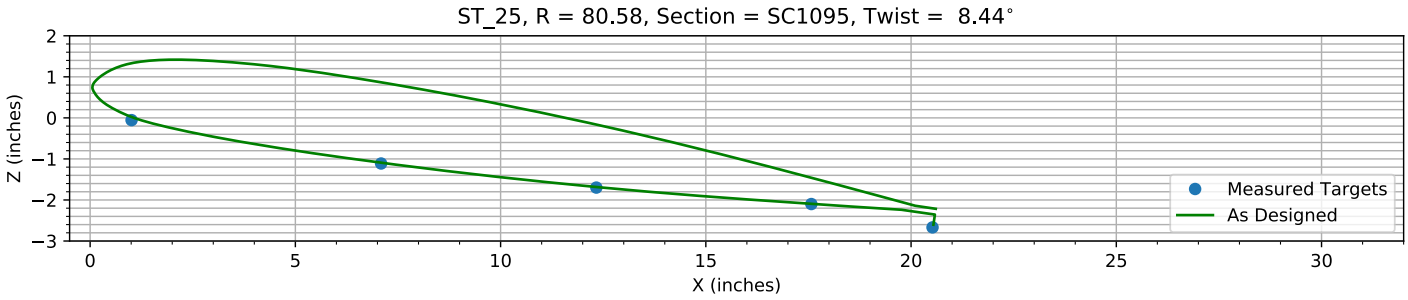

Figure 6-6. Target locations vs section profile at station 25.

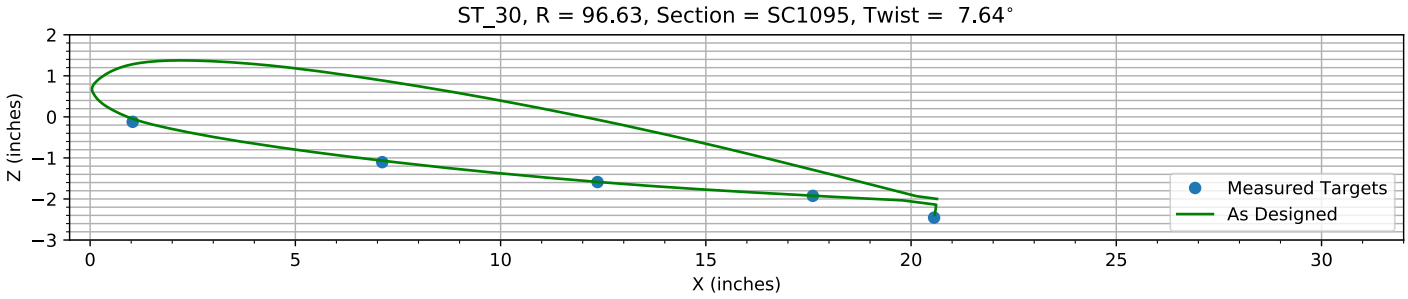

Figure 6-7. Target locations vs section profile at station 30.

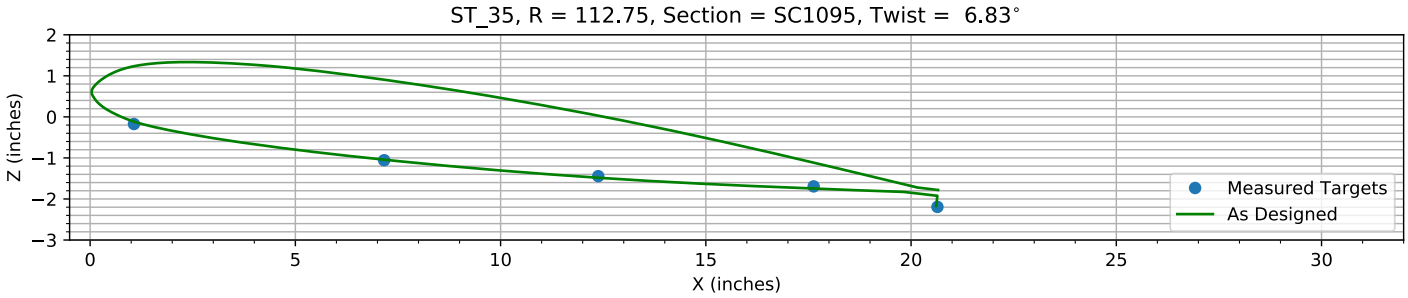

Figure 6-8. Target locations vs section profile at station 35.

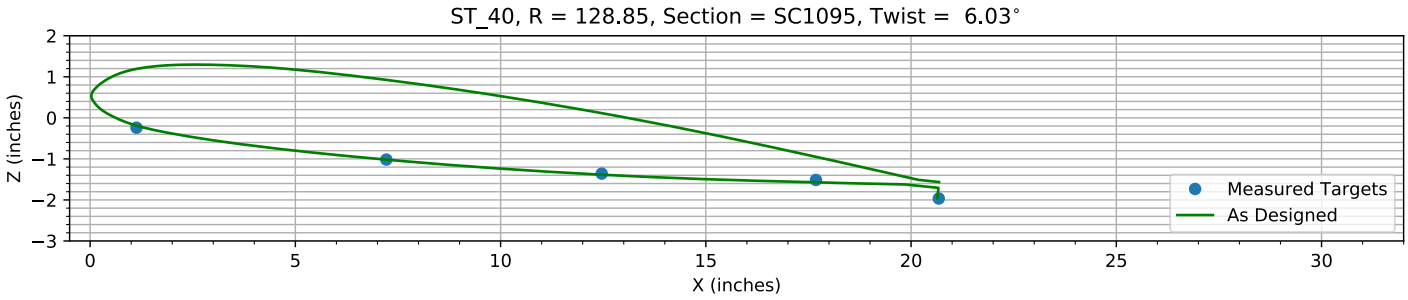

Figure 6-9. Target locations vs section profile at station 40.

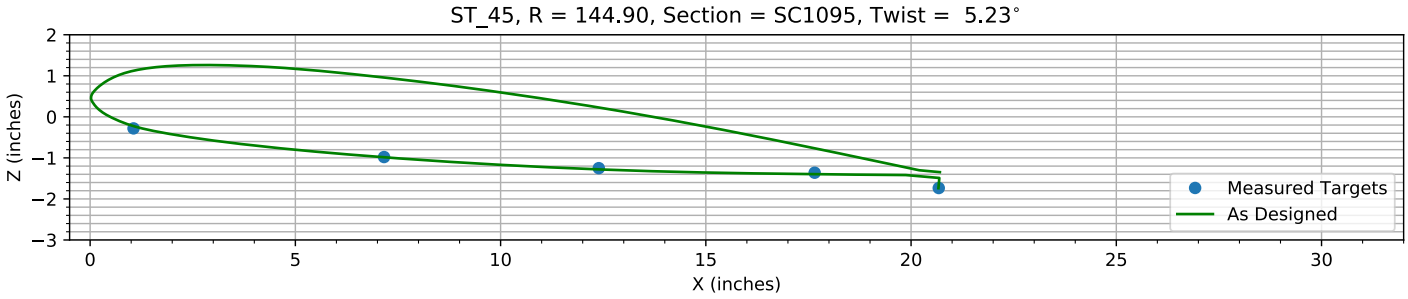

Figure 6-10. Target locations vs section profile at station 45.

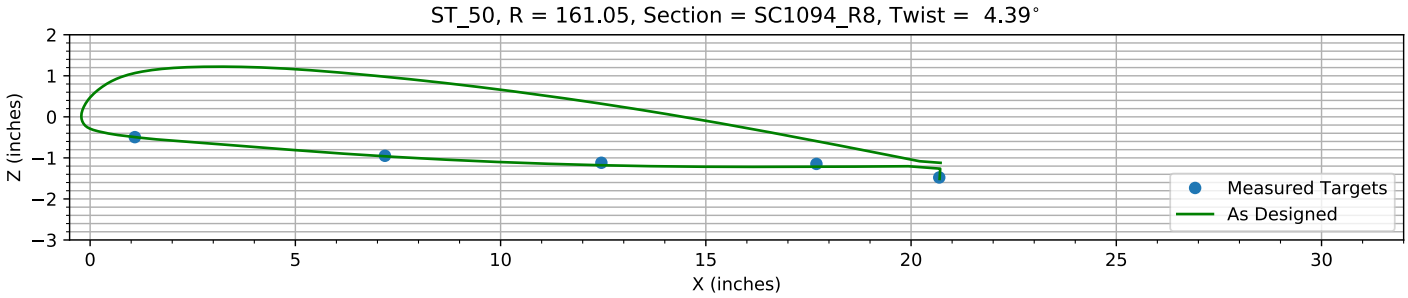

Figure 6-11. Target locations vs section profile at station 50.

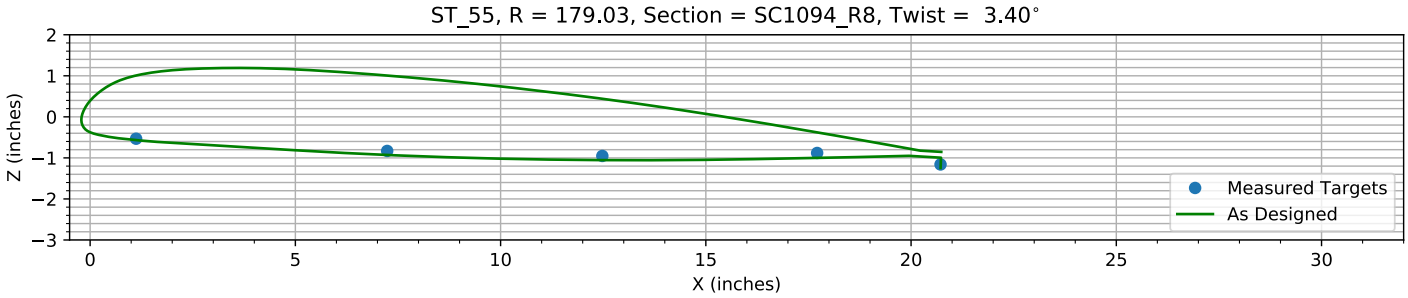

Figure 6-12. Target locations vs section profile at station 55.

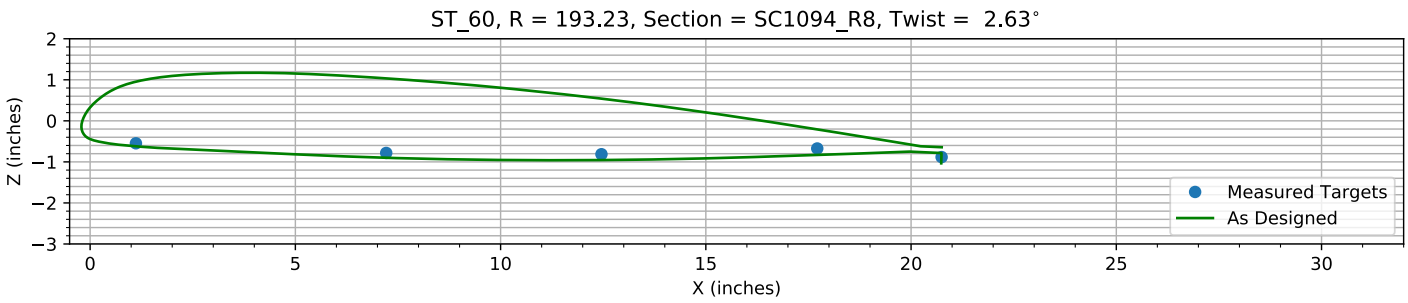

Figure 6-13. Target locations vs section profile at station 60.

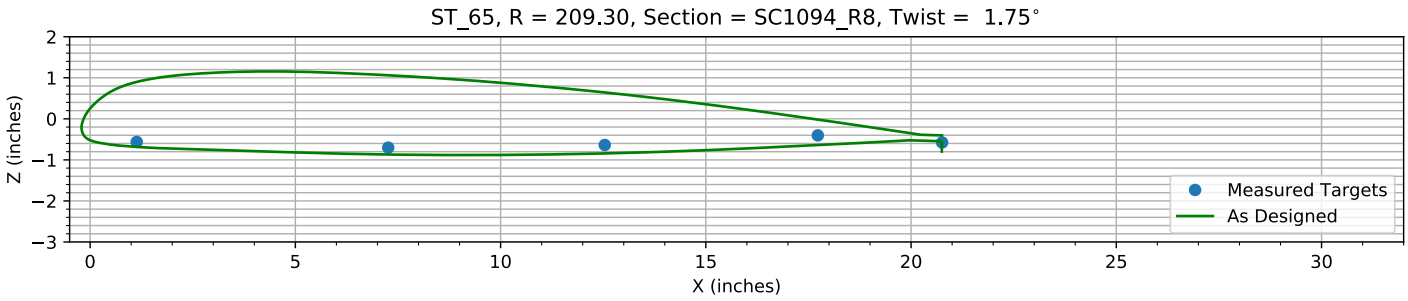

Figure 6-14. Target locations vs section profile at station 65.

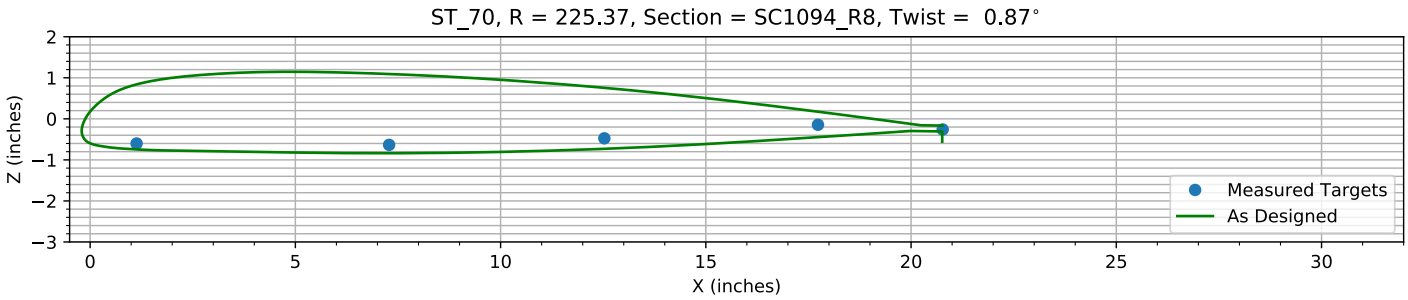

Figure 6-15. Target locations vs section profile at station 70.

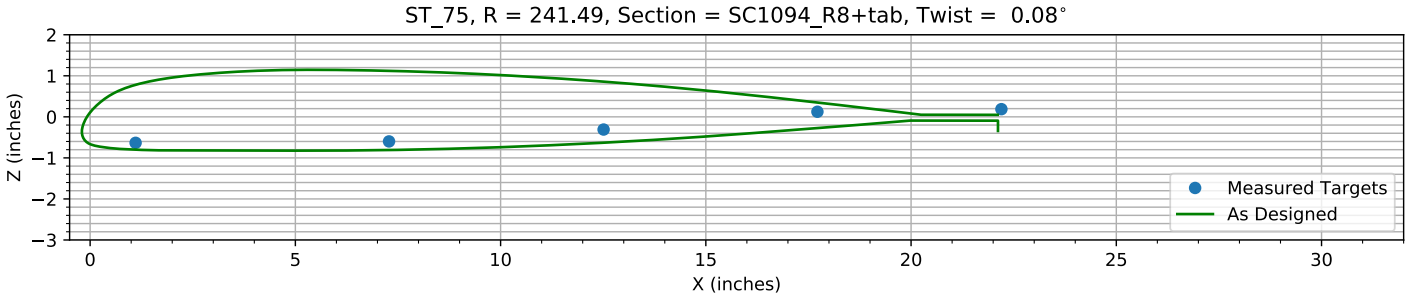

Figure 6-16. Target locations vs section profile at station 75.

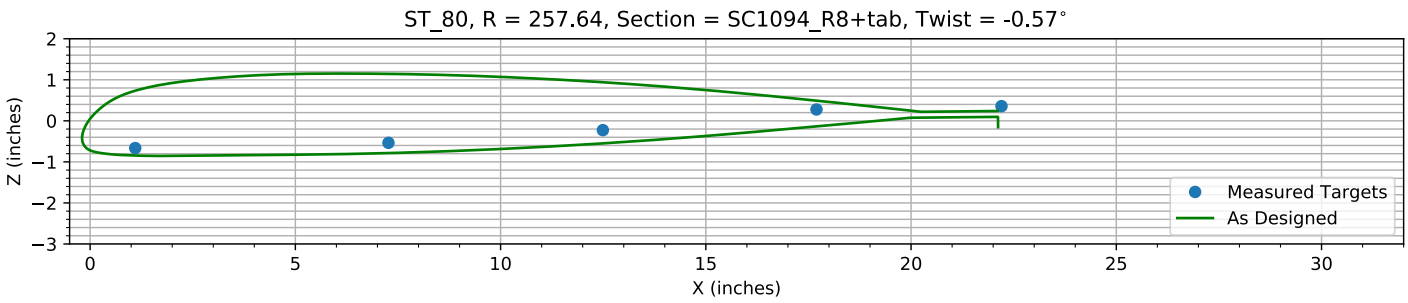

Figure 6-17. Target locations vs section profile at station 80.

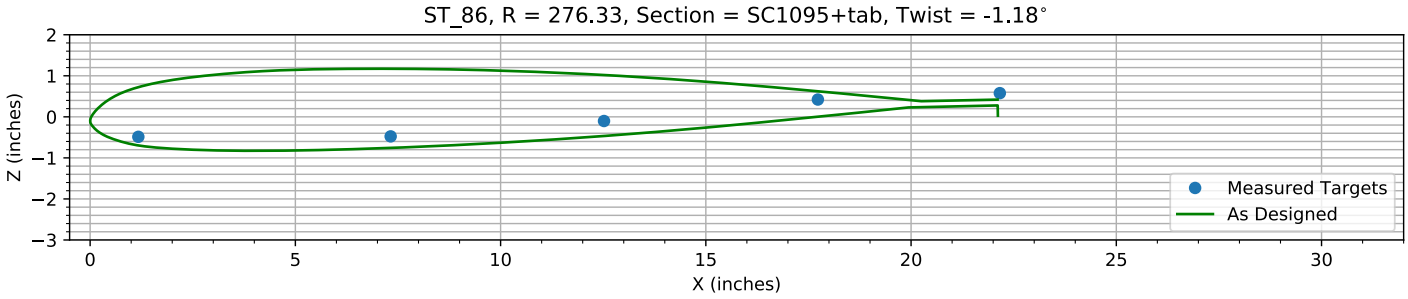

Figure 6-18. Target locations vs section profile at station 86.

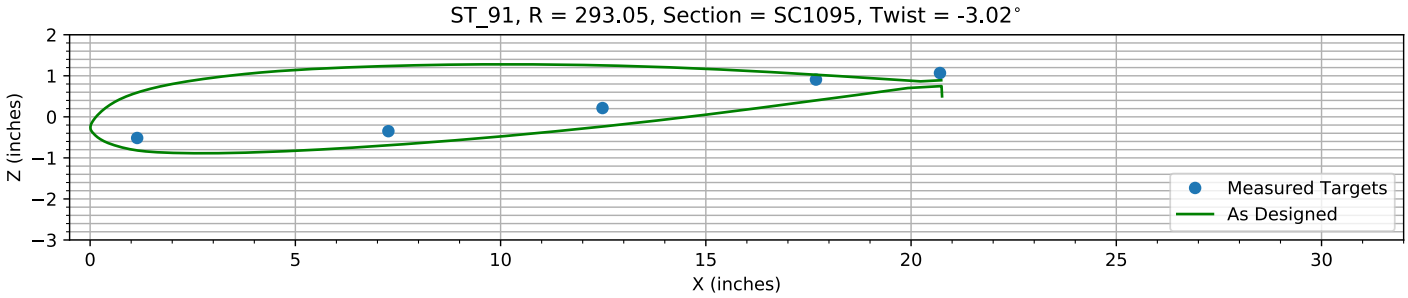

Figure 6-19. Target locations vs section profile at station 91.

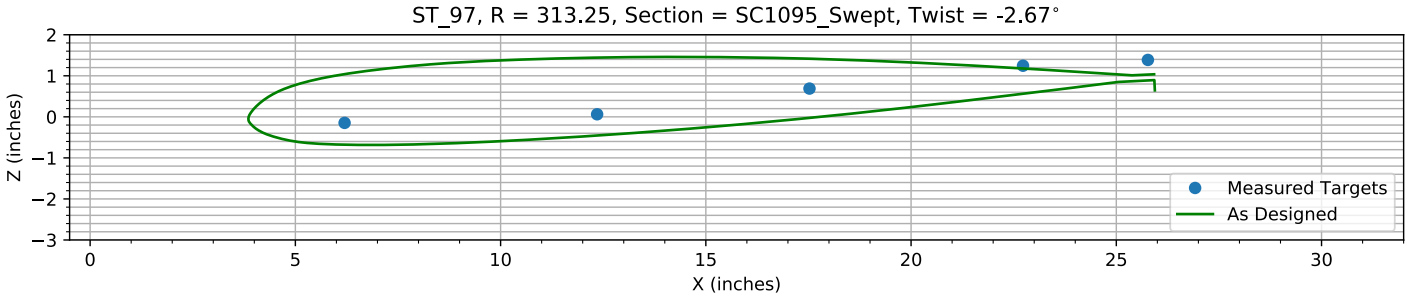

Figure 6-20. Target locations vs section profile at station 97.

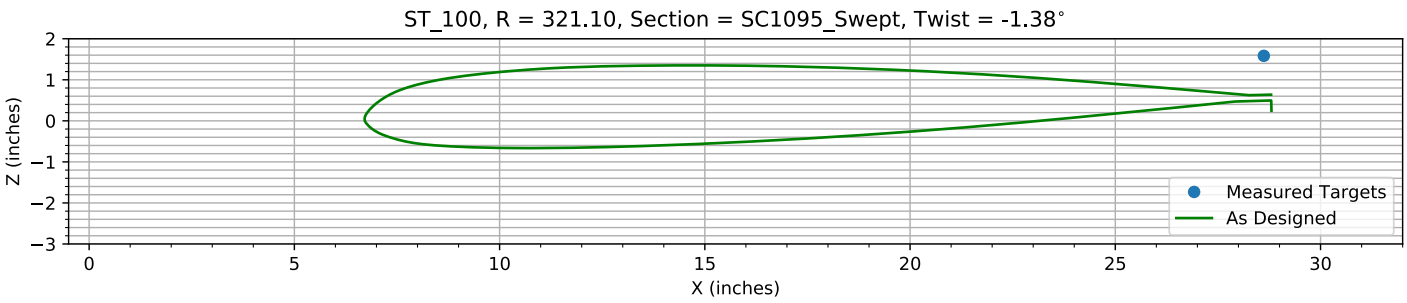

Figure 6-21. Target locations vs section profile at station 100.

Chapter 7: Flap and ΔZ Registration (15 rows)

The targets at the 15 spanwise stations nearest the root are used to determing the Z and flap offset.

The estimated Z error, -0.41464 inches, is within an allowed range of ±2.000 inches.

The estimated flap error is 0.32351°.

7.1: Target Location Errors After Flap Target Registration

Table 7-1. Measured(1) with flap registration vs as designed(2) in inches.

Name	X1	Y1	Z1	X2	Y2	Z2	dX	dY	dZ	dR
B4_R20_C05	1.0442	64.473	0.076456	1.0442	64.473	0.067261	0	0	0.0091951	0.0091951
B4_R20_C36	7.1162	64.431	-1.0668	7.1162	64.431	-1.1255	0	0	0.058627	0.058627
B4_R20_C61	12.289	64.424	-1.6677	12.289	64.424	-1.7833	0	0	0.11562	0.11562
B4_R20_C86	17.51	64.427	-2.1505	17.51	64.427	-2.2673	0	0	0.11682	0.11682
B4_R20_C99	20.483	64.388	-2.7112	20.506	64.388	-2.8207	-0.023021	0	0.10951	0.1119
B4_R25_C05	1.0092	80.602	-0.0074162	1.0092	80.602	0.021264	0	0	-0.02868	0.02868
B4_R25_C36	7.089	80.587	-1.0644	7.089	80.587	-1.0924	0	0	0.028011	0.028011
B4_R25_C61	12.333	80.576	-1.651	12.333	80.576	-1.6844	0	0	0.033402	0.033402
B4_R25_C86	17.57	80.578	-2.052	17.57	80.578	-2.0946	0	0	0.04258	0.04258
B4_R25_C99	20.523	80.577	-2.6206	20.544	80.577	-2.603	-0.021593	0	-0.017645	0.027885
B4_R30_C05	1.0372	96.674	-0.09957	1.0372	96.674	-0.047273	0	0	-0.052296	0.052296
B4_R30_C36	7.1163	96.669	-1.082	7.1163	96.669	-1.067	0	0	-0.01493	0.01493
B4_R30_C61	12.361	96.639	-1.5672	12.361	96.639	-1.5844	0	0	0.017208	0.017208
B4_R30_C86	17.606	96.635	-1.9031	17.606	96.635	-1.921	0	0	0.017942	0.017942
B4_R30_C99	20.561	96.576	-2.4339	20.579	96.576	-2.3879	-0.018187	0	-0.045906	0.049377
B4_R35_C05	1.0674	112.73	-0.17931	1.0674	112.73	-0.11497	0	0	-0.064339	0.064339
B4_R35_C36	7.1628	112.78	-1.0618	7.1628	112.78	-1.0431	0	0	-0.018712	0.018712
B4_R35_C61	12.379	112.74	-1.4495	12.379	112.74	-1.4832	0	0	0.033714	0.033714
B4_R35_C86	17.627	112.75	-1.6988	17.627	112.75	-1.746	0	0	0.047239	0.047239
B4_R35_C99	20.642	112.77	-2.1991	20.611	112.77	-2.1703	0.030743	0	-0.028785	0.042116
B4_R40_C05	1.1301	128.86	-0.27171	1.1301	128.86	-0.19106	0	0	-0.080654	0.080654
B4_R40_C36	7.2165	128.86	-1.0487	7.2165	128.86	-1.0188	0	0	-0.029884	0.029884
B4_R40_C61	12.463	128.87	-1.3906	12.463	128.87	-1.3853	0	0	-0.0052551	0.0052551
B4_R40_C86	17.682	128.82	-1.5458	17.682	128.82	-1.5724	0	0	0.026601	0.026601
B4_R40_C99	20.674	128.87	-1.9974	20.64	128.87	-1.9537	0.034133	0	-0.043699	0.055449
B4_R45_C05	1.0572	144.93	-0.33972	1.0572	144.93	-0.22612	0	0	-0.1136	0.1136
B4_R45_C36	7.1607	144.9	-1.0377	7.1607	144.9	-0.98524	0	0	-0.052412	0.052412
B4_R45_C61	12.392	144.89	-1.3083	12.392	144.89	-1.2803	0	0	-0.027928	0.027928
B4_R45_C86	17.651	144.91	-1.4194	17.651	144.91	-1.3968	0	0	-0.022621	0.022621
B4_R45_C99	20.674	144.9	-1.7927	20.666	144.9	-1.7379	0.0083948	0	-0.054776	0.055415
B4_R50_C05	1.0893	161.11	-0.57929	1.0893	161.11	-0.49444	0	0	-0.084848	0.084848
B4_R50_C36	7.1821	161.06	-1.0333	7.1821	161.06	-0.96166	0	0	-0.071684	0.071684
B4_R50_C61	12.455	161.04	-1.2036	12.455	161.04	-1.1793	0	0	-0.02432	0.02432
B4_R50_C86	17.694	161.03	-1.2311	17.694	161.03	-1.2161	0	0	-0.014926	0.014926
B4_R50_C99	20.686	161.05	-1.5616	20.695	161.05	-1.512	-0.0090074	0	-0.049612	0.050423
B4_R55_C05	1.1204	179.06	-0.64694	1.1204	179.06	-0.56686	0	0	-0.080081	0.080081
B4_R55_C36	7.2369	179.04	-0.94466	7.2369	179.04	-0.92896	0	0	-0.015706	0.015706
B4_R55_C61	12.478	179.04	-1.0668	12.478	179.04	-1.0541	0	0	-0.012658	0.012658

Name	X1	Y1	Z1	X2	Y2	Z2	dX	dY	dZ	dR
B4_R55_C86	17.712	179.02	-0.99424	17.712	179.02	-1.001	0	0	0.0067995	0.0067995
B4_R55_C99	20.718	178.99	-1.2744	20.719	178.99	-1.246	-0.0014372	0	-0.028418	0.028454
B4_R60_C05	1.1158	193.25	-0.68508	1.1158	193.25	-0.62091	0	0	-0.064174	0.064174
B4_R60_C36	7.2132	193.24	-0.91945	7.2132	193.24	-0.90005	0	0	-0.0194	0.0194
B4_R60_C61	12.457	193.23	-0.95056	12.457	193.23	-0.9556	0	0	0.00504	0.00504
B4_R60_C86	17.714	193.24	-0.81093	17.714	193.24	-0.83122	0	0	0.020293	0.020293
B4_R60_C99	20.744	193.2	-1.0203	20.734	193.2	-1.0352	0.0096235	0	0.014947	0.017777
B4_R65_C05	1.1355	209.3	-0.7261	1.1355	209.3	-0.68395	0	0	-0.042147	0.042147
B4_R65_C36	7.2627	209.33	-0.86497	7.2627	209.33	-0.86937	0	0	0.0043951	0.0043951
B4_R65_C61	12.537	209.32	-0.80004	12.537	209.32	-0.84219	0	0	0.04215	0.04215
B4_R65_C86	17.728	209.33	-0.56717	17.728	209.33	-0.63854	0	0	0.071366	0.071366
B4_R65_C99	20.756	209.27	-0.74021	20.749	209.27	-0.79656	0.0075881	0	0.056353	0.056861
B4_R70_C05	1.132	225.35	-0.79103	1.132	225.35	-0.74524	0	0	-0.045796	0.045796
B4_R70_C36	7.2839	225.38	-0.824	7.2839	225.38	-0.83749	0	0	0.013483	0.013483
B4_R70_C61	12.527	225.37	-0.66505	12.527	225.37	-0.73036	0	0	0.065308	0.065308
B4_R70_C86	17.732	225.39	-0.33443	17.732	225.39	-0.44653	0	0	0.1121	0.1121
B4_R70_C99	20.77	225.41	-0.45008	20.759	225.41	-0.55659	0.011385	0	0.10652	0.10712
B4_R75_C05	1.1079	241.5	-0.84942	1.1079	241.5	-0.80002	0	0	-0.049401	0.049401
B4_R75_C36	7.282	241.51	-0.81508	7.282	241.51	-0.80861	0	0	-0.0064714	0.0064714
B4_R75_C61	12.509	241.5	-0.52594	12.509	241.5	-0.6301	0	0	0.10416	0.10416
B4_R75_C86	17.718	241.51	-0.092647	17.718	241.51	-0.27434	0	0	0.18169	0.18169
B4_R80_C05	1.0986	257.63	-0.90627	1.0986	257.63	-0.84527	0	0	-0.061005	0.061005
B4_R80_C36	7.2681	257.66	-0.77864	7.2681	257.66	-0.78564	0	0	0.0069972	0.0069972
B4_R80_C61	12.491	257.67	-0.46961	12.491	257.67	-0.54926	0	0	0.079647	0.079647
B4_R80_C86	17.696	257.69	0.033482	17.696	257.69	-0.1354	0	0	0.16888	0.16888
B4_R86_C05	1.1744	276.34	-0.76025	1.1744	276.34	-0.69698	0	0	-0.063267	0.063267
B4_R86_C36	7.3217	276.34	-0.74995	7.3217	276.34	-0.7568	0	0	0.0068478	0.0068478
B4_R86_C61	12.519	276.34	-0.37533	12.519	276.34	-0.46655	0	0	0.091216	0.091216
B4_R86_C86	17.73	276.33	0.14781	17.73	276.33	0.0022884	0	0	0.14552	0.14552
B4_R91_C05	1.146	293.02	-0.81604	1.146	293.02	-0.81808	0	0	0.0020443	0.0020443
B4_R91_C36	7.2662	293.06	-0.65027	7.2662	293.06	-0.69348	0	0	0.043212	0.043212
B4_R91_C61	12.483	293.07	-0.086915	12.483	293.07	-0.23592	0	0	0.14901	0.14901
B4_R91_C86	17.683	293.07	0.60611	17.683	293.07	0.39974	0	0	0.20637	0.20637
B4_R91_C99	20.704	293.06	0.76667	20.755	293.06	0.49967	-0.051116	0	0.267	0.27185
B4_R97_C05	6.1992	313.23	-0.48131	6.1992	313.23	-0.67931	0	0	0.198	0.198
B4_R97_C36	12.351	313.21	-0.27173	12.351	313.21	-0.45474	0	0	0.18302	0.18302
B4_R97_C61	17.525	313.29	0.35438	17.525	313.29	-0.027675	0	0	0.38205	0.38205
B4_R97_C86	22.727	313.27	0.91126	22.727	313.27	0.56019	0	0	0.35108	0.35108
B4_R97_C99	25.77	313.29	1.0525	25.953	313.29	0.64376	-0.18288	0	0.40872	0.44777
HUB_LE	2.1813	30.003	-3.0853	2.19	30	-3.5	-0.0086618	0.0026453	0.41474	0.41483
HUB_TE	8.1763	30.002	-3.0856	8.19	30	-3.5	-0.013662	0.0020388	0.41444	0.41467
RMS Errors:							0.022556	0.00037576	0.12687	0.12886

7.2: Flap Registration Plots (15 rows)

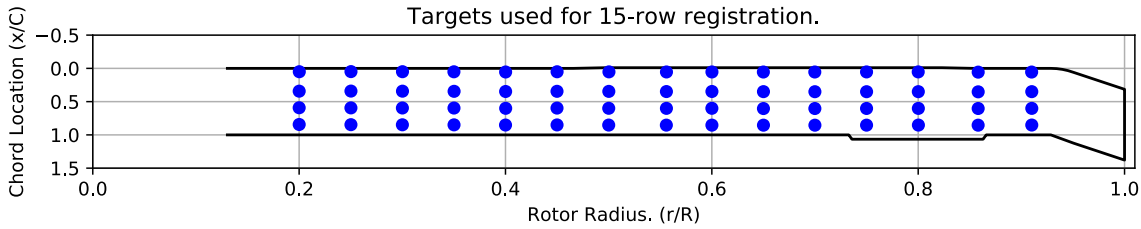

Figure 7-1. Targets used for 15 row root registration.

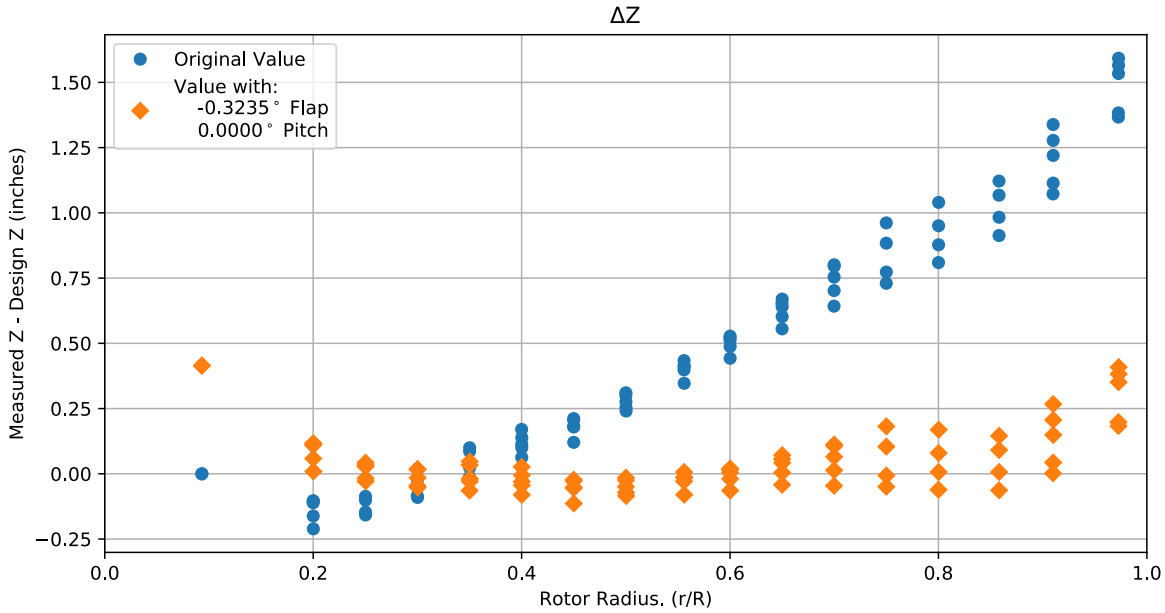

Figure 7-2. Flap target registration, ΔZ error vs rotor radius.

Note: the “as designed” geometry used for the swept tip may have some inaccuracies.

7.3: Estimated Bending and Twist at the Quarter Chord

The error bars shown represent the residual errors for fitting the measure target locations to the "as designed" geometry. These errors are generally much larger than those due to the VSTARS measurement errors. Therefore, the most likely source of these errors is the placement of the trailing-edge targets, differences between the "as designed" and "as built" geometries, and blade deformation during measurement. In the future, iterative adjustment of the "as designed" twist angle may be implemented to see if it reduces the fit error in delta twist. Note: The "as designed" geometry used for the swept tip may have some inaccuracies.

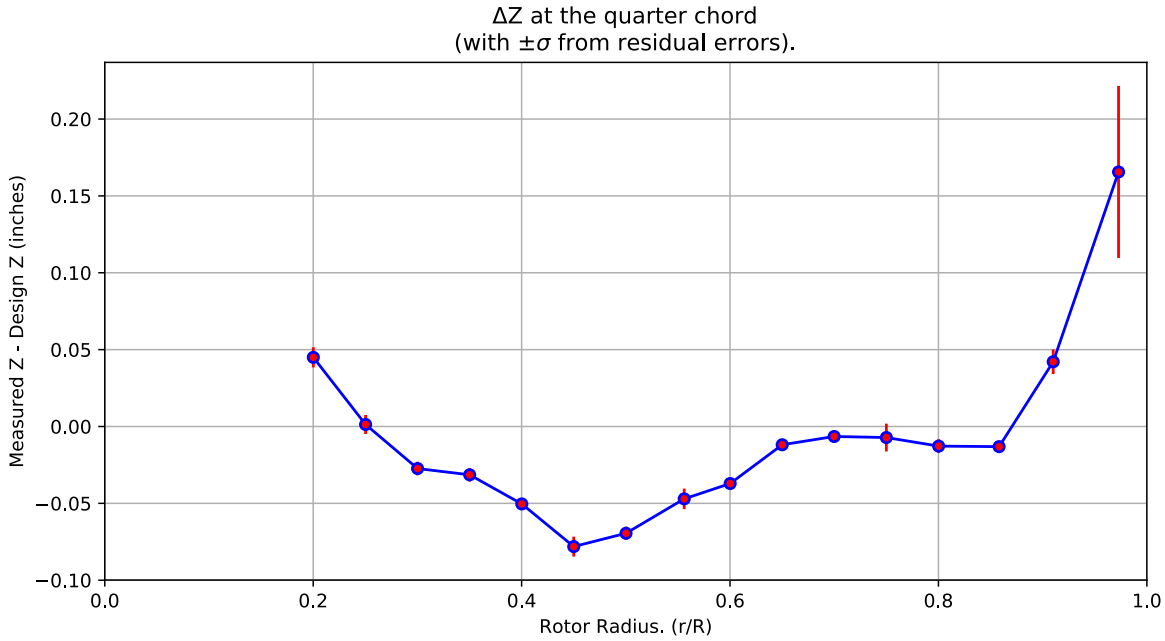

Figure 7-3. ΔZ error at the quarter chord vs rotor radius.

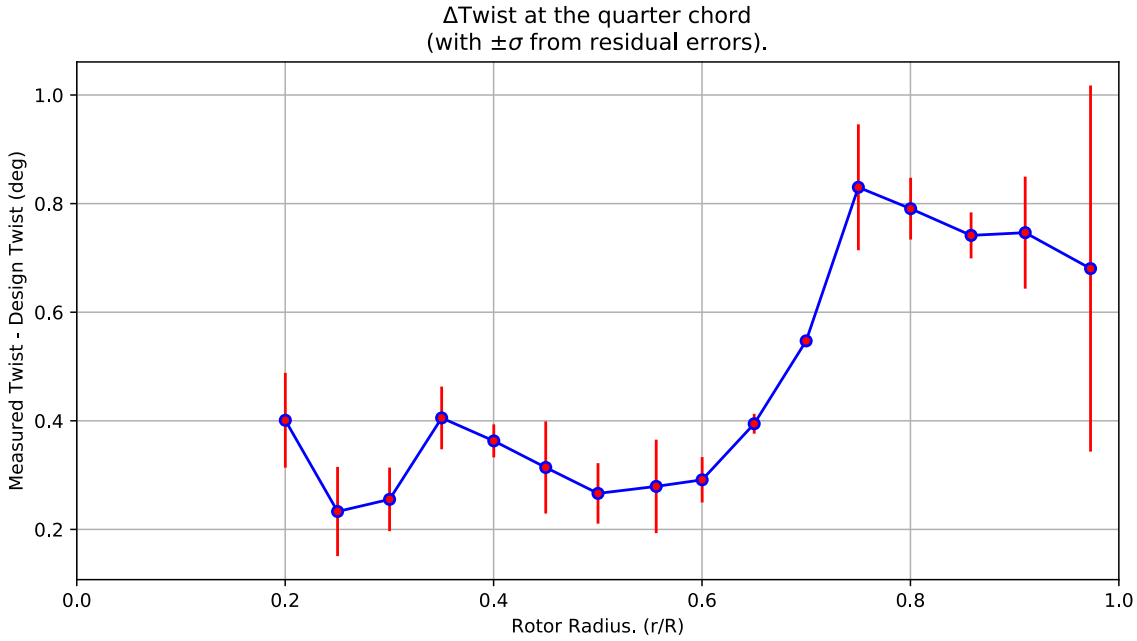

Figure 7-4. ΔTwist error at the quarter chord vs rotor radius.

Table 7-2. Quarter-chord bending and twist statistics.

r	r/R	dZ 1/4-chord	dT	sigma dZ meas	sigma dT meas	sigma dZ res	sigma dT res	n	t_conf
64.439	0.20012	0.04497	0.401	6.1154e-10	4.6917e-09	0.0065497	0.08727	4	4.3027
80.586	0.25027	0.0013025	0.23296	6.1073e-10	4.6617e-09	0.0061774	0.082114	4	4.3027
96.655	0.30017	-0.027362	0.25534	6.1204e-10	4.6595e-09	0.004435	0.058545	4	4.3027
112.75	0.35015	-0.03143	0.40528	6.136e-10	4.664e-09	0.0044023	0.057727	4	4.3027
128.85	0.40017	-0.050386	0.36302	6.166e-10	4.6634e-09	0.0023516	0.030392	4	4.3027
144.91	0.45002	-0.078123	0.31406	6.1345e-10	4.6542e-09	0.0064827	0.084891	4	4.3027
161.06	0.50018	-0.069465	0.26629	6.1506e-10	4.648e-09	0.0042946	0.05573	4	4.3027
179.04	0.55603	-0.047082	0.27922	6.1682e-10	4.6539e-09	0.0066776	0.086037	4	4.3027
193.24	0.60013	-0.037113	0.29135	6.1618e-10	4.6521e-09	0.0032394	0.041848	4	4.3027
209.32	0.65006	-0.011884	0.39459	6.1805e-10	4.6503e-09	0.0014281	0.01828	4	4.3027
225.37	0.69991	-0.0065032	0.54721	6.1822e-10	4.6507e-09	0.00055724	0.0071278	4	4.3027
241.51	0.75002	-0.0071871	0.83007	6.1746e-10	4.6486e-09	0.009038	0.11597	4	4.3027
257.66	0.80019	-0.012763	0.79068	6.1687e-10	4.6524e-09	0.0044162	0.05687	4	4.3027
276.34	0.8582	-0.013112	0.74148	6.1975e-10	4.6655e-09	0.0033217	0.042321	4	4.3027
293.06	0.91012	0.042118	0.7465	6.1789e-10	4.6687e-09	0.0080198	0.10314	4	4.3027
313.25	0.97282	0.16559	0.68041	9.2317e-10	4.6745e-09	0.055973	0.33716	4	4.3027

7.4: Section Plots

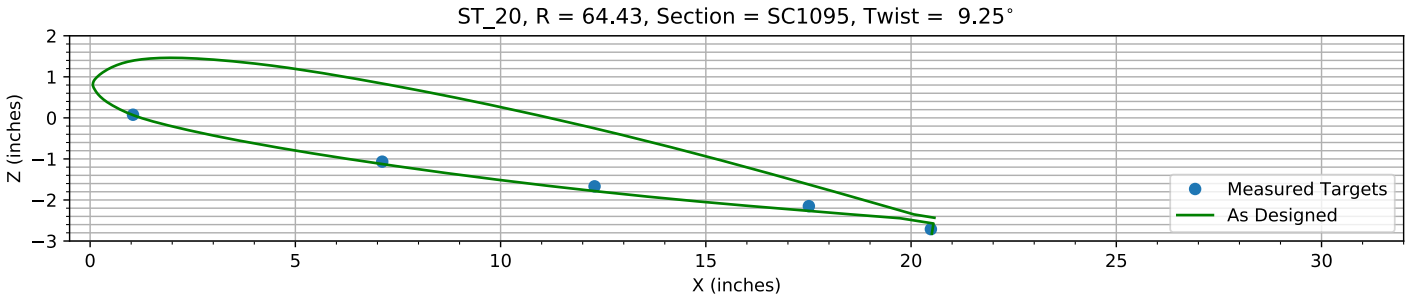

Figure 7-5. Target locations vs section profile at station 20.

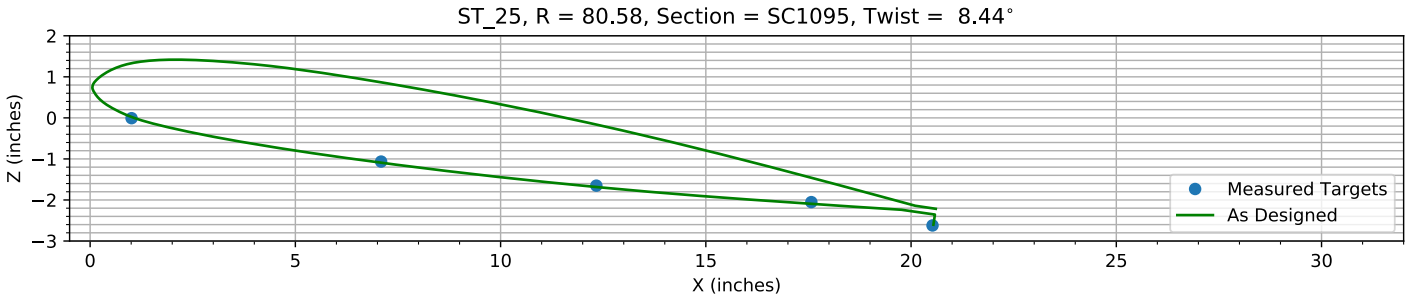

Figure 7-6. Target locations vs section profile at station 25.

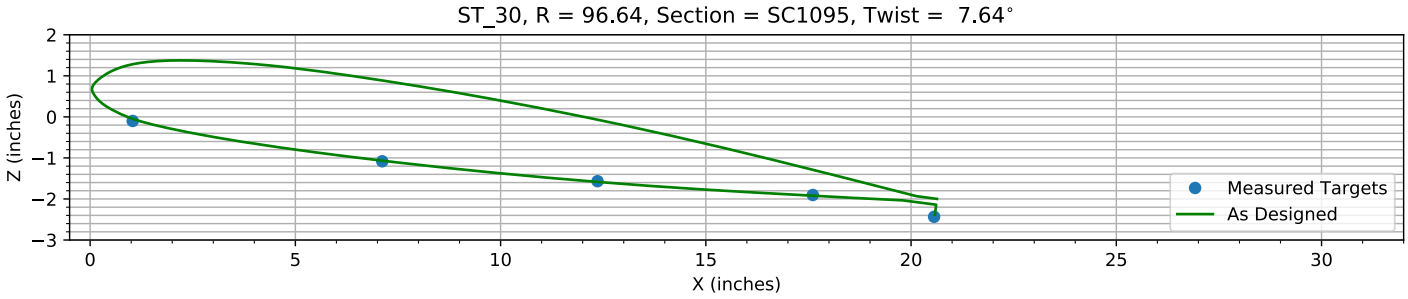

Figure 7-7. Target locations vs section profile at station 30.

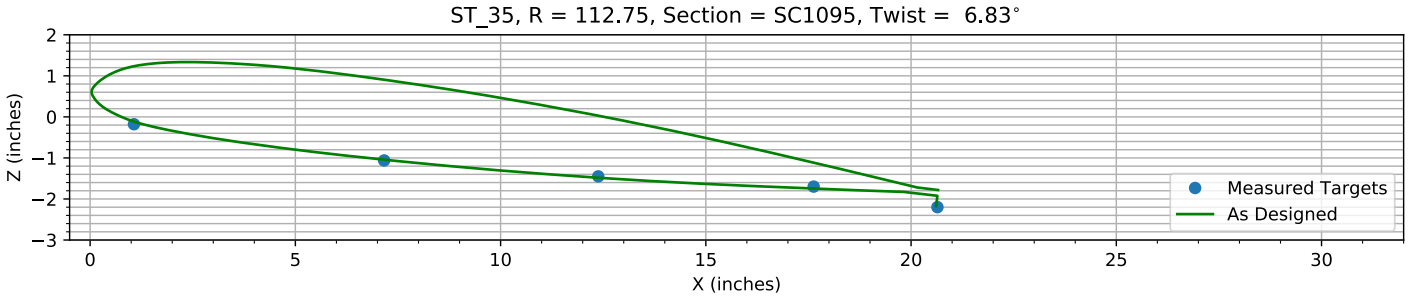

Figure 7-8. Target locations vs section profile at station 35.

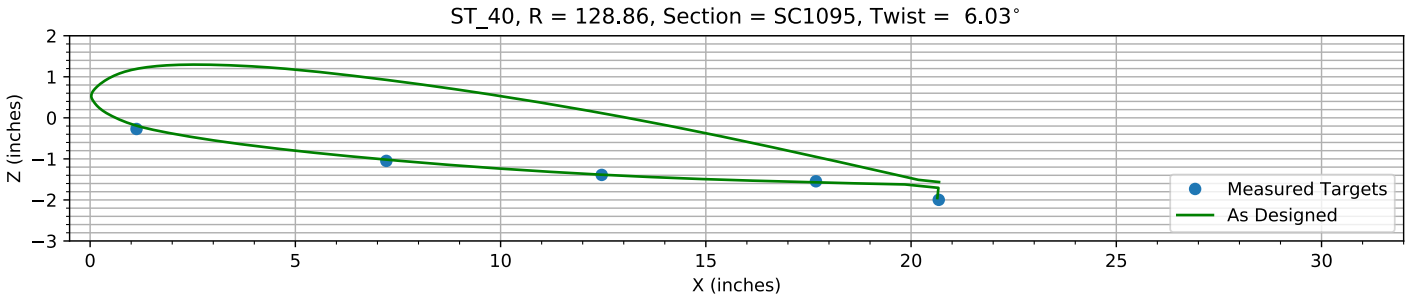

Figure 7-9. Target locations vs section profile at station 40.

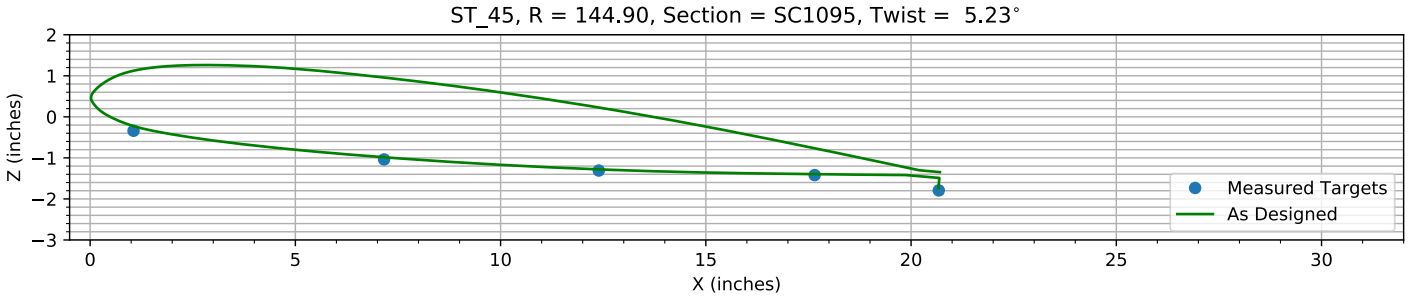

Figure 7-10. Target locations vs section profile at station 45.

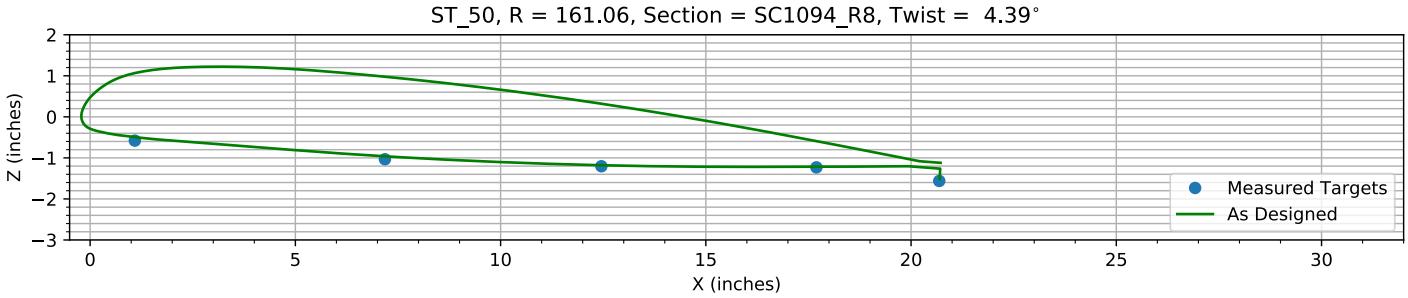

Figure 7-11. Target locations vs section profile at station 50.

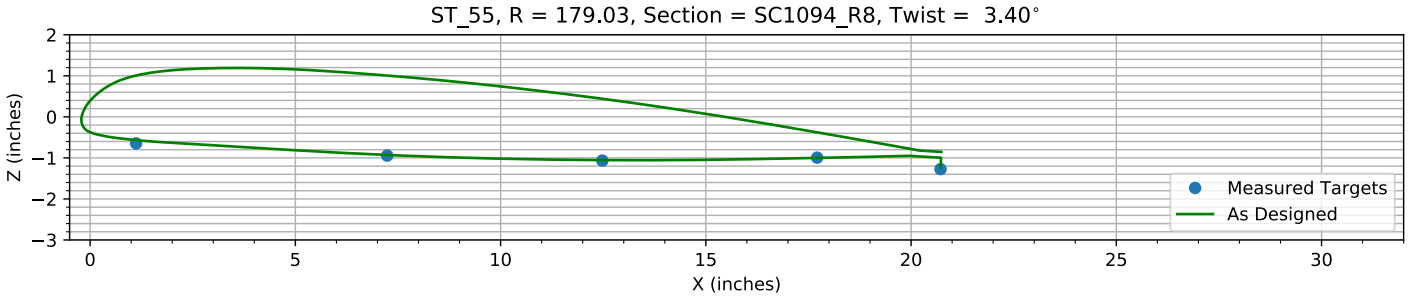

Figure 7-12. Target locations vs section profile at station 55.

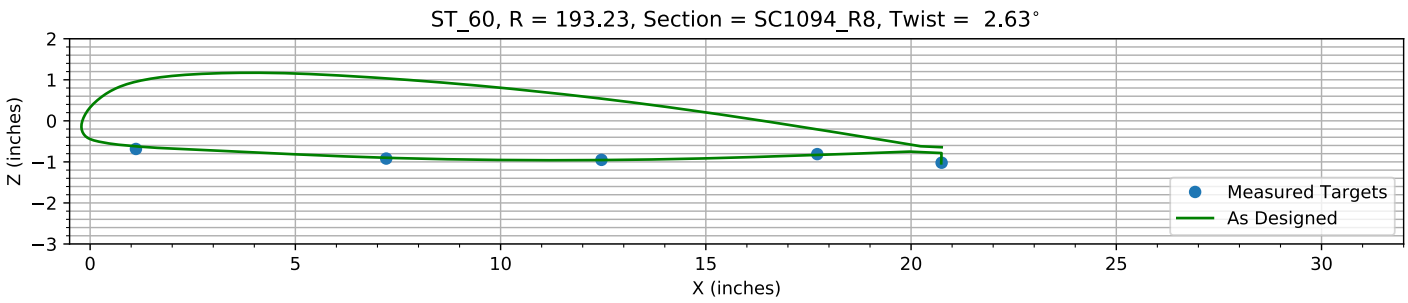

Figure 7-13. Target locations vs section profile at station 60.

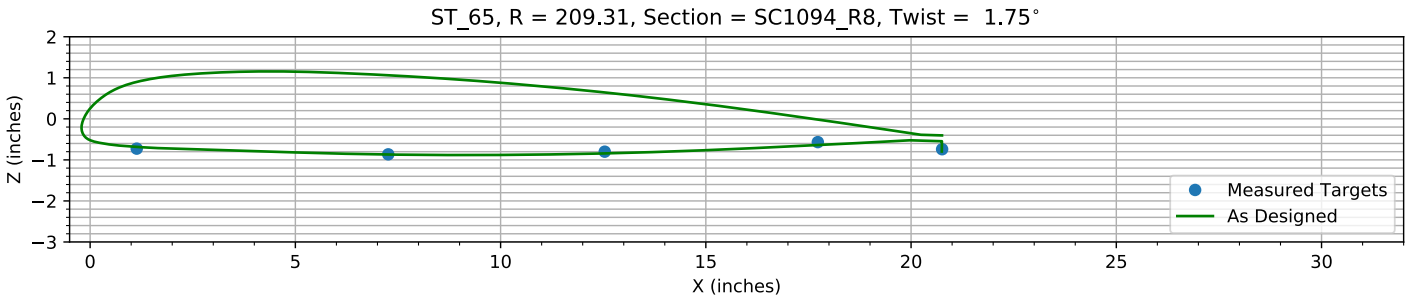

Figure 7-14. Target locations vs section profile at station 65.

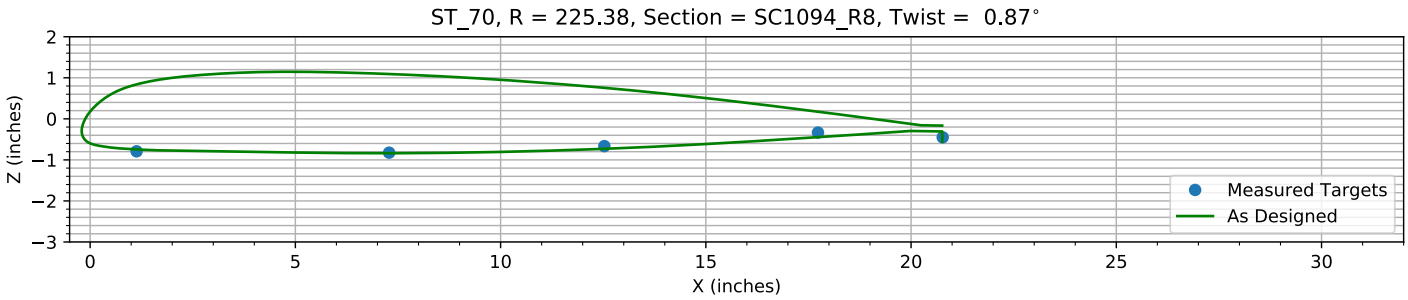

Figure 7-15. Target locations vs section profile at station 70.

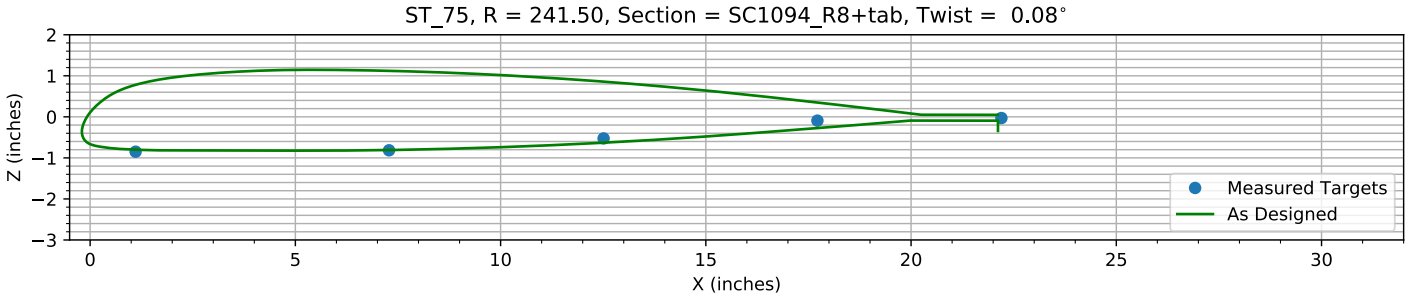

Figure 7-16. Target locations vs section profile at station 75.

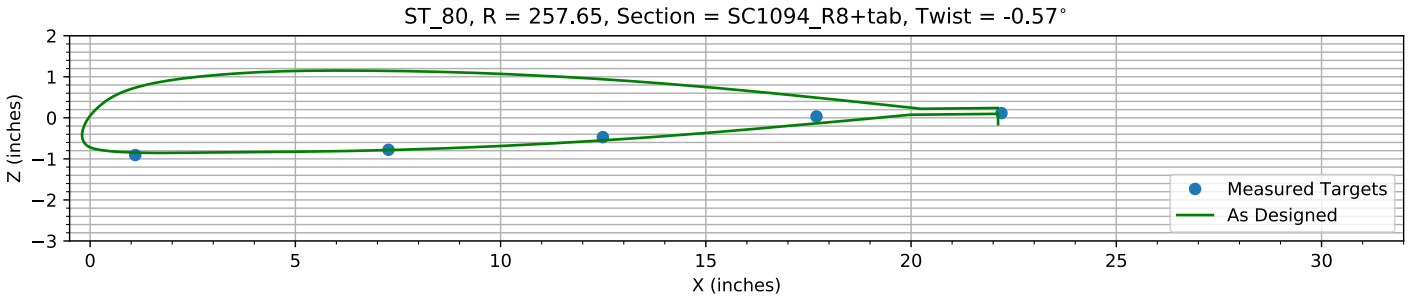

Figure 7-17. Target locations vs section profile at station 80.

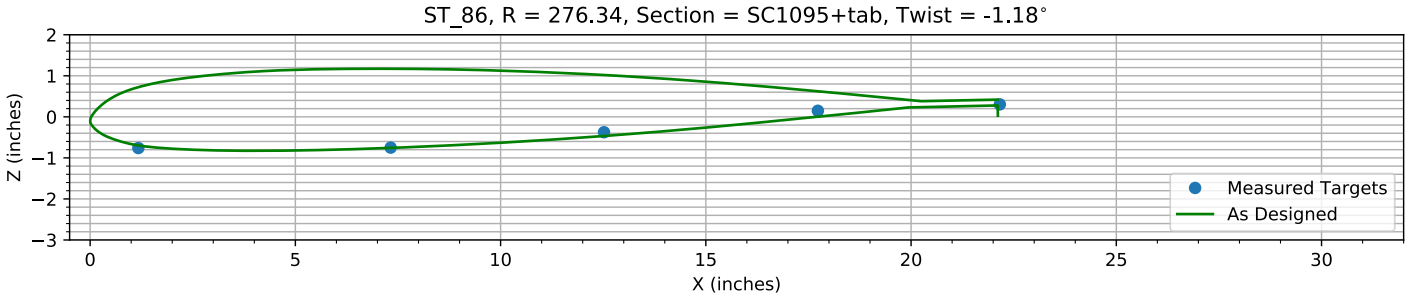

Figure 7-18. Target locations vs section profile at station 86.

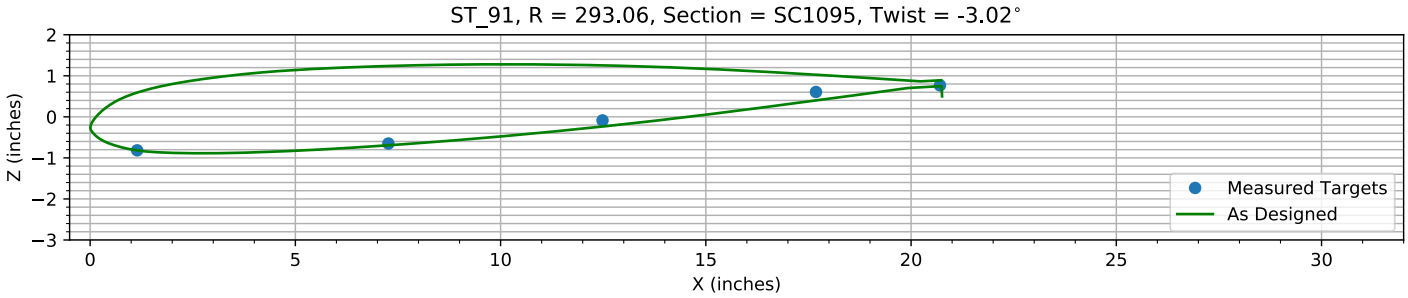

Figure 7-19. Target locations vs section profile at station 91.

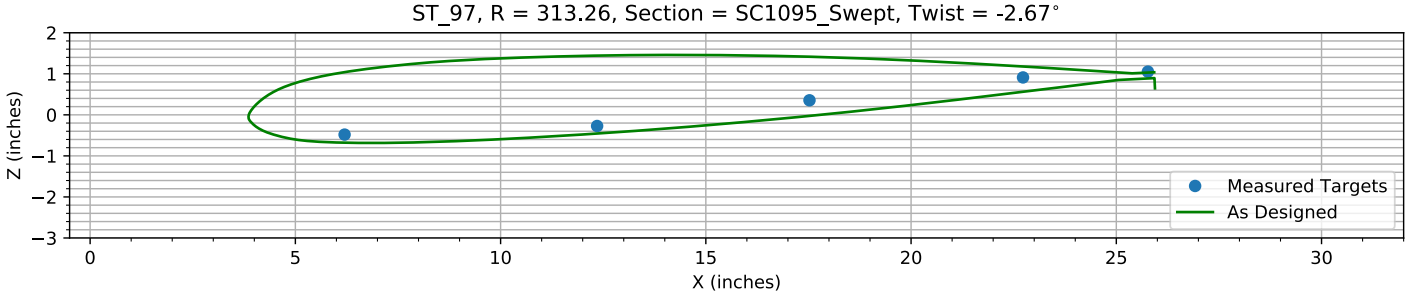

Figure 7-20. Target locations vs section profile at station 97.

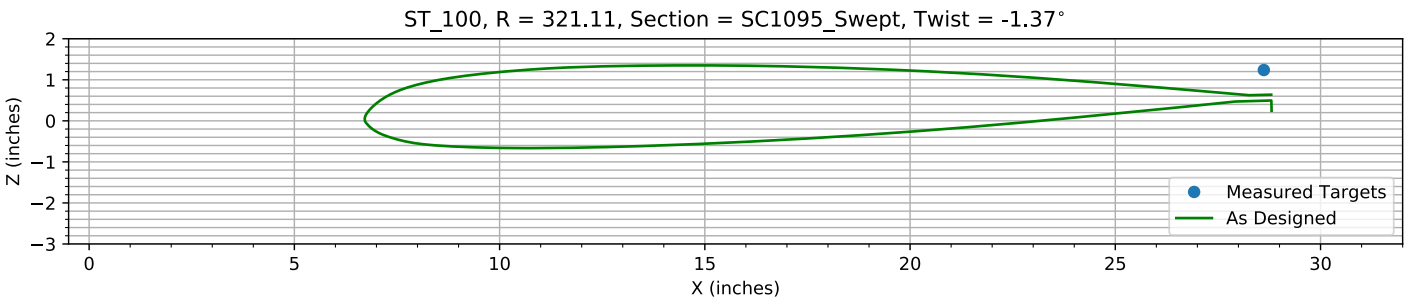

Figure 7-21. Target locations vs section profile at station 100.

Chapter 8: Pitch, Flap, and ΔZ Registration (6 rows)

The targets at the 6 spanwise stations nearest the root are used to determing the Z, flap, and pitch offset.

The estimated Z error, -0.28621 inches, is within an allowed range of ±2.000 inches.

The estimated flap error is 0.22328°.

The estimated pitch error is -0.12403°.

8.1: Target Location Errors After Target Registration

Table 8-1. Measured(1) with pitch and flap registration vs as designed(2) in inches.

Name	X1	Y1	Z1	X2	Y2	Z2	dX	dY	dZ	dR
B4_R20_C05	1.0518	64.466	0.017285	1.0518	64.466	0.064459	0	0	-0.047174	0.047174
B4_R20_C36	7.1213	64.426	-1.1392	7.1213	64.426	-1.1262	0	0	-0.013003	0.013003
B4_R20_C61	12.293	64.42	-1.7513	12.293	64.42	-1.7838	0	0	0.03247	0.03247
B4_R20_C86	17.513	64.424	-2.2454	17.513	64.424	-2.2676	0	0	0.022187	0.022187
B4_R20_C99	20.484	64.386	-2.8126	20.506	64.386	-2.8207	-0.021492	0	0.0081447	0.022983
B4_R25_C05	1.0167	80.595	-0.038295	1.0167	80.595	0.018536	0	0	-0.056831	0.056831
B4_R25_C36	7.0941	80.582	-1.1085	7.0941	80.582	-1.0931	0	0	-0.015363	0.015363
B4_R25_C61	12.336	80.572	-1.7064	12.336	80.572	-1.6848	0	0	-0.021632	0.021632
B4_R25_C86	17.573	80.575	-2.1188	17.573	80.575	-2.0948	0	0	-0.023944	0.023944
B4_R25_C99	20.524	80.575	-2.6938	20.544	80.575	-2.603	-0.019807	0	-0.090771	0.092907
B4_R30_C05	1.0445	96.668	-0.10239	1.0445	96.668	-0.049815	0	0	-0.052578	0.052578
B4_R30_C36	7.1215	96.664	-1.0979	7.1215	96.664	-1.0676	0	0	-0.030302	0.030302
B4_R30_C61	12.366	96.635	-1.5946	12.366	96.635	-1.5848	0	0	-0.0098209	0.0098209
B4_R30_C86	17.61	96.632	-1.9418	17.61	96.632	-1.9212	0	0	-0.02059	0.02059
B4_R30_C99	20.563	96.574	-2.4791	20.579	96.574	-2.388	-0.015936	0	-0.091123	0.092506
B4_R35_C05	1.0746	112.72	-0.15412	1.0746	112.72	-0.1173	0	0	-0.036821	0.036821
B4_R35_C36	7.1681	112.77	-1.0497	7.1681	112.77	-1.0436	0	0	-0.0060702	0.0060702
B4_R35_C61	12.384	112.74	-1.4488	12.384	112.74	-1.4836	0	0	0.034777	0.034777
B4_R35_C86	17.631	112.75	-1.7094	17.631	112.75	-1.7462	0	0	0.036831	0.036831
B4_R35_C99	20.645	112.76	-2.2162	20.611	112.76	-2.1703	0.033564	0	-0.045851	0.056823
B4_R40_C05	1.1372	128.86	-0.21843	1.1372	128.86	-0.19308	0	0	-0.025355	0.025355
B4_R40_C36	7.2219	128.85	-1.0086	7.2219	128.85	-1.0193	0	0	0.010704	0.010704
B4_R40_C61	12.468	128.87	-1.3618	12.468	128.87	-1.3856	0	0	0.023783	0.023783
B4_R40_C86	17.687	128.82	-1.5284	17.687	128.82	-1.5726	0	0	0.044149	0.044149
B4_R40_C99	20.678	128.86	-1.9864	20.64	128.86	-1.9537	0.037451	0	-0.032664	0.049694
B4_R45_C05	1.0642	144.92	-0.25817	1.0642	144.92	-0.22815	0	0	-0.030018	0.030018
B4_R45_C36	7.1662	144.89	-0.96938	7.1662	144.89	-0.98566	0	0	0.016283	0.016283
B4_R45_C61	12.397	144.89	-1.2513	12.397	144.89	-1.2805	0	0	0.029246	0.029246
B4_R45_C86	17.656	144.9	-1.3738	17.656	144.9	-1.3969	0	0	0.023073	0.023073
B4_R45_C99	20.678	144.89	-1.7536	20.666	144.89	-1.738	0.012217	0	-0.015693	0.019888
B4_R50_C05	1.0958	161.1	-0.46951	1.0958	161.1	-0.49518	0	0	0.025671	0.025671
B4_R50_C36	7.1876	161.06	-0.93683	7.1876	161.06	-0.96201	0	0	0.025177	0.025177
B4_R50_C61	12.46	161.03	-1.1185	12.46	161.03	-1.1794	0	0	0.060884	0.060884
B4_R50_C86	17.699	161.02	-1.1574	17.699	161.02	-1.2162	0	0	0.058814	0.058814
B4_R50_C99	20.691	161.05	-1.4943	20.695	161.05	-1.512	-0.0046233	0	0.017718	0.018311
B4_R55_C05	1.1268	179.05	-0.50583	1.1268	179.05	-0.56748	0	0	0.061649	0.061649

Name	X1	Y1	Z1	X2	Y2	Z2	dX	dY	dZ	dR
B4_R55_C36	7.2427	179.04	-0.81681	7.2427	179.04	-0.92922	0	0	0.11241	0.11241
B4_R55_C61	12.484	179.04	-0.95027	12.484	179.04	-1.0542	0	0	0.10391	0.10391
B4_R55_C86	17.717	179.02	-0.8891	17.717	179.02	-1.001	0	0	0.11188	0.11188
B4_R55_C99	20.723	178.99	-1.1758	20.719	178.99	-1.246	0.003636	0	0.070237	0.070331
B4_R60_C05	1.1222	193.24	-0.51913	1.1222	193.24	-0.62143	0	0	0.1023	0.1023
B4_R60_C36	7.2191	193.24	-0.76671	7.2191	193.24	-0.90024	0	0	0.13353	0.13353
B4_R60_C61	12.463	193.22	-0.80919	12.463	193.22	-0.95558	0	0	0.14639	0.14639
B4_R60_C86	17.72	193.24	-0.68092	17.72	193.24	-0.83108	0	0	0.15016	0.15016
B4_R60_C99	20.75	193.19	-0.89691	20.734	193.19	-1.0353	0.0153	0	0.13839	0.13924
B4_R65_C05	1.1419	209.29	-0.53211	1.1419	209.29	-0.68438	0	0	0.15226	0.15226
B4_R65_C36	7.2688	209.32	-0.6842	7.2688	209.32	-0.86946	0	0	0.18527	0.18527
B4_R65_C61	12.543	209.32	-0.63069	12.543	209.32	-0.84208	0	0	0.21139	0.21139
B4_R65_C86	17.735	209.32	-0.40905	17.735	209.32	-0.63828	0	0	0.22923	0.22923
B4_R65_C99	20.762	209.26	-0.58875	20.749	209.26	-0.79664	0.013931	0	0.20789	0.20836
B4_R70_C05	1.1384	225.34	-0.56896	1.1384	225.34	-0.74556	0	0	0.1766	0.1766
B4_R70_C36	7.2902	225.38	-0.61519	7.2902	225.38	-0.83749	0	0	0.2223	0.2223
B4_R70_C61	12.534	225.37	-0.46761	12.534	225.37	-0.73014	0	0	0.26253	0.26253
B4_R70_C86	17.739	225.38	-0.14823	17.739	225.38	-0.44613	0	0	0.2979	0.2979
B4_R70_C99	20.777	225.41	-0.27041	20.759	225.41	-0.55668	0.018416	0	0.28628	0.28687
B4_R75_C05	1.1141	241.49	-0.59904	1.1141	241.49	-0.80026	0	0	0.20122	0.20122
B4_R75_C36	7.2883	241.51	-0.57805	7.2883	241.51	-0.80852	0	0	0.23047	0.23047
B4_R75_C61	12.516	241.5	-0.30023	12.516	241.5	-0.62977	0	0	0.32953	0.32953
B4_R75_C86	17.726	241.5	0.12178	17.726	241.5	-0.27378	0	0	0.39556	0.39556
B4_R80_C05	1.1048	257.62	-0.62766	1.1048	257.62	-0.84544	0	0	0.21778	0.21778
B4_R80_C36	7.2746	257.65	-0.51334	7.2746	257.65	-0.78547	0	0	0.27214	0.27214
B4_R80_C61	12.498	257.66	-0.21559	12.498	257.66	-0.54883	0	0	0.33324	0.33324
B4_R80_C86	17.704	257.68	0.27627	17.704	257.68	-0.13471	0	0	0.41098	0.41098
B4_R86_C05	1.181	276.34	-0.44907	1.181	276.34	-0.69802	0	0	0.24896	0.24896
B4_R86_C36	7.3283	276.34	-0.45207	7.3283	276.34	-0.75655	0	0	0.30448	0.30448
B4_R86_C61	12.527	276.33	-0.088709	12.527	276.33	-0.46603	0	0	0.37732	0.37732
B4_R86_C86	17.738	276.33	0.42314	17.738	276.33	0.003109	0	0	0.42003	0.42003
B4_R91_C05	1.1525	293.02	-0.47561	1.1525	293.02	-0.81898	0	0	0.34337	0.34337
B4_R91_C36	7.2731	293.06	-0.32302	7.2731	293.06	-0.69302	0	0	0.37	0.37
B4_R91_C61	12.491	293.07	0.22906	12.491	293.07	-0.23516	0	0	0.46422	0.46422
B4_R91_C86	17.693	293.06	0.91082	17.693	293.06	0.40083	0	0	0.50999	0.50999
B4_R91_C99	20.714	293.05	1.0648	20.755	293.05	0.49943	-0.041206	0	0.56539	0.56689
B4_R97_C05	6.2065	313.22	-0.11648	6.2065	313.22	-0.67959	0	0	0.56311	0.56311
B4_R97_C36	12.359	313.21	0.079761	12.359	313.21	-0.45407	0	0	0.53383	0.53383
B4_R97_C61	17.534	313.28	0.69479	17.534	313.28	-0.026392	0	0	0.72118	0.72118
B4_R97_C86	22.737	313.26	1.2404	22.737	313.26	0.56204	0	0	0.67834	0.67834
B4_R97_C99	25.78	313.28	1.375	25.949	313.28	0.64408	-0.16903	0	0.73096	0.75025
HUB_LE	2.182	30.001	-3.2072	2.19	30	-3.5	-0.008035	0.0014193	0.29282	0.29293
HUB_TE	8.177	30.001	-3.2205	8.19	30	-3.5	-0.01305	0.0008133	0.27954	0.27985
RMS Errors:							0.021076	0.00018404	0.25827	0.25913

8.2: Pitch and Flap Registration Plots (6 rows)

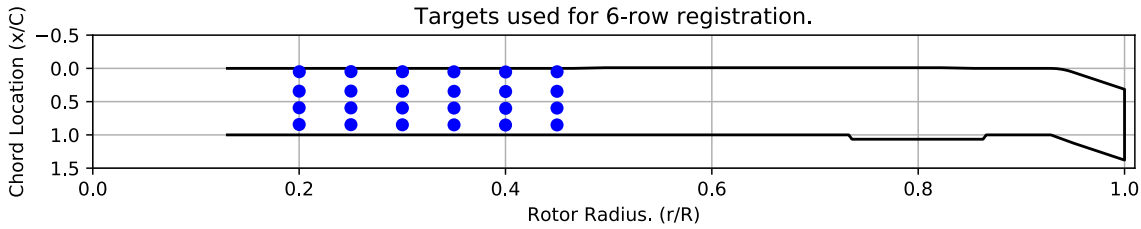

Figure 8-1. Targets used for 6 row root registration.

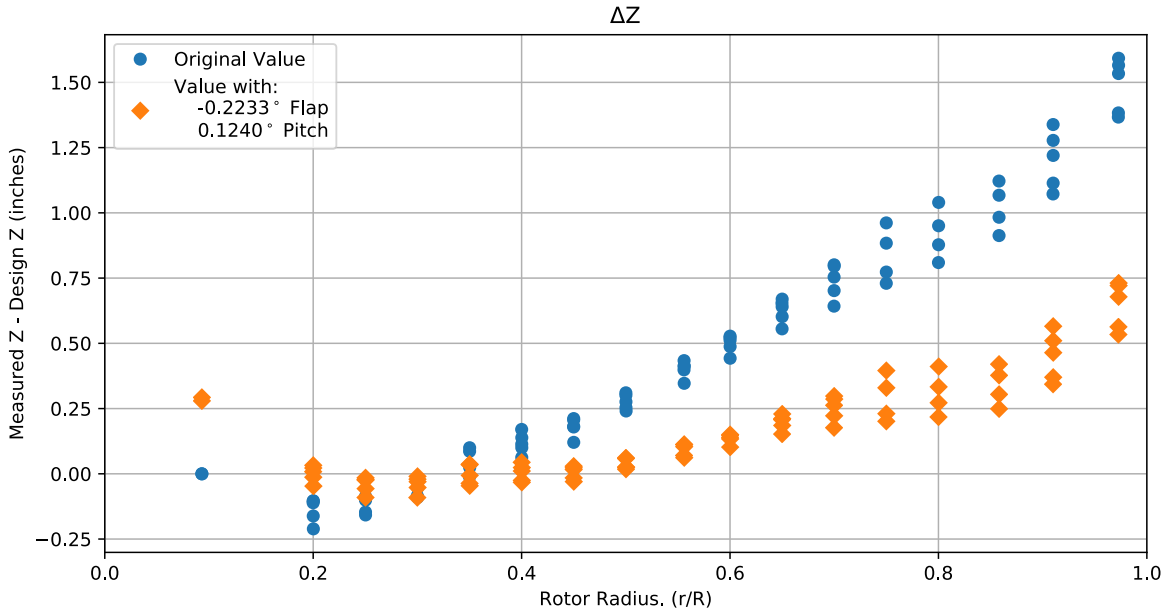

Figure 8-2. Pitch and flap target registration, ΔZ error vs rotor radius.

Note: the “as designed” geometry used for the swept tip may have some inaccuracies.

8.3: Estimated Bending and Twist at the Quarter Chord

The error bars shown represent the residual errors for fitting the measure target locations to the "as designed" geometry. These errors are generally much larger than those due to the VSTARS measurement errors. Therefore, the most likely source of these errors is the placement of the trailing-edge targets, differences between the "as designed" and "as built" geometries, and blade deformation during measurement. In the future, iterative adjustment of the "as designed" twist angle may be implemented to see if it reduces the fit error in delta twist. Note: The "as designed" geometry used for the swept tip may have some inaccuracies.

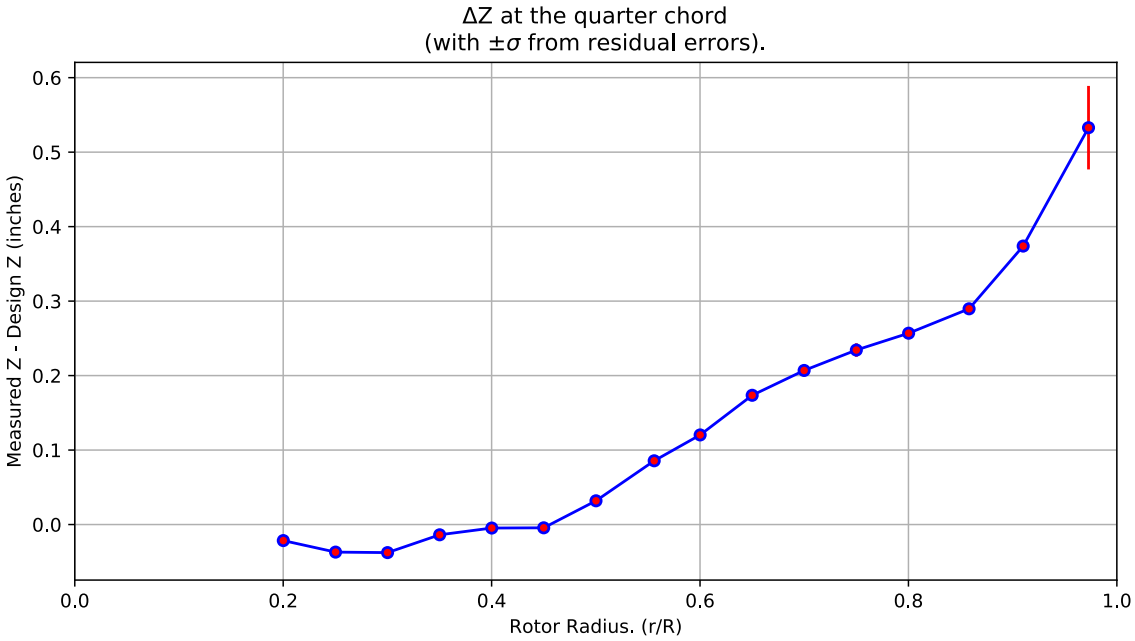

Figure 8-3. ΔZ error at the quarter chord vs rotor radius.

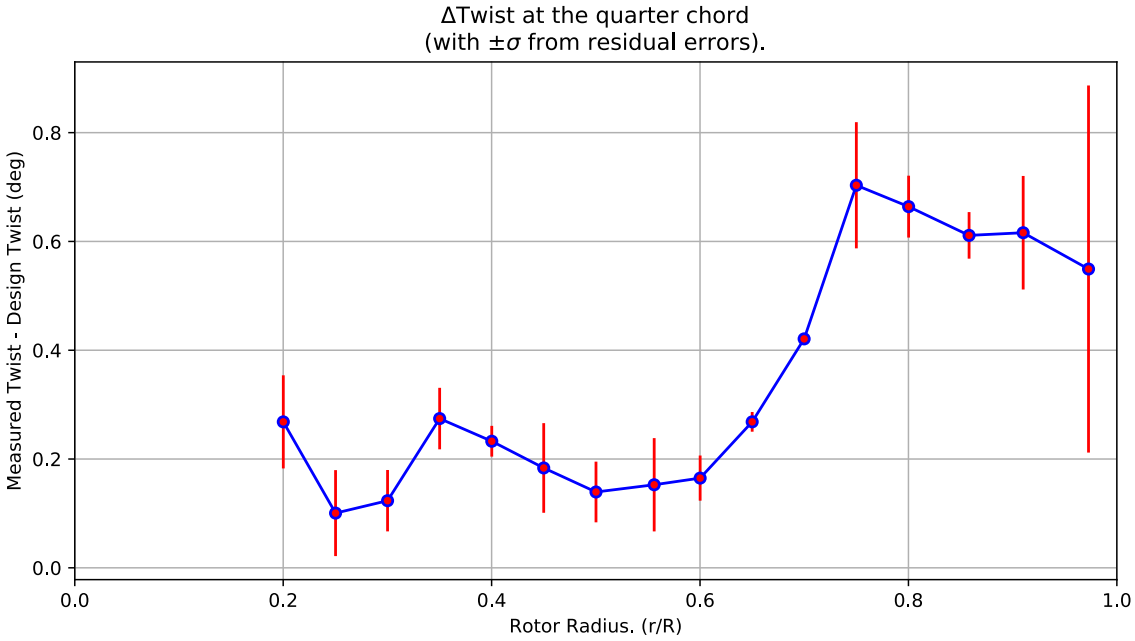

Figure 8-4. ΔTwist error at the quarter chord vs rotor radius.

Table 8-2. Quarter-chord bending and twist statistics.

r	r/R	dZ 1/4-chord	dT	sigma dZ meas	sigma dT meas	sigma dZ res	sigma dT res	n	t_conf
64.434	0.20011	-0.021538	0.2683	6.1183e-10	4.6932e-09	0.0064311	0.085596	4	4.3027
80.581	0.25025	-0.037017	0.10057	6.1101e-10	4.663e-09	0.0059516	0.079024	4	4.3027
96.65	0.30015	-0.037682	0.12341	6.1232e-10	4.6607e-09	0.0042795	0.056428	4	4.3027
112.74	0.35014	-0.013768	0.27436	6.1389e-10	4.6651e-09	0.0043159	0.056528	4	4.3027
128.85	0.40015	-0.004706	0.2327	6.1689e-10	4.6643e-09	0.0021909	0.028282	4	4.3027
144.9	0.45	-0.0043899	0.18357	6.1374e-10	4.655e-09	0.0062996	0.08239	4	4.3027
161.05	0.50017	0.031881	0.1394	6.1534e-10	4.6485e-09	0.0043044	0.055787	4	4.3027
179.04	0.55601	0.085596	0.15269	6.1711e-10	4.6542e-09	0.006665	0.085763	4	4.3027
193.24	0.60011	0.12031	0.16493	6.1648e-10	4.6523e-09	0.0032183	0.041519	4	4.3027
209.31	0.65005	0.17354	0.26835	6.1835e-10	4.6504e-09	0.0014179	0.018124	4	4.3027
225.37	0.6999	0.20688	0.42087	6.1852e-10	4.6506e-09	0.00054804	0.0070002	4	4.3027
241.5	0.75	0.23431	0.70327	6.1776e-10	4.6484e-09	0.0090524	0.11598	4	4.3027
257.65	0.80017	0.2569	0.664	6.1718e-10	4.6521e-09	0.0044239	0.056882	4	4.3027
276.33	0.85818	0.28966	0.61113	6.2008e-10	4.6652e-09	0.0033655	0.042812	4	4.3027
293.05	0.9101	0.37392	0.61602	6.1823e-10	4.6681e-09	0.0081292	0.10437	4	4.3027
313.24	0.9728	0.53285	0.54928	9.2364e-10	4.6738e-09	0.056068	0.33744	4	4.3027

8.4: Section Plots

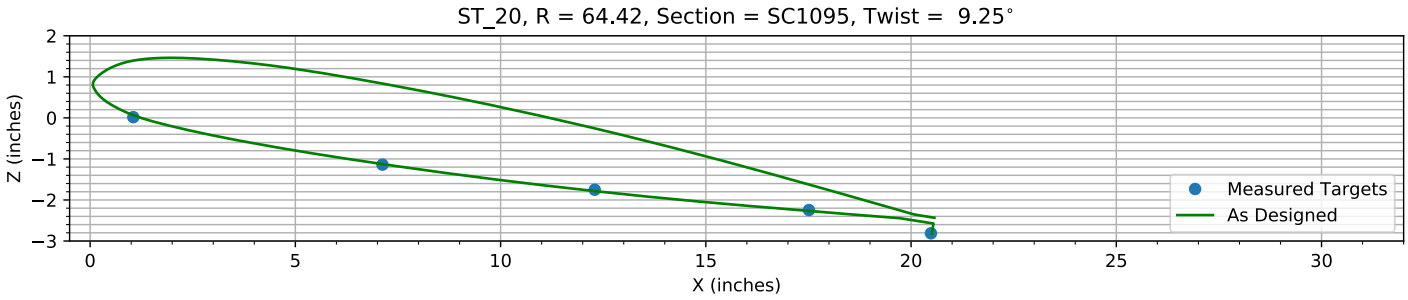

Figure 8-5. Target locations vs section profile at station 20.

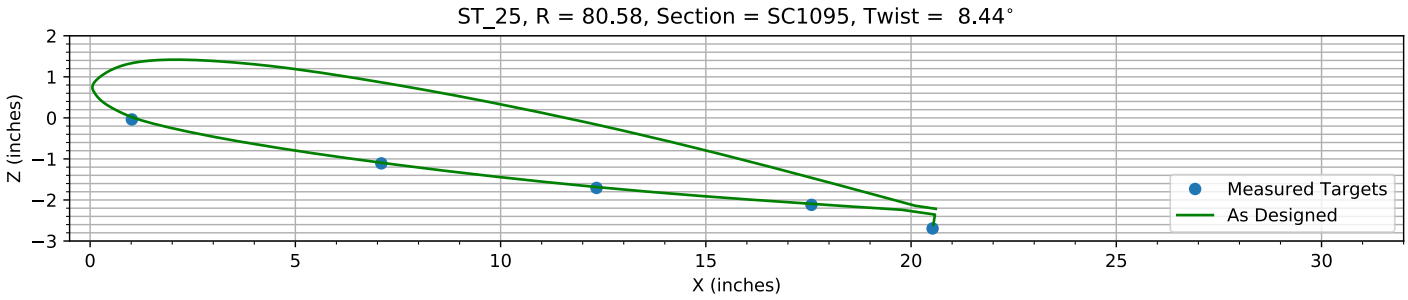

Figure 8-6. Target locations vs section profile at station 25.

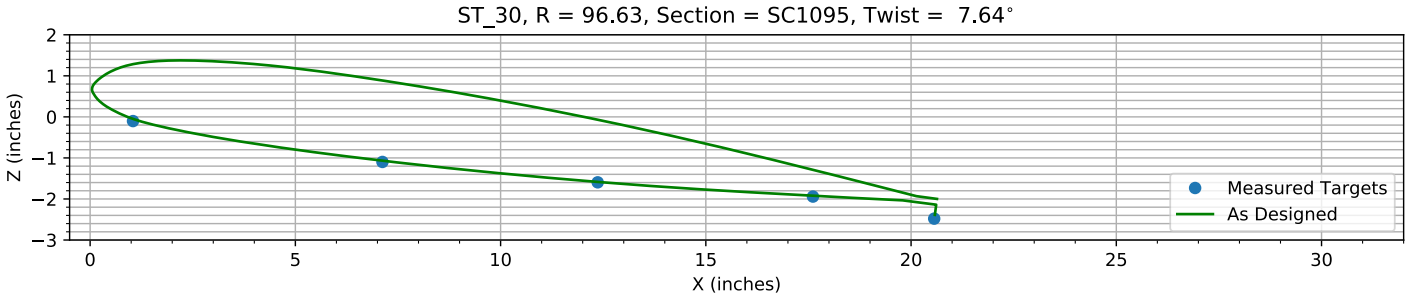

Figure 8-7. Target locations vs section profile at station 30.

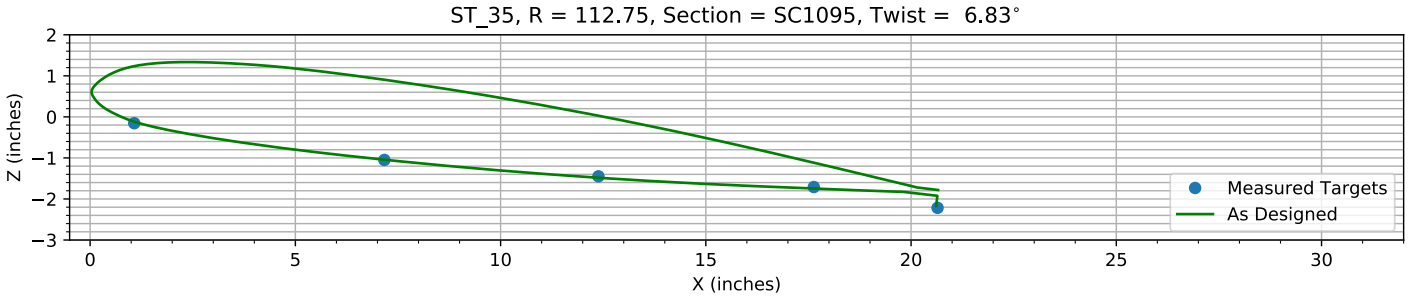

Figure 8-8. Target locations vs section profile at station 35.

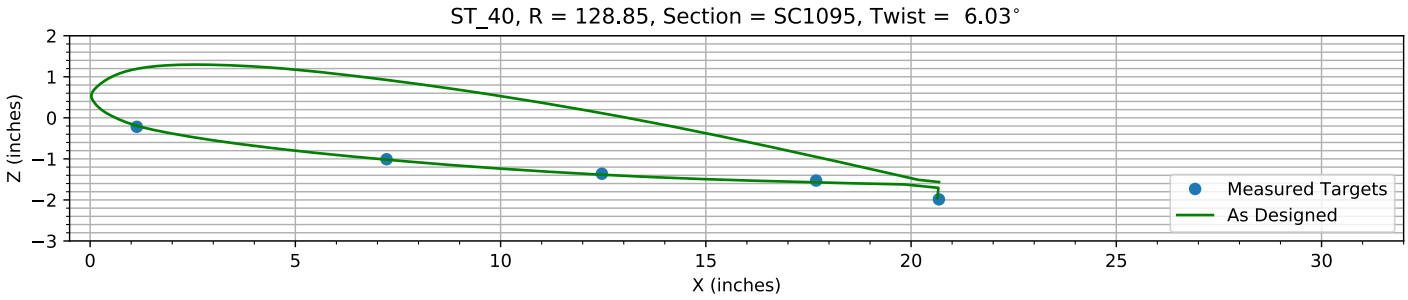

Figure 8-9. Target locations vs section profile at station 40.

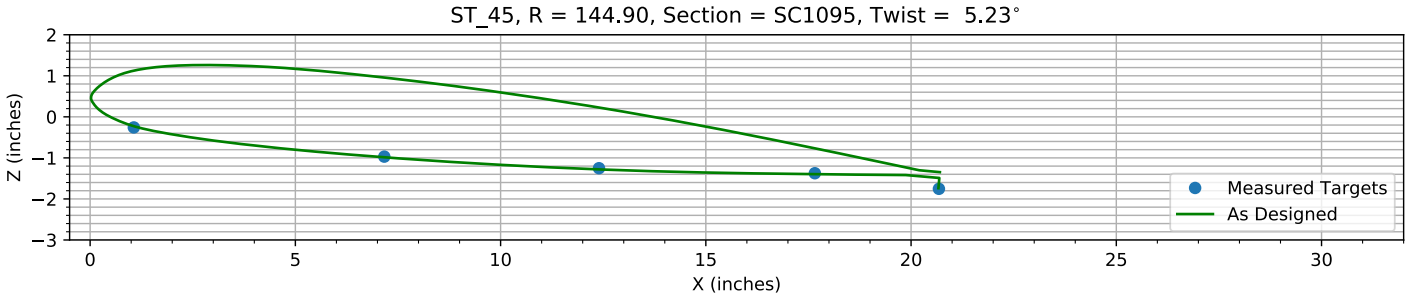

Figure 8-10. Target locations vs section profile at station 45.

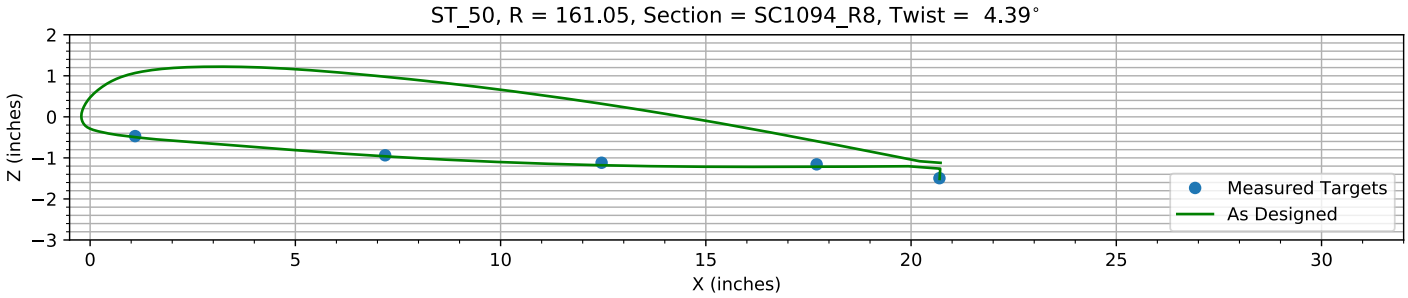

Figure 8-11. Target locations vs section profile at station 50.

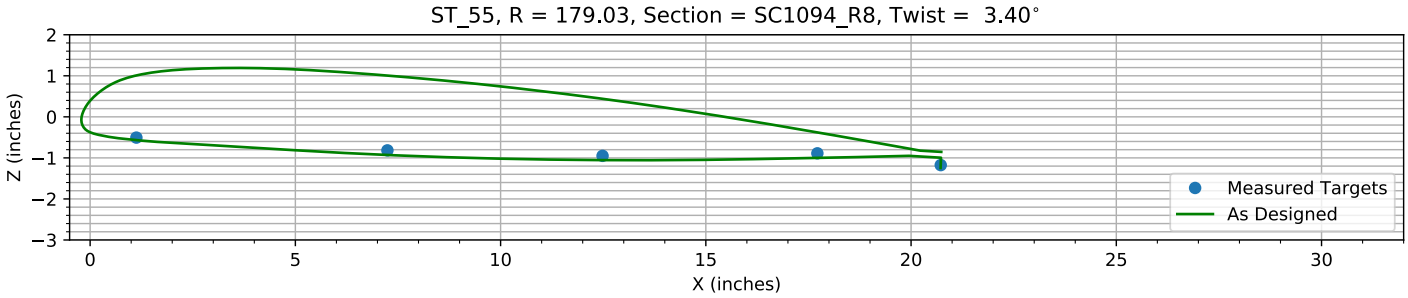

Figure 8-12. Target locations vs section profile at station 55.

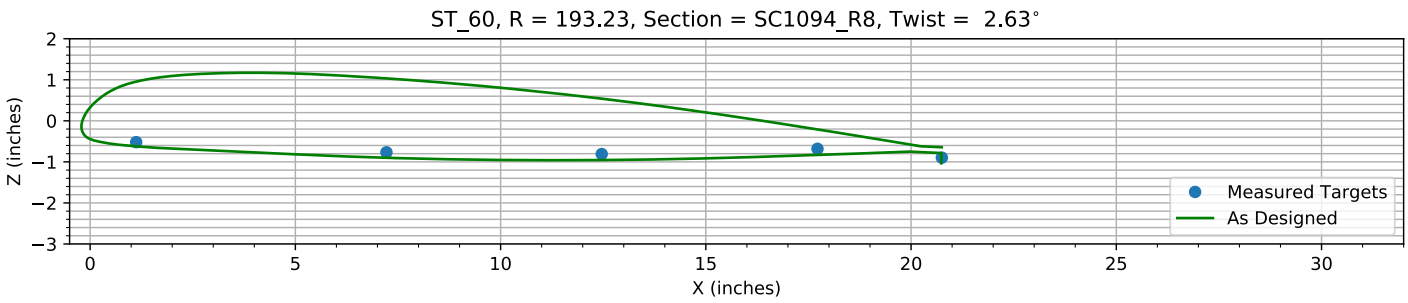

Figure 8-13. Target locations vs section profile at station 60.

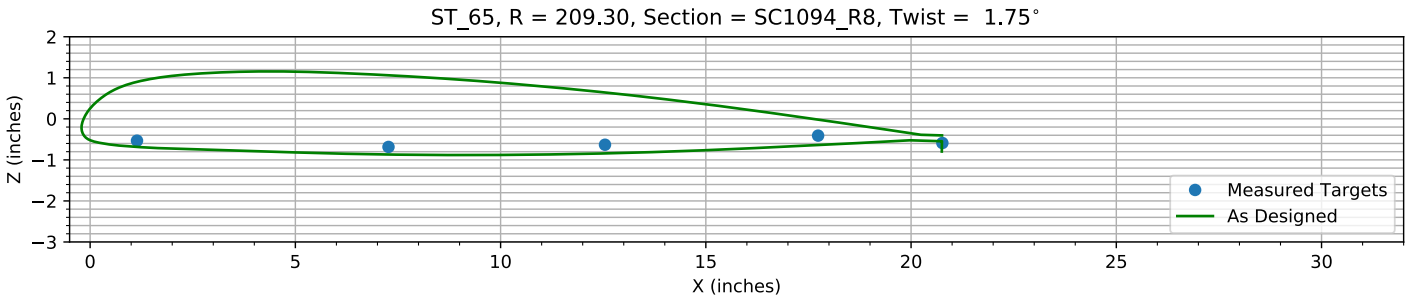

Figure 8-14. Target locations vs section profile at station 65.

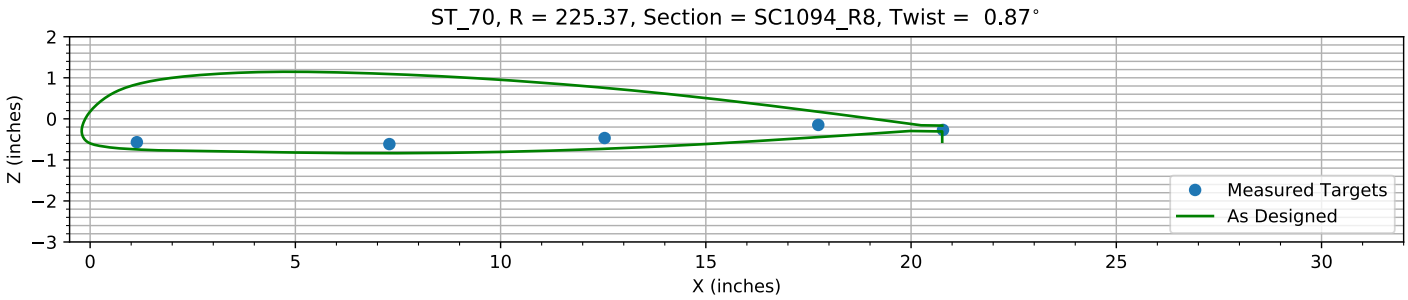

Figure 8-15. Target locations vs section profile at station 70.

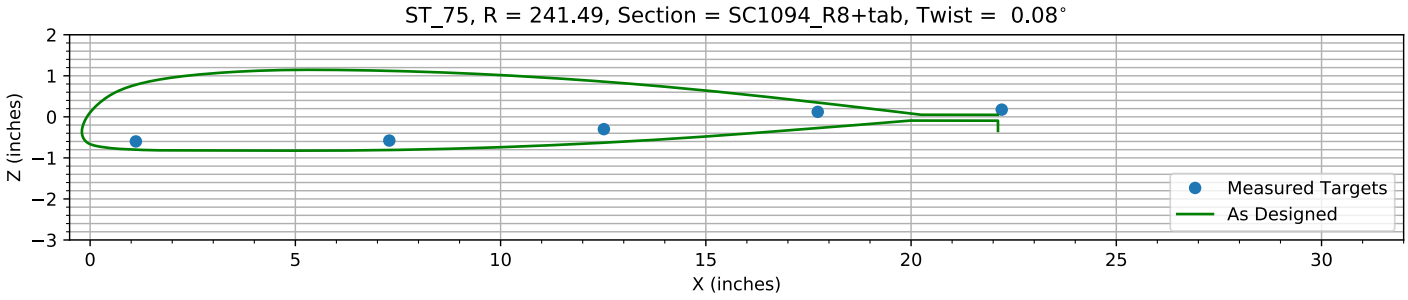

Figure 8-16. Target locations vs section profile at station 75.

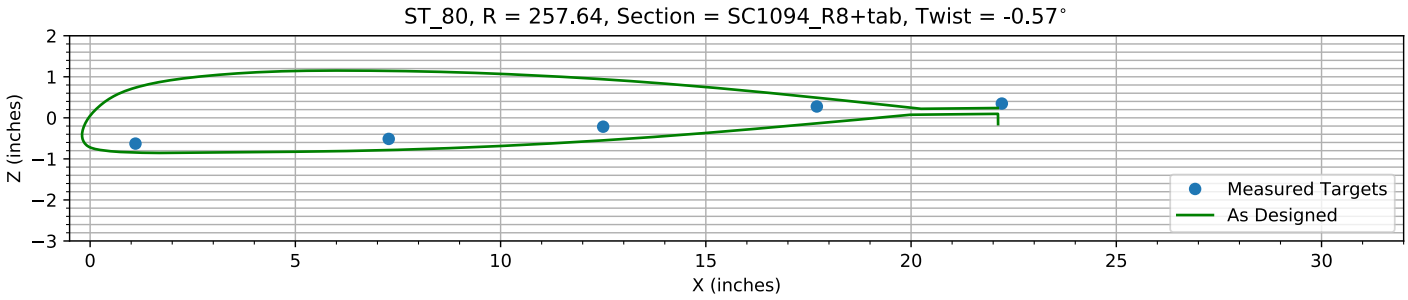

Figure 8-17. Target locations vs section profile at station 80.

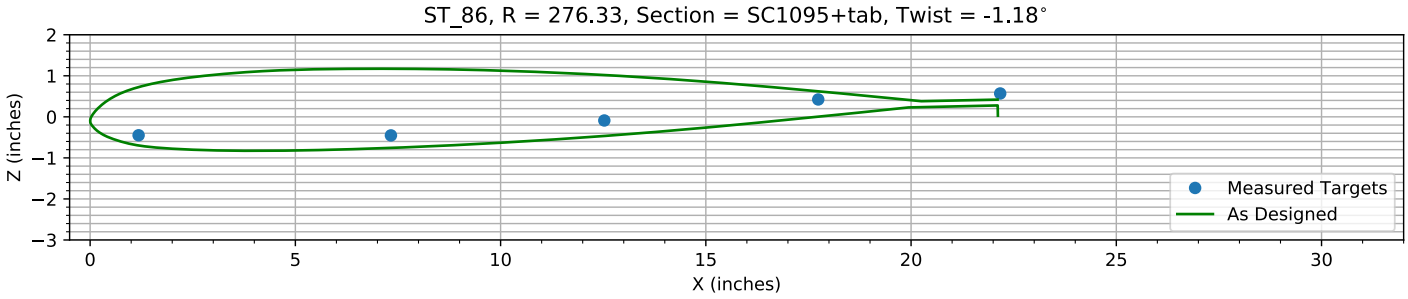

Figure 8-18. Target locations vs section profile at station 86.

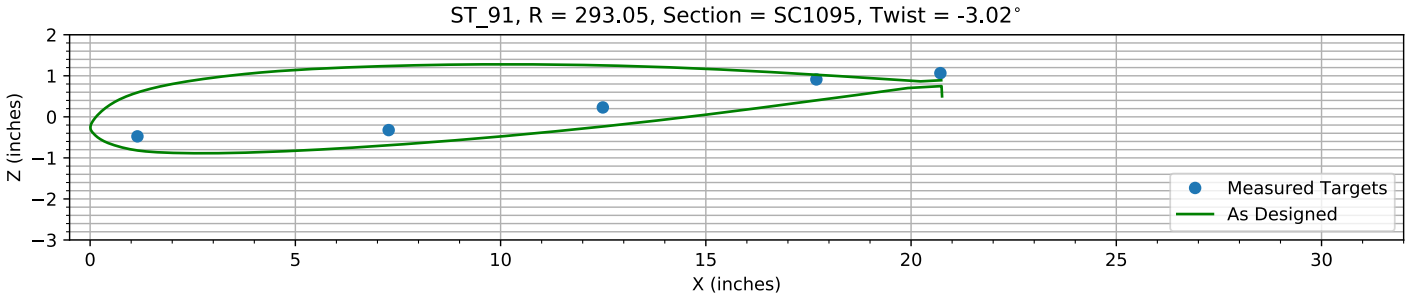

Figure 8-19. Target locations vs section profile at station 91.

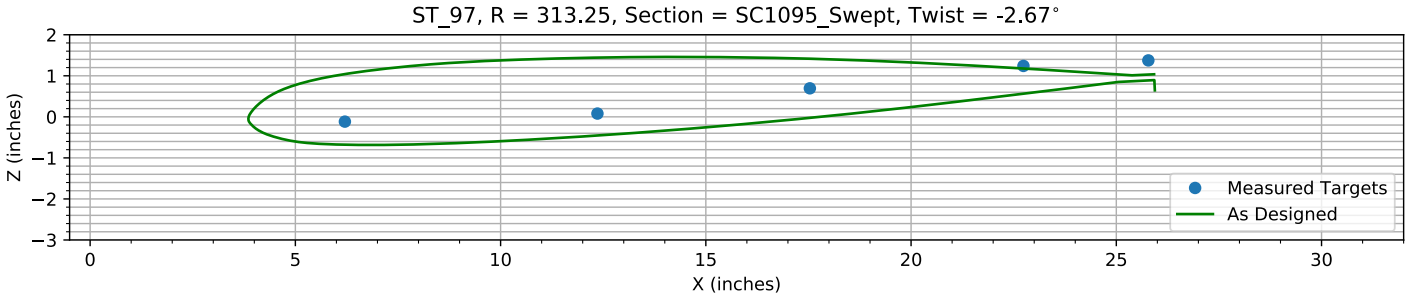

Figure 8-20. Target locations vs section profile at station 97.

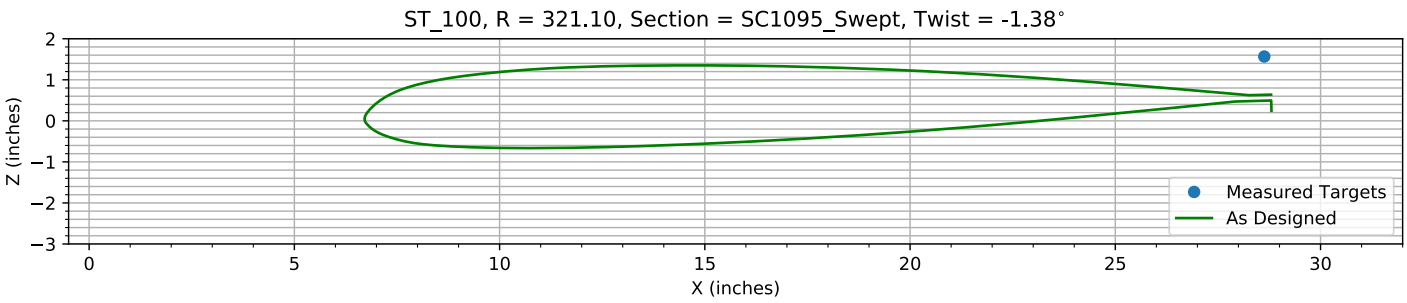

Figure 8-21. Target locations vs section profile at station 100.

Chapter 9: Pitch, Flap, and ΔZ Registration (15 rows)

The targets at the 15 spanwise stations nearest the root are used to determing the Z, flap, and pitch offset.

The estimated Z error, -0.42876 inches, is within an allowed range of ±2.000 inches.

The estimated flap error is 0.32547°.

The estimated pitch error is -0.15751°.

9.1: Target Location Errors After Target Registration

Table 9-1. Measured(1) with pitch and flap registration vs as designed(2) in inches.

Name	X1	Y1	Z1	X2	Y2	Z2	dX	dY	dZ	dR
B4_R20_C05	1.0541	64.473	0.10078	1.0541	64.473	0.063586	0	0	0.037193	0.037193
B4_R20_C36	7.1229	64.431	-1.0592	7.1229	64.431	-1.1264	0	0	0.06724	0.06724
B4_R20_C61	12.294	64.424	-1.6743	12.294	64.424	-1.7839	0	0	0.10959	0.10959
B4_R20_C86	17.514	64.427	-2.1715	17.514	64.427	-2.2676	0	0	0.096184	0.096184
B4_R20_C99	20.485	64.388	-2.7403	20.506	64.388	-2.8207	-0.020875	0	0.080403	0.083069
B4_R25_C05	1.0189	80.602	0.016452	1.0189	80.602	0.017713	0	0	-0.0012614	0.0012614
B4_R25_C36	7.0957	80.587	-1.0572	7.0957	80.587	-1.0933	0	0	0.03605	0.03605
B4_R25_C61	12.338	80.576	-1.6582	12.338	80.576	-1.6849	0	0	0.026634	0.026634
B4_R25_C86	17.574	80.579	-2.0737	17.574	80.579	-2.0949	0	0	0.021196	0.021196
B4_R25_C99	20.525	80.577	-2.6504	20.544	80.577	-2.603	-0.0192	0	-0.047412	0.051152
B4_R30_C05	1.0466	96.675	-0.076327	1.0466	96.675	-0.050536	0	0	-0.025791	0.025791
B4_R30_C36	7.1229	96.669	-1.0754	7.1229	96.669	-1.0678	0	0	-0.0076176	0.0076176
B4_R30_C61	12.367	96.64	-1.5751	12.367	96.64	-1.5848	0	0	0.0097584	0.0097584
B4_R30_C86	17.611	96.635	-1.9254	17.611	96.635	-1.9213	0	0	-0.0041238	0.0041238
B4_R30_C99	20.564	96.576	-2.4643	20.579	96.576	-2.3879	-0.015282	0	-0.076327	0.077841
B4_R35_C05	1.0766	112.73	-0.1567	1.0766	112.73	-0.11795	0	0	-0.038751	0.038751
B4_R35_C36	7.1695	112.78	-1.0559	7.1695	112.78	-1.0438	0	0	-0.012168	0.012168
B4_R35_C61	12.385	112.74	-1.458	12.385	112.74	-1.4836	0	0	0.025611	0.025611
B4_R35_C86	17.632	112.75	-1.7217	17.632	112.75	-1.7462	0	0	0.024525	0.024525
B4_R35_C99	20.646	112.77	-2.2303	20.611	112.77	-2.1703	0.034292	0	-0.059983	0.069094
B4_R40_C05	1.139	128.86	-0.24983	1.139	128.86	-0.19362	0	0	-0.056205	0.056205
B4_R40_C36	7.2233	128.86	-1.0435	7.2233	128.86	-1.0194	0	0	-0.024129	0.024129
B4_R40_C61	12.469	128.87	-1.3999	12.469	128.87	-1.3856	0	0	-0.014228	0.014228
B4_R40_C86	17.688	128.83	-1.5694	17.688	128.83	-1.5726	0	0	0.0031266	0.0031266
B4_R40_C99	20.679	128.87	-2.0292	20.64	128.87	-1.9537	0.038234	0	-0.075536	0.084662
B4_R45_C05	1.066	144.93	-0.31818	1.066	144.93	-0.22868	0	0	-0.089493	0.089493
B4_R45_C36	7.1675	144.9	-1.0329	7.1675	144.9	-0.98575	0	0	-0.047145	0.047145
B4_R45_C61	12.398	144.89	-1.3179	12.398	144.89	-1.2806	0	0	-0.03731	0.03731
B4_R45_C86	17.657	144.91	-1.4435	17.657	144.91	-1.3969	0	0	-0.04663	0.04663
B4_R45_C99	20.679	144.9	-1.8251	20.666	144.9	-1.7379	0.013058	0	-0.087162	0.088135
B4_R50_C05	1.0973	161.11	-0.55839	1.0973	161.11	-0.49537	0	0	-0.063013	0.063013
B4_R50_C36	7.1889	161.06	-1.0292	7.1889	161.06	-0.96207	0	0	-0.067123	0.067123
B4_R50_C61	12.461	161.04	-1.2139	12.461	161.04	-1.1794	0	0	-0.034524	0.034524
B4_R50_C86	17.7	161.03	-1.2558	17.7	161.03	-1.2161	0	0	-0.039694	0.039694
B4_R50_C99	20.692	161.05	-1.5946	20.695	161.05	-1.512	-0.0037107	0	-0.082585	0.082668
B4_R55_C05	1.1283	179.06	-0.62674	1.1283	179.06	-0.56764	0	0	-0.059106	0.059106

Name	X1	Y1	Z1	X2	Y2	Z2	dX	dY	dZ	dR
B4_R55_C36	7.2439	179.04	-0.94128	7.2439	179.04	-0.92926	0	0	-0.012017	0.012017
B4_R55_C61	12.485	179.04	-1.0778	12.485	179.04	-1.0542	0	0	-0.023648	0.023648
B4_R55_C86	17.718	179.02	-1.0196	17.718	179.02	-1.0009	0	0	-0.018752	0.018752
B4_R55_C99	20.724	179	-1.3081	20.719	179	-1.246	0.0046472	0	-0.062091	0.062264
B4_R60_C05	1.1236	193.25	-0.66535	1.1236	193.25	-0.62157	0	0	-0.043788	0.043788
B4_R60_C36	7.2203	193.24	-0.91649	7.2203	193.24	-0.90026	0	0	-0.016226	0.016226
B4_R60_C61	12.464	193.23	-0.962	12.464	193.23	-0.95553	0	0	-0.0064709	0.0064709
B4_R60_C86	17.721	193.24	-0.83683	17.721	193.24	-0.83097	0	0	-0.0058632	0.0058632
B4_R60_C99	20.751	193.2	-1.0545	20.734	193.2	-1.0352	0.016405	0	-0.019285	0.025319
B4_R65_C05	1.1432	209.3	-0.70697	1.1432	209.3	-0.68448	0	0	-0.022491	0.022491
B4_R65_C36	7.27	209.33	-0.86269	7.27	209.33	-0.86947	0	0	0.0067762	0.0067762
B4_R65_C61	12.544	209.32	-0.81226	12.544	209.32	-0.84201	0	0	0.029752	0.029752
B4_R65_C86	17.736	209.33	-0.59366	17.736	209.33	-0.63814	0	0	0.044474	0.044474
B4_R65_C99	20.764	209.27	-0.77502	20.749	209.27	-0.79656	0.015138	0	0.021537	0.026325
B4_R70_C05	1.1395	225.35	-0.77245	1.1395	225.35	-0.74564	0	0	-0.026806	0.026806
B4_R70_C36	7.2913	225.38	-0.82233	7.2913	225.38	-0.83748	0	0	0.015146	0.015146
B4_R70_C61	12.535	225.37	-0.67779	12.535	225.37	-0.73005	0	0	0.052259	0.052259
B4_R70_C86	17.741	225.39	-0.36148	17.741	225.39	-0.44596	0	0	0.084481	0.084481
B4_R70_C99	20.779	225.41	-0.48548	20.759	225.41	-0.55659	0.019731	0	0.071109	0.073796
B4_R75_C05	1.1152	241.5	-0.83131	1.1152	241.5	-0.80032	0	0	-0.030997	0.030997
B4_R75_C36	7.2894	241.51	-0.81395	7.2894	241.51	-0.8085	0	0	-0.0054569	0.0054569
B4_R75_C61	12.517	241.5	-0.53918	12.517	241.5	-0.62967	0	0	0.090485	0.090485
B4_R75_C86	17.728	241.51	-0.12021	17.728	241.51	-0.2736	0	0	0.15339	0.15339
B4_R80_C05	1.1058	257.63	-0.88869	1.1058	257.63	-0.84548	0	0	-0.043213	0.043213
B4_R80_C36	7.2756	257.66	-0.77803	7.2756	257.66	-0.78544	0	0	0.0074121	0.0074121
B4_R80_C61	12.5	257.67	-0.48336	12.5	257.67	-0.54872	0	0	0.065363	0.065363
B4_R80_C86	17.706	257.69	0.0054237	17.706	257.69	-0.13452	0	0	0.13995	0.13995
B4_R86_C05	1.182	276.34	-0.74352	1.182	276.34	-0.69818	0	0	-0.045345	0.045345
B4_R86_C36	7.3293	276.34	-0.75012	7.3293	276.34	-0.75651	0	0	0.0063897	0.0063897
B4_R86_C61	12.528	276.34	-0.38979	12.528	276.34	-0.46592	0	0	0.076129	0.076129
B4_R86_C86	17.74	276.33	0.11902	17.74	276.33	0.0032927	0	0	0.11573	0.11573
B4_R91_C05	1.1534	293.02	-0.7998	1.1534	293.02	-0.81914	0	0	0.019339	0.019339
B4_R91_C36	7.274	293.06	-0.65086	7.274	293.06	-0.69293	0	0	0.042071	0.042071
B4_R91_C61	12.492	293.07	-0.10185	12.492	293.07	-0.23493	0	0	0.13308	0.13308
B4_R91_C86	17.694	293.07	0.57687	17.694	293.07	0.40124	0	0	0.17563	0.17563
B4_R91_C99	20.716	293.06	0.72913	20.755	293.06	0.49967	-0.039431	0	0.22946	0.23282
B4_R97_C05	6.2075	313.23	-0.47966	6.2075	313.23	-0.67947	0	0	0.19981	0.19981
B4_R97_C36	12.36	313.21	-0.28699	12.36	313.21	-0.45416	0	0	0.16718	0.16718
B4_R97_C61	17.536	313.29	0.32489	17.536	313.29	-0.02665	0	0	0.35154	0.35154
B4_R97_C86	22.739	313.27	0.86747	22.739	313.27	0.56164	0	0	0.30583	0.30583
B4_R97_C99	25.782	313.29	1.0003	25.953	313.29	0.64375	-0.17052	0	0.35657	0.39525
HUB_LE	2.1825	30.003	-3.0629	2.19	30	-3.5	-0.0074715	0.0027397	0.43712	0.43719
HUB_TE	8.1775	30.002	-3.0797	8.19	30	-3.5	-0.012495	0.0021332	0.42034	0.42054
RMS Errors:							0.021232	0.00039066	0.1177	0.1196

9.2: Pitch and Flap Registration Plots (15 rows)

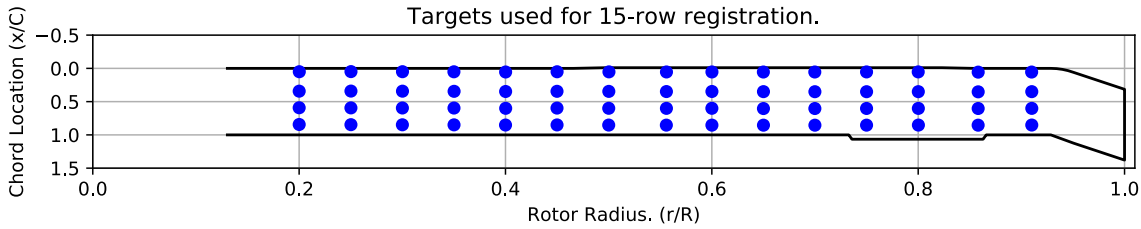

Figure 9-1. Targets used for 15 row root registration.

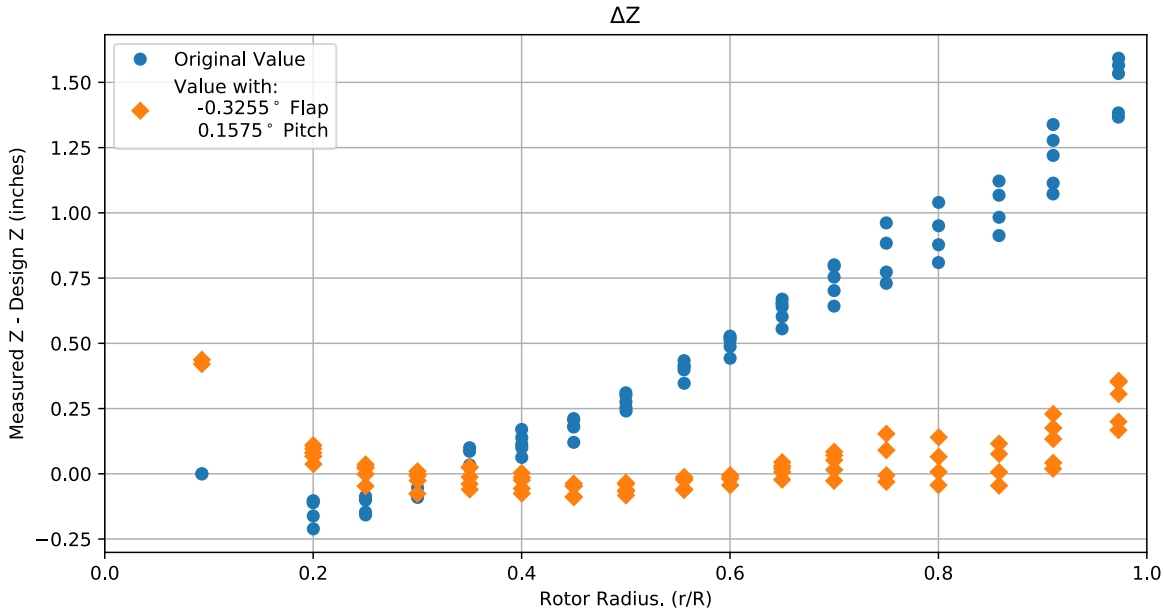

Figure 9-2. Pitch and flap target registration, ΔZ error vs rotor radius.

Note: the “as designed” geometry used for the swept tip may have some inaccuracies.

9.3: Estimated Bending and Twist at the Quarter Chord

The error bars shown represent the residual errors for fitting the measure target locations to the "as designed" geometry. These errors are generally much larger than those due to the VSTARS measurement errors. Therefore, the most likely source of these errors is the placement of the trailing-edge targets, differences between the "as designed" and "as built" geometries, and blade deformation during measurement. In the future, iterative adjustment of the "as designed" twist angle may be implemented to see if it reduces the fit error in delta twist. Note: The "as designed" geometry used for the swept tip may have some inaccuracies.

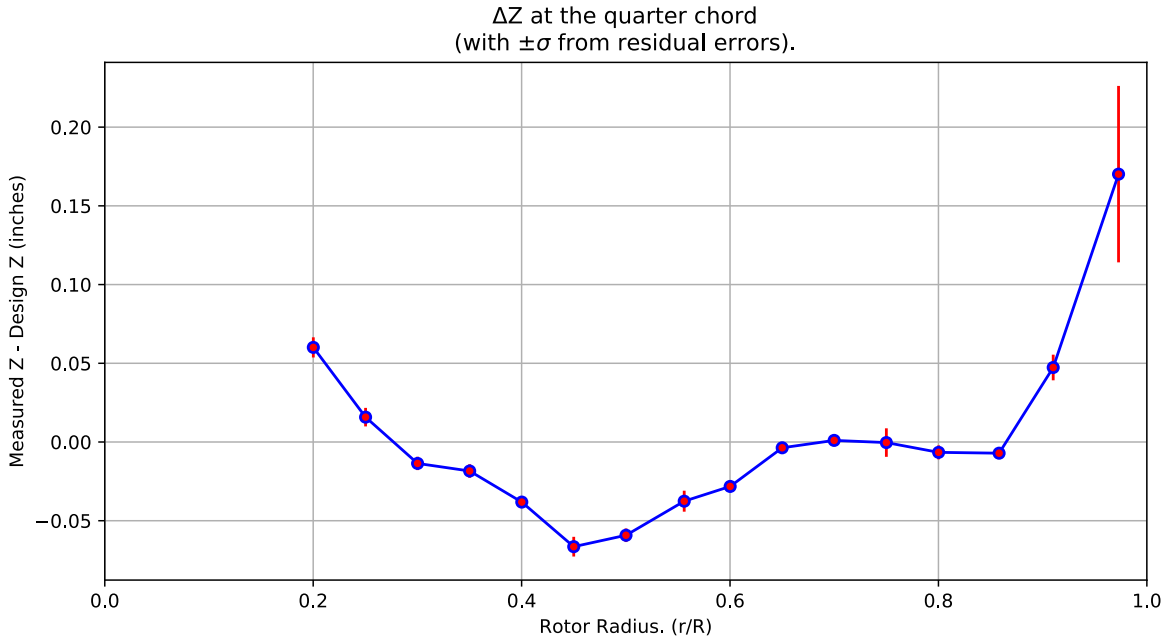

Figure 9-3. ΔZ error at the quarter chord vs rotor radius.

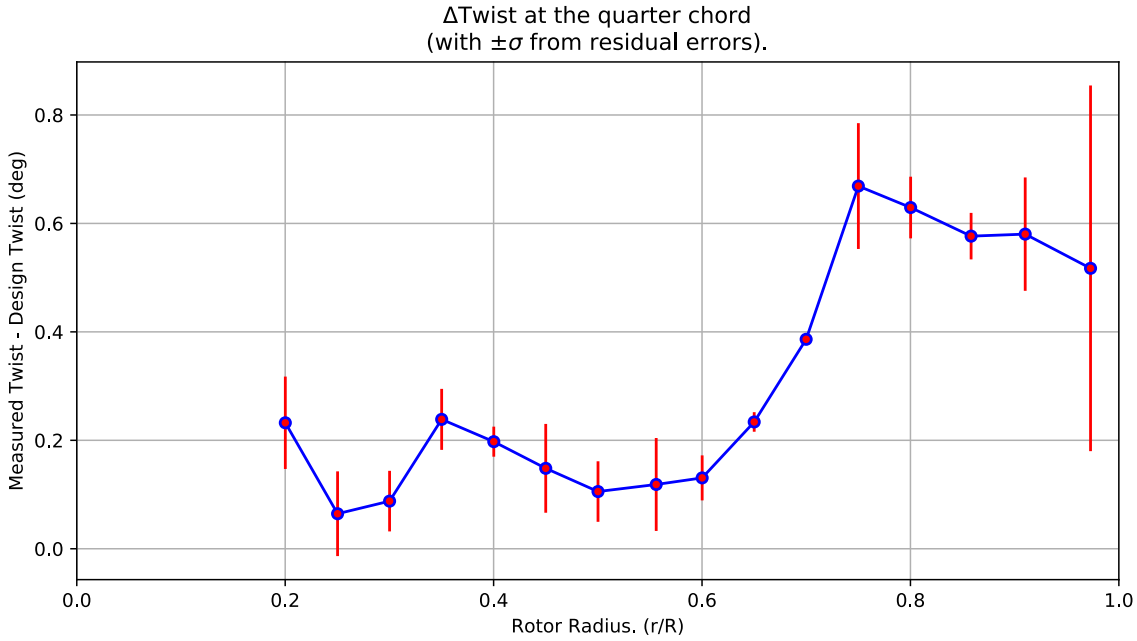

Figure 9-4. ΔTwist error at the quarter chord vs rotor radius.

Table 9-2. Quarter-chord bending and twist statistics.

r	r/R	dZ 1/4-chord	dT	sigma dZ meas	sigma dT meas	sigma dZ res	sigma dT res	n	t_conf
64.439	0.20012	0.060091	0.23232	6.1192e-10	4.6936e-09	0.0064026	0.085188	4	4.3027
80.586	0.25027	0.015788	0.064598	6.1109e-10	4.6633e-09	0.0058867	0.078136	4	4.3027
96.655	0.30017	-0.013608	0.087846	6.124e-10	4.661e-09	0.0042387	0.055871	4	4.3027
112.75	0.35015	-0.01842	0.23863	6.1397e-10	4.6653e-09	0.0042963	0.056255	4	4.3027
128.85	0.40017	-0.038163	0.1975	6.1697e-10	4.6645e-09	0.0021463	0.027698	4	4.3027
144.91	0.45002	-0.066489	0.14833	6.1381e-10	4.6552e-09	0.0062641	0.081903	4	4.3027
161.06	0.50018	-0.059232	0.10551	6.154e-10	4.6487e-09	0.004308	0.055819	4	4.3027
179.04	0.55603	-0.037596	0.11855	6.1717e-10	4.6542e-09	0.006662	0.085701	4	4.3027
193.24	0.60013	-0.02822	0.1307	6.1654e-10	4.6523e-09	0.0032182	0.041506	4	4.3027
209.32	0.65006	-0.0036722	0.23386	6.1841e-10	4.6504e-09	0.001412	0.018045	4	4.3027
225.37	0.69992	0.0010175	0.38632	6.1857e-10	4.6506e-09	0.0005498	0.0070208	4	4.3027
241.51	0.75002	-0.00036302	0.66891	6.1781e-10	4.6484e-09	0.009057	0.11601	4	4.3027
257.66	0.80019	-0.0065756	0.62932	6.1722e-10	4.652e-09	0.0044236	0.056864	4	4.3027
276.34	0.8582	-0.0071054	0.57654	6.2013e-10	4.6651e-09	0.0033726	0.042892	4	4.3027
293.06	0.91012	0.047326	0.58027	6.1827e-10	4.6679e-09	0.0081455	0.10455	4	4.3027
313.25	0.97282	0.17014	0.51722	9.237e-10	4.6737e-09	0.056036	0.3372	4	4.3027

9.4: Section Plots

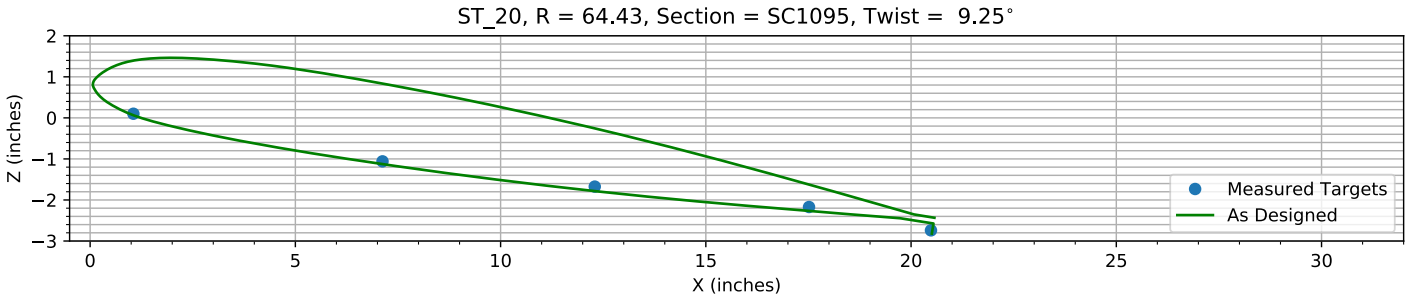

Figure 9-5. Target locations vs section profile at station 20.

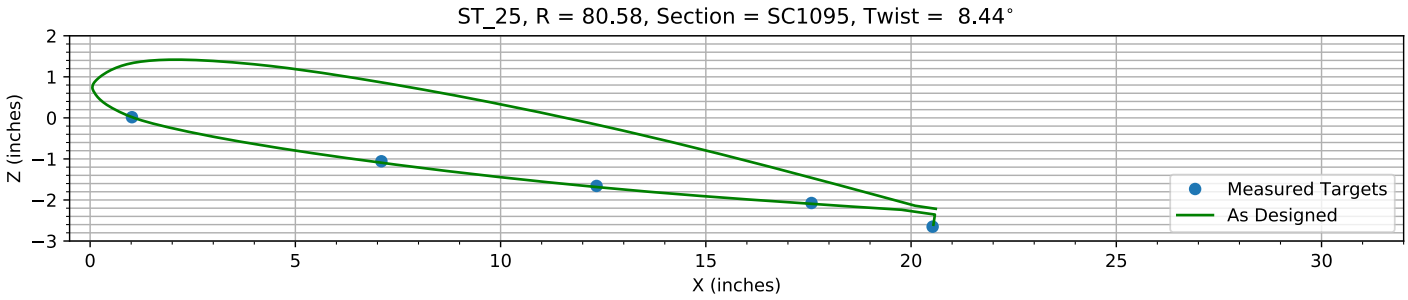

Figure 9-6. Target locations vs section profile at station 25.

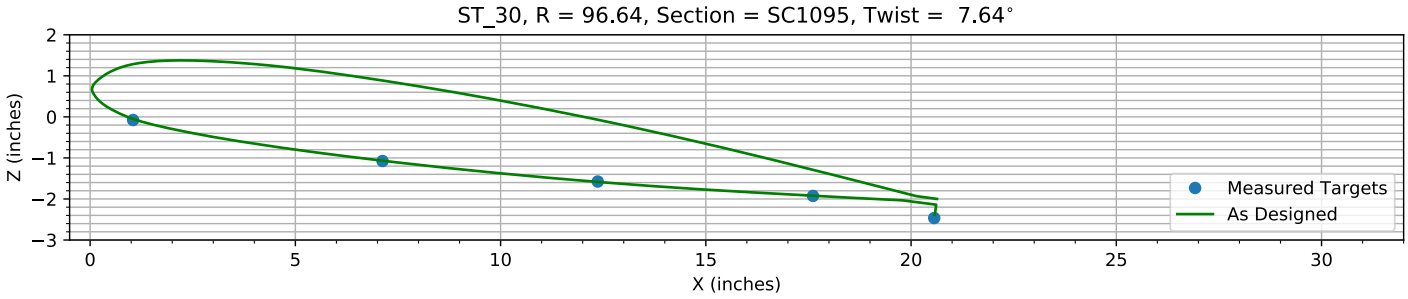

Figure 9-7. Target locations vs section profile at station 30.

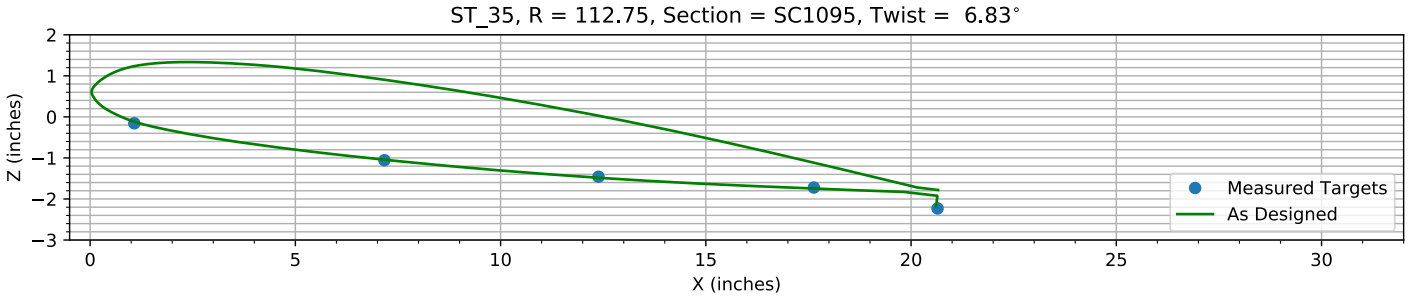

Figure 9-8. Target locations vs section profile at station 35.

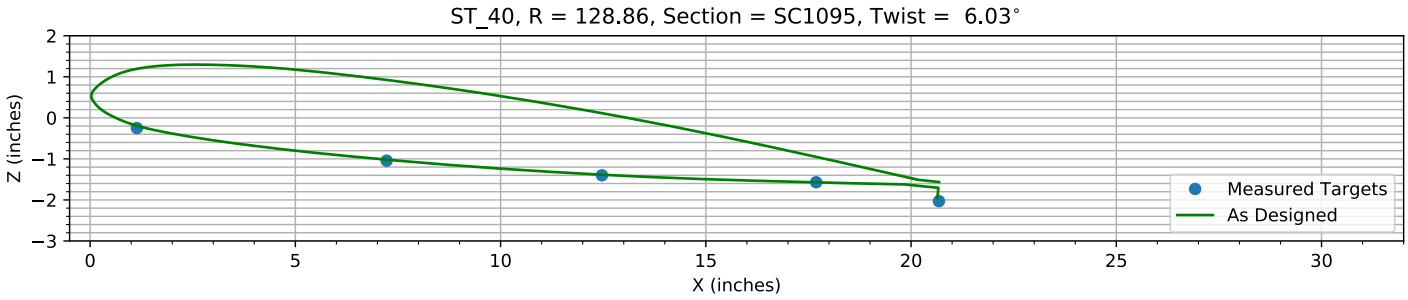

Figure 9-9. Target locations vs section profile at station 40.

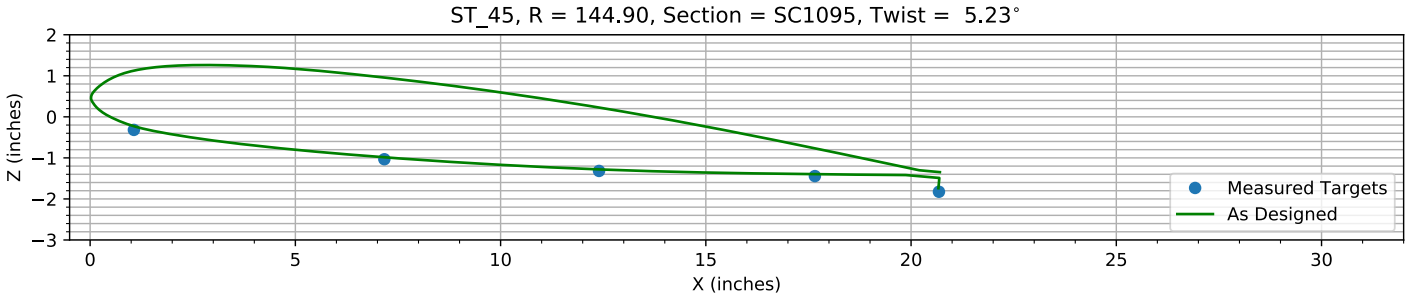

Figure 9-10. Target locations vs section profile at station 45.

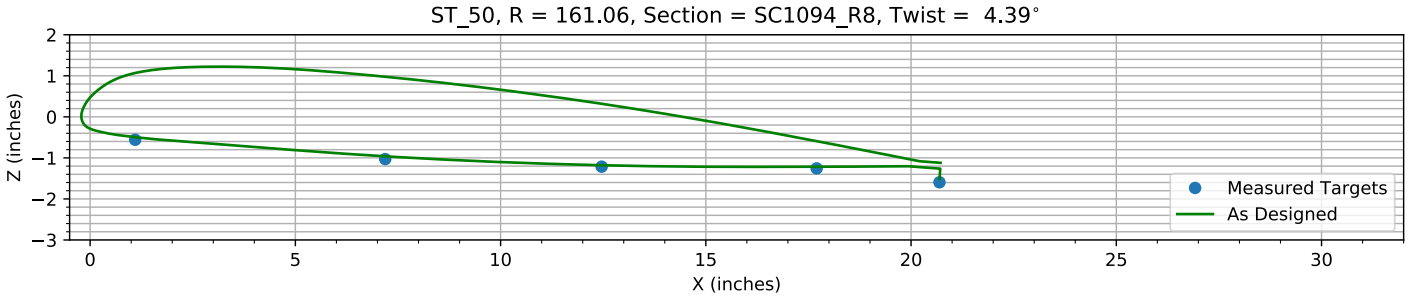

Figure 9-11. Target locations vs section profile at station 50.

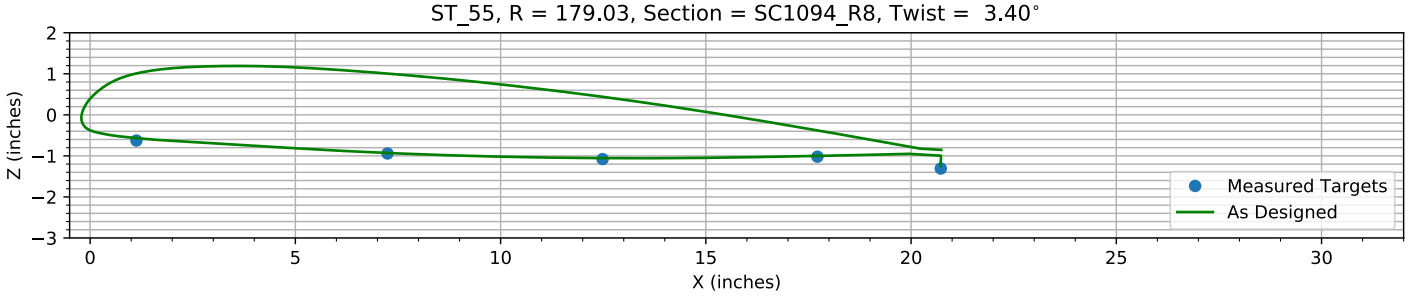

Figure 9-12. Target locations vs section profile at station 55.

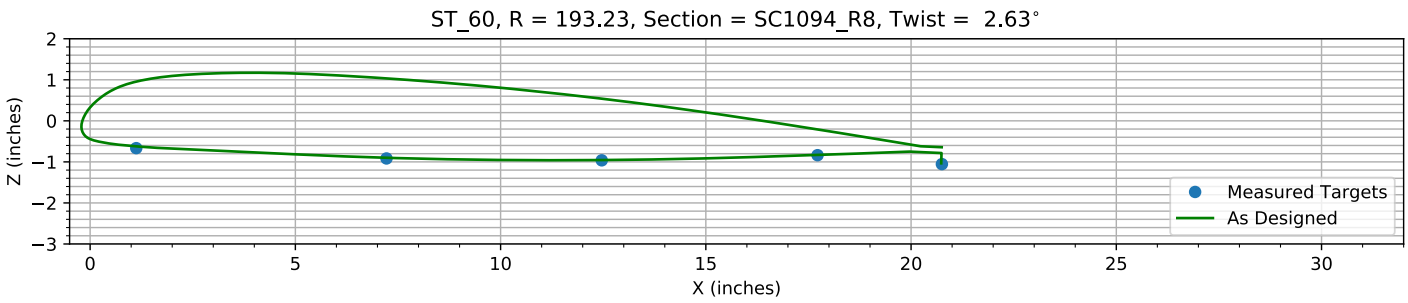

Figure 9-13. Target locations vs section profile at station 60.

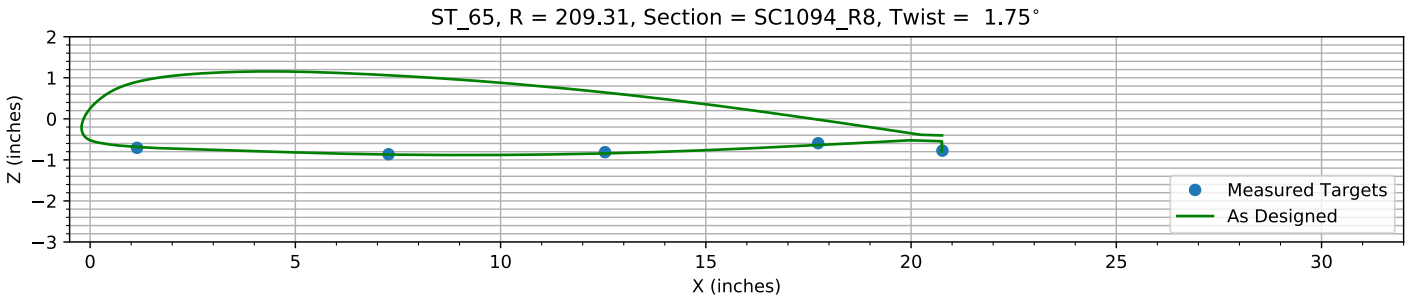

Figure 9-14. Target locations vs section profile at station 65.

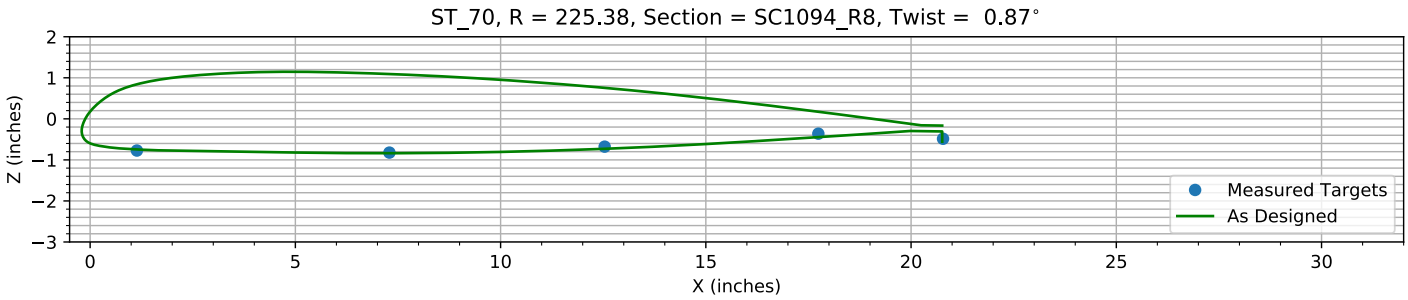

Figure 9-15. Target locations vs section profile at station 70.

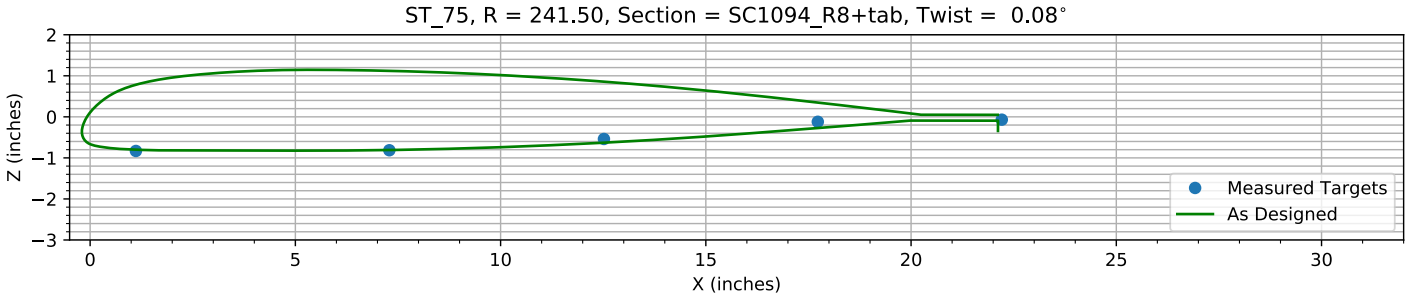

Figure 9-16. Target locations vs section profile at station 75.

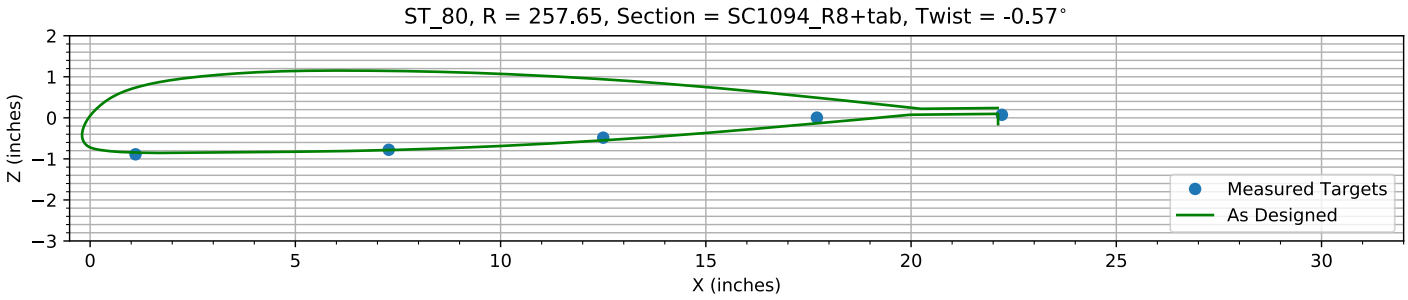

Figure 9-17. Target locations vs section profile at station 80.

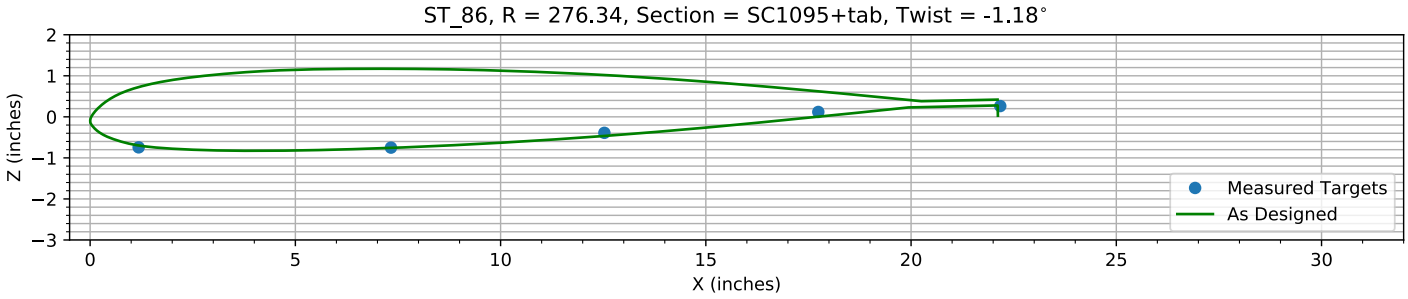

Figure 9-18. Target locations vs section profile at station 86.

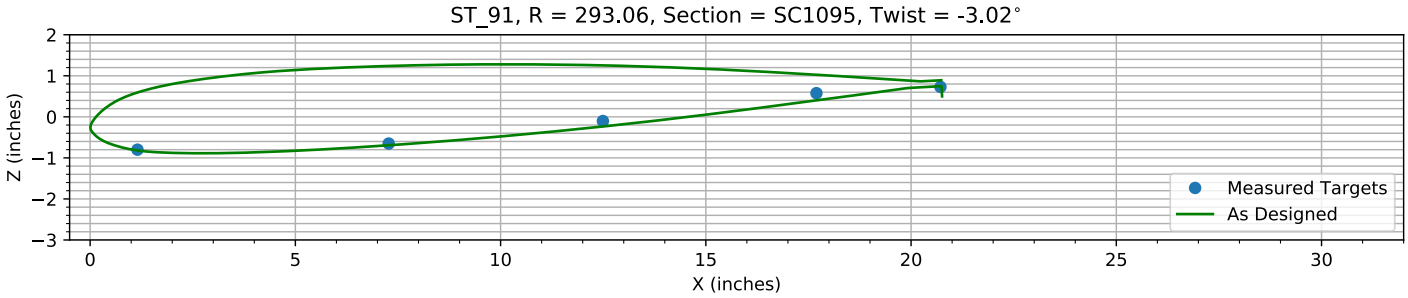

Figure 9-19. Target locations vs section profile at station 91.

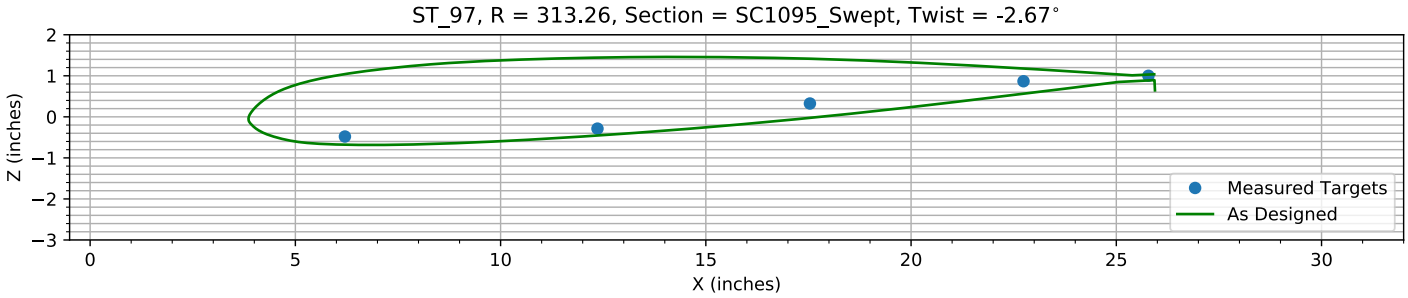

Figure 9-20. Target locations vs section profile at station 97.

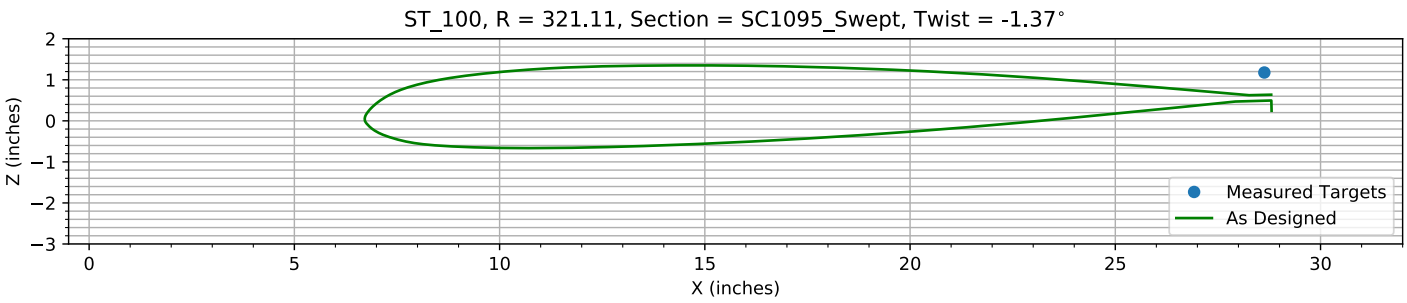

Figure 9-21. Target locations vs section profile at station 100.

REPORT DOCUMENTATION PAGE

Form Approved
OMB No. 0704–0188

1. REPORT DATE *(DD-MM-YYYY)*	2. REPORT TYPE	3. DATES COVERED *(From - To)*
01-08-2017	Technical Memorandum	

4. TITLE AND SUBTITLE
Blade Displacement Measurements During the NFAC UH-60A Airloads Test
Volume I—Methodology, System Development, and Data Analysis Techniques

5a. CONTRACT NUMBER

5b. GRANT NUMBER

5c. PROGRAM ELEMENT NUMBER

6. AUTHOR(S)
Larry A. Meyn, Anita I. Abrego, Danny A. Barrows and Alpheus W. Burner

5d. PROJECT NUMBER

5e. TASK NUMBER

5f. WORK UNIT NUMBER

7. PERFORMING ORGANIZATION NAME(S) AND ADDRESS(ES)
NASA Ames Research Center
Moffett Field, CA 94035-1000

8. PERFORMING ORGANIZATION REPORT NUMBER

9. SPONSORING/MONITORING AGENCY NAME(S) AND ADDRESS(ES)
National Aeronautics and Space Administration
Washington, DC 20546-0001

10. SPONSOR/MONITOR'S ACRONYM(S)
NASA

11. SPONSOR/MONITOR'S REPORT NUMBER(S)
NASA/TM—2017–219094

12. DISTRIBUTION/AVAILABILITY STATEMENT
Unclassified-Unlimited
Subject Category 05
Availability: NASA STI Program (757) 864-9658

13. SUPPLEMENTARY NOTES
An electronic version can be found at http://ntrs.nasa.gov.

14. ABSTRACT

Blade displacement measurements using multi-camera photogrammetry techniques were acquired for a full-scale UH-60A rotor, tested in the National Full-Scale Aerodynamics Complex (NFAC) 40- by 80-Foot Wind Tunnel. The measurements, acquired over the full rotor azimuth, encompassed a range of test conditions that included advance ratios from 0.15 to 1.0, thrust coefficient to rotor solidity ratios from 0.01 to 0.13, and rotor shaft angles from -10.0 to 8.0 degrees. The objective was to measure the blade displacements and deformations of the four rotor blades and provide a benchmark blade displacement database to be used in the development and validation of rotorcraft prediction techniques. The blade displacement measurement methodology, system development, and data analysis techniques are presented. Sample results are shown based on the final set of camera calibrations, data reduction procedures, and estimated corrections that account for registration errors due to blade elasticity.

15. SUBJECT TERMS
rotor, deformation, photogrammetry, measurement

16. SECURITY CLASSIFICATION OF:			17. LIMITATION OF ABSTRACT	18. NUMBER OF PAGES	19a. NAME OF RESPONSIBLE PERSON
a. REPORT	b. ABSTRACT	c. THIS PAGE			STI Information Desk (help@sti.nasa.gov)
U	U	U	UU	360	19b. TELEPHONE NUMBER *(Include area code)* (757) 864-9658